

Heinrich-Heine-Universität Düsseldorf



Derivation, characterization and application of human primary stem cells, iPSCs, and iPSC-derived MSCs for regenerative medicine and disease modelling

Inaugural-Dissertation

zur Erlangung des Doktorgrades
der Mathematisch-Naturwissenschaftlichen Fakultät
der Heinrich-Heine-Universität Düsseldorf

vorgelegt von

Lucas-Sebastian Spitzhorn
aus Düsseldorf

Düsseldorf, Januar 2020

aus dem Institut für Stammzellforschung und Regenerative Medizin des
Universitätsklinikums der Heinrich-Heine-Universität Düsseldorf

Gedruckt mit der Genehmigung der
Mathematisch-Naturwissenschaftlichen Fakultät der
Heinrich-Heine-Universität Düsseldorf

Berichtersteller:

1. Prof. Dr. James Adjaye

2. Prof. Dr. Henrike Heise

Tag der mündlichen Prüfung: 09.01.2020

Abstract

Mathematisch-Naturwissenschaftliche Fakultät

Institute for Stem Cell Research and Regenerative Medicine

Doctor rerum naturalium

Derivation, characterization and application of human primary stem cells, iPSCs, and iPSC-derived MSCs for regenerative medicine and disease modelling

by Lucas-Sebastian Spitzhorn

In today's research and medical practice, stem cells are of high relevance. They represent a promising alternative to whole organ transplantation and provide multiple ways of action and settings to be used in. The first aspect of this work was the derivation of stem cells from different sources. Bone marrow is a long-established source for stem cells such as mesenchymal stem cells (MSCs). Amniotic fluid and urine were investigated herein as alternative sources to receive MSCs originating from the kidney following detailed characterization of the isolated cells. These urine stem cells were furthermore reprogrammed into induced pluripotent stem cells (iPSCs) which are capable of differentiating into all cells of the human body. The suitability of iPSCs was further successfully tested for toxicology studies as well as for liver disease modelling (particularly non-alcoholic fatty liver disease- NAFLD).

For the purpose of *in vivo* studies within this work, mesenchymal stem cells were derived from iPSCs from different origins, termed iMSCs. These iMSCs were analysed upon their features compared to primary MSCs and were shown to represent rejuvenated and thus more potent cells than their native counterparts. The iMSCs were used in 2 independent animal models to study their potential to be used in translational regenerative medicine approaches.

The first model was the Gunn rat which lacks activity of the Ugt1a1 (UDP glucuronosyltransferase family 1 member A1) by spontaneous mutation, resulting in

increased bilirubin levels. To improve this liver disease phenotype human iMSCs (derived from iPSCs from human foetal MSCs) were transplanted by intra-spleenic injection after liver injury by partial hepatectomy. The transplanted human iMSCs differentiated into functional human liver cells and thereby contributed to liver regeneration and to the reduction of serum bilirubin levels in Gunn rats.

The second model, in which the iMSCs were applied, was a human-scale preclinical animal model for bone regeneration. iMSCs differentiated from human foreskin fibroblast-derived iPSCs were transplanted combined with calcium phosphate granules into a critical size defect in the tibiae of Göttingen mini pigs. The human iMSCs significantly supported bone regeneration and showed a similar effect than autologous bone marrow concentrate which consist of MSCs, immune cells and growth factors. In addition to the direct therapeutic effect by differentiation of the iMSCs it can be assumed that the paracrine release of signalling factors is another mode of action by iMSCs capable to suppress the host's immune system and to attract resident stem cells. This represents another clinically relevant property of MSCs.

Beside the MSC-derived immune-modulatory factors it was further shown that human foetal MSCs secrete factors which promote oligodendrogenesis in rat neural stem cells and iPSC-derived neuronal stem cells.

In conclusion, amniotic fluid and urine were qualified as sources for renal stem cells, iPSCs were generated and shown to be a promising tool for future research, iMSCs were shown to be rejuvenated and able to support regeneration of liver and bone *in vivo*. Additionally, MSCs were shown to be active in paracrine manner and by that were able to aid neuronal developmental processes. All findings reported herein by translational research qualify (i)MSCs for developing new therapeutic approaches.

Zusammenfassung

Für die heutige Forschung und klinische Anwendungen sind Stammzellen von hoher Relevanz. Sie sind gute Alternativen zur Transplantation ganzer Organe und können vielfältig eingesetzt werden. Der erste Teil dieser Arbeit bestand in der Gewinnung von Stammzellen aus verschiedenen Quellen. Das Knochenmark ist eine etablierte Quelle zur Gewinnung von Stammzellen wie den mesenchymalen Stammzellen (MSCs). Als alternative Stammzellquellen wurden in dieser Arbeit das Fruchtwasser sowie der Urin untersucht und die gewonnenen Stammzellen als MSCs mit Ursprung in der Niere charakterisiert. Diese Urinstammzellen wurden zusätzlich in induzierte pluripotente Stammzellen (iPSCs) reprogrammiert, die in der Lage sind, sich in alle Zellen des menschlichen Körpers zu differenzieren. Weiterhin wurde gezeigt, dass sich iPSCs hervorragend für Toxikologie-Studien sowie zur Modellierung von Leberkrankheiten (im speziellen nicht alkoholische Fettleber- NAFLD) eignen.

Zur Durchführung von *in vivo*-Studien innerhalb dieser Arbeit wurden MSCs aus iPSCs hergestellt; genannt iMSCs. Diese iMSCs wurden im Vergleich zu primären MSCs analysiert und als verjüngte MSCs identifiziert, die potenter sind als ihre primären Gegenstücke. Diese iMSCs wurden in zwei unabhängigen *in vivo*-Modellen eingesetzt, um ihr Potenzial für translationale regenerative Anwendungen zu untersuchen.

Das erste Modell war die Gunn-Ratte, bei der eine natürliche Mutation in dem Ugt1a1 Gen (UDP glucuronosyltransferase family 1 member A1) mit einem daraus resultierenden erhöhten Serum-Bilirubin-Wert vorliegt. Nach partieller Hepatektomie und anschließender Transplantation humaner iMSCs, die aus iPSCs von fötalen MSCs hergestellt wurden, konnte gezeigt werden, dass humane iMSCs in funktionale Leberzellen differenziert sind. Dadurch haben sie zur Regeneration der Leber und zur Senkung des erhöhten Bilirubin Spiegels beigetragen.

Als zweite *in vivo*-Studie wurden iMSCs, die aus iPSCs aus humanen Vorhaut Fibroblasten erzeugt wurden, in Kombination mit Kalziumphosphat-Granulat in einen Knochendefekt kritischer Größe in das Schienbein von Göttingen Minischweinen transplantiert. Die humanen iMSCs unterstützten die Knochenheilung in diesem prä-klinischen Tiermodell humaner Größe signifikant und zeigten vergleichbare Ergebnisse

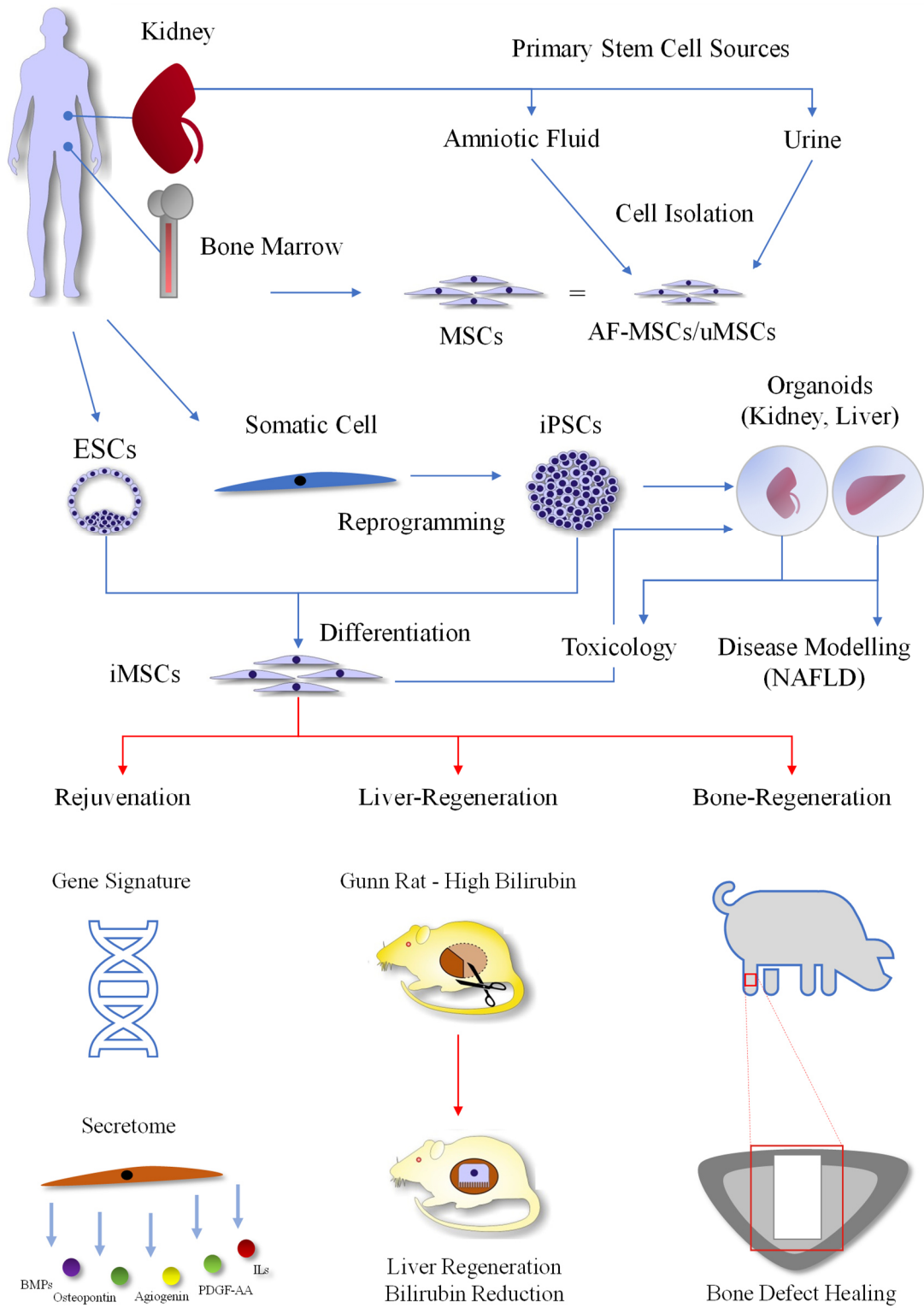
wie autologes Knochenmark-Konzentrat, das MSCs, Immunzellen und Wachstumsfaktoren beinhaltet.

Zusätzlich zu dem direkten therapeutischen Effekt der iMSCs durch Differenzierung kann auch ein parakriner Wirkmechanismus angenommen werden, wodurch das Immunsystem des Empfängers unterdrückt wird und körpereigene Stammzellen mobilisiert werden.

Es wurde zudem gezeigt, dass fötale MSCs zusätzlich zu immunmodulierenden Stoffen auch Faktoren sezernieren, die die Oligodendrogenese in neuronalen Zellen der Ratte und in neuronalen Stammzellen aus iPSCs fördern.

Zusammenfassend wurden Fruchtwasser und Urin als geeignete Quellen für Nierenstammzellen identifiziert. Pluripotente iPSCs wurden aus Urinstammzellen hergestellt und zeigten sich als vielversprechende Zellen für die zukünftige Forschung. iMSCs wurden als verjüngte Stammzellen beschrieben, die in der Lage sind *in vivo* zur Leber- und Knochenheilung beizutragen. Darüber hinaus wurden MSCs als parakrin-aktive Zellen beschrieben, die neuronale Entwicklungsprozesse unterstützen können. All diese Befunde zeichnen (i)MSCs unterschiedlicher Quellen für die translationale Forschung aus und stellen eine Basis für die Entwicklung neuer therapeutischer Ansätze dar.

Graphical Abstract



Contents

Abstract	3
Zusammenfassung	5
Graphical Abstract	7
Contents	8
List of Figures	10
Abbreviations	13
1. Introduction	
1.1 Stem Cells.....	16
1.2 Mesenchymal Stem Cells.....	17
1.3 Clinical Applications of MSCs.....	19
1.4 MSCs in Liver Regeneration.....	20
1.5 MSCs in Bone Regeneration.....	22
1.6 MSCs in Neurogenesis.....	22
1.7 Induced Pluripotent Stem Cells.....	23
1.8 In Human Application of iPSC-derived Cells.....	26
1.9 iPSC-derived MSCs (iMSCs).....	27
1.10 Amniotic Fluid as a Source of Stem Cells.....	29
1.11 Kidney Structure and Cell Types for Kidney-related Research.....	30
Aims of This Thesis	33
2. Results - Publications	
Part 1: Sources of Stem Cells	
2.1 <i>Isolation and Molecular Characterization of Amniotic Fluid-derived Mesenchymal Stem Cells obtained from Caesarean sections</i>	34
2.2 <i>The presence of human mesenchymal stem cells of renal origin in amniotic fluid increases with gestational time</i>	51
2.3 <i>Urine-derived stem cells as innovative platform for drug testing and disease modelling</i>	70
2.4 <i>Derivation and characterization of integration-free iPSC line ISRM-UM51 derived from SIX2-positive renal cells isolated from urine of an African male expressing the CYP2D6 *4/*17 variant which confers intermediate drug metabolizing activity</i>	76
Part 2: Translational Applications of iPSCs, MSCs and iMSCs <i>in vitro</i> and <i>in vivo</i>	
2.5 <i>Use of Stem Cells in Toxicology</i>	82
2.6 <i>Liver Disease Modelling</i>	103
2.7 <i>Generation of a 3D model to better mimic NAFLD in vitro</i>	124

2.8 <i>Constructing an Isogenic 3D Human Nephrogenic Progenitor Cell Model Composed of Endothelial, Mesenchymal, and SIX2-Positive Renal Progenitor Cells....</i>	129
2.9 <i>Human iPSC-derived MSCs (iMSCs) from aged individuals acquire a rejuvenation signature.....</i>	142
2.10 <i>Transplanted human pluripotent stem cell-derived mesenchymal stem cells support liver regeneration in Gunn rats.....</i>	163
2.11 <i>Human iPSC-derived iMSCs improve bone regeneration in mini-pigs.....</i>	186
2.12 <i>Human mesenchymal factors induce rat hippocampal- and human neural stem cell dependent oligodendrogenesis.....</i>	206
2.13 <i>Additional Publications.....</i>	224
Discussion	
Caesarean Section as Alternative Process to Obtain AF-MSCs.....	228
Amniotic Fluid as Source for Kidney-derived Stem Cells.....	229
Urine as a Source of Kidney Stem Cells with Industrial Potential for Personalized Research.....	231
The Future of iPSCs in Clinical Applications.....	234
Multicellular Organoids as Better <i>in vitro</i> Instruments for Disease Modelling.....	235
iMSCs as Rejuvenated MSCs with Clinical Application Potential.....	236
iMSCs as Promising Cells for Treatment of Liver Diseases.....	239
iMSC Transplantation as a Feasible Way to Regenerate Bone.....	241
MSCs for Treatment of Neurodegenerative Diseases.....	244
Further Research.....	245
Conclusion.....	248
Appendix – Talks, Poster Presentations and Prizes.....	249
Bibliography.....	252
Acknowledgements.....	274
Curriculum Vitae.....	275
Declaration of Authorship.....	277

List of Figures

1. Introduction

1.1 Modes of action of MSCs.....	18
1.2 Number and distribution of clinical trials employing MSCs	20
1.3 Derivation process of iPSCs and differentiation into organ-specific cells.....	25
1.4 Generation of human iMSCs from pluripotent stem cells.....	28

2. Results - Publications

2.1 Isolation and Molecular Characterization of Amniotic Fluid-derived Mesenchymal Stem Cells obtained from Caesarean sections

Amniotic Fluid Cell Preparation.....	40
<i>In vitro</i> differentiation potential and immunophenotype of AF-MSCs.....	41
Protein expression analysis of AF-MSCs.....	42
Secretome Analysis of AF-MSCs.....	43
Overlapping and distinct gene expression in AF-MSCs.....	44
AF-MSC specific genes.....	45
Network analysis of the 181 AF-MSC specific genes.....	46

2.2 The presence of human mesenchymal stem cells of renal origin in amniotic fluid increases with gestational time

Initially attached heterogeneous AFCs display homogenous cell morphology upon passaging and include typical kidney cell morphologies.....	56
Pluripotency-associated stem cell markers expression of AFCs in distinct media.....	58
AFCs express typical MSC-associated proteins as well as CK19 and show multi-lineage differentiation potential <i>in vitro</i>	60
Renal-specific marker expression in AF-MSCs.....	61
Functional characterization of AF-MSCs as renal cells.....	62
WNT mediated cell fate decisions in AF-MSCs.....	63
Expression levels of renal-specific genes in AFCs increase with gestational time.....	64
Third trimester AF-MSCs express genes associated with renal-specific biological processes and have high overlap with kidney cells.....	66

2.3 Urine-derived stem cells as innovative platform for drug testing and disease modelling

Molecular and cellular characteristics of uMSCs and uMSC-iPSCs.....	74
Gene expression profiles characterize renal developmental properties of uMSCs and uRETCs.....	75

2.4 Derivation and characterization of integration-free iPSC line ISRM-UM51 derived

<i>from SIX2-positive renal cells isolated from urine of an African male expressing the CYP2D6 *4/*17 variant which confers intermediate drug metabolizing activity</i>	
Characterisation of ISRM-UM51.....	79
<i>2.5 Use of stem cells in toxicology</i>	
iPS cells used in embryoid body-based differentiation into the three embryonic germ layers.....	88
Gene expression analysis of the ADME genes in iPSCs differentiated into cell types representative of endoderm, mesoderm, and ectoderm.....	96
<i>2.6 Liver disease modelling</i>	
<i>In vitro</i> differentiation of iPSCs into HLCs.....	109
Bioinformatic analysis of genes regulated in TD and NAFLD.....	117
<i>2.7 Liver disease modelling</i>	
Generation of a 3D liver model and mimicking NAFLD <i>in vitro</i>	127
<i>2.8 Constructing an Isogenic 3D Human Nephrogenic Progenitor Cell Model Composed of Endothelial, Mesenchymal, and SIX2-Positive Renal Progenitor Cells</i>	
UdRPC-iMSCs are MSCs and bear characteristic MSC features.....	134
Expression of MSC markers in UdRPC-iMSCs.....	135
Phase contrast image of UdRPCs and expression of kidney-related markers.....	135
Comparison of UdRPC-iECs with HUVECs.....	136
Overview of the formation of three-dimensional nephron progenitor cells (3D-NPCs).....	137
Expression of kidney markers (SIX2, PAX8, Nephryn, and Podocin), endothelial marker (CD31), mesenchymal markers (PDGFR- β and Vimentin), and pluripotency-associated markers (TRA-1-81, NANOG, and SSEA4) in 3D-NPCs.....	138
<i>2.9 Human iPSC-derived MSCs (iMSCs) from aged individuals acquire a rejuvenation signature</i>	
Characterization of fMSCs and aMSCs.....	150
Characterization of MSC-derived iPSCs.....	152
Characterization of fMSC-iMSCs, aMSC- iMSCs and ESC-iMSCs.....	153
Distinct and overlapping gene expression patterns between iMSCs and primary MSCs isolated from donors of distinct ages.....	155
Identification of rejuvenation and ageing signature.....	156
Protein-association network related to ageing and rejuvenation signatures of gene expression in iMSCs and parental MSCs.....	157
Comparative analyses of the secretome of fMSCs, iMSCs and aMSCs.....	158
<i>2.10 Transplanted human pluripotent stem cell-derived mesenchymal stem cells support liver regeneration in Gunn rats</i>	

Characterization of iMSCs by immunofluorescence and transcriptome analysis.....	170
Characterization of fMSCs and iMSCs by flow cytometry.....	171
Functional characterization of fMSCs and iMSCs.....	172
Transplanted human iMSCs acquired hepatocyte functions in host Gunn rats.....	173
Transplanted human iMSCs successfully engrafted in Gunn rat liver and expressed hepatocyte markers.....	174
Histological analysis of human iMSC-derived hepatocytes within the Gunn rat liver.....	175
Cluster analysis of gene expression arrays and short tandem repeat analysis.....	179
Assessment of cell proliferation by BrdU incorporation.....	180
FISH analysis of human and rat-specific sex chromosomes.....	181
Human iMSC transplantation caused no shift from taurine- to glycine-conjugated bile acids typical for humanized bile acid serum profile.....	182
Fibrosis-associated genes remained unchanged after human iMSC transplantation.....	183
2.11 Human iPSC-derived iMSCs improve bone regeneration in mini-pigs	
Characterization of HFF-derived iPSCs.....	190
Properties of HFF-iPSCs derived iMSCs.....	191
Microarray analysis of HFF-iMSCs.....	192
Histomorphometrical and radiological analysis of regenerated bone defects after 6 weeks..	193
Radiological analysis of regenerated bone defects after 6 weeks.....	194
Possible modes of action of HFF-iMSCs.....	196
HFF-iMSC differentiations.....	200
Pearson correlation values.....	200
Short-tandem-repeat Analysis.....	201
<i>In vitro</i> compatibility test of HFF-iMSC and CPG.....	201
Schematic of a histological section with the critical-size bone defect in the proximal tibia..	202
2.12 Human mesenchymal factors induce rat hippocampal- and human neural stem cell dependent oligodendrogenesis	
Localization of p57kip2 protein in the dentate gyrus of the rat adult brain.....	213
p57kip2 protein localization under oligodendroglial differentiation promoting conditions...	214
Induction of oligodendroglial differentiation by human mesenchymal stem cell factors.....	216
p57kip2 protein overexpression interferes with human MSC-derived oligodendrogenesis...	217
Myelination of adult neural stem cells.....	218
Transplantation of hippocampal aNSCs on cerebellar slices.....	219
Human MSC-CM enhances nuclear Olig2 protein expression in human iPSC-derived NSCs (hiPSC-NSCs).....	220

Abbreviations

AD	Alzheimer's disease
ADME	Absorption, distribution, metabolism, and excretion
AF	Amniotic fluid
AFCs	Amniotic fluid cells
AF-MSCs	Amniotic fluid mesenchymal stem cells
AFP	α -Fetoprotein
ALK	Anaplastic lymphoma kinase
ALT	Alanine transaminase
AKI	Acute kidney injury
AMED	Japan Agency for Medical Research and Development
aNSCs	Adult neural stem cells
AST	Aspartate transaminase
bFGF/FGF2	Basic fibroblast growth factor
BMC	Bone marrow concentrate
BM-MSCs	Bone marrow derived mesenchymal stem cells
BSEP	Bile salt export pump
CAS9	CRISPR-Associated endonuclease 9
CD	Cluster of differentiation
cDNA	Complementary deoxyribonucleic acid
CiRA	The Center for iPS Cell Research and Application
CITED1	Cbp/p300-interacting transactivator 1
CK18	Cytokeratin 18
CK19	Cytokeratin 19
CKD	Chronic kidney disease
c-Myc	Myelocytomatosis viral oncogene homologue
CNS	Central nervous system
CPG	Calcium phosphate granules
CRISPR	Clustered regularly interspaced short palindromic repeats
CYP	Cytochromes P450
CYP2D6	Cytochrome P450 family 2 subfamily D member 6
DAB	3,3'-Diaminobenzidine
DAVID	Database for Annotation, Visualization and Integrated Discovery
DE	Definitive endoderm
DILI	Drug-induced liver injury
DNA	Deoxyribonucleic acid

EB	Embryoid Body
EMT	Epithelial-to-mesenchymal transition
ESCs	Embryonic stem cells
FACS	Fluorescence-activated cell sorting
FGF	Fibroblast growth factor
FISH	Fluorescence in situ hybridization
fMSCs	Fetal mesenchymal stem cells
GEO	Gene Expression Omnibus
GMP	Good manufacturing practice
GO	Gene ontology
GSK-3β	Glycogen synthase kinase 3 beta
GST	Glutathione S-transferase
GvHD	Graft versus Host Disease
HE	Hepatic endoderm
HFF	Human foreskin fibroblasts
HGF	Hepatocyte growth factor
HLA	Human leukocyte antigen
HLCs	Hepatocyte-like cells
HNFα	Hepatocyte nuclear factor alpha
HREpCs	Human renal epithelial cell
HUVECs	Human umbilical vein endothelial cells
iMSCs	iPSC-derived mesenchymal stem cells
iPSCs	Induced pluripotent stem cells
IL	Interleukin
ISCT	International society for cellular therapy
KEGG	Kyoto Encyclopedia of Genes and Genomes
KLF4	Krueppel-like factor 4
LDH	Lactate dehydrogenase
LHX1	LIM homeobox 1
LIF	Leukemia inhibitory factor
LIN28	Lin-28 homologue A (<i>C. elegans</i>)
MET	Mesenchymal-to-epithelial transition
MHC	Major histocompatibility complex
MRP	Multidrug resistance-associated protein
NANOG	Nanog homeobox
NPCs	Neural progenitor cells

NTCP	Sodium-taurocholate cotransporting polypeptide
OCT4	Octamer-binding protein 4/POU class 5 homeobox 1
PAN	Protein association network
PAX8	Paired-Box-Protein 8
PDGF	Platelet-derived growth factor
PHH	Primary human hepatocytes
PODXL	Podocalyxin-like protein 1
PSG5	Pregnancy-specific beta-1-glycoprotein 5
RNA	Ribonucleic acid
RUNX2	Runt-related transcription factor 2
SOX2	Sex-determining region Y (SRY)-box 2
SRY	Sex determining region Y
SSEA4	Stage-specific embryonic antigen 4
STAT3	Signal transducer and activator of transcription 3
TALEN	Transcription activator-like effector nuclease
TGFβ	Transforming growth factor beta
TRA-1-60	Tumor-related antigen-1-60
TRA-1-81	Tumor-related antigen-1-81
UGT1A1	Uridine diphosphate glucuronosyltransferase 1 A 1
USCs	Urine stem cells
VEGF	Vascular Endothelial Growth Factor
WNT3a	Wingless-type MMTV integration site family, member 3a

1. Introduction

1.1 Stem Cells

The smallest structural unit of all living organisms is the cell. The human body is comprised of more than 200 different cell types which have their specific functions and appearances, and which form an inter-connected network [Ellinger and Ellinger, 2014]. A special subpopulation of cells, the stem cells, is characterized by their ability of indefinitely self-renewal and their potential to differentiate into cells with organ-specific functions. The self-renewing ability of stem cells is manifested in their ability to divide and give rise to cells with the same properties as the mother cell by symmetric cell division. Alternatively, asymmetric cell division of stem cells results in one daughter stem cell with identical properties to the mother stem cell and one cell primed to undergo further differentiation [McCaffrey and Macara, 2011]. These features are making stem cells enormously important for the organogenesis during development, tissue homeostasis and regeneration processes. Germ line stem cells are important for the reproduction and somatic stem cells are crucial for organogenesis.

Different types of stem cells exist which are distinguished by their differentiation potential. Totipotent stem cells can differentiate into all the cells of the body including extraembryonic tissue; pluripotent stem cells only lack the differentiation into extra embryonic tissue; multipotent stem cells can give rise to all types of a single germ layer whereas unipotent stem cells are tissue specific [Fuchs et al., 2004; Weissman, 2000]. In contrast to the restricted differentiation potential of adult stem cells, embryonic stem cells (derived from the inner cell mass of the blastocyst) have a pluripotent differentiation capacity covering ectodermal, mesodermal and endodermal cell lineages [Thomson et al., 1998; Chambers et al., 2004].

Stem cells reside in a special microenvironment – the stem cell niches [Li et al., 2005] which provide a milieu of interacting cellular and acellular factors determining the fate of the stem cells [Haque et al., 2013].

1.2 Mesenchymal Stem Cells

Alexander A. Maximow described the presence of cells within the bone marrow with features of fibroblast capable to support haematopoiesis [Maximow, 1924]. Friedenstein and colleagues isolated stem cells from bone marrow employing their ability of plastic adherence [Friedenstein et al., 1970]. The term “mesenchymal stem cells” (MSCs) was established by Arnold I. Caplan in the 1990’s [Caplan, 1991]. Originally, MSCs were derived from the perivascular region of the bone marrow [Bianco et al., 2013] but have now been isolated from other tissues such as blood [Campagnoli et al., 2001], adipose tissue [Zuk et al., 2002], umbilical cord blood [Rosada et al., 2003], placenta [Parolini et al., 2008], skin [Toma et al., 2005], teeth [Perry et al., 2008], liver [Wenceslau et al., 2011], pancreas [Seeberger et al., 2011] and urine [Spitzhorn et al., 2018].

MSCs are multipotent as shown by their differentiation potential into various mesenchymal lineages such as bone, cartilage and fat [Uccelli et al., 2008]. This fate determination and thus the switch from self-renewal to differentiation, is governed by growth factors, cytokines, adhesion molecules and extracellular matrix components which are present in the stem cell niche [Song et al., 2006]. MSCs have a great proliferation potential *in vitro* and have a spindle-shaped, fibroblastoid morphology. They are characterized by a distinct cell surface marker pattern including high levels of CD73, CD90 and CD105 by parallel lacking the hematopoietic markers CD14, CD20, CD34 and CD45. This specific morphology, immunophenotype and differentiation potential were set as the minimal criteria for MSCs by the international society for cellular therapy (ISCT) [Dominici et al., 2006]. Expression of CD146 as well as platelet-derived growth factor receptor β (PDGFR β) was further described for MSC identification [Crisan et al., 2008]. Additionally, MSCs were shown to be able to differentiate into other cells types such as cardiomyocytes [Makino et al., 1999], neuronal cells [Woodbury et al., 2000] or hepatocytes [Sato et al., 2005].

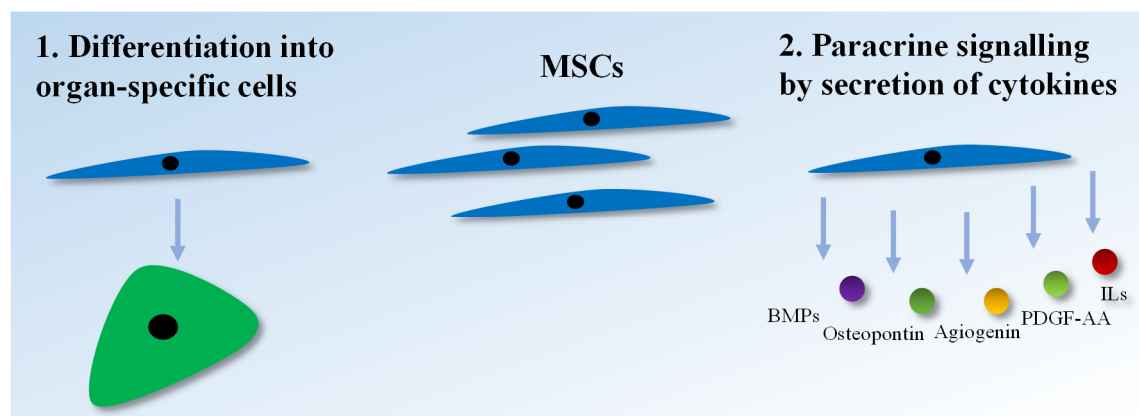


Figure 1.1: Modes of MSC action based on existing knowledge.

Apart from their differentiation capacity, MSCs have been shown to be paracrine active in various ways. By secretion of cytokines and growth factors they can support haematopoiesis in the bone marrow but also to modulate the immune system which also involves its suppression. Furthermore, MSCs are able to support regeneration processes by release of trophic factors [Li et al., 2015]. Chemokines and corresponding receptors are crucial in chemotaxis of leucocytes to sites of inflammation or injury [Miyasaka et al., 2004]. MSCs express many chemokine receptors contributing to their ability to home into injured tissue and to show a tropism towards injured tissue [Phinney et al., 2007; Hwang et al., 2009; Vogel et al., 2010] which makes them very useful in many (pre-)clinical regenerative therapies. Amongst factors secreted by MSCs there are pro-angiogenic cytokines and growth factors such as VEGF-A, IL-6, IL-8, HGF and PDGF [Takahashi et al., 2018].

Currently there is a big debate on the proper characterization of MSCs since recently the human skeletal stem cells were described for the first time. These skeletal stem cells have a distinct cell surface marker profile ($PDPN^+/CD146^-/CD73^+/CD164^+$) and are able to generate progenitor cells for the bone, cartilage and stroma lineage but not adipogenic lineage [Chan et al., 2018].

1.3 Clinical Applications of MSCs

Due to their secretion of different cytokines [Charbord et al., 2011] and the above described differentiation potential, MSCs are seen as key players in medical research and enable innovative therapeutic approaches. Their good *in vitro* propagation and their high plasticity endow them to be suitable for direct cell transplantation or to contribute to tissue engineering approaches for repair or replacement of injured or diseased organs [Mark et al., 2013].

Because of this broad range differentiation potential, MSCs are of high therapeutic relevance. Beside their regenerative properties MSCs can interact with cells of the innate as well as the adaptive immune system and thus modulate immunological effector functions resulting in immune-suppressive and anti-inflammatory ability. They can suppress the activation of natural killer cells, which are important for the innate immunity. On the level of the adaptive immunity they suppress the activation and maturation of dendritic cells, T-cells and B-cells [Uccelli et al., 2008]. Their function as paracrine effector cells is utilized by their application in acute Graft-versus-host disease (GvHD) in which T-cells which remained in the transplanted organ recognise cells of the recipient as foreign and attack them. In addition to this, they are used to support the growth of haematopoietic cells after bone marrow transplantation which is enabled by their stroma function [Zeiser et al., 2017; Le Blanc et al., 2008]. Haploidentical (only 50 percent match of HLA marker between donor and recipient) MSCs were transplanted into a young patient suffering from GvHD and could improve the patient's conditions without obvious side effects after 1 year [Le Blanc, 2008]. For treatment of immune-system-associated diseases such as Multiple sclerosis or Crohn's disease their function as immune modulators is employed [Uccelli et al., 2011; Duijvestein et al., 2010]. Furthermore, MSCs were shown to improve the success rate of allogenic transplantations [Nesselmann et al., 2011].

Especially for skeletal tissue engineering MSCs are widely used [Mirmalek-Sani et al., 2006; Rose et al., 2002; Oreffo et al., 2005]. Also, MSCs were shown to have positive effects in treatment of the genetic bone disease osteogenesis imperfecta [Horwitz et al., 2002]. MSCs regenerated tissue after myocardial infarction or neural diseases and support wound healing [Wu et al., 2010; Williams et al., 2011]. For the treatment of cancer, MSCs are used as carriers of anti-tumour agents since they home in into tumorous tissue

[Bexell et al., 2012;]. In a rat model of acute renal failure, injection of MSCs led to increased renal function by secretion of anti-inflammatory cytokines [Tögel et al., 2005]

More than 740 clinical trials employing MSCs were registered so far as either on-going or completed [<https://clinicaltrials.gov/>] to investigate the therapeutic potential of MSCs. Therefore, these cells have been transplanted into patients suffering from GvHD, multiple sclerosis or acute myocardial ischemia either autologous or allogenic [Squillaro et al., 2016; Wang et al., 2012]. Furthermore, MSCs have been implemented in many additional diseases affecting various organs emphasizing the multipotency of MSCs.

Clinical trials employing MSCs (27/03/2019)
Total: 742; thereof iMSCs: 2 (1 iPSC, 1 ESC)

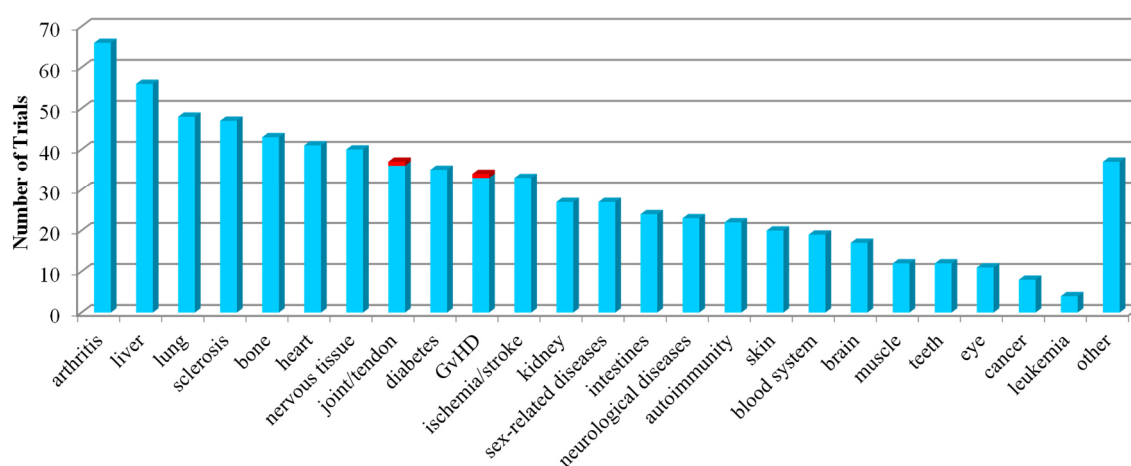


Figure 1.2: Number and distribution of clinical trials employing MSCs. The numbers were calculated based on the deposited information at <https://clinicaltrials.gov/>. Clinical trials using (a) MSCs are displayed in light blue and (b) iMSCs are displayed in red.

1.4 MSCs in Liver Regeneration

A healthy liver is crucial as it has several key functions like removal of toxins from the blood, synthesis of proteins and vitamin storage amongst others. Due to its detoxifying function, the liver has a remarkably high regenerative potential [Starzl et al., 1993]. Liver regeneration is impaired under pathological liver conditions such as viral infection, inflammation or inherited genetic metabolic diseases. Such situations trigger hepatic

progenitor cells to restore liver tissue [Duncan et al., 2009]. Although these cells are of high proliferation capacity and can differentiate into mature hepatocytes the intrinsic regeneration capacity of the liver might be insufficient [Chatzipantelis et al., 2008], or impaired upon tumour removal [Karoui et al., 2006]. An insufficient regeneration process could be explained by suppressed proliferation of the hepatocytes, which normally reconstitute the liver mass within days. If the hepatocyte proliferation and function is continuously impaired, whole organ transplantations might become necessary but there is an acute donor organ shortage.

Alternatively, cell transplantations could be done, which bear a lower risk of comorbidity but are also limited by the low number of available organs for cell isolation [Nussler et al., 2006]. As an opportunity to be used in cell-based therapies, MSCs are under critical evaluation for treating liver diseases. MSC transplantation could circumvent the above-mentioned shortcomings of primary liver cells. In addition to their well-known differentiation capacity into bone, fat and cartilage they can differentiate into functional liver cells *in vitro* and *in vivo* [Sato et al., 2005; Kuo et al., 2008; Kordes et al., 2015] furthermore liver resident MSCs were described which are also called hepatic stellate cells [Kordes et al., 2013; Michellotti et al., 2013; Kordes et al., 2014]. Thus, they can directly contribute to liver regeneration or promote liver recovery by releasing trophic factors [van Poll et al., 2008]. Triggered by the perfect microenvironment, it was shown that MSCs are able to differentiate into hepatocyte-like cells (HLCs) [Chivu et al., 2009; Li et al., 2013], expressed hepatocyte genes and were able to store glycogen and to produce urea [Lange et al., 2005; Schwartz et al., 2002; Lee et al., 2004]. Furthermore, pathological liver conditions such as liver fibrosis (pathological increment of collagen deposits) improved upon MSCs injection [Zhao et al., 2012]. One major condition in today's medicine with no promising treatment available, cirrhosis, which is a cause of long-term chronic liver injury, was improved in a rat model after transplantation of human MSCs [Jung et al., 2009]. After injection of MSCs via the portal or tail vein MSCs restored liver function indicated by albumin production after partial hepatectomy [Li et al., 2013]. Reduction of fibrosis was also achieved by hepatocyte-like cells (HLCs) derived from MSCs [Abdel Aziz et al., 2007]. As a next step for *in vitro* analysis of supportive effects of MSCs on liver function, three-dimensional organoids were generated through self-organization of endothelial cells, MSCs and hepatocytes. The

organoids could remarkably restore liver function upon transplantation into mice [Takebe et al., 2014].

1.5 MSCs in Bone Regeneration

Although healing of the most bone fractures happens without any problems, complications as skeletal bone defects or cases of non-union are challenges for orthopaedic surgeons. Fracture healing involves a complex cascade under the contribution of circulating blood cells [Kuroda et al., 2014], macrophages [Das et al., 2013], as well as stromal stem and progenitor cells. In these situations, usage of autologous bone grafts is the gold standard. But this treatment option is associated with several hurdles such as limited and suboptimal bone grafts and donor site comorbidity [Faour et al., 2011]. Autologous bone marrow concentrate which is composed of stem cells, immune cells, and growth factors was shown as promising alternative for treatment of bone defects [Hakimi et al., 2014; Herten et al., 2013]. Also, the single use of autologous MSCs which are able to differentiate into osteogenic lineage has been reported [Grayson et al., 2015; Hakimi et al., 2014]. Both alternatives were successfully applied in animal models for recovery of bone tissue in weight-bearing and non-weightbearing conditions [Hakimi et al., 2014; Bhumiratana et al., 2016]. For example, MSCs are used in preclinical large animal studies for facial bone regeneration [Bhumiratana et al., 2016] and further numerous clinical trials for MSCs are focussing on bone related research [<https://clinicaltrials.gov/>].

1.6 MSCs in Neurogenesis

Demyelination in the central nervous system (CNS) is characterized by the reduction of myelin sheaths of the neurons. It is associated with neurodegenerative diseases such as Multiple sclerosis. This loss of myelin can be counteracted by recruitment of new glial cells which are responsible for the myelination process [Jessen et al., 1980; Franklin, 2002] to a certain extent. Adult neural stem cells as well as oligodendroglial progenitor cells at the site of myelin loss are the most prominent cell types for repairing the myelin sheaths [Akkermann et al., 2016]. But this intrinsic repair process is limited [Kremer et al., 2011].

In the brain environment, MSCs were also successfully tested and their neuroprotective abilities have been reported [Karussis et al., 2008]. MSCs were shown to have a beneficial effect on animals suffering from neurodegenerative impairments [Jin et al., 2002]. External support of oligodendrogenesis was reported for the use of MSC-secreted factors [Kassis et al., 2008; Uccelli et al., 2008]. Both cell types involved in the myelin repair were susceptible for MSC-mediated stimuli to differentiate towards oligodendroglial direction [Rivera et al., 2006; Jadasz et al., 2013]. It was shown that factors secreted by human MSCs increased the level of oligodendrogenesis in adult neural stem cells (aNSCs) in rats as well as axonal tissue integration and wrapping. In the rat setting MSC conditioned media supported oligodendral differentiation of oligodendral progenitor cells by upregulated expression of myelin [Jadasz et al., 2013]. Moreover, conditioned media of human MSCs supported regeneration of demyelinated CNS upon injection in an animal model of Multiple sclerosis by HGF-driven generation of oligodendrocytes and neurons [Bai et al., 2012]. Additionally, it could be shown that hippocampal stem cells gain potential to differentiate into oligodendrocytes through MSC-mediated signalling [Munoz et al., 2005; Rivera et al., 2006]. In a model of spinal cord contusion, administration of MSCs resulted in an improved functional outcome [Chopp et al., 2000]. In experimental-induced autoimmune encephalomyelitis MSCs showed neuroprotective function and modulated the immune system [Kassis et al., 2008].

1.7 Induced Pluripotent Stem Cells

Since their first derivation in 1998 by James Thomson, embryonic stem cells (ESCs) have become the gold standard for researchers working on stem cells due to their unrestricted differentiation and proliferation capacity [Thomson et al., 1998]. ESCs represent the first isolated pluripotent stem cells. They are derived from the inner cell mass of the blastocysts (a structure formed 5 days after fertilization of the egg) which mostly is taken from spare embryos from *in vitro* fertilization in agreement with the donor [Shand et al., 2012]. For the human, this was done 1998 for the first time in a process in which the trophoblast, the outer layer of the blastocysts, was removed and the inner cell mass was taken out for subsequent processing and cultivation on inactivated mouse embryonic fibroblasts. The researchers themselves described the ethical issues attached to this technique [Thomson et al., 1998].

Pluripotent stem cells are characterized by the expression of OCT4 (octamer binding transcription factor 4), SOX2 (SRY (sex determining region Y)-box 2, NANOG and KLF4 (krueppel-like factor 4) and other pluripotency-associated genes and activated relevant signaling pathways such as leukemia inhibitory factor/ signal transducer and activator of transcription 3 (LIF/STAT3) to maintain stemness, formation of three dimensional embryoid bodies which can spontaneously differentiate into cells of all three germ layers and their ability to form teratomas (tumorous tissue which can include cells from all three germ layers) upon transplantation into immune-compromised mice [Alvarez et al., 2012; Thomson et al., 1998]. Other approaches to generate pluripotent cells from somatic cells include somatic cell nuclear transfer into oocytes [Wilmut et al., 1997], exposure of somatic cells with extracts from embryonic carcinoma cells or ESCs [Taranger et al., 2005] or the fusion of somatic cells with embryonic germ or stem cells [Tada et al., 2001; Cowan et al., 2005]. All these approaches rely on the use of embryonic cells or material which is wrought with massively ethical issues and concerns.

These problems could be overcome by the generation of induced pluripotent stem cells (iPSCs) by the Nobel Prize awarded researcher and physician Shinya Yamanaka. By ectopic expression via retroviruses of the transcription factors OCT4, SOX2, KLF4 and C-MYC (v-myc myelocytomatosis viral oncogene homolog), human dermal fibroblast cells could be reprogrammed into pluripotent stem cells [Takahashi et al., 2007]. This technique was described one year before for reprogramming of mouse fibroblasts [Takahashi and Yamanaka, 2006]. These iPSCs were morphologically identical to ESC by growing in flat colonies and expressed the pluripotency genes in comparable levels and had high telomerase activity levels [Takahashi et al., 2007].

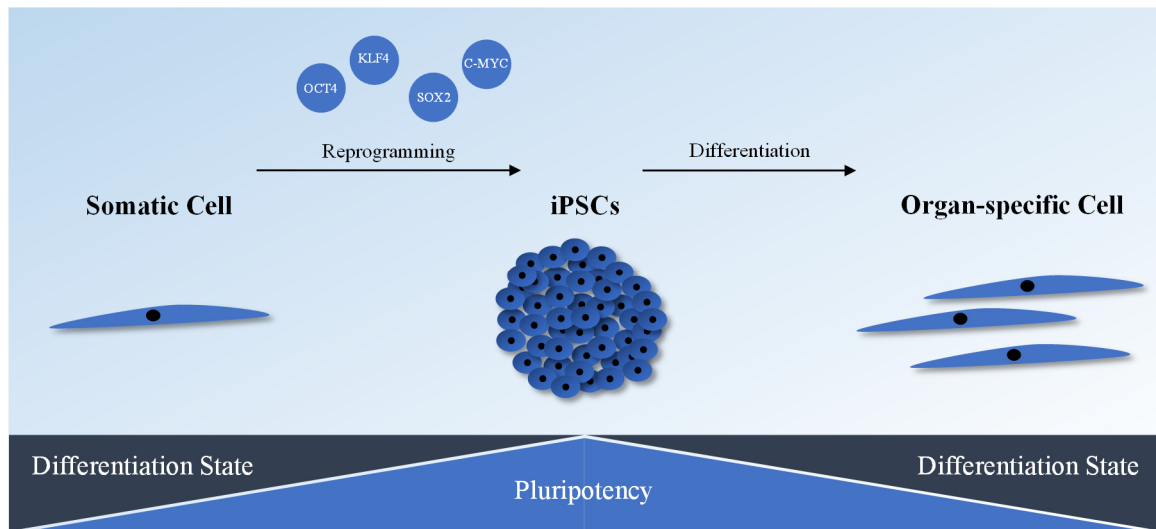


Figure 1.3: Derivation process of iPSCs and differentiation into organ-specific cells.

This reprogramming mechanism is associated with several key events such as increase of reactive oxygen species resulting in DNA damage and activated p53 which regulates cell cycle arrest, senescence and apoptosis [Mah et al., 2011]. The mesenchymal-to-epithelial transition (process in which mesenchymal cells switch their identity to epithelial cells) is another important step [Li et al., 2010]. Furthermore, epigenetic remodelling via alterations in CpG methylation patterns and histone modifications occur which subsequently leads to overall changes on the transcriptional level [Takahashi et al., 2007]. This comes along with changes in the bioenergetic metabolism in mitochondria where a shift from oxidative phosphorylation to glycolysis takes place [Prigione et al., 2010]. Telomere length is increased by reprogramming indicating a rejuvenation of the cells [Mahmoudi et al., 2012]. It could be shown that iPSCs preserve an epigenetic memory leading to an enhanced differentiation capacity into the cell lineage they were derived from [Hu et al., 2010].

The original reprogramming protocol was improved and redefined over the years to increase its efficacy. Therefore, the use of small molecules such as anaplastic lymphoma kinase (ALK) 4/5/7 inhibitor SB431542, the MEK inhibitor PD0325901 or the glycogen synthase kinase 3 (GSK-3) inhibitor CHIR99021 were described [Drews et al., 2012]. The single use of only one vector led to a reduction of integrations into the genome [Carey et al., 2009] and the use of non-integrating adenoviruses enabled it to receive an unmodified genome [Zhou et al., 2009]. To avoid the need for viruses, other

reprogramming ways were described using mini-circle DNA or the transcription factors were carried in the nucleus using episomal plasmids and electroporation [Yu et al., 2011]. It is important to avoid integration into the genome since integration events may result in inactivation of tumour suppressor genes or the activation of oncogenes causing tumour formation [Chatterjee et al., 2016]. Up to date, many different cell types were reprogrammed into iPSCs including cord blood and adult blood cells [Chou et al., 2011], amniotic fluid cells [Wolfrum et al. 2010], MSCs [Megges et al., 2015], chorionic villi-derived cells [Lichtner et al., 2015], epicardium-derived cells [Paulitschek et al., 2017] and urine-derived cells [Bohndorf et al., 2017].

1.8 In Human Application of iPSC-derived Cells

Due to their ability of indefinitely self-renewal and pluripotent differentiation potential, iPSCs have tremendous value for bio-medical research and clinical applications. Furthermore, new methods to model human diseases *in vitro* have arisen to study the underlying molecular mechanisms and to discover new drugs or diagnostics [Drews et al., 2012]. More and more, iPSCs replace primary human cells or human carcinoma cell lines in *in vitro* settings thereby circumventing limitation such as poor *in vitro* lifespan or genetic aberrations. They have been used to study a broad variety of diseases including Parkinson's disease [Miller et al., 2013], hepatitis c virus [Schöbel et al., 2018], retinitis pigmentosa [Jin et al., 2011], steatosis [Graffmann et al., 2015] and Alzheimer's disease [Israel et al., 2012].

The medical potential of iPSCs has not exclusively been analysed in cell culture. Within the last years some pioneer in-human trials using iPSC-derived cells were performed. In 2014, skin cells of an aged Japanese woman were reprogrammed into iPSCs which subsequently were differentiated into retinal cells in sheet architecture. They were transplanted into the patient's retina to treat age-related macular degeneration which is associated with gradual loss of sight up to blindness. One year post operation the survival of transplanted cells was reported without obvious side effects [Mandai et al., 2017]. A follow-up trial for the same disease was done using allogenic cells since the autologous cells were infringed by age-related genetic defects. The human leukocyte antigen (HLA) matched iPSCs were obtained from an iPSC bank and were as such chosen to minimize

the risk of rejection by the recipient's immune system. Since allogenic transplantations are more cost- and time-effective than personalized treatment, this study is of high importance to unveil the allogenic iPSC-based treatment for future applications [Cyranoski, 2017].

1.9 iPSC-derived MSCs (iMSCs)

As mentioned above, MSCs can be routinely obtained from bone marrow or other sources but these invasive procedures are associated with particular risks [Sheyn et al., 2016]. Especially in a clinical scenario with a high frequency of elderly patients several limitations reduce cell quality. These aged cells exhibit higher levels of genomic instability, cellular senescence, DNA damage, oxidative stress and immunogenicity [Zhou et al., 2008; Moskalev et al., 2013; Reuter et al., 2010; Brink et al., 2009]. These ageing-associated cellular changes reduce the proliferation and differentiation potential of the MSCs and thereby their therapeutic potential [Oreffo et al., 1998; Stolzing and Scutt, 2006; Wagner et al., 2009; Duscher et al., 2014]. Furthermore, their *in vitro* proliferation capacity is limited, by replicative senescence [Wagner et al., 2008], which can lead to an insufficient number of cells [Illich et al., 2011]. The therapeutic potential of MSCs decreases over *in vitro* culture time by decline of their differentiation capacity resulting from chronological ageing [Katsara et al., 2011; Duscher et al., 2014; Palumbo et al., 2014; Kasper et al., 2009; Stolzing et al., 2008]. Therefore, foetal MSCs have been shown to have better features than their adult counterparts [Mirmalek Sani et al., 2006] and showed better outcome in a mouse model of Multiple sclerosis [Scruggs et al., 2013]. Differences between the young and old stem cells have been shown in methylation pattern [Bork et al., 2010], telomere length [Wagner et al., 2008; 2010], growth factor production as well as altered oxidative stress levels and altered signalling pathways [Wilson et al., 2010].

These difficulties associated with MSCs from an aged background could be overcome by generation of MSCs from iPSCs [Frobel et al., 2014] since via reprogramming the cells undergo a rejuvenation process. These so called iMSCs can also be generated from ESCs and were shown to exhibit similar features than native MSCs related to their differentiation capacity and their potential use in regeneration processes [Chen et al.,

2012; Kimbrel et al., 2014]. As an alternative for primary MSCs, MSCs from iPSCs or ESCs (both termed iMSCs in the following chapters) were generated by the induction of epithelial-to-mesenchymal transition using the transforming growth factor beta (TGF β)-receptor inhibitor SB-431542 [Chen et al., 2012] amongst many other protocols. These iMSCs met the minimal criteria for MSCs by their ability to grow on plastic surfaces, cell surface marker composition and their multilineage differentiation potential [Villa-Diaz et al., 2012]. The differentiation potential of iMSCs into osteogenic and chondrogenic lineage was comparable to the native MSCs but iMSCs exhibited a weaker potential to differentiate into fat cells [Chen et al., 2012; Boyd et al., 2009; Kang et al., 2015].

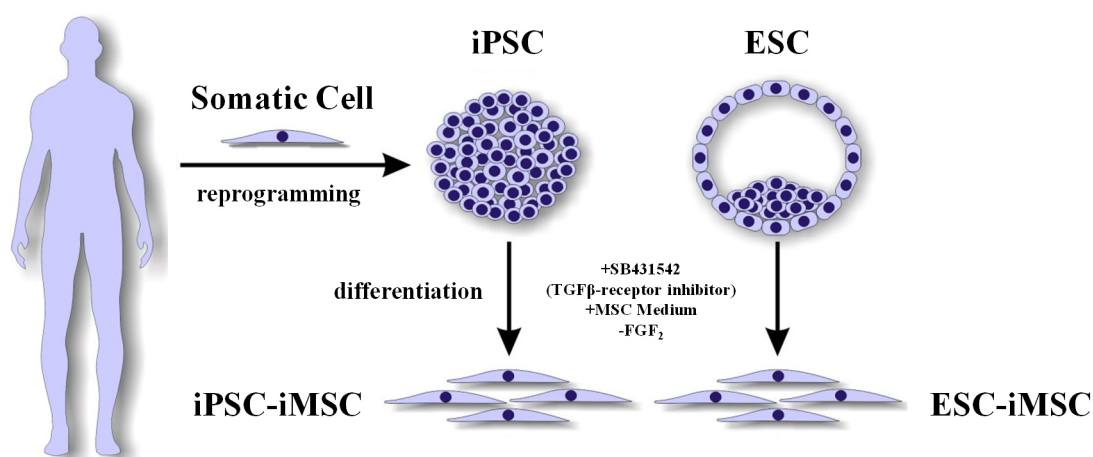


Figure 1.4: Generation of human iMSCs from pluripotent stem cells.

iMSCs have been employed in many pre-clinical studies such as the treatment of hind-limp ischemia where transplantation of iMSCs supported neovascularisation and myogenesis. Furthermore, iMSCs contributed to liver regeneration and differentiated into functional human liver cells in Gunn rats [Spitzhorn et al., 2018]. Additionally, it was shown that a rejuvenation effect occurs through reprogramming which also effects the resulting iMSCs to be in a younger state [Spitzhorn et al., 2019], which also was shown for patients' cells suffering from early onset ageing syndrome [Frobel et al., 2014; Cheung et al., 2014]. For transplantation safety is very important to note that iMSCs are not pluripotent and thus upon injection of iMSCs no teratoma formation was observed [Chen et al., 2012]. iMSCs contributed to regeneration in various animal disease models

such as hypoxic ischemia autoimmunity limb ischemia and multiple sclerosis [Kimbrel et al., 2014; Gruenloh et al., 2011; Lian et al., 2010; Hawkins et al., 2018; Wang et al., 2014]. iMSCs were shown to act directly by differentiation into bone cells and indirectly by the recruitment of resident host cells contributed to regeneration in a murine radial defect model [Sheyn et al., 2016]. Remarkably, two clinical trials have used iMSCs for the treatment of GvHD and meniscus injury [<https://clinicaltrials.gov/>].

1.10 Amniotic Fluid as a Source of Stem Cells

Amniotic fluid (AF) in the amniotic sac surrounds the embryo during pregnancy and is essential for the foetal development. Its main component is water (98-99%) but it also contains proteins, carbohydrates, lipids, electrolytes, enzymes and hormones. Amniotic fluid protects the foetus from external mechanical stimuli and contains nutrients and growth factors as well as substances for the innate immune system. Since the embryo is constantly breathing the amniotic fluid, it is essential for lung development [Underwood et al., 2005; Harding and Hoper, 1996]. Until the middle of the second trimester of gestation AF mainly results from maternal plasma and permeates the membranes of the embryo by osmosis and hydrostatic force [Underwood et al., 2005]. From this time point on until delivery, amniotic fluid composition is predominantly built up by the excretory fluids of the foetus such as urine, respiratory or gastrointestinal efflux [Olver and Strang, 1974]. Amniotic fluid is routinely collected during pregnancy in a process called amniocentesis for diagnostic purpose [De Coppi et al., 2007] but can also be obtained during caesarean sections [Spitzhorn et al., 2017; Rahman et al., 2018].

The AF contains differentiated and undifferentiated cells [Simoni and Colognato, 2009; Torricelli et al., 1993]. The AF harbours stem cells (AFSCs) which exhibit therapeutic potential [De Coppi et al., 2007]. These AFSCs are highly proliferative, have a broad *in vitro* differentiation capacity, low potential to provoke immunogenic reactions, have anti-inflammatory potential and are not tumorigenic [De Coppi et al., 2007; Antonucci et al., 2014]. There have been reports of AFSCs isolated from first/second trimester, describing these cells to express pluripotency factors OCT4, NANOG, KLF4, SOX2, CD133, stage-specific embryonic antigen 4 (SSEA4) and C-Kit [Moschidou et al., 2013; Koike et al., 2014]. Additional studies revealed their self-renewing potential, high plasticity and their

good susceptibility for reprogramming purposes [Hawkins et al., 2017; Moschidou et al., 2012]. Furthermore, they were characterized as paracrine effector cells by promoting angiogenesis, vasculogenesis and osteogenesis [Mirabella et al., 2011, 2013; Ranzoni et al., 2016]. Due to these features AFSCs are considered for therapeutically applications for example in improvement of wound healing by differentiation into keratinocytes [Sun et al., 2015].

Within the AFSCs, MSC-like cells (AF-MSCs), were identified which share MSC features of plastic adherence, morphology, immunophenotype and differentiation potential [Savickiene et al., 2015; Tsai et al., 2004; Kaviani et al., 2001; Tsai et al., 2007]. Very importantly, these AF-MSCs are of foetal and not maternal origin [In't Anker et al., 2004]. A comparative study of MSCs from different origins (amniotic fluid/membrane, cord blood and bone marrow) revealed overlapping potentials as well as transcriptomes. But each origin was manifested in gene expression profile by specifically upregulated genes. Amniotic fluid/membrane MSCs expressed genes associated with uterine maturation and homeostasis of fluids and electrolytes, cord blood derived MSCs showed upregulation of genes involved in innate immune system and bone marrow MSCs had upregulated bone formation genes [Tsai et al., 2007].

Several features of Amniotic fluid-derived MSCs make them suitable for regenerative medicine including (i) low immunogenicity and anti-inflammatory properties by low level expression of major histocompatibility complex (MHC) antigens [Kang et al., 2012], (ii) better *in vitro* propagation than bone marrow-derived MSCs [In't Anker et al., 2003; Roubelakis et al., 2007] (iii) genomic stability during *in vitro* culture [De Coppi et al., 2007] and (iv) a broader range of differentiation potential [Kang et al., 2012]. Furthermore, they can be banked comparable to cord blood cells until they are needed [Cananzi et al., 2009].

1.11 Kidney Structure and Cell Types for Kidney-related Research

The kidney harbours 26 different cell types and as such represents one of the most complex organs in the human body. The kidneys are necessary for electrolyte and pH homeostasis and clear the blood from toxins which are excreted via the urinary system [O'Brien and McMahon, 2014; Al-Awqati and Oliver, 2002; Hariharan et al. 2015;

Arcolino et al., 2015]. The functional units within the kidney are the nephrons which are located within the renal cortex and medulla and appear in a number of 1-1.5 million in a human adult kidney [McMahon, 2016]. A single nephron is built up by the renal corpuscle and the renal tubule system. The main part of the renal corpuscle is the Bowman's capsule which harbours the glomerulus which is rich of renal capillaries. Podocytes are located within and are essential for maintenance of the matrix for the blood filtration processes as their inter-connecting foot processes build up the slit diaphragms [Chuah and Zink, 2017].

The kidney is very challenging organ for researchers since it is composed of a high number of different cell types which are able to interchange identities by a highly complex signalling orchestration of cells from epithelial and stromal lineage [Little, 2016; Al-Awqati and Oliver, 2012]. Amongst these cells, mesenchymal cells from the kidney have been shown to express Cbp/p300-interacting transactivator 1 (CITED1) and SIX2 which are essential in maintaining self-renewal [Kobayashi et al., 2014; Combes et al., 2017]. In addition to these, more key regulators of the functional units, the nephrons, have been reported such as WT1, SALL1, BRN1, PAX2, Cytokeratin 19 (CK19), CD133, Podocalyxin-like protein 1 (PODXL), HOXD11, HNF1B, Lhx1 and Pax8 [Buzhor et al., 2013; Metsuyanin et al., 2009; Schedl, 2007; Higgins et al., 2004; Georgas et al., 2011; Hendry et al., 2011].

Since pathological kidney conditions are on the rise and current treatment relies on dialysis or transplantation, organ shortage drives the search for alternative treatment options. MSCs from the bone marrow showed beneficial outcome and have already been used to treat renal diseases [Casiraghi et al., 2016; Hamza et al., 2017]. In a model of acute kidney injury MSCs were able to suppress the immune system and contributed to restoration of kidney function [Večerić-Haler et al., 2017]. In other studies AF-MSCs from the second trimester were successfully used to build up kidney structures *in vitro* [Perin et al., 2007]. Furthermore, AF-MSCs improved kidney recovery in a rodent model of tubular necrosis [Perin et al., 2010; Sedrakyan et al., 2012; Rosner et al., 2012]. These findings were further confirmed and AF-MSCs showed comparable outcome than BM-MSCs [Hauser et al., 2010]. Second trimester AFCs were observed to express podocyte markers NPHS2 and CD2AP in addition to mesenchymal markers [Siegel et al., 2009; Perin et al., 2007] and as such can differentiate into podocytes [Da Sacco et al., 2017]. As a further step to generate kidney structures *in vitro*, species chimeric renal structures were

derived by combination of human AF-MSCs with murine embryonal kidney cells [Siegel et al, 2010].

Other alternatives for transplantations are renal progenitors isolated from the kidney directly or from urine [Acrolino et al., 2015; Spitzhorn et al., 2018]. As the kidney is connected to the urinary system, viable kidney cells such as podocytes, proximal tubular cells and urine stem cells (USCs) can be found in the urine [Arcolino et al., 2015]. Alternatively, these cells can also be obtained by biopsies of the kidney or the upper urogenital tract. USCs are essential for renewal of kidney tissue based on their stem cell characteristics including clonogenicity, multipotent differentiation potential and high proliferative potential [Zhang et al, 2014]. These USCs can form different cell types from the kidney and the remaining urogenital tract and express SIX2, CITED1, WT1, epCAM and Sall1; of which CITED1 and Sall1 are essential for maintenance of progenitor cell state whereas WT1 is important for differentiation processes [Acrolino et al., 2015, Bussolati and Camussi 2015]. Apart from renal marker expression these USCs are also able to differentiate into bone, cartilage and fat cells *in vitro*, this why they also have been called uMSCs [Spitzhorn et al., 2018]. They also share MSCs specific cell surface marker expression [Kloskowski et al., 2015]. Apart from their ability to differentiate into mature kidney cells they also were found to be immune-modulatory and paracrine active [Zhang et al., 2014]. In addition to primary renal stem cells from amniotic fluid and urine, iPSCs have been used to generate kidney cells or kidney organoids *in vitro* [Cruz et al., 2017; Nguyen et al., 2019].

Aims of This Thesis

Since stem cells are tremendously important for today's regenerative medical research and new stem cell sources have to be established, this thesis aimed to derive stem cells from amniotic fluid and urine and to analyse their origin as well as therapeutic potential. Furthermore, iPSCs should be generated from urine-derived stem cells and the potential of iPSC-derived cells for *in vitro* toxicology and liver disease modelling (NAFLD) should be elucidated. To add more clinical relevance, MSCs should be generated from pluripotent stem cells (iMSCs) and analysed if they represent an alternative to native MSCs. The therapeutic potential human iMSCs should be applied in translational *in vivo* models for inherited liver disease and critical bone defect. Additionally, the paracrine effect of human native MSCs on oligodendrogenesis should be investigated.

2. Results - Publications

Part 1: Sources of Stem Cells

2.1 Isolation and Molecular Characterization of Amniotic Fluid-derived Mesenchymal Stem Cells obtained from Caesarean sections

Lucas-Sebastian Spitzhorn*, Md Shaifur Rahman*, Laura Schwindt, Huyen-Tran Ho, Wasco Wruck, Martina Bohndorf, Silke Wehrmeyer, Audrey Ncube, Ines Beyer, Carsten Hagenbeck, Percy Balan, Tanja Fehm and James Adjaye

*These authors contributed equally to this work.

Abstract

Human amniotic fluid cells are immune-privileged with low immunogenicity and anti-inflammatory properties. They are able to self-renew, are highly proliferative, and have a broad differentiation potential, making them amenable for cell-based therapies. Amniotic fluid (AF) is routinely obtained via amniocentesis and contains heterogeneous populations of foetal-derived progenitor cells including mesenchymal stem cells (MSCs). In this study, we isolated human MSCs from AF (AF-MSCs) obtained during Caesarean sections (C-sections) and characterized them. These AF-MSCs showed typical MSC characteristics such as morphology, *in vitro* differentiation potential, surface marker expression, and secreted factors. Besides vimentin and the stem cell marker CD133, subpopulations of AF-MSCs expressed pluripotency-associated markers such as SSEA4, c-Kit, TRA-1-60, and TRA-1-81. The secretome and related gene ontology (GO) terms underline their immune modulatory properties. Furthermore, transcriptome analyses revealed similarities with native foetal bone marrow-derived MSCs. Significant KEGG pathways as well as GO terms are mostly related to immune function, embryonic skeletal system, and TGF β -signalling. An AF-MSC-enriched gene set included putative AF-MSC markers PSG5, EMX-2, and EVR-3. In essence, C-section-derived AF-MSCs can be routinely obtained and are amenable for personalized cell therapies and disease modelling.

Approximated total share of contribution: 40%

Publication Status: published in *Stem Cells International*; 2017:5932706.

Impact Factor: 3.989

This article is reproduced with permission.

Contribution on experimental design, realization and publication:

JA, TF, MSR, LSS conceived the idea and designed the experiments. IB, CH and PB collected the third trimester amniotic fluid samples. HTH and LS did pilot experiments and helped to establish the workflow. WW did the bioinformatic analysis. MSR and LSS isolated the AFCs from third trimester AF and characterized the AFCs/AF-MSCs (protein level, cell surface marker expression, secretome and *in vitro* differentiation potential). MSR and LSS made the figure and wrote the manuscript and JA edited it. The manuscript including all figures was subsequently reviewed, amended and approved by all co-authors.

Link to the publication:

<https://www.hindawi.com/journals/sci/2017/5932706/>

Hindawi
Stem Cells International
Volume 2017, Article ID 5932706, 15 pages
<https://doi.org/10.1155/2017/5932706>

Research Article

Isolation and Molecular Characterization of Amniotic Fluid-Derived Mesenchymal Stem Cells Obtained from Caesarean Sections

Lucas-Sebastian Spitzhorn,¹ Md Shaifur Rahman,¹ Laura Schwindt,¹ Huyen-Tran Ho,¹ Wasco Wruck,¹ Martina Bohndorf,¹ Silke Wehrmeyer,¹ Audrey Ncube,¹ Ines Beyer,² Carsten Hagenbeck,² Percy Balan,² Tanja Fehm,² and James Adjaye¹

¹Institute for Stem Cell Research and Regenerative Medicine, Heinrich Heine University Düsseldorf, Moorenstr. 5, 40225 Düsseldorf, Germany

²Department of Obstetrics and Gynaecology, Heinrich Heine University Düsseldorf, Moorenstr. 5, 40225 Düsseldorf, Germany

Correspondence should be addressed to James Adjaye; james.adjaye@med.uni-duesseldorf.de

Lucas-Sebastian Spitzhorn and Md Shaifur Rahman contributed equally to this work.

Received 29 June 2017; Revised 13 September 2017; Accepted 1 October 2017; Published 31 October 2017

Academic Editor: Valentina Russo

Copyright © 2017 Lucas-Sebastian Spitzhorn et al. This is an open access article distributed under the Creative Commons Attribution License, which permits unrestricted use, distribution, and reproduction in any medium, provided the original work is properly cited.

Human amniotic fluid cells are immune-privileged with low immunogenicity and anti-inflammatory properties. They are able to self-renew, are highly proliferative, and have a broad differentiation potential, making them amenable for cell-based therapies. Amniotic fluid (AF) is routinely obtained via amniocentesis and contains heterogeneous populations of foetal-derived progenitor cells including mesenchymal stem cells (MSCs). In this study, we isolated human MSCs from AF (AF-MSCs) obtained during Caesarean sections (C-sections) and characterized them. These AF-MSCs showed typical MSC characteristics such as morphology, *in vitro* differentiation potential, surface marker expression, and secreted factors. Besides vimentin and the stem cell marker CD133, subpopulations of AF-MSCs expressed pluripotency-associated markers such as SSEA4, c-Kit, TRA-1-60, and TRA-1-81. The secretome and related gene ontology (GO) terms underline their immune modulatory properties. Furthermore, transcriptome analyses revealed similarities with native foetal bone marrow-derived MSCs. Significant KEGG pathways as well as GO terms are mostly related to immune function, embryonic skeletal system, and TGF β -signalling. An AF-MSC-enriched gene set included putative AF-MSC markers *PSG5*, *EMX-2*, and *EVR-3*. In essence, C-section-derived AF-MSCs can be routinely obtained and are amenable for personalized cell therapies and disease modelling.

1. Introduction

Recent human AF research has shown that stem cells from the first and second trimester can be collected during amniocentesis (an invasive method of prenatal diagnosis of chromosomal abnormalities and foetal infections) [1]. The therapeutic potential including *in vitro* characterization of human amniotic fluid-derived stem cells (AFSCs) was first reported by the Atala group [2]. Because of their low immunogenicity, anti-inflammatory properties, and high proliferative and differentiation capacity *in vitro*, AFSCs are amenable for clinical application and tissue engineering. Furthermore, they

lack carcinogenesis after transplantation in nude mice and have the ability to create embryoid body-like structures after specific treatments. Their possible origin from epiblast, demonstrated by the presence of common features with primordial germ cells, is also under discussion [2, 3]. The AFSC populations are heterogeneous in nature, of foetal-derived-differentiated and undifferentiated progenitor cells [4]. In 1993, Torricelli and coworkers first reported a subpopulation of hematopoietic progenitor cells in AF [5]. Interestingly, in 2003, it was reported that a small subpopulation of AFSCs expresses the pluripotency-regulating marker, octamer-binding transcription factor 4 (OCT4) [6]. Later, Moschidou

coworkers reported that AFSCs isolated from the first trimester express other pluripotent stem cell-associated markers such as NANOG, sex-determining region Y-box 2 (SOX2), Krüppel-like factor 4 (KLF4), stage-specific embryonic antigen-4 (SSEA4), CD133, and c-Kit [7, 8]. Their self-renewal capabilities were also confirmed, thus indicating that AFSCs are of high plasticity and easily reprogrammable as our previous studies demonstrated [9, 10]. At the transcription level, it has also been shown that a subpopulation of AFSCs has high overlap with human ESCs as they share about 82% of transcriptome identity [11]. Additionally, AFSCs were found to be paracrine active as their conditioned media contain cytokines which have a profound effect on vasculogenesis, angiogenesis, and osteogenesis [12–14]. AFSCs have the potential for use in clinical applications as shown for example by keratinocyte differentiation and subsequent improvement of wound healing [15].

Mesenchymal stem cells (MSCs) are multipotent stromal stem cells [16, 17]. Morphologically, they are fibroblast-like and spindle-shaped cells. *In vitro*, these clonogenic cells easily adhere to plastic surfaces and have high-replicative capacity [17, 18]. Several sources are reported from adult and foetal tissues from which these types of MSCs can be obtained, for example, bone marrow (BM) and adipose tissue [19] and extraembryonic tissues such as umbilical cord blood [20, 21] and placental tissues such as amnion and decidua and furthermore from second and term amniotic fluid [22]. *In vitro* and *in vivo* MSCs differentiate into mesodermal cell types such as fibroblasts, osteoblasts, chondrocytes, and adipocytes [16, 23]. The International Society for Cellular Therapy (ISCT) postulated that for transplantation and cellular therapy, MSCs should not differentiate into blood cells and therefore not express any markers of hematopoietic lineage such as the surface markers CD14, CD34, and CD45. In contrast to this, bone marrow MSCs should express CD73, CD90, and CD105 referring to their minimal characterization criteria [24]. MSCs have been widely used for therapies such as graft versus host disease, precisely in over 700 clinical trials till date (<https://clinicaltrials.gov>). The frequency and differentiation capacity as well as proliferation potential from BM-MSCs has been shown to decrease with age [25].

A subpopulation of AFSCs with mesenchymal characteristics has been isolated from second and third-trimester AF and thus referred to as amniotic fluid mesenchymal stem cells (AF-MSCs). They were isolated based upon their plastic adherence and similar cell surface marker composition as MSCs from other sources. Furthermore, they were also able to differentiate into bone, cartilage, and fat cells *in vitro* [23, 26–28]. Various studies have shown that these AF-MSCs also express OCT4 [27, 28]; however, this is still controversial since no one has yet defined the self-renewal function of OCT4 in AF-MSCs as has been shown in human embryonic stem cells [29].

AF-MSCs are advantageous in terms of developmental stages but problematic with respect to the invasiveness of the collection procedures—amniocentesis and foetal infections. Therefore, C-section-derived AF could be an alternative source for these cells. However, the amniotic fluid is merely discarded during this procedure that is why few studies have isolated AFSCs at this stage of gestation. The question remains

as to whether full-term AF harbours AF-MSCs of similar potency as cells obtained in the first and second trimesters of pregnancy.

In this study, we characterized human AF-MSCs obtained from C-sections (third trimester) and tested their multilineage differentiation capacity *in vitro*, immunophenotype, expression of mesenchymal markers, multipotency markers, transcriptome, and their secretome. Our data suggests that AF obtained from C-sections may represent a promising source for stem cells of mesenchymal origin. Presently, the most common source of MSCs is the bone marrow (BM). However, harvesting and processing of BM-MSCs have major drawbacks and limitations. Thus, it is significant that AF collected during C-sections is an alternative source of AF-MSCs that are immature and possess high plasticity making them useful for clinical applications.

2. Materials and Methods

2.1. Preparation of Amniotic Fluid. Three amniotic fluid samples from healthy human donors were collected during full-term C-sections from the Obstetrics and Gynaecology faculty, Heinrich Heine University Düsseldorf, Germany, with patient consent as well as institutional ethical approval and kept at 4°C until processed. In general, the time between collection and processing was kept as short as possible to minimize cell death. First, AF was washed with PBS (Gibco; Thermo Fisher Scientific, Darmstadt, Germany) and centrifuged at 300 ×g for 5 min. The supernatant was discarded, and the pellet washed again with PBS and was dissolved in Ammonium chloride (University Hospital Düsseldorf; Pharmacy) to lyse the remaining erythrocytes. Thereafter, the cell solution was incubated at 4°C for 20 min and centrifuged again. This procedure was repeated until the pellet had a clear colour. Afterwards, the cells were cultured in Chang C Medium (Irvine Scientific, CA, USA) containing 88% α MEM (Minimum Essential Medium Eagle Alpha Modification; Sigma) with 10% FBS, 1% GlutaMAX, 1% penicillin/streptomycin (all Gibco), 10% Chang B Basal Medium, and 2% Chang C supplement (Irvine Scientific) at 37°C and 5% CO₂. Once attached, the cells were visible after 4–7 days and the medium was changed. Upon attainment of 90% confluency, the cells were detached using TrypLE Express (Thermo Fisher Scientific) and seeded into other plate formats or frozen.

2.2. Flow Cytometric Analysis of Amniotic Fluid Cells. The immunophenotyping of three independent AF preparations was done using the human MSC phenotyping kit (Miltenyi Biotec GmbH, Bergisch Gladbach, Germany) was done according to manufacturer's instructions. After harvesting, 2×10^5 AF-MSCs were transferred into two test tubes. 2 ml PBS was added to each tube and centrifuged at 300 ×g for 5 min. The supernatant was discarded and the pellet resuspended in 100 μ l PBS within the tubes. In one of the tubes, 0.5 μ l of the MSC phenotyping cocktail and the other tube 0.5 μ l of the isotype control cocktail were added and vortexed. The MSC phenotyping cocktail contained fluorochrome-conjugated monoclonal antibodies CD14-PerCP, CD20-PerCP, CD34-PerCP, CD45-PerCP,

CD73-APC, CD90-FITC, and CD105-PE. The isotype phenotyping cocktail contained fluorochrome-conjugated antibodies that should not specifically detect human antigens and was therefore used as a negative control. The tubes were incubated at 4°C for 10 min in the dark. To washout nonbinding antibodies, 1 ml PBS was added and centrifugation at 300 ×g for 5 min was performed. Afterwards, the cell pellet was fixed using 4% paraformaldehyde (PFA; Polysciences Inc., PA, USA). For flow cytometric analysis of the AF-MSCs for pluripotency-associated markers, TRA-1-60, TRA-1-81, and SSEA4 dye-coupled antibodies were used (anti-TRA-1-60-PE, human (clone: REA157), number 130-100-347; anti-TRA-1-81-PE, human (clone: REA246), number 130-101-410, and anti-SSEA-4-PE, human (clone: REA101), number 130-098-369; Miltenyi Biotec GmbH). The staining procedure was carried out as described above.

The cells were stored at 4°C in the dark until flow cytometric analysis via BD FACSCanto (BD Biosciences, Heidelberg, Germany) and CyAn ADP (Beckman Coulter, CA, USA) was done. Histograms were created using the FCSalyzer software version 0.9.3.

2.3. Immunofluorescence Staining. To analyse the cells for specific markers, AF-MSCs were cultured in 12- or 24-well plates. At 60–80% confluency, the cells were washed and subsequently fixed using 4% PFA for 15 min at room temperature (RT) on a rocking platform. The fixed cells were treated with 1% Triton X-100 (Carl Roth GmbH & Co. KG, Karlsruhe, Germany) for 5 min and blocking buffer was added to the cells. For intracellular staining, this buffer contained 10% normal goat serum (NGS; Sigma), 0.5% Triton X-100, 1% BSA (Sigma), and 0.05% Tween 20 (Sigma), all dissolved in PBS. If extracellular structures were to be stained, Triton and Tween were omitted. After blocking for 2 h at RT, the first antibodies OCT-4A (C30A3) rabbit mAb number 2840, SSEA4 (MC813) mouse mAb number 4755, E-cadherin (24E10) rabbit mAb number 3195, vimentin (5G3F10) mouse mAb number 3390, TRA-1-60 mouse mAb number 4746, TRA-1-81 mouse mAb number 4745 (Cell Signalling Technology, MA, USA), CD133 PA2049 (Boster Bio, PA, USA), and c-Kit (H-300) rabbit polyclonal IgG (Tebu Bio, Offenbach, Germany) were diluted in blocking buffer/PBS and added to the cells with an incubation time of 1 h at RT. After washing for three times with 0.05% Tween 20 in PBS, the appropriate secondary Cy3- or Alexa Fluor 488-labelled antibodies (Thermo Fisher Scientific) and Hoechst 33258 dye (Sigma-Aldrich Chemie GmbH, Taufkirchen, Germany, 1 : 5000 in blocking buffer) were applied for visualization of the primary antibodies and cell nuclei, respectively. Images were taken with a fluorescence microscope (LSM700; Zeiss, Oberkochen, Germany).

2.4. In Vitro Differentiation into Adipogenic, Chondrogenic, and Osteogenic Lineage. The differentiation of the AF-MSCs from passages 5 to 6 was carried out using the StemPro Adipogenesis differentiation Kit, StemPro Chondrogenesis differentiation Kit, and StemPro Osteogenesis differentiation Kit (Gibco, Life Technologies, CA, USA). The differentiation

media were formulated by mixing 90 ml of the respective basal media with 10 ml of their corresponding supplements and 1.1 ml of penicillin/streptomycin. At 60–70% confluency, cultivation of the cells in the differentiation media or Chang C media (control wells) was initiated. The medium was replaced every 2–3 days for three weeks. After this period, the medium was removed, and the cells were washed with PBS and fixed with 4% PFA for 30 min at RT on a rocking platform. Subsequently, the cells were stained for distinct developed structures.

2.5. Oil Red O Staining for Adipocytes. Fixed cells were washed with 50% ethanol and then 0.2% Oil Red O working solution was added to the wells and incubated for 30 min at RT on a rocking platform. This solution stained the developed fat vacuoles. The 0.2% Oil Red O working solution was prepared by diluting the 0.5% Oil Red O stock solution (Sigma) with distilled water and filtering it. After washing twice with 50% ethanol and at least 3 times with distilled water until all the excess Oil Red O solution was removed, cells were kept in PBS and images were taken with a light microscope.

2.6. Alcian Blue Staining of Chondrocytes. After fixation, cells should be stained with alcian blue which turns sulfated proteoglycans deposits in chondrocytes visibly blue. Cells were first washed with PBS and 1% alcian blue 8GX (Sigma) solution, prepared in 0.1 N hydrochloric acid (HCl), was added. The cells were stained for 30 min at RT on a rocking platform. Afterwards, the cells were washed three times with 0.1 N HCl solution and with distilled water until the alcian blue solution was completely removed. Cells were then kept in PBS for microscopic imaging.

2.7. Alizarin Red S Staining for Osteoblasts. Alizarin red S (Sigma) which specifically stains developed calcium deposits was used to stain the cells after osteogenic differentiation. Cells were washed after fixation with PBS, and 2% alizarin red S solution in distilled water was added. After 30 min incubation at RT on a rocking platform, the cells were washed with distilled water and then with PBS to remove the remaining dye. For light microscopic analysis, the cells were kept in PBS.

2.8. Secretome Analysis. For the detection of cytokines secreted by the AF-MSCs, the Proteome Profiler Human Cytokine Array Panel A (R&D Systems, MA, USA) was performed according to the manufacturer's instructions. Initially, 1.5 ml of conditioned medium (pooled equal volumes from the three independent AF-MSC samples used for this study) was used. The array was evaluated by detection of the emitted chemiluminescence. The pixel density of each spotted cytokine was analysed using the software ImageJ. All spots on the membrane including reference and negative control spots were measured separately. Correlation variations and *p* values were calculated based on the pixel density. The pixel density value of 50 was set as the threshold.

2.9. RNA Isolation. After incubation with TRIzol (Thermo Fisher) for 5 min at RT on a rocking platform, the cells were detached and frozen within this solution at –80°C.

The RNA was then isolated by using the Direct-zol RNA MiniPrep Kit (Zymo Research, CA, USA) which already contains DNase. The resulting RNA was dissolved in RNA/DNase free water and analysed using the NanoDrop 2000 (Thermo Fisher) spectrophotometer.

2.10. Transcriptome Analysis. Microarray experiments were performed on the PrimeView Human Gene Expression Array (Affymetrix, Thermo Fisher Scientific) for two samples of AF-MSCs (AF-MSC1, AF-MSC2), foetal bone marrow-derived MSCs (fMSC), and embryonic stem cells (H1, H9) as well as human foreskin fibroblast-derived induced pluripotent stem cells (iPSCs) and are provided online at the National Center of Biotechnology Information (NCBI) Gene Expression Omnibus (<https://www.ncbi.nlm.nih.gov/geo/query/acc.cgi?acc=GSE100448>). The unnormalized bead summary data was further processed via the R/Bioconductor [30] environment using the package *affy* (<http://bioconductor.org/packages/release/bioc/html/affy.html>) [31]. The obtained data was background-corrected, transformed to a logarithmic scale (to the base 2), and normalized by employing the Robust Multiarray Average method. Heatmaps and cluster analysis were generated using the *heatmap.2* function from the *gplots* package, and the correlation coefficients were measured using Pearson correlation as similarity measure (<http://CRAN.R-project.org/package=gplots>).

2.11. Gene Ontology, KEGG Pathway, and STRING Network Analysis. After transcriptome analysis gene ontology terms and associated KEGG pathways [32] for the different gene sets were generated using the DAVID tool (<https://david.ncifcrf.gov/>) [33], the STRING network tool was used for network cluster analysis (<https://string-db.org/>) [34].

3. Results

3.1. Isolation and Culture of C-Section-Derived AF-MSCs. During C-sections at full-term gestation, AF was collected using a syringe (Figure 1(a)) and transferred into 50 ml tubes. The red colour of the fluid indicates the presence of erythrocytes. The AF was washed twice with PBS (Figures 1(b) and 1(c)) then the remaining erythrocytes were lysed by resuspending the cell pellet in ammonium chloride (Figure 1(d)). After additional washing, the pellet had a whitish colour indicating successful removal of the remaining blood cells (Figure 1(e)). Microscopic analysis directly after the purification displayed a heterogeneous mixture of different cell types (Figure 1(f)). First, attached cells were visible after 4 to 7 days. After passaging them twice, the heterogeneous morphology of the cells (Figure 1(g)) became more homogeneous with spindle-shaped fibroblast-like forms (Figure 1(h)). Cells were cultured until they all showed a homogeneous MSC morphology and then used for further experiments.

3.2. In Vitro Differentiation Capacity and Cell Surface Marker Expression. To investigate their multipotent differentiation capacity, AF-MSCs from three independent preparations were challenged to differentiate into adipogenic, chondrogenic, and osteogenic directions by employing distinct differentiation media for 3 weeks. Successful differentiation into adipocytes

was observed by staining of emerging fat droplets with Oil Red O solution (Figure 2(a), A1). The fat vacuoles surrounded the cell nuclei. During chondrogenic differentiation, the cells aggregated and alcian blue staining showed the presence of emerged proteoglycans within the developed cell clusters of chondrocytes (Figure 2(a), A2) and osteogenic lineage differentiation was shown by alizarin red S staining of developed calcium deposits (Figure 2(a), A3). The visual mineralization of the cells started after the first week. Cells of the control wells remained fibroblast-like. Cells from all preparations showed a higher propensity to differentiate into the osteogenic lineage than into the other two investigated lineages as evidenced by differentiated areas within the cell culture dish of about 90%.

3.3. Flow Cytometric Analysis for Cell Surface Marker Expression. To analyse the cell surface marker presence on the AF-MSCs, the human MSC phenotyping kit (Miltenyi Biotec GmbH, Bergisch Gladbach, Germany) was used which contained antibodies against MSC-related markers CD73, CD90, and CD105 separately and antibodies against haematopoietic markers CD14, CD20, CD34, and CD45 in a combined cocktail. After staining, the cells were analysed using a flow cytometer. Within the three independent AF-MSC preparations, the presence of CD73, CD90, and CD105 positive cells was up to 90%. As expected, all cell preparations were devoid of the haematopoietic markers CD14, CD20, CD34, and CD45 (Figure 2(b)). Furthermore, AF-MSCs were analysed for the expression of pluripotency-associated cell surface markers. A subpopulation of approximately 33% of the cells was positive for SSEA4 whereas 14% of the cells was positive for TRA-1-60 and 8% was positive for TRA-1-81 (Figure 3(b), B1, B2, and B3).

3.4. Immunofluorescent-Based Analysis of Stem Cell Marker Expression in AF-MSCs. AF-MSCs had a spindle-shaped morphology and expressed the type III intermediate filament vimentin (Figure 3(a), A1) which is expressed by mesenchymal cells and widely used as a mesenchymal indicator [35]. In parallel, these cells were negative for E-cadherin (Figure 3(a), A2) as a marker for epithelial cells. The expression of CD133/prominin-1 (Figure 3(a), A3), a marker for multipotent progenitor cells including MSCs [36, 37], was detected. The populations we isolated did not express OCT4 or NANOG (Figure 3(a), A5 and A6). However, the AF-MSCs expressed c-Kit, SSEA4, TRA-1-60, and TRA-1-81 (Figure 3(a), A4, A7, A8, and A9). The percentage of cells positive for the investigated markers was consistent with the flow cytometric data.

3.5. Secretome Analysis. The ability of AF-MSCs to secrete cytokines was investigated employing a cytokine array. To achieve this, cell culture supernatants from three distinct AF-MSC preparations were pooled and analysed using the cytokine array. This revealed the presence of chemokine (C-C motif), ligand 2 (CCL2; MCP-1), C-X-C motif chemokine 1 (CXCL1; GRO α), CXCL12 (SDF-1), colony stimulating factor 2 (CSF2; GM-CSF), intercellular adhesion molecule 1 (ICAM1; CD54), interleukin-6 (IL-6), IL-8,

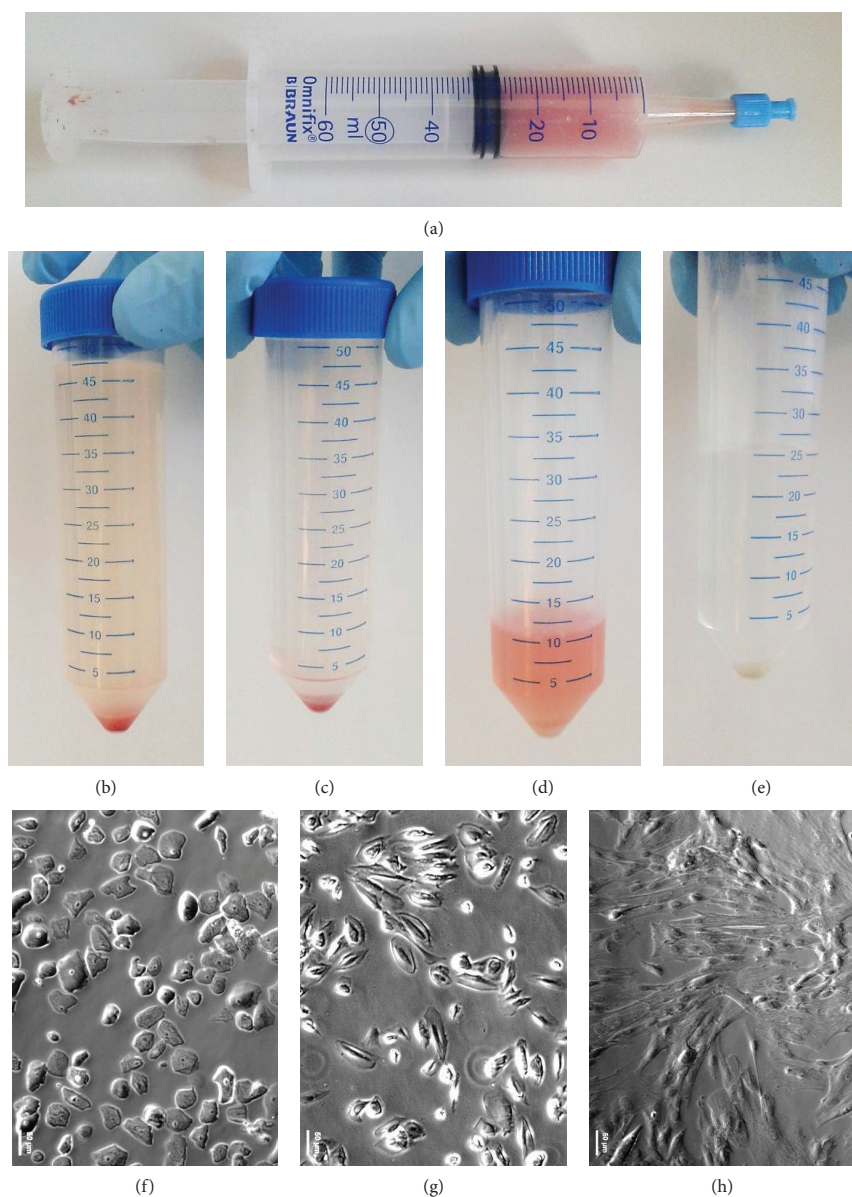


FIGURE 1: Amniotic fluid cell preparation. Amniotic fluid was collected during Caesarean sections using a 60 ml syringe (a). The AF was washed with PBS and centrifuged resulting in a reddish pellet (b, c). The red colour indicated the presence of erythrocytes which were then lysed using ammonium chloride at 4°C. The resulting white cell pellet (d, e) was transferred to cell culture vessels showing high level of heterogeneity (f). After, prolonged *in vitro* culture and passaging heterogeneous cell morphology (g) became uniform showing spindle-shaped fibroblast-like morphology (h).

IL-21, macrophage migration inhibitory factor (MIF), and plasminogen activator inhibitor-1 (PAI-1; SERPINE1) at distinct levels which were above background expression (Figures 4(a) and 4(b)). CCL2, CXCL1, IL-6, and IL-8 were the highest secreted cytokines. Average levels of secretion were found for CSF2, ICAM1, MIF, and SERPINE (PAI-1) whereas CXCL12 and IL-21 were expressed at the

lowest levels. Gene ontology term analysis of the secreted cytokines revealed terms associated with immune modulatory properties such as “immune response,” “chemotaxis,” and “inflammatory response” (Figure 4(c)).

3.6. *Overlapping, Distinct Gene Expression, Associated Gene Ontologies, and Pathways.* Hierarchical clustering

6

Stem Cells International

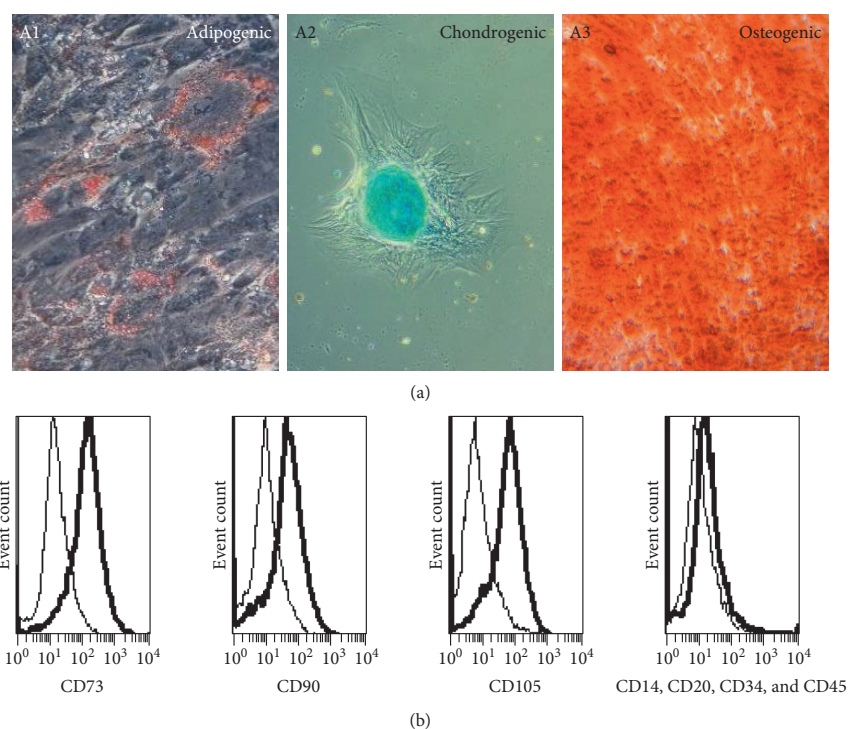


FIGURE 2: *In vitro* differentiation potential and immunophenotype of AF-MSCs. Multilineage differentiation potential of AF-MSCs was investigated by applying adipocyte, chondrocyte, and osteoblast differentiation media to the cells for 3 weeks. Staining of Oil Red O showed successful differentiation into adipogenic lineage with developed fat vacuoles surrounding the cell nucleus (A1). Chondrogenic differentiation was shown to be present by alcian blue staining of cell aggregates containing proteoglycan (A2). Osteoblast formation by AF-MSCs was indicated by alizarin red S staining of calcium deposits (A3). Flow cytometry was used for the analysis of cell surface marker expression. Histograms showed that MSC markers CD73, CD90, and CD105 were detected as cell surface proteins on AF-MSCs preparation derived from C-sections whereas hematopoietic marker expressions CD14, CD20, CD34, and CD45 were low (bold lines) (b). Antibody isotype controls are represented by thin lines.

(Figure 5(a)) based on the transcriptome profiles of AF-MSCs, fMSCs, and pluripotent stem cells (H1, H9, and iPSCs) revealed a closer relationship of AF-MSC1 and AF-MSC2 to native fMSCs than to pluripotent stem cells. The heatmap derived from the transcriptome data (Figure 5(b)) shows that the cells from both AF preparations are closer to fMSCs. The heatmap consists of 17 genes commonly up- and downregulated between AF-MSCs, fMSCs, and pluripotent cells. Genes which were expressed predominantly in AF-MSCs and fMSCs were vimentin (*VIM*), *CD44*, *CD73*, *CD105*, and *SERPINE1* as well as osteogenic markers runt-related transcription factor 2 (*RUNX2*) and growth/differentiation factor 5 (*GDF5*). In contrast to this, AF-MSCs and fMSCs were devoid of *E-Cadherin* and pluripotency markers *OCT4*, *SOX2*, and *NANOG*. Venn diagram analysis (Figure 5(c)) revealed an overlap of 11,148 genes among all cell types. Interestingly, AF-MSCs shared more genes (489) with pluripotent stem cells than with fMSCs (442). KEGG pathway analysis of genes shared between pluripotent stem cells and AF-MSCs showed the involvement of phosphatidylinositol pathway

and Notch signalling (Supplementary Figure S1 available online at <https://doi.org/10.1155/2017/5932706>). However, AF-MSCs distinctly expressed 181 genes.

Pearson correlation analysis of the transcriptome data (Figure 5(d)) revealed a high correlation (0.89 and 0.90) between AF-MSC1 and AF-MSC2 and fMSCs but low correlation (0.78–0.81) with the pluripotent cells. The significant KEGG pathways as well as gene ontology terms related to the shared genes between AF samples and fMSCs were related to immune function, skeletal development, and TGF β -signalling (Figure S2).

3.7. AF-MSC-Specific Gene Expression Analysis. A heatmap was derived using the 181 AF-MSC exclusive gene set (Figure 6(a)). One subset of these genes could be used to identify possible AF-MSC marker genes (Figure 6(b)) including *PSG5*, *C4orf26*, *C8orf4*, *EVR-3*, *EMX-2*, and *C15orf37*. Furthermore, gene ontology analysis focusing on biological processes (Figure 6(c)) showed the involvement of genes associated with skeletal system development and patterning. Tissue-specific gene distribution analysis (Figure 6(d))

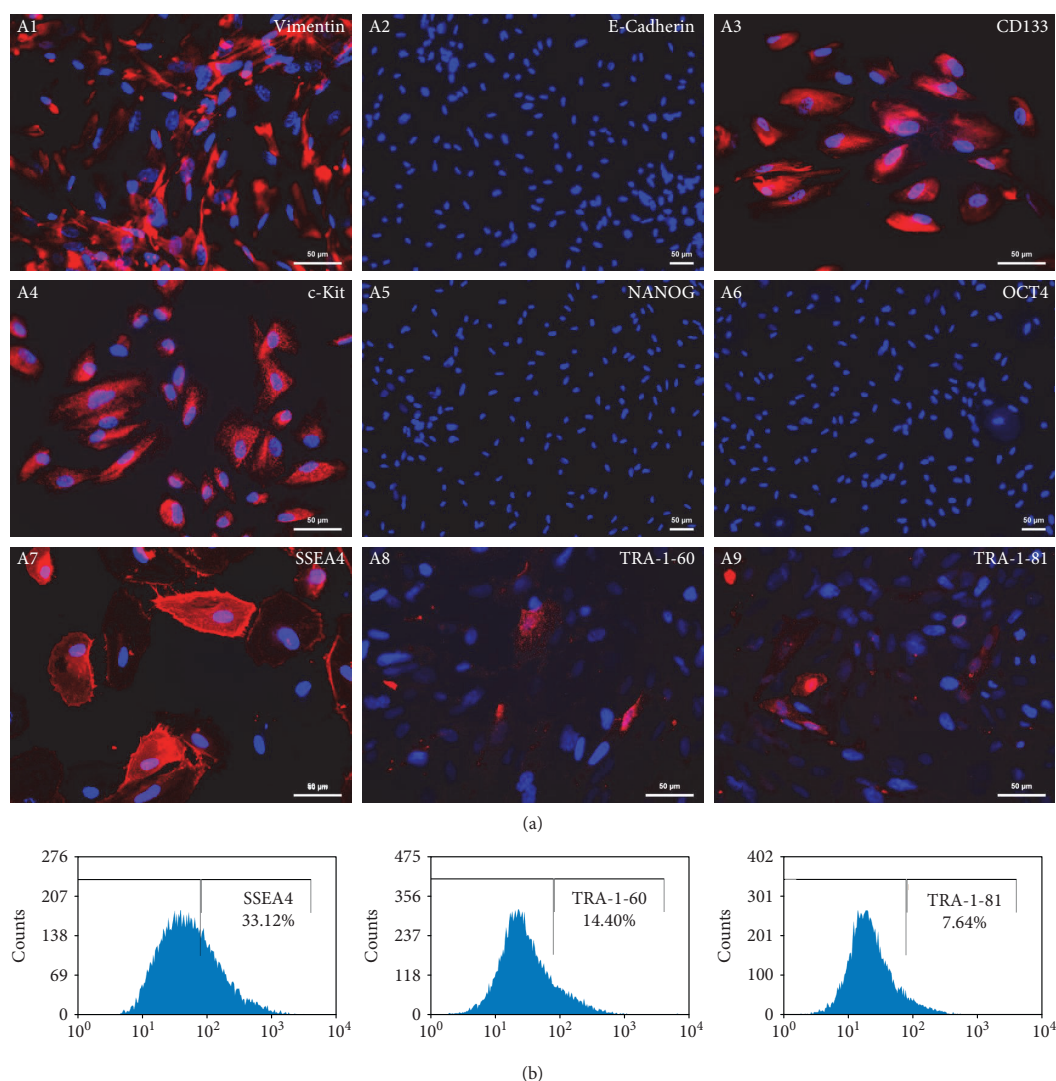


FIGURE 3: Protein expression analysis of AF-MSCs. (a) By immunofluorescent staining, AF-MSCs were found to express vimentin (A1), CD133 (A3), c-Kit (A4), SSEA4 (A7), TRA-1-60 (A8), and TRA-1-81 (A9) and by parallel absence of E-cadherin (A2), NANOG (A5), and OCT4 (A6). Cell nuclei were stained using Hoechst. (b) Flow cytometric analysis confirmed cell surface expression of SSEA4 (B1), TRA 1-60 (B2), and TRA-1-81 (B3).

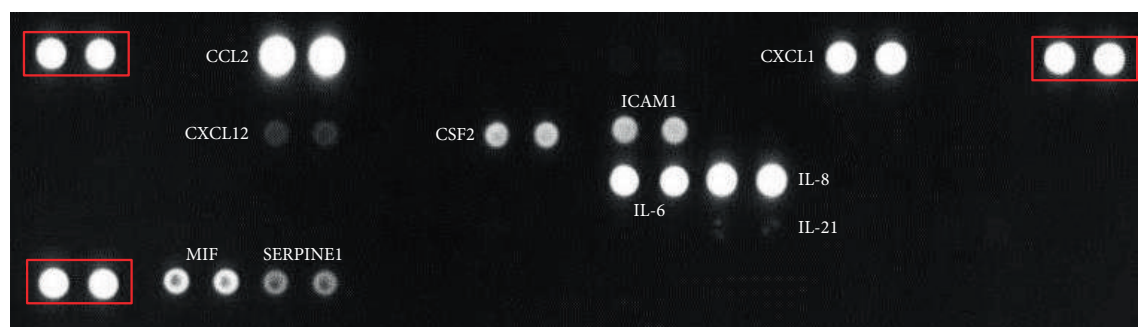
revealed the relationship between the 181 AF-MSC-specific genes and the different embryonic tissues. The most prominent tissues were the testis, kidney, and hypothalamus. The rest of the genes were distributed among the other organs. The AF-MSC-specific gene set (181 genes) was further compared to an already published transcriptome dataset of third-trimester AFSCs [11] and visualized with a Venn diagram (Figure 6(e)). 25 genes including *HOXB7*, *APBB1IP*, *HOXB8*, *PTHLH*, and *ZPLD1* were found to be expressed in common between these two gene sets. Referring to the associated gene ontology terms, these genes are mostly associated with embryonic skeletal system morphogenesis, positive regulation of

branching involved in ureteric bud morphogenesis, skeletal system development, and regulation of mesonephros development as well as anterior/posterior pattern specification.

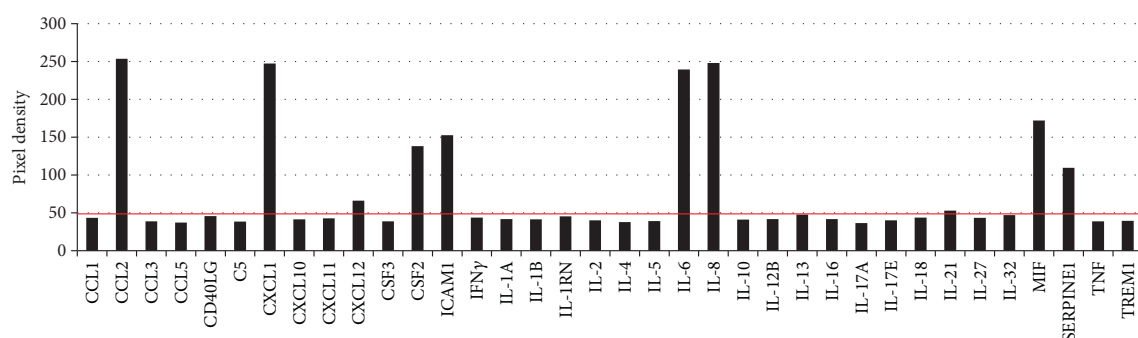
3.8. Network Analysis of 181 AF-MSC Exclusive Genes. The network analysis of the 181 AF-MSC-specific genes was done using the STRING tool and predicted 4 different clusters (Figure 7): cluster 1 displayed the patterning and embryonic development related HOX genes such as the homeobox B7 (*HOXB7*), cluster 2 contained the immunity-related gene (e.g., *CSF2*), and cluster 3 included the extracellular matrix- (ECM-) related gene set (e.g., laminin subunit

8

Stem Cells International



(a)



(b)

Category	Term	<i>p</i> value	Genes
GOTERM_CC_DIRECT	GO:0005615~extracellular space	8,74E-10	CXCL1, CSF2, ICAM1, IL6, CCL2, SERPINE1, IL21, CXCL12, and MIF
GOTERM_BP_DIRECT	GO:0071222~cellular response to lipopolysaccharide	1,33E-07	CSF2, ICAM1, IL6, CCL2, and SERPINE1
GOTERM_BP_DIRECT	GO:0006955~immune response	5,09E-07	CXCL1, CSF2, IL6, CCL2, IL21, and CXCL12
GOTERM_CC_DIRECT	GO:0005576~extracellular region	1,13E-05	CXCL1, CSF2, IL6, CCL2, SERPINE1, CXCL12, and MIF
GOTERM_MF_DIRECT	GO:0005102~receptor binding	1,23E-05	CXCL1, CCL2, SERPINE1, CXCL12, and MIF
GOTERM_BP_DIRECT	GO:0006954~inflammatory response	1,66E-05	CXCL1, IL6, CCL2, CXCL12, and MIF
GOTERM_BP_DIRECT	GO:0090026~positive regulation of monocyte chemotaxis	2,38E-05	CCL2, SERPINE1, and CXCL12
GOTERM_MF_DIRECT	GO:0008083~growth factor activity	4,69E-05	CXCL1, CSF2, IL6, and CXCL12
GOTERM_BP_DIRECT	GO:0070374~positive regulation of ERK1 and ERK2 cascade	6,00E-05	ICAM1, IL6, CCL2, and MIF
GOTERM_MF_DIRECT	GO:0005125~cytokine activity	6,00E-05	CSF2, IL6, IL21, and MIF
GOTERM_BP_DIRECT	GO:0043200~response to amino acid	9,17E-05	ICAM1, IL6, and CCL2
GOTERM_BP_DIRECT	GO:0009408~response to heat	2,22E-04	IL6, CCL2, and CXCL12
GOTERM_MF_DIRECT	GO:0008009~chemokine activity	2,29E-04	CXCL1, CCL2, and CXCL12
GOTERM_BP_DIRECT	GO:0060326~cell chemotaxis	4,07E-04	CXCL1, CCL2, and CXCL12

(c)

FIGURE 4: Secretome analysis of AF-MSCs. The cytokines CCL2, CXCL1, CXCL12, CSF2, ICAM, IL-6, IL-8, IL-21, MIF, and SERPINE1 were detected by protein arrays in cell culture supernatant from AF-MSCs. A membrane with spotted antibodies was used for detection. The three red-boxed spot pairs in the corners represent protein array quality controls (a). Densitometric analysis revealed specific pixel densities; the pixel density of 50 represents the threshold (red line) (b). Gene ontology analysis of secreted cytokines revealed the shown top 14 results with *p* values below 0.0005 (c).

alpha 3 (*LAMA 3*)) whereas cluster 4 showed the WNT pathway and signalling-related gene set which includes *WNT10A*. The network analysis also revealed functional biological process (BP) enrichment of regionalization, anterior/posterior pattern specification, chordate embryonic development, embryonic organ development, and embryonic skeletal system morphogenesis.

4. Discussion

In comparison to our results, it was shown that MSCs derived from the bone marrow attached to the cell culture dish within three days after plating whereas umbilical cord and adipose tissue-derived MSCs attached within the first 24 h [38]. The prolonged attachment time of the AF-MSCs

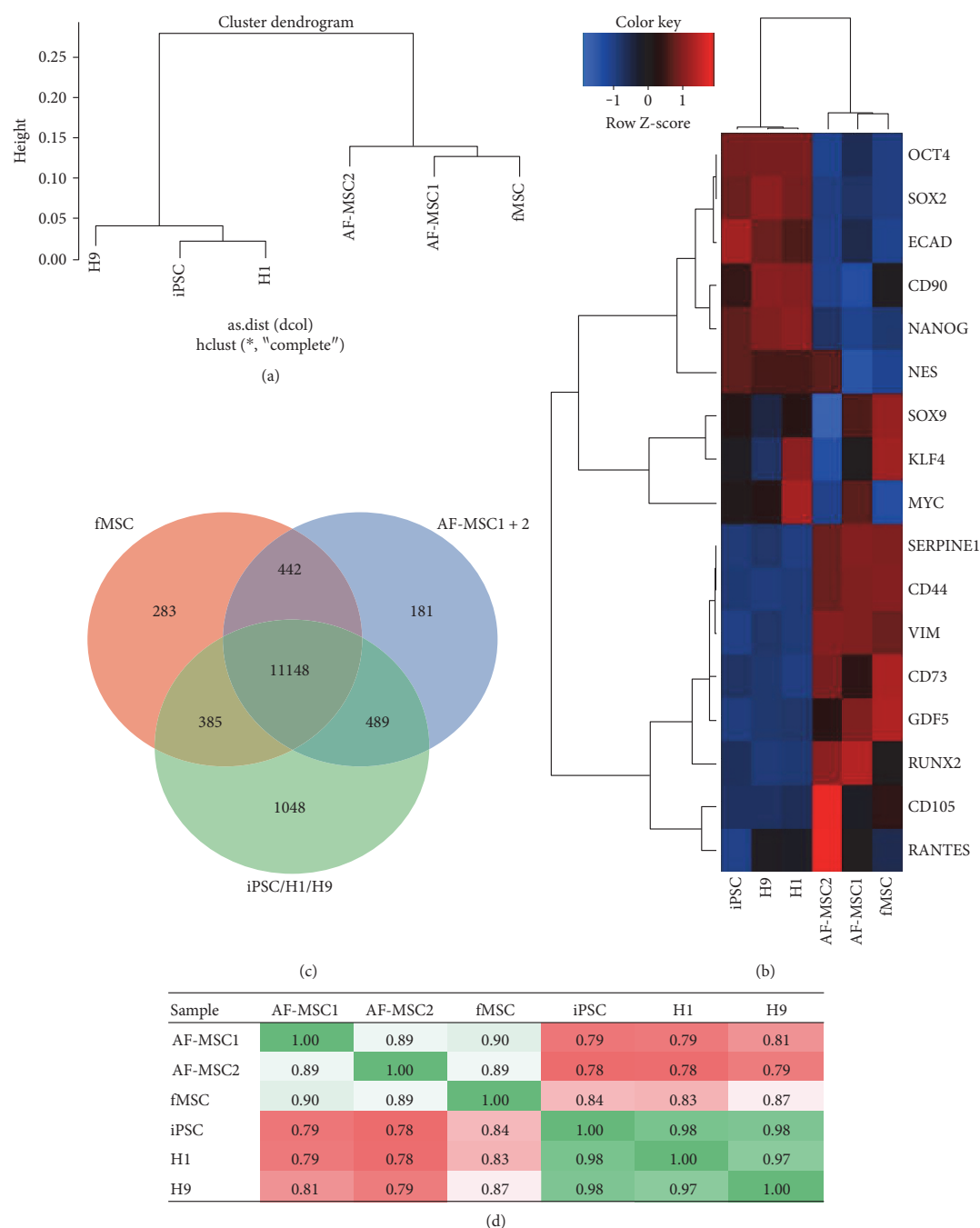


FIGURE 5: Overlapping and distinct gene expression in AF-MSCs. Dendrogram resulting from hierarchical clustering (a) of global gene expression profiles of AF-MSCs, fMSCs, and established pluripotent stem cells (H1, H9, and iPSCs). Transcriptomes of AF-MSC1 and AF-MSC2 cluster with fMSC while those of the H1, H9, and iPSCs cluster separately. The heatmap of 17 commonly up- or downregulated genes (b) shows similar gene expression of AF-MSCs and fMSCs. Venn diagram analysis revealed shared gene expression between fMSC, AF-MSCs, and pluripotent stem cells (c). Pearson's correlation coefficient was calculated based on the transcription data (d). Each replicate was pairwise compared with each other replicate. A value of 1 indicates perfect linear correlation while a value of 0 implies no correlation. Pearson correlation analysis of transcriptome data revealed a high correlation (green) of both AF-MSC1 and AF-MSC2 with fMSCs but low correlation (red) with pluripotent cells.

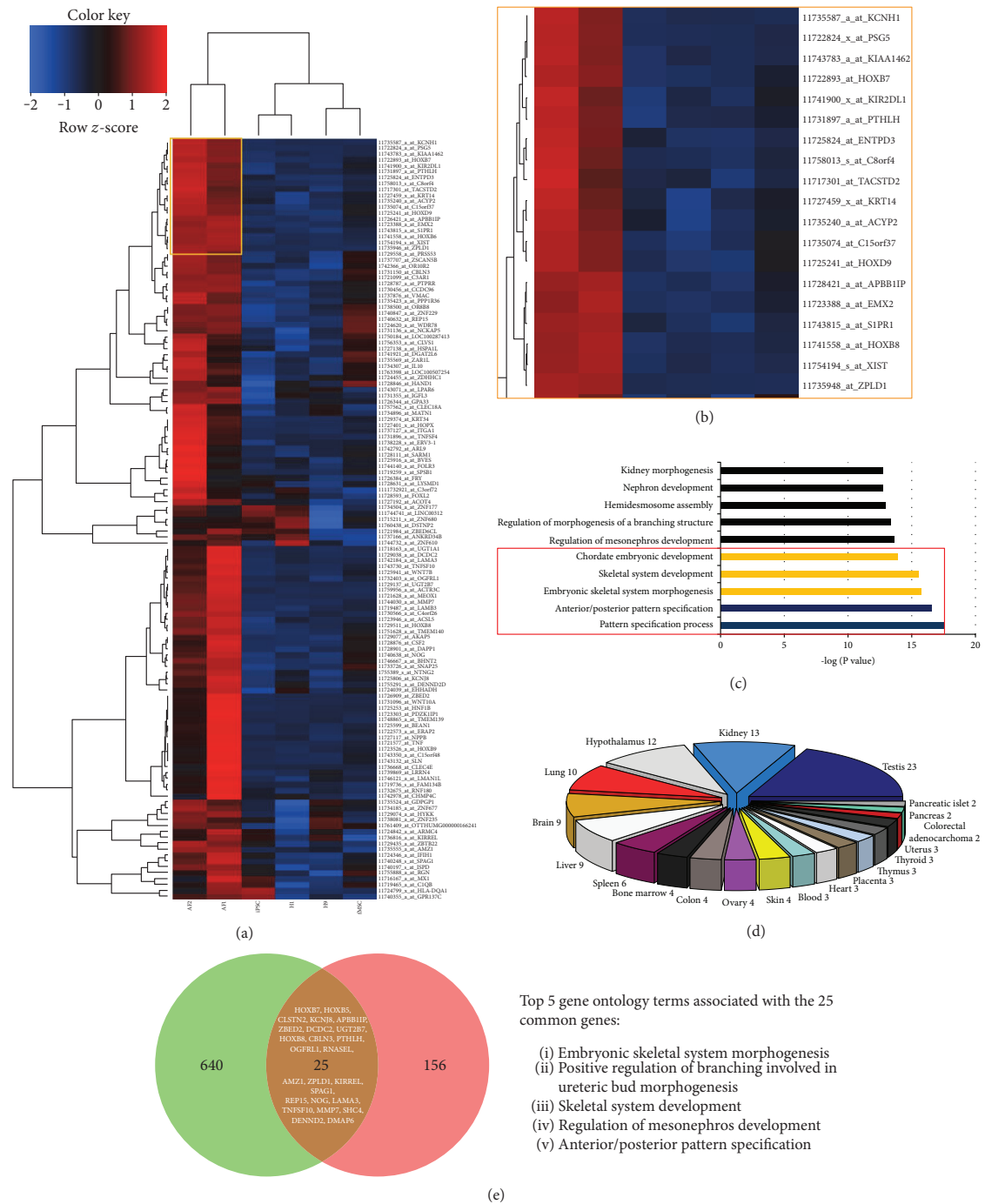


FIGURE 6: AF-MSC-specific genes. (a) Heatmap and clustering of the 181 genes exclusive for AF-MSCs (see Figure 5(c)). Zoom in on one cluster of the heatmap (b) showed possible AF-MSC markers (yellow box). Gene ontology (GO) analysis of the 181 AF-MSC exclusive genes using the DAVID tool for the GO terms associated with biological processes (c) with a maximum p value of 0.05. Significantly enriched GO terms for each category are shown with the $-\log$ of their p values. (d) Tissue distribution of the 181 exclusive AF-MSC-related genes. (e) Comparative analysis of 181 AF-MSC-specific genes and an already published data set of 665 AFSC-specific genes [11] via Venn diagram uncovered a common set of 25 genes.

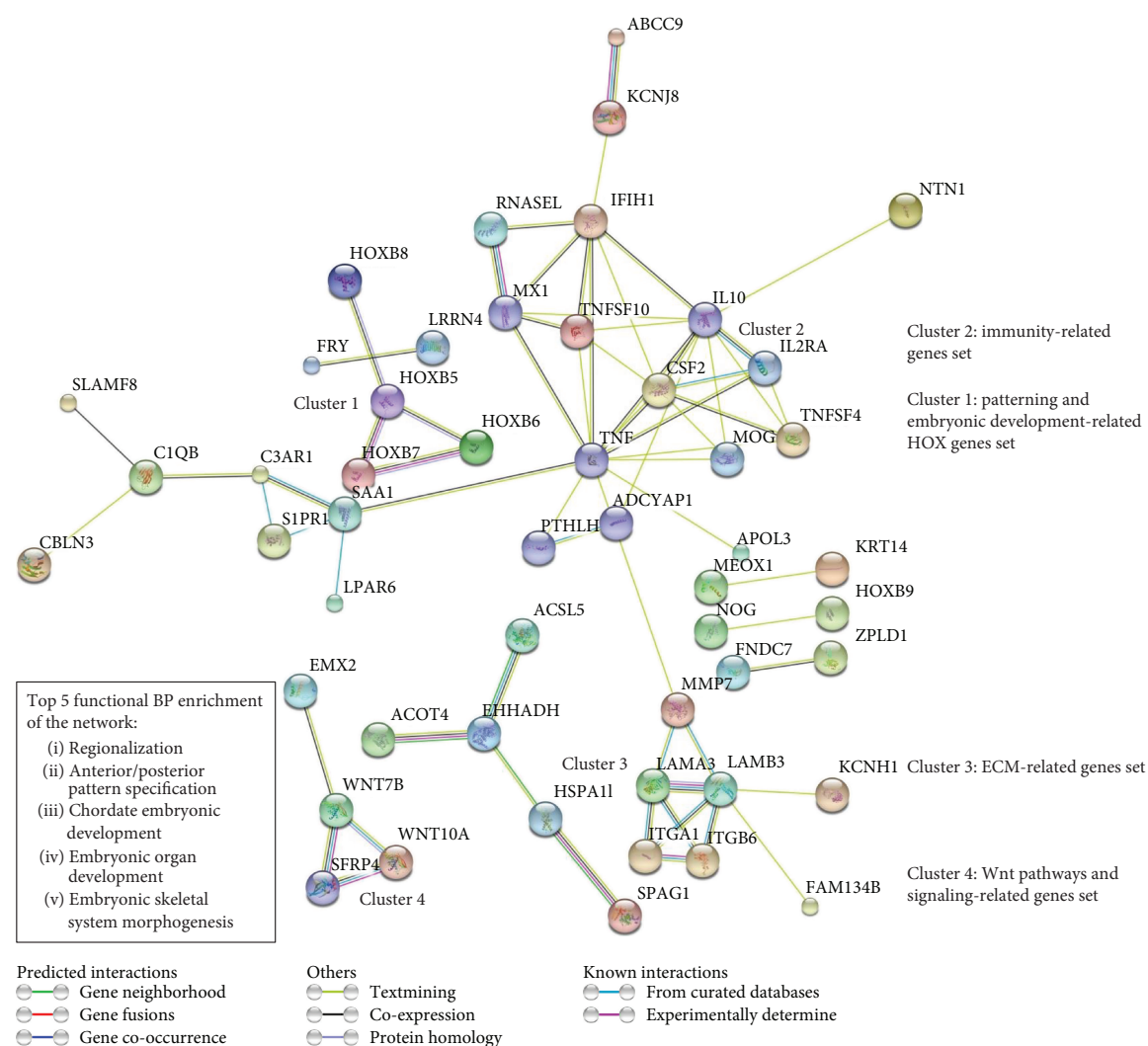


FIGURE 7: Network analysis of the 181 AF-MSC-specific genes. STRING network analysis revealed 4 distinct clusters: cluster 1 represents the genes involved in patterning and embryonic development which mainly involves the HOX genes. Cluster 2 contains genes related to immunity (e.g., TNF and IL-10). Extracellular matrix- (ECM-) related genes are found in cluster 3, and cluster 4 shows genes related to WNT signalling.

could be explained by the change of environment (micro-environment of amnion with distinct chemicals), the high heterogeneity of the cells, and a lower prevalence of stem cells within at term amniotic fluid when compared to the first and second-trimester amniotic fluid. In addition to the fibroblast-like cells, other cell morphologies were present in the AF preparation but these diluted out with time and increasing passage numbers (Figure 1). The remaining cells were of mesenchymal morphology and expressed vimentin and were devoid of E-cadherin (Figure 2(a), A1 and A2). Wolfrum et al. reported epithelial-like morphologies in senescent AFSCs [11]. Hoehn et al. similarly recognized different populations in second-trimester AF

that either possessed fibroblast-like or epithelial-like morphologies [39, 40]. Comparable proliferative capabilities of the populations, long-lasting ex vivo culture of the fibroblast-like cells which proliferated over 30 passages and the epithelial-like morphologies have also been observed. Nevertheless, most of the studies obtained AFSCs from amniocentesis. This procedure has restricted access to the fluid with a certain level of risk to the foetus and mother [41]. The collection of AF from full-term pregnancies or during deliveries as done in the present study could be a possible alternative option with higher prevalence of healthy diploid foetuses as compared to first- and second-trimester-derived AF.

The exhibited multilineage differentiation potential into bone, fat, and cartilage cells of the C-section-derived AF-MSCs (Figure 2(a), A1, A2, and A3) was also previously described for AFSCs derived from amniocentesis. The chondrogenic differentiation potential of AF-MSCs derived from amniocentesis has been reported [42] and especially osteogenic differentiation potential and further use in bone defect models underlines the potency of these cells to build up osteoblasts [43] and thus could be used for future bone related therapies.

The AF-MSCs obtained during C-sections showed the typical MSC cell surface marker expression of CD73, CD90, and CD105 by parallel absence of the haematopoietic markers CD14, CD20, CD34, and CD45 (Figure 2(b)) as described by the ISCT [24]. However, as shown in previous studies, different individuals and origins of MSCs, respectively, can lead to altered cell surface marker expressions [23].

The transcription factor OCT4 in association with NANOG and SOX2 has been shown to be the key driver of pluripotency [29]. However, the majority of AFSC studies published so far have focused on only expression but not function.

In contrast to other studies describing OCT4 and NANOG expression in third-trimester AF-derived cells, our analysis revealed these markers to be negative for caesarean-derived AF-MSCs [27, 28, 41]. In our case, we identified singular cytoplasmic OCT4 positive-expressing cells at passages 1-2, but after a few more passaging, these cells were diluted out (data not shown). This variability could be due to the number of passages, different protocols, culture methods, and media used.

It was previously shown that a subpopulation of AFSCs from the first and second trimester expresses the pluripotency markers OCT4, NANOG, SOX2, c-MYC, and KLF4 [6, 7, 10] thus indicating that first and second-trimester AFSCs are multipotent and express pluripotency-associated markers. Although, Prusa et al. claimed OCT4 expression by 5 out of 11 independent AF-MSCs (no passage numbers stated) as indicated by real-time PCR. Additionally, they only showed a single cell of their AF preparations being positive for OCT4. Furthermore, the functionality of this OCT4 positivity was not addressed [6].

However, first-trimester c-Kit-positive AFSCs were converted to a pluripotent state by supplementation with valproic acid in pluripotency supporting media and matrix. [10]. While valproic acid could induce pluripotency, these cells were distinct from hESCs as evidenced by microarray analysis [9]. Additional results [7] further support our observation that developmental potential of AFSCs decreases with gestation time. Also shown in our current study, transcriptome cluster analysis revealed clear separation between AFSCs and hESCs [7]. Thus it can be concluded that subpopulations of early term AFSCs are more susceptible for reprogramming events but are not pluripotent.

In this study, we have demonstrated the expression of SSEA4, an early embryonic glycolipid antigen by immunofluorescent and flow cytometric analysis (Figures 3(a), A7 and 3(b), B1). This protein does not play a critical role in maintaining pluripotency and has also been shown to be expressed

in adult BM-MSCs [44, 45]. Furthermore, the cells were found to be c-Kit positive (Figure 3(a), A4), which is essential for the maintenance and differentiation of hematopoietic stem cells and multipotent progenitor cells [46]. It has been reported that c-Kit-expressing cells show a subpopulation of MSCs derived from adipose tissue that possess a higher telomerase expression and differentiation potential [47]. Moreover, a subpopulation of the AF-MSCs from C-sections also expresses TRA-1-60 and TRA-1-81 as shown by immunofluorescent-based stainings as well as flow cytometric analysis (Figures 3(a), A8 and A9 and 3(b), B2 and B3). This relates to already existing studies of midtrimester AF preparations [48].

Chemokines and their correspondent receptors are important for attraction and homing of leukocytes to infections, injury, or inflammation sites [49]. MSCs express these receptors, and thus it has been shown that chemokines and growth factors are chemotactic for bone marrow-derived MSCs [50]. Due to their immune modulatory properties, MSCs are widely used in clinical application in graft versus host disease [51]. In accordance with our secretome data (Figure 3) revealing the release of at least 9 distinct cytokines from AF-MSCs, Mirabella et al. analysed AFSC-conditioned media and identified the presence of known proangiogenic and antiangiogenic factors such as vascular endothelial growth factor (VEGF), CXCL12, IL-8, CCL2, two angiogenesis inhibitors interferon gamma (IFN γ), and CXCL10 and IP-10 as secreted proteins [13]. Besides angiogenesis, AFSCs also contribute to osteogenesis either directly or indirectly by secreting distinct cytokines [14].

The therapeutic potential of AF-MSCs and their secreted molecules in mice with acute hepatic failure has been analysed, and numerous proinflammatory mediators, regulating cytokines and growth factors in AF-MSC-conditioned media such as IL-10, IL-27, IL-17E, IL-12p70, IL-1 β , and IL-1ra, were observed. Some tissue repair promoting factors, namely, SERPINE1, MCP-1, and SDF-1, were also identified [52]. Our results agree with the previous comparison of cytokines released from MSCs originating from the bone marrow, cord blood, and placenta. The pool of cytokines previously investigated was the same as that of our work. MIF, IL-8, SERPINE1, GRO α , and IL-6 were secreted by MSCs from all the investigated sources. Placental MSCs expressed ICAM-1 (CD54), and MCP-1 (CCL2) and bone marrow MSCs secreted MCP-1 (CCL2), and SDF-1 (CXCL12) in addition [53]. Other studies that investigated a larger pool of cytokines showed additional expression of RANTES, INF γ , IL-1 α , TGF β , angiogenin, and oncostatin M [54]. The trophic factors released by AF-MSCs are and will be of great importance for future therapies.

Cluster dendrogram analysis clearly demonstrated that the transcriptomes of the two AF-MSC samples clustered together with the fMSC sample while the pluripotent iPSCs and ESCs (H1, H9) clustered in a separate group (Figure 5(a)). Both AF-MSC preparations acquired the expression profile of native foetal MSCs (Figures 5(b) and 5(d)). They were devoid of pluripotency-associated markers OCT4, NANOG, and SOX2 but express the MSC markers CD44, CD73, CD105, and *vimentin*.

Recent studies investigating the gene expression pattern of AFSCs at different passages by illumina microarray detected 1970 differentially expressed genes and classified the expression profile into 9 distinct clusters. Genes with gradually increasing expression and higher passages included *CXCL12*, *CDH6*, and *FOLR3*. On the other hand, the important downregulated genes were *CCND2*, *K8*, *IGF2*, *BNP-B*, and *CRABP1* [55]. The Venn diagram of the analysed data sets in the present study showed a group of genes which are exclusively expressed by the AF-MSCs samples (Figure 5(c)). From the heatmap of the 181 AF-MSCs-specific genes (Figure 6(a)) identified by transcriptome analysis, a group of potential AF-MSCs marker genes was extracted. This group contained *PSG5*, *C4orf26*, *C8orf4*, *EVR-3*, *EMX-2*, and *C15orf37* amongst others (Figure 6(b)), of which some such as *C8orf4* have not been characterized yet. Using these 181 genes, gene ontology analysis was conducted and most of the terms within the top 10 results of the biological processes were related to bone and skeletal development (Figure 6(c)). Global gene expression of AFSCs compared with AF-iPSCs and ESCs revealed genes related to self-renewal and pluripotency (1299 genes, e.g., *POU5F1*, *SOX2*, *NANOG*, and *microRNA-binding protein LIN28*) as well as AFSC-specific genes (665 genes, e.g., *OXTR*, *HHAT*, *RGS5*, *NF2*, *CD59*, *TNFSF10*, and *NT5E*) were identified in AFSCs [11]. The AF-MSCs-specific genes from our study were further investigated using the STRING tool which built up 4 different clusters (Figure 7): patterning and embryonic development-related HOX genes, immunity-related genes, ECM-related genes, and a WNT pathway and signalling-related gene set which is in line with the KEGG pathway analysis (Figure S3). Compared to the previous identified 665 AFSC-specific genes, we could show an overlap of 25 genes (Figure 6(e)) which include *HOXB7*, *APBB1IP*, *HOXB8*, *PTHLH*, and *ZPLD1* which were also present within the highest expressed genes within our samples (Figure 6(b)). These genes are mainly involved in skeletal development (Figure 6(e) and Table S1). This subset of genes represents putative marker genes for AF-MSCs selection procedures in the future.

5. Conclusion

In this study, we have demonstrated that a subpopulation of human AFSCs (AF-MSCs) isolated from AF collected during C-sections is indeed MSCs meeting the accepted criteria and definition [16]. In addition, we show that the transcriptomes of AF-MSCs are more similar to that of BM-MSCs (Pearson's correlation of 0.9) than to bona fide pluripotent stem cells (human embryonic stem cell lines H1 and H9 and a dermal fibroblast-derived iPSC line) even though they express well-known pluripotency-associated markers. We finally demonstrated their ability to secrete a plethora of cytokines and growth factors crucial for paracrine signalling. Overall, Caesarean section-derived amniotic fluid which in contrast to that obtained from amniocentesis is of no risk to the foetus and contain AF-MSCs with great potential for clinical applications.

Conflicts of Interest

The authors declare that there is no conflict of interest regarding the publication of this paper.

Authors' Contributions

Lucas-Sebastian Spitzhorn and Md Shaifur Rahman contributed equally to this work.

Acknowledgments

Professor Dr. James Adjaye and Professor Dr. Tanja Fehm acknowledge support from the Medical Faculty, Heinrich-Heine-Universität Düsseldorf. In addition, Professor Dr. James Adjaye acknowledges support from the German Academic Exchange Service (DAAD) (91607303).

References

- [1] M. C. Renda, E. Fecarotta, G. Schillaci et al., "Mesenchymal fetal stem cells (FMSC) from amniotic fluid (AF): expansion and phenotypic characterization," *Blood*, vol. 126, p. 4758, 2015.
- [2] P. de Coppi, G. Bartsch Jr., M. M. Siddiqui et al., "Isolation of amniotic stem cell lines with potential for therapy," *Nature Biotechnology*, vol. 25, no. 1, pp. 100–106, 2007.
- [3] I. Antonucci, R. Di Pietro, M. Alfonsi et al., "Human second trimester amniotic fluid cells are able to create embryoid body-like structures in vitro and to show typical expression profiles of embryonic and primordial germ cells," *Cell Transplantation*, vol. 23, no. 12, pp. 1501–1515, 2014.
- [4] G. Simoni and R. Colognato, "The amniotic fluid-derived cells: the biomedical challenge for the third millennium," *Journal of Prenatal Medicine*, vol. 3, no. 3, pp. 34–36, 2009.
- [5] F. Torricelli, L. Brizzi, P. A. Bernabei et al., "Identification of hematopoietic progenitor cells in human amniotic fluid before the 12th week of gestation," *Italian Journal of Anatomy and Embryology*, vol. 98, no. 2, pp. 119–126, 1993.
- [6] A. R. Prusa, E. Marton, M. Rosner, G. Bernaschek, and M. Hengstschläger, "Oct-4-expressing cells in human amniotic fluid: a new source for stem cell research?," *Human Reproduction*, vol. 18, no. 7, pp. 1489–1493, 2003.
- [7] D. Moschidou, K. Drews, A. Eddaoudi, J. Adjaye, P. de Coppi, and P. V. Guillot, "Molecular signature of human amniotic fluid stem cells during fetal development," *Current Stem Cell Research & Therapy*, vol. 8, no. 1, pp. 73–81, 2013.
- [8] C. Koike, K. Zhou, Y. Takeda et al., "Characterization of amniotic stem cells," *Cellular Reprogramming*, vol. 16, no. 4, pp. 298–305, 2014.
- [9] K. E. Hawkins, D. Moschidou, D. Faccenda et al., "Human amniocytes are receptive to chemically induced reprogramming to pluripotency," *Molecular Therapy*, vol. 25, no. 2, pp. 427–442, 2017.
- [10] D. Moschidou, S. Mukherjee, M. P. Blundell et al., "Valproic acid confers functional pluripotency to human amniotic fluid stem cells in a transgene-free approach," *Molecular Therapy*, vol. 20, no. 10, pp. 1953–1967, 2012.
- [11] K. Wolfrum, Y. Wang, A. Prigione, K. Sperling, H. Lehrach, and J. Adjaye, "The LARGE principle of cellular reprogramming: lost, acquired and retained gene expression in foreskin

- and amniotic fluid-derived human iPS cells," *PLoS One*, vol. 5, no. 10, article e13703, 2010.
- [12] M. Teodelinda, C. Michele, C. Sebastiano, C. Ranieri, and G. Chiara, "Amniotic liquid derived stem cells as reservoir of secreted angiogenic factors capable of stimulating neo-arteriogenesis in an ischemic model," *Biomaterials*, vol. 32, no. 15, pp. 3689–3699, 2011.
- [13] T. Mirabella, C. Gentili, A. Daga, and R. Cancedda, "Amniotic fluid stem cells in a bone microenvironment: driving host angiogenic response," *Stem Cell Research*, vol. 11, no. 1, pp. 540–551, 2013.
- [14] A. M. Ranzoni, M. Corcelli, K. L. Hau et al., "Counteracting bone fragility with human amniotic mesenchymal stem cells," *Scientific Reports*, vol. 6, no. 6, article 39656, 2016.
- [15] Q. Sun, F. Li, H. Li et al., "Amniotic fluid stem cells provide considerable advantages in epidermal regeneration: B7H4 creates a moderate inflammation microenvironment to promote wound repair," *Scientific Reports*, vol. 5, article 11560, 2015.
- [16] M. F. Pittenger, A. M. Mackay, S. C. Beck et al., "Multilineage potential of adult human mesenchymal stem cells," *Science*, vol. 284, no. 5411, pp. 143–147, 1999.
- [17] A. J. Friedenstein, I. I. Piatetzky-Shapiro, and K. V. Petrakova, "Osteogenesis in transplants of bone marrow cells," *Journal of Embryology and Experimental Morphology*, vol. 16, no. 3, pp. 381–390, 1966.
- [18] A. J. Friedenstein, U. F. Deriglasova, N. N. Kulagina et al., "Precursors for fibroblasts in different populations of hematopoietic cells as detected by the in vitro colony assay method," *Experimental Hematology*, vol. 2, pp. 83–92, 1974.
- [19] M. Mimeault and S. K. Batra, "Concise review: recent advances on the significance of stem cells in tissue regeneration and cancer therapies," *Stem Cells*, vol. 24, no. 11, pp. 2319–2345, 2006.
- [20] K. Bieback, S. Kern, H. Kluter, and H. Eichler, "Critical parameters for the isolation of mesenchymal stem cells from umbilical cord blood," *Stem Cells*, vol. 22, no. 4, pp. 625–634, 2004.
- [21] J. W. Kim, S. Y. Kim, S. Y. Park et al., "Mesenchymal progenitor cells in the human umbilical cord," *Annals of Hematology*, vol. 83, no. 12, pp. 733–738, 2004.
- [22] P. S. In 't Anker, S. A. Scherjon, C. Kleijburg-van der Keur et al., "Isolation of mesenchymal stem cells of fetal or maternal origin from human placenta," *Stem Cells*, vol. 22, no. 7, pp. 1338–1345, 2004.
- [23] M. S. Tsai, S. M. Hwang, K. D. Chen et al., "Functional network analysis of the transcriptomes of mesenchymal stem cells derived from amniotic fluid, amniotic membrane, cord blood, and bone marrow," *Stem Cells*, vol. 25, no. 10, pp. 2511–2523, 2007.
- [24] M. Dominici, K. Le Blanc, I. Mueller et al., "Minimal criteria for defining multipotent mesenchymal stromal cells. The International Society for Cellular Therapy position statement," *Cytotherapy*, vol. 8, no. 4, pp. 315–317, 2006.
- [25] A. Stolzing, E. Jones, D. McGonagle, and A. Scutt, "Age-related changes in human bone marrow-derived mesenchymal stem cells: consequences for cell therapies," *Mechanisms of Ageing and Development*, vol. 129, no. 3, pp. 163–173, 2008.
- [26] J. Savickiene, G. Treigyte, S. Baronaite et al., "Human amniotic fluid mesenchymal stem cells from second- and third-trimester amniocentesis: differentiation potential, molecular signature, and proteome analysis," *Stem Cells International*, vol. 2015, Article ID 319238, 15 pages, 2015.
- [27] Q. You, X. Tong, Y. Guan et al., "The biological characteristics of human third trimester amniotic fluid stem cells," *The Journal of International Medical Research*, vol. 37, no. 1, pp. 105–112, 2009.
- [28] M. S. Tsai, J. L. Lee, Y. J. Chang, and S. M. Hwang, "Isolation of human multipotent mesenchymal stem cells from second-trimester amniotic fluid using a novel two-stage culture protocol," *Human Reproduction*, vol. 19, no. 6, pp. 1450–1456, 2004.
- [29] Y. Babaie, R. Herwig, B. Greber et al., "Analysis of Oct4-dependent transcriptional networks regulating self-renewal and pluripotency in human embryonic stem cells," *Stem Cells*, vol. 25, no. 2, pp. 500–510, 2007.
- [30] R. C. Gentleman, V. J. Carey, D. M. Bates et al., "Bioconductor: open software development for computational biology and bioinformatics," *Genome Biology*, vol. 5, no. 10, article R80, 2004.
- [31] L. Gautier, L. Cope, B. M. Bolstad, and R. A. Irizarry, "affy—analysis of *Affymetrix GeneChip* data at the probe level," *Bioinformatics*, vol. 20, no. 3, pp. 307–315, 2004.
- [32] M. Kanehisa, M. Furumichi, M. Tanabe, Y. Sato, and K. Morishima, "KEGG: new perspectives on genomes, pathways, diseases and drugs," *Nucleic Acids Research*, vol. 45, no. D1, pp. D353–D361, 2017.
- [33] D. W. Huang, B. T. Sherman, and R. A. Lempicki, "Systematic and integrative analysis of large gene lists using DAVID bioinformatics resources," *Nature Protocols*, vol. 4, no. 1, pp. 44–57, 2009.
- [34] D. Szklarczyk, A. Franceschini, S. Wyder et al., "STRING v10: protein–protein interaction networks, integrated over the tree of life," *Nucleic Acids Research*, vol. 43, no. D1, Database issue, pp. D447–D452, 2015.
- [35] M. G. Mendez, S. Kojima, and R. D. Goldman, "Vimentin induces changes in cell shape, motility, and adhesion during the epithelial to mesenchymal transition," *FASEB Journal*, vol. 24, no. 6, pp. 1838–1851, 2010.
- [36] A. B. Balaji, K. Jamil, G. M. Ram, and G. S. Raju, "Pluripotent lineage of CD133 stem cells isolated from human skin samples," *Indian Journal of Experimental Biology*, vol. 51, no. 2, pp. 107–115, 2013.
- [37] T. Tondreau, N. Meuleman, A. Delforge et al., "Mesenchymal stem cells derived from CD133-positive cells in mobilized peripheral blood and cord blood: proliferation, Oct4 expression, and plasticity," *Stem Cells*, vol. 23, no. 8, pp. 1105–1112, 2005.
- [38] S. Kern, H. Eichler, J. Stoeve, H. Kluter, and K. Bieback, "Comparative analysis of mesenchymal stem cells from bone marrow, umbilical cord blood, or adipose tissue," *Stem Cells*, vol. 24, no. 5, pp. 1294–1301, 2006.
- [39] H. Hoehn, E. M. Bryant, L. E. Karp, and G. M. Martin, "Cultivated cells from diagnostic amniocentesis in second trimester pregnancies. I. Clonal morphology and growth potential," *Pediatric Research*, vol. 8, no. 8, pp. 746–754, 1974.
- [40] H. Hoehn and D. Salk, "Chapter 2. Morphological and biochemical heterogeneity of amniotic fluid cells in culture," *Methods in Cell Biology*, vol. 26, pp. 11–34, 1982.
- [41] A. A. Hamid, M. K. Joharry, H. Mun-Fun et al., "Highly potent stem cells from full-term amniotic fluid: a realistic perspective," *Reproductive Biology*, vol. 17, no. 1, pp. 9–18, 2017.
- [42] J. S. Park, M. S. Shim, S. H. Shim et al., "Chondrogenic potential of stem cells derived from amniotic fluid, adipose tissue, or

- bone marrow encapsulated in fibrin gels containing TGF- β 3," *Biomaterials*, vol. 32, no. 32, pp. 8139–8149, 2011.
- [43] K. M. Dupont, K. Sharma, H. Y. Stevens, J. D. Boerckel, A. J. García, and R. E. Gulberg, "Human stem cell delivery for treatment of large segmental bone defects," *Proceedings of the National Academy of Sciences of the United States of America*, vol. 107, no. 8, pp. 3305–3310, 2010.
- [44] S. N. Brimble, E. S. Sherrer, E. W. Uhl et al., "The cell surface glycosphingolipids SSEA-3 and SSEA-4 are not essential for human ESC pluripotency," *Stem Cells*, vol. 25, no. 1, pp. 54–62, 2007.
- [45] E. J. Gang, D. Bosnakovski, C. A. Figueiredo, J. W. Visser, and R. C. Perlingeiro, "SSEA-4 identifies mesenchymal stem cells from bone marrow," *Blood*, vol. 109, no. 4, pp. 1743–1751, 2007.
- [46] J. Zayas, D. S. Spassov, R. G. Nachtman, and R. Jurecic, "Murine hematopoietic stem cells and multipotent progenitors express truncated intracellular form of c-kit receptor," *Stem Cells and Development*, vol. 17, no. 2, pp. 343–353, 2008.
- [47] A. Blazquez-Martinez, M. Chiesa, F. Arnalich, J. Fernandez-Delgado, M. Nistal, and M. P. de Miguel, "c-Kit identifies a subpopulation of mesenchymal stem cells in adipose tissue with higher telomerase expression and differentiation potential," *Differentiation*, vol. 87, no. 3-4, pp. 147–160, 2014.
- [48] D. Moschidou, S. Mukherjee, M. P. Blundell et al., "Human mid-trimester amniotic fluid stem cells cultured under embryonic stem cell conditions with valproic acid acquire pluripotent characteristics," *Stem Cells and Development*, vol. 22, no. 3, pp. 444–458, 2013.
- [49] M. Miyasaka and T. Tanaka, "Lymphocyte trafficking across high endothelial venules: dogmas and enigmas," *Nature Reviews Immunology*, vol. 4, no. 5, pp. 360–370, 2004.
- [50] J. F. Ji, B. P. He, S. T. Dheen, and S. S. Tay, "Interactions of chemokines and chemokine receptors mediate the migration of mesenchymal stem cells to the impaired site in the brain after hypoglossal nerve injury," *Stem Cells*, vol. 22, no. 3, pp. 415–427, 2004.
- [51] C. Balbi, M. Piccoli, L. Barile et al., "First characterization of human amniotic fluid stem cell extracellular vesicles as a powerful paracrine tool endowed with regenerative potential," *Stem Cells Translational Medicine*, vol. 6, no. 5, pp. 1340–1355, 2017.
- [52] D. S. Zagoura, M. G. Roubelakis, V. Bitsika et al., "Therapeutic potential of a distinct population of human amniotic fluid mesenchymal stem cells and their secreted molecules in mice with acute hepatic failure," *Gut*, vol. 61, no. 6, pp. 894–906, 2012.
- [53] J. H. Hwang, S. S. Shim, O. S. Seok et al., "Comparison of cytokine expression in mesenchymal stem cells from human placenta, cord blood, and bone marrow," *Journal of Korean Medical Science*, vol. 24, no. 4, pp. 547–554, 2009.
- [54] J. A. Potian, H. Aviv, N. M. Ponzio, J. S. Harrison, and P. Rameshwar, "Veto-like activity of mesenchymal stem cells: functional discrimination between cellular responses to alloantigens and recall antigens," *Journal of Immunology*, vol. 171, no. 7, pp. 426–434, 2003.
- [55] Y. W. Kim, H. J. Kim, S. M. Bae et al., "Time-course transcriptional profiling of human amniotic fluid-derived stem cells using microarray," *Cancer Research and Treatment*, vol. 42, no. 2, pp. 82–94, 2010.

2.2 The presence of human mesenchymal stem cells of renal origin in amniotic fluid increases with gestational time

Md Shaifur Rahman*, Lucas-Sebastian Spitzhorn*, Wasco Wruck, Carsten Hagenbeck, Percy Balan, Nina Graffmann, Martina Bohndorf, Audrey Ncube, Pascale V. Guillot, Tanja Fehm and James Adjaye

*These authors contributed equally to this work.

Abstract

Background: Established therapies for managing kidney dysfunction such as kidney dialysis and transplantation are limited due to the shortage of compatible donated organs and high costs. Stem cell-based therapies are currently under investigation as an alternative treatment option. As amniotic fluid is composed of fetal urine harboring mesenchymal stem cells (AF-MSCs), we hypothesized that third-trimester amniotic fluid could be a novel source of renal progenitor and differentiated cells.

METHODS: Human third-trimester amniotic fluid cells (AFCs) were isolated and cultured in distinct media. These cells were characterized as renal progenitor cells with respect to cell morphology, cell surface marker expression, transcriptome and differentiation into chondrocytes, osteoblasts and adipocytes. To test for renal function, a comparative albumin endocytosis assay was performed using AF-MSCs and commercially available renal cells derived from kidney biopsies. Comparative transcriptome analyses of first, second and third trimester-derived AF-MSCs were conducted to monitor expression of renal-related genes.

RESULTS: Regardless of the media used, AFCs showed expression of pluripotency-associated markers such as SSEA4, TRA-1-60, TRA-1-81 and C-Kit. They also express the mesenchymal marker Vimentin. Immunophenotyping confirmed that third-trimester AFCs are bona fide MSCs. AF-MSCs expressed the master renal progenitor markers SIX2 and CITED1, in addition to typical renal proteins such as PODXL, LHX1, BRN1 and PAX8. Albumin endocytosis assays demonstrated the functionality of AF-MSCs as renal cells. Additionally, upregulated expression of BMP7 and downregulation of WT1, CD133, SIX2 and C-Kit were observed upon activation of WNT signaling by treatment with the GSK-3 inhibitor CHIR99201. Transcriptome analysis and semiquantitative PCR

revealed increasing expression levels of renal-specific genes (e.g., SALL1, HNF4B, SIX2) with gestational time. Moreover, AF-MSCs shared more genes with human kidney cells than with native MSCs and gene ontology terms revealed involvement of biological processes associated with kidney morphogenesis.

CONCLUSIONS: Third-trimester amniotic fluid contains AF-MSCs of renal origin and this novel source of kidney progenitors may have enormous future potentials for disease modeling, renal repair and drug screening.

Publication Status: published in *Stem Cell Research & Therapy*. 2018 Apr 25;9(1):113.

Impact Factor: 4.963

This article is reproduced with permission.

Approximated total share of contribution: 40%

Contribution on experimental design, realization and publication:

JA, TF, MSR, LSS conceived the idea and designed the experiments. CH and PB collected the third trimester amniotic fluid samples. PG collected first and second trimester amniotic fluid samples and prepared the corresponding RNA. MB performed immunofluorescence stainings of the hREPCs and designed the renal specific primers. NG performed the real time PCR analysis. WW did the bioinformatic analysis. AN performed the analysis of the CHIR99021 treated AF-MSCs and hREPCs. MSR and LSS isolated the AFCs from third trimester AF and characterized the AFCs/AF-MSCs. MSR and LSS wrote the manuscript and JA edited it. All authors have read and approved the manuscript.

Link to the publication:

<https://stemcellres.biomedcentral.com/articles/10.1186/s13287-018-0864-7>

RESEARCH

Open Access



The presence of human mesenchymal stem cells of renal origin in amniotic fluid increases with gestational time

Md Shaifur Rahman^{1†}, Lucas-Sebastian Spitzhorn^{1†}, Wasco Wruck¹, Carsten Hagenbeck², Percy Balan², Nina Graffmann¹, Martina Bohndorf¹, Audrey Ncube¹, Pascale V. Guillot³, Tanja Fehm² and James Adjaye^{1*}

Abstract

Background: Established therapies for managing kidney dysfunction such as kidney dialysis and transplantation are limited due to the shortage of compatible donated organs and high costs. Stem cell-based therapies are currently under investigation as an alternative treatment option. As amniotic fluid is composed of fetal urine harboring mesenchymal stem cells (AF-MSCs), we hypothesized that third-trimester amniotic fluid could be a novel source of renal progenitor and differentiated cells.

Methods: Human third-trimester amniotic fluid cells (AFCs) were isolated and cultured in distinct media. These cells were characterized as renal progenitor cells with respect to cell morphology, cell surface marker expression, transcriptome and differentiation into chondrocytes, osteoblasts and adipocytes. To test for renal function, a comparative albumin endocytosis assay was performed using AF-MSCs and commercially available renal cells derived from kidney biopsies. Comparative transcriptome analyses of first, second and third trimester-derived AF-MSCs were conducted to monitor expression of renal-related genes.

Results: Regardless of the media used, AFCs showed expression of pluripotency-associated markers such as SSEA4, TRA-1-60, TRA-1-81 and C-Kit. They also express the mesenchymal marker Vimentin. Immunophenotyping confirmed that third-trimester AFCs are bona fide MSCs. AF-MSCs expressed the master renal progenitor markers SIX2 and CITED1, in addition to typical renal proteins such as PODXL, LHX1, BRN1 and PAX8. Albumin endocytosis assays demonstrated the functionality of AF-MSCs as renal cells. Additionally, upregulated expression of *BMP7* and downregulation of *WT1*, *CD133*, *SIX2* and C-Kit were observed upon activation of WNT signaling by treatment with the GSK-3 inhibitor CHIR99201. Transcriptome analysis and semiquantitative PCR revealed increasing expression levels of renal-specific genes (e.g., *SALL1*, *HNF4B*, *SIX2*) with gestational time. Moreover, AF-MSCs shared more genes with human kidney cells than with native MSCs and gene ontology terms revealed involvement of biological processes associated with kidney morphogenesis.

Conclusions: Third-trimester amniotic fluid contains AF-MSCs of renal origin and this novel source of kidney progenitors may have enormous future potentials for disease modeling, renal repair and drug screening.

Keywords: Amniotic fluid, Kidney, Renal progenitor cells, SIX2, Mesenchymal stem cells, Albumin endocytosis, Third trimester

* Correspondence: james.adjaye@med.uni-duesseldorf.de

[†]Equal contributors

¹Institute for Stem Cell Research and Regenerative Medicine, Medical Faculty, Heinrich Heine University, Moorenstraße 5, 40225 Düsseldorf, Germany
Full list of author information is available at the end of the article



© The Author(s). 2018 **Open Access** This article is distributed under the terms of the Creative Commons Attribution 4.0 International License (<http://creativecommons.org/licenses/by/4.0/>), which permits unrestricted use, distribution, and reproduction in any medium, provided you give appropriate credit to the original author(s) and the source, provide a link to the Creative Commons license, and indicate if changes were made. The Creative Commons Public Domain Dedication waiver (<http://creativecommons.org/publicdomain/zero/1.0/>) applies to the data made available in this article, unless otherwise stated.

Background

A functional kidney is essential for healthy living due to its major role in toxin and drug filtration. Globally, each year millions of patients require rapid kidney transplantation or dialysis to restore renal function [1, 2]. But the shortage of compatible organs, donor-associated diseases, ageing-associated factors and high cost of transplantation/dialysis are major hurdles [3]. Kidney-associated dysfunctions are now a prioritized health concern and research area. A potential alternative source of renal cells are those derived from embryonic and induced pluripotent stem cells (ESCs and iPSCs) [4–9]. Clinical applications of pluripotent stem cell technologies are constrained by the risk of tumor formation, immunological rejection, legal as well as ethical concerns. In light of this, it is therefore important to find other sources of stem cells which are not tumorigenic, bear a broad differentiation potential and have a high renal regenerative potential.

The architecture and organization of the kidney is very complex and consists of numerous cell types [10] which can interchange identities by a very complex reciprocal interplay and interactions of stromal and epithelial cell lineages [9, 11]. Kidney mesenchymal cells have been demonstrated to express SIX2 and Cbp/p300-interacting transactivator 1 (*CITED1*) which are crucial for the self-renewing capability [11, 12]. Furthermore, the main kidney nephron-regulatory genes have been described, such as *SALL1*, *PAX2*, *WT1*, Cytokeratin 19 (*CK19*), *CD133*, Podocalyxin-like protein 1 (*PODXL*), *HOXD11*, *HNF1B*, *BRN1*, *Lhx1* and *Pax8* [13–18]. Adult and fetal bone marrow-derived mesenchymal stem cells (BM-MSCs) have been shown to be capable of repairing renal function deficits [19, 20]. BM-MSCs have potent immunosuppressive properties and their potential application in acute kidney injury animal models has been studied recently [21]. However, the use of adult BM-MSCs has some limitations such as the low number of MSCs in adult bone marrow, expression of ageing-associated factors, slow expansion rate, early senescence, inactive telomerase, shorter telomeres and restricted differentiation potential [22]. Due to the increasing number of patients with kidney diseases and limited cell-based therapeutic options, alternative renal progenitor cells and sources are clearly in need [23]. Amniotic fluid contains fetal-derived differentiated and undifferentiated progenitor cells. In vitro, they can be expanded in distinct media formulations and exhibit a heterogeneous morphology with a preponderance of epithelioid and fibroblastoid mesenchymal-like cell shape [24]. In 2007, Perin et al. [25] demonstrated the potency of second-trimester amniotic fluid-derived MSCs (AF-MSCs) to form embryonic kidney structures in vitro. Later, they also showed that human AF-MSCs help in regenerating kidneys

undergoing acute tubular necrosis in a rodent model [26–28]. In an animal model of acute renal injury, Camussi's research group confirmed these results and could show comparable efficacy between BM-MSCs and AF-MSCs [29]. Remarkably, the renal differentiation potential of AF-MSCs was demonstrated by producing chimeric organotypic renal structures from murine embryonic kidney cells and human AF-MSCs [30]. Although properties of human amniotic fluid cells such as the lack of immunogenicity and tumorigenicity, their anti-inflammatory properties and their high proliferative and differentiation potential are well described [31, 32], the exact origin of AF-MSCs is still unknown and controversial [33]. Before use in clinical applications, it is mandatory to elucidate the origin of AF-MSCs. Due to the fact that term amniotic fluid consists mostly of fetal urine [34], we hypothesized that AF-MSCs originate from the kidney and accumulate in the AF during fetal nephrogenesis.

Adult and neonatal human urine has been described as a source of kidney progenitor cells [35, 36]. Second-trimester AFCs have been described as an alternative source of podocytes [37] which express mesenchymal markers as well as the podocyte markers *CD2AP* and *NPHS2* [25, 38]. In this study we isolated third-trimester human AF-MSCs and cultured them in distinct supporting media. AF-MSCs were characterized as a multipotent population of renal cells. By combining cellular, molecular, functional and transcriptome data, we conclude that third-trimester amniotic fluid harbors MSCs originating from the fetal kidney. These cells should be considered promising sources for studies on kidney development, nephrotoxicity tests, disease modeling, drug screening and future kidney-related cellular therapies.

Methods

Isolation and culture of human amniotic fluidic cells

Healthy donors who provided the first and second-trimester amniotic fluid in this study provided written informed consent in accordance with the Declaration of Helsinki. Ethical approval was given by the Research Ethics Committees of Hammersmith & Queen Charlotte's Hospitals (2001/6234) in compliance with UK national guidelines (Review of the Guidance on the Research Use of Fetuses and Fetal Material (1989), also known as the Polkinghorne Guidelines, Her Majesty's Stationery Office, London, 1989: Cm762) for the collection of fetal tissue for research. Third-trimester amniotic fluid samples from healthy donors were collected from the Department of Obstetrics and Gynaecology, Medical Faculty, Heinrich Heine University Düsseldorf, Germany, with informed patient consent as well as institutional ethical approval. Amniotic fluids were processed and AF-MSCs were isolated as described previously [32]. In

brief, the cells were cultured in Prime XV or Chang C Medium (both Irvine Scientific, CA, USA), α MEM (Minimum Essential Medium Eagle Alpha Modification; Sigma) containing 10% FBS, 1% GlutaMAX and 1% penicillin/streptomycin (Penstrep), MG30 (Cell Lines Service, Germany) or renal cell medium (RCM) consisting of high-glucose Dulbecco's Modified Eagle's Medium (DMEM) supplemented with 1% Penstrep, 1% glutamine, 10% FBS and SingleQuot Kit CC-4127 REGM at 37 °C, 5% CO₂ and 5% O₂ (Lonza) [39, 40].

After the appearance of initially attached cells (days 4–7), the medium was changed and cells grew until reaching almost full confluency. The cells were then detached using TrypLE Express (Thermo Fisher Scientific) and prepared for further passaging and experiments. Urine-derived kidney progenitor cells and corresponding iPSCs (UM51, ISRM-UM51 [40]) and human renal epithelial cells from a biopsy (HREpCs; PromoCell, Heidelberg, Germany) were used as control cells.

Immunofluorescence staining

To analyze the cells for pluripotency, mesenchymal stem cell and renal cell specific markers, AF-MSCs were cultured in 12-well plates. After a washing step using PBS (Gibco), 4% paraformaldehyde (PFA; Polysciences Inc., PA, USA) was used to fix the cells for 15 min at room temperature (RT). To increase the cell membranes' permeability, 1% Triton X-100 (Carl Roth GmbH & Co. KG, Karlsruhe, Germany) was applied to the fixed cells for 5 min followed by blocking of unspecific binding sites for 2 h. For staining of intracellular proteins, this blocking buffer contained 10% normal goat serum (NGS; Sigma), 0.5% Triton X-100, 1% BSA (Sigma) and 0.05% Tween 20 (Sigma), all dissolved in PBS. Triton and Tween were omitted when extracellular proteins were stained. Afterward, the primary antibodies (presented in Additional file 1: Table S1) were diluted in blocking buffer/PBS and incubated with the cells for 1 h at RT followed by several washing steps using 0.05% Tween 20 in PBS. The corresponding secondary Cy3-labeled or Alexa Fluor 488-labeled antibodies (Thermo Fisher Scientific) and Hoechst 33,258 dye (Sigma-Aldrich Chemie GmbH, Taufkirchen, Germany) or DAPI (Southern Biotech) were added under light exclusion. For the actin filament staining, the toxin phalloidin 488 (A12370; Life Technologies) was used in a dilution of 1:200. A fluorescence microscope (LSM700; Zeiss, Oberkochen, Germany) was used for taking the pictures. All pictures were processed with the ZenBlue 2012 Software Version 1.1.2.0. (Carl Zeiss Microscopy GmbH, Jena, Germany).

In-vitro differentiation assay

In-vitro differentiation of the AF-MSCs into adipocytes, chondrocytes and osteoblasts was done employing the

StemPro Adipogenesis, Chondrogenesis, and Osteogenesis differentiation Kits (Gibco, Life Technologies, CA, USA). Media were replaced 2–3 times per week for 3 weeks, and the formation of intracellular lipid droplets (adipocytes), calcium mineralization (osteoblasts) and cellular aggregation toward clusters (chondrocytes) was observed from 14 to 21 days. After the differentiation process, fixation of the cells was done using 4% PFA for 30 min at RT. Subsequently, the cells were stained with Oil Red O for adipocytes, Alcian Blue for chondrocytes, and Alizarin Red S for osteoblasts as described previously [32]. A light microscope was used for imaging.

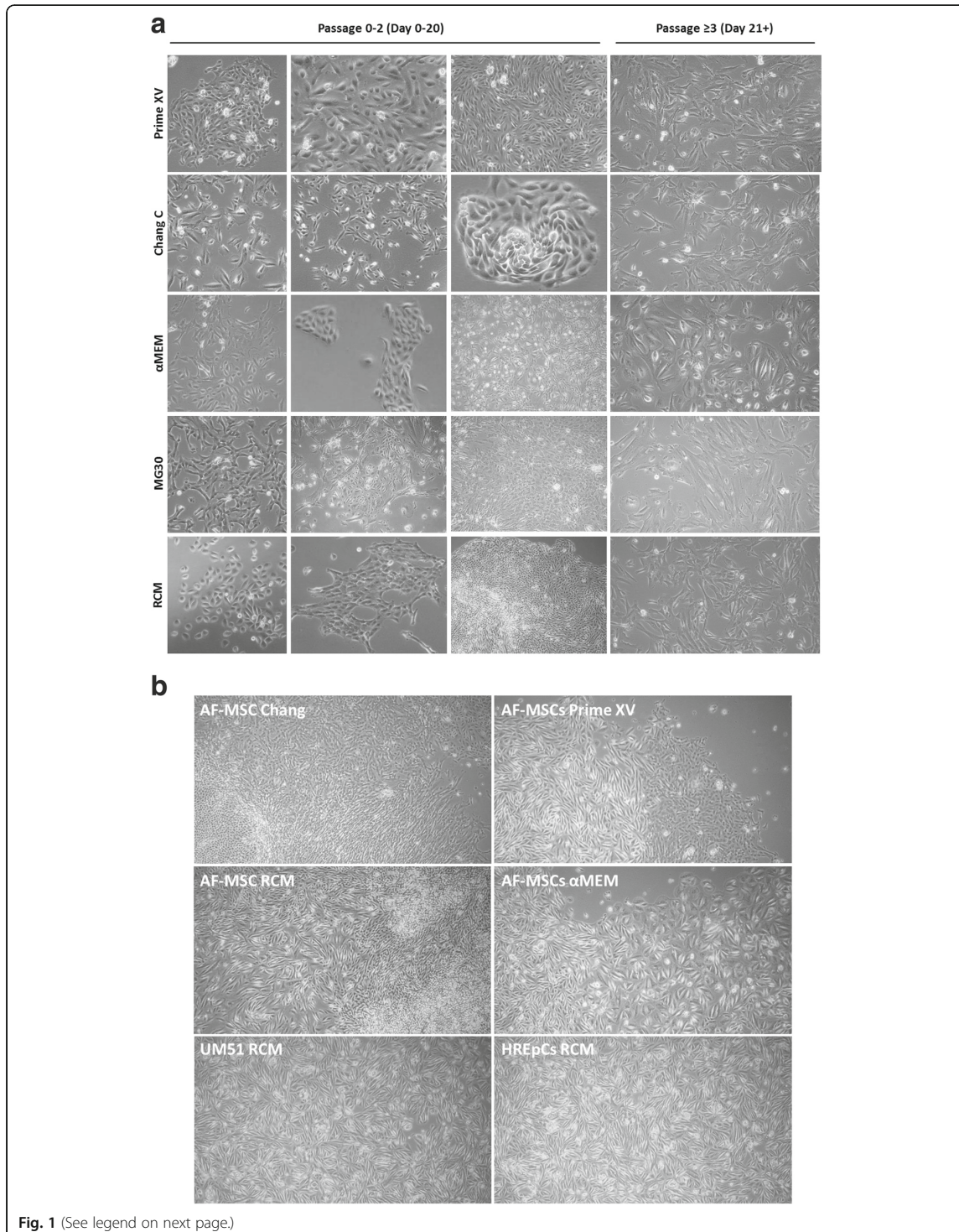
Flow cytometric analysis

The human MSC phenotyping kit (Miltenyi Biotec GmbH, Bergisch Gladbach, Germany) was used to analyze the cell surface marker composition of the AF-MSC samples (2×10^5 cells were used for each analysis), according to the manufacturer's instructions. The cells were washed with PBS and centrifuged at $300 \times g$ for 5 min. After resuspending the pellet in 100 μ l PBS, 0.5 μ l of the MSC phenotyping cocktail or of the isotype control cocktail were added and the tubes were mixed thoroughly. The MSC phenotyping cocktail is composed of a mixture of fluorochrome-coupled antibodies against various cell surface proteins (CD14-PerCP, CD20-PerCP, CD34-PerCP, CD45-PerCP, CD73-APC, CD90-FITC and CD105-PE). The isotype phenotyping cocktail served as a negative control. The antibody binding took place at 4 °C for 10 min in the dark. Nonbound antibodies were washed out using 1 ml PBS. After centrifugation at $300 \times g$ for 5 min, cell fixation using 4% PFA was done.

To analyze the AF-MSCs for pluripotency-associated cell surface markers (TRA-1-60, TRA-1-81, stage-specific embryonic antigen 4 (SSEA4)), corresponding prelabeled antibodies (anti-TRA-1-60-PE, human (clone REA157), number 130-100-347; anti-TRA-1-81-PE, human (clone REA246), number 130-101-410, and anti-SSEA-4-PE, human (clone REA101), number 130-098-369; Miltenyi Biotec GmbH, Bergisch Gladbach, Germany) were used. The staining procedure was carried out as already described. Until analysis via BD FACSCanto (BD Biosciences, Heidelberg, Germany) and CyAn ADP (Beckman Coulter, CA, USA), stained cells were kept at 4 °C in the dark. The FCSalyzer software version 0.9.3 and Summit 4.3 software were used for data analysis.

RNA isolation and quantitative PCR

After single washing with PBS, TRIzol (Thermo Fisher) was added to the cells for 5 min at RT, and the cells were scraped off and stored at -80 °C. For isolation of the RNA, the Direct-zol RNA Miniprep Kit (Zymo Research, CA, USA) was used according to the manufacturer's instructions. All of the primers used were



(See figure on previous page.)

Fig. 1 Initially attached heterogeneous AFCs display homogeneous cell morphology upon passaging and include typical kidney cell morphologies. Phenotypical complexity of AFCs observed, regardless of culture media composition within first two passages. Upon further passaging, cells became homogeneous with fibroblast-like morphology (a). During culture, subpopulation of cells observed which had similar morphology to distinct renal-originated progenitor cells UM51 and HREpCs (b). AF-MSC amniotic fluid mesenchymal stem cell, HREpC human renal epithelial cell, α MEM minimum essential medium alpha modification, RCM renal cell medium

purchased from MWG (primer sequences and predicted sizes of amplicons presented in Additional file 1: Table S2). After checking the quality of mRNA, complementary DNA (cDNA) was synthesized with the TaqMan Reverse Transcription Kit (Applied Biosystems). A sample of 500 ng of RNA was used for cDNA synthesis. The prepared mix of 20 μ l per sample consisted of 7.70 μ l H₂O, 2 μ l reverse transcriptase buffer, 4.4 μ l MgCl₂ (25 mM), 1 μ l Oligo (dT)/random hexamer (50 μ M), 4 μ l dNTP mix (10 mM), 0.4 μ l RNase inhibitor (20 U/ μ l) and 0.5 μ l reverse transcriptase (50 U/ μ l). For semi-qPCR, a mixture of 25 μ l per sample contained the following: 11.375 μ l H₂O, 5 μ l of 1 \times Go-Taq G2 Hot Start Green PCR buffer, 4 μ l of 4 mM MgCl₂, 0.5 μ l dNTP-Mix (10 mM each), 1 μ l forward primer (0.3 μ M), 1 μ l reverse primer (0.3 μ M), 0.125 μ l (0.625 U) Hotstart Taq polymerase (5 U/ μ l) and 2 μ l cDNA. A PCR thermal cycler (PEQLAB, Erlangen Germany) was employed. After an initial denaturation step at 95 °C for 2 min, 30 cycles followed with a denaturation step at 95 °C for 30 s, an annealing step at the temperature specific for each primer (ranging from 55 to 63 °C) for 30–35 s and an extension step at 72 °C for 30–40 s. Detection of semi-qPCR amplification products was performed by size fractionation on 2% agarose gel electrophoresis. Real-time quantitative PCR was performed in technical triplicates with Power SYBR Green Master Mix (Life Technologies) on a VIIA7 (Life Technologies) machine. Mean values were normalized to levels of the house-keeping gene ribosomal protein L37A. Results are depicted as mean values (% of untreated control) with 95% confidence interval.

Albumin endocytosis assay

To analyze the functional ability of the AF-MSCs to endocytose exogenous albumin, cells were plated at a density of 30% in 12-well plates without coating. After 2 days, media were supplemented with 10 μ M CHIR dissolved in DMSO or the same volume of DMSO alone and the cells were allowed to differentiate for 2 days. After this time period the cells were washed once with PBS and incubated in new medium supplemented with 20 μ g/ml of albumin from bovine serum (BSA), Alexa Fluor™ 488 conjugate (catalog no. A13100; Thermo Fischer) for 1 h. As endocytosis is an energy-dependent process, incubations were performed at 37 °C. After 1 h of incubation, however, cells were washed three times

with ice-cold PBS and fixed with 4% PFA for 15 min. Cell-associated fluorescence was analyzed using an excitation wavelength of 488 nm and an emission wavelength of 540 nm and imaged using a fluorescence microscope (LSM700; Zeiss, Oberkochen, Germany). All pictures were analyzed with ZenBlue 2012 Software Version 1.1.2.0. (Carl Zeiss Microscopy GmbH, Jena, Germany). Human fetal foreskin cell line HFF1 (SCRC-1041; ATCC) and fMSCs (kindly gifted from Prof. Richard O. C. Oreffo, Southampton, UK) served as control.

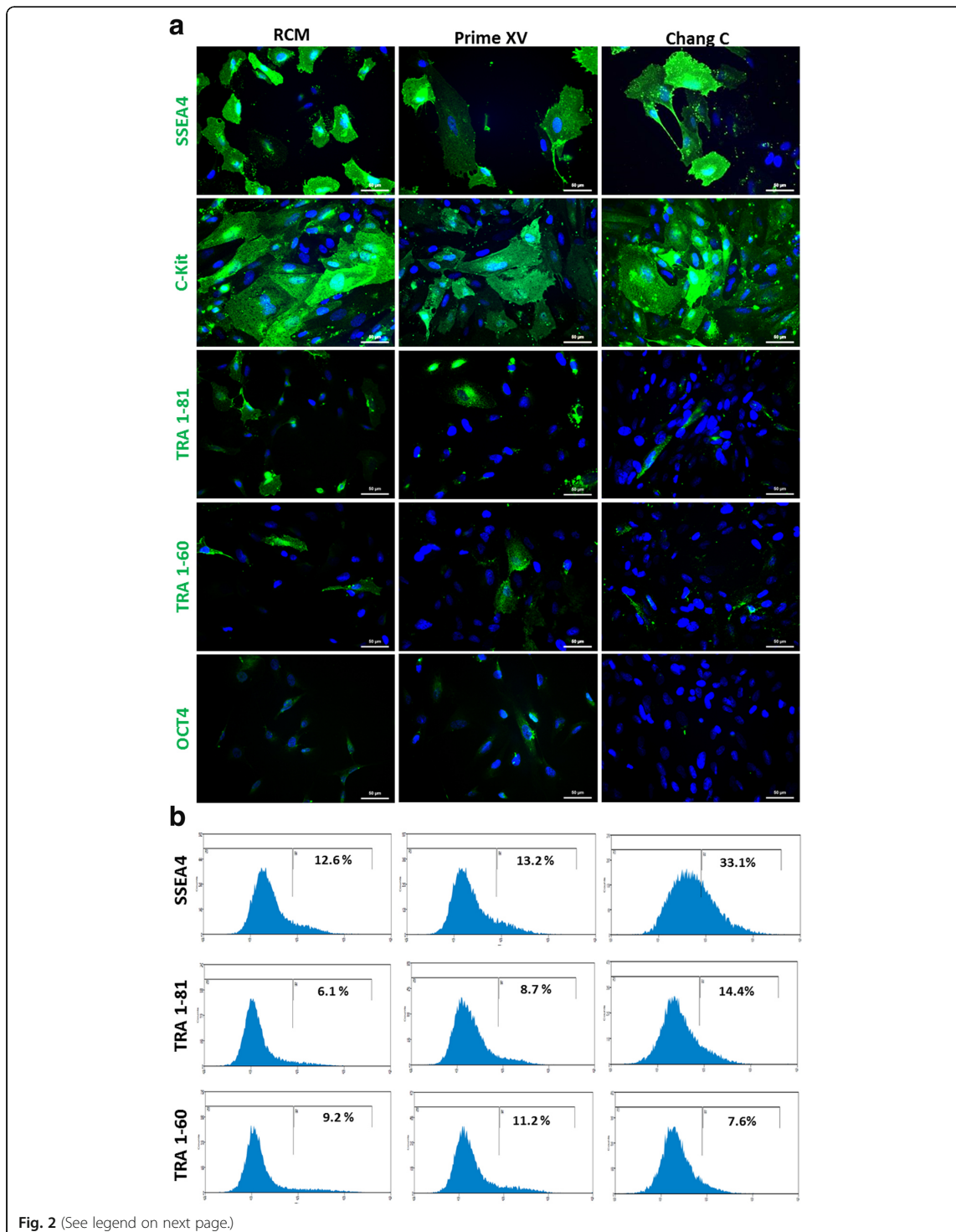
Transcriptome analysis

PrimeView Human Gene Expression Array Chips (Affymetrix; Thermo Fisher Scientific) were used for microarray experiments (conducted by Biologisch-Medizinisches Forschungszentrum, Düsseldorf, Germany). The gene expression profile for AF-MSCs, HREpCs, fMSCs, UM51 and ISRM-UM51 are provided online at the National Center of Biotechnology Information Gene Expression Omnibus. The affy package of the R/Bioconductor environment [41, 42] was used for further processing of the unnormalized bead summary data. After background correction, the data were transformed to a logarithmic scale (to base 2), and normalized by employing the robust multiarray average method. The heatmap.2 function from the gplots package (<http://CRAN.R-project.org/package=gplots>) was employed to create cluster analysis and heatmaps. The correlation coefficients were calculated with Pearson correlation as a similarity measure (<http://CRAN.R-project.org/package=gplots>). Based on the results of the transcriptome analysis, the DAVID tool (<https://david.ncifcrf.gov/>) [43] was used to generate gene ontology terms and associated KEGG pathways [44] for the distinct gene sets.

Results

AFCs become homogeneous after several passages and contain a renal cell-like subpopulation

In-vitro growth of AFCs in monolayers preserves diversity of cell types irrespective of media, in particular within the first two passages. AFCs were isolated and expanded in various media (RCM, Prime XV, Chang C, MG30, α MEM) under hypoxic conditions. Bright-field microscopic observation revealed a mixture of distinct cell types with a morphology of mesenchymal-like, epithelioid, spindle, cobble-stone and tubular shapes, of fetal-derived differentiated and undifferentiated progenitor cells (Fig. 1a). After



(See figure on previous page.)

Fig. 2 Pluripotency-associated stem cell marker expression of AFCs in distinct media. Immunofluorescent-based staining showed similar stem cell-related protein expression in all three media conditions (RCM, Prime XV, Chang C). AFCs express SSEA4, C-Kit, TRA-1-60 and TRA-1-81. Cell nuclei stained using Hoechst (a). Flow cytometric analysis confirmed cell surface expression of SSEA4, TRA-1-60 and TRA-1-81 (b). RCM renal cell medium

passaging 3–4 times, the cells became more homogeneous with fibroblastic mesenchymal-like morphologies in all media except α MEM and MG30. In α MEM and MG30, cells attained an oval/egg-shaped morphology and had significantly decreased growth rates (Fig. 1a). Based on morphology, renal progenitor, undifferentiated and differentiated cell types were observed as subpopulations. The commercially available human kidney cell line HREpC as well as urine-derived renal cells (UM51) served as controls (Fig. 1b).

AFCs express pluripotency-associated proteins

To analyze the presence of pluripotent stem cell-associated markers in AFCs, both immunofluorescence staining and flow cytometry were performed. The AFC populations cultured in RCM, Prime XV and Chang C media were found to express SSEA4, C-Kit, TRA-1-60 and TRA-1-81. Expression of cytoplasmic and no nuclear octamer-binding transcription factor 4 (OCT4) was observed at early passages in RCM and Prime XV (Fig. 2a). However, the percentages of cells positive for the investigated markers (SSEA4, C-Kit, TRA-1-60 and TRA-1-81) were consistent with the flow cytometric data. Approximately 13% of the RCM cultured cells were positive for SSEA4, 9% for TRA-1-60 and 6% for TRA-1-81. AFCs cultured in Prime XV showed positivity rates of 13.2% for SSEA4, 8.7% for TRA-1-60 and 11.2% for TRA-1-81. Previously performed flow cytometric analysis for cells cultured in Chang C media revealed 33.1% SSEA4, 14.4% TRA-1-60 and 7.6% TRA-1-81 positive cells [32] (Fig. 2b).

AFCs express proteins related to MSCs as well as CK19 and show multilineage differentiation potential in vitro

AFCs cultured in all three media compositions (RCM, Prime XV and Chang C) expressed the typical mesenchymal marker Vimentin and not E-Cadherin. Additionally, subpopulations of the cells were positive for CK19, a marker for renal epithelial cells. The expression of CD133/Prominin-1, as a marker for multipotent progenitor cells, was also observed in all conditions. HREpCs, derived from kidney biopsies, were used as renal reference cells and also showed positivity for Vimentin, CD133 and CK19 (Fig. 3a). To analyze the typical MSC surface marker expression in AFCs, flow cytometric analysis was conducted. The presence of CD73, CD90 and CD105 could be identified in all cases; interestingly, cells in RCM had the highest level of

expression. However, all cell preparations were devoid of the hematopoietic markers CD14, CD20, CD34 and CD45 (Fig. 3b, [32]). These features establish and confirm these cells as bona fide AF-MSCs.

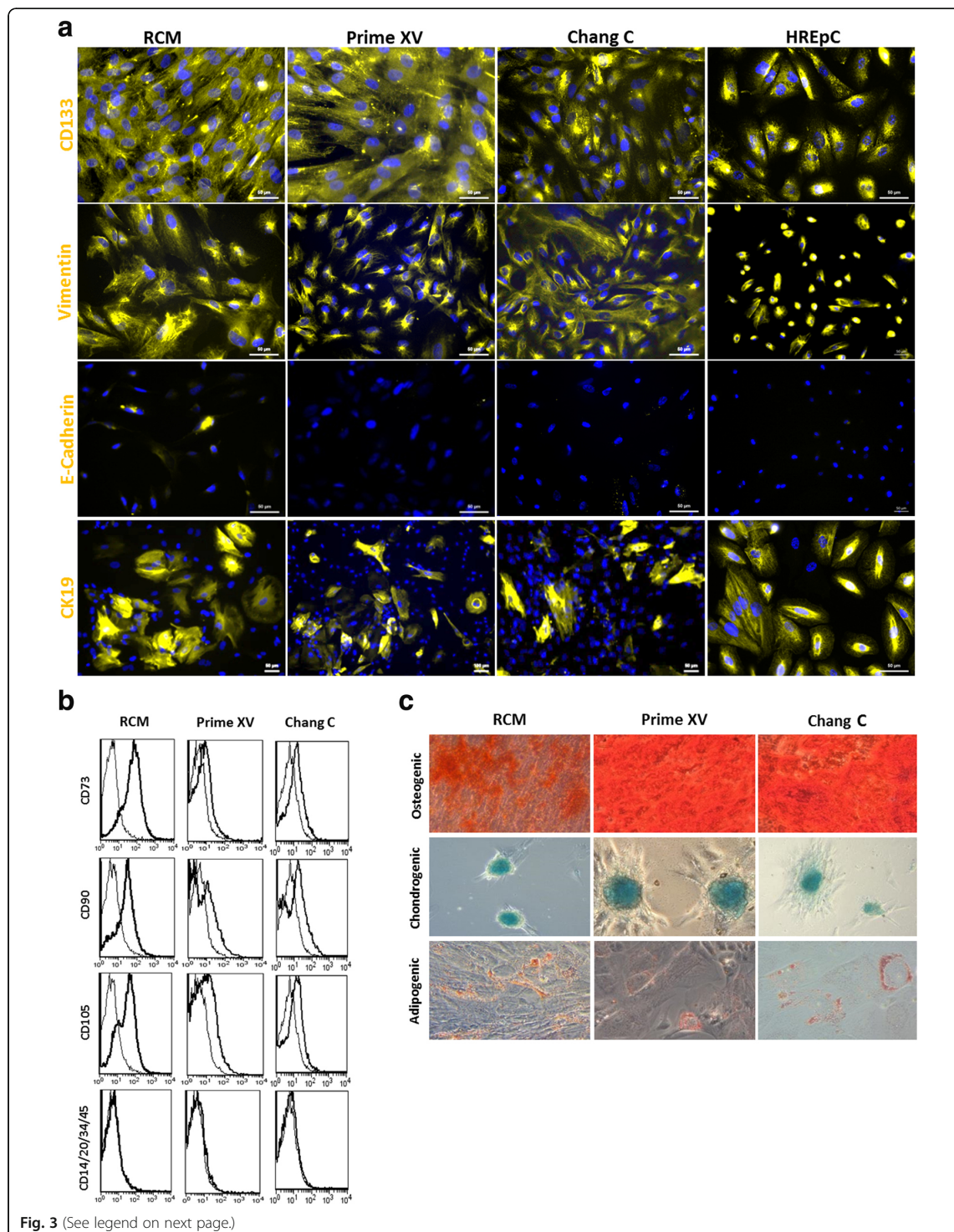
To investigate the differentiation capacity of the AFCs, the cells were subjected to adipocyte, chondrocyte and osteoblast differentiation for 3 weeks. Successful differentiation into adipocytes was observed by Oil Red O staining of emerging fat droplets surrounding the cell nuclei. During chondrogenic differentiation the cells aggregated, and Alcian Blue staining showed the presence of emerged proteoglycans within the developed cell clusters. Osteogenic lineage differentiation was shown by Alizarin Red S staining of developed calcium deposits (Fig. 3c).

AF-MSCs express renal markers irrespective of in-vitro culture media composition

To validate our hypothesis that third-trimester AF-MSCs harbor renal progenitor cells, we analyzed AF-MSCs cultured in RCM, which is a medium formulated for kidney cells, for the expression of kidney-associated markers SIX2, CITED1, LHX1, PODXL, BRN1 and Paired-Box-Protein 8 (PAX8)—these were positive. Prime XV and Chang C, specialized for AFC culture, also supported expression of the renal markers. The commercially bought human kidney cells HREpCs served as a positive control. These results imply that AF-MSCs are of nephrogenic origin and the phenotype is maintained irrespective of the media used (Fig. 4).

AF-MSCs are able to transport albumin

Albumin endocytosis is a criterion defining renal cells. To analyze the ability of AF-MSCs to take up and release albumin, fluorescent dye-coupled Alexa Fluor™ 488-labeled albumin was used. It could be shown that the temperature-dependent (37 °C) uptake of albumin (1 h incubation) by AF-MSCs was higher in comparison to fetal MSCs (fMSCs) and human fetal foreskin cell HFF1. This held true for both progenitor and differentiated cells (Fig. 5a). To differentiate AF-MSCs, we treated the cells with 10 μ M CHIR99021 (WNT pathway activation by GSK3 inhibition) for 2 days and observed morphological changes from fibroblastic to elongated tubular shape (Fig. 5b), resulting in decreased expression of progenitor markers C-Kit and SIX2. The expression and localization of WT1 switched from nuclear to cytoplasmic upon CHIR99021 treatment whereas Nephryn (NPHS1) expression was stable (Fig. 5c) as detected at



(See figure on previous page.)

Fig. 3 AFCs express typical MSC-associated proteins as well as CK19 and show multilineage differentiation potential in vitro. AFCs cultured in distinct media compositions stained positive for Vimentin and CD133 but negative for E-Cadherin. CK19, an established kidney epithelial marker, also expressed. Cell nuclei stained using Hoechst/DAPI (a). Flow cytometry-based analysis confirmed expression of MSC markers CD73, CD90 and CD105, and negativity for hematopoietic markers CD14, CD20, CD34 and CD45 (antibody isotype controls represented by thin lines; bold lines indicate histograms of distinct proteins) (b). Analysis of multilineage differentiation capacity of AF-MSCs revealed Alizarin Red staining of osteoid matrix-like structure in osteogenic medium, Alcian Blue staining of proteoglycans in chondrogenic media and lipid droplet formation around the cells in adipogenic media (c). HREpC human renal epithelial cell, RCM renal cell medium

the protein level via immunofluorescent-based staining. Real-time RT PCR revealed downregulation of *SIX2*, *WT1* and *CD133* and activation of kidney-associated bone morphogenic protein 7 (*BMP7*) (Fig. 5d). Based on our experimental data we derive a scheme describing CHIR99021-mediated WNT activation and its influence on differentiation or self-renewal (Fig. 6). Self-renewal (inactive WNT signaling) is maintained by elevated

expression of the renal progenitor markers *SIX2*, *WT1* and *CD133* (stem cell proliferation marker) and down-regulated expression of *BMP7*. In contrast, upon activation of canonical WNT signaling by GSK3 β inhibition with CHIR99021, AF-MSCs exit self-renewal and differentiate as a consequence of elevated *BMP7* expression and downregulation of *SIX2*, *WT1* and *CD133* respectively.

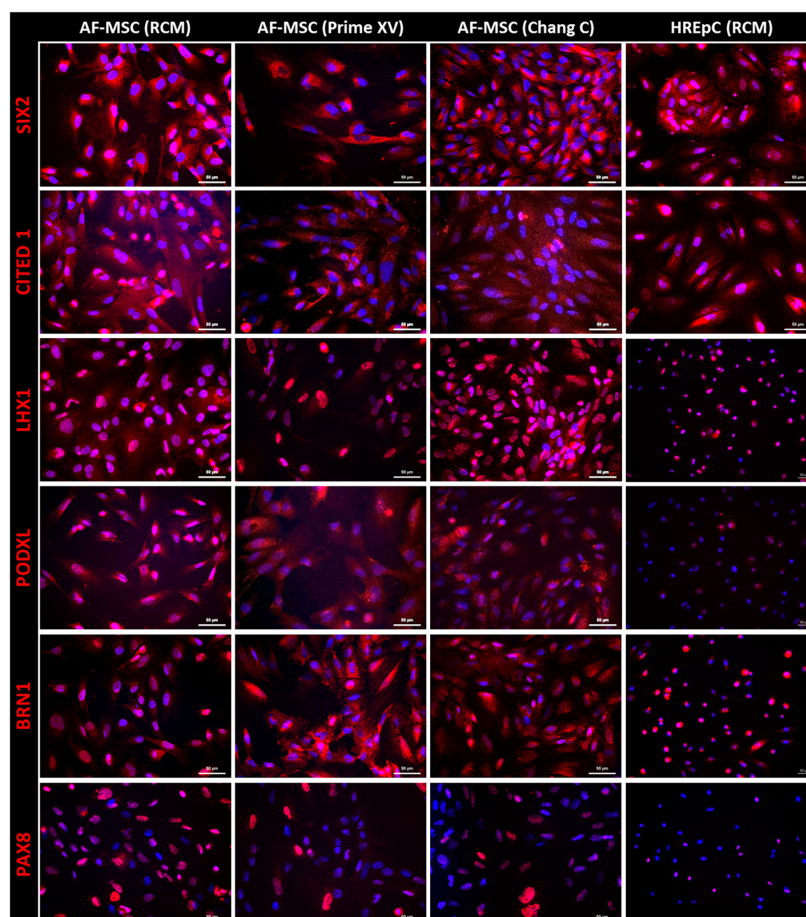


Fig. 4 Renal-specific marker expression in AF-MSCs. Immunofluorescent-based images showing expression and localization of *SIX2*, *CITED1*, *PAX8*, *BRN1*, *PODXL* and *LHX1* in AF-MSCs cultured in either RCM, PrimeXV or Chang C. HREpCs cells served as positive control. Cell nuclei stained using Hoechst/DAPI. AF-MSC amniotic fluid mesenchymal stem cell, HREpC human renal epithelial cell, RCM renal cell medium

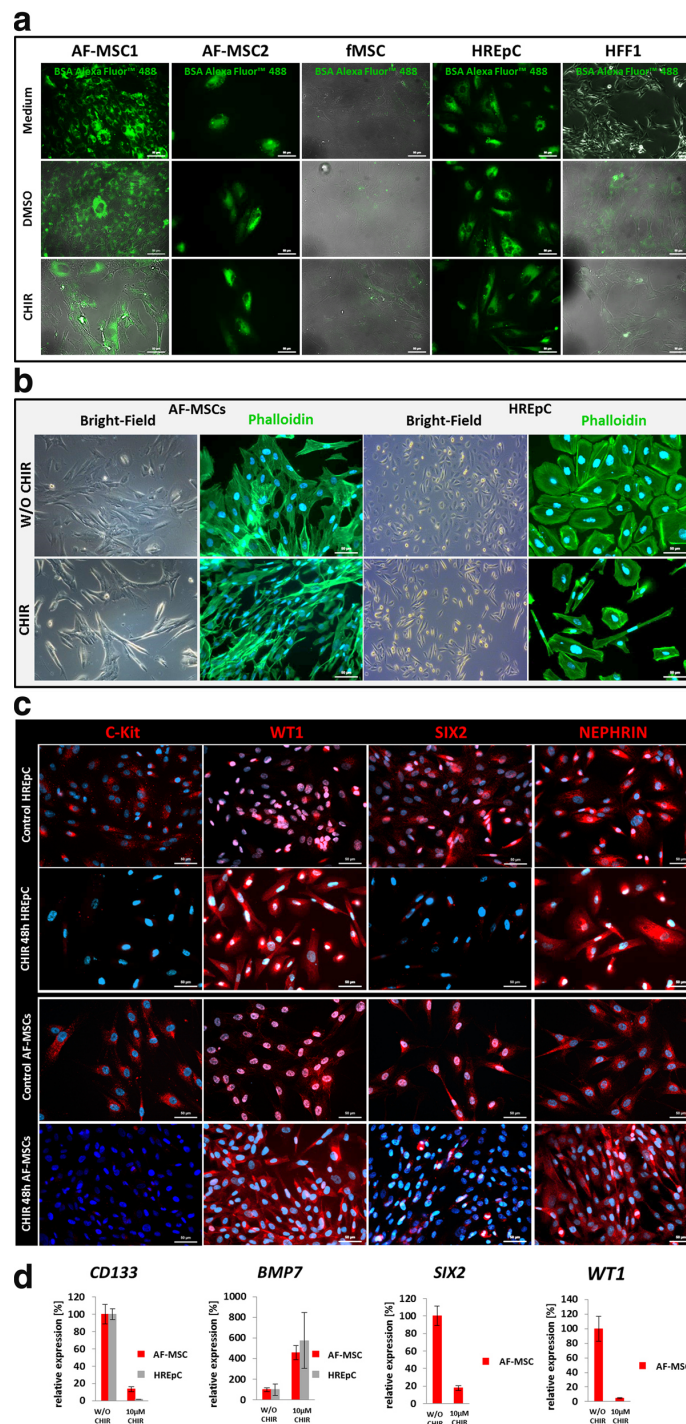


Fig. 5 (See legend on next page.)

(See figure on previous page.)

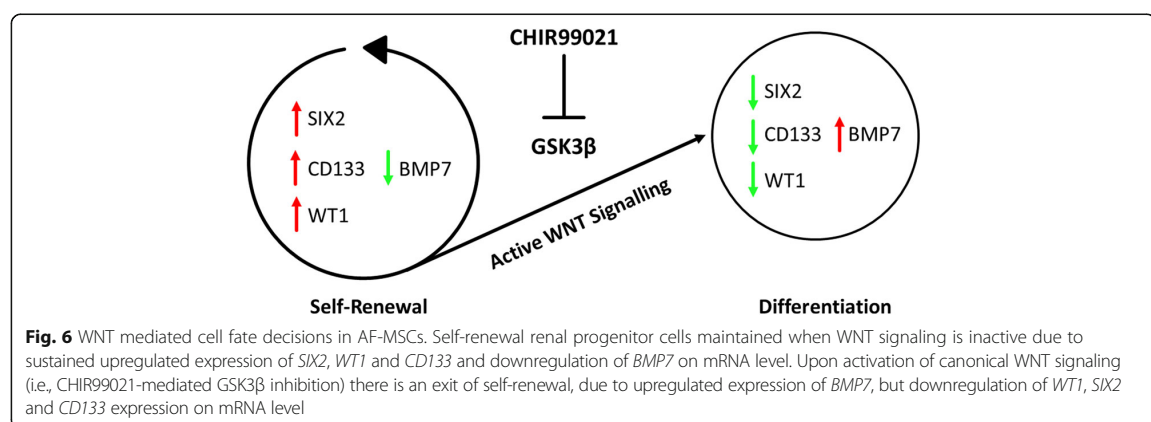
Fig. 5 Functional characterization of AF-MSCs as renal cells. Regardless of differentiated or undifferentiated AF-MSC status, functional albumin endocytosis observed at significantly higher levels than in HFF1 and fetal MSCs (fMSC) when cells incubated with albumin at 37 °C (a). Activation of WNT signaling by supplementation with GSK3-inhibitor CHIR99021 led to differentiation into tubular looking cells, shown by phalloidin staining (b). WT1 localization switch from nucleus to cytoplasm, Nephrin expression retained and C-Kit and SIX2 expression decreased (c). Cell nuclei stained using Hoechst/DAPI. qRT-PCR of CHIR differentiated cells clearly showed downregulation of renal undifferentiated progenitor markers *CD133*, *SIX2* and *WT1* and upregulation of the differentiation marker *BMP7* (d). AF-MSC amniotic fluid mesenchymal stem cell, DMSO dimethylsulfoxide, fMSC fetal mesenchymal stem cell, HFF human foreskin fibroblast, HREpC human renal epithelial cell, w/o without

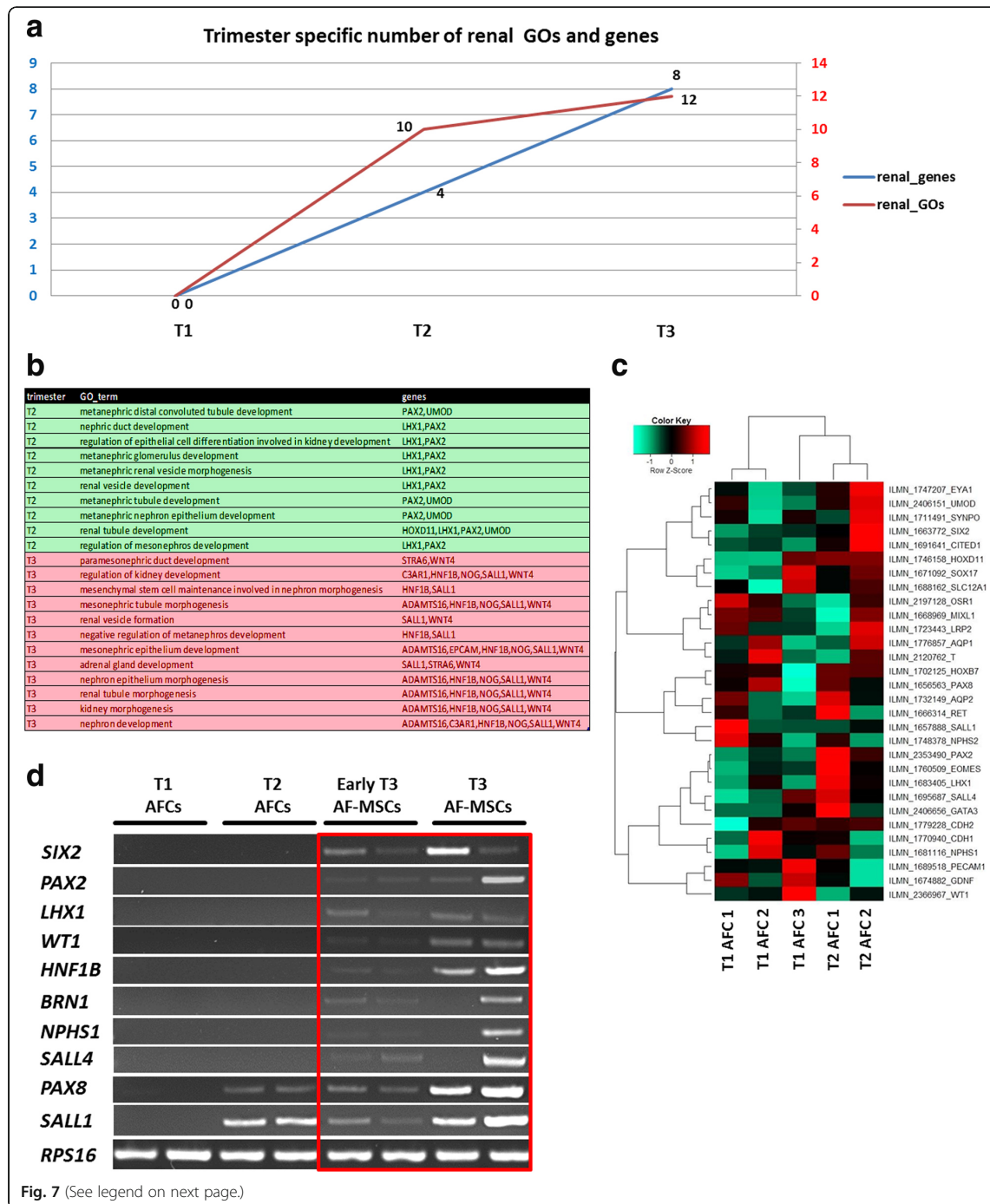
Increased appearance of renal-associated genes in AFCs correlates with gestational time

Taking advantage of previously published transcriptome data [45], related to renal system development from first and second-trimester AFCs, we analyzed gene set enrichments and related GOs from T1 (first trimester), T2 (second trimester) and T3 (third trimester). Interestingly, the number of expressed kidney-associated genes increased with gestational time. From the predictions based on the datasets, we observed that most of the renal developmental-related genes (eight genes) were expressed in the third trimester. Subsequently, only four genes were identified to be present in the second trimester and none was predicted to be expressed in the first trimester. In line with this, no kidney development-related GO terms were found for AFC samples from the first trimester, 10 GOs were shown for the second and 12 GOs in the third trimester, thus implying an increasing renal expression pattern during fetal kidney development which is also shown in a heatmap generated from the transcriptome data (Fig. 7a–c). These data were validated by semi-qPCR of cDNA samples obtained from the mRNA of AFCs/AF-MSCs from the first, second, early third and late third trimesters. We did not detect renal gene expression from the first-trimester samples; in contrast, *PAX8* and *SALL1* could be detected in the second and third-trimester samples. In contrast to this, third-trimester cells exclusively expressed *SIX2*, *PAX2*, *LHX1*, *WT1*, *HNF1B*, *BRN1*, *NPHS1* and *SALL4* (Fig. 7d).

Transcriptome analysis of third-trimester AF-MSCs reveals involvement in kidney specific biological processes

To reveal the AF-MSC identity, the cells' transcriptomes were compared to HREpCs, UM51 (urine-derived SIX2-positive renal cells) and UM51-derived iPSCs (ISRM-UM51). Using cluster dendrogram analysis, AF-MSCs were shown to cluster together with two different kidney cells and apart from the iPSCs (Fig. 8a). This is also shown by Pearson correlation coefficient calculation (Fig. 8b), revealing a value of 0.9095 for AF-MSC 1 and UM51 and a value of 0.955 for AF-MSC 1 and HREpCs. Next, we wanted to focus on genes shared amongst the AF-MSCs and the other two renal cell types. Since UM51, HREpCs and AF-MSCs showed expression of MSC markers, a sample of bone marrow-derived fetal MSCs was included in the Venn diagram, to allow focus on commonly expressed genes in AF-MSCs, UM51 and HREpCs but not in fMSCs (409 genes) (Fig. 8c). Using these genes, a GO term analysis was conducted. Among the top 20 GOs (Fig. 8d), 11 GOs were connected to kidney development-related biological processes such as “renal tubule development” and “nephron epithelium development”. The significant KEGG pathways resulting from the 409 shared genes are shown in Fig. 8e, revealing stem cell-related pathways such as “TGF-beta signaling pathway” and “Hedgehog signaling pathway”. The complete gene lists, GOs (BP, CC, MF) and the KEGG pathways for each single group as well as for a group





(See figure on previous page.)

Fig. 7 Expression levels of renal-specific genes in AFCs increase with gestational time. Number of renal-enriched genes (blue line) and GOs of trimester-specific AFCs (red line) indicates increasing pattern during fetal kidney development (a). Differentially expressed genes involved in nephron development in second and third-trimester AFCs. Gene-set enrichment analysis revealed expression of genes from different renal developmental compartments such as metanephros development (*ADAMTS16, EPCAM, HNF1B, NOG, SALL1, WNT4*), metanephric mesenchyme development (*HNF1B, SALL1*), renal tubule development (*HOXD11, LHX1, PAX2, UMOD*), metanephric nephron and tubule development (*PAX2, UMOD*), and metanephric glomerulus and mesonephros development (*LHX1, PAX2*) (b). Heatmap showing relative expression of genes involved in nephrogenesis from existing published data of AFCs from first and second trimester (c). Semi-qPCR of renal genes in AFC/AF-MSc samples from first, second, early third and late third trimester. Gel bands indicating enriched expression of renal genes in third trimester boxed in red (d). AFC amniotic fluid cell, AF-MSc amniotic fluid mesenchymal stem cell, GO gene ontology, T1 first trimester, T2 second trimester, T3 third trimester

consisting of AF-MSCs, UM51 and HREpCs are provided in Additional files 2, 3 and 4.

Discussion

Amniotic fluid cells display a spectrum of morphologies (Fig. 1a) depicting their composition of fetal-derived differentiated and undifferentiated progenitor cells [24, 33]. In the majority of studies, the heterogeneity of AF-derived cells has led to conflicting results and uncertainty regarding the identity of the cell population, in particular the origin of the third-trimester AFCs [37]. In our earlier work it could be shown that first-trimester AFCs have a germ cell origin [45]. Remarkably, we observed that third-trimester AFCs have similar morphologies when compared to urine-derived cells and human kidney biopsy-derived cells (Fig. 1b), as shown by others [46–50]. It is well known that AF contains various cell types which originate mostly from fetal urine [34, 51] and the appearance of cells in the amniotic fluid/fetal urine increases in number with gestational age. Furthermore, it has also been shown recently that urine cells have a kidney origin [35–37, 40]. In studies on full-term male fetal AF-MSc transcriptomes, we and others found that most of the expressed genes were related to kidney and skeletal system development [32, 37]. Nevertheless, the phenotypes of AFCs obtained during culture were dictated by culture conditions [52] and by the passage number. Initially, we cultured the cells in five distinct media, namely RCM, Prime XV, Chang C, MG30 and α MEM. Regardless of the media used, homogeneous spindle-shaped mesenchymal like cells were observed after a few passages, except for α MEM and MG30 which also led to decreased growth rates. So, these media were excluded from further analysis.

In this study, the third-trimester AFCs were shown to maintain expression of pluripotency-associated stem cell markers C-Kit, SSEA4, TRA-1-60 and TRA-1-81 but not nuclear OCT4 (Fig. 2a), which has also been shown for a subpopulation of urine-derived stem cells [46, 48]. C-kit was also identified to be expressed at the loop of Henley and distal tubules of murine kidney [53]. Second-trimester human nephron progenitor cells were shown to have elevated expression of NANOG and OCT4 [14].

These data suggests that pluripotency-associated gene/protein expression decreases with gestational time.

Third-trimester AFCs investigated in the present work expressed the mesenchymal marker Vimentin, typical MSC cell surface markers CD73, CD90, and CD105 as well as the stem cell marker CD133. Furthermore, the cells differentiated into adipocytes, osteocytes and chondrocytes (Fig. 3a–c), which has also been reported for cells derived from human kidneys [13], and hence we refer to the cells as AF-MSCs. In support of our findings, AFCs as well as cells derived from preterm neonatal urine were described to be positive for Vimentin and CD133 but negative for hematopoietic cell markers [35], which also was confirmed for fetal and adult kidney-derived cells [13, 14, 54]. In addition, our AF-MSCs also express CK19 (Fig. 3a) as shown previously for human kidney cells [53]. It has been described that subpopulations of renal cells exist with MSC-specific morphology and marker expression (CD73, CD105) which additionally express metanephric mesenchyme markers such as SIX2, CITED1 and PAX2 [37, 54].

As the AF-MSCs share similar properties with neonatal urine cells and human renal cells with respect to pluripotency-associated and mesenchymal marker expression, and multipotent differentiation potential, we assumed, as shown in the 1970s [51], that AFCs originate from fetal kidney. This hypothesis is supported by a recent review describing that cells leave the fetal kidney during the transition from the pronephron to the metanephron, and reside within AF [37]. To confirm, we investigated AF-MSCs cultured in RCM, Chang C and Prime XV for the expression of typical renal markers such as SIX2, CITED1, PODXL, LHX1, BRN1 and PAX8. Irrespective of the used media, the third-trimester AF-MSCs expressed all of these markers (Fig. 4). In line with our results, nephron progenitor cells derived from the developing human kidney as well as from neonatal urine were previously reported to express the investigated marker [14, 15, 35, 55, 56].

We also investigated uptake of exogenous albumin as a key kidney function, which has been shown for human renal cells [57–59] as well neonatal urine cells [35]. Third-trimester AF-MSCs and HREpCs showed albumin endocytosis whereas fMSCs and HFF1 did not

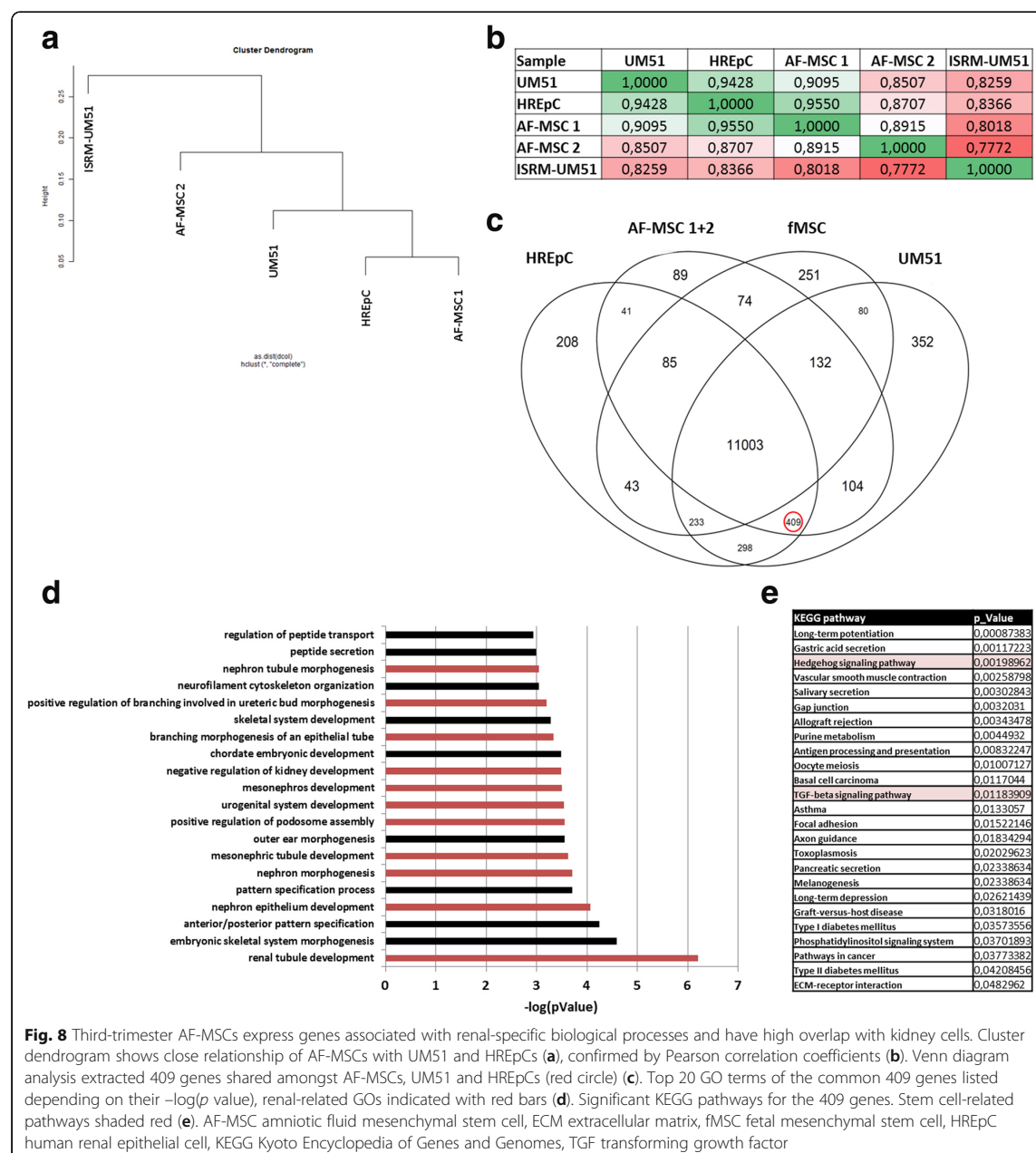


(Fig. 5a). Further, we analyzed the changes in morphology and protein/gene expression in the AF-MSCs upon differentiation by activation of WNT signaling as a consequence of inhibition of GSK3 using CHIR99201. Cell shapes became elongated and expression of renal progenitor markers C-KIT and SIX2 decreased, WT1 expression translocated from the nucleus to the cytoplasm and Nephron expression remained cytoplasmic,

which was also confirmed for cells isolated directly from a human kidney biopsy [37, 60]. The translocation of WT1 expression from the nucleus to cytoplasm has been described previously [61]. The cytoplasmic expression of WT1 will denote a loss of transcription factor activity.

Moreover, qRT-PCR revealed that the differentiated AF-MSCs acquired upregulated *BMP7* expression with

parallel decreased *SIX2*, *WT1* and *CD133* expression (Fig. 5d), as shown previously [62, 63]. One possible explanation for our observations could be that the antibody recognizes an epitope present on a variant of WT1 which we could not detect with our primers. Of course this is speculation and more studies are required to substantiate this observation.

Since nephrons are generated during the second and third trimesters [64], a synergistic relation between expression of kidney-associated genes in AF-MSCs and the gestational period can be postulated. To address this, we analyzed gene expression from previously published transcriptome data [32, 45] and performed a semiquantitative PCR of first, second and third-trimester samples to investigate any possible relationship between gradual expressions of renal genes with gestational time. The third-trimester AF-MSCs expressed increasing number of genes and GOs compared to second-trimester cells (Fig. 7a, b, d). For future research it would be of high value to have AF samples obtained from gestational week-wise time points to better understand the impact of the temporal developmental stage of the fetal kidney on the composition of the AF and likewise the identity of AF-MSCs. Cluster dendrogram analysis based on the transcriptome data showed that AF-MSCs cluster apart from pluripotent cells and cluster together with kidney-derived cells (Fig. 8a, b). In line with this, AF-MSCs shared more genes with human kidney cells UM51 and HREpCs than with fetal MSCs (Fig. 8c). Furthermore, GO analysis focusing on biological processes revealed the involvement of genes associated mostly with kidney development (Fig. 8d), which also can be observed in our previous analysis of AF specific genes [32].

Since the kidney is a complex organ and is composed of a multitude of different cell types, sorting and specification of distinct kidney cells from the amniotic fluid needs to be investigated.

Nevertheless, our results identify third-trimester human amniotic fluid-derived mesenchymal stem cells as of renal origin. As we have demonstrated before that these AF-MSCs also secrete immunomodulatory factors, they are highly suitable for transplantation, for example in chronic/acute kidney disease or graft versus host disease. These findings qualify these cells and the iPSCs derived from them as potent cells that can be used in the future for research on nephrogenesis, for modeling kidney-related diseases and for drug screening in combination with tissue engineering approaches such 3D organoid formation to further improve mimicking of kidney features in vitro.

Conclusions

We have demonstrated that third-trimester human AFCs originated from fetal kidney are mesenchymal stem cells

(AF-MSCs) with retained renal cell gene expression and functionality. AFCs/AF-MSCs have been widely investigated; however, to date only a limited number of studies have attempted to reveal their enigmatic origin. Our results add an important milestone for the usefulness of these cells as a suitable source for future studies related to nephrogenesis, derivation of iPSCs, nephrotoxicity tests and kidney disease-related cell replacement therapies.

Additional files

Additional file 1: Table S1. Antibodies used in this study **Table S2.** Primers used for semiquantitative and quantitative real-time PCR. (DOCX 18 kb)
Additional file 2: Gene list of exclusive groups and shared genes of AF-MSCs, HREpCs and UM51. (XLS 995 kb)
Additional file 3: GOs of exclusive groups and shared genes of AF-MSCs, HREpCs and UM51. (XLS 331 kb)
Additional file 4: KEGG pathways of exclusive groups and shared genes of AF-MSCs, HREpCs and UM51. (XLSX 76 kb)

Abbreviations

AF: Amniotic fluid; AFC: Amniotic fluid cell; AF-MSC: Amniotic fluid mesenchymal stem cell; BM-MSC: Bone marrow-derived mesenchymal stem cell; BSA: Bovine serum albumin; CD: Cluster of differentiation; DAVID: Database for Annotation, Visualization and Integrated Discovery; ESC: Embryonic stem cell; FBS: Fetal bovine serum; fMSC: Fetal mesenchymal stem cell; GO: Gene ontology; HFF: Human foreskin fibroblast; HREpC: Human renal epithelial cell; iPSC: Induced pluripotent stem cell; KEGG: Kyoto Encyclopedia of Genes and Genomes; αMEM: Minimum essential medium alpha modification; MSC: Mesenchymal stem cell; PBS: Phosphate buffered saline; PCR: Polymerase chain reaction; RCM: Renal cell medium; REGM: Renal epithelial growth medium; RT: Room temperature; T1: First trimester; T2: Second trimester; T3: Third trimester

Acknowledgements

The authors thank Prof. Richard O. C. Oreffo, Centre for Human Development, Stem Cells and Regeneration, Faculty of Medicine, University of Southampton, UK for providing the fMSCs.

Funding

JA and TF acknowledge support from the Medical Faculty, Heinrich-Heine-University, Düsseldorf, Germany. In addition, JA and MSR acknowledge support from the German Academic Exchange Service (DAAD-91607303).

Availability of data and materials

The data and cells described in this manuscript can be made available upon request. The transcriptome data are available online at the National Center of Biotechnology Information (NCBI) Gene Expression Omnibus.

Authors' contributions

JA, TF, MSR and L-SS conceived the idea and designed the experiments. CH and PB collected third-trimester amniotic fluid samples. PVG collected first and second-trimester amniotic fluid samples and prepared the corresponding RNA. MB performed immunofluorescence staining of the HREpCs, and designed the renal specific primers. NG performed real-time PCR analysis. WW performed bioinformatic analysis. AN performed analysis of the CHIR99021-treated AF-MSCs and HREpCs. MSR and L-SS isolated the AFCs from third-trimester AF and characterized the AFCs/AF-MSCs. MSR and L-SS wrote the manuscript and JA edited it. All authors read and approved the manuscript.

Ethics approval and consent to participate

Full-term amniotic fluid samples from healthy donors were collected from the Department of Obstetrics and Gynaecology, Medical Faculty, Heinrich Heine University Düsseldorf, Germany, with informed patient consent as well as institutional ethical approval.

Consent for publication

All authors have agreed to submit this manuscript for publication.

Competing interests

The authors declare that they have no competing interests.

Publisher's Note

Springer Nature remains neutral with regard to jurisdictional claims in published maps and institutional affiliations.

Author details

¹Institute for Stem Cell Research and Regenerative Medicine, Medical Faculty, Heinrich Heine University, Moorenstraße 5, 40225 Düsseldorf, Germany.

²Department of Obstetrics and Gynaecology, Medical Faculty, Heinrich Heine University Düsseldorf, Moorenstraße 5, 40225 Düsseldorf, Germany. ³Institute for Women's Health, Maternal and Fetal Medicine Department, University College London, London WC1E 6HX, UK.

Received: 24 January 2018 Revised: 19 March 2018

Accepted: 10 April 2018 Published online: 25 April 2018

References

- Kellum JA, Hoste EA. Acute kidney injury: epidemiology and assessment. *Scand J Clin Lab Invest Suppl.* 2008;241:6–11.
- Hoste EA, Schurgers M. Epidemiology of acute kidney injury: how big is the problem? *Crit Care Med.* 2008;36(4 Suppl):S146–51.
- Saidi RF, Kenari SKH. Challenges of organ shortage for transplantation: solutions and opportunities. *Int J Organ Transplant Med.* 2014;5(3):87–96.
- Xia Y, Nivet E, Sancho-Martinez I, Gallegos T, Suzuki K, Okamura D, et al. Directed differentiation of human pluripotent cells to ureteric bud kidney progenitor-like cells. *Nat Cell Biol.* 2013;5(12):1507–15.
- Taguchi A, Kaku Y, Ohmori T, Sharmin S, Ogawa M, Sasaki H, et al. Redefining the in vivo origin of metanephric nephron progenitors enables generation of complex kidney structures from pluripotent stem cells. *Cell Stem Cell.* 2014;14(1):53–67.
- Freedman BS. Modeling kidney disease with iPSC cells. *Biomark Insights.* 2015;10(Suppl 1):153–69.
- Lam AQ, Freedman BS, Morizane R, Lerou PH, Valerius MT, Bonventre JV. Rapid and efficient differentiation of human pluripotent stem cells into intermediate mesoderm that forms tubules expressing kidney proximal tubular markers. *J Am Soc Nephrol.* 2014;25(6):1211–25.
- Schutgens F, Verhaar MC, Rookmaaker MB. Pluripotent stem cell-derived kidney organoids: an in vivo-like in vitro technology. *Eur J Pharmacol.* 2016; 790:12–20.
- Little MH. Generating kidney tissue from pluripotent stem cells. *Cell Death Discovery.* 2016;2:16053.
- Al-Awqati Q, Oliver JA. Stem cells in the kidney. *Kidney Int.* 2002;61(2):387–95.
- Kobayashi A, Mugford JW, Krautzbarger AM, Naiman N, Liao J, McMahon AP. Identification of a multipotent self-renewing stromal progenitor population during mammalian kidney organogenesis. *Stem Cell Reports.* 2014;3(4):650–62.
- Combes AN, Wilson S, Phipson B, Binnie BB, Ju A, Lawlor KT, et al. Haploinsufficiency for the *Six2* gene increases nephron progenitor proliferation promoting branching and nephron number. *Kidney Int.* 2017; 17:30763–69.
- Buzhor E, Omer D, Harari-Steinberg O, Dotan Z, Vax E, Pri-Chen S, et al. Reactivation of NCAM1 defines a subpopulation of human adult kidney epithelial cells with clonogenic and stem/progenitor properties. *Am J Pathol.* 2013;183(5):1621–33.
- Metsuyanin S, Harari-Steinberg O, Buzhor E, Omer D, Pode-Shakked N, Ben-Hur H, et al. Expression of stem cell markers in the human fetal kidney. *PLoS One.* 2009;4(8):e6709.
- Schedl A. Renal abnormalities and their developmental origin. *Nat Rev Genet.* 2007;8:791–802.
- Higgins JP, Wang L, Kambham N, Montgomery K, Mason V, Vogelmann SU, et al. Gene expression in the normal adult human kidney assessed by complementary DNA microarray. *Mol Biol Cell.* 2004;15(2):649–56.
- Georgas KM, Chiu HS, Lesieur E, Rumballe BA, Little MH. Expression of metanephric nephron-patterning genes in differentiating mesonephric tubules. *Dev Dyn.* 2011;240(6):1600–12.
- Hendry C, Rumballe B, Moritz K, Little MH. Defining and redefining the nephron progenitor population. *Pediatr Nephrol.* 2011;26(9):1395–406.
- Casiraghi F, Perico N, Cortinovis M, Remuzzi G. Mesenchymal stromal cells in renal transplantation: opportunities and challenges. *Nat Rev Nephrol.* 2016; 12(4):241–53.
- Hamza AH, Al-Bishri WM, Damiati LA, Ahmed HH. Mesenchymal stem cells: a future experimental exploration for recession of diabetic nephropathy. *Ren Fail.* 2017;39(1):67–76.
- Večerić-Haler Ž, Cerar A, Perše M. (Mesenchymal) Stem cell-based therapy in cisplatin induced acute kidney injury animal model: risk of immunogenicity and tumorigenicity. *Stem Cells Int.* 2017;2017:7304643.
- Guillot PV, Gotherstrom C, Chan J, Kurata H, Fisk NM. Human first-trimester fetal MSC express pluripotency markers and grow faster and have longer telomeres than adult MSC. *Stem Cells.* 2007;25(3):646–54.
- Romagnani P. Kidney regeneration: any prospects? *Contrib Nephrol.* 2011; 170:228–36.
- Cananzi M, De Coppi P. CD117+ amniotic fluid stem cells: state of the art and future perspectives. *Organ.* 2012;8(3):77–88.
- Perin L, Giuliani S, Jin D, Sedrakyan S, Carraro G, Habibian R, et al. Renal differentiation of amniotic fluid stem cells. *Cell Prolif.* 2007;40:936–48.
- Perin L, Sedrakyan S, Giuliani S, Da Sacco S, Carraro G, Shiri L, et al. Protective effect of human amniotic fluid stem cells in an immunodeficient mouse model of acute tubular necrosis. *PLoS One.* 2010;5(2):e9357.
- Sedrakyan S, Da Sacco S, Milanese A, Shiri L, Petrosyan A, Varimezova R, et al. Injection of amniotic fluid stem cells delays progression of renal fibrosis. *J Am Soc Nephrol.* 2012;23(4):661–73.
- Rosner M, Schipany K, Gundacker C, Shanmugasundaram B, Li K, Fuchs C, et al. Renal differentiation of amniotic fluid stem cells: perspectives for clinical application and for studies on specific human genetic diseases. *Eur J Clin Invest.* 2012;42:677–84.
- Hauser PV, De Fazio R, Bruno S, Sdei S, Grange C, Bussolati B, Benedetto C, Camussi G. Stem cells derived from human amniotic fluid contribute to acute kidney injury recovery. *Am J Pathol.* 2010;177(4):2011–21.
- Siegel N, Rosner M, Unbekandt M, Fuchs C, Slabina N, Dolznig H, et al. Contribution of human amniotic fluid stem cells to renal tissue formation depends on mTOR. *Hum Mol Genet.* 2010;19(17):3320–31.
- De Coppi P, Bartsch G Jr, Siddiqui MM, Xu T, Santos CC, Perin L, et al. Isolation of amniotic stem cell lines with potential for therapy. *Nat Biotechnol.* 2007;25(1):100–6.
- Spitzhorn LS, Rahman MS, Schwindt L, Ho HT, Wruck W, Bohndorf M, et al. Isolation and molecular characterization of amniotic fluid-derived mesenchymal stem cells obtained from caesarean sections. *Stem Cells Int.* 2017;2017:5932706.
- Loukogeorgakis SP, De Coppi P. Amniotic fluid stem cells: the known, the unknown, and potential regenerative medicine applications. *Stem Cells.* 2017;35:1663–73.
- Underwood MA, Gilbert WM, Sherman MP. Amniotic fluid: not just fetal urine anymore. *J Perinatol.* 2005;25:341–8.
- Arcolino FO, Zia S, Held K, Papadimitriou E, Theunis K, Bussolati B, et al. Urine of preterm neonates as a novel source of kidney progenitor cells. *J Am Soc Nephrol.* 2016;27(9):2762–70.
- Zhang D, Wei G, Li P, Zhou X, Zhang Y. Urine-derived stem cells: a novel and versatile progenitor source for cell-based therapy and regenerative medicine. *Genes Dis.* 2014;1(1):8–17.
- Da Sacco S, Perin L, Sedrakyan S. Amniotic fluid cells: current progress and emerging challenges in renal regeneration. *Pediatr Nephrol.* 2017;1–11.
- Siegel N, Valli A, Fuchs C, Rosner M, Hengstschlagger M. Induction of mesenchymal/epithelial marker expression in human amniotic fluid stem cells. *Reprod BioMed Online.* 2009;19(6):838–46.
- Zhou T, Benda C, Duzinger S, Huang Y, Li X, Li Y, et al. Generation of induced pluripotent stem cells from urine. *J Am Soc Nephrol.* 2011;22(7):1221–8.
- Bohndorf M, Ncube A, Spitzhorn LS, Enczmann J, Wruck W, Adjaye J. Derivation and characterization of integration-free iPSC line ISRM-UM51 derived from *SIX2*-positive renal cells isolated from urine of an African male expressing the CYP2D6 *4/*17 variant which confers intermediate drug metabolizing activity. *Stem Cell Res.* 2017;25:18–21.
- Gentleman C, Carey VJ, Bates DM, et al. Bioconductor: open software development for computational biology and bioinformatics. *Genome Biol.* 2004;5(10):R80.
- Gautier L, Cope L, Bolstad BM, Irizarry RA. affy-analysis of Affymetrix GeneChip data at the probe level. *Bioinformatics.* 2004;20:307–15.
- Huang DW, Sherman BT, Lempicki RA. Systematic and integrative analysis of large gene lists using DAVID bioinformatics resources. *Nat Protoc.* 2009;4(1):44–57.

44. Kanehisa M, Furumichi M, Tanabe M, et al. KEGG: new perspectives on genomes, pathways, diseases and drugs. *Nucleic Acids Res.* 2017;45(D1):D353–61.
45. Moschidou D, Drews K, Eddaoudi A, Adjaye J, De Coppi P, Guillot PV. Molecular signature of human amniotic fluid stem cells during fetal development. *Curr Stem Cell Res Ther.* 2013;8(1):73–81.
46. Zhang Y, McNeill E, Tian H, Soker S, Andersson KE, Yoo JJ, et al. Urine derived cells are a potential source for urological tissue reconstruction. *J Urol.* 2008;180:2226–33.
47. Lang R, Liu G, Shi Y, Bharadwaj S, Leng X, Zhou X, et al. Self-renewal and differentiation capacity of urine-derived stem cells after urine preservation for 24 hours. *PLoS One.* 2013;8(1):e53980.
48. Bharadwaj S, Liu G, Shi Y, Wu R, Yang B, He T, et al. Multipotential differentiation of human urine-derived stem cells: potential for therapeutic applications in urology. *Stem Cells.* 2013;31(9):1840–56.
49. Kim EY, Page P, Dellefave-Castillo LM, McNally EM, Wyatt EJ. Direct reprogramming of urine-derived cells with inducible MyoD for modeling human muscle disease. *Skelet Muscle.* 2016;6:32.
50. Qin D, Long T, Deng J, Zhang Y. Urine-derived stem cells for potential use in bladder repair. *Stem Cell Res Ther.* 2014;5(3):69.
51. Sutherland GR, Bain AD. Culture of cells from the urine of newborn children. *Nature.* 1972;239:231.
52. Zagoura DS, Trohatou O, Bitsika V, Makridakis M, Pappa KI, Vlahou A, et al. AF-MSCs fate can be regulated by culture conditions. *Cell Death Dis.* 2013;4:e571.
53. Bussolati B, Camussi G. Therapeutic use of human renal progenitor cells for kidney regeneration. *Nat Rev Nephrol.* 2015;11:695–706.
54. Wang H, Gomez JA, Klein S, Zhang Z, Seidler B, Yang Y, et al. Adult renal mesenchymal stem cell-like cells contribute to juxtaglomerular cell recruitment. *J Am Soc Nephrol.* 2013;24(8):1263–73.
55. Rosenblum ND. Developmental biology of the human kidney. *Semin Fetal Neonatal Med.* 2008;13(3):125–32.
56. Tong GX, Yu WM, Beaubier NT, Weeden EM, Hamele-Bena D, Mansukhani MM, et al. Expression of PAX8 in normal and neoplastic renal tissues: an immunohistochemical study. *Mod Pathol.* 2009;22(9):1218–27.
57. Tojo A, Kinugasa S. Mechanisms of glomerular albumin filtration and tubular reabsorption. *Int J Nephrol.* 2012;2012:481520.
58. Eyre J, Ioannou K, Grubb BD, Saleem MA, Mathieson PW, Brunskill NJ, et al. Statin-sensitive endocytosis of albumin by glomerular podocytes. *Am J Physiol Renal Physiol.* 2007;292:F674–81.
59. Xinaris C, Benedetti V, Novelli R, Abbate M, Rizzo P, Conti S, et al. Functional human podocytes generated in organoids from amniotic fluid stem cells. *J Am Soc Nephrol.* 2016;27(5):1400–11.
60. Musah S, Mammoto A, Ferrante TC, Jeanty SSF, Hirano-Kobayashi M, Mammoto T, et al. Mature induced-pluripotent-stem-cell-derived human podocytes reconstitute kidney glomerular-capillary-wall function on a chip. *Nat Biomed Eng.* 2017;1:0069.
61. Depping R, Schindler SG, Jacobi C, Kirschner KM, Scholz H. Nuclear transport of Wilms' tumour protein Wt1 involves importins α and β . *Cell Physiol Biochem.* 2012;29(1–2):223–32.
62. Park JS, Ma W, O'Brien LL, Chung E, Guo JJ, Cheng JG, et al. Six2 and Wnt regulate self-renewal and commitment of nephron progenitors through shared gene regulatory networks. *Dev Cell.* 2012;23(3):637–51.
63. Zeisberg M. Bone Morphogenic protein 7 and the kidney: current concepts and open questions. *Nephrol Dial Transplant.* 2006;21:568–73.
64. Little MH, McMahon AP. Mammalian kidney development: principles, progress, and projections. *Cold Spring Harb Perspect Biol.* 2012;4:4.

Ready to submit your research? Choose BMC and benefit from:

- fast, convenient online submission
- thorough peer review by experienced researchers in your field
- rapid publication on acceptance
- support for research data, including large and complex data types
- gold Open Access which fosters wider collaboration and increased citations
- maximum visibility for your research: over 100M website views per year

At BMC, research is always in progress.

Learn more biomedcentral.com/submissions



2.3 Urine-derived stem cells as innovative platform for drug testing and disease modelling

Lucas-Sebastian Spitzhorn, Md Shaifur Rahman, Lisa Nguyen, Audrey Ncube, Martina Bohndorf, Wasco Wruck and James Adjaye

Abstract

Kidney-related diseases and associated health costs are on the rise. Due to the shortage of compatible organ donors, stem cell-based therapies are considered as alternative treatment options. To date, several adult stem cell sources have been established such as bone marrow, cord blood and amniotic fluid. Although these sources harbor stem cells with great regenerative potential there are some limitations. Cord blood and amniotic fluid can only be accessed before and at birth and bone marrow requires invasive procedures associated with risks and pain for the patient. So far, kidney biopsies are used to derive human kidney cells for research purposes. Recent investigations have shown that urine represents an alternative source of renal stem cells and differentiated cells originating from shed cells within the kidney. These include urine-derived mesenchymal stem cells (uMSCs) and renal epithelial tubular cells (uRETCs). These cells can be collected without the need of invasive or complex procedures. In this review, we describe the cellular and molecular features of these cells and emphasize possible future applications in drug-screening and development, nephrotoxicity tests and disease modelling.

Publication Status: published in *Drug Target Review*, Summer 2018, Issue 02

Impact Factor: -

This article is reproduced with permission.

Approximated total share of contribution: 50%

Contribution on experimental design, realization and publication:

JA, LSS, MSR and MB conceived the idea and designed the experiments. MB isolated urine derived stem cells. MB and AN generated iPSCs from the urine stem cells (uMSCs). LSS and MSR performed the stainings for renal markers and the differentiation of uMSCs into bone, cartilage and fat. LN differentiated the uMSC-iPSCs into endothelial cells and generated kidney organoids. WW did the bioinformatic analysis. LSS designed the figures and wrote the manuscript and JA edited it. All authors have read and approved the manuscript.

Link to the publication:

<https://www.drugtargetreview.com/article/32611/urine-derived-stem-cells/>

IN-DEPTH FOCUS | STEM CELLS

Urine-derived stem cells as innovative platform for drug testing and disease modelling

Lucas-Sebastian Spitzhorn, Lisa Nguyen and Wasco Wruck

Institute for Stem Cell Research and Regenerative Medicine, Medical faculty, Heinrich Heine University Düsseldorf, Germany

Shaifur Rahman

Doctoral Student, Institute for Stem Cell Research and Regenerative Medicine, Medical faculty, Heinrich Heine University Düsseldorf, Germany

Audrey Ncube

Scientific Research Associate, Institute for Stem Cell Research and Regenerative Medicine, Medical faculty, Heinrich Heine University Düsseldorf, Germany

Martina Bohndorf

Qualified Medical Technical Assistant, Institute for Stem Cell Research and Regenerative Medicine, Medical faculty, Heinrich Heine University Düsseldorf, Germany

James Adjaye

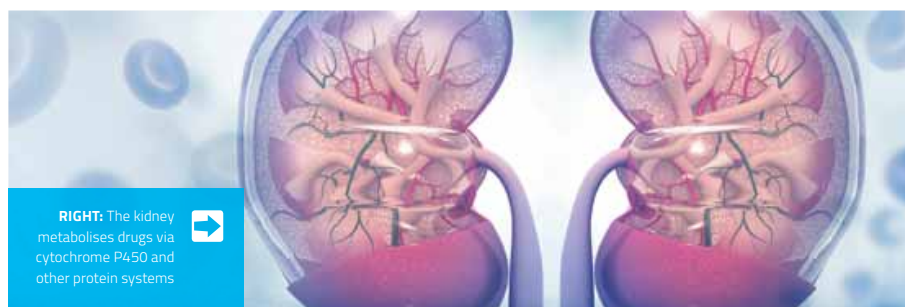
Director Institute for Stem Cell Research and Regenerative Medicine, Medical faculty, Heinrich Heine University Düsseldorf, Germany

Kidneys are crucial for filtration of drugs and toxins and their proper function is essential for overall health. Unfortunately, due to disease and improper function, kidney transplantation or dialysis are necessary for millions of patients annually all over the world.^{1,2}

BIOGRAPHY



SHAIFUR RAHMAN, Md, has a BSc and an MSc degree in Biotechnology and Genetic Engineering from Khulna University, Bangladesh. Additionally, he has an Erasmus Mundus Master degree in BioHealth Computing from University Joseph Fourier, France. He is now working as a doctoral student at the Institute for Stem Cell Research and Regenerative Medicine at Heinrich-Heine-University Düsseldorf, Germany and investigating therapeutic potentials of amniotic fluid cells.



RIGHT: The kidney metabolises drugs via cytochrome P450 and other protein systems

CLINICIANS face several hurdles, such as limited organ donors and high financial demands, during the course of administering the necessary treatment options.³ The kidney metabolises drugs via cytochrome P450 and other protein systems.⁴ The increasing prevalence of acute kidney injury (AKI) is associated with medical and economic burdens.⁵ AKI, of which 19-26% are induced by drugs, can result in chronic kidney disease (CKD),^{6,7} which increases the probability of developing renal cell carcinoma.⁸ Nephrotoxicity caused by drugs is an important causative factor in the development of AKI and CKD.⁹ It causes failure of about 7% of newly developed drugs, thus emphasising that pre-clinical models have to be improved.¹⁰

Several drugs are nephrotoxic per se. These side effects could be increased by prolonged medication and synergistic effects with other drugs, such as cephalosporins plus aminoglycosides, which are used in cancer treatment.¹¹ Although there are models such as cisplatin treatment¹² to investigate drug induced nephrotoxicity, more prospective studies and novel *in vitro* models are warranted to validate these approaches.

Embryonic and induced pluripotent stem cells (ESCs / iPSCs) have been differentiated into kidney-related cells, thus representing a potential alternative to native cells.¹³⁻¹⁵

The kidney is an organ of high complexity consisting of many cell types.¹⁶ One key regulator

of nephrogenesis, SIX2, has been shown to be expressed in umbilical cord mesenchymal stem cells (uMSCs).¹⁷ Bone marrow-derived mesenchymal stem cells (MSCs) have been successfully used to restore renal function deficits.¹⁸ It has been shown that renal cells can be isolated from urine as well as from third trimester amniotic fluid, which mostly consists of foetal urine. Obtaining kidney biopsy-derived cells from patients is difficult; thus urine represents a substitution which enables personalised research approaches for kidney-related drug screening and toxicity tests. Building upon previous work showing that amniotic fluid mostly consist of foetal urine,¹⁹ amniotic fluid-derived stem cells were recently also described as MSCs of renal origin²⁰ and have been used to generate podocytes.²¹

Urine is a source of stem cells

Derivation of patient-specific stem cells from urine has many advantages over other established stem cell sources. These autologous or human leukocyte

antigens (HLA)-matched uMSCs are ideal for transplantation purposes. Additionally, it is possible to generate vast amounts of these cells because the source is nearly infinite and can be expanded *in vitro* on a large scale in a good manufacturing practice (GMP) setting. In case of infants and older patients with impaired wound healing, urine cells can be obtained non-invasively, without wounding, cost-effectively and easily cultured. uMSCs or uRETCs can be reprogrammed into iPSCs¹⁷ also under GMP conditions.

Urine-derived stem cells have features of MSCs and kidney cells

Cellular and molecular characterisation of the uMSCs and uRETCs revealed similarities with amniotic fluid-derived MSCs.²⁰ Furthermore, they are able to differentiate into osteoblasts, adipocytes and chondrocytes and secreted cytokines capable of modulating the immune system and support healing processes. Besides their MSC marker expression, these cells express kidney-related ▶

BIOGRAPHY



LUCAS-SEBASTIAN SPITZHORN has a BSc and an MSc degree in Biology from Heinrich-Heine University, Düsseldorf. Currently, he is finishing his PhD thesis, which includes work on bone-marrow-derived MSCs, amniotic fluid cells, urine-derived stem cells and liver cells at the Institute for Stem Cell Research and Regenerative Medicine at Heinrich-Heine-University Düsseldorf, Germany.

EXPERT VIEW



Liz Quinn

Associate Director,
Stem Cell Marketing,
Takara Bio USA

“This fundamental limitation restricts the utility of hpheps in multiple applications, including drug metabolism and metabolic disease research”

Overcoming the problems of working with human primary hepatocytes

Human primary hepatocytes (hpheps) are the gold standard for *in vitro* evaluation of drug metabolism, drug-drug interactions, and metabolic disease research. However, hpheps don't survive in standard 2D culture for very long – no longer than two or three days.

EXPERIMENTS are therefore limited due to their rapid loss of function when cultured *in vitro*, which is especially problematic for chronic toxicity studies that require longer usage windows to observe the effects of drugs.

This fundamental limitation restricts the utility of hpheps in multiple applications, including drug metabolism and metabolic disease research. To address this problem, 3D sandwich cultures with matrix overlays (Liu *et al.* 1999), bioreactors (Hoffman *et al.* 2012), and 3D spheroid cultures (Proctor *et al.* 2017) have been developed. Although these approaches can maintain some hepatocyte functions for several weeks *in vitro*, they do not

entirely overcome the limitations of hpheps because these culture systems restrict the types of assays that can be performed. Further, they require advanced and expensive lab equipment, are not easy to use, or are not generally applicable to hpheps from different donors.

Another problem is the large variation between donors and a finite number of harvestable cells – normally from patient biopsies – from each donor. It is now possible to obtain batches of hpheps from commercial vendors. Though commercial vendors might provide a more convenient and reliable source of cells, each batch of isolated cells is donor-specific and, as such,

needs to be pre-screened by the vendors and qualified for different functions (eg, transporter-mediated uptake, metabolic activity, CYP enzyme induction).

And to complicate things even further, each vendor provides their own culture medium to go with the cells, which can lead to variable results when comparing results from different vendors, donors and experiments. As a result, no matter what the source of hpheps, no universally accepted culture system currently exists and researchers need to pre-qualify each lot of cells prior to their experiments, which influences the ability to interpret their results. ■

IN-DEPTH FOCUS | STEM CELLS

BIOGRAPHY



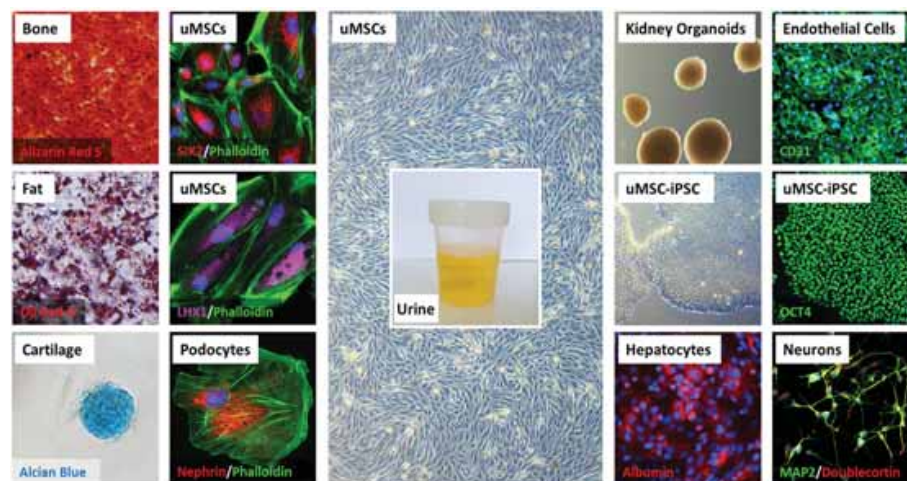
LISA NGUYEN has a BSc in Biology from Heinrich-Heine University, Düsseldorf. She is currently working on her MSC thesis at the Institute for Stem Cell Research and Regenerative Medicine at Heinrich-Heine-University Düsseldorf, Germany. Her thesis is based on modelling nephrogenesis using urine-derived renal progenitor cells.

BIOGRAPHY



WASCO WRUCK has a diploma in computer science and a diploma in architecture from Technische Universität Berlin, Germany. He worked as a software developer with Siemens AG and BULL AG before joining the Max-Planck-Institute for Molecular Genetics in Berlin. There he worked as a Bioinformatician on microarray-based image analysis, application development and to evaluate various types of high-throughput genomics experiments. He then worked on a European Systems Biology research project at Charité Universitätsmedizin Berlin and was elected chair of the ERASysBio+ initiative's data management group. He currently works at the Institute for Stem Cell Research and Regenerative Medicine at Heinrich-Heine-University Düsseldorf, Germany.

FIGURE 1



ABOVE: Molecular and cellular characteristics of uMSCs and uMSC-iPSCs. (Middle column) uMSCs with grain-like morphology were isolated from urine. (Left columns) They are able to differentiate into fat (Oil Red O), cartilage (Alcian Blue) and bone cells (Alizarin Red S) and additionally express renal markers SIX2, LHX1 and Nephrin and can be differentiated into podocyte-like cells. (Right columns) uMSC-iPSCs are positive for OCT4 and can be differentiated into endothelial cells (CD31), neuronal cells (MAP2 and Doublecortin), hepatocytes (Albumin) and form kidney organoids. Cell nuclei were stained using DAPI or Hoechst 33258

markers such as SIX2, Nephrin and LHX1 and can be differentiated into podocyte-like cells (**Figure 1**). Furthermore, it was possible to efficiently generate iPSCs from these cells.¹⁷ These uMSC-iPSCs can be differentiated into all cell types within the body including hepatocytes, neurons and endothelial cells (**Figure 1**).

Gene expression analysis confirms kidney origin of urine cells

Figure 2 shows a heatmap representation of genes associated with (A) pluri- and multipotency, (B) renal developmental processes, (C) encoding the core ADME (absorption, distribution, metabolism, and excretion) enzymes and (D) of the cytochrome P450 family. The heatmaps are based on uMSC transcriptome data sets described in the research^{17,20} and also uRETCs obtained directly from urine using a selective medium for differentiated cells. Drugs up-regulate the enzyme systems responsible for their degradation or activation (Phase I) and conjugation (Phase II) to biochemical forms that can be excreted in bile or urine.²²⁻²⁴ Genes coding Phase I and Phase II enzymes are included in the absorption, distribution, metabolism, and excretion (ADME) genes. The high similarity between both cell types is demonstrated by the predominantly consistent expression between both cell types. However, clustering of renal developmental genes shows a separation of uMSCs and uRETCs pointing to differences in these cells in nephrogenesis. These

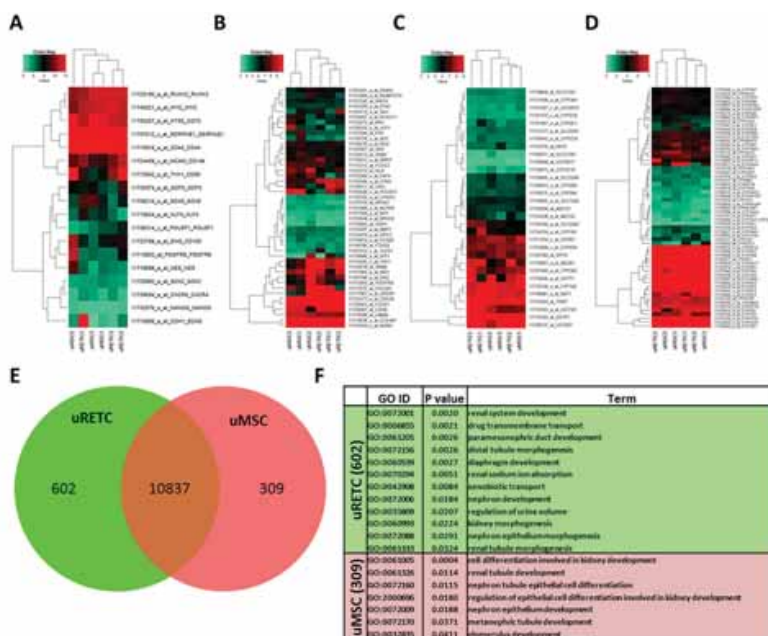
differences are shown in **Figure 2E**. The subsets of genes exclusively expressed in uMSCs or uRETCs were further subjected to gene ontology (GO) analysis and revealed differences in kidney developmental processes, such as the GO-terms drug transmembrane transport, paramesonephric duct development, distal tubule morphogenesis for uRETCs and metanephric tubule development, glomerulus development for uMSCs (**Figure 2F**).

Improve disease modelling, drug screening and nephrotoxicity tests using 3D-based kidney organoids

Ethical concerns and the limited predictability of cross-species translation of research results increase the importance of *in vitro* models as an alternative to *in vivo* pre-clinical testing. Recent 3D approaches increase assay relevance but still need improvement.²⁵

Moreover, uMSC-iPSCs are the basis for generating 3D kidney organoids. To resemble the complex kidney structure, it is useful to combine different cell types. We have generated 3D kidney organoids (**Figure 1**) by combining uMSCs as renal cells with uMSC-iPSCs differentiated endothelial cells (iECs) and mesenchymal stem cells (iMSCs) originating from the same individual.¹⁷ This approach may enable researchers to better mimic human physiology in contrast to standard 2D cell culture systems. For future research and therapy, it is important to increase maturity, and thus functionality, in order to attain predictive

FIGURE 2



ABOVE: Gene expression profiles characterise renal developmental properties of uMSCs and uRETcs. Heatmap-based representations of co-regulated expression of distinct gene sets associated with (A) pluripotency, (B) renal developmental processes, (C) the core ADME genes (http://pharmaadme.org/joomla/index.php?option=com_content&task=view&id=14&Itemid=29) and (D) cytochrome P450 genes. uMSCs and uRETcs have high similarity. However, the clustering related to renal development demonstrates differences between both cell types (C). Values on the color key scales are logarithmic (base 2). (E) Venn diagram analysis of genes expressed in uMSCs and uRETcs identified 10837 genes expressed in common, 309 genes expressed in uMSCs and 602 genes expressed in uRETcs. (F) Genes exclusively expressed in uMSCs or uRETcs reveal many kidney-related terms which point to their distinct developmental potential.

value. Recent studies have shown bio-printing^{26,27} and kidney-on-a-chip technology²⁸ as improved means of generating better *in vitro* models.

Perspectives

Urine is a source of stem cells that can be accessed non-invasively, with no pain and risk for the patient; has nearly unlimited availability; and is cost-efficient. Urine should be considered as an alternative to established stem cell sources such as bone marrow and cord blood. Most importantly, uMSCs and uRETcs originate from the kidney and, thus, by-pass the need for donated kidneys. Combined with HLA analysis and analysis of the patient's CYP variants, the cells are perfectly suited for individualised drug screening, dose determination, disease modelling *in vitro* and eventually kidney-associated cell therapies.

ACKNOWLEDGEMENTS

James Adjaye acknowledges support from the medical faculty of the Heinrich Heine University- Düsseldorf, Germany. Md Shaifur Rahman acknowledges support from the German Academic Exchange Service (DAAD-91607303).

@DrugTargetRev

BIOGRAPHY



PROFESSOR DR JAMES AFFRAM ADJAYE has a BSc degree in Biochemistry from University College of Cardiff, Wales, and an MSc in Biochemistry from University of Sussex, Brighton. He has a PhD in Biochemistry from King's College, London. Professor Adjaye was head of the Molecular Embryology and Aging group at the Max Planck Institute for Molecular Genetics, Berlin, Germany. He is now Director of the Institute for Stem Cell Research and Regenerative Medicine within the Faculty of Medicine at the Heinrich-Heine-University, Düsseldorf, Germany. He is involved in systems biology-based projects, both at the national and international level where iPSCs are used to model Alzheimer's disease and Non-Alcoholic Fatty Liver Disease (NAFLD) and Nijmegen Breakage Syndrome.

BIOGRAPHY



MARTINA BOHNDORF is a Qualified Medical Technical Assistant working at the Institute for Stem Cell Research and Regenerative Medicine- Heinrich-Heine-University Düsseldorf, Germany. She has extensive experience in culturing pluripotent stem cells and was instrumental in the development of the protocols for isolation and expansion of urine-derived stem cells.

BIOGRAPHY



AUDREY NOZITHELO NCUBE has a BSc in Applied Biology and MSc in Biomedical Sciences from Hochschule Bonn-Rhein-Sieg, Germany. The practical lab work for the two degrees was conducted at the Institute for Stem Cell Research and Regenerative Medicine at Heinrich-Heine-University Düsseldorf, Germany where she is now working as a Scientific Research Associate since 2016.

“ In case of infants and older patients with impaired wound healing, urine cells can be obtained non-invasively, without wounding, cost-effectively and easily cultured ”

REFERENCES

To view references, please visit: drugtargetreview.com/2-18-Adjaye

2.4 Derivation and characterization of integration-free iPSC line ISRM-UM51 derived from SIX2-positive renal cells isolated from urine of an African male expressing the CYP2D6 *4/*17 variant which confers intermediate drug metabolizing activity

Martina Bohndorf*, Audrey Ncube*, Lucas-Sebastian Spitzhorn, Jürgen Enczmann, Wasco Wruck and James Adjaye

*These authors contributed equally to this work.

Abstract

SIX2-positive renal cells isolated from urine from a 51year old male of African origin bearing the CYP2D6 *4/*17 variant were reprogrammed by nucleofection of a combination of two episomal-based plasmids omitting pathway (TGF β , MEK and GSK3 β) inhibition. The induced pluripotent stem cells (iPSCs) were characterized by immunocytochemistry, embryoid body formation, DNA-fingerprinting and karyotype analysis. Comparative transcriptome analyses with human embryonic stem cell lines H1 and H9 revealed a Pearson correlation of 0.9243 and 0.9619 respectively.

Publication Status: published in *Stem Cell Research*. 2017 Dec;25:18-21.

Impact Factor: 1.829

This article is reproduced with permission.

Approximated total share of contribution: 10%

Contribution on experimental design, realization and publication:

JA and MB conceived the idea and designed the experiments. MB isolated renal cells from urine and generated the iPSCs. MB isolated genomic DNA of the iPSCs, stained the iPSCs and generated the embryonic bodies generated. LSS and MB performed the flow-cytometric analysis. JE and LSS did the HLA analysis. AN evaluated the CYP2D6 genotyping and phenotyping. WW did the bioinformatic analysis. LSS designed the figures. MB, AN and LSS wrote the manuscript and JA edited it. All authors have read and approved the manuscript.

Link to the publication:

<https://www.sciencedirect.com/science/article/pii/S187350611730209X?via%3Dihub>



Contents lists available at ScienceDirect

Stem Cell Research

journal homepage: www.elsevier.com/locate/scr

Lab Resource: Stem Cell Line

Derivation and characterization of integration-free iPSC line ISRM-UM51 derived from SIX2-positive renal cells isolated from urine of an African male expressing the CYP2D6 *4/*17 variant which confers intermediate drug metabolizing activity



Martina Bohndorf^{a,1}, Audrey Ncube^{a,1}, Lucas-Sebastian Spitzhorn^a, Jürgen Enczmann^b, Wasco Wruck^a, James Adjaye^{a,*}

^a Institute for Stem Cell Research and Regenerative Medicine, Medical Faculty, Heinrich Heine University, 40225 Düsseldorf, Germany

^b Institute of Transplantation Diagnostics and Cell Therapeutics, Medical Faculty, Heinrich Heine University, 40225 Düsseldorf, Germany

ARTICLE INFO

Article history:

Received 29 June 2017

Received in revised form 7 September 2017

Accepted 3 October 2017

Available online 07 October 2017

ABSTRACT

SIX2-positive renal cells isolated from urine from a 51 year old male of African origin bearing the CYP2D6 *4/*17 variant were reprogrammed by nucleofection of a combination of two episomal-based plasmids omitting pathway (TGf β , MEK and GSK3 β) inhibition. The induced pluripotent stem cells (iPSCs) were characterized by immunocytochemistry, embryoid body formation, DNA-fingerprinting and karyotype analysis. Comparative transcriptome analyses with human embryonic stem cell lines H1 and H9 revealed a Pearson correlation of 0.9243 and 0.9619 respectively.

© 2017 The Authors. Published by Elsevier B.V. This is an open access article under the CC BY-NC-ND license (<http://creativecommons.org/licenses/by-nc-nd/4.0/>).

Resource table.

Unique stem cell line identifier	HHUUKDi001-A
Alternative name of stem cell line	ISRM-UM51
Institution	Institute for Stem Cell Research and Regenerative Medicine
Contact information of distributor	James Adjaye, James.Adjaye@med.uni-duesseldorf.de
Type of cell line	iPSC
Origin	Human
Additional origin info	Applicable for human ESC or iPSC Age: 51 Sex: Male Ethnicity if known: African
Cell Source	SIX2-positive renal cells isolated from urine
Method of reprogramming	Episomal-based plasmid expressing OCT4, SOX2, NANOG, KLF4, c-MYC and LIN28
Associated disease	none
Method of modification	n/a
Gene correction	NO
Name of transgene or resistance	none
Inducible/constitutive system	n/a

(continued)

Date archived/stock date	08.10.2016
Cell line repository/bank	n/a
Ethical approval	Ethical committee of the medical faculty of Heinrich Heine University, Düsseldorf, Germany Approval number: 5704

Resource utility

SIX2-positive renal cells derived iPSCs are more efficient for the differentiation into distinct kidney cell types. Furthermore, the African origin and CYP2D6 *4/*17 variant will enable better screening for drugs and toxicology studies.

Resource details

SIX2 and CD133 positive renal cells (Fig. 1A) isolated from urine of a 51 year old male (UM51) were reprogrammed by nucleofection of a combination of two episomal-based plasmids (7F1) expressing OCT4, SOX2, NANOG, LIN28, c-MYC and KLF-4. The resulting iPSC line ISRM-UM51 (Fig. 1B) expresses the pluripotency-associated transcription factors OCT4, NANOG, SOX2 and cell surface markers SSEA-4, TRA-1-60 and TRA-1-81 (Fig. 1C). Pluripotency was further demonstrated by SSEA4 flow cytometry (Fig. 1E) and also *in vitro* by embryoid body (EB)-based differentiation into cell types representative of the three

* Corresponding author.

E-mail address: james.adjaye@med.uni-duesseldorf.de (J. Adjaye).¹ These authors contributed equally to the work.

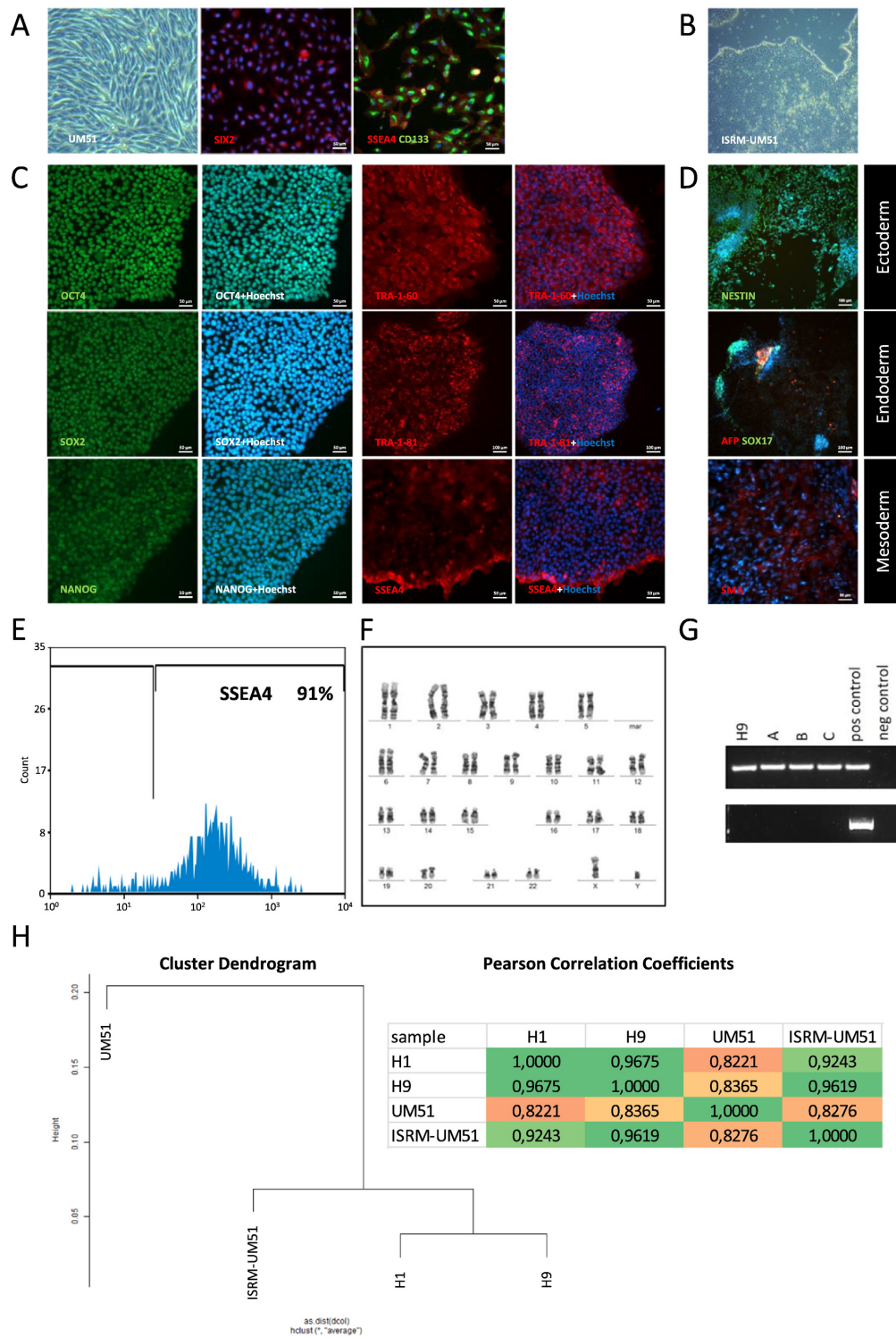


Fig. 1. Characterisation of ISRM-UM51.

Table 1
Characteristics of ISRM-UM51.

Classification	Test	Result	Data
Morphology Phenotype	Photography	Normal	Fig. 1 panel B
	Immunocytochemistry	Expression of pluripotency- associated markers: OCT4, NANOG, SOX2, TRA-1-G0, TRA-1-81 and SSEA4	Fig. 1 panel C
Genotype	Flow cytometry	Expression of pluripotency marker SSEA4	Fig. 1 panel E
	Karyotype (G-banding) and resolution	46 XY 150–300 Bd	Fig. 1 panel F
Identity	Microsatellite PCR (mPCR)	Not tested	–
	STR analysis	PCR, two sites tested, matched	Supplementary File 1
Mutation analysis (IF APPLICABLE)	Sequencing	Not tested	–
	Southern Blot OR WGS	Not tested	–
Microbiology and virology	Mycoplasma	Mycoplasma testing by PCR	Supplementary File 2
		Negative	–
Differentiation potential	Embryoid body formation OR Teratoma formation OR Scorecard	Expression of germ layer-specific proteins Ectoderm: Nestin Endoderm: AFP/SOX17 Mesoderm: SMA	Fig. 1 panel D
Donor screening (OPTIONAL)	HIV 1 + 2 Hepatitis B, Hepatitis C	Not tested	–
Genotype additional info (OPTIONAL)	Blood group genotyping	Not tested	–
	HLA tissue typing	A*03:01,33:01 B*08:01,53:01C*04:01/09N,07:02 DRB1*07:01,13:01 DQB1*02:02,06:03.	–

germ layers- endoderm (SOX17 and AFP), ectoderm (NESTIN) and mesoderm (SMA) (Fig. 1D). Chromosomal content analysis revealed a normal 46, XY karyotype (Fig. 1F). Confirmation of vector dilution in ISRM-UM51 was carried out by analysing mRNA expression of endogenous *OCT4* (top panel) and exogenous/vector expressed *OCT4* (lower panel) (Fig. 1G). Comparative transcriptome and cluster analysis with the human embryonic stem cell lines H1 and H9 revealed a Pearson correlation of 0.9243 and 0.9619 respectively (Fig. 1H). DNA fingerprinting confirmed the origin of ISRM-UM51 based on the primers D17S1290 and D21S2055 (Supplementary File 1). A PCR-based Mycoplasma contamination test was negative (Supplementary File 2).

The HLA-genotype of UM51 is: A*03:01,33:01 B*08:01,53:01C*04:01/09N,07:02 DRB1*07:01,13:01 DQB1*02:02,06:03. For further functional analysis, the CYP2D6 variant was determined. CYP2D6 is a highly polymorphic gene, with more than 70 distinct allele variants. It is involved in the metabolism of nearly all drugs; genetic variability affects the impact of drugs, which might lead to deficiencies or toxicity. For individuals with high CYP2D6 activity usual drug doses are not sufficient, as medication is degraded quickly. In contrast, individuals with low or missing CYP2D6 activity normal drug doses might be toxic. The four distinct CYP2D6 phenotypes are defined as poor metabolizer (PM), intermediate metabolizer (IM), extensive metaboliser (EM) and ultra-rapid metaboliser (UM) (Pinto and Dolan, 2011). UM51 has the CYP2D6 *4/*17 genotype conferring an intermediate metabolizing activity. This knowledge can be used for future personalized drug testing, screening and toxicology studies (Supplementary File 3).

Materials and methods

Cell culture

Approximately 200 ml of fresh urine (UM51) were centrifuged at 400g for 10 min. Thereafter the supernatant was discarded then 2 ml (in each well of a 6 well plate) of expansion medium consisting of high-glucose Dulbecco's Modified Eagle's Medium (DMEM) supplemented with 1% Penicillin-Streptomycin (Penstrep), 1% Glutamine, 10% fetal calf serum and SingleQuot Kit CC-4127 REGM (Lonza) added to resuspend cell pellet. The cells were cultured at 37 °C, 5% CO₂ and 5% O₂. This protocol is a modification from Zhou et al. (2011).

ISRM-UM51, HESC-H1 and H9 were cultured in StemMACS iPS-Brew XF Medium with 1% Penstrep on Matrigel at 37 °C and 5% CO₂. All cell lines were split once per week.

Derivation of iPSCs

Approximately 250,000 SIX2-positive renal cells derived from UM51 were reprogrammed into iPSCs by nucleofection of an episomal-based plasmid combination (Kobayashi et al., 2008; Yu et al., 2011), but omitting pathway inhibitors: TGFβ/SB431245, MEK/PD0325901 and GSK3β/CHIR99021. Vector dilution was confirmed by PCR (Fig. 1G) (Table 1).

DNA fingerprinting analysis

The STR analysis was performed by PCR using primers D17S1290 and D21S2055 (Supplementary File 1). Primer sequences are shown in Table 2.

CYP2D6 genotyping and phenotyping

The assay was carried on genomic DNA outsourced to CeGat GmbH-Germany (Supplementary File 3). The pharmacogenetics (PGx) profile (Table A) gives information on a patient's genotype and phenotype based on tested pharmacogenetic markers. Genotype information is derived from genetic analysis, from which the phenotype can be determined. The Organization (CPIC or DPWG) indicates where the genotype/phenotype interpretation is derived from.

Under foreseeable drug-PGx interactions (Table B) are variant phenotypes and related drugs for which dosage guidelines exist. Additionally the FDA/EMA drug label contains relevant PGx information classified as "required, recommended or actionable". Genetic variants may influence drug efficacy or the risk of adverse drug reactions, hence guidelines of drug label recommendations should be considered when prescribing such drugs.

Embryoid body (EB) formation

To confirm pluripotency of the cultured iPSCs, EB formation was performed. First, iPSCs were cultured normally on Matrigel coated plates until sub-confluent. The cells were further cultured for a week in a T25 flask in high glucose DMEM, containing 1% NEAA. Afterwards, EBs were settled for 3–4 days on a gelatin coated 12-well plate in preparation for antibody staining. Cells were fixed with 4% paraformaldehyde (PFA) and immunocytochemistry (ICC) performed. To visualize differentiated cells, markers for all three germ layers were employed. The

Table 2
Antibodies used for immunocytochemistry/flow-cytometry.

	Antibody	Dilution	Company Cat # and RRID
Flow-cytometry	Anti-SSEA-4-PE	1:11	Miltenyi Biotec Cat# 130-098-369, RRID:AB_2653519
Renal progenitor marker	SIX2	1:200	Proteintech Group Cat# 11562-1-AP, RRID:AB_2189084
Pluripotency markers	CD133	1:500	US Biological Cat# C2514-90B, RRID:AB_2284567Boster Biological; PA2049
Pluripotency markers	Rabbit anti-OCT4	1:400	Cell Signaling Technology Cat# 2840S, RRID:AB_2167691
Pluripotency markers	Rabbit anti-SOX2	1:400	Cell Signaling Technology Cat# 3579S, RRID:AB_2195767
Pluripotency markers	Rabbit anti-NANOG	1:800	Cell Signaling Technology Cat# 4903S, RRID:AB_10559205
Pluripotency markers	Mouse anti-Tra-1-60	1:1000	Cell Signaling Technology Cat# 4746S, RRID:AB_2119059
Pluripotency markers	Mouse anti-Tra-1-81	1:1000	Cell Signaling Technology Cat# 4745S, RRID:AB_2119060
Pluripotency markers	Mouse anti-SSEA4	1:1000	Cell Signaling Technology Cat# 4755S, RRID:AB_1264259
Differentiation markers	Mouse anti-Sox17	1:50	R and D Systems Cat# AF1924, RRID:AB_355060
Differentiation markers	Rabbit anti-AFP	1:200	Cell Signaling Technology Cat# 2137S, RRID:AB_2209744
Differentiation markers	anti-Nestin	1:250	Sigma-Aldrich Cat# N5413, RRID:AB_1841032
Differentiation markers	anti-aSMA	1:1000	Dako Cat# M0851, RRID:AB_2223500
Secondary antibodies	anti-mouse-Cy3	1:2000	Thermo Fisher Scientific Cat# A10521, RRID:AB_2534030
Secondary antibodies	anti-rabbit-Alexa488	1:2000	Thermo Fisher Scientific Cat# A27034, RRID:AB_2536097
Nuclear Co-Staining	Hoechst	1:5000	Thermo Fisher Scientific Cat# H3569, RRID:AB_2651133
Primers			
	Target		Forward/Reverse primer (5'-3')
Episomal Plasmids (qPCR)	OCT4 Plasmid		AGTGAGAGGCAACTGGAGA/AGGAAGCTGCTTCCTCACGA
Fingerprinting	D17S1290		GCAACAGAGCAAGACTGTC/GGAAAACAGTAAATGGCCAA
Fingerprinting	D21S2055		AACAGAACCAATAGGCTATCTATC/TACAGTAAATCACTTGGTAGGAGA
Mycoplasma	16 S rRNA gene		GGGAGCAACAGGATTAGATACCTC/TGCACCATCTGCTACTCTGTTAACCTC

primary antibodies used were incubated overnight at 4 °C; SMA (mesoderm), SOX17 and AFP (endoderm) and NESTIN (ectoderm). After washing, secondary antibody (Cy3, Alexa488) incubation followed for 1 h at room temperature (RT). Co-staining was accomplished using nuclear Hoechst. Dilutions and companies are shown in Table 2. Images were captured using a fluorescence microscope (LSM700; Zeiss).

Flow-cytometry and immunofluorescence-based detection of pluripotency associated proteins

Flow-cytometric analysis using a PE-labelled SSEA4 antibody was carried out using the CyAn device from Dako. To confirm pluripotency of the cultured iPSCs, ICC for pluripotency-associated markers was performed. Primary antibodies SOX2, OCT4, NANOG, TRA-1-60, TRA-1-81 and SSEA4 were used. After fixation of the cells with 4% paraformaldehyde and blocking of unspecific binding-sites with a self-made blocking buffer (10% normal goat serum, 1% bovine serum albumin, 0.5% Triton, 0.05% Tween in PBS) the primary antibodies were incubated overnight at 4 °C, followed by secondary antibody (Alexa488, Cy3) incubation as described above.

Karyotype analysis

Analysis of the karyotype was performed at the Institute of Human Genetics and Anthropology, Heinrich-Heine-University, Düsseldorf.

Microarray-based transcriptome analysis

Global gene expression analysis was carried out on the Affymetrix microarray platform. Total RNA (1 µg) preparations and hybridizations were carried out by the Biologisch-medizinisches Forschungszentrum (BMFZ), Heinrich-Heine University, Düsseldorf. The dendrogram calculated using the package affy of the R/Bioconductor software (Gentleman et al., 2004).

HLA-genotyping analysis

The HLA-Genotyping of UM51 was performed on genomic DNA isolated from cultured cells as well as on cells derived from a buccal swab of the corresponding donor. HLA-typing was done at the Institute for Transplantation Diagnostics and Cell Therapeutics (ITZ) at the University Hospital Düsseldorf which represents an American Society for Histocompatibility and Immunogenetics (AHSI) accredited laboratory.

Acknowledgements

J.A. acknowledges support from the Medical faculty of Heinrich-Heine University Düsseldorf and the Bundesministerium für Wirtschaft und Energie (BMWi) FKZ: ZF4047101AJ5.

Appendix A. Supplementary data

Supplementary data to this article can be found online at <https://doi.org/10.1016/j.scr.2017.10.004>.

References

- Gentleman, R.C., Carey, V.J., Bates, D.M., Bolstad, B., Dettling, M., Dudoit, S., Ellis, B., Gautier, L., Ge, Y., Gentry, J., Hornik, K., Hothorn, T., Huber, W., Iacus, S., Irizarry, R., Leisch, F., Li, C., Maechler, M., Rossini, A.J., Sawitzki, G., Smyth, C., Smyth, G., Tierney, L., Yang, J.Y.H., Zhang, J., 2004. Bioconductor: open software development for computational biology and bioinformatics. *Genome Biol.* 5, R80.
- Kobayashi, A., Valerius, M.T., Mugford, J.W., Carroll, T.J., Self, M., Oliver, G., McMahon, A.P., 2008. Six2 defines and regulates a multipotent self-renewing nephron progenitor population throughout mammalian kidney development. *Cell Stem Cell* 3 (2), 169–181.
- Pinto, N., Dolan, M.E., 2011. Clinically relevant genetic variations in drug metabolizing enzymes. *Curr. Drug Metab.* 12, 487–497.
- Yu, J., Chau, K.F., Vodyanik, M.A., Jiang, J., Jiang, Y., 2011. Efficient feeder-free episomal reprogramming with small molecules. *PLoS One* 6:e17557. <https://doi.org/10.1371/journal.pone.0017557>.
- Zhou, T., Benda, C., Duzinger, S., Huang, Y., Li, X., Li, Y., Guo, X., Cao, G., Chen, S., Hao, L., Chan, Y.-C., Ng, K.-M., Ho, J.C., Wieser, M., Wu, J., Redl, H., Tse, H.-F., Grillari, J., Grillari-Voglauer, R., Pei, D., Esteban, M.A., 2011. Generation of induced pluripotent stem cells from urine. *J. Am. Soc. Nephrol.* JASN 22, 1221–1228.

Part 2: Translational Applications of iPSCs, MSCs and iMSCs *in vitro* and *in vivo*

2.5 Use of Stem Cells in Toxicology

Peggy Matz, Lucas-Sebastian Spitzhorn, Jörg Otte, Marie-Ann Kawala, Julia Woestmann, Hatice Yigit, Wasco Wruck and James Adjaye

Introduction

Within the context of animal experimentation, the 3Rs are acronyms for replace, reduce, and refine meaning that animal tests - ordered by priority - should be replaced, be reduced, or at least take place under the best possible conditions for the animals (refine). To date, toxicology screens necessitate the use of significant numbers of animals, for example, the EU program REACH Registration, Evaluation, Authorisation and Restriction of Chemicals (REACH) shall assess the hazard risk of 30,000 chemicals involving estimated up to 54 million additional animals. Alternative testing strategies in the spirit of the 3Rs can achieve a reduction to below 10 million animals. Such an approach is based on human induced pluripotent stem cell (iPSC)-derived cell types for toxicity testing and drug development. iPSCs have the unique capacity to self-renew in the undifferentiated state *in vitro* while maintaining their ability to differentiate into a broad number of cell types. In addition, iPSCs can be generated from somatic cells of existing individuals with known genetic characteristics. These iPSC-derived hepatocytes, cardiomyocytes, or neuronal cells can model *in vitro* the patient's genetic disease or metabolic capability, thereby adding a further dimension to the current toxicity testing platforms. An iPSC-HLC-based strategy thus allows large-scale studies impossible to perform in mice, on human primary cell cultures, or from biopsies and also enables studies on hepatocytes genetically susceptible to drug-induced liver injury as *in vitro* models with genotypic relevance for toxicology screening. By employing patient-specific iPSC-derived hepatocytes, neurons, or cardiomyocytes and systems biology models, we can find strategies to reduce or -where possible- to replace animal tests. Systems biology modelling can provide whole-body human toxicokinetic data by *in silico* and *in vitro*

methods assessing absorption, distribution, metabolism, and excretion (ADME) processes. These human-specific models can partly circumvent drawbacks of animal models, which cannot fully reflect the human condition.

Publication Status: published in Samuel Chackalamannil, David P Rotella and Simon E Ward, (eds.) *Comprehensive Medicinal Chemistry III* vol. 4, pp. 177–194. Oxford: Elsevier. ISBN: 9780128032008

Impact Factor (2017): -

This article is reproduced with permission.

Approximated total share of contribution: 15%

Contribution on experimental design, realization and publication:

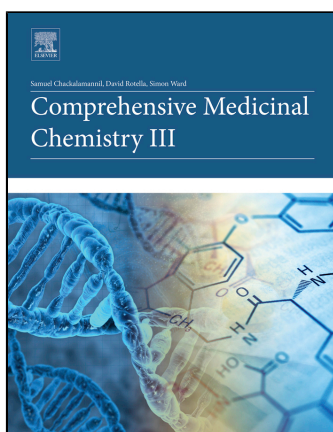
LSS was responsible for the section “4.10.3 Induced Pluripotent Stem Cell-Derived Hepatocytes”. All authors have read and approved the manuscript.

Link to the publication:

<http://dx.doi.org/10.1016/B978-0-12-409547-2.12380-7>

**Provided for non-commercial research and educational use.
Not for reproduction, distribution or commercial use.**

This article was originally published in *Comprehensive Medicinal Chemistry III*, published by Elsevier, and the attached copy is provided by Elsevier for the author's benefit and for the benefit of the author's institution, for non-commercial research and educational use including without limitation use in instruction at your institution, sending it to specific colleagues who you know, and providing a copy to your institution's administrator.



All other uses, reproduction and distribution, including without limitation commercial reprints, selling or licensing copies or access, or posting on open internet sites, your personal or institution's website or repository, are prohibited. For exceptions, permission may be sought for such use through Elsevier's permissions site at:

<https://www.elsevier.com/about/our-business/policies/copyright/permissions>

From Matz, P., Spitzhorn, L. S., Otte, J., Kawala, M. A., Woestmann, J., Yigit, H., Wruck, W., Adjaye, J. (2017) Use of Stem Cells in Toxicology. In: Samuel Chackalamannil, David P Rotella and Simon E Ward, (eds.) *Comprehensive Medicinal Chemistry III* vol. 4, pp. 177–194. Oxford: Elsevier. <http://dx.doi.org/10.1016/B978-0-12-409547-2.12380-7>

ISBN: 9780128032008

Copyright © 2017 Elsevier Ltd. All rights reserved

Elsevier

4.10 Use of Stem Cells in Toxicology

P Matz, L-S Spitzhorn, J Otte, M-A Kawala, J Woestmann, H Yigit, W Wruck, and J Adjaye, Institute for Stem Cell Research and Regenerative Medicine, Düsseldorf, Germany

© 2017 Elsevier Ltd. All rights reserved.

4.10.1	Introduction	178
4.10.2	Pluripotent Stem Cells	178
4.10.3	Induced Pluripotent Stem Cell-Derived Hepatocytes	180
4.10.4	Induced Pluripotent Stem Cell-Derived Neuronal Cells	182
4.10.5	Induced Pluripotent Stem Cell-Derived Cardiomyocytes	183
4.10.6	Induced Pluripotent Stem Cell-Derived Organoids	183
4.10.6.1	Liver Organoids	186
4.10.6.2	Brain Organoids	186
4.10.6.3	Heart Organoids	187
4.10.7	Use of Induced Pluripotent Stem Cells for Toxicogenomics	187
4.10.8	The 3Rs	189
References		189

Abbreviations

ABC Adenosine triphosphate-binding cassette	EGF Epidermal growth factor
AD Alzheimer's disease	ESCs Embryonic stem cells
ADME Absorption, distribution, metabolism, and excretion	EURL-ECVAM The European Union Reference Laboratory for alternatives to animal testing
AFP α -Fetoprotein	FBS Fetal bovine serum
ALK Transforming growth factor beta receptor (TGFBR)	GSK-3 β Glycogen synthase kinase 3 beta
ALS Amyotrophic lateral sclerosis	GST Glutathione S-transferase
AP Action potential	HDAC Histone deacetylase
aspirin Acetylsalicylic acid	hESCs Human embryonic stem cells
ATP Adenosine triphosphate	HGF Hepatocyte growth factor
bFGF Basic fibroblast growth factor	HIF Hypoxia inducible factor
BMP4 Bone morphogenetic protein 4	HIF PHD1 Hypoxia-inducible factor PHD1
CAS9 CRISPR- Associated endonuclease 9	HLA Human leukocyte antigen
CAT Catalase	HLCs Hepatocyte-like cells
CBR Carbonyl reductase	ICM Inner cell mass
CDA Cytidine deaminase	iHeps Induced hepatocyte cells
CHST Carbohydrate sulfotransferase	iPSCs Induced pluripotent stem cells
CRISPR Clustered regularly interspaced short palindromic repeats	iPSC-CM Induced pluripotent stem cell-derived cardiomyocytes
CYP Cytochromes	JLNS Jervell and Lange-Nielsen syndrome
CYP2D6 Cytochrome P450 family 2 subfamily D member 6	KCNH2 Potassium voltage-gated channel subfamily H member 2
CYP3A4 Cytochrome P450 family 3 subfamily A member 4	KLF4 Krueppel-like factor 4
DEX Dexamethasone	LIN28 Lin-28 homologue A (<i>C. elegans</i>)
DHRS Dehydrogenase/reductase	LQT2 Long QT syndrome
DILI Drug-induced liver injury	LSD1 Zinc finger protein
DMSO Dimethyl sulfoxide	MEA Microelectrode array
DNA Deoxyribonucleic acid	MEF Mouse embryonic fibroblast
DNMT DNA (cytosine-5)-methyltransferase	c-Myc Myelocytomatosis viral oncogene homologue
3-D Three-dimensional	mRNA Messenger ribonucleic acid
EBs Embryoid bodies	miRNA Micro-ribonucleic acid
EBNA-1 Epstein-Barr nuclear antigen 1	MRP Multidrug resistance-associated protein
ECM Extracellular matrix	NANOG Nanog homeobox

NAT N-acetyltransferase	SOD Superoxide dismutase
NES Nestin	SOX2 Sex-determining region Y (SRY)-box 2
NPCs Neural progenitor cells	SOX17 Sex-determining region Y (SRY)-box 17
OCT4 Octamer-binding protein 4/POU class 5 homeobox 1	SSEA-4 Stage-specific antigene 4
OECD Organisation for Economic Co-operation and Development	SULT Sulfotransferase
oriP Origin of plasmid replication	SVM Support vector machine
OSM Oncostatin M	SV40LT Simian virus 40 large T antigen
PBTK Physiologically based toxicokinetic	TALEN Transcription activator-like effector nuclease
PDK1 Pyruvate dehydrogenase kinase 1	TdP Torsades de pointes
PHH Primary human hepatocytes	TG-GATE Toxicogenomics database
PPARD Peroxisome proliferator-activated receptor delta	TGF β Transforming growth factor β
PPARG Peroxisome proliferator-activated receptor gamma	TGP Japanese Toxicogenomics Project consortium
p53 Tumor protein p53	TK Toxicokinetic
QSAR Quantitative structure–activity relationship	TRA-1-60 Tumor-related antigen-1–60
REACH Registration, Evaluation, Authorisation and Restriction of Chemicals	TRA-1-81 Tumor-related antigen-1–81
ROS Reactive oxygen species	TRA-2-49 Tumor-related antigen-2–49, alkaline phosphatase
RXRA Retinoid X receptor alpha	TUJ1 Neuron-specific class III β -tubulin, β -tubulin III
SERPINA7 Serpin family A member 7	UDP Uridine diphosphate
SLC Solute carrier	UGT Uridine diphosphate glucuronosyltransferase
α -SMA α -Smooth muscle actin	WNT3a Wingless-type MMTV integration site family, member 3a
SNP Single nucleotide polymorphism	

4.10.1 Introduction

Within the context of animal experimentation, the 3Rs are acronyms for replace, reduce, and refine meaning that animal tests—ordered by priority—should be replaced, be reduced, or at least take place under the best possible conditions for the animals (refine). To date, toxicology screens necessitate the use of significant numbers of animals, for example, the EU program REACH Registration, Evaluation, Authorisation and Restriction of Chemicals (REACH) shall assess the hazard risk of 30,000 chemicals involving estimated up to 54 million additional animals. Alternative testing strategies in the spirit of the 3Rs can achieve a reduction to below 10 million animals. Such an approach is based on human induced pluripotent stem cell (iPSC)-derived cell types for toxicity testing and drug development. iPSCs have the unique capacity to self-renew in the undifferentiated state in vitro while maintaining their ability to differentiate into a broad number of cell types. In addition, iPSCs can be generated from somatic cells of existing individuals with known genetic characteristics. These iPSC-derived hepatocytes, cardiomyocytes, or neuronal cells can model in vitro the patient's genetic disease or metabolic capability, thereby adding a further dimension to the current toxicity testing platforms. An iPSC–HLC-based strategy thus allows large-scale studies impossible to perform in mice, on human primary cell cultures, or from biopsies and also enables studies on hepatocytes genetically susceptible to drug-induced liver injury as in vitro models with genotypic relevance for toxicology screening. By employing patient-specific iPSC-derived hepatocytes, neurons, or cardiomyocytes and systems biology models, we can find strategies to reduce or—where possible—to replace animal tests. Systems biology modeling can provide whole-body human toxicokinetic data by in silico and in vitro methods assessing absorption, distribution, metabolism, and excretion (ADME) processes. These human-specific models can partly circumvent drawbacks of animal models, which cannot fully reflect the human condition.

4.10.2 Pluripotent Stem Cells

The focus of this article will be on the application of human pluripotent stem cells, which encompass both embryonic and induced pluripotent stem cells.

Human embryonic stem cells (hESCs) are derived from the inner cell mass (ICM) of blastocyst-stage embryos. hESCs can be differentiated into all cell types present in the three embryonic germ layers, endoderm (e.g., cells of the gastrointestinal tract), ectoderm (e.g., cells of the nervous system), mesoderm (e.g., cells of the bone and muscle), and also germ cells.

Currently, there are over 400 human embryonic stem cell (hESC) lines established but only a few of these are well characterized (lines H1 and H9) and used by most laboratories worldwide.^{1,2}

To bypass ethical and moral concerns, scientists searched for alternative ways to derive embryonic stem cell-like cells. Takahashi and Yamanaka were the first to successfully derive induced pluripotent cells (iPSCs) from mouse fibroblasts. In 2006, they published the reprogramming of mouse fibroblasts to iPSCs employing retroviral transduction and coerced expression of transcription factors, which are normally only expressed in embryonic stem cells.³ Shortly after that, two groups managed the reprogramming of human adult fibroblasts with viral transfection and overexpression of four transcription factors OCT4, SOX2, KLF4, and c-MYC⁴ or OCT4, SOX2, NANOG, and LIN28.⁵

To generate iPSCs, transformation is attained by the use of *KLF4* and *c-MYC*. *c-MYC* affects p53-dependent apoptosis in fibroblasts, which is in all probability repressed by *KLF4*. *KLF4* activates *p21* and affects proliferation. For this reason, the balance between *c-MYC* and *KLF4* during the reprogramming process is critical. Furthermore, *c-MYC* enhances the expression of embryonic stem cell-specific genes by activating histone acetylase complexes. The enforced expression of *c-MYC* and *KLF4* can lead to the formation of tumors. Probably OCT4 channels the cell from tumor to induced pluripotent cells. OCT4 and SOX2 synergistically activate target pluripotency-associated genes during the reprogramming process.^{6,7}

The requirement of specified amounts of each transcription factor needed for the reprogramming process is realized in a small number of transfected cells. This could also be an explanation for the low efficiency of iPSC generation (>1%). Each cell type needs maybe another combination of factors and different amounts of each factor to achieve higher efficiencies of reprogramming.³

Induced pluripotent stem cells have the same properties as human embryonic stem cells, which are pluripotency, self-renewal, and the expression of surface markers such as SSEA-4, TRA-1-60, TRA-1-81, and TRA-2-49 (alkaline phosphatase) and transcription factors, for example, OCT4, NANOG, and SOX2.^{4,5,8} Pluripotency is assayed both in vivo by the formation of teratomas when they are injected into immunodeficient mice and also in vitro by the formation of embryoid bodies (EBs). These EBs have the innate capacity to differentiate into endodermal lineages (expressing the marker genes *SOX17* and *AFP*), mesodermal lineages (expressing the marker genes α -SMA and *brachyury*), and ectodermal lineages (expressing the marker genes *TUJ1* and *Nestin*).⁴ A typical assay to demonstrate pluripotency in vitro is shown in Fig. 1.

The efficiency of reprogramming human fibroblasts to iPSCs by using retroviruses to transduce OCT4, SOX2, KLF4, and *c-MYC* is approximately 0.02%.³ The reprogramming of human fibroblasts to iPSCs through transduction of lentiviral constructs carrying OCT4, SOX2, NANOG, and LIN28 had an efficiency of 0.02–0.0095%.⁵ Both methods are robust due to the fact that numerous groups have been able to reproduce the protocols. In addition, there are still unresolved problems, such as the random integration of proviruses into the genome of the reprogrammed cells and the fact that *KLF4* and *c-MYC* are oncogenes that could be reactivated. These conditions cause a high probability of genomic instability and mutagenesis in iPSCs.¹⁰ To enable regenerative medicine applications in the future, safer reprogramming by using fewer factors with OCT4, SOX2, and *KLF4* but omitting *c-MYC* has been suggested.¹¹ To increase the efficiency of the viral reprogramming method, additional factors have been used such as the viral oncogene SV40LT, which enhances the efficiency of iPSC generation from fibroblasts by inhibition of p53. It has been demonstrated that the inhibition of p53 enhances the iPSC generation from human fibroblasts up to 100-fold.¹² Furthermore, Wang and Adjaye demonstrated that transient inhibition of p53 can increase the efficiency of reprogramming human dermal fibroblasts by approximately sevenfold.¹³

Over the years, a large number of somatic cell types have been reprogrammed, for example, fibroblasts, keratinocytes, amniotic fluid cells, and chorionic villi cells.^{5,14–17} The integration of proviruses into genome of viral-derived iPSCs is a risk factor for clinical applications in the future.¹⁸ To avoid this, nonviral integration protocols have been established.¹⁹ Additionally, mRNA, miRNA, and protein-based reprogramming have been established as reviewed in Tavernier et al.²⁰

Nonintegration reprogramming methods are established and standardized. Reagents and kits of various methods are also available on the market. One can select from the following methods: Sendai viral, episomal, and mRNA transfection. Sendai virus particles are used to infect the donor cells with RNA, which encode the reprogramming factors *OCT4*, *SOX2*, *c-MYC*, and *KLF4* without integration into the host genome.²¹ The episomal vectors are derived from the Epstein–Barr virus without the viral packaging. These oriP/EBNA1 vectors contain DNA of the reprogramming factors *OCT4*, *SOX2*, *NANOG*, *LIN28A*, *c-MYC*, and *KLF4* and express these independently.^{22,23} In vitro transcribed mRNAs of *OCT4*, *SOX2*, *LIN28A*, *c-MYC*, and *KLF4* have been transfected using the mRNA reprogramming method.²⁴ The mRNA method is the most inefficient and cumbersome protocol for reprogramming and is not applicable to all cell types. Due to the very short half-life of the mRNAs, daily, up to 7 days transfections are necessary to induce pluripotent stem cells. However, the main advantage of using mRNA to derive iPSCs is the absence of any exogenous viral or plasmid DNA in the host genome.²⁵

Recently, numerous studies have been published in demonstrating reprogramming somatic cells with supplementation with small molecules, in addition to the Yamanaka factors.^{26,27} Small molecules such as the cyclic AMP analog 8-Br-cAMP, valproic acid (a histone deacetylase inhibitor), and thiazovivin enhance reprogramming efficiency of human somatic cells.^{10,13,26} Additionally, there exists a list of small-molecule compounds with the potential for replacing the Yamanaka factors. However, most compounds to date function more in reprogramming mouse cells.²⁸ Table 1 lists a selection of small molecules, which increase the efficiency of reprogramming human somatic cells (modified from Lin and Wu 2015).²⁸

In summary, iPSCs are promising in vitro tools for the application in tissue replacement therapies, for the generation of disease models, and for drug screening and toxicology studies.

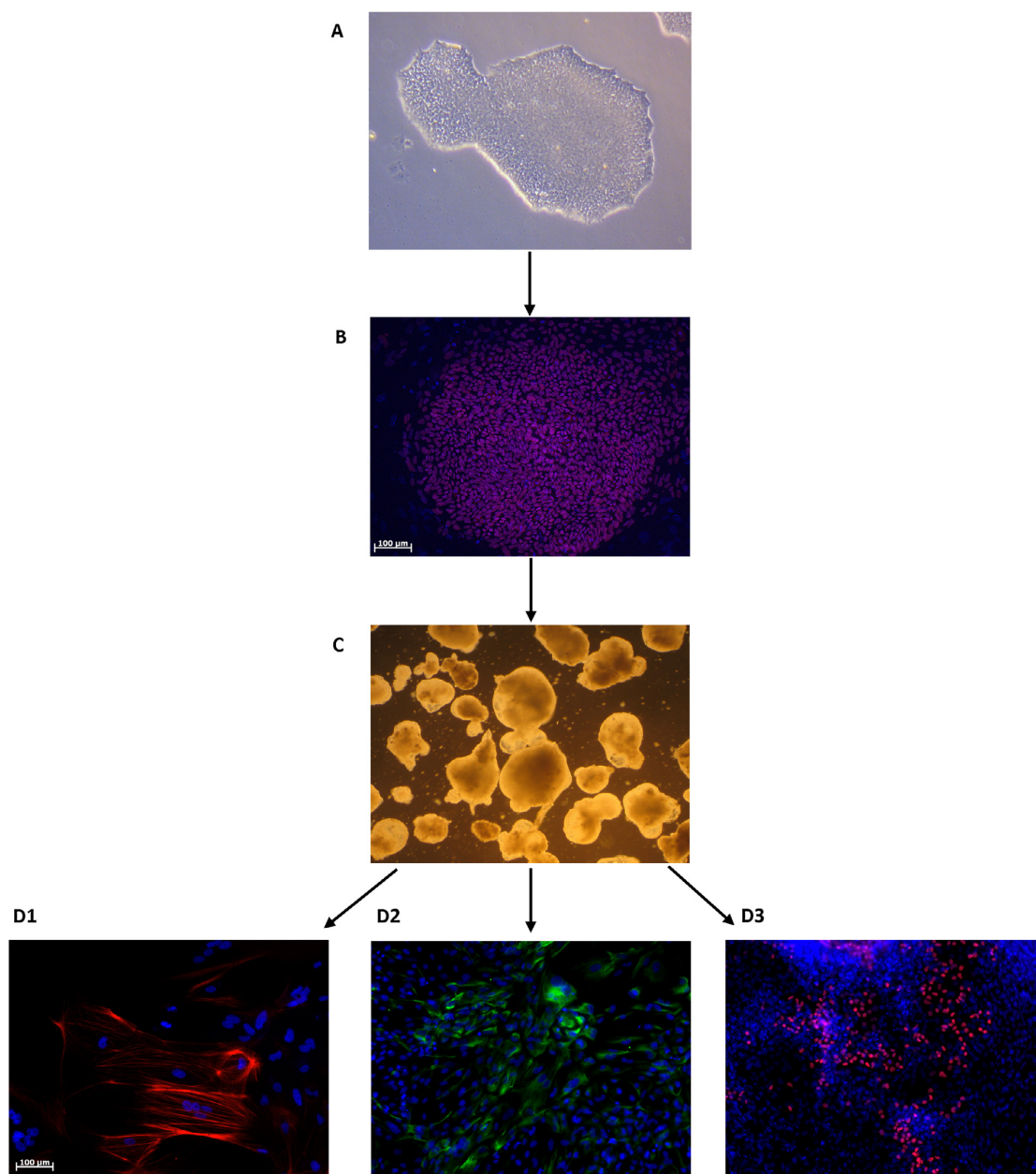


Fig. 1 iPS cells used in embryoid body-based differentiation into the three embryonic germ layers. Induced pluripotent stem cell (*iPSC*) colonies (A) express pluripotency-associated transcription factors such as OCT4 (B) and can be differentiated via embryoid bodies (*EBs*) (C) into cell types representative of the three germ layers (D). Immunofluorescence-based detection of expression of alpha-smooth muscle actin (α -*SMA*) identifies the mesoderm germ layer (D1), Nestin (*NES*) ectoderm (D2), and SOX17 endoderm (D3).

4.10.3 Induced Pluripotent Stem Cell-Derived Hepatocytes

The liver is the largest internal organ and is responsible for several key bodily functions such as metabolizing glucose and fatty acids and degradation of exogenous and endogenous toxins. There are several liver-associated diseases such as fatty liver, steatosis, and hepatitis. A broad range of mechanisms are associated with xenobiotic hepatotoxicity, for example, reactive metabolites, formation of reactive oxygen species (ROS) and impaired transporter, and cytochrome activities.^{35,36}

Table 1 Small molecules used for increasing the efficiency of reprogramming human somatic cells into iPSCs

Signaling pathway or target	Name of compound	Efficiency	Ref
ALK4, ALK5, ALK7 inhibitors	SB431542	~200-fold	26
cAMP-dependent protein kinase activator	8-Br-cAMP	6.5-fold	29
DNMT inhibitor, histone deacetylase inhibitor	RSC133	Threefold	30
GSK-3 β inhibitor, LSD1 inhibitor	LICL	>10-fold	29
HDAC inhibitor	Sodium butyrate	100-fold	31
HDAC inhibitor	VPA	>100-fold	32
HIF PHD1 and PHD2 inhibitors	<i>N</i> -Oxalylglycine	3.5-fold	33
PDK1 activator	5-(4-Chloro-phenyl)-3-phenyl-pent-2-enoic acid (PS48)	15-fold	33
Phosphofructokinase 1 activator	Fructose-2,6-bisphosphate	Twofold	33
Rho-associated protein kinase inhibitor	Thiazovivin	~200-fold	26
Rho-associated protein kinase inhibitor	Y27632	Improved generation	34
Selective MEK/ERK inhibitor	PD0325901	~200-fold	26
TGF- β inhibitor	A83-01	Sevenfold	33

Modified from Lin, T.; Wu, S., Reprogramming With Small Molecules Instead of Exogenous Transcription Factors. *Stem Cells Int.* **2015**, *2015*, 794632.

Numerous studies have shown that findings in animals cannot be directly extrapolated to human because of species–species differences.³⁷ Current available in vitro models such as liver cancer cell lines and primary human hepatocytes (PHH) have been established to circumvent animal studies.³⁸ Advantages of PHHs are the functional cellular architecture, but unfortunately, these cells cannot be kept in culture for long periods.³⁹ Primary hepatocytes of course are ideal for appropriate drug and toxicity screens due to their high metabolic and functional properties.⁴⁰ However, there are several shortfalls associated with the use of primary hepatocytes, among these are variability between donors, low number of donors, and rapid decrease of cell-specific function in vitro.³⁵ The lack of healthy liver sample donors and the high variability between the samples are shortfalls associated with the use of primary liver cell. Due to this and the poor expandability, these cells are of limitation for high-throughput drug screening and toxicological studies. The current available human liver cell models are somehow limited, and thus, it is of prime importance to find alternatives.⁴¹ Generation of hepatocyte-like cells (HLCs) from induced pluripotent stem cells (iPSCs) could circumvent these drawbacks.^{42,43}

Protocols for generating HLCs are based on stepwise differentiation protocols resembling the developmental process in vivo. Most of these so far developed protocols are dependent on cytokines and growth factors, which try to mirror the partial differentiation stages cells go through to become hepatocytes. The first differentiation stage is the definitive endoderm, which is accomplished by supplementation with activin A and in some protocols WNT3a, bFGF, and BMP4. The second stage is the differentiation into hepatic endoderm, which resembles the bipotential hepatoblast stage in vivo. To attain a certain level of maturity, HGF, OSM, DEX, and insulin are used to advance from the hepatic endoderm to HLC stage. Several protocols for deriving HLCs in vitro have been published (Table 2).^{42,45,46,50–52} Besides the improvement of supplements for derivation of hepatocytes from iPSC, there are several engineering approaches such as micropatterning, microfluidics, and synthetic biomaterials to improve hepatocyte culture for longer periods.³⁸ Another improvement of iPSC-derived hepatocytes with respect to maturity is culturing in three-dimensional (3-D) spheroids in contrast to the standard 2-D culture.⁵² The leading reason why drugs are withdrawn from the market is the induction of drug-induced liver injury (DILI). HLCs could be powerful in predicting such reactions. Numerous groups have shown the functional ability of HLCs to metabolize drugs, which makes it possible to use these cells for toxicology studies.⁵⁴ HLCs can also be used to study host and virus interaction during an infection process like hepatitis C.⁵⁵ The use of iPSC-derived hepatocytes can also enlighten risk potentials of drugs for pregnant women and the fetus. Furthermore, it has been demonstrated that these cells are functional by metabolizing specific drugs although they do not reach the same level of metabolic activity like primary human hepatocytes, which was also shown on gene expression level.^{42,56–59} iPSC-derived hepatocytes are used for drug screening and toxicity tests. Using this approach, it is possible to investigate the influence of the genetics of the outcome of different compounds.⁴³ For example, it has been shown that HLCs with an SNP in CYP2D6 have a higher persistence to tamoxifen, which is metabolized by CYP2D6 into toxic products. In parallel, these cells had a higher sensitivity to desipramine, which is detoxified by this enzyme. Derivation of a panel of HLCs bearing distinct genetic variations and polymorphisms would be a great tool for the evaluation of specific drug dosages for the particular individual.⁵² Furthermore, such a panel of HLCs bearing distinct SNPs and HLA types would be a great tool for high-throughput drug screening and assays on drug metabolism.⁴³ Recently established methods allow gene editing by CRISPR/Cas9 and TALENs, which could be used for the creation of a pool of genetically distinct iPSC-derived hepatocytes.^{43,60} Although transcriptome analysis showed that HLCs share more genes with fetal liver than with adult liver (underlining the lack of maturity in those cells), in vitro HLC differentiation can be used to study the molecular pathways involved in the liver development.

For the future, it will be important to mimic human physiological liver environment in vitro as close as possible to improve the maturity and function of HLCs and thus ensure a better prediction potential for drug screening and toxicology studies.⁴³ The number of studies using iPSC-derived hepatocytes is increasing with more improved protocols and approaches that try to mimic the liver environment. Future research will provide many possibilities for personalized medicine such as specific drug screenings

Table 2 Overview of protocols used to sequentially differentiate iPSCs into HLCs

Surface	Endoderm	Hepatic ectoderm	Hepatic maturation	References
MEF	Activin A, albumin fraction V (1 day) Activin A, albumin fraction V, ITS (2 days)	FGF4, BMP2 (5 days)	HGF (5 days) OSM, DEX (5 days)	44
MEF Matrigel	Activin A (5 days) Activin A (5 days)	FGF4, HGF (6 days) 2BME, DMSO (7 days)	FGF4, HGF, OSM, DEX (9 days) Hydrocortisone 21-hemisuccinate, insulin, HGF, OSM (5 days)	45 46
MEF	Activin A, albumin fraction V (1 day) Activin A, albumin fraction V, ITS (2 days)	FGF2, BMP2 (4 days)	HGF, KGF (6 days) OSM, DEX, (5 days) OSM, DEX 2BME (3 days)	47
Fibronectin	Activin A, FGF2, BMP4, LY294002 (3 days)	FGF10 (3 days) FGF10, RA, SB43452 (2 days)	FGF4, HGF, EGF (10 days)	48
Matrigel	Activin A (5 days)	BMP4, FGF2 (5 days)	HGF (5 days) OSM (5 days)	49
Gelatine	Activin A, bFGF, LY (3 days) Activin A, bFGF (1 day) Activin A (3 days)	BMP4, FGF10 (4 days)	HGF, OSM (19 days)	50
Fibronectin/Matrigel	Activin A, CHIR, PI-103 (1 day) Activin A, DM3189 (2 days)	DM3189 IWP2, PD0325901, RA (1 day) BMP4, A-83-01, IWP2, RA (3 days)	BMP4 (2 days) DEX, OSM (10 days)	51
Matrigel	L-Wnt3A-expressing cells (ATCC, CRL2647), activin A (4 days)	BMP4, FGF4 (5 days) ITS, nicotinamide, NaHCO ₃ , HGF, EGF (6 days)	HGF (5 days) OSM (11 days)	52
Matrigel/laminin- 521/laminin-111	Activin A, Wnt3a (3 days)	DMSO (1 day)	HGF, OSM, hydrocortisone (11 days)	53

to identify the impact of specific genetic alterations for liver function; generation of HLCs from iPSCs from distinct genotypes makes it possible to evaluate new drugs.^{61,62}

4.10.4 Induced Pluripotent Stem Cell-Derived Neuronal Cells

Worldwide, approximately one billion people are currently affected by a brain disorder.⁶³ Neurodegenerative- or neurodevelopmental-diseased persons suffer from the loss of cognitive function, movement, or muscle strength. Intellectual abilities such as communication and behavior are often impaired. Although neurological diseases are widespread, little is known about the underlying molecular mechanisms and hence the lack of effective therapies. Studies into neurological diseases are mostly carried out in animal models and transformed cell lines and tissues from aborted fetuses or poor-quality brain biopsies.^{64,65} Experimental data obtained from animals and transformed cells are not representative of human neurological function due to the greater complexity of the human brain and interspecies physiological differences. Furthermore, neurons from different species behave differently with respect to electrophysiology.⁶⁶ For example, thalidomide and 13-*cis*-retinoic acid are well-known human teratogens but are harmless in murine models.^{67, 68} The sensitivity of the human brain, chemical compounds, environmental changes, and naturally occurring substances has to be addressed in future studies.

Human induced pluripotent stem cell (iPSC)-derived neurons are more representative of human neural physiology than other model systems. They can recapitulate the *in vivo* conditions of neurodegenerative disorders *in vitro* and provide a promising tool for drug screening and neurotoxicological tests. In recent years, several neuronal disease models based on patient-specific iPSCs have been established and described.⁶⁹⁻⁷¹

One of the pioneering examples was the establishment of *in vitro* models of amyotrophic lateral sclerosis (ALS) by differentiation of human embryonic stem cells and iPSCs into motor neurons.^{68, 69} Currently, *in vitro* drug treatment has shown restoration of normal distribution of affected protein(s) for several neuronal diseases such as spinal muscular atrophy, Parkinson's disease, Rett syndrome, mucopolysaccharidosis type IIIB, schizophrenia, and Alzheimer's disease.⁷⁰⁻⁷⁵ Utilizing iPSC-derived neuronal cells enables characterization of the effect of potential drugs and toxins on distinct cell types present in the human brain. Therefore, neuronal differentiation protocols, which are stepwise and produce distinct cell types of the brain (e.g., neural progenitor cells (NPCs)), represent a tool for neurotoxicity screening assay due to the highly sensitive response to neurotoxins as compared with other neural lineages.⁷⁶ So far, neurospheres developed from NPCs have been used to analyze migration, proliferation, viability, and differentiation of neural cells in the presence of different chemicals. Methylmercury chloride was identified as neurotoxic, which negatively impacts differentiation into neural cell types and inhibits the migration.⁷⁷

More effort is needed to realize the promise of human iPSC-derived neurons in enhanced and cost-effective drug discovery and toxicology test for clinical use. A major obstacle is the low homogeneity and immature phenotype of the iPSC-derived neurons. To

develop reliable model system for drug discovery, the derivation of homogenous and more mature cell types is necessary in addition to establishing standardized and optimized protocols.

4.10.5 Induced Pluripotent Stem Cell-Derived Cardiomyocytes

Cardiotoxicity is a major problem not only for drugs targeting heart diseases but also for other compounds that act by systemic administration. Despite extensive testing with a variety of in vitro and animal models, nearly 40% of all drugs in clinical trials have to be withdrawn due to unanticipated cardiotoxic effects.^{61,78} A reliable cardiotoxicity screening identifying adverse side effects on the cardiovascular system early in the drug discovering process is needed to reduce time and cost in the development of new compounds.

The action potential of a cardiomyocyte and thereby the overall electric activity of the myocardium originate from the complex interplay of multiple ionic currents. Every second case of cardiotoxicity-related drug withdrawal is caused by a risk of arrhythmia,⁷⁹ namely, an extension of the repolarization of the cell membrane detectable with an electrocardiogram as a prolongation of the QT interval. This delayed repolarization might cause a life-threatening ventricular arrhythmia termed *torsades de pointes* (TdP). In this very aspect of membrane repolarization, animal cardiac physiology relies on different currents making rat, mouse, or guinea pig an inappropriate model for human drug testing.⁸⁰ Not only in addressing safety concerns animal models lack important qualities but also today's advanced medicine uses monoclonal antibodies specifically designed against human drug targets.⁸¹

Cardiac physiology is difficult to mimic in vitro; there are high interspecies variation in cardiovascular physiology, which inhibits efficient preclinical testing. The main disadvantage of human adult cardiomyocytes is the limited proliferation rate, and therefore, this postmitotic cell type cannot be cultured for the durations needed for drug screenings.⁸¹ New hopes for better drug screenings, diagnostics, and therapeutic options have been raised by induced pluripotent stem cell-derived cardiomyocytes (iPSC-CM). Theoretically, they provide an endless source of cardiomyocytes that can be kept in culture also for long-term experiments. Grown as a monolayer, iPSC-CM fit into two-dimensional assays and embryoid bodies (EBs), which constitute a three-dimensional assay system. The differentiation of cardiomyocytes from iPSCs is a complicated and multifactorial process. Since the first derivation of iPSC-CM from mouse iPSCs in 2008^{81,82} and from human in 2009,⁸³ many improved protocols have been established (Table 2).⁸⁴ Besides recent advantages in the differentiation process, today's iPSC-CM is still immature and resembles more a fetal-like phenotype of a cardiomyocyte than a fully mature adult cell type. This immaturity is, among other features, characterized by an altered current channel density manifesting in the spontaneous release of action potentials due to the less-negative resting potential of fetal cardiomyocytes.⁸⁰ Furthermore, the derived population of cardiomyocytes is heterogeneous as it usually consists of the three major subtypes of an atrial-, ventricular-, or nodal-like phenotype. Differences of these phenotypes manifest in different morphologies of the action potential and its response to drugs.^{81,85} However, functional assays such as the treatment with cardioactive drugs (e.g., adrenaline, isoproterenol, and verapamil) can be conducted as iPSC-derived cardiomyocytes show a synchronized response in terms of changes in the contractility and the beating rate.⁸⁶ Additionally, at the single-cell level, the intracellular transmembrane potential can be measured with a detailed characterization of electrophysiological effects.⁸⁰ Even a higher resolution can be provided by the long-established patch clamp technique allowing the recording of current changes of single ion channels. On a larger scale, the extracellular field potential is often measured by a microelectrode array (MEA).⁸⁷ The MEA technique has been validated for iPSC-CM models showing a reliable detection of drug-induced arrhythmias and changes in the electric properties.^{87,88} In addition to electrophysiological effects on cardiomyocytes caused by drug treatment, a contractile and structural cardiotoxicity (also termed as biochemical cardiotoxicity) is sometimes caused by chemotherapeutics as anthracyclines or kinase-targeted cancer drugs like trastuzumab.⁸⁹ Cardiotoxic side effects of noncardiac drugs are often not detected in preclinical or stage I trials. They only become significant during long-term treatment. Furthermore, the aged heart of older cancer patients might be more susceptible to an adverse reaction.

It has been shown in recent studies that long-term culture of iPSC-CM is possible and this results in increased maturity. A vascular coculture and newly designed biometrics also applying mechanical and electric forces have generated cardiomyocytes of higher maturation.^{84,90} iPSC lines from patient-derived somatic cells have already been established (Table 3).^{100,102} Critical mutations, like a missense mutation in the KCNH2 gene that causes one type of the long QT syndrome (LQT2), have been analyzed in functional assays for their response to corresponding drugs. Using MEA analysis, it has been shown that blocking calcium channels in LQT2 patients with nifedipine lead to a shortening of the AP duration and reduce arrhythmic activity.^{81,103}

Recent breakthroughs in technological possibilities of genome editing using CRISPR/Cas9 and TALEN further allow the specific insertion or correction of critical mutations.¹⁰⁰ This will lead to a deeper understanding of cardiac disease and drug-target interactions and hold great promise for preclinical safety testing.

4.10.6 Induced Pluripotent Stem Cell-Derived Organoids

Cellular models based on using distinct cell lines, explanted tissues, or animal models all exhibit several limitations.^{104–106} Established cell lines are usually immortalized or possess a malignant specimen origin.¹⁰⁷ Due to their long-term cultivation, they acquire several mutations or contaminations, and these probably limit their true biological relevance.^{108,109} Furthermore, cell lines that are cultured in a two-dimensional system are not able to mimic human tissue since cells behave differently due to the lack of cell-cell

Table 3 Overview of protocols used to sequentially differentiate iPSCs into cardiomyocytes

Differentiation condition	Cardiogenic factors	Small molecules	References
EB formation	FBS		83
EB—suspension culture	FGF2, activin A, DKK1, BMP4	L-ascorbic acid, SB431542	91
Increased EB formation, forced aggregation	FBS/HSA, FGF2, BMP4	Polyvinyl alcohol, L-ascorbic acid	84
EB—suspension culture	FBS	L-ascorbic acid	92
Monolayer on gelatin		KY02111	93
Monolayer on Matrigel/Synthemax		IWP2/IWP4, CHIR99021, SB431542, DMH1	94
Monolayer on Matrigel		Purmorphamine, CHIR99021, IWR-1 endo, SB431542	95
Monolayer on Matrigel/Synthemax		L-ascorbic acid, CHIR99021, WNT-C59	96
EB—suspension culture	Activin A, BMP4	L-ascorbic acid, IWR-1, blebbistatin	97
Rotated Erlenmeyer flasks		CHIR99021, IWP2/IWP4	98
Spinner flask		SB431542, purmorphamine, CHIR99021, IWR-1	99
Increased EB formation, forced aggregation	FGF2, activin A, BMP4	CHIR99021, IWP2, WNT-C59	100
Patient-derived (JLNS)/genetic engineered-derived, Monolayer on Matrigel/EB formation	Activin A, BMP4, (FGF2)	CHIR99021, XAV939, (IWP-2)	101
Patient-derived (LQT3), EB formation	FGF2, activin A, BMP4	Polyvinyl alcohol, L-ascorbic acid, IWP-2	102

JLNS, Jervell and Lange-Nielsen syndrome.

and cell–matrix interactions.^{104,106} Explanted tissues are particularly limited by their availability and their short-term nature.¹¹⁰ Additionally, primary cell populations can lose their phenotype when they are cultured in two-dimensional systems.¹⁰⁶ In animal models, the performance of drug tests and modeling of diseases can demonstrate the effect on a complete organism. However, certain human diseases have been extremely difficult to model in animals due to their anatomical and physiological divergence.¹¹¹ In view of these limitations, attempts are being made to generate more relevant *in vitro* biological model systems.

In the 1960s, small aggregates of dissociated embryonic cells were shown to reconstitute tissues with an architecture resembling that of the original tissue.¹¹² Recently, this knowledge was applied into several studies, and in 2009, Sato et al. were able to create an organotypic culture system.¹¹³ These gave rise to an epithelium-only organoid based on a single intestinal cell, which was isolated from murine intestinal crypts. They used Matrigel as an extracellular matrix (ECM) substitute and supplemented the culture medium with key growth factors of the intestinal stem cell niche, such as WNT, Noggin, R-spondin, and EGF. This culture system, referred to as the R-spondin method, appeared to be a major technological advance to the stem cell field. These organoids exhibited near-physiological and self-renewing capabilities and showed similar architecture to the native organ.¹¹³ Observing these principles, organoids resembling tissues such as the eye, gut, breast, pancreas, prostate, liver, kidney, lung, or stomach have been generated by imitating the specific stem cell niche.¹⁰⁴ However, most organoids still lack several key cell types, for example, mesenchymal and endothelial.¹⁰⁵ In addition, they only mimic the very early developmental stages of the organ under investigation.¹⁰⁴ Consequently, these organoids are still limited for scientific research with respect to the physiology of the whole organism. Nevertheless, organoids provide an important bridge between traditional *in vitro* and *in vivo* models.

Historically, the term organoid was used for all three-dimensional organotypic cultures.^{114,115} Recently, the definition of an organoid has changed. Organoids have to contain more than one cell type, organized similarly to the modeled tissue, and exhibit some functions that are specific to the native organ.¹¹⁶ In their review, Lancaster and Knoblich defined organoids as cell clusters that “containing several cell types that develop from stem cells or organ progenitors and self-organize through cell sorting and spatially restricted lineage commitment, similar to the process *in vivo*.”¹¹⁶ Consequently, organoids represent a methodical evolution of an *in vitro* system called embryoid body (EB). EBs are three-dimensional aggregates of pluripotent stem cells that undergo initial developmental specification as almost identical to the pregastrulating embryo and can further differentiate to form various organized tissues. Nevertheless, not all three-dimensional organoid culture systems make use of an initial EB formation.¹¹⁷ The term spheroid refers to another traditional three-dimensional culture system. However, spheroids lack the presence of relevant stem or progenitor cell populations performing self-renewal to sustain the three-dimensional cluster.¹⁰⁶

Self-organization can be realized in organoids due to a growing movement away from the two-dimensional culture, which particularly relies on an artificial ECM. Here, Matrigel is a common and important component that provides a scaffold and additional supplementation of signaling cues.¹¹⁸ Laminin, fibronectin, and collagen build a physical framework of tissues and influence cell behavior.¹¹⁹ Due to the fact that Matrigel is not well defined, it disregards special ECM cues, which are required by different tissue types.¹⁰⁶ Current developed biotechnologies allow the incorporation of essential signals from native ECMs into synthetic matrices and produce designer ECMs. These synthetic scaffolds can be constructed from natural macromolecules and synthetic polymers.¹¹⁹ Here, mechanical signaling can be mimicked by a hydrogel that contains technologies like light-mediated patterning. When exposed to light, photolabile cross-links can undergo local degradation and thereby soften the gel, whereas photoinitiators will cause local stiffness due to additional cross-linking.¹²⁰ Moreover, three-dimensional bioprinting is a new technique. The ink comprises a biomaterial with living cells that is precisely positioned in an additive layer-by-layer approach in order to create

Table 4 Advantages and limitations of three-dimensional organoid culture

<i>Advantages</i>	<i>Limitations</i>
Near-physiological model system	The lack of native microenvironment
High purity with minimal contributions from other cell types	The absence of several key cell types (e.g., mesenchymal, stromal, immune, neuronal cells)
Can be propagated for a long time without genomic alterations	Currently depend on mouse sarcoma-derived Matrigel (precludes transplantation into human)
Amenable to variety of established experimental techniques for 2-D culture systems	Inability to mimic in vivo growth factor/signaling gradients in Matrigel matrix
Can be derived from multiple sources (ESCs, iPSCs, primary cells/tissue)	Organoids in the same culture are heterogeneous in terms of viability, size, and shape
Limited amounts of starting material can be expanded	Inability to address questions regarding the whole organism
Human diseases that are difficult to model in animals can be studied with patient-derived organoids	Some tissues still remain resistant to 3-D organoid culture

Modified from Fatehullah, A.; Tan, S. H.; Barker, N., Organoids as an in vitro model of human development and disease. *Nat. Cell Biol.* **2016**, *18* (3), 246–254.

three-dimensional biological structures that mimic the structure and function of native tissues and organs.¹²¹ By using this method, researchers were recently able to create a beating heart organoid.¹⁰⁶

During organoid formation, several factors such as growth factors and small-molecule-based pathway activators or repressors are used to assist self-organization by controlling self-renewal and differentiation of stem cells. This is possible by mimicking the specific stem cell niche that contains ECM and cell–cell interactions and biophysical and biochemical signals.¹⁰⁶ However, cell–cell and cell–matrix interactions are difficult to control. Microfluidic devices, microbeads, and degradable vehicles in the culture matrices can deliver soluble growth factors and ligands by forming a gradient through manipulations.^{106, 122} Furthermore, an important consideration in developing functional organoids is permitting sufficient nutrient and oxygen supply. Most attempts to create in vitro vascularization have been a combination of neoangiogenesis and synthetic scaffolds that are used to create micro-engineered three-dimensional structures.^{123,124} An essential function is the cellular memory that enables the storage of otherwise transient responses. In this regard, sophisticated memory devices have been a key development to mimic cellular memory via genomic integrated circuits. Many synthetic circuits have been designed by using digital logic gates, relying on transcriptional control using activators, repressors, and other novel mechanisms.¹²⁵

However, there are still tissues that remain to be resolved in three-dimensional organoid culture; among these is the heterogeneous nature of cultured organoids in terms of viability, size, and shape.¹⁰⁵ Regardless, the three-dimensional culture systems of organoids have advantages over the two-dimensional culture systems but still with some limitations (**Table 4**).¹⁰⁵

The field of three-dimensional (3-D) organoids derived from human pluripotent stem cells is evolving rapidly, and there are many possibilities for potential applications (**Table 5**). The organoids have the potential to model adult homeostasis, and disease modeling will probably be a primary focus of future organoid-based studies.¹¹⁶ The testing of efficacy and toxicity of drug components will be an important aspect, too. This could be applied to organoids that represent models for degenerative conditions. In particular, the development of, for example, human liver organoids would be of enormous relevance, because the liver often metabolizes drugs and animal-based toxicity tests often exhibit other metabolism-related pathways. Therefore, methods to screen

Table 5 Application of organoids¹²⁶

<i>Organoid</i>	<i>Understanding of development</i>	<i>Understanding of diseases</i>	<i>Source of tissue transplantation/therapeutic cells</i>	<i>Identifying patient-tailored drugs</i>
Cerebral cortex	X	X		
Intestine				X
Optic cup			X	
Pituitary gland			X	
Kidney			X	X
Liver			X	X
Pancreas				X
Neural tube	X		X	
Stomach	X	X		
Prostate				X
Breast		X		
Heart	X			X
Lung	X	X		

Modified from Willyard et al. Rise of the Organoids. *Nature* **2015**, *523*, 520–522.

Table 6 Already established organoid in vitro models for human diseases

<i>Organoids</i>	<i>Types of human disease modeling</i>
Lingual	Lingual carcinoma
Taste bud	–
Salivary gland	Hyposalivation
Esophagus	Barrett's esophagus
Stomach	<i>H. pylori</i> infection, cancer
Intestine	Cancer, cystic fibrosis, infection model for viral and bacterial infection
Colon	IBD, cancer
Liver	Alagille syndrome, cystic fibrosis
Pancreas	Cancer
Prostate	Cancer
Lung	Cystic fibrosis
Retina	–
Inner ear	–
Brain	Autism, microcephaly
Kidney	–

Reproduced from Fatehullah, A.; Tan, S. H.; Barker, N. Organoids as an in vitro Model of Human Development and Disease. *Nat. Cell Biol.* **2016**, *18* (3), 246–254.

components in an in vitro 3-D human liver model are under investigation. This could be a great opportunity as an alternative in the drug discovery process.¹²⁷ So far, several organoid systems have been established, which are associated with human disease modeling (Table 6).¹⁰⁵

4.10.6.1 Liver Organoids

Primary and adult liver cells are difficult to cultivate, and for decades, laboratory studies have failed to generate vascularized, functional, and complex organotypic cell cultures that resemble native liver.¹²⁸ Previous reported three-dimensional hepatic cell clusters were entirely composed of epithelial structures and lacked complex structures such as blood vessels.¹²⁹

The embryonal gastrointestinal tract consists of foregut, midgut, and hindgut.¹²⁹ Each of these regions gives rise to different tissues and organs. The foregut gives rise to the oral cavity, pharynx, esophagus, stomach, liver, pancreas, and proximal duodenum. The midgut and hindgut give rise to the distal duodenum, jejunum, ileum, colon, anal canal, urethra, and bladder.¹²⁹ During liver development, ductal epithelium and hepatocytes arise from liver progenitor cells, referred to as hepatoblasts.¹³⁰ In order to attain maturity, these cells rely on a complex symphony of signals from other nearby cells. This leads to the initiation of human liver-bud formation in the third or fourth week of gestation.¹²⁸ By recapitulating these principals, Takebe et al. were recently able to create in vitro liver buds via cocultivation of hepatoblasts with mesenchymal and endothelial cells.¹¹² They plated the different cell types in two-dimensional conditions, and these cells self-organized into macroscopically visible three-dimensional clusters after 2 days of culture. They detected that the lack of one cell type results in failure of three-dimensional organoid formation. The created organoids were mechanically stable, could be manipulated physically, and were cultivated for 2 months while exhibiting a higher albumin production rate compared with traditional two-dimensional cultures. Takebe et al. discovered that the transplantation of these liver buds into mice led to maturation of the organoids into vascularized and functional human liver. Transplanted liver buds were capable of rescuing drug-induced liver failure in mice.¹¹²

More advanced methods like 3-D architecture of HLC derivatives in vitro show improvements in experimental outcome. Liver functions such as urea synthesis and activity of distinct cytochromes were higher in the 3-D organoids than in the 2-D culture approaches. Furthermore, these 3-D iPSC-derived hepatocyte-like cells (HLCs) were more susceptible for most of the tested drugs in comparison with the monolayer culture.⁵² Furthermore, liver-bud-like tissue generation by self-organization of genetically engineered iPSCs is possible. These organoids are able to perform several liver key functions.¹³¹

Based on these advances, it is evident that three-dimensional organoid culture systems may be suitable not only for disease modeling, drug test performance, and developmental research but also for cell replacement therapies in the near future.

4.10.6.2 Brain Organoids

The brain is a complex organ. It derives from the neural ectoderm,¹³² which gives rise to the neural plate which folds and fuses to form the neural tube. The neural tube is an epithelium with apical–basal polarity that is organized around fluid-filled lumen that likely represents the brain ventricles. The axes are built through concentration gradients and because of these axes the epithelial tube can subdivide into four major brain regions: the forebrain, midbrain, hindbrain, and spinal cord.¹¹⁶ In general, neural stem cells that are resident next to the ventricles differentiate into neurons.¹³³ The neural stem cells expand through symmetric proliferative

and asymmetric divisions that give rise to self-renewing progenitors and differentiated cell types which migrate to other zones to generate stratified structures.^{116, 134}

In previous studies, *in vitro*-derived neural stem cells from pluripotent stem cells were used to better decipher the mechanisms of neural differentiation.¹³⁵ These homogenous neural stem cells were generated in classical two-dimensional culture systems and could neither show the characteristic apical–basal polarity nor recapitulate the complicated lineage of neural stem cells. To gain knowledge in this field, protocols for generating neurospheres have been developed.¹³⁶ Neurospheres are aggregates of neural stem cells and have a self-renewing capacity. Though, neurospheres are not well organized and are limited in their capacity to generate different aspects of brain development.¹¹⁶ Furthermore, neural tubelike structures and the neural rosettes have also been established. Neural rosettes derive from isolated neuroepithelium or directed differentiation of pluripotent stem cells.^{137,138} They have the ability to recapitulate apical–basal polarity and exhibit radial organization similar to that of the neural tube. They show a higher capacity to recapitulate many aspects of brain development including the production of intermediate progenitor cells and the timed production of layer identities similar to those *in vivo*.¹³⁹ However, the two-dimensional aspect of this method results in many limitations in modeling the organization of the developing brain; hence, three-dimensional (3-D) culture methods were established to help overcome some of these limitations.^{116,128,140–144} These methods have the potential to recapitulate brain tissue formation. To obtain the 3-D cultures, first, embryoid bodies have to be generated from pluripotent stem cells. Second, after embedding them in Matrigel, which provides an environment that is similar to the extracellular matrix, the embryonic bodies exhibit an outgrowth of large buds of neuroepithelium. These buds have the ability to expand and develop into various brain regions. The cerebral organoids can reach the size of a few millimeters and can be further maintained for over a year by using a bioreactor that provides sufficient oxygen and nutrient supply.^{116,145} Cerebral organoids are able to mimic the development and disease conditions.¹⁴³ Furthermore, they offer potential for drug testing and even future organ replacement strategies.¹⁴⁶ However, like all *in vitro* systems, the method does not contain all crucial factors necessary for proper brain development. The surrounding embryonic tissues that have great importance on the interplay of neural and nonneural tissue are missing.¹⁴⁵

4.10.6.3 Heart Organoids

Heart organogenesis and morphogenesis are complex anatomical processes. In the adult heart, myocardial cells are generated from mesodermal precursors during the embryonic period of heart growth.¹⁴⁷ Distinct signaling pathways lead to the formation of the first and second heart fields and afterward to the four-chambered heart.^{148–150} After the forming of the early heart shape, some mesodermal cells from the proepicardium build the epicardium, which is a single layer of cells that envelope the heart.¹⁵¹ Then, epicardial cells become migratory mesenchymal cells and enter the underlying myocardium and differentiate.¹⁴⁷

There are three main points to consider, that is, scaffold, cell sources, and signaling factors, when generating three-dimensional (3-D) cardiac tissue for use in cardiovascular therapy or toxicological testing.¹⁴⁷ The differentiation of pluripotent stem cells into cardiomyocytes follows a distinct developmental lineage after mesoderm induction. Generating organoids involve mimicking the 3-D setting of an evolving embryo using embryoid bodies as intermediates.¹⁵² These aggregates of cells are exposed to various growth factors and hypoxic environment for initiating the developmental processes. Other scaffold-free constructs are used by a relatively new developed method: the cell sheet engineering technique. There, a temperature-responsive culture surface is used that detaches myocardial layers as a confluent sheet. This is achieved by lowering the temperature, which then results in the stacking of myocardial layers to produce a 3-D cardiac construct.¹⁵³ The monolayers can rapidly attach and form cell–cell connections. However, the thickness of the 3-D construct is limited to three layers.¹⁵⁴ In contrast to the use of embryonic bodies and the cell sheet engineering technique, a scaffold can be used to obtain organoids via other pathways. A scaffold represents the structural platform for a new cellular microenvironment and supports new tissue formation. It provides cell attachment, migration, differentiation, and organization.¹⁵⁵ Biometric scaffolds are made of natural or synthetic polymers or hybrid copolymer and are similar to the native components of the extracellular matrix.¹⁵⁶ In general, biometric scaffolds should not be immunogenic but mechanically stable. They should mimic cardiac tissue flexibility and allow physiological electric propagation and sufficient oxygen and nutrient delivery to the cells and a degradation rate that is appropriate to the rate of native extracellular matrix replacement.^{115,157} The biometric scaffolds are used alone or in combination with cells.^{158–161} To gain success, the selection of cell types and scaffold material and the incorporation of bioactive molecules and bioreactors should be noted.¹⁴⁷ Another method for generating a 3-D cardiac tissue is the decellularization. Therefore, the success of this depends on specific requirements of the application as high density, high pressure, and stiffness.^{162,163} The commonly used methods are microwave radiation and chemical, enzymatic, mechanical, and physical separation. The combination of physical, chemical, and enzymatic methods leads to better results in the decellularization process in whole organ and small tissues in cardiac applications.^{164,165} In order to decellularize and recellularize an organ to serve as a scaffold, detergent or an enzymatic solution is first used to remove cellular material and then the stem cell of choice is applied to repopulate the scaffold in the presence of an appropriate culture environment.¹⁴⁷

4.10.7 Use of Induced Pluripotent Stem Cells for Toxicogenomics

Toxicogenomics—an interdisciplinary between toxicology and genomics—is concerned with identification of potential human and environmental toxicants and their putative mechanisms of action through the use of genomic resources.¹⁶⁶ Measurements on the proteome, genome, and transcriptome level target at the prediction of toxicity, the finding of biomarkers, and the detection of

genetic variants associated with higher predisposition to toxicity. A broader concept of toxicogenomics also includes metabolomics.¹⁶⁷ A plethora of studies have demonstrated the advantages of the toxicogenomic approach.¹⁶⁸ For instance, McBurney et al. proposed a systems toxicology approach to discover toxicogenomic biomarkers to detect a drug's potential for human idiosyncratic drug-induced liver injury and could show that the molecular analyses employed in the study were detecting substantial "off-target" markers.¹⁶⁹ Ellinger-Ziegelbauer et al. could distinguish genotoxic carcinogens from nongenotoxic carcinogens via a toxicogenomic approach employing gene expression profiles from treated rat liver.¹⁷⁰ Based on the gene expression profiles and a support vector machine (SVM), classifiers of the carcinogens were determined in what would have usually required a 2-year evaluation with rodent lifetime bioassays. Obviously, in toxicogenomics, the accessibility of a large amount of existing toxicological information plays an important role. Hence, there is a need for databases making this knowledge accessible to the community and integrating newly acquired knowledge. Here, as an example, the Japanese Toxicogenomics Project consortium (TGP) provides a large-scale toxicogenomics database (open TG-GATEs) consisting of data from 170 compounds (mostly drugs) with the aim of improving and enhancing drug safety assessment.¹⁷¹ The database (<http://toxico.nibio.go.jp/english/index.html>) comprises data and metadata including gene expression profiles and pathology and is freely available.

Although toxicity can affect various tissues such as neurotoxicity or kidney toxicity, the liver as a key metabolic organ plays a major role for toxicity studies. Most drugs promote their own metabolism by upregulating the enzyme systems responsible for their activation (phase I) and conjugation (phase II) to biochemical forms that can be excreted in bile or urine. The majority of drugs that are metabolized by the liver through such detoxification pathways induce particular subsets of cytochromes (CYP) P450.¹⁷² The most ubiquitous of these, CYP3A4, is responsible for metabolizing a large fraction of hepatotoxic drugs, and indeed, CYP3A4 induction can be used as an index of exposure to them. The Adjaye group demonstrated the expression of cytochrome P450 family members in induced pluripotent stem cells (iPSCs) and embryonic stem cell (ESC)-derived hepatocyte-like cells, and others have shown the prediction of interindividual differences in hepatic functions and drug sensitivity by using human iPSC-derived hepatocytes.^{42,52,58,173} These studies among others have provided evidence that human iPSC-derived hepatocytes can be used as an in vitro hepatocyte model for use in pharmacology and toxicology. Fig. 2 shows expression of the drug-metabolism-associated absorption, distribution, metabolism, and excretion (ADME) genes in iPSCs differentiated into hepatocytes, cardiomyocytes, and neurons.^{41,42,71,100,174} The iPSC-based strategy is also exploited by companies by providing human iPSC-derived hepatocyte cells (iHeps) for use in toxicology screening and studies.¹⁷³ The ADME genes have been shown to be associated with drug metabolism and can be grouped into four distinct categories (<http://www.pharmaadme.org/>):³⁵

1. Phase I metabolism enzymes: CYP, DHRS, and CBR
2. Phase II metabolism enzymes: GST, SULT, UGT, CHST, and NAT, which are responsible for the modification of functional groups and the conjugation with endogenous moieties
3. Transporters: SLC, ABC, and MRP, which are responsible for the uptake and excretion of drugs in and out of cells
4. Modifiers: CAT, CDA, RXRA, PPARG, PPARD, SOD, and SERPINA7, which can have dual functions, that is, regulate the expression of other ADME genes or modulate the biochemistry of ADME enzymes

ADME genes can be employed to derive parameters from in vitro models, which can be combined with toxicokinetic (TK) parameters from in vivo models, which increasingly can be derived from physiologically based toxicokinetic (PBTK) modeling.¹⁷⁵

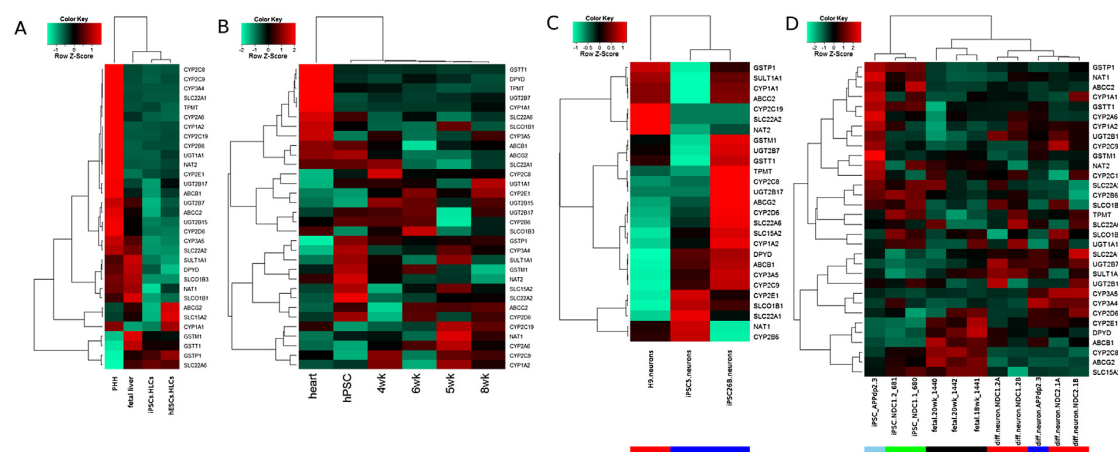


Fig. 2 Gene expression analysis of the ADME genes in iPSCs differentiated into cell types representative of endoderm, mesoderm, and ectoderm. The heatmaps represent genes encoding the core ADME enzymes based on the transcriptome data sets of iPSC- and ESC-derived HLCs (A),⁴² cardiomyocytes (B),¹⁰⁰ and neurons for Alzheimer's disease models (C¹⁷⁴ and D).⁷¹ The ADME genes have been shown to be associated with drug metabolism (http://pharmaadme.org/joomla/index.php?option=com_content&task=view&id=14&Itemid=29),⁴¹ Color bars: *blue*, iPSC-derived neuron from AD; *red*, iPSC-derived neuron from healthy control; *light blue*, iPSC from AD; *green*, iPSCs from healthy control; black, fetal brain.

ADME-derived parameters depend on the tested chemicals and can be integrated with chemical-independent physiological and anatomical information in PBTK models to simulate TK profiles. Employing quantitative structure–activity relationship (QSAR) models and in vitro methods, ADME parameters can be determined. PBTK models are valuable tools for extrapolating in vitro results either interspecies or interindividuals and thus are gaining importance in toxicity testing.

4.10.8 The 3Rs

The 3Rs are first mentioned in a report by Russell and Burch originally published in 1959 and are acronyms for replace, reduce, and refine.¹⁷⁶ The first R means that as far as possible, animal tests should be replaced. If that is not possible, they should be reduced, and if that is also not possible, the experiments should at least take place under the best possible conditions for the animals (refine).

To date, toxicology screens necessitate the use of significant numbers of animals. In the EU program Registration, Evaluation, Authorisation and Restriction of Chemicals (REACH), the hazard risk of 30,000 chemicals shall be assessed, which had not been tested before. This testing of chemicals required under the REACH regulations has been variously estimated to require up to 54 million additional animals, therefore necessitating the development of alternative testing strategies (http://ec.europa.eu/enterprise/sectors/chemicals/reach/index_en.htm), which could achieve a reduction to below 10 million animals.¹⁷⁷

3R approaches could tackle this problem by employing patient-specific iPSC-derived hepatocytes, neurons, or cardiomyocytes in order to reduce or—where possible—to replace animal tests. In a strategy paper, the European Union Reference Laboratory for alternatives to animal testing (EURL-ECVAM) outlines the possible use of physiologically based toxicokinetic (PBTK) models for toxicological tests with respect to the 3Rs.¹⁷⁵ These models have the potential to provide whole-body human toxicokinetic data by in silico and in vitro methods assessing ADME processes. Standardization and an infrastructure for these methods are important issues that when properly solved, could leverage their acceptance and use, thus leading to a more efficient use of available human and animal data. Höfer et al. mention the importance of databases and data management to ensure a more ubiquitous accessibility of existing data.¹⁷⁷ Adequate data management strategies are an issue for many scientific disciplines where large amounts of data are generated and, in particular for modern biology disciplines such as toxicogenomics and systems biology, where novel techniques produce data in high throughput.¹⁷⁸

Predictions based on animals models not always reflect the human reactions but instead display sometimes qualitative and also quantitative differences in their physiology and metabolism; for example, animal test data for acetylsalicylic acid (aspirin) demonstrated that it could cause severe problems in rats but it is harmless to humans.^{179–182} Would these animal experiments have been used to test the safety of aspirin, it may not have been permitted for clinical trials. Already in 1988, Lave et al. criticized the reliability and the cost-effectiveness of rodent models for carcinogenicity testing.¹⁸³ The report *Toxicity Testing in the 21st Century: A Vision and a Strategy* released by the US National Academy of Sciences envisioned toxicity testing firmly based on human biology and thus reducing animal testing.¹⁸⁴ Computational models would simulate dose–response behavior and extrapolate in vitro results to in vivo human blood and tissue concentrations. Thus, human relevance of test results would be increased.

However, a full replacement of animal tests at the moment is not feasible as the models still cannot fully reflect the in vivo reality. This is demonstrated by the demand for animal tests in most guidelines for toxicity testing, for example, the Organisation for Economic Co-operation and Development (OECD) guidelines for the testing of chemicals. In general, guideline methods such as OECD TGs 417 and 427 are based on animal tests.^{175,185,186} Only OECD TG 428 for the in vitro method for skin absorption is an exception.¹⁸⁷ However, with the continuous improvement of the toxicological models, replacement can be envisioned as a long-term goal, and meanwhile, the two other Rs—reduction and refinement—should be followed as far as possible.

References

1. Jensen, J.; Hyllner, J.; Bjorquist, P. Human Embryonic Stem Cell Technologies and Drug Discovery. *J. Cell. Physiol.* **2009**, *219* (3), 513–519.
2. Lai, D.; Wang, Y.; Sun, J.; Chen, Y.; Li, T.; Wu, Y.; Guo, L.; Wei, C. Derivation and Characterization of Human Embryonic Stem Cells on Human Amnion Epithelial Cells. *Sci. Rep.* **2015**, *5*, 10014.
3. Takahashi, K.; Yamanaka, S. Induction of Pluripotent Stem Cells From Mouse Embryonic and Adult Fibroblast Cultures by Defined Factors. *Cell* **2006**, *126* (4), 663–676.
4. Takahashi, K.; Okita, K.; Nakagawa, M.; Yamanaka, S. Induction of Pluripotent Stem Cells From Fibroblast Cultures. *Nat. Protoc.* **2007**, *2* (12), 3081–3089.
5. Yu, J.; Vodyanik, M. A.; Smuga-Otto, K.; Antosiewicz-Bourget, J.; Frane, J. L.; Tian, S.; Nie, J.; Jonsdottir, G. A.; Ruotti, V.; Stewart, R.; Slukvin, I. I.; Thomson, J. A. Induced Pluripotent Stem Cell Lines Derived From Human Somatic Cells. *Science* **2007**, *318* (5858), 1917–1920.
6. Jung, M.; Peterson, H.; Chavez, L.; Kahlem, P.; Lehrach, H.; Vilo, J.; Adjaye, J. A Data Integration Approach to Mapping OCT4 Gene Regulatory Networks Operative in Embryonic Stem Cells and Embryonal Carcinoma Cells. *PLoS One* **2010**, *5* (5), e10709.
7. Goke, J.; Jung, M.; Behrens, S.; Chavez, L.; O'Keeffe, S.; Timmermann, B.; Lehrach, H.; Adjaye, J.; Vingron, M. Combinatorial Binding in Human and Mouse Embryonic Stem Cells Identifies Conserved Enhancers Active in Early Embryonic Development. *PLoS Comput. Biol.* **2011**, *7* (12), e1002304.
8. Thomson, J. A.; Itskovitz-Eldor, J.; Shapiro, S. S.; Waknitz, M. A.; Swiergiel, J. J.; Marshall, V. S.; Jones, J. M. Embryonic Stem Cell Lines Derived From Human Blastocysts. *Science* **1998**, *282* (5391), 1145–1147.
9. Yamanaka, S. Strategies and New Developments in the Generation of Patient-Specific Pluripotent Stem Cells. *Cell Stem Cell* **2007**, *1* (1), 39–49.
10. Wang, Y.; Mah, N.; Prigione, A.; Wolfrum, K.; Andrade-Navarro, M. A.; Adjaye, J. A Transcriptional Roadmap to the Induction of Pluripotency in Somatic Cells. *Stem Cell Rev.* **2010**, *6* (2), 282–296.
11. Masato Nakagawa, M. K.; Tanabe, K.; Takahashi, K.; Ichisaka, T.; Takashi Aoi, K. O.; Mochizuki, Y.; Takizawa, N.; Yamanaka, S. Generation of Induced Pluripotent Stem Cells Without Myc From Mouse and Human Fibroblasts. *Nat. Biotechnol.* **2008**, *26* (1), 101–106.

12. Zhao, Y.; Yin, X.; Qin, H.; Zhu, F.; Liu, H.; Yang, W.; Zhang, Q.; Xiang, C.; Hou, P.; Song, Z.; Liu, Y.; Yong, J.; Zhang, P.; Cai, J.; Liu, M.; Li, H.; Li, Y.; Qu, X.; Cui, K.; Zhang, W.; Xiang, T.; Wu, Y.; Zhao, Y.; Liu, C.; Yu, C.; Yuan, K.; Lou, J.; Ding, M.; Deng, H. Two Supporting Factors Greatly Improve the Efficiency of Human iPSC Generation. *Cell Stem Cell* **2008**, *3* (5), 475–479.
13. Wang, Y.; Adjaye, J. A Cyclic AMP Analog, 8-Br-cAMP, Enhances the Induction of Pluripotency in Human Fibroblast Cells. *Stem Cell Rev.* **2011**, *7* (2), 331–341.
14. Maherali, N.; Ahfeldt, T.; Rigamonti, A.; Utikal, J.; Cowan, C.; Hochedlinger, K. A High-Efficiency System for the Generation and Study of Human Induced Pluripotent Stem Cells. *Cell Stem Cell* **2008**, *3* (3), 340–345.
15. Prigione, A.; Fauler, B.; Lurz, R.; Lehrach, H.; Adjaye, J. The Senescence-Related Mitochondrial/Oxidative Stress Pathway Is Repressed in Human Induced Pluripotent Stem Cells. *Stem Cells* **2010**, *28* (4), 721–733.
16. Wolfrum, K.; Wang, Y.; Prigione, A.; Sperling, K.; Lehrach, H.; Adjaye, J. The Large Principle of Cellular Reprogramming: Lost, Acquired and Retained Gene Expression in Foreskin and Amniotic Fluid-Derived Human Ips Cells. *PLoS One* **2010**, *5* (10), e13703.
17. Lichtner, B.; Knaus, P.; Lehrach, H.; Adjaye, J. BMP10 as a Potent Inducer of Trophoblast Differentiation in Human Embryonic and Induced Pluripotent Stem Cells. *Biomaterials* **2013**, *34* (38), 9789–9802.
18. Chen, L.; Liu, L. Current Progress and Prospects of Induced Pluripotent Stem Cells. *Sci. Chin.* **2009**, *52* (7), 622–636.
19. Kiskinis, E.; Eggan, K. Progress Toward the Clinical Application of Patient-Specific Pluripotent Stem Cells. *J. Clin. Invest.* **2010**, *120* (1), 51–59.
20. Tavernier, G.; Wolfrum, K.; Demeester, J.; De Smedt, S. C.; Adjaye, J.; Rejman, J. Activation of Pluripotency-Associated Genes in Mouse Embryonic Fibroblasts by Non-Viral Transfection With In Vitro-Derived mRNAs Encoding Oct4, Sox2, Klf4 and cMyc. *Biomaterials* **2012**, *33* (2), 412–417.
21. Fusaki, N.; Ban, H.; Nishiyama, A.; Saeki, K.; Hasegawa, M. Efficient Induction of Transgene-Free Human Pluripotent Stem Cells Using a Vector Based on Sendai Virus, an RNA Virus That Does Not Integrate Into the Host Genome. *Proc. Jpn. Acad. Ser. B Phys. Biol. Sci.* **2009**, *85* (8), 348–362.
22. Yu, J.; Hu, K.; Smuga-Otto, K.; Tian, S.; Stewart, R.; Slukvin, I. I.; Thomson, J. A. Human Induced Pluripotent Stem Cells Free of Vector and Transgene Sequences. *Science* **2009**, *324* (5928), 797–801.
23. Okita, K.; Matsumura, Y.; Sato, Y.; Okada, A.; Morizane, A.; Okamoto, S.; Hong, H.; Nakagawa, M.; Tanabe, K.; Tezuka, K.; Shibata, T.; Kunisada, T.; Takahashi, M.; Takahashi, J.; Saiji, H.; Yamanaka, S. A More Efficient Method to Generate Integration-Free Human iPS Cells. *Nat. Methods* **2011**, *8* (5), 409–412.
24. Warren, L.; Manos, P. D.; Ahfeldt, T.; Loh, Y. H.; Li, H.; Lau, F.; Ebina, W.; Mandal, P. K.; Smith, Z. D.; Meissner, A.; Daley, G. Q.; Brack, A. S.; Collins, J. J.; Cowan, C.; Schläeger, T. M.; Rossi, D. J. Highly Efficient Reprogramming to Pluripotency and Directed Differentiation of Human Cells With Synthetic Modified mRNA. *Cell Stem Cell* **2010**, *7* (5), 618–630.
25. Schläeger, T. M.; Dameron, L.; Brickler, T. R.; Entwisle, S.; Chan, K.; Cianci, A.; DeVine, A.; Ettenger, A.; Fitzgerald, K.; Godfrey, M.; Gupta, D.; McPherson, J.; Malwadkar, P.; Gupta, M.; Bell, B.; Doi, A.; Jung, N.; Li, X.; Lynes, M. S.; Brookes, E.; Cherry, A. B.; Demirbas, D.; Tsankov, A. M.; Zon, L. I.; Rubin, L. L.; Feinberg, A. P.; Meissner, A.; Cowan, C. A.; Daley, G. Q. A Comparison of Non-Integrating Reprogramming Methods. *Nat. Biotechnol.* **2015**, *33* (1), 58–63.
26. Lin, T.; Ambasudhan, R.; Yuan, X.; Li, W.; Hilcove, S.; Abujarour, R.; Lin, X.; Hahm, H. S.; Hao, E.; Hayek, A.; Ding, S. A Chemical Platform for Improved Induction of Human iPSCs. *Nat. Methods* **2009**, *6* (11), 805–808.
27. Marson, A.; Foreman, R.; Chevalier, B.; Bilodeau, S.; Kahn, M.; Young, R. A.; Jaenisch, R. Wnt Signaling Promotes Reprogramming of Somatic Cells to Pluripotency. *Cell Stem Cell* **2008**, *3* (2), 132–135.
28. Lin, T.; Wu, S. Reprogramming With Small Molecules Instead of Exogenous Transcription Factors. *Stem Cells Int.* **2015**, *2015*, 794632.
29. Wang, Q.; Xu, X.; Li, J.; Liu, J.; Gu, H.; Zhang, R.; Chen, J.; Kuang, Y.; Fei, J.; Jiang, C.; Wang, P.; Pei, D.; Ding, S.; Xie, X. Lithium, an Anti-Psychotic Drug, Greatly Enhances the Generation of Induced Pluripotent Stem Cells. *Cell Res.* **2011**, *21* (10), 1424–1435.
30. Lee, J.; Xia, Y.; Son, M. Y.; Jin, G.; Seol, B.; Kim, M. J.; Son, M. J.; Do, M.; Lee, M.; Kim, D.; Lee, K.; Cho, Y. S. A Novel Small Molecule Facilitates the Reprogramming of Human Somatic Cells Into a Pluripotent State and Supports the Maintenance of an Undifferentiated State of Human Pluripotent Stem Cells. *Angew. Chem.* **2012**, *51* (50), 12509–12513.
31. Mali, P.; Chou, B. K.; Yen, J.; Ye, Z.; Zou, J.; Dowey, S.; Brodsky, R. A.; Ohm, J. E.; Yu, W.; Baylin, S. B.; Yusa, K.; Bradley, A.; Meyers, D. J.; Mukherjee, C.; Cole, P. A.; Cheng, L. Butyrate Greatly Enhances Derivation of Human Induced Pluripotent Stem Cells by Promoting Epigenetic Remodeling and the Expression of Pluripotency-Associated Genes. *Stem Cells* **2010**, *28* (4), 713–720.
32. Huangfu, D.; Maehr, R.; Guo, W.; Eijkelenboom, A.; Snitow, M.; Chen, A. E.; Melton, D. A. Induction of Pluripotent Stem Cells by Defined Factors Is Greatly Improved by Small-Molecule Compounds. *Nat. Biotechnol.* **2008**, *26* (7), 795–797.
33. Zhu, S.; Li, W.; Zhou, H.; Wei, W.; Ambasudhan, R.; Lin, T.; Kim, J.; Zhang, K.; Ding, S. Reprogramming of Human Primary Somatic Cells by OCT4 and Chemical Compounds. *Cell Stem Cell* **2010**, *7* (6), 651–655.
34. Claassen, D. A.; Desler, M. M.; Rizzino, A. ROCK Inhibition Enhances the Recovery and Growth of Cryopreserved Human Embryonic Stem Cells and Human Induced Pluripotent Stem Cells. *Mol. Reprod. Dev.* **2009**, *76* (8), 722–732.
35. Gomez-Lechon, M. J.; Donato, M. T.; Castell, J. V.; Jover, R. Human Hepatocytes as a Tool for Studying Toxicity and Drug Metabolism. *Curr. Drug Metab.* **2003**, *4* (4), 292–312.
36. Gunawan, B. K.; Kaplowitz, N. Mechanisms of Drug-Induced Liver Disease. *Clin. Liver Dis.* **2007**, *11* (3), 459–475. v.
37. Olson, H.; Betton, G.; Robinson, D.; Thomas, K.; Monro, A.; Kolaja, G.; Lilly, P.; Sanders, J.; Sipes, G.; Bracken, W.; Dorato, M.; Van Deun, K.; Smith, P.; Berger, B.; Heller, A. Concordance of the Toxicity of Pharmaceuticals in Humans and in Animals. *Regul. Toxicol. Pharmacol.* **2000**, *32* (1), 56–67.
38. Khetani, S. R.; Berger, D. R.; Ballinger, K. R.; Davidson, M. D.; Lin, C.; Ware, B. R. Microengineered Liver Tissues for Drug Testing. *J. Lab. Autom.* **2015**, *20* (3), 216–250.
39. LeCluyse, E. L.; Wittek, R. P.; Andersen, M. E.; Powers, M. J. Organotypic Liver Culture Models: Meeting Current Challenges in Toxicity Testing. *Crit. Rev. Toxicol.* **2012**, *42* (6), 501–548.
40. Dambach, D. M.; Andrews, B. A.; Moulin, F. New Technologies and Screening Strategies for Hepatotoxicity: Use of in vitro Models. *Toxicol. Pathol.* **2005**, *33* (1), 17–26.
41. Graffmann, N.; Matz, P.; Wruck, W.; Adjaye, J. The Promise of Induced Pluripotent Stem Cells for Liver Disease, Toxicology and Drug Discovery. *Drug Target Rev.* **2015**, *2* (1), 8–11.
42. Jozefczuk, J.; Prigione, A.; Chavez, L.; Adjaye, J. Comparative Analysis of Human Embryonic Stem Cell and Induced Pluripotent Stem Cell-Derived Hepatocyte-Like Cells Reveals Current Drawbacks and Possible Strategies for Improved Differentiation. *Stem Cells Dev.* **2011**, *20* (7), 1259–1275.
43. Davidson, M. D.; Ware, B. R.; Khetani, S. R. Stem Cell-Derived Liver Cells for Drug Testing and Disease Modeling. *Discov. Med.* **2015**, *19* (106), 349–358.
44. Cai, J.; Zhao, Y.; Liu, Y.; Ye, F.; Song, Z.; Qin, H.; Meng, S.; Chen, Y.; Zhou, R.; Song, X.; Guo, Y.; Ding, M.; Deng, H. Directed Differentiation of Human Embryonic Stem Cells Into Functional Hepatic Cells. *Hepatology* **2007**, *45* (5), 1229–1239.
45. Agarwal, S.; Holtan, K. L.; Lanza, R. Efficient Differentiation of Functional Hepatocytes From Human Embryonic Stem Cells. *Stem Cells* **2008**, *26* (5), 1117–1127.
46. Hay, D. C.; Zhao, D.; Fletcher, J.; Hewitt, Z. A.; McLean, D.; Urruticoechea-Uriguen, A.; Black, J. R.; Elcombe, C.; Ross, J. A.; Wolf, R.; Cui, W. Efficient Differentiation of Hepatocytes From Human Embryonic Stem Cells Exhibiting Markers Recapitulating Liver Development In Vivo. *Stem Cells* **2008**, *26* (4), 894–902.
47. Song, Z.; Cai, J.; Liu, Y.; Zhao, D.; Yong, J.; Duo, S.; Song, X.; Guo, Y.; Zhao, Y.; Qin, H.; Yin, X.; Wu, C.; Che, J.; Lu, S.; Ding, M.; Deng, H. Efficient Generation of Hepatocyte-Like Cells From Human Induced Pluripotent Stem Cells. *Cell Res.* **2009**, *19* (11), 1233–1242.
48. Touboul, T.; Hannan, N. R.; Corbineau, S.; Martinez, A.; Martinet, C.; Branchereau, S.; Mainot, S.; Strick-Marchand, H.; Pedersen, R.; Di Santo, J.; Weber, A.; Vallier, L. Generation of Functional Hepatocytes From Human Embryonic Stem Cells Under Chemically Defined Conditions That Recapitulate Liver Development. *Hepatology* **2010**, *51* (5), 1754–1765.
49. Si-Tayeb, K.; Noto, F. K.; Nagaoka, M.; Li, J.; Battle, M. A.; Duris, C.; North, P. E.; Dalton, S.; Duncan, S. A. Highly Efficient Generation of Human Hepatocyte-Like Cells From Induced Pluripotent Stem Cells. *Hepatology* **2010**, *51* (1), 297–305.

50. Hannan, N. R.; Segeritz, C. P.; Touboul, T.; Vallier, L. Production of Hepatocyte-Like Cells From Human Pluripotent Stem Cells. *Nat. Protoc.* **2013**, *8* (2), 430–437.
51. Loh, K. M.; Ang, L. T.; Zhang, J.; Kumar, V.; Ang, J.; Auyeong, J. Q.; Lee, K. L.; Choo, S. H.; Lim, C. Y.; Nichane, M.; Tan, J.; Noghabi, M. S.; Azola, L.; Ng, E. S.; Durruthy-Durruthy, J.; Sebastiano, V.; Poellinger, L.; Elefanty, A. G.; Stanley, E. G.; Chen, O.; Prabhakar, S.; Weissman, I. L.; Lim, B. Efficient Endoderm Induction From Human Pluripotent Stem Cells by Logically Directing Signals Controlling Lineage Bifurcations. *Cell Stem Cell* **2014**, *14* (2), 237–252.
52. Takayama, K.; Morisaki, Y.; Kuno, S.; Nagamoto, Y.; Harada, K.; Furukawa, N.; Ohtaka, M.; Nishimura, K.; Imagawa, K.; Sakurai, F.; Tachibana, M.; Sumazaki, R.; Noguchi, E.; Nakanishi, M.; Hirata, K.; Kawabata, K.; Mizuguchi, H. Prediction of Interindividual Differences in Hepatic Functions and Drug Sensitivity by Using Human iPS-Derived Hepatocytes. *Proc. Natl. Acad. Sci. U. S. A.* **2014**, *111* (47), 16772–16777.
53. Cameron, K.; Tan, R.; Schmidt-Heck, W.; Campos, G.; Lyall, M. J.; Wang, Y.; Lucendo-Villarín, B.; Szkolnicka, D.; Bates, N.; Kimber, S. J.; Hengstler, J. G.; Godoy, P.; Forbes, S. J.; Hay, D. C. Recombinant Laminins Drive the Differentiation and Self-Organization of HESC-Derived Hepatocytes. *Stem Cell Rep.* **2015**, *5* (6), 1250–1262.
54. Takayama, K.; Inamura, M.; Kawabata, K.; Katayama, K.; Higuchi, M.; Tashiro, K.; Nonaka, A.; Sakurai, F.; Hayakawa, T.; Furue, M. K.; Mizuguchi, H. Efficient Generation of Functional Hepatocytes From Human Embryonic Stem Cells and Induced Pluripotent Stem Cells by HNF4 α Transduction. *Mol. Ther.* **2012**, *20* (1), 127–137.
55. Yoshida, T.; Takayama, K.; Kondoh, M.; Sakurai, F.; Tani, H.; Sakamoto, N.; Matsuura, Y.; Mizuguchi, H.; Yagi, K. Use of Human Hepatocyte-Like Cells Derived From Induced Pluripotent Stem Cells as a Model for Hepatocytes in Hepatitis C Virus Infection. *Biochem. Biophys. Res. Commun.* **2011**, *416* (1–2), 119–124.
56. Ulvestad, M.; Nordell, P.; Asplund, A.; Rehnstrom, M.; Jacobsson, S.; Holmgren, G.; Davidsson, L.; Brolen, G.; Edsbacke, J.; Bjorquist, P.; Kuppers-Munther, B.; Andersson, T. B. Drug Metabolizing Enzyme and Transporter Protein Profiles of Hepatocytes Derived From Human Embryonic and Induced Pluripotent Stem Cells. *Biochem. Pharmacol.* **2013**, *86* (5), 691–702.
57. Medine, C. N.; Lucendo-Villarín, B.; Storck, C.; Wang, F.; Szkolnicka, D.; Khan, F.; Pernagallo, S.; Black, J. R.; Marriage, H. M.; Ross, J. A.; Bradley, M.; Iredale, J. P.; Flint, O.; Hay, D. C. Developing High-Fidelity Hepatotoxicity Models From Pluripotent Stem Cells. *Stem Cells Transl. Med.* **2013**, *2* (7), 505–509.
58. Holmgren, G.; Sjogren, A. K.; Barragan, I.; Sabirsh, A.; Sartip, P.; Synnergren, J.; Bjorquist, P.; Ingelman-Sundberg, M.; Andersson, T. B.; Edsbacke, J. Long-Term Chronic Toxicity Testing Using Human Pluripotent Stem Cell-Derived Hepatocytes. *Drug Metab. Dispos.* **2014**, *42* (9), 1401–1406.
59. Sirenko, O.; Hesley, J.; Rusyn, I.; Cromwell, E. F. High-Content Assays for Hepatotoxicity Using Induced Pluripotent Stem Cell-Derived Cells. *Assay Drug Dev. Technol.* **2014**, *12* (1), 43–54.
60. Smith, C.; Abalde-Atristain, L.; He, C.; Brodsky, B. R.; Braunstein, E. M.; Chaudhari, P.; Jang, Y. Y.; Cheng, L.; Ye, Z. Efficient and Allele-Specific Genome Editing of Disease Loci in Human iPSCs. *Mol. Ther.* **2015**, *23* (3), 570–577.
61. Anson, B. D.; Kolaja, K. L.; Kamp, T. J. Opportunities for Use of Human iPS Cells in Predictive Toxicology. *Clin. Pharmacol. Ther.* **2011**, *89* (5), 754–758.
62. Dianat, N.; Steichen, C.; Vallier, L.; Weber, A.; Dubart-Kupperschmitt, A. Human Pluripotent Stem Cells for Modelling Human Liver Diseases and Cell Therapy. *Curr. Gene Ther.* **2013**, *13*, 120–132.
63. Aarli, J. A.; Janca, A.; Muscetta, A. *Neurological Disorders: Public Health Challenges*; World Health Organization: Geneva, 2006.
64. Breier, J. M.; Gassmann, K.; Kayser, R.; Stegeman, H.; De Groot, D.; Fritsche, E.; Shafer, T. J. Neural Progenitor Cells as Models for High-Throughput Screens of Developmental Neurotoxicity: State of the Science. *Neurotoxicol. Teratol.* **2010**, *32* (1), 4–15.
65. Yap, M. S.; Nathan, K. R.; Yeo, Y.; Lim, L. W.; Poh, C. L.; Richards, M.; Lim, W. L.; Othman, I.; Heng, B. C. Neural Differentiation of Human Pluripotent Stem Cells for Nontherapeutic Applications: Toxicology, Pharmacology, and in vitro Disease Modeling. *Stem Cells Int.* **2015**, *2015*, 105172.
66. Steffenhagen, C.; Kraus, S.; Dechant, F. X.; Kandasamy, M.; Lehner, B.; Poehler, A. M.; Furtner, T.; Siebzehnrubl, F. A.; Couillard-Despres, S.; Strauss, O.; Aigner, L.; Rivera, F. J. Identity, Fate and Potential of Cells Grown as Neurospheres: Species Matters. *Stem Cell Rev.* **2011**, *7* (4), 815–835.
67. NAU, H. Correlation of Transplacental and Maternal Pharmacokinetics of Retinoids During Organogenesis With Teratogenicity. *Methods Enzymol.* **1990**, *190*, 437–448.
68. Di Giorgio, F. P.; Carrasco, M. A.; Siao, M. C.; Maniatis, T.; Eggan, K. Non-Cell Autonomous Effect of Glia on Motor Neurons in an Embryonic Stem Cell-Based ALS Model. *Nat. Neurosci.* **2007**, *10* (5), 608–614.
69. Dimos, J. T.; Rodolfa, K. T.; Niakan, K. K.; Weisenthal, L. M.; Mitsumoto, H.; Chung, W.; Croft, G. F.; Saphier, G.; Leibel, R.; Goland, R.; Wichterle, H.; Henderson, C. E.; Eggan, K. Induced Pluripotent Stem Cells Generated From Patients With ALS Can Be Differentiated Into Motor Neurons. *Science* **2008**, *321*, 1218–1221.
70. Ebert, A. D.; Yu, J.; Rose, F. F., Jr.; Mattis, V. B.; Lorson, C. L.; Thomson, J. A.; Svendsen, C. N. Induced Pluripotent Stem Cells From a Spinal Muscular Atrophy Patient. *Nature* **2009**, *457* (7227), 277–280.
71. Israel, M. A.; Yuan, S. H.; Bardy, C.; Reyna, S. M.; Mu, Y.; Herrera, C.; Hefferan, M. P.; Van Gorp, S.; Nazor, K. L.; Boscolo, F. S.; Carson, C. T.; Laurent, L. C.; Marsala, M.; Gage, F. H.; Remes, A. M.; Koo, E. H.; Goldstein, L. S. Probing Sporadic and Familial Alzheimer's Disease Using Induced Pluripotent Stem Cells. *Nature* **2012**, *482* (7384), 216–220.
72. Hargus, G.; Cooper, O.; Deleidi, M.; Levy, A.; Lee, K.; Marlow, E.; Yow, A.; Soldner, F.; Hockemeyer, D.; Hallett, P. J.; Osborn, T.; Jaenisch, R.; Isacson, O. Differentiated Parkinson Patient-Derived Induced Pluripotent Stem Cells Grow in the Adult Rodent Brain and Reduce Motor Asymmetry in Parkinsonian Rats. *Proc. Natl. Acad. Sci. U. S. A.* **2010**, *107* (36), 15921–15926.
73. Hotta, A.; Cheung, A. Y.; Farra, N.; Vijayaragavan, K.; Seguin, C. A.; Draper, J. S.; Pasceri, P.; Maksakova, I. A.; Mager, D. L.; Rossant, J.; Bhatia, M.; Ellis, J. Isolation of Human iPS Cells Using EOS Lentiviral Vectors to Select for Pluripotency. *Nat. Methods* **2009**, *6* (5), 370–376.
74. Lemonnier, T.; Blanchard, S.; Toli, D.; Roy, E.; Bigou, S.; Froissart, R.; Rouvet, I.; Vitry, S.; Heard, J. M.; Bohl, D. Modeling Neuronal Defects Associated With a Lysosomal Disorder Using Patient-Derived Induced Pluripotent Stem Cells. *Hum. Mol. Genet.* **2011**, *20* (18), 3653–3666.
75. Brennand, K. J.; Simone, A.; Jou, J.; Gelboin-Burkhardt, C.; Tran, N.; Sangar, S.; Li, Y.; Mu, Y.; Chen, G.; Yu, D.; McCarthy, S.; Sebat, J.; Gage, F. H. Modelling Schizophrenia Using Human Induced Pluripotent Stem Cells. *Nature* **2011**, *473* (7346), 221–225.
76. Llorens, J.; Li, A. A.; Ceccatelli, S.; Sunol, C. Strategies and Tools for Preventing Neurotoxicity: To Test, to Predict and How to Do It. *Neurotoxicology* **2012**, *33* (4), 796–804.
77. Moors, M.; Rockel, T. D.; Abel, J.; Cline, J. E.; Gassmann, K.; Schreiber, T.; Schuwald, J.; Weinmann, N.; Fritsche, E. Human Neurospheres as Three-Dimensional Cellular Systems for Developmental Neurotoxicity Testing. *Environ. Health Perspect.* **2009**, *117* (7), 1131–1138.
78. (a) Kola, I.; Landis, J. Can the Pharmaceutical Industry Reduce Attrition Rates? *Nat. Rev. Drug Discov.* **2004**, *3* (8), 711–716; (b) MacDonald, J. S.; Robertson, R. T. Toxicity Testing in the 21st Century: A View From the Pharmaceutical Industry. *Toxicol. Sci.* **2009**, *110* (1), 40–46.
79. Mandenius, C. F.; Steel, D.; Noor, F.; Meyer, T.; Heinzle, E.; Asp, J.; Arain, S.; Kraushaar, U.; Bremer, S.; Class, R.; Sartip, P. Cardiotoxicity Testing Using Pluripotent Stem Cell-Derived Human Cardiomyocytes and State-of-the-Art Bioanalytics: A Review. *J. Appl. Toxicol.* **2011**, *31* (3), 191–205.
80. Gintant, G.; Sager, P. T.; Stockbridge, N. Evolution of Strategies to Improve Preclinical Cardiac Safety Testing. *Nat. Rev. Drug Discov.* **2016**, *15* (7), 457–471. <http://dx.doi.org/10.1038/nrd.2015.34>.
81. Khan, J. M.; Lyon, A. R.; Harding, S. E. The Case for Induced Pluripotent Stem Cell-Derived Cardiomyocytes in Pharmacological Screening. *Br. J. Pharmacol.* **2013**, *169* (2), 304–317.
82. (a) Mauritz, C.; Schwanke, K.; Reppel, M.; Neef, S.; Katsimtak, K.; Maier, L. S.; Nguemo, F.; Menke, S.; Hausteiner, M.; Heschler, J.; Hasenfuss, G.; Martin, U. Generation of Functional Murine Cardiac Myocytes From Induced Pluripotent Stem Cells. *Circulation* **2008**, *118* (5), 507–517; (b) Narazaki, G.; Uosaki, H.; Teranishi, M.; Okita, K.; Kim, B.; Matsuoka, S.; Yamanaka, S.; Yamashita, J. K. Directed and Systematic Differentiation of Cardiovascular Cells From Mouse Induced Pluripotent Stem Cells. *Circulation* **2008**, *118* (5), 498–506.
83. Zhang, J.; Wilson, G. F.; Soerens, A. G.; Koonce, C. H.; Yu, J.; Palecek, S. P.; Thomson, J. A.; Kamp, T. J. Functional Cardiomyocytes Derived From Human Induced Pluripotent Stem Cells. *Circ. Res.* **2009**, *104* (4), e30–e41.
84. Burridge, P. W.; Keller, G.; Gold, J. D.; Wu, J. C. Production of De Novo Cardiomyocytes: Human Pluripotent Stem Cell Differentiation and Direct Reprogramming. *Cell Stem Cell* **2012**, *10* (1), 16–28.
85. Birket, M. J.; Mummery, C. L. Pluripotent Stem Cell Derived Cardiovascular Progenitors—A Developmental Perspective. *Dev. Biol.* **2015**, *400* (2), 169–179.

86. Yokoo, N.; Baba, S.; Kaichi, S.; Niwa, A.; Mima, T.; Doi, H.; Yamanaka, S.; Nakahata, T.; Heike, T. The Effects of Cardioactive Drugs on Cardiomyocytes Derived From Human Induced Pluripotent Stem Cells. *Biochem. Biophys. Res. Commun.* **2009**, *387* (3), 482–488.
87. Bedada, F. B.; Wheelwright, M.; Metzger, J. M. Maturation Status of Sarcomere Structure and Function in Human iPSC-Derived Cardiac Myocytes. *Biochim. Biophys. Acta* **2015**, *1863*, 1829–1838.
88. Nakamura, Y.; Matsuo, J.; Miyamoto, N.; Ojima, A.; Ando, K.; Kanda, Y.; Sawada, K.; Sugiyama, A.; Sekino, Y. Assessment of Testing Methods for Drug-Induced Repolarization Delay and Arrhythmias in an iPSC Cell-Derived Cardiomyocyte Sheet: Multi-Site Validation Study. *J. Pharmacol. Sci.* **2014**, *124* (4), 494–501.
89. (a) Wadhwa, D.; Fallah-Rad, N.; Grenier, D.; Krahn, M.; Fang, T.; Ahmadi, R.; Walker, J. R.; Lister, D.; Arora, R. C.; Barac, I.; Morris, A.; Jassal, D. S. Trastuzumab Mediated Cardiotoxicity in the Setting of Adjuvant Chemotherapy for Breast Cancer: A Retrospective Study. *Breast Cancer Res. Treat.* **2009**, *117* (2), 357–364; (b) Albini, A.; Pennesi, G.; Donatelli, F.; Cammarota, R.; De Flora, S.; Noonan, D. M. Cardiotoxicity of Anticancer Drugs: The Need for Cardio-Oncology and Cardio-Oncological Prevention. *J. Natl. Cancer Inst.* **2010**, *102* (1), 14–25.
90. 79 (a) Hirt, M. N.; Boeddinghaus, J.; Mitchell, A.; Schaaf, S.; Bornchen, C.; Muller, C.; Schulz, H.; Hubner, N.; Stenzig, J.; Stoehr, A.; Neuber, C.; Eder, A.; Luther, P. K.; Hansen, A.; Eschenhagen, T. Functional Improvement and Maturation of Rat and Human Engineered Heart Tissue by Chronic Electrical Stimulation. *J. Mol. Cell. Cardiol.* **2014**, *74*, 151–161; Vunjak Novakovic, G.; Eschenhagen, T.; Mummery, C. Myocardial Tissue Engineering: in vitro Models. *CSH Perspect Med J.* **2014**, *4* (3), a014076; (c) Tulloch, N. L.; Muskheili, V.; Razumova, M. V.; Korte, F. S.; Regnier, M.; Hauch, K. D.; Pabon, L.; Reinecke, H.; Murry, C. E. Growth of Engineered Human Myocardium With Mechanical Loading and Vascular Coculture. *Circ. Res.* **2011**, *109* (1), 47–59.
91. Kattman, S. J.; Witty, A. D.; Gagliardi, M.; Dubois, N. C.; Niapour, M.; Hotta, A.; Ellis, J.; Keller, G. Stage-Specific Optimization of Activin/Nodal and BMP Signaling Promotes Cardiac Differentiation of Mouse and Human Pluripotent Stem Cell Lines. *Cell Stem Cell* **2011**, *8* (2), 228–240.
92. Cao, N.; Liu, Z.; Chen, Z.; Wang, J.; Chen, T.; Zhao, X.; Ma, Y.; Qin, L.; Kang, J.; Wei, B.; Wang, L.; Jin, Y.; Yang, H. T. Ascorbic Acid Enhances the Cardiac Differentiation of Induced Pluripotent Stem Cells Through Promoting the Proliferation of Cardiac Progenitor Cells. *Cell Res.* **2012**, *22* (1), 219–236.
93. Minami, I.; Yamada, K.; Otsuji, T. G.; Yamamoto, T.; Shen, Y.; Otsuka, S.; Kadota, S.; Morone, N.; Barve, M.; Asai, Y.; Tenkova-Heuser, T.; Heuser, J. E.; Uesugi, M.; Aiba, K.; Nakatsuji, N. A Small Molecule That Promotes Cardiac Differentiation of Human Pluripotent Stem Cells Under Defined, Cytokine- and Xeno-Free Conditions. *Cell Rep.* **2012**, *2* (5), 1448–1460.
94. Xiaojun Lian, C. H.; Wilson, G.; Zhu, K.; Hazeltine, L. B.; Azarin, S. M.; Raval, K. K.; Zhang, J.; Kamp, T. J.; Palecek, S. P. Robust Cardiomyocyte Differentiation From Human Pluripotent Stem Cells via Temporal Modulation of Canonical Wnt Signaling. *Proc. Natl. Acad. Sci. U. S. A.* **2012**, *109* (27), E1848–E1857.
95. Gonzalez, R.; Lee, J. W.; Schultz, P. G. Stepwise Chemically Induced Cardiomyocyte Specification of Human Embryonic Stem Cells. *Angew. Chem. Int. Ed.* **2011**, *50* (47), 11181–11185.
96. BurrIDGE, P. W.; Matsa, E.; Shukla, P.; Lin, Z. C.; Churko, J. M.; Ebert, A. D.; Lan, F.; Diecke, S.; Huber, B.; Mordwinkin, N. M.; Plews, J. R.; Abilez, O. J.; Cui, B.; Gold, J. D.; Wu, J. C. Chemically Defined Generation of Human Cardiomyocytes. *Nat. Methods* **2014**, *11* (8), 855–860.
97. Karakikes, I.; Senyei, G. D.; Hansen, J.; Kong, C. W.; Azeloglu, E. U.; Stillitano, F.; Lieu, D. K.; Wang, J.; Ren, L.; Hulot, J. S.; Iyengar, R.; Li, R. A.; Hajjar, R. J. Small Molecule-Mediated Directed Differentiation of Human Embryonic Stem Cells Toward Ventricular Cardiomyocytes. *Stem Cells Transl. Med.* **2014**, *3* (1), 18–31.
98. Kempf, H.; Olmer, R.; Kropp, C.; Ruckert, M.; Jara-Avaca, M.; Robles-Diaz, D.; Franke, A.; Elliott, D. A.; Wojciechowski, D.; Fischer, M.; Roa Lara, A.; Kensah, G.; Gruh, I.; Haverich, A.; Martin, U.; Zweigerdt, R. Controlling Expansion and Cardiomyogenic Differentiation of Human Pluripotent Stem Cells in Scalable Suspension Culture. *Stem Cell Rep.* **2014**, *3* (6), 1132–1146.
99. Fonoudi, H.; Ansari, H.; Abbasalizadeh, S.; Larjani, M. R.; Kiani, S.; Hashemizadeh, S.; Zarchi, A. S.; Bosman, A.; Blue, G. M.; Pahlavan, S.; Perry, M.; Orr, Y.; Mayorchak, Y.; Vandenberg, J.; Talkhabi, M.; Winlaw, D. S.; Harvey, R. P.; Aghdami, N.; Baharvand, H. A Universal and Robust Integrated Platform for the Scalable Production of Human Cardiomyocytes From Pluripotent Stem Cells. *Stem Cells Transl. Med.* **2015**, *4* (12), 1482–1494.
100. Zhang, M.; Schulte, J. S.; Heinick, A.; Piccini, I.; Rao, J.; Quaranta, R.; Zeuschner, D.; Malan, D.; Kim, K. P.; Ropke, A.; Sasse, P.; Arauzo-Bravo, M.; Seeböhm, G.; Scholer, H.; Fabritz, L.; Kirchhof, P.; Müller, F. U.; Greber, B. Universal Cardiac Induction of Human Pluripotent Stem Cells in Two and Three-Dimensional Formats: Implications for in vitro Maturation. *Stem Cells* **2015**, *33* (5), 1456–1469.
101. Zhang, M.; D'Aniello, C.; Verkerk, A. O.; Wrobel, E.; Frank, S.; Ward-van Oostwaard, D.; Piccini, I.; Freund, C.; Rao, J.; Seeböhm, G.; Atsma, D. E.; Schulze-Bahr, E.; Mummery, C. L.; Greber, B.; Bellin, M. Recessive Cardiac Phenotypes in Induced Pluripotent Stem Cell Models of Jervell and Lange-Nielsen Syndrome: Disease Mechanisms and Pharmacological Rescue. *Proc. Natl. Acad. Sci. U. S. A.* **2014**, *111* (50), E5383–E5392.
102. Malan, D.; Zhang, M.; Stallmeyer, B.; Müller, J.; Fleischmann, B. K.; Schulze-Bahr, E.; Sasse, P.; Greber, B. Human iPSC Cell Model of Type 3 Long QT Syndrome Recapitulates Drug-Based Phenotype Correction. *Basic Res. Cardiol.* **2016**, *111* (2), 14.
103. Matsa, E.; Rajamohan, D.; Dick, E.; Young, L.; Mellor, I.; Staniforth, A.; Denning, C. Drug Evaluation in Cardiomyocytes Derived From Human Induced Pluripotent Stem Cells Carrying a Long QT Syndrome Type 2 Mutation. *Eur. Heart J.* **2011**, *32* (8), 952–962.
104. Willyard, C. The Boom in Mini Stomachs, Brains, Breasts, Kidneys and More. *Nature* **2015**, *523* (7562), 520–522.
105. Fatehullah, A.; Tan, S. H.; Barker, N. Organoids as an in vitro Model of Human Development and Disease. *Nat. Cell Biol.* **2016**, *18* (3), 246–254.
106. Yin, X.; Mead, B. E.; Safaee, H.; Langer, R.; Karp, J. M.; Levy, O. Engineering Stem Cell Organoids. *Cell Stem Cell* **2016**, *18* (1), 25–38.
107. Paul, E. C. A.; Hochman, J.; Quaroni, A. Conditionally Immortalized Intestinal Epithelial Cells: Novel Approach for Study of Differentiated Enterocytes. *Am. J. Physiol.* **1993**, *266*–278.
108. Marx, V. Cell-Line Authentication Demystified. *Nat. Methods* **2014**, *11* (5), 483–488.
109. Masters, J. R.; Stacey, G. N. Changing Medium and Passaging Cell Lines. *Nat. Protoc.* **2007**, *2* (9), 2276–2284.
110. Randall, K. J.; Turton, J.; Foster, J. R. Explant Culture of Gastrointestinal Tissue: A Review of Methods and Applications. *Cell Biol. Toxicol.* **2011**, *27* (4), 267–284.
111. Shanks, N.; Greek, R.; Greek, J. Are Animal Models Predictive for Humans? *Philos. Ethics Humanit. Med.* **2009**, *4*, 2.
112. Takebe, T.; Enomura, M.; Yoshizawa, E.; Kimura, M.; Koike, H.; Ueno, Y.; Matsuzaki, T.; Yamazaki, T.; Toyohara, T.; Osafune, K.; Nakauchi, H.; Yoshikawa, H. Y.; Taniguchi, H. Vascularized and Complex Organ Buds From Diverse Tissues via Mesenchymal Cell-Driven Condensation. *Cell Stem Cell* **2015**, *16* (5), 556–565.
113. Sato, T.; Vries, R. G.; Snippert, H. J.; van de Wetering, M.; Barker, N.; Stange, D. E.; van Es, J. H.; Abo, A.; Kujala, P.; Peters, P. J.; Clevers, H. Single Lgr5 Stem Cells Build Crypt-Villus Structures in vitro Without a Mesenchymal Niche. *Nature* **2009**, *459* (7244), 262–265.
114. Hachitanda, Y.; Tsuneyoshi, M. Neuroblastoma With a Distinct Organoid Pattern. *Hum. Pathol.* **1994**, *25* (1), 67–72.
115. Zimmermann, W. H.; Melnychenko, I.; Eschenhagen, T. Engineered Heart Tissue for Regeneration of Diseased Hearts. *Biomaterials* **2004**, *25* (9), 1639–1647.
116. Lancaster, M. A.; Knoblich, J. A. Organogenesis in a Dish: Modeling Development and Disease Using Organoid Technologies. *Science* **2014**, *345* (6194), 1247125.
117. Weitzer, G. Embryonic Stem Cell-Derived Embryoid Bodies: An in vitro Model of Eutherian Pregastrulation Development and Early Gastrulation. *Handb. Exp. Pharmacol.* **2006**, *174*, 21–51.
118. Xu, C.; Inokuma, M. S.; Denham, J.; Golds, K.; Kundu, P.; Gold, J. D.; Carpenter, M. K. Feeder-Free Growth of Undifferentiated Human Embryonic Stem Cells. *Nat. Biotechnol.* **2001**, *19*, 971–974.
119. Vazin, T.; Schaffer, D. V. Engineering Strategies to Emulate the Stem Cell Niche. *Trends Biotechnol.* **2010**, *28* (3), 117–124.
120. Guvendiren, M.; Burdick, J. A. Stiffening Hydrogels to Probe Short- and Long-Term Cellular Responses to Dynamic Mechanics. *Nat. Commun.* **2012**, *3*, 792.
121. Atala, A.; Yoo, J. Bioprinting: 3D Printing Comes to Life. *Manuf. Eng.* **2015**, 63–66.
122. Stephan, M. T.; Irvine, D. J. Enhancing Cell Therapies From the Outside in: Cell Surface Engineering Using Synthetic Nanomaterials. *Nano Today* **2011**, *6* (3), 309–325.
123. Golden, A. P.; Tien, J. Fabrication of Microfluidic Hydrogels Using Molded Gelatin as a Sacrificial Element. *Lab Chip* **2007**, *7* (6), 720–725.

124. Visconti, R. P.; Kasyanov, V.; Gentile, C.; Zhang, J.; Markwald, R. R.; Mironov, V. Towards Organ Printing: Engineering an Intra-Organ Branched Vascular Tree. *Expert Opin. Biol. Ther.* **2010**, *10* (3), 409–420.
125. Purcell, O.; Lu, T. K. Synthetic Analog and Digital Circuits for Cellular Computation and Memory. *Curr. Opin. Biotechnol.* **2014**, *29*, 146–155.
126. Willyard, C. Rise of the Organoids. *Nature* **2015**, *523*, 520–522.
127. Luni, C.; Serena, E.; Elvassore, N. Human-on-Chip for Therapy Development and Fundamental Science. *Curr. Opin. Biotechnol.* **2014**, *25*, 45–50.
128. Takebe, T.; Sekine, K.; Enomura, M.; Koike, H.; Kimura, M.; Ogaeri, T.; Zhang, R. R.; Ueno, Y.; Zheng, Y. W.; Koike, N.; Aoyama, S.; Adachi, Y.; Taniguchi, H. Vascularized and Functional Human Liver From an iPSC-Derived Organoid Transplant. *Nature* **2013**, *499* (7459), 481–484.
129. Dedhia, P. H.; Bertaux-Skeirik, N.; Zavros, Y.; Spence, J. R. Organoid Models of Human Gastrointestinal Development and Disease. *Gastroenterology* **2016**, *150*, 1098–1112.
130. Miyajima, A.; Tanaka, M.; Itoh, T. Stem/Progenitor Cells in Liver Development, Homeostasis, Regeneration, and Reprogramming. *Cell Stem Cell* **2014**, *14* (5), 561–574.
131. Sarada Devi Ramachandran, K. S.; Münst, B.; Heinz, S.; Ghafoory, S.; Wölfl, S.; Simon-Keller, K.; Marx, A.; Ionica Øie, C.; Ebert, M. P.; Walles, H.; Braspenning, J.; BreitkopfHeinlein, K. In Vitro Generation of Functional Liver Organoid-Like Structures Using Adult Human Cells. *PLoS One* **2015**, *10* (10), e0139345.
132. Gilbert, S. F. *Developmental Biology*, 6th ed.; Sinauer Associates: Sunderland, MA, 2000.
133. Lehtinen, M. K.; Walsh, C. A. Neurogenesis at the Brain-Cerebrospinal Fluid Interface. *Annu. Rev. Cell Dev. Biol.* **2011**, *27*, 653–679.
134. Lancaster, M. A.; Knoblich, J. A. Spindle Orientation in Mammalian Cerebral Cortical Development. *Curr. Opin. Neurobiol.* **2012**, *22* (5), 737–746.
135. Conti, L.; Cattaneo, E. Neural Stem Cell Systems: Physiological Players or in vitro Entities? *Nat. Rev. Neurosci.* **2010**, *11* (3), 176–187.
136. Reynolds, B. A.; Weiss, S. Generation of Neurons and Astrocytes From Isolated Cells of the Adult Mammalian Central Nervous System. *Science* **1992**, *255* (5052), 1707–1710.
137. Zhang, S. C.; Wernig, M.; Duncan, I. D.; Brustle, O.; Thomson, J. A. In Vitro Differentiation of Transplantable Neural Precursors From Human Embryonic Stem Cells. *Nat. Biotechnol.* **2001**, *19* (12), 1129–1133.
138. Elkabetz, Y.; Panagiotakos, G.; Al Shamy, G.; Succi, N. D.; Tabar, V.; Studer, L. Human ES Cell-Derived Neural Rosettes Reveal a Functionally Distinct Early Neural Stem Cell Stage. *Genes Dev.* **2008**, *22* (2), 152–165.
139. Gaspard, N.; Bouschet, T.; Hourez, R.; Dimidschstein, J.; Naeije, G.; van den Aemele, J.; Espuny-Camacho, I.; Herpoel, A.; Passante, L.; Schiffmann, S. N.; Gaillard, A.; Vanderhaeghen, P. An Intrinsic Mechanism of Corticogenesis From Embryonic Stem Cells. *Nature* **2008**, *455* (7211), 351–357.
140. Nakano, T.; Ando, S.; Takata, N.; Kawada, M.; Muguruma, K.; Sekiguchi, K.; Saito, K.; Yonemura, S.; Eiraku, M.; Sasai, Y. Self-Formation of Optic Cups and Storable Stratified Neural Retina From Human ESCs. *Cell Stem Cell* **2012**, *10* (6), 771–785.
141. Cyranoski, D. Tissue Engineering: The Brainmaker. *Nature* **2012**, *488* (7412), 444–446.
142. Spence, J. R.; Mayhew, C. N.; Rankin, S. A.; Kuhar, M. F.; Vallance, J. E.; Tolle, K.; Hoskins, E. E.; Kalinichenko, V. V.; Wells, S. I.; Zorn, A. M.; Shroyer, N. F.; Wells, J. M. Directed Differentiation of Human Pluripotent Stem Cells Into Intestinal Tissue In Vitro. *Nature* **2011**, *470* (7332), 105–109.
143. Lancaster, M. A.; Renner, M.; Martin, C. A.; Wenzel, D.; Bicknell, L. S.; Hurler, M. E.; Homfray, T.; Penninger, J. M.; Jackson, A. P.; Knoblich, J. A. Cerebral Organoids Model Human Brain Development and Microcephaly. *Nature* **2013**, *501* (7467), 373–379.
144. Humphreys, B. D. Kidney Structures Differentiated From Stem Cells. *Nat. Cell Biol.* **2014**, *16* (1), 19–21.
145. Lancaster, M. A.; Knoblich, J. A. Generation of Cerebral Organoids From Human Pluripotent Stem Cells. *Nat. Protoc.* **2014**, *9* (10), 2329–2340.
146. Belen, D. Cerebral Organoids Will Play an Essential Role in Understanding the Development of the Brain. *Turk. Neurosurg.* **2014**, *24* (5), 637–638.
147. Alrefai, M. T.; Murali, D.; Paul, A.; Ridwan, K. M.; Connell, J. M.; Shum-Tim, D. Cardiac Tissue Engineering and Regeneration Using Cell-Based Therapy. *Stem Cells Cloning* **2015**, *8*, 81–101.
148. Perez-Pomares, J. M.; de la Pompa, J. L. Signaling During Epicardium and Coronary Vessel Development. *Circ. Res.* **2011**, *109* (12), 1429–1442.
149. Tian, X.; Hu, T.; Zhang, H.; He, L.; Huang, X.; Liu, Q.; Yu, W.; Yang, Z.; Zhang, Z.; Zhong, T. P.; Yang, X.; Yan, Y.; Baldini, A.; Sun, Y.; Lu, J.; Schwartz, R. J.; Evans, S. M.; Gittenberger-de Groot, A. C.; Red-Horse, K.; Zhou, B. Subepicardial Endothelial Cells Invade the Embryonic Ventricle Wall to Form Coronary Arteries. *Cell Res.* **2013**, *23* (9), 1075–1090.
150. Cossette, S.; Misra, R. The Identification of Different Endothelial Cell Populations Within the Mouse Proepicardium. *Dev. Dyn.* **2011**, *240* (10), 2344–2353.
151. Tomanek, R. J. Formation of the Coronary Vasculature: A Brief Review. *Cardiovasc. Res.* **1996**, *31*, Spec No. E46–51.
152. Yang, L.; Soonpaa, M. H.; Adler, E. D.; Roepke, T. K.; Kattman, S. J.; Kennedy, M.; Henckaerts, E.; Bonham, K.; Abbott, G. W.; Linden, R. M.; Field, L. J.; Keller, G. M. Human Cardiovascular Progenitor Cells Develop From a KDR+ Embryonic-Stem-Cell-Derived Population. *Nature* **2008**, *453* (7194), 524–528.
153. Vunjak-Novakovic, G.; Tandon, N.; Godier, A.; Maidhof, R.; Marsano, A.; Martens, T. P.; Radisic, M. Challenges in Cardiac Tissue Engineering. *Tissue Eng. Part B Rev.* **2010**, *16* (2), 169–187.
154. Shimizu, T.; Sekine, H.; Yang, J.; Isoi, Y.; Yamato, M.; Kikuchi, A.; Kobayashi, E.; Okano, T. Polysurgery of Cell Sheet Grafts Overcomes Diffusion Limits to Produce Thick, Vascularized Myocardial Tissues. *FASEB J.* **2006**, *20* (6), 708–710.
155. Reddi, A. H.; Huggins, C. B. Influence of Geometry of Transplanted Tooth and Bone on Transformation of Fibroblasts. *Proc. Soc. Exp. Biol. Med.* **1973**, *143* (3), 634–637.
156. Lutolf, M. P.; Hubbell, J. A. Synthetic Biomaterials as Instructive Extracellular Microenvironments for Morphogenesis in Tissue Engineering. *Nat. Biotechnol.* **2005**, *23* (1), 47–55.
157. Leor, J.; Amsalem, Y.; Cohen, S. Cells, Scaffolds, and Molecules for Myocardial Tissue Engineering. *Pharmacol. Ther.* **2005**, *105* (2), 151–163.
158. Christman, K. L.; Lee, R. J. Biomaterials for the Treatment of Myocardial Infarction. *J. Am. Coll. Cardiol.* **2006**, *48* (5), 907–913.
159. Davis, M. E.; Hsieh, P. C.; Grodzinsky, A. J.; Lee, R. T. Custom Design of the Cardiac Microenvironment With Biomaterials. *Circ. Res.* **2005**, *97* (1), 8–15.
160. Huang, N. F.; Yu, J.; Sievers, R.; Li, S.; Lee, R. J. Injectable Biopolymers Enhance Angiogenesis After Myocardial Infarction. *Tissue Eng.* **2005**, *11* (11–12), 1860–1866.
161. Reffelmann, T.; Kloner, R. A. Cellular Cardiomyoplasty—Cardiomyocytes, Skeletal Myoblasts, or Stem Cells for Regenerating Myocardium and Treatment of Heart Failure? *Cardiovasc. Res.* **2003**, *58* (2), 358–368.
162. Henning, R. J.; Burgos, J. D.; Vasko, M.; Alvarado, F.; Sanberg, C. D.; Sanberg, P. R.; Morgan, M. B. Human Cord Blood Cells and Myocardial Infarction: Effect of Dose and Route of Administration on Infarct Size. *Cell Transplant.* **2007**, *16* (9), 907–917.
163. Fu, R. H.; Wang, Y. C.; Liu, S. P.; Shih, T. R.; Lin, H. L.; Chen, Y. M.; Sung, J. H.; Lu, C. H.; Wei, J. R.; Wang, Z. W.; Huang, S. J.; Tsai, C. H.; Shyu, W. C.; Lin, S. Z. Decellularization and Recellularization Technologies in Tissue Engineering. *Cell Transplant.* **2014**, *23* (4–5), 621–630.
164. Guyette, J. P.; Gilpin, S. E.; Charest, J. M.; Tapias, L. F.; Ren, X.; Ott, H. C. Perfusion Decellularization of Whole Organs. *Nat. Protoc.* **2014**, *9* (6), 1451–1468.
165. Venkatasubramanian, R. T.; Grassl, E. D.; Barocas, V. H.; Lafontaine, D.; Bischof, J. C. Effects of Freezing and Cryopreservation on the Mechanical Properties of Arteries. *Ann. Biomed. Eng.* **2006**, *34* (5), 823–832.
166. Nuwaysir, E. F.; Bittner, M.; Trent, J.; Barrett, J. C.; Afshari, C. A. Microarrays and Toxicology: The Advent of Toxicogenomics. *Mol. Carcinog.* **1999**, *24* (3), 153–159.
167. Afshari, C. A.; Hamadeh, H. K.; Bushel, P. R. The Evolution of Bioinformatics in Toxicology: Advancing Toxicogenomics. *Toxicol. Sci.* **2011**, *120* (Suppl 1), S225–S237.
168. Chen, M.; Zhang, M.; Borlak, J.; Tong, W. A Decade of Toxicogenomic Research and Its Contribution to Toxicological Science. *Toxicol. Sci.* **2012**, *130* (2), 217–228.
169. McBurney, R. N.; Hines, W. M.; VonTungeln, L. S.; Schnackenberg, L. K.; Beger, R. D.; Moland, C. L.; Han, T.; Fuscoe, J. C.; Chang, C. W.; Chen, J. J.; Su, Z.; Fan, X. H.; Tong, W.; Booth, S. A.; Balasubramanian, R.; Courchesne, P. L.; Campbell, J. M.; Graber, A.; Guo, Y.; Juhasz, P.; Li, T. Y.; Lynch, M. D.; Morel, N. M.; Plasterer, T. N.; Takach, E. J.; Zeng, C.; Beland, F. A. The Liver Toxicity Biomarker Study Phase I: Markers for the Effects of Tolcapone or Entacapone. *Toxicol. Pathol.* **2012**, *40* (6), 951–964.
170. Ellinger-Ziegelbauer, H.; Gmuender, H.; Bandenburg, A.; Ahr, H. J. Prediction of a Carcinogenic Potential of Rat Hepatocarcinogens Using Toxicogenomics Analysis of Short-Term in vivo Studies. *Mutat. Res.* **2008**, *637* (1–2), 23–39.
171. Igarashi, Y.; Nakatsu, N.; Yamashita, T.; Ono, A.; Ohno, Y.; Urushidani, T.; Yamada, H. Open TG-GATES: A Large-Scale Toxicogenomics Database. *Nucleic Acids Res.* **2015**, *43* (Database issue), D921–D927.

172. Gerets, H. H.; Tilmant, K.; Gerin, B.; Chanteux, H.; Depelchin, B. O.; Dhalluin, S.; Atienzar, F. A. Characterization of Primary Human Hepatocytes, HepG2 Cells, and HepaRG Cells at the mRNA Level and CYP Activity in Response to Inducers and Their Predictivity for the Detection of Human Hepatotoxins. *Cell Biol. Toxicol.* **2012**, *28* (2), 69–87.
173. Berger, D. R.; Ware, B. R.; Davidson, M. D.; Allsup, S. R.; Khetani, S. R. Enhancing the Functional Maturity of Induced Pluripotent Stem Cell-Derived Human Hepatocytes by Controlled Presentation of Cell–Cell Interactions In Vitro. *Hepatology* **2015**, *61* (4), 1370–1381.
174. Hossini, A. M.; Megges, M.; Prigione, A.; Lichtner, B.; Toliat, M. R.; Wruck, W.; Schroter, F.; Nuernberg, P.; Kroll, H.; Makrantonaki, E.; Zouboulis, C. C.; Adjaye, J. Induced Pluripotent Stem Cell-Derived Neuronal Cells From a Sporadic Alzheimer's Disease Donor as a Model for Investigating AD-Associated Gene Regulatory Networks. *BMC Genomics* **2015**, *16*, 84.
175. Bessems, J.; Coeckey, S.; Gouliarmou, V.; Whelan, M.; Worth, A. *EURL ECVAM Strategy for Achieving 3Rs Impact in the Assessment of Toxicokinetics and Systemic Toxicity*; Publications Office: Luxembourg, 2015.
176. Russell, W. M. S.; Burch, R. L. *The Principles of Humane Experimental Technique*; Methuen: London, 1959. (Reprinted by UFAW, 1992: 8 Hamilton Close, South Mimms, Potters Bar, Herts EN6 3QD England.
177. Hofer, T.; Gerner, I.; Gundert-Remy, U.; Liebsch, M.; Schulte, A.; Spielmann, H.; Vogel, R.; Wettig, K. Animal Testing and Alternative Approaches for the Human Health Risk Assessment Under the Proposed new European Chemicals Regulation. *Arch. Toxicol.* **2004**, *78* (10), 549–564.
178. Wruck, W.; Peuker, M.; Regenbrecht, C. R. Data Management Strategies for Multinational Large-Scale Systems Biology Projects. *Brief. Bioinform.* **2014**, *15* (1), 65–78.
179. Pelkonen, O.; Tolonen, A.; Rousu, T.; Tursas, L.; Turpeinen, M.; Hokkanen, J.; Uusitalo, J.; Bouvier d'Yvoire, M.; Coecke, S. Comparison of Metabolic Stability and Metabolite Identification of 55 ECVAM/ICCVAM Validation Compounds Between Human and Rat Liver Homogenates and Microsomes—A Preliminary Analysis. *Altox* **2009**, *26* (3), 214–222.
180. Greek, R.; Menache, A. Systematic Reviews of Animal Models: Methodology Versus Epistemology. *Int. J. Med. Sci.* **2013**, *10* (3), 206–221.
181. Saker, B. M.; Kincaid-Smith, P. Papillary Necrosis in Experimental Analgesic Nephropathy. *Br. Med. J.* **1969**, *1* (5637), 161–162.
182. Gupta, U.; Cook, J. C.; Tassinari, M. S.; Hurtt, M. E. Comparison of Developmental Toxicology of Aspirin (Acetylsalicylic Acid) in Rats Using Selected Dosing Paradigms. *Birth Defects Res. B Dev. Reprod. Toxicol.* **2003**, *68* (1), 27–37.
183. Lave, L. B.; Rosenkranz, H. S.; Omenn, G. S. Information Value of the Rodent Bioassay. *Nature* **1988**, *336* (6200), 631–633.
184. Krewski, D.; Acosta, D., Jr.; Andersen, M.; Anderson, H.; Bailar, J. C., 3rd; Boekelheide, K.; Brent, R.; Charnley, G.; Cheung, V. G.; Green, S., Jr.; Kelsey, K. T.; Kerkvliet, N. I.; Li, A. A.; McCray, L.; Meyer, O.; Patterson, R. D.; Pennie, W.; Scala, R. A.; Solomon, G. M.; Stephens, M.; Yager, J.; Zeise, L. Toxicity Testing in the 21st Century: A Vision and a Strategy. *J. Toxicol. Environ. Health B Crit. Rev.* **2010**, *13* (2–4), 51–138.
185. Organisation for Economic Co-operation and Development. Test No. 427 skin absorption: in vivo method.
186. Organisation for Economic Co-operation and Development. Test no. 417: toxicokinetics.
187. Organisation for Economic Co-operation and Development. Skin absorption In vitro method.

2.6 Liver Disease Modelling

Nina Graffmann, Lucas-Sebastian Spitzhorn, Audrey Ncube, Wasco Wruck and James Adjaye

Abstract

This chapter describes how in vitro generated hepatic cells that are derived from induced pluripotent stem cells (iPSCs) or embryonic stem cells (ESCs) can be used for modelling liver disease.

We will introduce you to the essential liver functions and the different cell types in the liver. You will learn how the liver develops in vivo and how this is reflected in in vitro differentiation protocols. We will present you a widely used protocol for in vitro differentiation of iPSCs into hepatocyte-like cells (HLCs) and will then discuss advantages and disadvantages of iPSC derived hepatic cells for disease modelling. Next, we will introduce in vitro models for several diseases affecting hepatic cells or manifesting primarily in distant organs. You will learn how these models can be used to improve our knowledge of these diseases and to test novel treatment strategies.

Finally, we will demonstrate the use of bioinformatic tools to systematically analyse transcriptome data related to these disease models.

Publication Status: Brand-Saberi B. (eds) Essential Current Concepts in Stem Cell Biology. Learning Materials in Biosciences. Springer, Cham. ISBN 9783030339227

Impact Factor: -

This article is reproduced with permission.

Approximated total share of contribution: 20%

Contribution on experimental design, realization and publication:

LSS wrote the section “11.6.1 Liver diseases that affect hepatocytes” and contributed to the improvement of the whole manuscript. All authors have read and approved the manuscript.

Link to the publication:

https://link.springer.com/chapter/10.1007/978-3-030-33923-4_11



Liver Disease Modelling

Nina Graffmann, Lucas-Sebastian Spitzhorn, Audrey Ncube, Wasco Wruck, and James Adjaye

- 11.1 The Functions of the Liver – 190**
- 11.2 Cell Types in the Liver – 190**
- 11.3 Liver Development *in vivo* – 191**
- 11.4 *In vitro* Hepatocyte Differentiation – 192**
- 11.5 Advantages and Disadvantages of Modelling Liver Diseases with iPSC Derived Cells – 194**
- 11.6 Examples of Liver Diseases Modelled with iPSC Derived Hepatic Cells – 195**
 - 11.6.1 Liver Diseases That Affect Hepatocytes – 195
 - 11.6.2 Diseases That Affect Hepatocytes, But Manifest Primarily in Other Organs – 197
 - 11.6.3 Diseases That Affect Cholangiocytes – 198
- 11.7 Bioinformatic Analysis – 199**
 - 11.7.1 Datasets from Public Repositories – 199
 - 11.7.2 Comparison of Gene Expression Datasets – 200
 - 11.7.3 Gene Ontology (GO) and Pathway Analysis – 202
- References – 203**

What You Will Learn in This Chapter

This chapter describes how *in vitro* generated hepatic cells that are derived from induced pluripotent stem cells (iPSCs) or embryonic stem cells (ESCs) can be used for modelling liver disease.

We will introduce you to the essential liver functions and the different cell types in the liver. You will learn how the liver develops *in vivo* and how this is reflected in *in vitro* differentiation protocols. We will present you a widely used protocol for *in vitro* differentiation of iPSCs into hepatocyte-like cells (HLCs) and will then discuss advantages and disadvantages of iPSC derived hepatic cells for disease modelling. Next, we will introduce *in vitro* models for several diseases affecting hepatic cells or manifesting primarily in distant organs. You will learn how these models can be used to improve our knowledge of these diseases and to test novel treatment strategies.

Finally, we will demonstrate the use of bioinformatic tools to systematically analyse transcriptome data related to these disease models.

11.1 The Functions of the Liver

The liver is a versatile organ involved in many essential metabolic processes in the body and its high secretory activity classifies it as the biggest gland. One of the liver's main functions is the storage and release of micro- and macro-nutrients according to the needs of the body. It is capable of synthesizing, storing and breaking down the main energy sources for the body, namely glucose and fatty acids. Under the control of the insulin counterpart glucagon -a hormone which signals low blood glucose levels to the liver- it produces glucose either out of stored glycogen or by gluconeogenesis, thus providing a constant energy supply to the body and especially the brain (Rui 2014). Fatty acids which are derived either from the diet or from lipolysis taking place in adipocytes are taken up by the liver and stored as triacylglycerides in lipid droplets. From there, they can be released into the blood or they are used directly for energy generation via β -oxidation (Rui 2014).

In addition, the liver synthesizes and secretes many proteins, e.g. albumin -the major blood protein -, clotting factors, and factors related to immune reactions (Barle et al. 1997). It also produces bile acids which are stored in the gall bladder and released into the gut after food uptake (Chiang 2013). Furthermore, the liver plays a major role in detoxification of natural and synthetic compounds. Protein catabolism takes place in the liver and toxic ammonia originating from this process is transformed into urea which can be safely excreted (Mian and Lee 2002). In addition, the large family of cytochrome P-450 (CYP) enzymes is responsible for detoxifying a plethora of molecules, including drugs (Danielson 2002). In the latter case, CYP enzymes are not only needed for detoxification but also to generate the metabolically active form of the drug in the first place (Danielson 2002).

11.2 Cell Types in the Liver

The liver performs versatile functions and has an intricate architecture essential for this role. The adult human liver is composed of four lobes which consist of many small functional units, the so-called liver-lobules (Kruepunga et al. 2019).

About 70% of the cells in the liver are hepatocytes which are responsible for the metabolic and de-toxifying functions of the liver. Due to the anatomy of the liver lobule, the

oxygen level of the blood that passes the hepatocytes decreases from the periphery to the centre of the liver lobules and this is accompanied by functional alterations of the hepatocytes. Periportal hepatocytes are more active in oxygen consuming tasks like β -oxidation of fatty acids and they are involved in gluconeogenesis and glucose delivery, while perivenous hepatocytes perform glycolysis, and metabolize drugs with their active CYP enzymes (Hijmans et al. 2014; Kietzmann 2017).

Cholangiocytes are the second characteristic cell type in the liver (Tabibian et al. 2013). They line the intra-hepatic bile ducts and modify primary bile as it flows towards the gall bladder by transporting ions, solutes, and water across their membranes (Tabibian et al. 2013).

In addition to these so-called parenchymal cells, the liver consists of several non-parenchymal cells as well. These are sinusoidal endothelial cells which line the small blood vessels inside the liver (Wisse et al. 1996), Kupffer cells which belong to the macrophage lineage (Bilzer et al. 2006), and hepatic stellate cells, a population of mesenchymal stem cells (MSCs) which store retinoic acid and fat soluble vitamins and play an important role during liver regeneration and fibrosis (Bansal 2016; Kordes et al. 2014).

As the liver performs many distinct functions, it is also affected by a wide variety of diseases, ranging from genetic disorders affecting either hepatocytes or cholangiocytes themselves or peripheral organs which lack proteins synthesized by the liver to metabolically induced diseases as for example steatosis, fibrosis, cirrhosis or hepatocellular carcinoma. Currently, there are approximately 29 million people in the European Union afflicted with chronic liver diseases (Blachier et al. 2013). In order to further increase our meagre knowledge on the development and treatment options of these diseases, *in vitro* models based on hepatocyte-like cells (HLCs) derived from induced pluripotent stem cells (iPSCs) have emerged as tools for studying the aetiology of these diseases.

11.3 Liver Development *in vivo*

All *in vitro* differentiation protocols are based on insights from development *in vivo*. In human, the onset of liver development is within the third week of gestation, when the endoderm emerges from the anterior primitive streak (Gordillo et al. 2015; Lemaigre 2009; Zorn 2008). Driven by WNT3A and high levels of Activin/Nodal signalling, cells specify towards definitive endoderm (DE) and migrate towards the anterior of the embryo. Nodal signalling induces the expression of the endoderm-associated transcription factors SOX17 and FOXA1–3 (Tsankov et al. 2015). Afterwards, the DE cells form a tube comprising the foregut, hindgut and midgut, which become specified according to gradients of BMP2/4, FGF, and WNT secreted by the adjacent mesoderm cells (Dessimoz et al. 2006; McLin et al. 2007; Tiso et al. 2002). Only low to intermediate concentrations of these factors induce foregut development. Foregut cells then develop into liver, whilst also giving rise to the ventral pancreas, stomach, lungs and thyroid (Gordillo et al. 2015; Lemaigre 2009; Zorn 2008).

Between day 23 and 26 of human development, the liver diverticulum arises from the ventral foregut adjacent to the cardiac mesoderm (Gordillo et al. 2015; Lemaigre 2009; Zorn 2008). This process is guided by FGF signalling from the cardiac mesoderm and BMP2/4 signalling from the septum transversum while low levels of WNT signalling are required. At this point the cells specify into hepatic endoderm (HE). Next, the monolayer of HE cells develops into a multilayer of hepatoblasts -bipotential cells that can develop

192 N. Graffmann et al.

into hepatocytes or cholangiocytes. They form the so called liver bud by invading the septum transversum. Hepatoblast proliferation and migration is promoted by hepatocyte growth factor (HGF) signalling (Bladt et al. 1995; Michalopoulos et al. 2003; Schmidt et al. 1995).

Hepatoblasts express beside the fetal liver characteristic protein α -fetoprotein (AFP) and the more general factors hepatic nuclear factor (HNF) 4 α and cytokeratin (CK) 18 also albumin (ALB) which is characteristic for mature adult hepatocytes. In addition, they express markers characteristic for cholangiocytes e.g. CK19. They start differentiating into hepatocytes and cholangiocytes between day 56–58 of gestation. A gradient of TGF β , Notch, WNT, BMP, and FGF signalling from the portal vein area to the periphery is responsible for driving the cells into one of the two fates (Antoniou et al. 2009; Raynaud et al. 2011). Cholangiocyte precursors reside at the so-called ductal plate which is located next to the portal vein. Under the influence of the above mentioned cytokines, especially Notch2, they mature into cholangiocytes, bud off from the ductal plate (which eventually regresses) and form tubules (Antoniou et al. 2009; Raynaud et al. 2011). Cells at the periphery of this signalling gradient develop into hepatocytes (Raynaud et al. 2011). This process is guided by glucocorticoid hormones in combination with the liver specific cytokines oncostatin M (OSM) and HGF as well as WNT (Kamiya et al. 2001; Michalopoulos et al. 2003).

11.4 *In vitro* Hepatocyte Differentiation

11

Obtaining liver biopsies of healthy adult primary human hepatocytes (PHH) or cholangiocytes for *in vitro* studies is complicated due to ethical issues and the fact that healthy individuals rarely undergo liver biopsies. Thus, in almost all cases the biopsies will be from a diseased individual. An even stronger obstacle for using these cells for *in vitro* models is the fact that they immediately start to dedifferentiate in cell culture which precludes any long term experiments (Godoy et al. 2016).

Therefore, many research groups have developed protocols for the differentiation of ESCs and iPSCs into hepatocyte-like cells (HLCs) or cholangiocyte-like cells (CLCs) based on our knowledge of signalling pathways active during liver development (Agarwal et al. 2008; Graffmann et al. 2016; Hannan et al. 2013; Jozefczuk et al. 2011; Matz et al. 2017; Sauer et al. 2014; Sgodda et al. 2017; Sgodda et al. 2013; Si-Tayeb et al. 2010; Siller et al. 2015; Wang et al. 2017).

There are many laboratory-specific variations of a common core protocol for HLC differentiation such that we cannot explain all in detail in this book chapter. We will focus on the common scheme used in one of these protocol types. Besides HLC differentiation, numerous laboratories have also established protocols for CLC differentiation, however, this is not the subject of this chapter (Dianat et al. 2014; Ogawa et al. 2015; Sampaziotis et al. 2017).

Most HLC differentiation schemes are based on the three major steps of differentiation DE, HE and HLC stage (■ Fig. 11.1).

Step 1: From iPSCs to DE

In the first step, iPSCs are directed towards DE by Activin A and WNT signalling. The latter can be either induced by directly adding WNT3A to the medium or by inhibiting GSK3 β with CHIR99021 and thus activating β -catenin which enters the nucleus and initiates a WNT-specific transcriptional program.

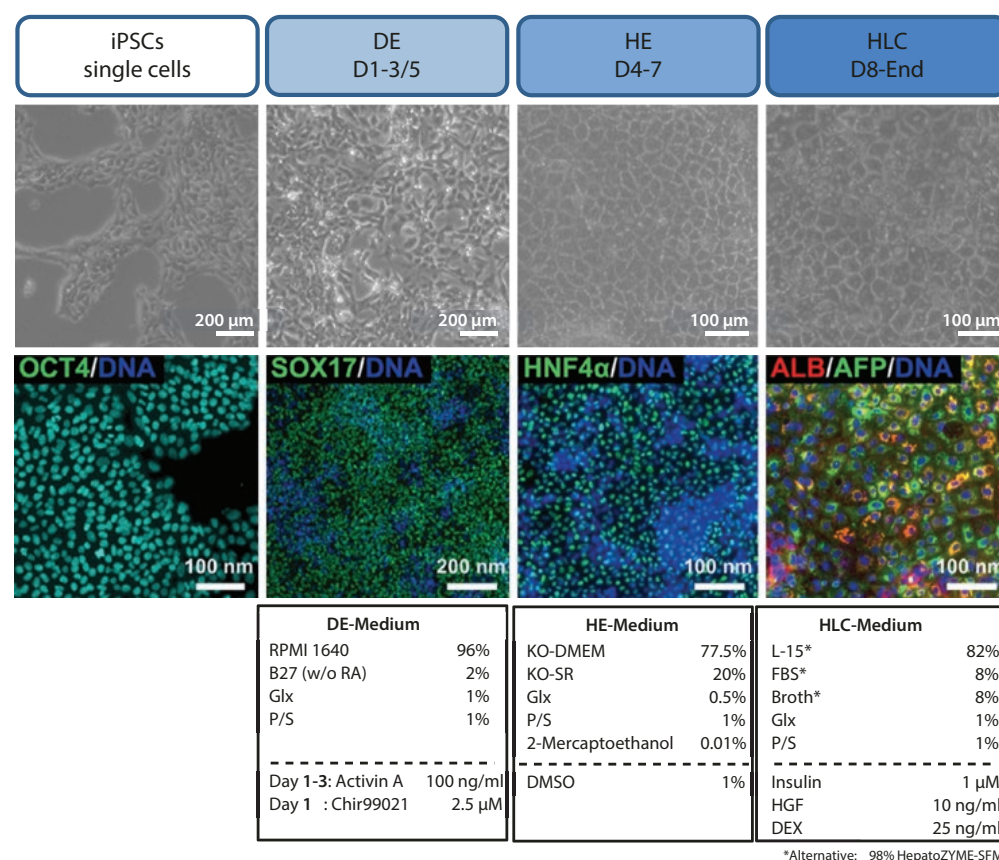


Fig. 11.1 *In vitro* differentiation of iPSCs into HLCs. Upper lane: Bright-field images demonstrating the changes in morphology during the differentiation process. Middle lane: Immunocytochemistry confirming the expression of characteristic markers for the respective state. Lower lane: Medium composition for each step (Graffmann et al. 2016)

At this stage, some groups additionally modulate FGF2 and/or BMP4 signalling to reduce self-renewal and increase differentiation. After 3–5 days of high proliferation accompanied by substantial cell death, the cells develop the typical petal like shape of DE. Successful accomplishment of this step can be confirmed by staining for the endoderm specific transcription factor SOX17 or for the surface marker CXCR4.

Step 2: From DE to HE

In the next step, HE is induced by adding DMSO to the medium for 4 days. In addition, it is possible to also include BMP2 or 4 and/or FGF4 or 10. The morphology of the cells further changes and they acquire a polygonal shape which is characteristic of hepatocytes. At this stage they express the hepatic transcription factor HNF4 α and sometimes even the early hepatocyte marker AFP.

Step 3: From HE to HLCs

Differentiation into HLCs is promoted by HGF, dexamethasone, and insulin. At this stage most protocols include also OSM, although this has been strongly questioned recently. While early data suggest that OSM is needed for differentiation and especially albumin secretion (Kamiya et al. 1999, 2001), recent studies indicate that differentiation efficiency is not reduced in the absence of OSM (Sgodda et al. 2017).

194 N. Graffmann et al.

Overall, HLCs usually appear 12–15 days after the start of differentiation. However, maturation increases till about day 21 and in most instances cells start to de-differentiate beyond this period. Mature HLCs are positive for CK18, ALB, E-Cadherin, as well as many more hepatocyte markers (Agarwal et al. 2008; Graffmann et al. 2016; Matz et al. 2017). In addition, they express AFP which is not detectable in adult primary hepatocytes and thus classifies the *in vitro* cells as more fetal. HLCs also have functional activities. They synthesize urea, uptake and release indocyanine dye and store glycogen. In addition, some of the CYP enzymes are active, especially the more fetal ones (Cameron et al. 2015; Graffmann et al. 2016; Hay et al. 2011; Matz et al. 2017).

Numerous factors besides the medium have an influence on the success of the differentiation. In earlier protocols, cells were seeded onto matrigel coated dishes for the differentiation process. However, these days a 1:3 mixture of Laminin 521 and 111 is preferred as this increases differentiation efficiency and is a step towards a xeno-free protocol (Cameron et al. 2015). In all cases it is important to maintain the cells at a high density, in order to prevent them from developing into large and granular endoderm-derived epithelial cells of unknown function (Graffmann et al. 2018).

Overall, HLCs in 2D cultures lack maturity and therefore it is the “Holy Grail” in this field of research to direct the cells towards a more adult phenotype similar to liver-biopsy derived mature hepatocytes. 3D cultures are very promising to achieve this stage of maturity. They comprise methods where cells are embedded in a collagen sandwich (Gieseck et al. 2014) as well as techniques with floating hepatic organoids under constant agitation or stirring (Sgodda et al. 2017). Finally, it is possible to include other cell types in the organoid in order to mimic the *in vivo* structures with sinusoids and mesenchymal cells (Camp et al. 2017; Nie et al. 2018).

11

11.5 Advantages and Disadvantages of Modelling Liver Diseases with iPSC Derived Cells

Disease modelling with *in vitro* derived HLCs or CLCs is still in a relatively early phase and there is no consensus model that can be used for all diseases. Rather, every laboratory has optimized their models in order to fit best for the disease under investigation. Despite this heterogeneity, there are many advantages of iPSC derived liver cells for disease modelling over traditional ways, which include animal models, transformed cancer cell lines, and primary human hepatocytes (PHH) (Table 11.1).

Table 11.1 Advantages and disadvantages of iPSC derived hepatic cells for disease modelling

Advantages	Disadvantages
<ul style="list-style-type: none"> iPSCs are available from all genetic backgrounds Minor risks for the patient Limited ethical considerations Unlimited expansion of cells, unrestricted availability of cells Differentiation into distinct tissues/cell types from one donor Increased lifetime of <i>in vitro</i> derived HLCs over primary hepatocytes Multifactorial diseases can be analysed 	<ul style="list-style-type: none"> Differentiated cells resemble the fetal instead of the adult state Ageing effects are diluted out during reprogramming Epigenetic memory influences differentiation efficiency

11.6 Examples of Liver Diseases Modelled with iPSC Derived Hepatic Cells

11.6.1 Liver Diseases That Affect Hepatocytes

In recent years, several diseases have been modelled with iPSC derived hepatic cells, however, we can only present a selection of these in this chapter.

11.6.1.1 Steatosis

Steatosis is a metabolic disease which is associated with the accumulation of fat within hepatocytes. Steatosis or fatty liver generally has two distinct aetiologies: Alcoholic liver disease is triggered by high and regular intakes of alcohol, while nonalcoholic fatty liver disease (NAFLD) depends on imbalances between calorie intake and expenditure. Since obesity as well as insulin resistance lead to chronic inflamed adipocyte tissue, they are the major risk factors which promote NAFLD. In later stages this disease can lead to steatohepatitis (NASH), liver fibrosis, cirrhosis and cancer (Basaranoglu et al. 2013; Perry et al. 2015). Besides nutrition and alcohol drugs (e.g. valproic acid, tetracycline, amiodarone) are also crucial factors for steatosis development (Szalowska et al. 2014). Although there are some mice models, they fail to recapitulate all aspects of the disease since the murine metabolism reacts differently upon diet changes compared to the human setting which does not allow to analyse all levels of the disease in a single mouse model (Machado et al. 2015; Takahashi et al. 2012).

In vitro modulation of this condition was done by generation of iPSC derived HLCs. Upon addition of oleic acid these HLCs incorporated fat leading to changes in the expression of metabolic associated genes and upregulation of lipid associated proteins (Graffmann et al. 2016).

Being a multifactorial disease, NAFLD is not caused by a single mutation. In this setting it is of particular interest to study the mechanisms underlying the disease in HLCs derived from a variety of patients in order to identify common disease associated pathways (Jozefczuk et al. 2012).

11.6.1.2 Hepatitis B/C

Even-though vaccination and therapy against hepatitis B virus (HBV) have been developed, approximately 260 million people are affected with chronic infection leading to a variety of outcomes. In some cases, the patient is symptom-free in other cases liver cirrhosis or hepatocellular carcinoma ensue (Reville et al. 2016; Zeng et al. 2008).

Apart from man only chimpanzees are fully susceptible for this infection which has a high tropism towards the liver. This fact makes it very challenging to study the disease. Since the research on great apes is limited other experimental models are needed (Allweiss and Dandri 2016). Efforts have been made to generate transgenic mice which are susceptible for the virus infection due to genetic modifications (Chisari et al. 1985; Yang et al. 2014). A more advanced approach is the generation of chimeric mice harbouring human hepatocytes as well as human immune cells and this has made it possible to study the interplay between human hepatocytes and the adaptive immune response (Bility et al. 2014).

Successful HBV models with iPSC-derived HLCs have been described (Shlomai et al. 2014). Shlomai et al. demonstrated that HLCs can be infected with HBV and observed changes over a time course of 24 days. In 2018, HLCs derived from human iPSCs in combina-

tion with human umbilical vein endothelial cells (HUVECs) and MSCs were used to derive liver organoids for modelling HBV infection. These 3D structures were more permissive for HBV and the virus propagation maintained for a longer time span than the 2D cultured HLCs. This personalized model enabled the modulation of HBV infection and mirrored virus induced hepatic dysfunction as well as the life cycle of the HBV (Nie et al. 2018).

Hepatitis C virus (HCV) is also a major health burden all over the world affecting approximately 550 million people and leading to secondary liver malfunctions. Established medication can suppress the replication of the virus and recently even drugs that cure the disease have been developed, although they are not affordable for the majority of the patients (Hayes and Chayama 2017). HCV infection is particularly hard to deal with because symptoms frequently only occur 15–20 years post-infection which limits treatment options. Many patients eventually need a liver transplant because of high levels of liver cirrhosis. However, the reinfection rate of transplanted liver is 100% (Garcia-Retortillo et al. 2002).

As for HBV, it could be shown that HLCs from iPSCs are a relevant tool for mimicking host-HCV interplay, allowing insights into innate immune response as well as the synthesis of lipoproteins (Schobel et al. 2018). In contrast to the Huh7.5 cell line, HLCs have been infected with various HCV strains isolated from patients, thus enabling a more detailed study of infection and replication modes (Wu et al. 2012). It has also been shown that shRNA mediated repression of receptors important for the infection with HCV only prevented the infection with wild-type virus strains and not with mutated ones (Wu et al. 2012).

Another level of HLC mediated disease modelling for both viruses is the combination of the HLC approach with the chimeric mice approach. Chimeras harbouring human HLCs were created for investigating the pathogenesis of HBV and HCV and as a platform to test anti-viral components (Carpentier et al. 2014; Yuan et al. 2018).

11.6.1.3 Wilsons Disease

Wilson's disease (WD) is caused by accumulation of copper in the liver and the brain. It is a rare autosomal recessive disease manifesting in a mutated *ATP7B* gene. This gene is crucial within the biliary excretion pathway of copper. Due to this impaired excretion, copper accumulates over time and primarily manifests in the brain and the liver of patients leading to hepatitis, cirrhosis, liver failure or neurological malfunctions (Brewer and Askari 2005).

To date, four established rodent models of WD exist, but they do not carry the most frequent missense mutation of the *ATP7B* gene (de Bie et al. 2007). Furthermore, the metabolic pathways in these animals are distinct to that observed in human (Ranucci et al. 2017).

Zhang et al. differentiated iPSCs from a Chinese patient suffering from WD with a Chinese hotspot mutation into HLCs. These HLCs mimicked the disease phenotype *in vitro* by showing impaired ATP7B proteins in the cytoplasm and thus resulting in reduced levels of copper transport. Using a lentivirus expressing the functional version of ATP7B it was possible to cure the disease *in vitro*. Furthermore, addition of the chaperone drug curcumin in the cell culture medium could rescue the disease phenotype (Zhang et al. 2011).

Yi et al. derived iPSCs from a patient carrying a Caucasian hotspot mutation. These cells were differentiated into neurons and HLCs expressing the gene defect thereby modelling both major affected cell types in WD (Yi et al. 2012).

11.6.1.4 Drug Induced Hepatic Toxicity

Although drug-induced liver injury (DILI) is a small factor for acute liver injury it causes most of the acute liver failures (Larrey and Pageaux 2005). DILI is also one of the main reasons for non-approval of drugs, terminations of clinical trials as well as withdrawing drugs from the market (Stevens and Baker 2009). During DILI, metabolites of the drugs and patients' proteins form adducts. These are presented on the cell surface as neo-antigens leading either to an immune-allergic reaction or to non-allergic toxic reactions (Kaplowitz 2005). The subsequent hepatic reaction cascades include impairment of transporters, elevated levels of oxidative stress, and pro-inflammatory cytokines (Rusmann et al. 2010). Especially anti-cancer drugs such as protein kinase inhibitors, immune checkpoint inhibitors or the epidermal growth factor receptor tyrosine kinase inhibitor can cause severe hepatic damages (Takeda et al. 2015), although the commonly used pain relieve medication paracetamol (acetaminophen) is the leading causative drug in the UK and the US (Larrey and Pageaux 2005).

In vitro cell models including PHH, hepatic cell lines, and HLCs in 2D and 3D composition have been used to promote DILI research (Gomez-Lechon et al. 2010; Lu et al. 2015). With these cell-based models it has been possible to gain insights into DILI-associated mechanisms such as endoplasmic and oxidative stress and transporter inhibition (Bell et al. 2017; Godoy et al. 2013; Schadt et al. 2015). In addition, it has been shown that HLCs derived from patients with alpha-1-antitrypsin deficiency (see ► Sect. 11.6.2.1.) react much more sensitive to several common drugs than those derived from healthy controls (Wilson et al. 2015). In line with the need for in depth knowledge about pharmacokinetics of certain drugs in a specific environment, iPSCs have been derived from donors with distinct known cytochrome P450 genotypes in order to generate HLCs which can be used for drug testing (Bohndorf et al. 2017). To enable high throughput screening of drugs, HLC differentiation has been achieved in 384 wells (Carpentier et al. 2016).

11.6.1.5 Tangier Disease

Tangier disease (TD) is a rare disease first found on Tangier island in Virginia where an isolated community of descendants from settlers live. TD patients have no high density lipoprotein (HDL) and thus cholesterol efflux is disturbed. TD symptoms due to cholesterol ester deposits range from orange tonsils over hepatosplenomegaly and neuropathy to cardiovascular disease. TD is caused by mutation in the gene *ABCA1* which regulates cholesterol efflux via HDL (Brooks-Wilson et al. 1999; Scott 1999) and an iPSC-based model has been reported (Bi et al. 2017). The authors of the study generated iPSCs from TD patients and matched healthy individuals and subsequently differentiated them into HLCs. TD iPSC-derived HLCs had impaired HDL production and cholesterol efflux and increased triacylglycerol secretion. This iPSC-derived HLC model of TD has been instrumental in confirming the involvement of *ABCA1* in the molecular mechanisms controlling cholesterol efflux.

11.6.2 Diseases That Affect Hepatocytes, But Manifest Primarily in Other Organs

Some liver diseases have extrahepatic manifestations, meaning that other organs besides the liver are affected.

11.6.2.1 Alpha-1-Antitrypsin Deficiency

Alpha-1-antitrypsin deficiency (A1AD) is a genetic disorder with a worldwide prevalence of 1:2500. It is caused by mutations in the *SERPINA1* gene. This gene codes for the protein alpha-1-anti-trypsin (A1AT) mainly synthesized in hepatocytes. A1AT is responsible for the protection against the enzyme neutrophil elastase, which is released by neutrophils during immune response, but also damages normal tissue if not carefully regulated by A1AT (Brantly et al. 1988). Lack of A1AT's anti-protease activity results in uncontrolled circulating neutrophil elastase that destroys lung air sacs leading to emphysema or chronic obstructive pulmonary disease (COPD). In addition, mutated A1AT protein forms insoluble precipitates in hepatocytes which cause damage, thus resulting in scarring and chronic liver disease.

Using multiple donors to model the disease, Wilson et al. showed differential expression of 135 genes between HLCs derived from patients carrying the mutation and healthy controls (Wilson et al. 2015). They and others could show that A1AT forms insoluble aggregates in patient derived HLCs and is not exported efficiently. They could improve the phenotype by treating the cells with a proteasome inhibitor or by increasing autophagy (Rashid et al. 2010; Wilson et al. 2015). In addition, they also showed that HLCs derived from A1AD patients are more sensitive for common drugs like paracetamol (acetaminophen) than those from healthy controls (Wilson et al. 2015).

11.6.2.2 Transthyretin-Related Hereditary Amyloidosis

Transthyretin (TTR) amyloidosis (or familial amyloidotic polyneuropathy (FAP)) is a systemic familiarly hereditary disorder caused by mutations that destabilise the TTR protein in the liver (Ando et al. 2013). Misfolded and aggregated amyloid fibrils consisting of TTR – a plasma protein produced in the liver to transport thyroxine and vitamin A– are deposited and accumulate in various organs and tissues, such as in the nervous system and cardiac tissue, leading to inherent dysfunction. It is characterised by a slowly progressive peripheral sensory motor and autonomic neuropathy, and later involves visceral organs such as the kidney, hence becoming fatal (Ando et al. 2013).

Leung et al. generated TTR patient-specific iPSCs which were further directly differentiated into hepatic, cardiac and neuronal lineages, to model three tissue types involved in the disease. The HLCs produced and secreted mutant TTR protein, which caused cell death of neurons and cardiac cells incubated with the TTR containing supernatant. Treatment with stabilizers of TTR improved the phenotype. In essence, Leung et al. proved that this iPSC-based system is an ideal platform for further investigating the role of the liver in TTR (Leung et al. 2013).

11.6.3 Diseases That Affect Cholangiocytes

11.6.3.1 Cystic Fibrosis

Cystic fibrosis (CF) is a hereditary disease caused by mutations in the gene encoding the CF transmembrane conductance regulator (CFTR). It involves several organ systems, with manifestations mostly as lung disease but it also affects the liver (Accurso 2006). In the liver, the *CFTR* gene expression occurs only at the level of the epithelium of the bile ducts and the CFTR protein anchors on the apical membrane of the cholangiocytes and regulates electrolyte and water content in the bile. Mutations in CFTR result in impaired secre-

tion and thick viscous bile causing damage to both the cholangiocytes and hepatocytes – periportal fibrosis, which over the years leads to cirrhosis (van Mourik 2017). Obstruction of the intra-hepatic bile ductules with thick mucus, leads to the development of conditions such as progressive cholestasis or multi-lobular biliary cirrhosis (O'Brien et al. 1992).

In vitro differentiation of iPSCs into cholangiocyte-like cells (CLCs) in a 3D system resulted in spheres and cysts which had functional activity measured by rhodamine uptake and swelling of the cysts (Ogawa et al. 2015; Sampaziotis et al. 2015). Patient derived CLCs did not only show reduced cyst formation, but also had impaired functions related to dye uptake and swelling due to the defects in CFTR function. In the *in vitro* assays, the function could be partly restored by treating the cysts with small molecules promoting proper folding of CFTR (Ogawa et al. 2015; Sampaziotis et al. 2015). Thus, this system is suitable for *in vitro* drug testing.

11.6.3.2 Alagille Syndrome

Alagille syndrome (ALGS) is a rare genetic disorder with varying severity, where bile duct formation is impaired. It is considered a multi-system disorder as it also affects the liver, skeleton, eyes and heart. It is predominantly caused by mutations in the gene *Jagged 1* (*JAG1*) which is a ligand in the Notch signalling pathway and thus essential for cholangiocyte development (Kamath et al. 2010). Typical symptoms such as cholestasis, jaundice, itching, as well as heart and skeletal problems manifest during the first 3 months of life with the severe form, with cholestasis being a direct consequence due to insufficient bile ducts.

To improve our understanding of the mechanisms that cause ALGS liver pathology, studies using hepatic organoids from iPSCs were recently carried out by Guan et al. (2017). The organoids comprised a mixture of HLCs and CLCs. Organoid formation and function was massively impaired in ALGS patient derived iPSCs. Inducing a disease causing mutation in wildtype iPSCs by CRISPR (Clustered Regularly Interspaced Short Palindromic Repeats) lead to the same phenotype as observed in ALGS patient derived organoids. In addition, it was also possible to correct the mutation in ALGS patient derived cells which reverted the phenotype and thus proved that the mutation was responsible for the disease (Guan et al. 2017).

11.7 Bioinformatic Analysis

11.7.1 Datasets from Public Repositories

Bioinformatic methods enable meta-analysis of a plethora of datasets available at public repositories such as the ones shown in ■ Table 11.2.

For a more comprehensive compilation of public repositories we refer to the list recommended by the journal Scientific Data: ► <https://www.nature.com/sdata/policies/repositories>. For liver disease modeling there exist datasets generated from liver biopsies or from iPSC-derived HLCs.

In this example, we focus on a dataset based on HLCs derived from Tangier disease (TD, see ► Sect. 11.6.1.5) patients for which no liver biopsies or primary hepatocytes existed (Bi et al. 2017). We compare the transcriptome data of these cells with transcriptomes of liver biopsies from NAFLD and NASH patients with the intention of gaining in

Table 11.2 Selection of repositories for transcriptome and genome data

Repository	URL	Comments
National Center for biotechnology information (NCBI) gene expression omnibus (GEO)	▶ https://www.ncbi.nlm.nih.gov/geo	Microarrays and sequencing data
NCBI sequence read archive (SRA)	▶ https://www.ncbi.nlm.nih.gov/sra	Sequencing data
European Bioinformatic institute (EMBL-EBI) ArrayExpress	▶ https://www.ebi.ac.uk/arrayexpress/	Microarrays and sequencing data
1000 genomes project	▶ http://www.internationalgenome.org/	Sequencing data

depth insights on cholesterol reverse transport which is disabled in TD patients due to a lack of HDL.

Previous bioinformatic analyses have unveiled a gene signature which correlates with the progression of NAFLD to NASH (Wruck et al. 2017). This gene signature was functionally annotated with cholesterol-related processes. Similar, although not as dramatic as in TD, high plasma triacylglyceride levels and low HDL cholesterol often can be observed in NAFLD patients (Arguello et al. 2015). This indicates that both diseases have a common phenotype and that bioinformatic comparisons of genome-wide gene expression can increase our understanding of both diseases. The role of *ABCA1* in reverse cholesterol transport suggests that its decreased expression in NAFLD/NASH may result in increased liver triacylglycerides (Arguello et al. 2015; Vega-Badillo et al. 2016).

11.7.2 Comparison of Gene Expression Datasets

Employing a venn diagram analysis, we identified common genes that correlated to the progression of NAFLD and were also differentially expressed in the iPSC-derived HLC model of TD (▶ Fig. 11.2a). Each fraction in this diagram represents the number of genes that are either uniquely expressed in one sample or shared by the indicated samples. The overlap common to the TD model and all NAFLD datasets consists only of two genes: *LRRC31* and *C3orf58* (▶ Fig. 11.2b).

The classical way to gain a deeper insight into the functions of these genes is to review publications, however, for these two factors the number of publications is rather limited. Another way is to check which gene ontologies (GOs) are assigned to the gene of interest. GOs specify the biological role of genes (Ashburner et al. 2000) and starting with the top categories biological process (BP), cellular component (CC) and molecular function (MF) stepwise refine these roles to very detailed terms, e.g. the BP “somatotropin secreting cell differentiation”.

C3orf58, one of the genes present in all datasets related to the progression of NAFLD to NASH, is associated with GO terms which can be roughly grouped to Golgi, coat protein (COP) I coated vesicles and phosphatidylinositol 3-kinase signaling. COPI and COPII coated vesicles perform the retrograde and anterograde transport of proteins between the Golgi

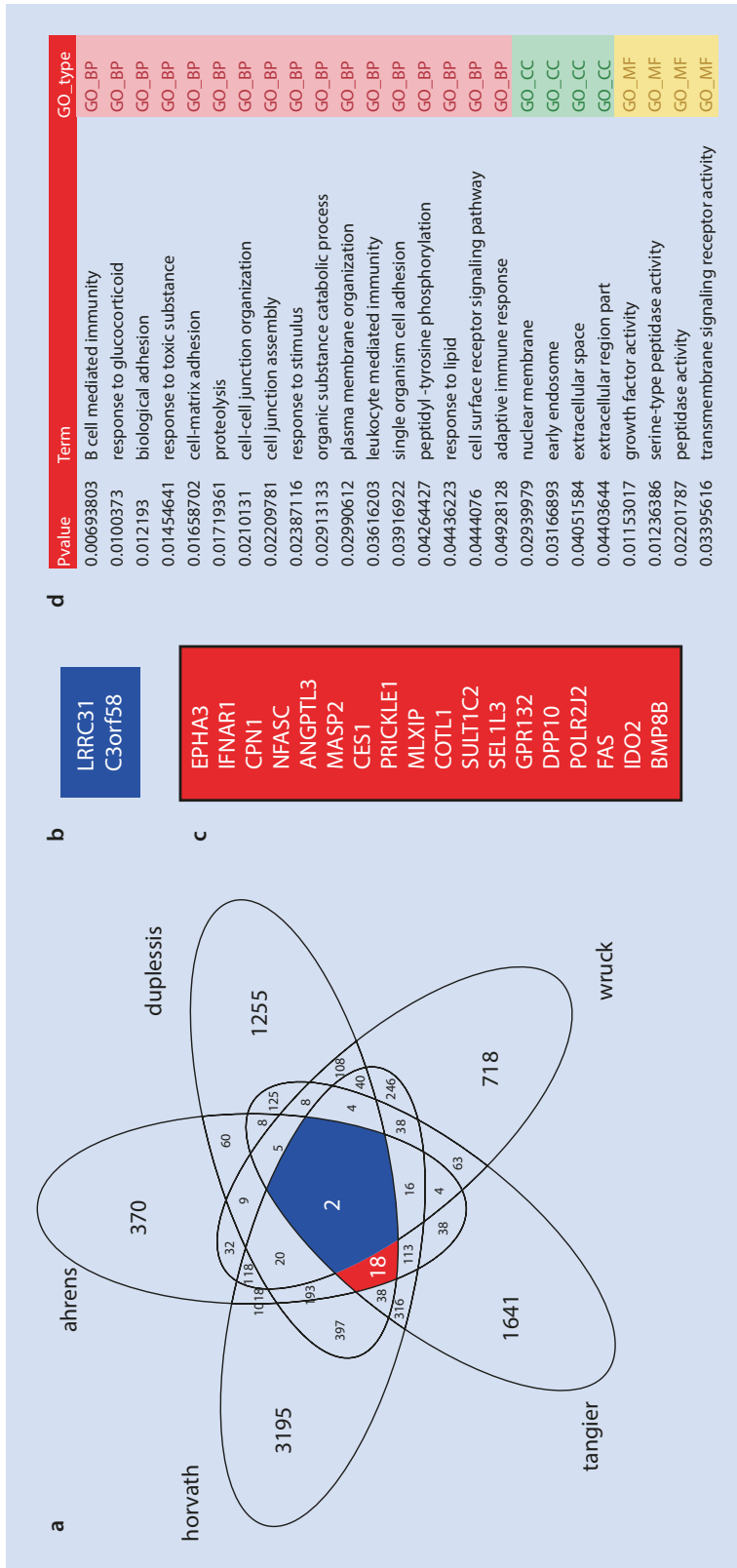


Fig. 11.2 Bioinformatic analysis of genes regulated in TD and NAFLD. **a** Liver transcriptome datasets related to the progression of NAFLD to NASH (Ahrens et al. 2013; du Plessis et al. 2015; Horvath et al. 2014; Wruck et al. 2015) and TD (Bi et al. 2017) were compared in a venn diagram. **b** The genes *C3orf58* and *LRRC31* were found in the intersection of all datasets. **c** 18 genes were found in the intersection of all NASH-related datasets and the TD dataset but not the high- vs low-grade NAFLD dataset. **d** Gene ontologies (GOs) overrepresented in the 18-gene-set in **c**

202 N. Graffmann et al.

complex and the endoplasmic reticulum (ER). COPII coated vesicles play an important role in cholesterol regulation because at low sterol levels in the ER they transport the sterol regulatory element binding protein (SREBP) to the Golgi for proteolytic release as transcription factor (Ikonen 2008). Further investigation of these proteins may shed light on hitherto unknown mechanisms of cholesterol transport regulation and progression of NAFLD.

Three of the steatosis datasets were related to NASH while one (Wruck et al. 2015) was related to a distinction between high and low grade steatosis. We were also interested in the comparison between TD and the three NASH datasets only. This resulted in a set of 18 genes (■ Fig. 11.2c) including also the gene *ANGPTL3* – an inhibitor of lipoprotein lipase - which Bi et al. have highlighted in their publication about the TD model (Bi et al. 2017).

11.7.3 Gene Ontology (GO) and Pathway Analysis

Gene sets like the 18 genes from the venn diagram can be further analyzed to find functionality associated with them. This functionality can be given by other gene sets annotated with specific functions, such as KEGG-pathways (► <https://www.genome.jp/kegg/pathway.html>) (Kanehisa et al. 2017) or GOs. The gene sets determined from the analysis of experiments can be connected to the functionally annotated gene sets by so-called “overrepresentation analysis”. Overrepresentation analysis uses statistical tests, such as Fisher’s exact test or the hypergeometric test, to determine if the genes from the set appear more often in a functional group of genes than in the background of all annotated genes. Usually, in gene expression analysis genes are categorized as (differentially) expressed/not (differentially) expressed and in the pathway (GO)/not in the pathway (GO). The number of genes in these categories are subjected to statistical tests (e.g. hypergeometric test or Fisher’s exact test) to determine their significance. A modified version of Fisher’s exact test is employed in the highly frequented web tool DAVID (► <https://david.ncifcrf.gov/>) (Huang da et al. 2009) which detects overrepresented gene sets in a plethora of dataset including pathways, GOs, transcription factors, chromosomal regions, etc.

In our example, an over-representation analysis of GOs using this set of 18 genes revealed several GO terms (■ Fig. 11.2d) which can be grouped into immune-related (e.g. B cell mediated immunity) cell junction-related (e.g. cell-cell-junction organization), and response-related (response to toxic substance/stimulus/lipid) categories.

11

Take Home Message

1. The liver is a complex organ with essential functions for metabolism and drug detoxification
2. Its main functional cells –hepatocytes and cholangiocytes- can be generated *in vitro* from pluripotent stem cells to model a wide variety of diseases
3. Disease models recapitulate the disease phenotype and help us to understand underlying mechanisms
4. They can be used for (high throughput) drug testing and are a step towards personalized medicine
5. 3D models generally reflect the *in vivo* situation better than 2D models
6. Bioinformatic tools allow the analysis of a wide spectrum of data. The comparison of related diseases can give hints towards common disease mechanisms

References

- Accurso, F. J. (2006). Update in cystic fibrosis 2005. *American Journal of Respiratory and Critical Care Medicine*, *173*, 944–947.
- Agarwal, S., Holton, K. L., & Lanza, R. (2008). Efficient differentiation of functional hepatocytes from human embryonic stem cells. *Stem Cells*, *26*, 1117–1127.
- Ahrens, M., Ammerpohl, O., von Schonfels, W., Kolarova, J., Bens, S., Itzel, T., Teufel, A., Herrmann, A., Brosch, M., Hinrichsen, H., et al. (2013). DNA methylation analysis in nonalcoholic fatty liver disease suggests distinct disease-specific and remodeling signatures after bariatric surgery. *Cell Metabolism*, *18*, 296–302.
- Allweiss, L., & Dandri, M. (2016). Experimental in vitro and in vivo models for the study of human hepatitis B virus infection. *Journal of Hepatology*, *64*, S17–S31.
- Ando, Y., Coelho, T., Berk, J. L., Cruz, M. W., Ericzon, B. G., Ikeda, S., Lewis, W. D., Obici, L., Plante-Bordeneuve, V., Rapezzi, C., et al. (2013). Guideline of transthyretin-related hereditary amyloidosis for clinicians. *Orphanet Journal of Rare Diseases*, *8*, 31.
- Antoniou, A., Raynaud, P., Cordi, S., Zong, Y., Tronche, F., Stanger, B. Z., Jacquemin, P., Pierreux, C. E., Clotman, F., & Lemaigre, F. P. (2009). Intrahepatic bile ducts develop according to a new mode of tubulogenesis regulated by the transcription factor SOX9. *Gastroenterology*, *136*, 2325–2333.
- Arguello, G., Balboa, E., Arrese, M., & Zanlungo, S. (2015). Recent insights on the role of cholesterol in non-alcoholic fatty liver disease. *Biochimica et Biophysica Acta*, *1852*, 1765–1778.
- Ashburner, M., Ball, C. A., Blake, J. A., Botstein, D., Butler, H., Cherry, J. M., Davis, A. P., Dolinski, K., Dwight, S. S., Eppig, J. T., et al. (2000). Gene ontology: Tool for the unification of biology. The Gene Ontology Consortium. *Nature Genetics*, *25*, 25–29.
- Bansal, M. B. (2016). Hepatic stellate cells: Fibrogenic, regenerative or both? Heterogeneity and context are key. *Hepatology International*, *10*, 902–908.
- Barle, H., Nyberg, B., Essen, P., Andersson, K., McNurlan, M. A., Wernerman, J., & Garlick, P. J. (1997). The synthesis rates of total liver protein and plasma albumin determined simultaneously in vivo in humans. *Hepatology*, *25*, 154–158.
- Basaranoglu, M., Basaranoglu, G., & Senturk, H. (2013). From fatty liver to fibrosis: A tale of “second hit”. *World Journal of Gastroenterology: WJG*, *19*, 1158–1165.
- Bell, C. C., Lauschke, V. M., Vorrink, S. U., Palmgren, H., Duffin, R., Andersson, T. B., & Ingelman-Sundberg, M. (2017). Transcriptional, functional, and mechanistic comparisons of stem cell-derived hepatocytes, HepaRG cells, and three-dimensional human hepatocyte spheroids as predictive in vitro systems for drug-induced liver injury. *Drug Metabolism and Disposition: The Biological Fate of Chemicals*, *45*, 419–429.
- Bi, X., Pashos, E. E., Cuchel, M., Lyssenko, N. N., Hernandez, M., Picataggi, A., McParland, J., Yang, W., Liu, Y., Yan, R., et al. (2017). ATP-binding cassette transporter A1 deficiency in human induced pluripotent stem cell-derived hepatocytes abrogates HDL biogenesis and enhances triglyceride secretion. *eBioMedicine*, *18*, 139–145.
- Bility, M. T., Cheng, L., Zhang, Z., Luan, Y., Li, F., Chi, L., Zhang, L., Tu, Z., Gao, Y., Fu, Y., et al. (2014). Hepatitis B virus infection and immunopathogenesis in a humanized mouse model: Induction of human-specific liver fibrosis and M2-like macrophages. *PLoS Pathogens*, *10*, e1004032.
- Bilzer, M., Roggel, F., & Gerbes, A. L. (2006). Role of Kupffer cells in host defense and liver disease. *Liver International: Official Journal of the International Association for the Study of the Liver*, *26*, 1175–1186.
- Blachier, M., Leleu, H., Peck-Radosavljevic, M., Valla, D. C., & Roudot-Thoraval, F. (2013). The burden of liver disease in Europe: A review of available epidemiological data. *Journal of Hepatology*, *58*, 593–608.
- Bladt, F., Riethmacher, D., Isenmann, S., Aguzzi, A., & Birchmeier, C. (1995). Essential role for the C-met receptor in the migration of myogenic precursor cells into the limb bud. *Nature*, *376*, 768–771.
- Bohndorf, M., Ncube, A., Spitzhorn, L. S., Enczmann, J., Wruck, W., & Adjaye, J. (2017). Derivation and characterization of integration-free iPSC line ISRM-UM51 derived from SIX2-positive renal cells isolated from urine of an African male expressing the CYP2D6 *4/*17 variant which confers intermediate drug metabolizing activity. *Stem Cell Research*, *25*, 18–21.
- Brantly, M., Nukiwa, T., & Crystal, R. G. (1988). Molecular basis of alpha-1-antitrypsin deficiency. *The American Journal of Medicine*, *84*, 13–31.
- Brewer, G. J., & Askari, F. K. (2005). Wilson's disease: Clinical management and therapy. *Journal of Hepatology*, *42*(Suppl), S13–S21.

204 N. Graffmann et al.

- Brooks-Wilson, A., Marcil, M., Clee, S. M., Zhang, L. H., Roomp, K., van Dam, M., Yu, L., Brewer, C., Collins, J. A., Molhuizen, H. O., et al. (1999). Mutations in ABC1 in Tangier disease and familial high-density lipoprotein deficiency. *Nature Genetics*, *22*, 336–345.
- Cameron, K., Tan, R., Schmidt-Heck, W., Campos, G., Lyall, M. J., Wang, Y., Lucendo-Villarin, B., Szkolnicka, D., Bates, N., Kimber, S. J., et al. (2015). Recombinant laminins drive the differentiation and self-organization of hESC-derived hepatocytes. *Stem Cell Reports*, *5*, 1250–1262.
- Camp, J. G., Sekine, K., Gerber, T., Loeffler-Wirth, H., Binder, H., Gac, M., Kanton, S., Kageyama, J., Damm, G., Seehofer, D., et al. (2017). Multilineage communication regulates human liver bud development from pluripotency. *Nature*, *546*(7659), 533.
- Carpentier, A., Tesfaye, A., Chu, V., Nimgaonkar, I., Zhang, F., Lee, S. B., Thorgeirsson, S. S., Feinstone, S. M., & Liang, T. J. (2014). Engrafted human stem cell-derived hepatocytes establish an infectious HCV murine model. *The Journal of Clinical Investigation*, *124*, 4953–4964.
- Carpentier, A., Nimgaonkar, I., Chu, V., Xia, Y., Hu, Z., & Liang, T. J. (2016). Hepatic differentiation of human pluripotent stem cells in miniaturized format suitable for high-throughput screen. *Stem Cell Research*, *16*, 640–650.
- Chiang, J. Y. (2013). Bile acid metabolism and signaling. *Comprehensive Physiology*, *3*, 1191–1212.
- Chisari, F. V., Pinkert, C. A., Milich, D. R., Filippi, P., McLachlan, A., Palmiter, R. D., & Brinster, R. L. (1985). A transgenic mouse model of the chronic hepatitis B surface antigen carrier state. *Science*, *230*, 1157–1160.
- Danielson, P. B. (2002). The cytochrome P450 superfamily: Biochemistry, evolution and drug metabolism in humans. *Current Drug Metabolism*, *3*, 561–597.
- de Bie, P., Muller, P., Wijmenga, C., & Klomp, L. W. (2007). Molecular pathogenesis of Wilson and Menkes disease: Correlation of mutations with molecular defects and disease phenotypes. *Journal of Medical Genetics*, *44*, 673–688.
- Dessimoz, J., Opoka, R., Kordich, J. J., Grapin-Botton, A., & Wells, J. M. (2006). FGF signaling is necessary for establishing gut tube domains along the anterior-posterior axis in vivo. *Mechanisms of Development*, *123*, 42–55.
- Dianat, N., Dubois-Pot-Schneider, H., Steichen, C., Desterke, C., Leclerc, P., Raveux, A., Combettes, L., Weber, A., Corlu, A., & Dubart-Kupferschmitt, A. (2014). Generation of functional cholangiocyte-like cells from human pluripotent stem cells and HepaRG cells. *Hepatology*, *60*, 700–714.
- du Plessis, J., van Pelt, J., Korf, H., Mathieu, C., van der Schueren, B., Lannoo, M., Oyen, T., Topal, B., Fetter, G., Nayler, S., et al. (2015). Association of adipose tissue inflammation with histologic severity of nonalcoholic fatty liver disease. *Gastroenterology*, *149*, 635–648.e614.
- Garcia-Retortillo, M., Fornis, X., Feliu, A., Moitinho, E., Costa, J., Navasa, M., Rimola, A., & Rodes, J. (2002). Hepatitis C virus kinetics during and immediately after liver transplantation. *Hepatology*, *35*, 680–687.
- Gieseck, R. L., 3rd, Hannan, N. R., Bort, R., Hanley, N. A., Drake, R. A., Cameron, G. W., Wynn, T. A., & Vallier, L. (2014). Maturation of induced pluripotent stem cell derived hepatocytes by 3D-culture. *PLoS One*, *9*, e86372.
- Godoy, P., Hewitt, N. J., Albrecht, U., Andersen, M. E., Ansari, N., Bhattacharya, S., Bode, J. G., Bolleyn, J., Borner, C., Bottger, J., et al. (2013). Recent advances in 2D and 3D in vitro systems using primary hepatocytes, alternative hepatocyte sources and non-parenchymal liver cells and their use in investigating mechanisms of hepatotoxicity, cell signaling and ADME. *Archives of Toxicology*, *87*, 1315–1530.
- Godoy, P., Widera, A., Schmidt-Heck, W., Campos, G., Meyer, C., Cadenas, C., Reif, R., Stober, R., Hammad, S., Putter, L., et al. (2016). Gene network activity in cultivated primary hepatocytes is highly similar to diseased mammalian liver tissue. *Archives of Toxicology*, *90*(10), 2513–2529.
- Gomez-Lechon, M. J., Lahoz, A., Gombau, L., Castell, J. V., & Donato, M. T. (2010). In vitro evaluation of potential hepatotoxicity induced by drugs. *Current Pharmaceutical Design*, *16*, 1963–1977.
- Gordillo, M., Evans, T., & Gouon-Evans, V. (2015). Orchestrating liver development. *Development*, *142*, 2094–2108.
- Graffmann, N., Ring, S., Kawala, M. A., Wruck, W., Ncube, A., Trompeter, H. I., & Adjaye, J. (2016). Modeling nonalcoholic fatty liver disease with human pluripotent stem cell-derived immature hepatocyte-like cells reveals activation of PLIN2 and confirms regulatory functions of peroxisome proliferator-activated receptor alpha. *Stem Cells and Development*, *25*, 1119–1133.
- Graffmann, N., Ncube, A., Wruck, W., & Adjaye, J. (2018). Cell fate decisions of human iPSC-derived bipotential hepatoblasts depend on cell density. *PLoS One*, *13*, e0200416.
- Guan, Y., Xu, D., Garfin, P. M., Ehmer, U., Hurwitz, M., Enns, G., Michie, S., Wu, M., Zheng, M., Nishimura, T., et al. (2017). Human hepatic organoids for the analysis of human genetic diseases. *JCI Insight*, *2*, 94954.

Liver Disease Modelling

- Hannan, N. R., Segeritz, C. P., Touboul, T., & Vallier, L. (2013). Production of hepatocyte-like cells from human pluripotent stem cells. *Nature Protocols*, *8*, 430–437.
- Hay, D. C., Pernagallo, S., Diaz-Mochon, J. J., Medine, C. N., Greenhough, S., Hannoun, Z., Schrader, J., Black, J. R., Fletcher, J., Dalgetty, D., et al. (2011). Unbiased screening of polymer libraries to define novel substrates for functional hepatocytes with inducible drug metabolism. *Stem Cell Research*, *6*, 92–102.
- Hayes, C. N., & Chayama, K. (2017). Why highly effective drugs are not enough: The need for an affordable solution to eliminating HCV. *Expert Review of Clinical Pharmacology*, *10*, 583–594.
- Hijmans, B. S., Grefhorst, A., Oosterveer, M. H., & Groen, A. K. (2014). Zonation of glucose and fatty acid metabolism in the liver: Mechanism and metabolic consequences. *Biochimie*, *96*, 121–129.
- Horvath, S., Erhart, W., Brosch, M., Ammerpohl, O., von Schonfels, W., Ahrens, M., Heits, N., Bell, J. T., Tsai, P. C., Spector, T. D., et al. (2014). Obesity accelerates epigenetic aging of human liver. *Proceedings of the National Academy of Sciences of the United States of America*, *111*, 15538–15543.
- Huang da, W., Sherman, B. T., & Lempicki, R. A. (2009). Systematic and integrative analysis of large gene lists using DAVID bioinformatics resources. *Nature Protocols*, *4*, 44–57.
- Ikonen, E. (2008). Cellular cholesterol trafficking and compartmentalization. *Nature Reviews Molecular Cell Biology*, *9*, 125–138.
- Jozefczuk, J., Prigione, A., Chavez, L., & Adjaye, J. (2011). Comparative analysis of human embryonic stem cell and induced pluripotent stem cell-derived hepatocyte-like cells reveals current drawbacks and possible strategies for improved differentiation. *Stem Cells and Development*, *20*, 1259–1275.
- Jozefczuk, J., Kashofer, K., Ummanni, R., Henjes, F., Rehman, S., Geenen, S., Wruck, W., Regenbrecht, C., Daskalaki, A., Wierling, C., et al. (2012). A systems biology approach to deciphering the etiology of steatosis employing patient-derived dermal fibroblasts and iPS cells. *Frontiers in Physiology*, *3*, 339.
- Kamath, B. M., Schwarz, K. B., & Hadzic, N. (2010). Alagille syndrome and liver transplantation. *Journal of Pediatric Gastroenterology and Nutrition*, *50*, 11–15.
- Kamiya, A., Kinoshita, T., Ito, Y., Matsui, T., Morikawa, Y., Senba, E., Nakashima, K., Taga, T., Yoshida, K., Kishimoto, T., et al. (1999). Fetal liver development requires a paracrine action of oncostatin M through the gp130 signal transducer. *EMBO Journal*, *18*, 2127–2136.
- Kamiya, A., Kinoshita, T., & Miyajima, A. (2001). Oncostatin M and hepatocyte growth factor induce hepatic maturation via distinct signaling pathways. *FEBS Letters*, *492*, 90–94.
- Kanehisa, M., Furumichi, M., Tanabe, M., Sato, Y., & Morishima, K. (2017). KEGG: New perspectives on genomes, pathways, diseases and drugs. *Nucleic Acids Research*, *45*, D353–D361.
- Kaplowitz, N. (2005). Idiosyncratic drug hepatotoxicity. *Nature Reviews. Drug Discovery*, *4*, 489–499.
- Kietzmann, T. (2017). Metabolic zonation of the liver: The oxygen gradient revisited. *Redox Biology*, *11*, 622–630.
- Kordes, C., Sawitzka, I., Gotze, S., Herebian, D., & Haussinger, D. (2014). Hepatic stellate cells contribute to progenitor cells and liver regeneration. *The Journal of Clinical Investigation*, *124*, 5503–5515.
- Kruepunga, N., Hakvoort, T. B. M., Hikspoors, J., Kohler, S. E., & Lamers, W. H. (2019). Anatomy of rodent and human livers: What are the differences? *Biochemistry Biophysics Acta Molecular Basis of Disease*, *1865*(5), 869–878. Amsterdam, Netherlands.
- Larrey, D., & Pageaux, G. P. (2005). Drug-induced acute liver failure. *European Journal of Gastroenterology & Hepatology*, *17*, 141–143.
- Lemaigre, F. P. (2009). Mechanisms of liver development: Concepts for understanding liver disorders and design of novel therapies. *Gastroenterology*, *137*, 62–79.
- Leung, A., Nah, S. K., Reid, W., Ebata, A., Koch, C. M., Monti, S., Genereux, J. C., Wiseman, R. L., Wolozin, B., Connors, L. H., et al. (2013). Induced pluripotent stem cell modeling of multisystemic, hereditary transthyretin amyloidosis. *Stem Cell Reports*, *1*, 451–463.
- Lu, J., Einhorn, S., Venkatarangan, L., Miller, M., Mann, D. A., Watkins, P. B., & LeCluyse, E. (2015). Morphological and functional characterization and assessment of iPSC-derived hepatocytes for in vitro toxicity testing. *Toxicological Sciences: An Official Journal of the Society of Toxicology*, *147*, 39–54.
- Machado, M. V., Michelotti, G. A., Xie, G., de Almeida, T. P., Boursier, J., Bohnic, B., Guy, C. D., & Diehl, A. M. (2015). Mouse models of diet-induced nonalcoholic steatohepatitis reproduce the heterogeneity of the human disease. *PLoS One*, *10*, e0127991.
- Matz, P., Wruck, W., Fauler, B., Herebian, D., Mielke, T., & Adjaye, J. (2017). Footprint-free human fetal fore-skin derived iPSCs: A tool for modeling hepatogenesis associated gene regulatory networks. *Scientific Reports*, *7*, 6294.

206 N. Graffmann et al.

- McLin, V. A., Rankin, S. A., & Zorn, A. M. (2007). Repression of Wnt/beta-catenin signaling in the anterior endoderm is essential for liver and pancreas development. *Development*, *134*, 2207–2217.
- Mian, A., & Lee, B. (2002). Urea-cycle disorders as a paradigm for inborn errors of hepatocyte metabolism. *Trends in Molecular Medicine*, *8*, 583–589.
- Michalopoulos, G. K., Bowen, W. C., Mule, K., & Luo, J. (2003). HGF-, EGF-, and dexamethasone-induced gene expression patterns during formation of tissue in hepatic organoid cultures. *Gene Expression*, *11*, 55–75.
- Nie, Y. Z., Zheng, Y. W., Miyakawa, K., Murata, S., Zhang, R. R., Sekine, K., Ueno, Y., Takebe, T., Wakita, T., Ryo, A., et al. (2018). Recapitulation of hepatitis B virus-host interactions in liver organoids from human induced pluripotent stem cells. *eBioMedicine*, *35*, 114–123.
- O'Brien, S., Keogan, M., Casey, M., Duffy, G., McErlean, D., Fitzgerald, M. X., & Hegarty, J. E. (1992). Biliary complications of cystic fibrosis. *Gut*, *33*, 387–391.
- Ogawa, M., Ogawa, S., Bear, C. E., Ahmadi, S., Chin, S., Li, B., Grompe, M., Keller, G., Kamath, B. M., & Ghanekar, A. (2015). Directed differentiation of cholangiocytes from human pluripotent stem cells. *Nature Biotechnology*, *33*, 853–861.
- Perry, R. J., Camporez, J. P., Kursawe, R., Titchenell, P. M., Zhang, D., Perry, C. J., Jurczak, M. J., Abudukadier, A., Han, M. S., Zhang, X. M., et al. (2015). Hepatic acetyl CoA links adipose tissue inflammation to hepatic insulin resistance and type 2 diabetes. *Cell*, *160*, 745–758.
- Ranucci, G., Polishchuck, R., & Iorio, R. (2017). Wilson's disease: Prospective developments towards new therapies. *World journal of gastroenterology: WJG*, *23*, 5451–5456.
- Rashid, S. T., Corbineau, S., Hannan, N., Marciniak, S. J., Miranda, E., Alexander, G., Huang-Doran, I., Griffin, J., Ahrlund-Richter, L., Skepper, J., et al. (2010). Modeling inherited metabolic disorders of the liver using human induced pluripotent stem cells. *The Journal of Clinical Investigation*, *120*, 3127–3136.
- Raynaud, P., Carpentier, R., Antoniou, A., & Lemaigre, F. P. (2011). Biliary differentiation and bile duct morphogenesis in development and disease. *The International Journal of Biochemistry & Cell Biology*, *43*, 245–256.
- Revill, P., Testoni, B., Locarnini, S., & Zoulim, F. (2016). Global strategies are required to cure and eliminate HBV infection. *Nature Reviews. Gastroenterology & Hepatology*, *13*, 239–248.
- Rui, L. (2014). Energy metabolism in the liver. *Comprehensive Physiology*, *4*, 177–197.
- Russmann, S., Jetter, A., & Kullak-Ublick, G. A. (2010). Pharmacogenetics of drug-induced liver injury. *Hepatology*, *52*, 748–761.
- Sampaziotis, F., Cardoso de Brito, M., Madrigal, P., Bertero, A., Saeb-Parsy, K., Soares, F. A., Schruppf, E., Melum, E., Karlsen, T. H., Bradley, J. A., et al. (2015). Cholangiocytes derived from human induced pluripotent stem cells for disease modeling and drug validation. *Nature Biotechnology*, *33*(8), 845–852.
- Sampaziotis, F., de Brito, M. C., Geti, I., Bertero, A., Hannan, N. R., & Vallier, L. (2017). Directed differentiation of human induced pluripotent stem cells into functional cholangiocyte-like cells. *Nature Protocols*, *12*, 814–827.
- Sauer, V., Roy-Chowdhury, N., Guha, C., & Roy-Chowdhury, J. (2014). Induced pluripotent stem cells as a source of hepatocytes. *Current Pathobiology Reports*, *2*, 11–20.
- Schadt, S., Simon, S., Kustermann, S., Boess, F., McGinnis, C., Brink, A., Lieven, R., Fowler, S., Youdim, K., Ullah, M., et al. (2015). Minimizing DILI risk in drug discovery – A screening tool for drug candidates. *Toxicology In Vitro An International Journal Published in Association with BIBRA*, *30*, 429–437.
- Schmidt, C., Bladt, F., Goedecke, S., Brinkmann, V., Zschiesche, W., Sharpe, M., Gherardi, E., & Birchmeier, C. (1995). Scatter factor/hepatocyte growth-factor is essential for liver development. *Nature*, *373*, 699–702.
- Schobel, A., Rosch, K., & Herker, E. (2018). Functional innate immunity restricts hepatitis C virus infection in induced pluripotent stem cell-derived hepatocytes. *Scientific Reports*, *8*, 3893.
- Scott, J. (1999). Heart disease – Good cholesterol news. *Nature*, *400*, 816.
- Sgodda, M., Mobus, S., Hoepfner, J., Sharma, A. D., Schambach, A., Greber, B., Ott, M., & Cantz, T. (2013). Improved hepatic differentiation strategies for human induced pluripotent stem cells. *Current Molecular Medicine*, *13*, 842–855.
- Sgodda, M., Dai, Z., Zweigerdt, R., Sharma, A.D., Ott, M., & Cantz, T. (2017). *A scalable approach for the generation of human pluripotent stem cell-derived hepatic organoids with sensitive hepatotoxicity features. Stem cells and development*. New York, USA.
- Shlomai, A., Schwartz, R. E., Ramanan, V., Bhatta, A., de Jong, Y. P., Bhatia, S. N., & Rice, C. M. (2014). Modeling host interactions with hepatitis B virus using primary and induced pluripotent stem cell-derived hepatocellular systems. *Proceedings of the National Academy of Sciences of the United States of America*, *111*, 12193–12198.

Liver Disease Modelling

- Siller, R., Greenhough, S., Naumovska, E., & Sullivan, G.J. (2015). *Small-molecule-driven hepatocyte differentiation of human pluripotent stem cells*. Stem cell reports. Bar Harbor, USA.
- Si-Tayeb, K., Noto, F. K., Nagaoka, M., Li, J., Battle, M. A., Duris, C., North, P. E., Dalton, S., & Duncan, S. A. (2010). Highly efficient generation of human hepatocyte-like cells from induced pluripotent stem cells. *Hepatology*, *51*, 297–305.
- Stevens, J. L., & Baker, T. K. (2009). The future of drug safety testing: Expanding the view and narrowing the focus. *Drug Discovery Today*, *14*, 162–167.
- Szalowska, E., van der Burg, B., Man, H. Y., Hendriksen, P. J., & Peijnenburg, A. A. (2014). Model steatogenic compounds (amiodarone, valproic acid, and tetracycline) alter lipid metabolism by different mechanisms in mouse liver slices. *PLoS One*, *9*, e86795.
- Tabibian, J. H., Masyuk, A. I., Masyuk, T. V., O'Hara, S. P., & LaRusso, N. F. (2013). Physiology of cholangiocytes. *Comprehensive Physiology*, *3*, 541–565.
- Takahashi, Y., Soejima, Y., & Fukusato, T. (2012). Animal models of nonalcoholic fatty liver disease/nonalcoholic steatohepatitis. *World journal of gastroenterology: WJG*, *18*, 2300–2308.
- Takeda, M., Okamoto, I., & Nakagawa, K. (2015). Pooled safety analysis of EGFR-TKI treatment for EGFR mutation-positive non-small cell lung cancer. *Lung Cancer*, *88*, 74–79.
- Tiso, N., Filippi, A., Pauls, S., Bortolussi, M., & Argenton, F. (2002). BMP signalling regulates anteroposterior endoderm patterning in zebrafish. *Mechanisms of Development*, *118*, 29–37.
- Tsankov, A. M., Gu, H., Akopian, V., Ziller, M. J., Donaghey, J., Amit, I., Gnirke, A., & Meissner, A. (2015). Transcription factor binding dynamics during human ES cell differentiation. *Nature*, *518*, 344–349.
- van Mourik, I. D. M. (2017). Liver disease in cystic fibrosis. *Paediatrics and Child Health*, *27*, 552–555.
- Vega-Badillo, J., Gutierrez-Vidal, R., Hernandez-Perez, H. A., Villamil-Ramirez, H., Leon-Mimila, P., Sanchez-Munoz, F., Moran-Ramos, S., Larrieta-Carrasco, E., Fernandez-Silva, I., Mendez-Sanchez, N., et al. (2016). Hepatic miR-33a/miR-144 and their target gene ABCA1 are associated with steatohepatitis in morbidly obese subjects. *Liver International*, *36*, 1383–1391.
- Wang, Y., Alhaque, S., Cameron, K., Meseguer-Ripolles, J., Lucendo-Villarin, B., Rashidi, H., and Hay, D.C. (2017). Defined and scalable generation of hepatocyte-like cells from human pluripotent stem cells. *Journal of Visualized Experiments: JoVE*.
- Wilson, A.A., Ying, L., Liesa, M., Segeritz, C.P., Mills, J.A., Shen, S.S., Jean, J., Lonza, G.C., Liberti, D.C., Lang, A.H., et al. (2015). *Emergence of a stage-dependent human liver disease signature with directed differentiation of alpha-1 antitrypsin-deficient iPSCs*. Stem cell reports. Bar Harbor, USA.
- Wisse, E., Braet, F., Luo, D., De Zanger, R., Jans, D., Crabbe, E., & Vermoesen, A. (1996). Structure and function of sinusoidal lining cells in the liver. *Toxicologic Pathology*, *24*, 100–111.
- Wruck, W., Kashofer, K., Rehman, S., Daskalaki, A., Berg, D., Gralka, E., Jozefczuk, J., Drews, K., Pandey, V., Regenbrecht, C., et al. (2015). Multi-omic profiles of human non-alcoholic fatty liver disease tissue highlight heterogenic phenotypes. *Scientific Data*, *2*, 150068.
- Wruck, W., Graffmann, N., Kawala, M. A., & Adjaye, J. (2017). Concise review: Current status and future directions on research related to nonalcoholic fatty liver disease. *Stem Cells*, *35*, 89–96.
- Wu, X., Robotham, J. M., Lee, E., Dalton, S., Kneteman, N. M., Gilbert, D. M., & Tang, H. (2012). Productive hepatitis C virus infection of stem cell-derived hepatocytes reveals a critical transition to viral permissiveness during differentiation. *PLoS Pathogens*, *8*, e1002617.
- Yang, D., Liu, L., Zhu, D., Peng, H., Su, L., Fu, Y. X., & Zhang, L. (2014). A mouse model for HBV immunotolerance and immunotherapy. *Cellular and molecular immunology*, *11*, 71–78.
- Yi, F., Qu, J., Li, M., Suzuki, K., Kim, N. Y., Liu, G. H., & Belmonte, J. C. (2012). Establishment of hepatic and neural differentiation platforms of Wilson's disease specific induced pluripotent stem cells. *Protein & Cell*, *3*, 855–863.
- Yuan, L., Liu, X., Zhang, L., Li, X., Zhang, Y., Wu, K., Chen, Y., Cao, J., Hou, W., Zhang, J., et al. (2018). A chimeric humanized mouse model by engrafting the human induced pluripotent stem cell-derived hepatocyte-like cell for the chronic hepatitis B virus infection. *Frontiers in Microbiology*, *9*, 908.
- Zeng, Z., Guan, L., An, P., Sun, S., O'Brien, S. J., Winkler, C. A., & consortium H.B.V.s. (2008). A population-based study to investigate host genetic factors associated with hepatitis B infection and pathogenesis in the Chinese population. *BMC Infectious Diseases*, *8*, 1.
- Zhang, S., Chen, S., Li, W., Guo, X., Zhao, P., Xu, J., Chen, Y., Pan, Q., Liu, X., Zychlinski, D., et al. (2011). Rescue of ATP7B function in hepatocyte-like cells from Wilson's disease induced pluripotent stem cells using gene therapy or the chaperone drug curcumin. *Human Molecular Genetics*, *20*, 3176–3187.
- Zorn, A.M. (2008). *Liver development*. StemBook (Ed) The Stem Cell Research Community, StemBook.

2.7 Generation of a 3D model to better mimic NAFLD in vitro

Lucas-Sebastian Spitzhorn, Marie-Ann Kawala and James Adjaye

Abstract

Introduction: Non-alcoholic fatty liver disease (NAFLD) has become one of the major risks for the development of hepatocellular carcinoma (HCC). Simple steatosis, which is the first stage of NAFLD, is characterized by abnormal lipid accumulation in hepatocytes. As the molecular processes which lead to steatosis and further progression to non-alcoholic steatohepatitis (NASH), fibrosis, cirrhosis and HCC, are currently not completely understood, many *in vivo* and *in vitro* models have been established. However, current existing *in vitro* models are wrought with limitations. Liver-biopsy derived primary hepatocytes have several limitations: They (i) are rare with a low number of healthy donors, (ii) have high inter-donor variability, (iii) show limited expansion in culture and (iv) rapid decline in function. Thus, the generation of hepatocyte like cells (HLCs) from induced pluripotent stem cells (iPSCs) can provide an alternative cell source. So far, these cells lack full maturity even though they express ALBUMIN and cytochrome P450 family members. Mature HLCs are needed to maximize the relevance of the experimental outcome and applicability of these cells for toxicology and drug screening. Improved maturity and functionality of human iPSC-derived HLCs has been achieved employing three-dimensional (3D) approaches incorporating MSCs and endothelial cells.

Methods: Our preliminary proof of principle experiments involved mixing of iPSC-derived mesenchymal stem cells (iMSCs) with human umbilical vein endothelial cells (HUVECs) and HepG2 cells to generate 3D *in vitro* liver organoids. Furthermore, it is planned to generate MSCs, HLCs and endothelial cells from the same iPSC line (same genetic background). Additionally, spinner flasks were used to provide better medium flow and to improve liver bud growth. These liver buds were then challenged with high levels of glucose and insulin to mimic steatosis.

Results: Within three weeks these cells aggregated and formed vascularized liver buds when cultured on artificial extracellular matrices. These buds secrete urea, express ALBUMIN, VIMENTIN (MSC marker) and CD31 – an endothelial specific marker. Fat

droplet formation after challenging with glucose and insulin resulted in activated expression of steatosis-associated genes.

Discussion/Conclusion: These iPSC-derived liver organoids have the added advantage of having present mesenchymal and endothelial cells from the same individual. Further studies are underway to better characterize these liver buds both molecular and biochemically for liver associated genes, pathways and functions. This 3D iPSC-based approach is a good model to study steatosis and complements our current iPSC-based 2D model.

Publication Status: published in *Zeitschrift für Gastroenterologie* 2016; 54(12): 1343-1404.

Impact Factor: 1.612

This article is reproduced with permission.

Approximated total share of contribution: 80%

Contribution on experimental design, realization and publication:

JA and LSS conceived the idea and designed the experiments. LSS generated the HLCs, the iMSCs and the liver buds and did the subsequent analysis. LSS and MAK performed the oleic acid and glucose tests. LSS prepared the figures.

Link to the publication:

<https://www.thieme-connect.com/products/ejournals/abstract/10.1055/s-0036-1597423>

3.3

Generation of a 3D model to better mimic NAFLD in vitroSpitzhorn LS¹, Kawala MA¹, Adjaye J¹¹Heinrich Heine University Duesseldorf, Institute for Stem Cell Research and Regenerative Medicine, Duesseldorf, Germany

Introduction: Non-alcoholic fatty liver disease (NAFLD) has become one of the major risks for the development of hepatocellular carcinoma (HCC). Simple steatosis, which is the first stage of NAFLD, is characterized by abnormal lipid accumulation in hepatocytes. As the molecular processes which lead to steatosis and further progression to non-alcoholic steatohepatitis (NASH), fibrosis, cirrhosis and HCC, are currently not completely understood, many in vivo and in vitro models have been established. However, current existing in vitro models are wrought with limitations. Liver-biopsy derived primary hepatocytes have several limitations: They (i) are rare with a low number of healthy donors, (ii) have high inter-donor variability, (iii) show limited expansion in culture and (iv) rapid decline in function. Thus, the generation of hepatocyte like cells (HLCs) from induced pluripotent stem cells (iPSCs) can provide an alternative cell source. So far these cells lack full maturity even though they express ALBUMIN and cytochrome P450 family members. Mature HLCs are needed to maximize the relevance of the experimental outcome and applicability of these cells for toxicology and drug screening. Improved maturity and functionality of human iPSC-derived HLCs has been achieved employing three-dimensional (3D) approaches incorporating MSCs and endothelial cells. **Methods:** Our preliminary proof of principle experiments involved mixing of iPSC-derived mesenchymal stem cells (iMSCs) with human umbilical vein endothelial cells (HUVECs) and HepG2 cells to generate 3D in vitro liver organoids. Furthermore it is planned to generate MSCs, HLCs and endothelial cells from the same iPSC line (same genetic background). Additionally spinner flasks were used to provide better medium flow and to improve liver bud growth. These liver buds were then challenged with high levels of glucose and insulin to mimic steatosis. **Results:** Within three weeks these cells aggregated and formed vascularized liver buds when cultured on artificial extracellular matrices. These buds secrete urea, express ALBUMIN, VIMENTIN (MSC marker) and CD31 – an endothelial specific marker. Fat droplet formation after challenging with glucose and insulin resulted in activated expression of steatosis-associated genes. **Discussion/Conclusion:** These iPSC-derived liver organoids have the added advantage of having present mesenchymal and endothelial cells from the same individual. Further studies are underway to better characterize these liver buds both molecular and biochemically for liver associated genes, pathways and functions. This 3D iPSC-based approach is a good model to study steatosis and complements our current iPSC-based 2D model.

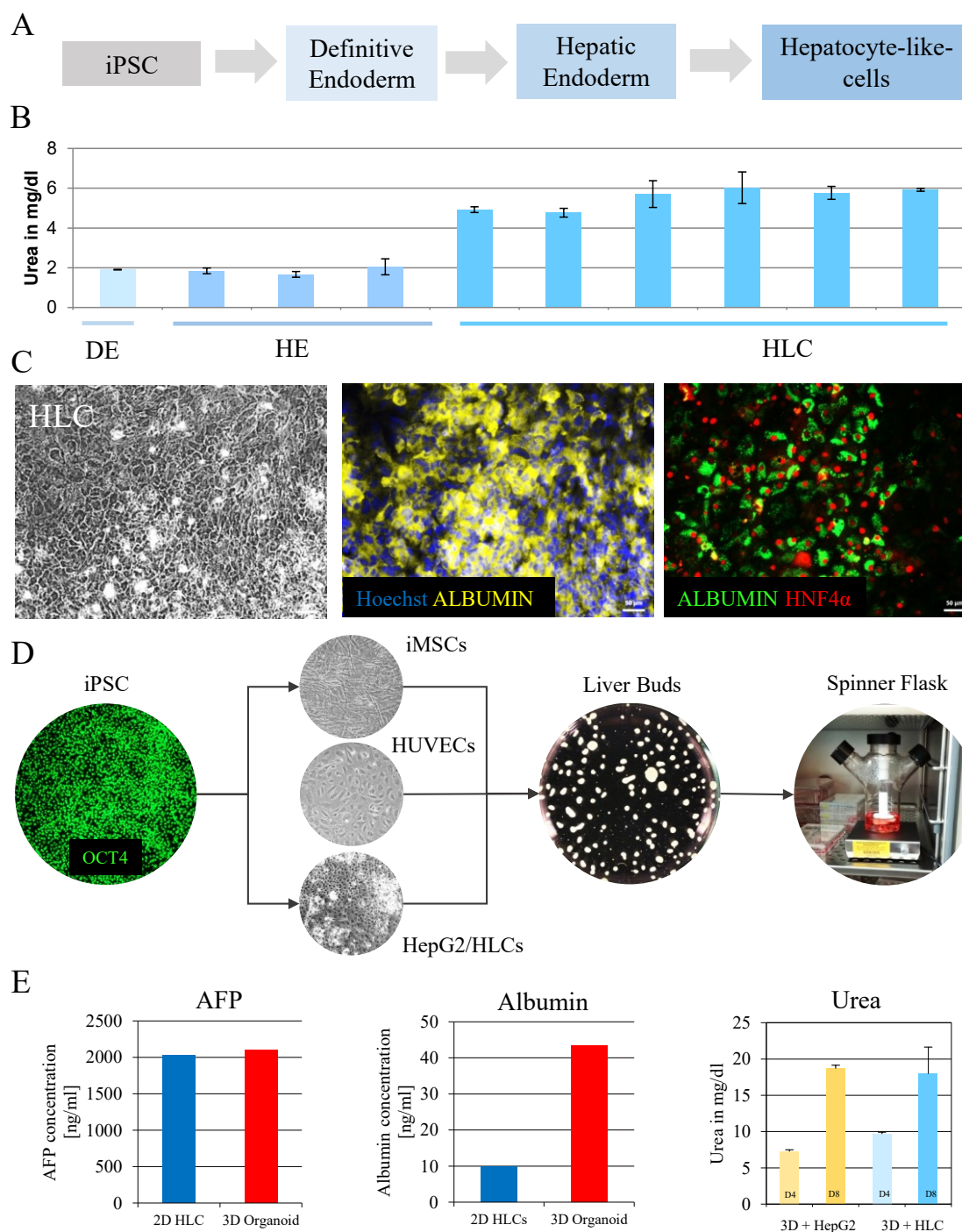


Figure 1a: Generation of a 3D liver model and mimicking NAFLD in vitro. (A) Scheme of the generation of HLCs from iPSCs including the intermediate steps definitive endoderm (DE) and hepatic endoderm (HE). (B) Urea production level increases from DE to HE and peaks at the HLC stage. (C) HLCs exhibit a hepatocyte-like, cobble stone morphology and express liver markers Albumin (yellow and green) and HNF4a (red). Cell nuclei were stained using Hoechst (blue). (D) Generation of liver buds by mixing iMSCs, HUVECs and HepG2/HLCs in a distinct ratio. Liver buds resulted from self-condensation processes. To ensure good nutrient flow, liver buds were cultivated in a spinner flask. (E) 3D liver buds express equal amounts of AFP than 2D HLCs but higher levels of Albumin. Liver buds secrete Urea in similar amounts than HepG2 cells and secretion levels alleviate over time.

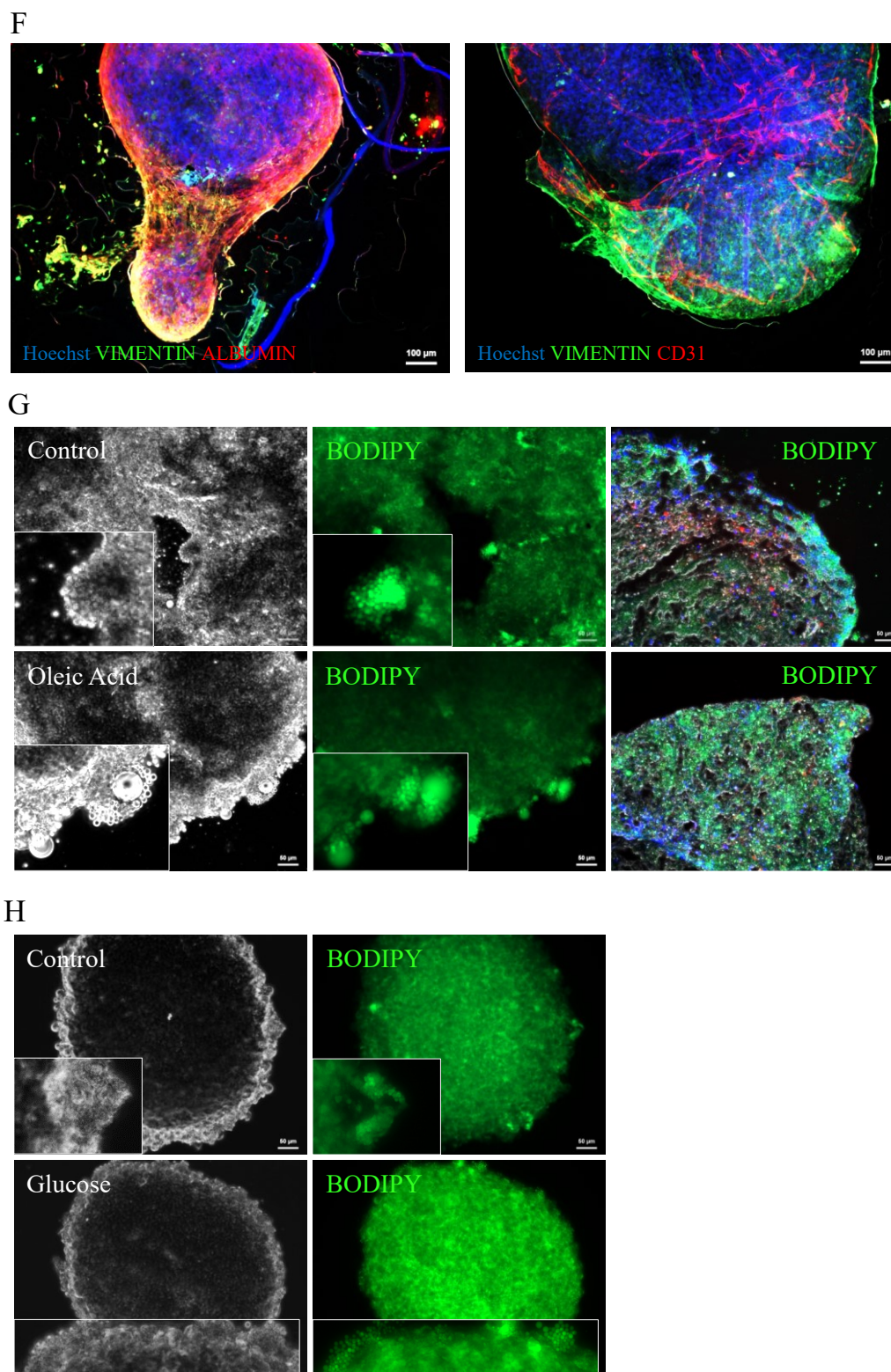


Figure 1b: Generation of a 3D liver model and mimicking NAFLD *in vitro*. (F) Cells within the liver buds were positive for the MSC Marker Vimentin (green), the liver Marker Albumin (red) and the endothelial cell marker CD31 (red) which was present in a network-like distribution. Cell nuclei were stained using Hoechst. (G, H) Liver buds challenged with Oleic acid or Glucose show higher number of fat droplets than the control as indicated by BODIPY staining thereby mimicking NAFLD *in vitro*.

2.8 Constructing an Isogenic 3D Human Nephrogenic Progenitor Cell Model Composed of Endothelial, Mesenchymal, and SIX2-Positive Renal Progenitor Cells

Lisa Nguyen, Lucas-Sebastian Spitzhorn and James Adjaye

Abstract

Urine has become the source of choice for noninvasive renal epithelial cells and renal stem cells which can be used for generating induced pluripotent stem cells. The aim of this study was to generate a 3D nephrogenic progenitor cell model composed of three distinct cell types—urine-derived SIX2-positive renal progenitor cells, iPSC-derived mesenchymal stem cells, and iPSC-derived endothelial cells originating from the same individual. Characterization of the generated mesenchymal stem cells revealed plastic adherent growth and a trilineage differentiation potential to adipocytes, chondrocytes, and osteoblasts. Furthermore, these cells express the typical MSC markers CD73, CD90, and CD105. The induced endothelial cells express the endothelial cell surface marker CD31. Upon combination of urine-derived renal progenitor cells, induced mesenchymal stem cells, and induced endothelial cells at a set ratio, the cells self-condensed into three-dimensional nephrogenic progenitor cells which we refer to as 3D-NPCs. Immunofluorescence-based stainings of sectioned 3D-NPCs revealed cells expressing the renal progenitor cell markers (SIX2 and PAX8), podocyte markers (Nephrin and Podocin), the endothelial marker (CD31), and mesenchymal markers (Vimentin and PDGFR- β). These 3D-NPCs share kidney progenitor characteristics and thus the potential to differentiate into podocytes and proximal and distal tubules. As urine-derived renal progenitor cells can be easily obtained from cells shed into urine, the generation of 3D-NPCs directly from renal progenitor cells instead of pluripotent stem cells or kidney biopsies holds a great potential for the use in nephrotoxicity tests, drug screening, modelling nephrogenesis and diseases.

Publication Status: published in *Stem Cells International*, Volume 2019, Article ID 3298432

Impact Factor: 3.989

This article is reproduced with permission.

Approximated total share of contribution: 10%

Contribution on experimental design, realization and publication:

JA and LN conceived the idea and designed the experiments. LSS did pilot experiments for generation organoids via self-condensation. LN derived and characterized the UdRPC-iECs and UdRPC-iMSCs. LN generated and stained the 3D-NPCs. LSS helped characterizing the UdRPC-iMSCs, making the figures and edited the manuscript. The manuscript including all figures was subsequently reviewed by JA.

Link to the publication:

<https://www.hindawi.com/journals/sci/2019/3298432/>

Hindawi
Stem Cells International
Volume 2019, Article ID 3298432, 11 pages
<https://doi.org/10.1155/2019/3298432>



Research Article

Constructing an Isogenic 3D Human Nephrogenic Progenitor Cell Model Composed of Endothelial, Mesenchymal, and SIX2-Positive Renal Progenitor Cells

Lisa Nguyen , Lucas-Sebastian Spitzhorn, and James Adjaye 

Institute for Stem Cell Research and Regenerative Medicine, University Hospital Duesseldorf, 40225 Duesseldorf, Germany

Correspondence should be addressed to James Adjaye; james.adjaye@med.uni-duesseldorf.de

Received 20 December 2018; Accepted 20 March 2019; Published 2 May 2019

Academic Editor: Stefan Liebau

Copyright © 2019 Lisa Nguyen et al. This is an open access article distributed under the Creative Commons Attribution License, which permits unrestricted use, distribution, and reproduction in any medium, provided the original work is properly cited.

Urine has become the source of choice for noninvasive renal epithelial cells and renal stem cells which can be used for generating induced pluripotent stem cells. The aim of this study was to generate a 3D nephrogenic progenitor cell model composed of three distinct cell types—urine-derived SIX2-positive renal progenitor cells, iPSC-derived mesenchymal stem cells, and iPSC-derived endothelial cells originating from the same individual. Characterization of the generated mesenchymal stem cells revealed plastic adherent growth and a trilineage differentiation potential to adipocytes, chondrocytes, and osteoblasts. Furthermore, these cells express the typical MSC markers CD73, CD90, and CD105. The induced endothelial cells express the endothelial cell surface marker CD31. Upon combination of urine-derived renal progenitor cells, induced mesenchymal stem cells, and induced endothelial cells at a set ratio, the cells self-condensed into three-dimensional nephrogenic progenitor cells which we refer to as 3D-NPCs. Immunofluorescence-based stainings of sectioned 3D-NPCs revealed cells expressing the renal progenitor cell markers (SIX2 and PAX8), podocyte markers (Nephrin and Podocin), the endothelial marker (CD31), and mesenchymal markers (Vimentin and PDGFR- β). These 3D-NPCs share kidney progenitor characteristics and thus the potential to differentiate into podocytes and proximal and distal tubules. As urine-derived renal progenitor cells can be easily obtained from cells shed into urine, the generation of 3D-NPCs directly from renal progenitor cells instead of pluripotent stem cells or kidney biopsies holds a great potential for the use in nephrotoxicity tests, drug screening, modelling nephrogenesis and diseases.

1. Introduction

Many disease conditions, including renal diseases, require replacement of tissues or organs. Organ or tissue transplantation is the only effective and most widely used medical treatment [1]. As stem cells can be used for the generation of autologous, specialized cell types, stem cell-based therapies are an alternative to transplantation [2]. However, both treatments face major problems: worldwide donor shortage, poor immunohistocompatibility between the donor and recipient, and the probability of side effects such as teratoma and tumor formation upon stem cell therapy. An alternative to kidney transplantations is the use of renal progenitor cells, which can be isolated from human urine [1], in order to generate kidney cell types and subsequently transplantable renal tissues. Physiological processes in the kidney result in

thousands of viable kidney cells being shed into the urine [1, 3]. The cell type of interest, i.e., urine stem cell or urine-derived renal progenitor cell (UdRPC), is required for the renewal of kidney cells [4]. UdRPCs have a rice grain-like morphology [3] and share stem cell characteristics including clonogenicity, high expansion capacity, multipotent differentiation potency, and self-renewal driven by SIX2 [3, 5, 6]. In addition, these cells have the potential to be differentiated into numerous cell types present within the kidney.

The three-dimensional organoid technology is another alternative. Here, cells of the organ of interest, such as heart, liver, or kidney, are generated from induced pluripotent stem cells (iPSCs) in a 3D manner, named organoids. Because these organoids are composed of organ-specific cells which can self-organize, they are able to recapitulate some of the typical organ structures and functions [7, 8]. Other three-

dimensional models include gastruloids, defined as *in vitro* multicellular models capable of mimicking the gastrulation process [9]. Published reports have shown successful generation of organoids derived from tissues such as the optic cup [10], hypophysis epithelium [11], intestine [12], cerebrum [13], and kidney [14]. Current shortfalls of existing organoid models include the lack of vascularization and the associated supply with nutrients and oxygen through blood flow as well as the organization of complex structures. Moreover, this kind of tissue engineering is based on the use of specific inducing factors and scaffolds, which cannot fully recapitulate the *in vivo* microenvironment needed for cell-cell interactions in the changing fluidity during organogenesis [15]. In light of these shortfalls, the generation of organoids by imitating the multicellular interactions in the *in vivo* organ is the next step needed to enhance organoid technology, especially in the kidney.

Here, we describe the generation and characterization of 3D-NPCs (three-dimensional nephron progenitor cells) composed of three cell types—SIX2-positive urine-derived renal progenitor cells (UdRPCs), UdRPC-iPSC-derived mesenchymal stem cells (UdRPC-iMSCs), and endothelial cells (UdRPC-iECs) to mimic the multicellular organization of the *in vivo* organ. The combination of the aforementioned cell types resulted in self-condensed 3D-NPCs, maintaining the expression of the renal progenitor marker SIX2 when cultured in self-renewal supportive medium. 3D-NPCs can be harnessed for efficient generation of kidney organoids useful as a platform for studying nephrogenesis, kidney disease modelling, and nephrotoxicity testing.

2. Materials and Methods

2.1. iPSCs from Urine-Derived Renal Progenitor Cells (UdRPCs). The iPSC line used, ISRM-UM51, here called UdRPC-iPSCs, was reprogrammed from renal progenitor cells (UdRPCs) isolated from urine samples as described before [16, 17]. ISRM-UM51 is of known HLA and has a CYP2D6 status of an intermediate metabolizer [17].

2.2. Differentiation of UdRPC-iPSCs to Endothelial Cells (UdRPC-iECs). Prior to differentiation, UdRPC-iPSCs were adapted to E8 medium (STEMCELL Technologies) on Matrigel-coated plates (Corning Incorporated, #354277). At 80–90% confluency, cells were dissociated with 0.05% EDTA/PBS and single cells were seeded on Matrigel-coated plates with an addition of ROCK inhibitor Y-27632 (10 μ M) (Tocris Bioscience, #1254/1) for the first 24 h to improve cell survival. When the cell density reached 70–80%, mesoderm formation was induced for 44 h by cultivating the cells in E8 medium containing 25 ng/ml activin A (PeproTech, #120-14E), 5 ng/ml BMP4 (PeproTech, #120-05ET), and 1 μ M CHIR99021 (Tocris Bioscience, #TB4423-GMP/10) [18]. The medium was changed to E7 medium (STEMCELL Technologies, #05910) supplemented with 50 ng/ml BMP4, 5 μ M SB431542 (Tocris Bioscience, #1614), and 50 ng/ml VEGF-A (PeproTech, #100-200) for three to five days. Endothelial cells were maintained in E7 medium supplemented with 50 ng/ml VEGF-A or Medium 200 (Gibco, #M200500) at 37°C and 5%

CO₂. Human umbilical cord vein endothelial cells (HUVECs) were used as a control.

2.3. Differentiation of UdRPC-iPSCs to Mesenchymal Stem Cells (UdRPC-iMSCs). The UdRPC-iPSCs were split into single cells at a confluency of 90–100% by incubating with TrypLE (Gibco, #12604021) for 4 min. Single cells were seeded on Matrigel-coated 6-well plates. As described before, differentiation was prepared at 60–70% confluency [19, 20]. Maintenance medium was replaced with mesenchymal stem cell (MSC) differentiation medium composed of Minimum Essential Medium Eagle (α -MEM) (Sigma-Aldrich, #M8042-6x500ml), 10% FBS (Gibco, #10500064), 1% P/S (Invitrogen, #15140122), 1% GlutaMAX (Gibco, #35050061), and 10 μ M of the TGF β -receptor inhibitor SB431542. Cell differentiation was carried out for 14 days, and medium was changed every second day. Afterwards, the cells were passaged with TrypLE and were plated onto uncoated flasks. Passaging was continued until the cells attained an MSC-like morphology. The cells were kept in MSC cultivation medium (α -MEM, 10% FBS, 1% P/S, and 1% GlutaMAX) lacking SB431542. Differentiation of resulting UdRPC-iMSCs was carried out afterwards to evaluate their trilineage differentiation potential. In addition, the expression of typical MSC cell surface markers and the absence of hematopoietic markers were analysed via flow cytometry.

2.4. In Vitro Differentiation Assays

2.4.1. Adipogenesis. Induction of adipogenesis was performed by incubating UdRPC-iMSCs in adipogenic medium (Gibco, #A1007001) for three weeks with medium changes every second day. Formation of lipid droplets was detected via Oil Red O staining (Sigma-Aldrich, #1320-06-5).

2.4.2. Chondrogenesis. Chondrogenesis of UdRPC-iMSCs was induced with chondrogenic medium (Gibco, #A1007101), and cells were cultivated for three weeks with regular medium changes every second day. Cartilage formation was confirmed with Alcian Blue staining (Sigma-Aldrich, #33864-99-2).

2.4.3. Osteogenesis. UdRPC-iMSCs were seeded in two wells of a 24-well plate and were incubated in osteogenic medium (Gibco, #A1007201) for three weeks with medium changes every second day. To demonstrate the successful differentiation, calcium deposits were identified with Alizarin Red staining (Sigma-Aldrich, #130-22-3).

2.5. Immunophenotyping of UdRPC-iMSCs. For the immunophenotyping, two biological replicates per cell type, namely, UdRPC-iMSCs, native UdRPCs and native human fetal MSCs [21], were analysed. Each replicate was divided into two aliquots, each containing 1×10^5 cells. MSC phenotyping cocktail (cocktail of fluorochrome-conjugated monoclonal antibodies: CD14-PerCP, CD20-PerCP, CD34-PerCP, CD45-PerCP, CD73-APC, CD90-FITC, and CD105-PE) or the isotype control cocktail (cocktail of fluorochrome-conjugated monoclonal antibodies: mouse IgG1-FITC, mouse IgG1-PE, mouse IgG1-APC, mouse IgG1-PerCP, and mouse IgG2a-PerCP) was added to the samples. The

TABLE 1: List of antibodies and dilution for immunofluorescence staining.

Immunofluorescence antibody	Specificity	Dilution	Company	Cat. No.
CD31	Mouse	1 : 300	R&D	BBA7
NPHS1	Rabbit	1 : 200	Invitrogen	PA5-20330
NPHS2	Rabbit	1 : 400	Proteintech	20384-1-AP
PAX8	Rabbit	1 : 200	Cell Signaling	59019
PDGFR- β	Rabbit	1 : 100	Cell Signaling	3169
SIX2	Rabbit	1 : 200	Proteintech	11562-1-AP
Vimentin	Rabbit	1 : 200	Cell Signaling	5741
Alexa 488	Rabbit	1 : 500	Invitrogen	A-11034
Alexa 555	Rabbit	1 : 500	Invitrogen	A-21428
Cy3	Mouse	1 : 500	Invitrogen	A10521
NANOG	Rabbit	1 : 800	Cell Signaling	4903T
SSEA4	Mouse	1 : 1000	Cell Signaling	4755T
TRA-1-81	Mouse	1 : 1000	Cell Signaling	4745T

cells were incubated with the respective antibody cocktail for 10 min at 4°C in the dark with occasional swaying of the tubes. Cells were washed afterwards, and the fixed samples were measured using the CyAn ADP (Beckman Coulter, CA, USA) and analysed using the Summit 4.3 software.

2.6. Immunofluorescence-Based Staining. Paraformaldehyde (Polysciences, #18814-10) fixed samples were washed with 1% Triton X-100/PBS (Merck, #9002-93-1). If staining for cell surface markers was intended, washing was done with PBS instead. After this step, samples were washed twice with PBS. To block unspecific binding sites, the sample was incubated with blocking buffer for 2 h at room temperature.

The primary antibody was incubated overnight at 4°C. The respective antibody was diluted following the instructions in Table 1. The following day, samples were washed three times with 0.05% Tween/PBS (Merck, #9005-64-5). The secondary antibody (solved 1:500 in blocking buffer/PBS of a ratio 1:2) and Hoechst (Thermo Fisher, #H3570) (1:5000) were added and incubated for 1 h in the dark at room temperature. After washing the samples twice with 0.05% Tween/PBS, the plates were kept in 1% PS/PBS at 4°C until evaluation under a fluorescence microscope X-Cite series 120 Lumen Dynamics (Zeiss).

2.7. Generation of 3D-NPCs Based on the Coculture of UdrPCs, UdrPC-iMSCs, and UdrPC-iECs. The medium for 3D-NPC maintenance was prepared by adding 5 ng/ml VEGF-A, 1 μ g/ml heparin, and 5 ng/ml EGF (PeproTech, #100-47) to renal progenitor maintenance medium (RPM) [16, 17]. Confluent wells of UdrPCs, UdrPC-iMSCs, and UdrPC-iECs were incubated with TrypLE at 37°C until cells detached; thereafter, RPM was added to stop the enzymatic reaction. UdrPCs and UdrPC-iMSCs were centrifuged at 250 \times g for 5 min, and UdrPC-iECs were centrifuged at 150 \times g for 5 min. After aspirating the supernatant and replenishing with fresh medium, cells were counted. The seeding ratio between the three cell types was 10:7:2 (UdrPCs, UdrPC-iMSCs, and UdrPC-iECs). The required

cell number of one combination process was as follows: 1×10^6 UdrPCs, 0.7×10^6 UdrPC-iMSCs, and 0.2×10^6 UdrPC-iECs. The cell types were resuspended in 1 ml RPM. After mixing the three cell types, the cell suspension was added to a T25 flask with 7 ml RPM, filling up to a total volume of 10 ml. ROCK inhibitor Y-27632 (10 μ M) was added on day one to ensure cell survival. The flask was placed in an upright position in the incubator at 37°C and 5% CO₂. After 14 days of cultivation, condensed 3D-NPCs were transferred into a petri dish and kept at 37°C and 5% CO₂ in a rotating incubator. Approximately 90% of the condensation experiments resulted in three-dimensional, non-adherent 3D-NPCs.

3. Results and Discussion

3.1. Derivation of UdrPC-iMSCs from UdrPC-iPSCs. In this study, UdrPC-iMSCs were successfully generated from the iPSC line UM51 reprogrammed from UdrPCs [17]. The criteria defining mesenchymal stem cells include plastic adherence, trilineage differentiation potential to adipocytes, chondrocytes, and osteoblasts, expression of cell surface markers CD73, CD90, and CD105 (95% and higher), and absence of hematopoietic markers CD14, CD20, CD34, and CD45 [22]. The UdrPC-iMSCs displayed a fibroblast-like and spindle-shaped morphology and were able to adhere to plastic surfaces (Figure 1(a)). Their potential to differentiate to clinical relevant chondrogenic and osteogenic fate was observed by Alcian Blue and Alizarin Red staining (Figure 1(a)). Additionally, the potential to differentiate into adipocytes was shown by Oil Red O staining (Figure 1(a)).

Immunophenotyping of the UdrPC-iMSCs confirmed the expression of the typical MSC cell surface markers CD73, CD90, and CD105 and absence of the hematopoietic markers CD14/CD20/CD34/CD45 ($1.59 \pm 0.7\%$, Figure 1(b)). The levels of CD73 and CD105 were $98.30 \pm 0.3\%$ and $98.27 \pm 0.3\%$, respectively (Figure 1(b)). UdrPC-iMSCs had a lower level CD90 ($25.25 \pm 6.1\%$) compared to bone marrow MSCs (Figure 1(b)). The reference gold standard bone

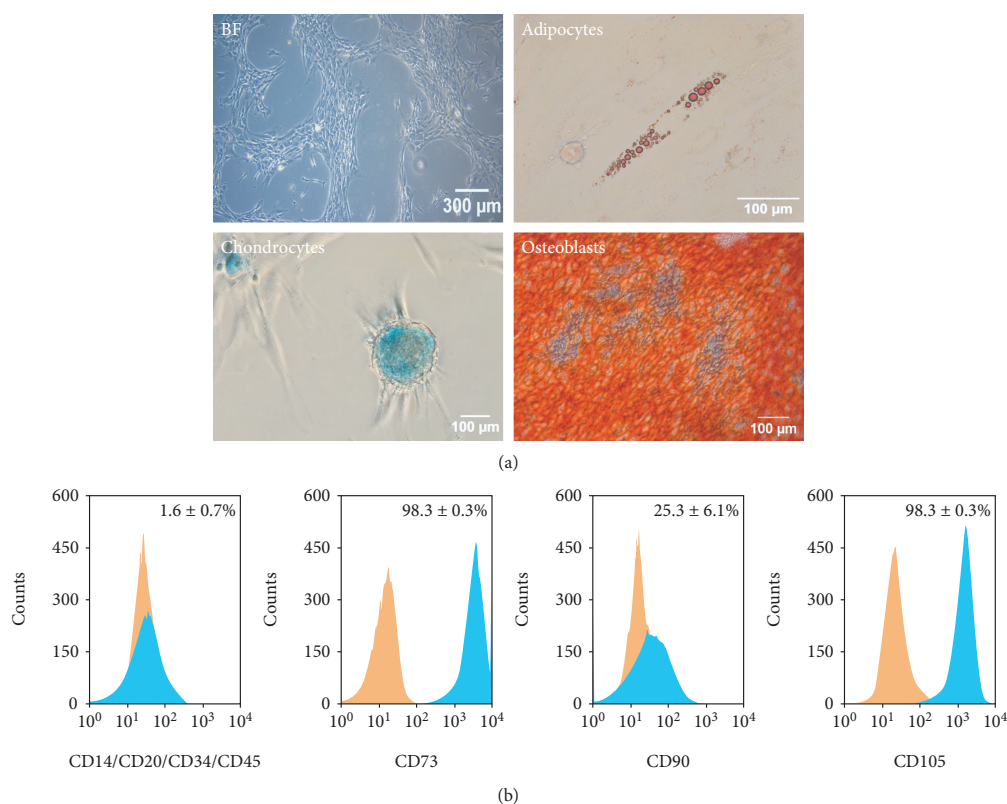


FIGURE 1: UdrPC-iMSCs are MSCs and bear characteristic MSC features. (a) Cell morphology and trilineage differentiation potential of UdrPC-iMSCs. UdrPC-iMSCs are elongated and spindle-shaped and possess trilineage differentiation potential to adipocytes, chondrocytes, and osteoblasts. (b) Immunophenotype of the generated UdrPC-iMSC line. Expression of MSC cell surface markers CD73, CD90, and CD105 and the hematopoietic markers CD14, CD20, CD34 and CD45 was analysed. Histograms of IgG control are displayed in orange, and histograms of MSC markers are displayed in blue ($n = 2$).

marrow-derived MSCs have more than 95% CD90⁺ cells (Figure S1A). However, MSCs isolated from distinct organs and origins are known to express a diverse set of MSC cell surface markers and even with varying degrees of expression [23]. In contrast, the native UdrPCs, from which the UdrPC-iMSCs originate, have high levels of CD73 ($99.11 \pm 0.3\%$) and CD90 ($79.28 \pm 3.6\%$) and a low level of CD105 ($10.92 \pm 0.6\%$) (Figure S1B). Urine-derived stem cells have been described to express high levels of CD29, CD44, and CD73 (>98%) and a variable expression of CD54, CD90, CD105, and CD166 [24, 25]. These variations between MSCs may be due to inherent functional differences and the fact that the cells are part of a heterogeneous subpopulation within tissues [23]. Since UdrPC-iMSCs bear MSC features other than 95% CD90 expression, i.e., plastic adherence and the trilineage differentiation to adipogenic, chondrogenic, and osteogenic fate, UdrPC-iMSCs are considered MSC-like.

Additionally, immunofluorescence-based staining also revealed the expression of the MSC markers α -SMA, Vimentin, and PDGFR- β (Figure 2). As MSCs are found in almost

all tissues of the human body, UdrPC-iMSCs are perfectly suited for the generation of organoids consisting of distinct cell types. MSCs have been described to be important for the process of self-condensation in the generation of organoids where contractions of the actomyosin cytoskeletal axis of MSCs play the key role [2, 26]. Condensation did not occur in the absence of MSCs and organoids could not form [2]. This observation was also made in this study; even though UdrPCs are MSCs, incubation of UdrPCs alone only led to emerging 3D cell aggregates without the typical round organoid structures with borders typical of 3D-NPCs (data not shown). It is known from embryonic invagination that Myosin II is active during this developmental process which leads to inward dislocation of cell-cell junctions [2, 26]. Takebe et al. were able to show that in MSCs, Myosin II was highly expressed just before condensation took place [2]. Furthermore, it has been shown that progressive recruitment of mesenchymal progenitors plays a fundamental role in cell fate acquisition during nephrogenesis in mice and human [27]. Another important role of MSCs was described by Tögel et al., where MSCs were injected into rat models

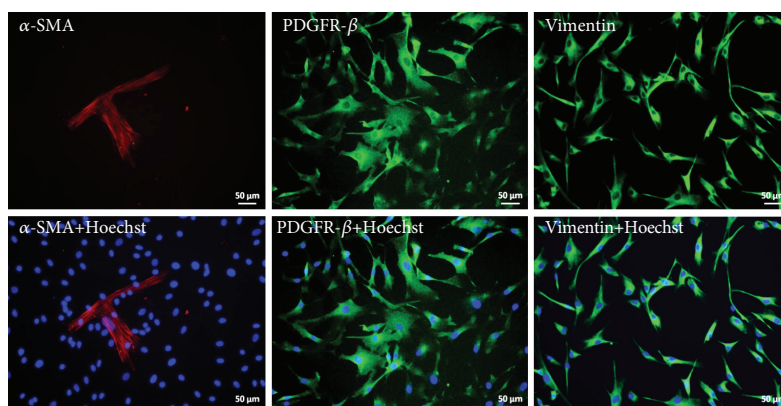


FIGURE 2: Expression of MSC markers in UdrPC-iMSCs. Stainings were carried out for the expression of the mesenchymal markers— α -SMA, Vimentin, and PDGFR- β . Cell nuclei were stained with Hoechst. Pictures were taken under 20x magnification.

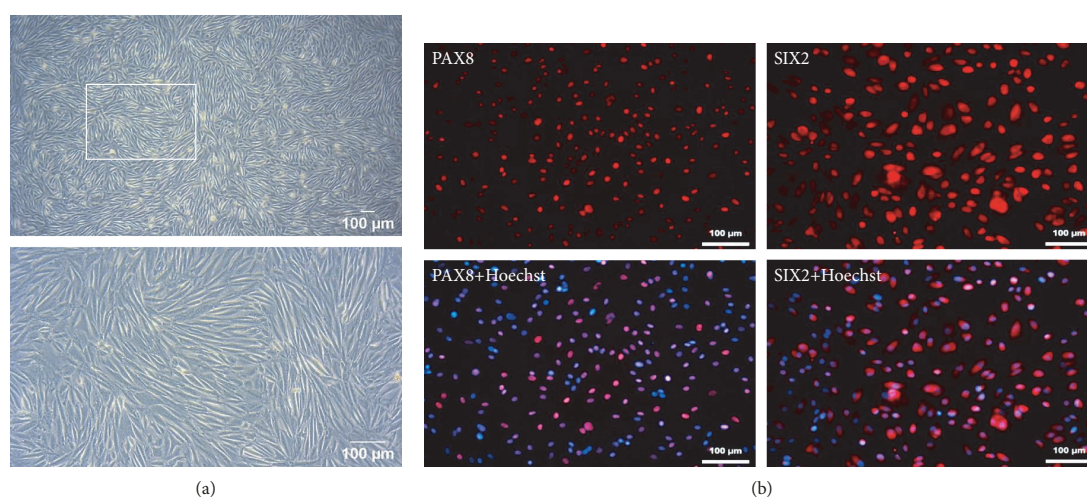


FIGURE 3: Phase contrast image of UdrPCs and expression of kidney-related markers. (a) Cell morphology of UdrPCs. (b) Stainings were carried out for PAX8 and the nephron progenitor marker SIX2. Cell nuclei were stained with Hoechst. Pictures were taken under 10x and 20x magnification.

suffering from reperfusion-induced acute renal failure [28]. The injected MSCs were able to protect renal cells from further damage and partly restored renal functions by secretion of anti-inflammatory factors.

3.2. Urine-Derived Renal Progenitor Cells (UdrPCs). UdrPCs were isolated from voided urine of a male donor of African origin [17]. When kept in proliferation medium, they retained the typical rice grain-like morphology (Figure 3(a)) and expressed PAX8 and SIX2 (Figure 3(b)).

3.3. Generation of Endothelial Cells from UdrPC-iPSCs. UdrPC-iPSCs were differentiated to endothelial cells (UdrPC-iECs) using a modified two-step protocol [18].

The differentiated cells had a cobblestone-like morphology with broad cell bodies and grew as a thin adherent cell layer (Figure 4(a)). Like HUVECs, UdrPC-iECs uniformly expressed the endothelial cell surface marker CD31 (Figure 4(b)). Cell sizes of UdrPC-iECs were smaller than those of HUVECs (Figure 4(b)) which could be explained by a lower passage number and the fact that they were derived from iPSCs which are small in size themselves. Since *in vivo* vasculature for nutrient and oxygen supply is established in the early embryonal development, UdrPC-iECs were used for the formation of kidney pre-organoids which should support the sufficient availability with nutrients and oxygen and allow further maturation of kidney structures.

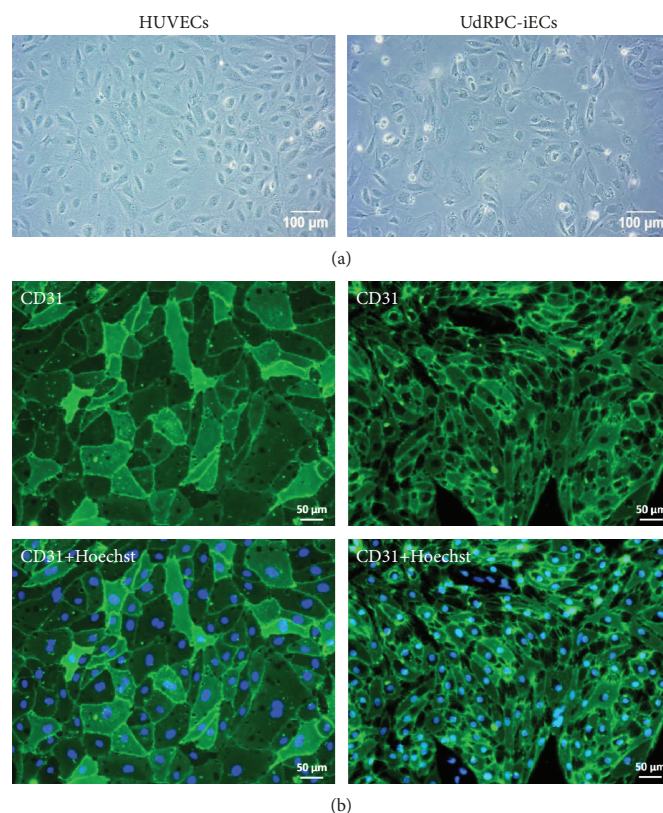


FIGURE 4: Comparison of UdrPC-iECs with HUVECs. (a) UdrPC-iECs had a broad, cobblestone-like morphology similar to HUVECs. (b) Expression of the endothelial cell surface marker CD31 in HUVECs and UdrPC-iECs. Cell nuclei were stained with Hoechst.

3.4. Formation of 3D-Nephron Progenitor Cells. Three-dimensional nephron progenitor cells (3D-NPCs) were generated by combining urine-derived SIX2-positive renal progenitor cells (UdrPCs), UdrPC-iMSCs, and UdrPC-iECs at a ratio of 10:7:2. The cell mixture self-condensed after 2 to 4 days forming round-shaped, three-dimensional structures with sharp borders (Figure 5). The 3D-NPCs were transferred to petri dishes 14 days after the respective cells were combined.

3.5. Expression of Renal, Endothelial, and Mesenchymal Markers in 3D-NPCs. After three to four weeks of cultivation, 3D-NPCs were fixed, dehydrated, and subsequently embedded in the preparation of cryosectioning. The sections were then stained for the expression of several kidney-specific markers, such as SIX2, PAX8, Nephlin, and Podocin, endothelial marker- CD31, and mesenchymal markers, PDGFR- β and Vimentin (Figure 6).

3D-NPCs express the renal progenitor marker SIX2 which in mice has been shown to be expressed during early kidney development, especially in the cap mesenchyme, a region consisting of progenitor cells committed to the nephron fate [27, 29]. This gene is involved in the

maintenance of the progenitor state, and the depletion of SIX2 leads to the differentiation of the progenitor cells towards cell types making up the nephron, the functional unit of the kidney, including podocytes and distal and proximal tubules.

The early renal marker PAX8 is uniformly expressed in 3D-NPCs (Figure 6). PAX8 expression is maintained throughout nephron morphogenesis, emerging at the renal vesicle stage, and regulates kidney organogenesis [30, 31]. Cytoplasmic expression of Nephlin was not as uniform as seen for SIX2 and PAX8, but more localized (Figure 6). Nephlin is a protein of the immunoglobulin superfamily of cell adhesion receptors and is present in epithelial podocytes which wrap around the glomeruli and are part of the glomerular filtration barrier [32]. The podocytic foot processes are interconnected via slit diaphragms which are formed by Nephlin, Podocin, TRPC6, and FAT1 [33, 34]. Expression of the membrane protein Podocin, encoded by *NPFS2*, was detected on the plasma membrane of cells within the 3D-NPCs (Figure 6). It has to be noted that native UdrPCs express SIX2 [17], Nephlin, and Podocin (data not shown); therefore, it is further evidence in support of our generated 3D-NPCs.

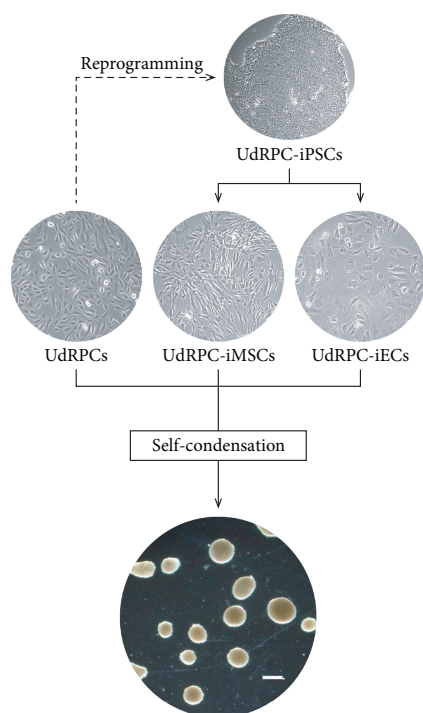


FIGURE 5: Overview of the formation of three-dimensional nephron progenitor cells (3D-NPCs). Isogenic 3D-NPCs were generated from three cell types namely SIX2-positive UdRPCs, UdRPC-iMSCs, and UdRPC-iECs of the same genetic background. The scale bar corresponds to a length of 500 μm .

Furthermore, 3D-NPCs harbour endothelial cells which express the cell surface marker CD31 (Figure 6). CD31 is also known as PECAM-1, a glycoprotein, and besides being present on the cell surface of endothelial cells, CD31 can also be found on platelets and some leukocytes [35]. This protein is involved in the adhesion between the endothelial cells by intercellular junctions [35]. Expression of the MSC markers Vimentin and PDGFR- β was not uniformly distributed as seen for PAX8. Vimentin is a type III intermediate filament, which forms the cytoskeleton together with microtubules and actin filaments. This protein is important for the maintenance of cell and tissue integrity [36]. Vimentin was also found to contribute to epithelial to mesenchymal transition (EMT) by upregulating the expression of EMT-related genes [37]. PDGFR- β is a receptor protein for the mitogen PDGF [38] and is involved in the development of mesenchymal stem cells. As mentioned before, MSCs are essential for self-condensation of organoids. In this case, UdRPC-iMSCs might have been involved in the condensation process where the contractile force of the cytoskeleton leads to 3D formation [2]. The addition of UdRPC-iMSCs should also be beneficial for the vascularization of 3D-NPCs. MSCs are in

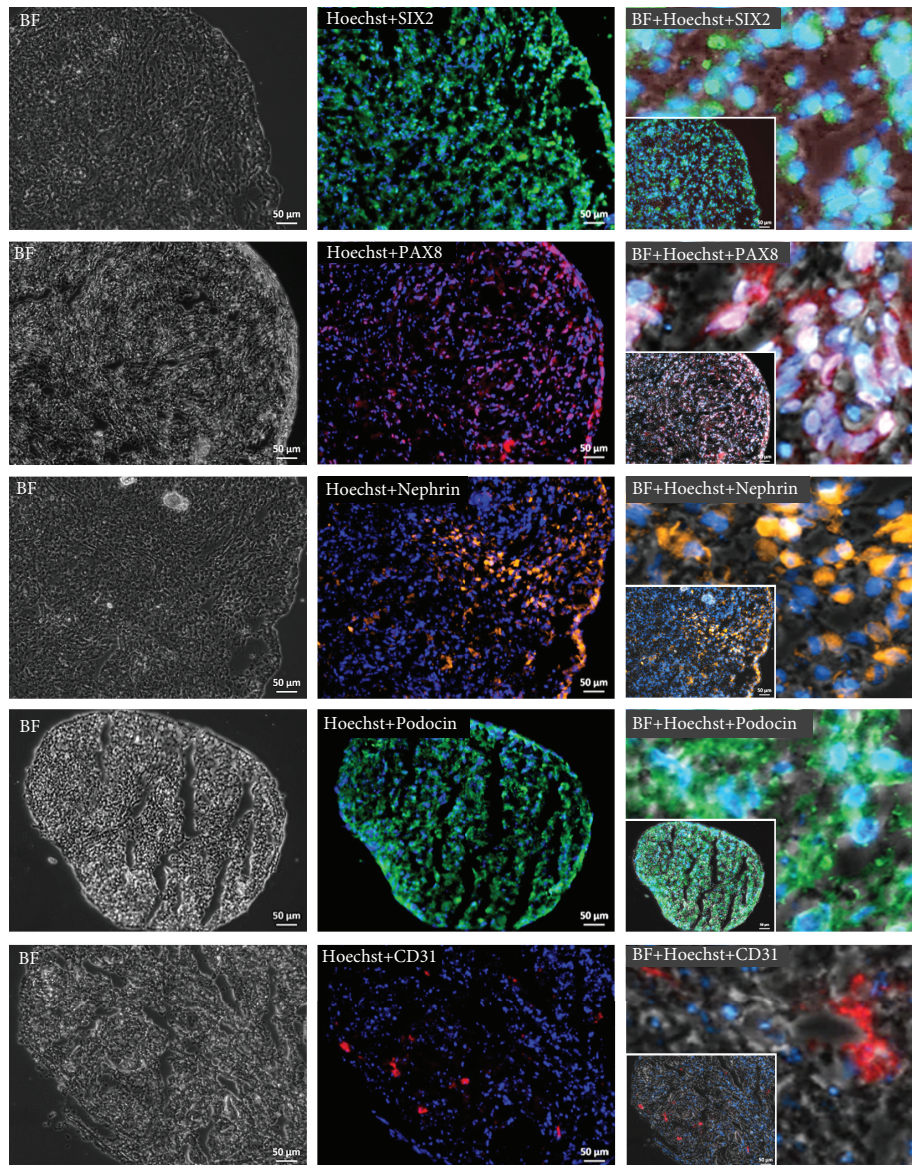
particular known to secrete a variety of growth factors and cytokines, some of them with proangiogenic properties such as VEGF-A, interleukin- (IL-) 6, IL-8, HGF, and PDGF [19, 38, 39].

Additionally, the sections were also stained for the expression of the pluripotency-associated proteins TRA-1-81, SSEA4, and NANOG (Figure 6). We chose to analyse NANOG expression because the cytoplasmic variant is known to be expressed in the kidney [40].

3.6. The Generation of 3D Kidney Organoids. The generation of kidney organoids has advanced in recent years. Compared to the 2D approach to cultivate renal tissues, 3D culture systems better mimic the *in vivo* configuration. Most protocols are based on the use of human pluripotent stem cells (ESCs and iPSCs) differentiated via formation of the intermediate mesoderm into renal structures [14, 41]. Alternatively, kidney tissues have been generated with a two-step protocol, starting with the formation of pluripotent stem cell-derived embryoid bodies followed by chemical-induced differentiation to kidney cell lineages including podocytes, cells of proximal and distal tubules, and collecting ducts [42]. In order to capture the complexity of the kidney organ, multicellular kidney spheroids from a coculture of PSCs, MSCs, and HUVECs driven by mesenchymal cell condensation were engineered by Takebe et al. [26] and Takahashi et al. [38]. Upon transplantation into mice, an *in vivo* environment, connection to the donor vasculature and self-organization into functional tissues fulfilling organ functions such as urine production were observed [26]. Moreover, instead of pluripotent stem cells, murine and human primary kidney cells isolated from biopsies have been described for the generation of three-dimensional renal structures *in vitro* [43, 44]. As renal development is completed before birth, isolation of human NPCs however is difficult. Several groups have worked on optimizing this isolation process as well as the *in vitro* cultivation conditions. Methods for the isolation of human NPCs from the human fetal kidney as well as long-term 3D culture of isolated fetal NPCs with retained nephrogenic potential have been described [45, 46]. With a similar nephrogenic potential as primary NPCs, our novel approach for the generation of 3D-NPCs was based on the use of UdRPCs in combination with isogenic UdRPC-iMSCs and UdRPC-iECs. As urine is an excretion product, isolation of UdRPCs is non-invasive, cost-effective, and indefinite [3]. Moreover, they can be isolated from every donor regardless of age, gender, and health condition. Additionally, even though these cells have moderate telomerase activity, they do not form teratomas or tumors [3, 5].

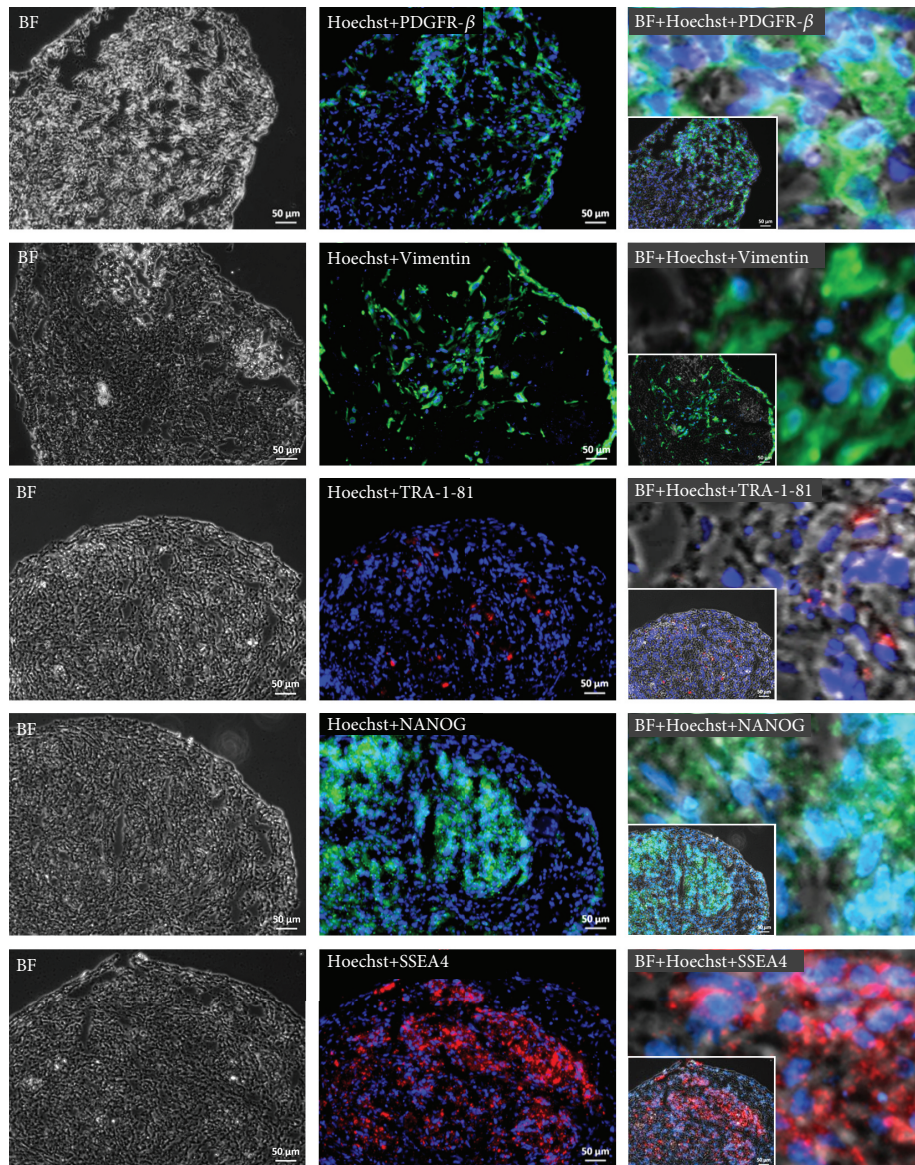
4. Conclusion

Summarizing our study, heterotypic 3D-NPCs were generated by combining UdRPCs, UdRPC-iPSC-derived UdRPC-iMSCs, and UdRPC-iECs originating from the same genetic background, hence isogenic. An immunofluorescence-based analysis demonstrated the expression of the renal progenitor markers (SIX2 and PAX8), the glomerular marker (Nephrin



(a)

FIGURE 6: Continued.



(b)

FIGURE 6: Expression of kidney markers (SIX2, PAX8, Nephritin, and Podocin), endothelial marker (CD31), mesenchymal markers (PDGFR- β and Vimentin), and pluripotency-associated markers (TRA-1-81, NANOG, and SSEA4) in 3D-NPCs. Cell nuclei were stained with Hoechst. Zoom-in pictures show the subcellular localization of the respective proteins. Pictures were taken under 20x magnification. The scale bars represent a length of 50 μ m.

and Podocin), and the endothelial marker (CD31) as well as the mesenchymal markers (Vimentin and PDGFR- β). 3D-NPCs have renal progenitor characteristics and therefore have the potential to generate several cell types of the kidney lineage. As the 3D-NPCs arose from isogenic cell types, inducing the differentiation of renal cell types with subsequent organoid formation could lead to future use in cell replacement therapies, drug screening, and

nephrotoxicity studies as well as kidney-associated disease modelling.

Data Availability

The photo and plot data used to support the findings of this study are included within the article and in the supplementary files.

Conflicts of Interest

The authors declare that there is no conflict of interest regarding the publication of this paper.

Acknowledgments

We thank Martina Bohndorf for technical support and Katharina Raba for technical advice on FACS analyses. Prof. Dr. James Adjaye acknowledges support from the Medical Faculty of the Heinrich-Heine-Universität, Düsseldorf. We thank Prof. Richard Oreffo, Southampton University, UK, for providing the fetal MSCs used in this study.

Supplementary Materials

Immunophenotype of fetal MSCs and native UdRPCs. Expression of MSC cell surface markers CD73, CD90, and CD105 and hematopoietic markers CD14, CD20, CD34, and CD45 was analysed. (A) Fetal MSCs. (B) Native UdRPCs. Histograms of IgG control are displayed in orange, and histograms of MSC markers are displayed in blue ($n = 2$). (Supplementary Materials)

References

- [1] F. Oliveira Arcolino, A. T. Piella, E. Papadimitriou et al., "Human urine as a noninvasive source of kidney cells," *Stem Cells International*, vol. 2015, 7 pages, 2015.
- [2] T. Takebe, R. R. Zhang, H. Koike et al., "Vascularized and functional human liver from an iPSC-derived organ bud transplant," *Nature*, vol. 499, no. 7459, pp. 481–484, 2013.
- [3] G. Liu, Y. Zhang, and C. Deng, "Urine-derived stem cells: biological characterization and potential clinical applications," in *Stem Cells: Current Challenges and New Directions*, Stem Cell Biology and Regenerative Medicine, K. Turksen, Ed., pp. 19–28, Humana Press, New York, NY, USA, 2013.
- [4] B. Bussolati and G. Camussi, "Therapeutic use of human renal progenitor cells for kidney regeneration," *Nature Reviews Nephrology*, vol. 11, no. 12, pp. 695–706, 2015.
- [5] D. Zhang, G. Wei, P. Li, X. Zhou, and Y. Zhang, "Urine-derived stem cells: a novel and versatile progenitor source for cell-based therapy and regenerative medicine," *Genes & Diseases*, vol. 1, no. 1, pp. 8–17, 2014.
- [6] A. Kobayashi, M. T. Valerius, J. W. Mugford et al., "Six2 defines and regulates a multipotent self-renewing nephron progenitor population throughout mammalian kidney development," *Cell Stem Cell*, vol. 3, no. 2, pp. 169–181, 2008.
- [7] S. Bartfeld and H. Clevers, "Stem cell-derived organoids and their application for medical research and patient treatment," *Journal of Molecular Medicine*, vol. 95, no. 7, pp. 729–738, 2017.
- [8] A. Fatehullah, S. H. Tan, and N. Barker, "Organoids as an in vitro model of human development and disease," *Nature Cell Biology*, vol. 18, no. 3, pp. 246–254, 2016.
- [9] M. Simunovic and A. Brivanlou, "Embryoids, organoids and gastruloids: new approaches to understanding embryogenesis," *Development*, vol. 144, no. 6, pp. 976–985, 2017.
- [10] M. Eiraku, N. Takata, H. Ishibashi et al., "Self-organizing optic-cup morphogenesis in three-dimensional culture," *Nature*, vol. 472, no. 7341, pp. 51–56, 2011.
- [11] H. Suga, T. Kadoshima, M. Minaguchi et al., "Self-formation of functional adenohypophysis in three-dimensional culture," *Nature*, vol. 480, no. 7375, pp. 57–62, 2011.
- [12] T. Sato and H. Clevers, "Growing self-organizing mini-guts from a single intestinal stem cell: mechanism and applications," *Science*, vol. 340, no. 6137, pp. 1190–1194, 2013.
- [13] M. A. Lancaster and J. A. Knoblich, "Organogenesis in a dish: modeling development and disease using organoid technologies," *Science*, vol. 345, no. 6194, article 1247125, 2014.
- [14] M. Takasato, P. X. Er, H. S. Chiu, and M. H. Little, "Generation of kidney organoids from human pluripotent stem cells," *Nature Protocols*, vol. 11, no. 9, pp. 1681–1692, 2016.
- [15] T. Takebe, R. R. Zhang, H. Koike et al., "Generation of a vascularized and functional human liver from an iPSC-derived organ bud transplant," *Nature Protocols*, vol. 9, no. 2, pp. 396–409, 2014.
- [16] T. Zhou, C. Benda, S. Duzinger et al., "Generation of human induced pluripotent stem cells from urine samples," *Nature Protocols*, vol. 7, no. 12, pp. 2080–2089, 2012.
- [17] M. Bohndorf, A. Ncube, L.-S. Spitzhorn, J. Enczmann, W. Wruck, and J. Adjaye, "Derivation and characterization of integration-free iPSC line ISRM-UM51 derived from SIX2-positive renal cells isolated from urine of an African male expressing the CYP2D6 *4/*17 variant which confers intermediate drug metabolizing activity," *Stem Cell Research*, vol. 25, pp. 18–21, 2017.
- [18] J. Zhang, M. P. Schwartz, Z. Hou et al., "A genome-wide analysis of human pluripotent stem cell-derived endothelial cells in 2D or 3D culture," *Stem Cell Reports*, vol. 8, no. 4, pp. 907–918, 2017.
- [19] L.-S. Spitzhorn, C. Kordes, M. Megges et al., "Transplanted human pluripotent stem cell-derived mesenchymal stem cells support liver regeneration in Gunn rats," *Stem Cells and Development*, vol. 27, no. 24, pp. 1702–1714, 2018.
- [20] Y. S. Chen, R. A. Pelekanos, R. L. Ellis, R. Horne, E. J. Wolvetang, and N. M. Fisk, "Small molecule mesengenic induction of human induced pluripotent stem cells to generate mesenchymal stem/stromal cells," *Stem Cells Translational Medicine*, vol. 1, no. 2, pp. 83–95, 2012.
- [21] S.-H. Mirmalek-Sani, R. S. Tare, S. M. Morgan et al., "Characterization and multipotentiality of human fetal femur-derived cells: implications for skeletal tissue regeneration," *Stem Cells*, vol. 24, no. 4, pp. 1042–1053, 2009.
- [22] M. Dominici, K. Le Blanc, I. Mueller et al., "Minimal criteria for defining multipotent mesenchymal stromal cells. The International Society for Cellular Therapy position statement," *Cytotherapy*, vol. 8, no. 4, pp. 315–317, 2006.
- [23] R. Hass, C. Kasper, S. Böhm, and R. Jacobs, "Different populations and sources of human mesenchymal stem cells (MSC): a comparison of adult and neonatal tissue-derived MSC," *Cell Communication and Signaling*, vol. 9, no. 1, p. 12, 2011.
- [24] S. Bharadwaj, G. Liu, Y. Shi et al., "Multipotential differentiation of human urine-derived stem cells: potential for therapeutic applications in urology," *Stem Cells*, vol. 31, no. 9, pp. 1840–1856, 2013.
- [25] R. Lang, G. Liu, Y. Shi et al., "Self-renewal and differentiation capacity of urine-derived stem cells after urine preservation for 24 hours," *PLoS One*, vol. 8, no. 1, article e53980, 2013.
- [26] T. Takebe, M. Enomura, E. Yoshizawa et al., "Vascularized and complex organ buds from diverse tissues via mesenchymal

- cell-driven condensation," *Cell Stem Cell*, vol. 16, no. 5, pp. 556–565, 2015.
- [27] N. O. Lindström, G. De Sena, T. Tran et al., "Progressive recruitment of mesenchymal progenitors reveals a time-dependent process of cell fate acquisition in mouse and human nephrogenesis," *Developmental Cell*, vol. 45, no. 5, pp. 651–660.e4, 2018.
- [28] F. Tögel, Z. Hu, K. Weiss, J. Isaac, C. Lange, and C. Westenfelder, "Administered mesenchymal stem cells protect against ischemic acute renal failure through differentiation-independent mechanisms," *American Journal of Physiology Renal Physiology*, vol. 289, no. 1, pp. F31–F42, 2005.
- [29] M. Self, O. V. Lagutin, B. Bowling et al., "Six2 is required for suppression of nephrogenesis and progenitor renewal in the developing kidney," *The EMBO Journal*, vol. 25, no. 21, pp. 5214–5228, 2006.
- [30] M. H. Little and A. P. McMahon, "Mammalian kidney development: principles, progress, and projections," *Cold Spring Harbor Perspectives in Biology*, vol. 4, no. 5, article a008300, 2012.
- [31] M. L. Barr, L. B. Jilaveanu, R. L. Camp, A. J. Adeniran, H. M. Kluger, and B. Shuch, "PAX-8 expression in renal tumours and distant sites: a useful marker of primary and metastatic renal cell carcinoma?," *Journal of Clinical Pathology*, vol. 68, no. 1, pp. 12–17, 2015.
- [32] M. Narlis, D. Grote, Y. Gaitan, S. K. Boualia, and M. Bouchard, "Pax2 and Pax8 regulate branching morphogenesis and nephron differentiation in the developing kidney," *Journal of the American Society of Nephrology*, vol. 18, no. 4, pp. 1121–1129, 2007.
- [33] M. Ristola and S. Lehtonen, "Functions of the podocyte proteins nephrin and Neph3 and the transcriptional regulation of their genes," *Clinical Science*, vol. 126, no. 5, pp. 315–328, 2014.
- [34] T. J. Rabelink, H. J. L. Heerspink, and D. Zeeuw, "Chapter 9 - the pathophysiology of proteinuria," in *Chronic Renal Disease*, P. L. K. M. Rosenberg, Ed., pp. 92–105, Academic Press, 2015.
- [35] S. Weber, "Chapter 13 - hereditary nephrotic syndrome," in *Comprehensive Pediatric Nephrology*, D. F. Geary and F. B. T.-C. P. N. Schaefer, Eds., pp. 219–228, Mosby, 2008.
- [36] J. K. C. Chuah and D. Zink, "Stem cell-derived kidney cells and organoids: recent breakthroughs and emerging applications," *Biotechnology Advances*, vol. 35, no. 2, pp. 150–167, 2017.
- [37] C.-Y. Liu, H.-H. Lin, M.-J. Tang, and Y.-K. Wang, "Vimentin contributes to epithelial-mesenchymal transition cancer cell mechanics by mediating cytoskeletal organization and focal adhesion maturation," *Oncotarget*, vol. 6, no. 18, pp. 15966–15983, 2015.
- [38] Y. Takahashi, K. Sekine, T. Kin, T. Takebe, and H. Taniguchi, "Self-condensation culture enables vascularization of tissue fragments for efficient therapeutic transplantation," *Cell Reports*, vol. 23, no. 6, pp. 1620–1629, 2018.
- [39] M. S. Rahman, L.-S. Spitzhorn, W. Wruck et al., "The presence of human mesenchymal stem cells of renal origin in amniotic fluid increases with gestational time," *Stem Cell Research & Therapy*, vol. 9, no. 1, p. 113, 2018.
- [40] S. Das, S. Jena, and D. N. Levasseur, "Alternative splicing produces Nanog protein variants with different capacities for self-renewal and pluripotency in embryonic stem cells," *Journal of Biological Chemistry*, vol. 286, no. 49, pp. 42690–42703, 2011.
- [41] M. Takasato, P. X. Er, M. Becroft et al., "Directing human embryonic stem cell differentiation towards a renal lineage generates a self-organizing kidney," *Nature Cell Biology*, vol. 16, no. 1, pp. 118–126, 2014.
- [42] A. Przepiorski, V. Sander, T. Tran et al., "A simple bioreactor-based method to generate kidney organoids from pluripotent stem cells," *Stem Cell Reports*, vol. 11, no. 2, pp. 470–484, 2018.
- [43] A. Joraku, K. A. Stern, A. Atala, and J. J. Yoo, "In vitro generation of three-dimensional renal structures," *Methods*, vol. 47, no. 2, pp. 129–133, 2009.
- [44] N. K. Guimaraes-Souza, L. M. Yamaleyeva, T. AbouShwareb, A. Atala, and J. J. Yoo, "In vitro reconstitution of human kidney structures for renal cell therapy," *Nephrology Dialysis Transplantation*, vol. 27, no. 8, pp. 3082–3090, 2012.
- [45] S. Da Sacco, M. E. Thornton, A. Petrosyan et al., "Direct isolation and characterization of human nephron progenitors," *Stem Cells Translational Medicine*, vol. 6, no. 2, pp. 419–433, 2016.
- [46] Z. Li, T. Araoka, J. Wu et al., "3D culture supports long-term expansion of mouse and human nephrogenic progenitors," *Cell Stem Cell*, vol. 19, no. 4, pp. 516–529, 2016.

2.9 Human iPSC-derived MSCs (iMSCs) from aged individuals acquire a rejuvenation signature

Lucas-Sebastian Spitzhorn*, Matthias Megges*, Wasco Wruck, Md Shaifur Rahman, Jörg Otte, Özer Degistirici, Roland Meisel, Richard O.C. Oreffo and James Adjaye

*These authors contributed equally to this work.

Abstract

Background: Primary mesenchymal stem cells (MSCs) are fraught with ageing-related shortfalls. Human induced pluripotent stem cells (iPSCs) - derived MSCs (iMSCs) have been shown to be a useful clinically relevant source of MSCs that circumvent these ageing-associated drawbacks. To date, the extent of the retention of ageing-hallmarks in iMSCs differentiated from iPSCs derived from elderly donors remains unclear.

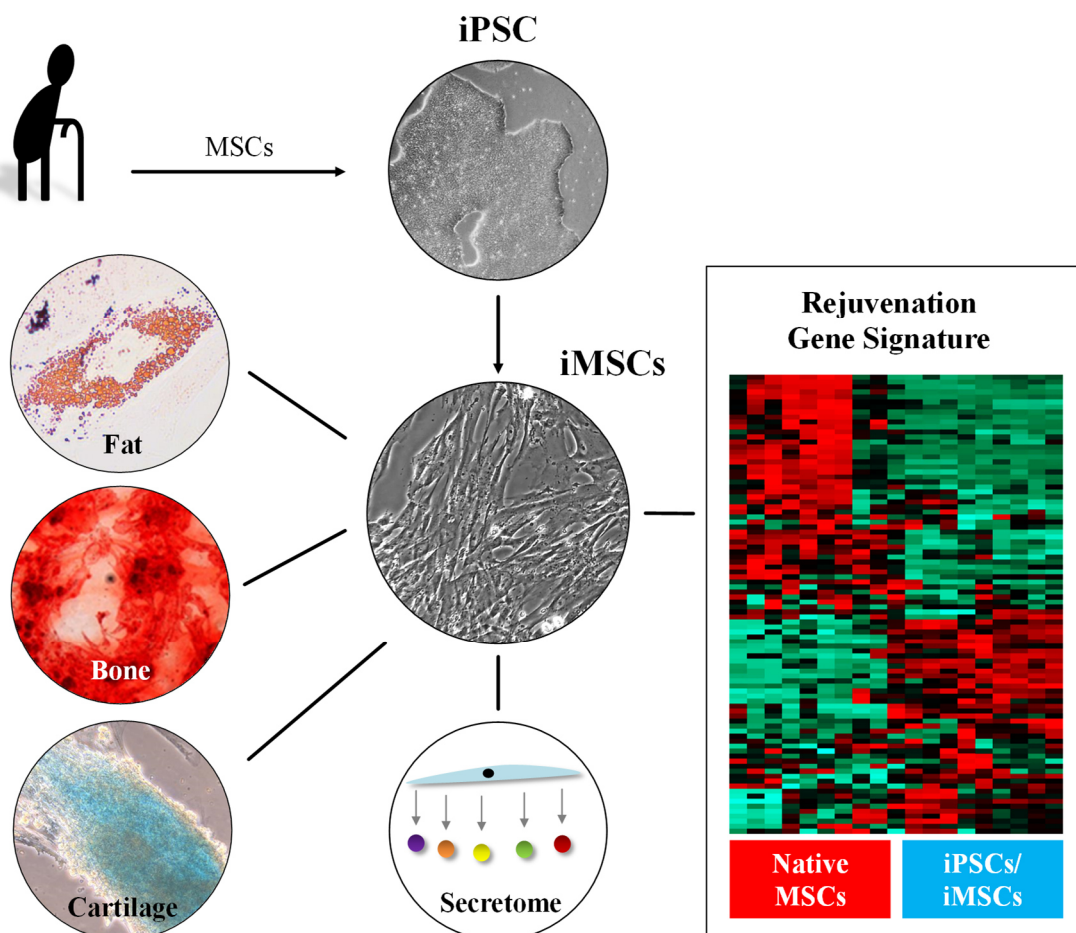
Methods: Fetal femur-derived MSCs (fMSCs) and adult bone-marrow MSCs (aMSCs) were isolated, corresponding iPSCs were generated, and iMSC were differentiated from fMSC-iPSCs, aMSC-iPSCs and from human embryonic stem cells (ESCs) H1. In addition, typical MSC characterization such as cell surface marker expression, differentiation capacity, secretome profile and transcriptome analysis were conducted for the three distinct iMSC preparations- fMSC-iMSCs, aMSC-iMSCs and ESC-iMSCs. To verify these results, previously published data sets were used as well as additional aMSCs and iMSCs were analysed.

Results: fMSCs and aMSCs both express the typical MSC cell surface markers, and can be differentiated into osteogenic, adipogenic and chondrogenic lineages *in vitro*. However, the transcriptome analysis revealed overlapping and distinct gene expression patterns and showed that fMSCs express more genes in common with ESCs than with aMSCs. fMSC-iMSCs, aMSC-iMSCs and ESC-iMSCs met the criteria set out for MSCs. Dendrogram analyses confirmed that the transcriptomes of all iMSCs clustered together with the parental MSCs and separated from the MSC-iPSCs and ESCs. iMSCs irrespective of donor age and cell type acquired a rejuvenation-associated gene signature, specifically, the expression of *INHBE*, *DNMT3B*, *POU5F1P1*, *CDKN1C*, *GCNT2* which are also expressed in pluripotent stem cells (iPSCs and ESC) but not in the parental aMSCs. iMSCs expressed more genes in common with fMSCs than with aMSCs.

Independent real-time PCR comparing aMSCs, fMSCs and iMSCs confirmed the differential expression of the rejuvenation (*COX7A*, *EZA2*, *TMEM119*) and ageing (*CXADR*, *IGSF3*) signatures. Importantly, in terms of regenerative medicine, iMSCs acquired a secretome (e.g. Agiogenin, DKK-1, IL-8, PDGF-AA, Osteopontin, SERPINE1 and VEGF) similar to that of fMSCs, thus highlighting their ability to act via paracrine signaling.

Conclusions: iMSCs irrespective of donor age and cell source acquire a rejuvenation gene signature. The iMSC concept could allow circumventing the drawbacks associated with the use of adult MSCs and thus provide a promising tool for use in various clinical settings in the future.

Graphical Abstract



Publication Status: published in *Stem Cell Research & Therapy*. 2019 Mar 18;10(1):100.

Impact Factor: 4.963

This article is reproduced with permission.

Approximated total share of contribution: 30%

Contribution on experimental design, realization and publication:

JA, RO, MM and LSS conceived the idea and designed the experiments. MM and LSS performed the characterization of primary MSCs, generation/ characterization of iPSCs/ iMSCs. MM, LSS, and MSR analyzed the results and wrote the draft manuscript. OD and RM provided RNA from MSCs of an aged individual (56 years) and JO performed the real time PCR analysis. WW did the Bioinformatical analysis. RVS provided aged MSCs for the cytokine array. JA edited and finally approved the manuscript. All authors reviewed and approved the submitted version.

Link to the publication:

<https://stemcellres.biomedcentral.com/articles/10.1186/s13287-019-1209-x>

RESEARCH

Open Access

Human iPSC-derived MSCs (iMSCs) from aged individuals acquire a rejuvenation signature



Lucas-Sebastian Spitzhorn^{1†}, Matthias Megges^{1†}, Wasco Wruck¹, Md Shaifur Rahman¹, Jörg Otte¹, Özer Degistirici², Roland Meisel², Rüdiger Volker Sorg³, Richard O. C. Oreffo⁴ and James Adjaye^{1*}

Abstract

Background: Primary mesenchymal stem cells (MSCs) are fraught with aging-related shortfalls. Human-induced pluripotent stem cell (iPSC)-derived MSCs (iMSCs) have been shown to be a useful clinically relevant source of MSCs that circumvent these aging-associated drawbacks. To date, the extent of the retention of aging-hallmarks in iMSCs differentiated from iPSCs derived from elderly donors remains unclear.

Methods: Fetal femur-derived MSCs (fMSCs) and adult bone marrow MSCs (aMSCs) were isolated, corresponding iPSCs were generated, and iMSCs were differentiated from fMSC-iPSCs, from aMSC-iPSCs, and from human embryonic stem cells (ESCs) H1. In addition, typical MSC characterization such as cell surface marker expression, differentiation capacity, secretome profile, and transcriptome analysis were conducted for the three distinct iMSC preparations—fMSC-iMSCs, aMSC-iMSCs, and ESC-iMSCs. To verify these results, previously published data sets were used, and also, additional aMSCs and iMSCs were analyzed.

Results: fMSCs and aMSCs both express the typical MSC cell surface markers and can be differentiated into osteogenic, adipogenic, and chondrogenic lineages in vitro. However, the transcriptome analysis revealed overlapping and distinct gene expression patterns and showed that fMSCs express more genes in common with ESCs than with aMSCs. fMSC-iMSCs, aMSC-iMSCs, and ESC-iMSCs met the criteria set out for MSCs. Dendrogram analyses confirmed that the transcriptomes of all iMSCs clustered together with the parental MSCs and separated from the MSC-iPSCs and ESCs. iMSCs irrespective of donor age and cell type acquired a rejuvenation-associated gene signature, specifically, the expression of *INHBE*, *DNMT3B*, *POU5F1P1*, *CDKN1C*, and *GCNT2* which are also expressed in pluripotent stem cells (iPSCs and ESC) but not in the parental aMSCs. iMSCs expressed more genes in common with fMSCs than with aMSCs. Independent real-time PCR comparing aMSCs, fMSCs, and iMSCs confirmed the differential expression of the rejuvenation (*COX7A*, *EZA2*, and *TMEM119*) and aging (*CXADR* and *IGSF3*) signatures. Importantly, in terms of regenerative medicine, iMSCs acquired a secretome (e.g., angiogenin, DKK-1, IL-8, PDGF-AA, osteopontin, SERPINE1, and VEGF) similar to that of fMSCs and aMSCs, thus highlighting their ability to act via paracrine signaling.

Conclusions: iMSCs irrespective of donor age and cell source acquire a rejuvenation gene signature. The iMSC concept could allow circumventing the drawbacks associated with the use of adult MSCs and thus provide a promising tool for use in various clinical settings in the future.

Keywords: Aged MSC, Fetal MSCs, iPSCs, iMSCs, Transcriptome, Secretome, Rejuvenation, Aging

* Correspondence: james.adjaye@med.uni-duesseldorf.de

[†]Lucas-Sebastian Spitzhorn and Matthias Megges contributed equally to this work.

¹Institute for Stem Cell Research and Regenerative Medicine, Medical Faculty, Heinrich Heine University, Düsseldorf, Moorenstr. 5, 40225 Düsseldorf, Germany

Full list of author information is available at the end of the article



Background

Primary human bone marrow-derived stem cells (MSCs) contain a sub-population of multipotent stem cells which retain osteogenic, chondrogenic, and adipogenic differentiation potential [1, 2]. Apart from the adult sources, these multipotent MSCs have been isolated from fetal femur [3]. Due to highly proliferative, immune-modulatory properties, and paracrine orchestration, MSCs offer significant therapeutic potential for an increasing aging demographic [4].

Although the bone marrow can be collected routinely to isolate MSCs, there are several drawbacks associated with the use of MSCs from aged individuals. Aging involves enhanced cellular senescence, instability of the genome, accumulation of DNA damage, changes in DNA repair pathways, oxidative stress, metabolic instability, and activated immune response [5–8]. In line with this, the expansion possibilities and application potential of primary MSCs are limited, in part, by changes in the differentiation/response potential and function of MSCs isolated from aged donors [9–11]. However, to date, it remains unclear whether there are any age-related differences in transcriptome and secretome signatures between human fetal MSCs and MSCs from elderly donors.

Recent studies have shown that the shortfalls associated with primary MSCs can be circumvented by reprogramming them to induced pluripotent stem cells (iPSCs) [12–14]. iPSCs have the potential to self-renew, bypass senescence and are similar to human embryonic stem cells (ESCs). However, the parental somatic aging signature and secretome properties and subsequent reflection in iPSC derivatives are unknown [15–17]. An iPSC-derived cell type that is of prime interest for circumventing shortfalls associated with primary MSCs are MSCs differentiated from iPSCs and ESCs (iMSCs). The similarity of iMSCs to primary MSCs and their regenerative potential *in vivo* has already been demonstrated [18, 19]. Moreover, the reflection of donor age in iMSCs was shown to be reverted into a younger state and at the same time reflected in iMSCs from patients with early onset aging syndromes [13, 20]. Although the paracrine effects of iMSCs have been indicated [21], relatively little is known about the potential to rejuvenate the paracrine features of MSCs from elderly patients via iMSC generation.

In view of this, there is a dire need to clarify in more detail whether age-related features inherent to primary MSCs isolated from elderly patients are retained in the corresponding iMSCs at the transcriptional, secretome, and functional level. In this study, we report the age-associated differences between fetal MSC (fMSC) populations and MSCs isolated from elderly donors with respect to their transcriptomes. We successfully reprogrammed fMSCs (55 days post conception) and adult

MSC (aMSC; 60–74 years) to iPSCs and, subsequently, generated the corresponding iMSCs. In addition, iMSCs were also derived from ESCs. The iMSCs were similar although not identical to primary MSCs. We unraveled a putative rejuvenation and aging gene expression signature. We show that iMSCs irrespective of donor age and cell type re-acquired a similar secretome to that of their parental MSCs, thus re-enforcing their capabilities of context-dependent paracrine signaling relevant for tissue regeneration.

Methods

MSC preparations used in this study

Fetal femur-derived MSCs were obtained at 55 days post-conception as previously described [3] following informed, written patient consent. Approval was obtained by the Southampton and South West Hampshire Local Research Ethics Committee (LREC 296100). Mesenchymal stem cells, used for generation of iPSCs and iMSCs, were isolated from the bone marrow of a 74-year-old female donor as described before [22] after written informed consent. The corresponding protocol was approved by the research ethics board of the Charite-Universitätsmedizin, Berlin (IRB approval EA2/126/07). Aged MSCs (60 years, 62 years, and 70 years) were isolated as previously described [23]. Isolation of mesenchymal stem cells from 60 to 70-year-old individuals was approved under the Southampton and South West Hampshire Local Research Ethics Committee (LREC 194/99). Three primary fetal MSC preparations, fMSC1, fMSC2, and fMSC3, derived from different donors, were compared to MSCs isolated from elderly donors between 60 and 74 years of age; aMSC1, aMSC2, aMSC3, and aMSC4 (Additional file 1: Table S1). For meta-analyses, we included published transcriptome datasets of adult human MSCs which are referred to as MSC1, MSC2, and MSC3 [24] and adult MSCs from donors aged 29, 48, 60, and 76 years are referred to as MSC4, MSC5, MSC6, and MSC7 [25]. For the purpose of comparing the secretomes of iMSCs, fMSCs, and aMSCs, three additional MSC preparations from donors aged 62, 64, and 69 years were used, which had been generated and characterized (data not shown) at the Institute for Transplantation Diagnostics and Cell Therapeutics at Heinrich Heine University Hospital, Düsseldorf with patient consent and approval of the Ethics commission of the medical faculty Heinrich Heine University (Study number: 5013).

Cell culture

The culture of MSCs and iMSCs was carried out in α MEM, nucleosides, GlutaMAX with addition of 10% fetal bovine serum (Biochrom AG, Germany), penicillin/streptomycin, and nonessential amino acids (all from

Life Technologies, California, USA). MSCs and iMSCs were expanded with a seeding density of 1000 cells per cm^2 . iMSCs were cultured in the same conditions starting from passage four [22].

Pluripotent stem cells (iPSCs and ESCs H1 and H9 (#WA01 and #WA09, respectively)) were cultured in unconditioned medium. The medium contained KO-DMEM, supplementation of 20% serum replacement, sodium pyruvate, nonessential amino acids, L-glutamine, penicillin/streptomycin, and 0.1mM β -mercaptoethanol (all from Life Technologies). Supplementation with basic fibroblast growth factor (bFGF) (Preprotech, USA) to a final concentration of 8 ng/ml was carried out before media change every day. Passaging of pluripotent stem cells was carried out with a splitting ratio of 1:3 to 1:10. Passaging was conducted manually using a syringe needle and a pipette under a binocular microscope or using a cell scraper and PBS (-). Mitomycin-C inactivated mouse embryonic fibroblasts were used as feeder cells seeded on cell culture dishes coated with Matrigel (BD) to culture iPSCs and ESCs. MSC culture was carried out at 37 °C and 5% CO_2 in a humidified atmosphere. Pluripotent stem cell culture was carried out under the same condition with additional hypoxic conditions in 5% O_2 [26].

In vitro differentiation of parental MSCs and iMSCs

Adipocyte differentiation was carried out using the StemPro Adipogenesis Differentiation Kit (Life technologies, USA). The MSCs were seeded at an initial density of 1×10^4 cells per cm^2 and induced to the adipogenic fate with differentiation medium and cultured for 21 days. Lipid filled vacuoles were visualized with Oil red O after adipogenic induction. Osteoblast differentiation was performed with the StemPro Osteogenesis Differentiation Kit (Life Technologies). Calcified matrix was visualized with Alizarin Red after osteogenic induction. The MSCs were seeded at a density of 5×10^3 cells per cm^2 in osteogenic induction media and cultured for 21 days. Chondrocyte differentiation was carried out using StemPro Chondrogenesis Differentiation Kit (Life Technologies). Acidic mucosubstances were visualized by Alcian Blue staining after chondrogenic induction.

Derivation of iPSCs from MSCs

fMSC-iPSC1, fMSC-iPSC2, and aMSC-iPSC1 were generated as previously described [22, 26]. Retroviral pluripotency induction in fetal femur-derived MSCs was carried out using pMX vector-based expression of *OCT4*, *SOX2*, *KLF4*, and *c-MYC*. Retrovirus generation was carried out in Phoenix cells using FuGENE HD Transfection Reagent (PROMEGA). Two hundred thousand MSCs were transduced. After transduction, MSCs were seeded onto Matrigel-coated cell culture plates

with feeder cells (inactivated MEFs) at a density of 4000 cells per cm^2 for pluripotency induction. To reprogram them, the transduced MSCs were cultured in N2B27-based medium with additions of 20% serum replacement, sodium pyruvate, nonessential amino acids, L-glutamine, penicillin/streptomycin, and 0.1mM β -mercaptoethanol (all from Life Technologies, USA) and bFGF (Preprotech, USA). After 14 days, the media was switched to mTeSR1 (Stem Cell Technologies, USA) as previously described [27]. The cells were cultured until ESC-like colonies became visible. The colonies were isolated manually and expanded for characterization. The resulting iPSCs were termed fMSC-iPSC3.

So termed, aMSC-iPSC2, were generated by using episomal plasmid-based reprogramming using the previously described combination of episomal plasmids 7F-2 [27]. The plasmids were delivered to aMSCs (62 years) by nucleofection using the Human MSC (Mesenchymal Stem Cell) Nucleofector Kit (Lonza, VPE-1001) and the Amaxa Nucleofector II (Lonza) following the manufacturer's instructions. aMSCs were cultured until passage two and the combination of 3 μg of pEP4 EO2S EN2K, 3.2 μg of pEP4 EO2S ET2K, and 2.4 μg of pCEP4-M2L was mixed with the 1×10^6 MSCs and nucleofected using the program U-23. Nucleofected aMSCs were expanded in MSC medium for 6 days and replated with a density of 6×10^4 cells per well of a six-well plate onto Matrigel and feeder cell-coated culture vessels. Further culture was carried out in N2B27-based medium as already described. Fifty micrograms per milliliter of L-ascorbic acid (Sigma-Aldrich) was added to the medium [28] with a media change every other day. After 14 days, the media was switched to mTeSR1 (Stem Cell Technologies) as previously described [27]. Further culture was carried out until ESC-like colonies could be isolated. ESC-like cell colonies were isolated manually with a syringe needle and pipette under a stereo microscope.

The isolated colonies were seeded onto freshly prepared feeder cell-coated plates as described previously [29, 30]. The characterization of the iPSC clones was initiated after six passages. The isolated iPSC colonies were characterized as previously described [22]. The pluripotency of iPSCs generated from MSCs was tested in a similar fashion as previously described for the tool PluriTest (<http://www.pluritest.org>) [31] by cluster analysis within the R statistical programming environment [32] using function *hclust* to show similarity with embryonal stem cells within a dendrogram.

Embryoid body-based in vitro differentiation

iPSCs were seeded into low attachment culture dishes (Corning) and cultured in DMEM with additional 10% fetal bovine serum (Biochrom AG), sodium pyruvate,

L-glutamine, nonessential amino acids, and penicillin/streptomycin (all from Life Technologies) without bFGF for the generation of embryoid bodies (EBs). EBs were transferred onto gelatin-coated culture dishes after 10 days and cultured further for 10 days using the same conditions. Next, the cells were fixed in 4% paraformaldehyde (PFA) and stained using immunofluorescence-based detection of germ layer-specific markers.

Generation of iMSCs

iMSCs were generated from iPSCs and ESC line H1 as previously described [18]. In brief, iPSCs and ESCs were cultured without feeder cells on Matrigel. When confluency was reached, the medium was switched to unconditioned medium without bFGF supplementation or α MEM and with addition of 10 μ M SB-431542 (Sigma-Aldrich) with a media change every day for 10 days. Next, the cells were trypsinized and seeded at a density of 4×10^4 cells per cm^2 onto uncoated culture dishes in MSC expansion medium. Subsequently, the cells were passaged and reseeded at a density of 2×10^4 cells per cm^2 under the same culture conditions. Finally, the cells were passaged and seeded at a density of 1×10^4 cells per cm^2 . The seeding density was maintained in every further passage.

Flow cytometry

The surface marker expression of MSCs and iMSCs was analyzed using MSC Phenotyping Kit (Miltenyi). The cells were trypsinized, washed with PBS and stained with labeled antibodies as well as analyzed according to the manufacturer's instructions. For the analysis of the stained cells, fluorescence-activated cell sorting (FACS) caliber (BD) flow cytometer was used, the program CellQuestPro for data acquisition, and the softwares Cyflogic (<http://www.cyflogic.com>) and Microsoft Excel for data analysis.

Quantitative real-time polymerase chain reaction

The Power SYBR Green Master Mix (Life technologies) was used for quantitative real-time PCR analysis. Three hundred eighty-four-well format plates were used, and the reaction mixture had final volume of 10 μ l as recommended in the manufacturer's protocol. An amount of 10 ng of cDNA was used for each reaction. The experiments were done in technical replicates. The ViiA7 (Life technologies) system was used to run the PCR with these conditions: 95°C for 10 min; 35 cycles of 95°C, 60°C, and 72°C with 30 s each step. Melting curves were generated after all cycles were completed. The $^{-\Delta\Delta\text{Ct}}$ method was used to calculate relative gene expression levels using the CT mean values as an input. Normalization was done based on the housekeeping gene RPL37A. Table S2 shows primer sequences.

Immunofluorescence staining

Immunofluorescence staining was used to detect pluripotency markers in iPSCs and to detect expression of germ layer-specific marker in cells differentiated from iPSCs in an embryonic body-based in vitro pluripotency test. The cells were fixed at room temperature with 4% PFA for 20 min. Subsequently, the cells were washed three times in PBS and incubated in 1% Triton X-100 in PBS for 10 min at room temperature. Next, the cells were incubated in blocking solution: 10% FCS (Vector) and 0.1% Triton X-100 (Sigma-Aldrich) in PBS for 1 h. Then, the cells were incubated with the primary antibody at 4°C in blocking solution overnight followed by three washes with PBS. Next, the cells were incubated with the secondary antibody at room temperature for 1 h followed by three more washes with PBS and a final incubation with DAPI (200 ng/ml, Invitrogen) in PBS for 20 min at room temperature. This was followed by image acquisition using a confocal microscope LSM510 (Carl Zeiss). A list of the used antibodies is provided in the supplement (Additional file 1: Table S3).

Gene expression analysis

The DNA+RNA+Protein Extraction Kit (Roboklon) was used to extract total RNA. The linear amplification kit (Ambion) was used to produce biotin-labeled cRNA form 500 ng of total RNA per sample. The samples were further processed using the Illumina BeadStation 500 platform (Illumina) following the manufacturer's protocol for hybridization and Cy3-streptavidin staining. HumanHT-12 v3.0 Gene Expression Bead Chips (Illumina) were used to hybridize the samples. Bead-level data was summarized to bead-summary data using the Gene Expression Module of the software GenomeStudio (Illumina) without normalization and background correction. Bead-summary data was imported into the R/Bioconductor [33] environment where it was background-corrected and normalized with quantile normalization from the package *lumi* [34]. The R_builtin function *cor* was used to compute the Pearson correlation values between the transcriptomes detected by microarray. Significant gene expression was calculated by determining the detection *p* value based on the difference to negative control beads. A gene with a detection *p* value ≤ 0.05 was considered to be expressed. Venn diagrams and heatmaps were generated employing the R/Bioconductor packages *VennDiagram* [35] and *gplots* [36]. Lists of human gene sets annotated to the Gene Ontology (GO)-terms cell cycle, senescence, response to oxidative stress, DNA damage repair, and aging were generated using AmiGO 2 version 2.3.1 (<http://amigo2.berkeleybop.org/amigo>) [37] and used to extract GO term-specific gene expression data sets which were analyzed by hierarchical clustering analysis. The data set of

the gene expression analysis will be accessible at the Gene Expression Omnibus (GEO) repository under the accession number GSE97311 (www.ncbi.nlm.nih.gov/geo/query/acc.cgi?acc=GSE97311).

Determination of differential expression

The linear models for microarrays from the R/Bioconductor *limma* package [38] were used to compute the differential p value to determine the significance of the difference between gene expression values. The computed differential p value was adjusted in R/Bioconductor with the q value false discovery rate (FDR) correction algorithm [39]. Genes with a FDR-corrected differential p value of ≤ 0.05 were considered significantly different. The up- or downregulation of these genes was calculated by determining the ratio of the average signals. A ratio higher than 1.33 was considered as upregulated, and a ratio lower than 0.75 was considered as downregulated.

Determination of the aged and rejuvenation gene signatures

Two gene signatures were determined which are characterizing the aging and rejuvenation processes. The gene signatures were identified based on combinations of gene expression of MSCs in differing age-related stages. The aged gene signature was defined by gene expression in the MSCs but not in the iMSCs and iPSCs, given by the combination of detection p values: $p_{\text{-MSC}} < 0.001 \wedge p_{\text{-iMSC}} > 0.1 \wedge p_{\text{-iPSC}} > 0.1$. The rejuvenation gene signature was defined by gene expression in the iMSCs and iPSCs but not in the MSCs, given by the combination of detection p values: $p_{\text{-MSC}} > 0.1 \wedge p_{\text{-iMSC}} < 0.001 \wedge p_{\text{-iPSC}} < 0.001$.

Functional annotation of gene sets

Database for Annotation, Visualization and Integrated Discovery (DAVID) Bioinformatics resources 6.7 (<http://david.abcc.ncifcrf.gov>) [40] was used for functional annotation analysis of gene sets. Lists of official gene symbols or Illumina IDs were used as input against human background. The default settings of DAVID Bioinformatics resources 6.7 were used. The option Kyoto Encyclopedia of Genes and Genomes (KEGG) terms was used for the annotation to pathways. The option GO_BP_Direct or GO_BP_Fat was used for annotation to gene ontology terms of biological processes.

Protein association network

Based on the aged and rejuvenation gene signatures, two protein interaction networks were constructed. The interactions are based upon the Biogrid database version 3.4.161 [41] filtered for the taxonomy id 9606 (*Homo sapiens*). From the Biogrid dataset, all protein interactions containing at least one protein coded by the above

mentioned aged and rejuvenation signatures were extracted separately for each signature. Both resulting networks were reduced by adding only the $n = 30$ interacting proteins with the most interactions to proteins coded by genes from the original sets. The R package *network* [42] was employed to visualize these interactions marking proteins from the original sets in green. Communities of related proteins within the networks were detected via an in-betweenness clustering analysis with the method *cluster_edge_betweenness* from the R package *igraph* [43].

Secretome analysis

The cell culture supernatants of three distinct fMSCs, three independent iMSCs, and three distinct aMSCs were collected, and 1.5 ml each was used for subsequent analysis. The Proteome Profiler™ Array Human (XL) Cytokine Array kit (R&D Systems, catalog number ARY022) was carried out according to the user's manual. Two reference spots showing successful performed analysis were located in three positions on the cytokine membrane (in upper left, lower left, and the lower right-corner). Horseradish peroxidase substrate and luminol enhancer solution (GE healthcare UK limited) were used to visualize protein distribution and amount on the membranes. The pictures were taken with Fusion-EX microscope (Fischer Biotec). The pixel density of the spots was measured using ImageJ, the background intensity was subtracted, and the values were finally calculated as percentage of the reference spots intensity. Values above 5% were classified as secreted. Cytokines with values above 20% of the reference were considered abundantly expressed.

Statistical analysis

The comparison of two groups was carried out using a two-tailed unpaired Student's t test. Significant difference was defined with p values ≤ 0.05 . For microarray data analysis, a gene with an expression p value ≤ 0.01 was considered significantly expressed. A gene with a differential p value ≤ 0.01 was considered significantly different in terms of expression. Functional annotation was considered significant with a p value of ≤ 0.05 .

Results

Mesenchymal stem cells of fetal and aged background differ in transcriptome level

Irrespective of donor age, fMSCs and aMSCs showed a typical MSC surface marker profile by expression of CD73, CD90, and CD105 and the absence of the hematopoietic markers CD14, CD20, CD34, and CD45 at the gene expression and protein level (Fig. 1a, b). ESCs H1 which were used as a negative control did not show expression of CD73 and CD105 at the gene

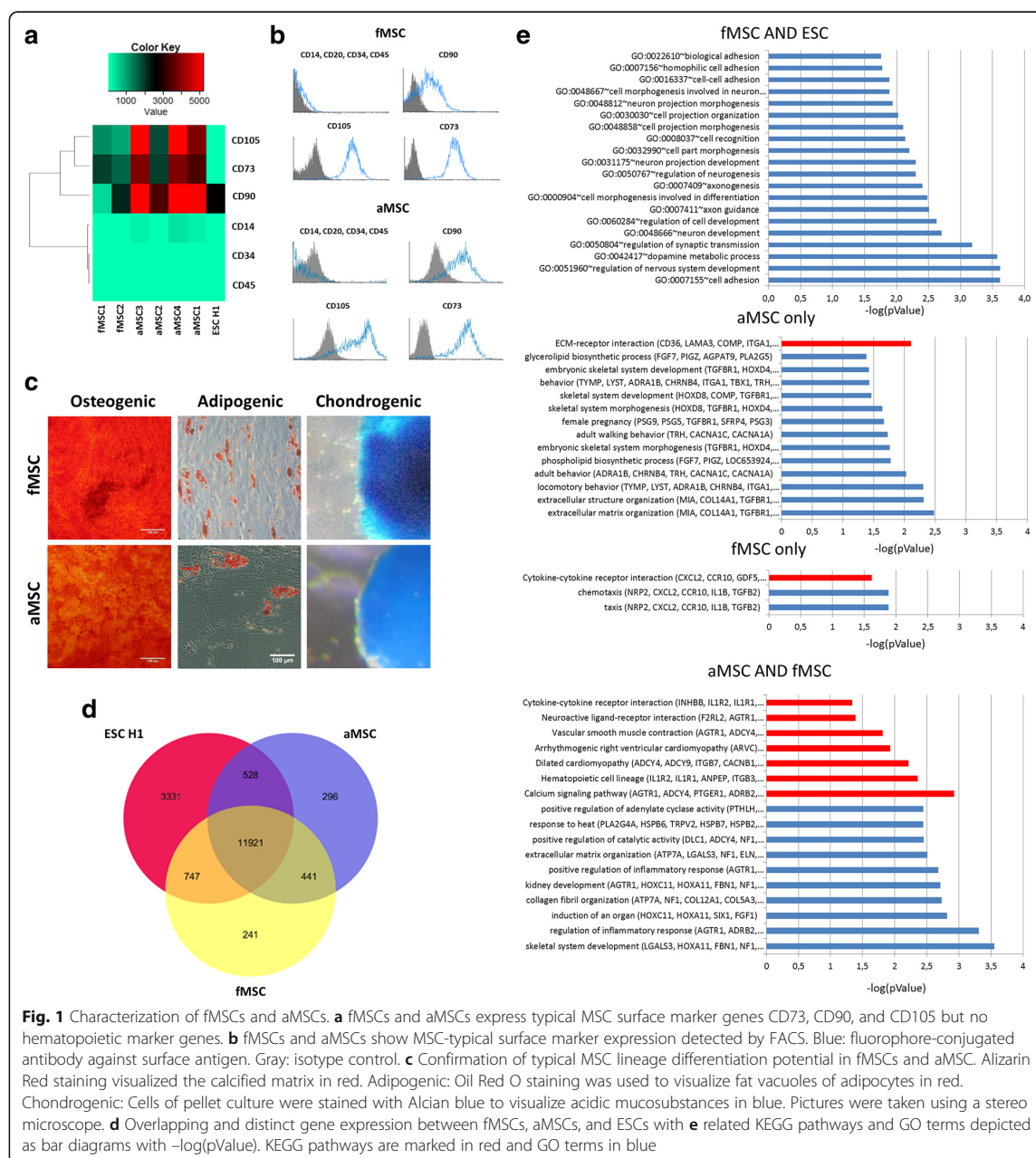


Fig. 1 Characterization of fMSCs and aMSCs. **a** fMSCs and aMSCs express typical MSC surface marker genes CD73, CD90, and CD105 but no hematopoietic marker genes. **b** fMSCs and aMSCs show MSC-typical surface marker expression detected by FACS. Blue: fluorophore-conjugated antibody against surface antigen. Gray: isotype control. **c** Confirmation of typical MSC lineage differentiation potential in fMSCs and aMSC. Alizarin Red staining visualized the calcified matrix in red. Adipogenic: Oil Red O staining was used to visualize fat vacuoles of adipocytes in red. Chondrogenic: Cells of pellet culture were stained with Alcian blue to visualize acidic mucosubstances in blue. Pictures were taken using a stereo microscope. **d** Overlapping and distinct gene expression between fMSCs, aMSCs, and ESCs with **e** related KEGG pathways and GO terms depicted as bar diagrams with $-\log(p\text{Value})$. KEGG pathways are marked in red and GO terms in blue

expression level and had a lower expression of CD90 than the MSCs. Additionally, MSCs of both age groups could be differentiated into osteoblasts, adipocytes, and chondrocytes and stained positive for Alizarin Red S (bone), Oil Red O (fat), and Alcian Blue (cartilage), respectively (Fig. 1c).

Venn diagram-based analysis of the transcriptome data revealed a higher number of genes expressed in common

between fMSCs and ESCs (747 genes) compared to the overlap of aMSCs and ESCs (Fig. 1d). The 747 genes were annotated to GO terms such as cell adhesion with a p value below 0.01. In addition, genes expressed in common between fMSCs and aMSCs (441) were annotated to KEGG pathways such as calcium signaling and GO terms such as skeletal system development with p values below 0.01. Genes exclusively expressed in fMSCs

(241) were annotated to the KEGG pathway cytokine-cytokine receptor interaction with a p value below 0.05, whereas the genes exclusively expressed in aMSCs (296) were annotated to ECM-receptor interaction and extracellular matrix organization with p values below 0.01 (Fig. 1e).

Derivation and characterization of iPSCs from fMSCs and aMSCs

We previously established two iPSC lines from fetal MSCs [26], named fMSC-iPSC1 and fMSC-iPSC2. Additionally, we have described an iPSC line from MSCs of a 74-year-old donor (aMSC-iPSC1) [22]. In the present study, MSCs isolated from a 62-year-old donor were successfully reprogrammed into iPSCs (aMSC-iPSC2) as well as a new iPSC line from fMSCs was created (fMSC-iPSC3).

Transcriptome analysis of the native MSCs, the corresponding iPSCs, and the ESC line H1 revealed two separated clusters. The first cluster included all MSC population irrespective of the donor age which was separated from the second cluster which includes the ESCs and all MSC-iPSCs (Fig. 2a). At the transcriptome level, there was a distinct level of heterogeneity in the results since MSCs and MSC-iPSCs did not show a separation by donor-cell age. All iPSC lines expressed pluripotency-associated markers (Additional file 1: Figure S1) and a transcriptome similar to ESCs (Fig. 2b). Moreover, both fMSC-iPSC3 and aMSC-iPSC2 expressed pluripotency marker at the protein level and formed embryoid bodies and differentiated into cell types representative of the three embryonic germ layers (Additional file 1: Figure S1).

iMSC from MSC-iPSCs of distinct age backgrounds and ESCs have MSC-typical marker expression and differentiation potential

fMSC-iPSC3, aMSC-iPSC2, and ESC line H1 were differentiated into MSCs and named fMSC-iMSCs, aMSC-iMSCs, and ESC-iMSCs. iMSCs displayed spindle-shaped morphologies comparable to primary MSCs (Fig. 3a). In addition, all iMSCs derived from primary MSCs expressed the MSC markers CD73, CD90, and CD105 but not the hematopoietic markers CD14, CD20, CD34, and CD45 (Fig. 3b). Oil Red O-positive fat droplets were detected in all iMSC preparations upon adipogenic induction. In addition, Alizarin Red-positive calcified matrix and Alcian Blue staining were detected following culture in osteogenic and chondrogenic medium, respectively (Fig. 3c). Although iMSCs were derived from pluripotent cells, they had a lower expression of pluripotency markers than the iPSC and ESCs they were derived from (Fig. 3d). Finally, comparison of the transcriptomes revealed a higher correlation co-efficient

(R^2) between iMSCs and primary MSCs (0.917–0.964) than between iMSCs and iPSCs/ESCs (0.879–0.914). Moreover, we detected a higher similarity between the transcriptomes of fMSCs and ESCs (0.925–0.939) than between aMSCs and ESCs (0.855–0.885) (Additional file 1: Figure S2).

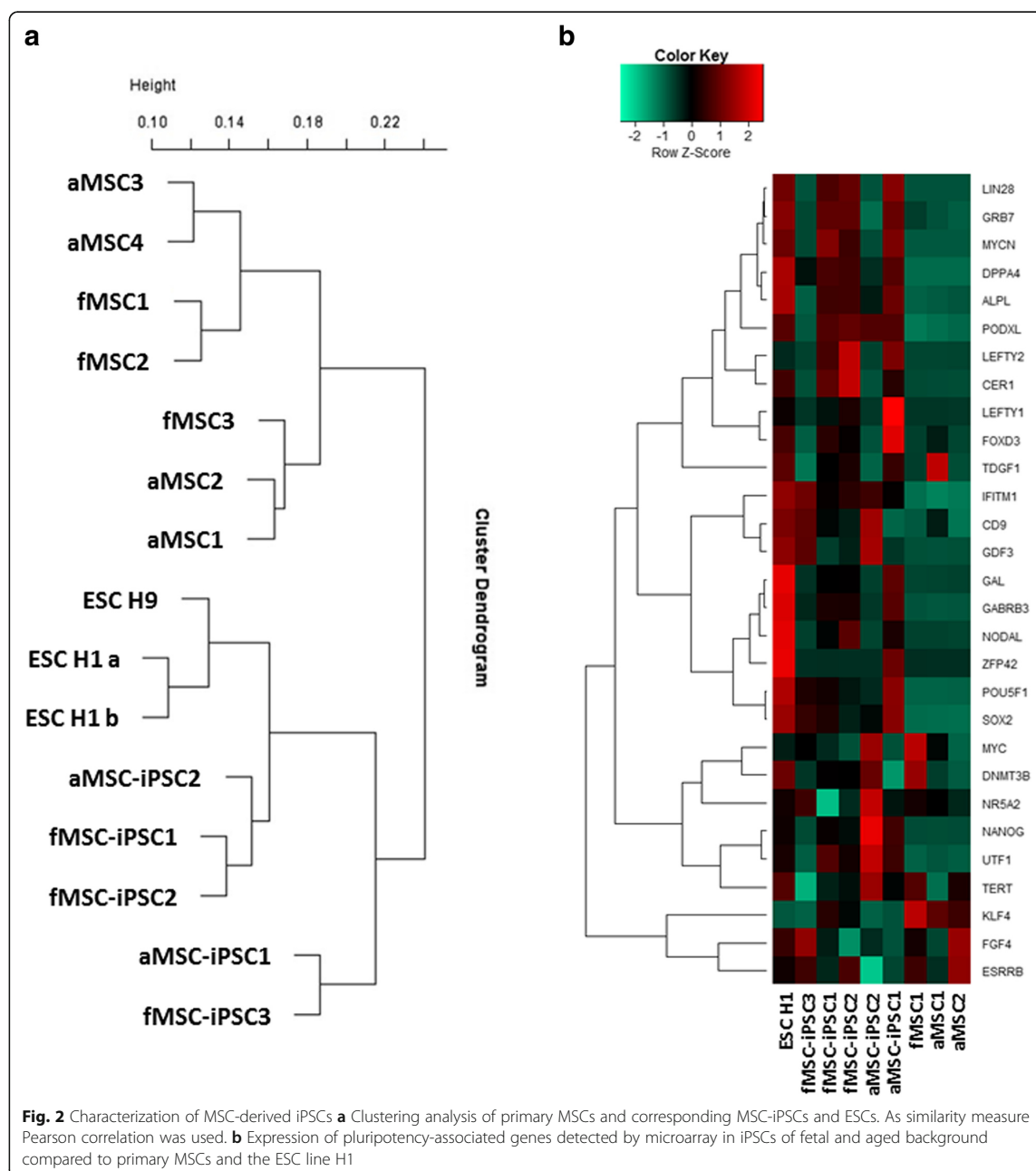
Primary MSCs and iMSCs have overlapping and distinct gene expression patterns revealing higher similarity between iMSCs and fMSCs

A Venn diagram-based representation of transcriptome data identified 12,487 genes commonly expressed between the fMSC-iMSCs, aMSC-iMSCs, and ESC-iMSCs. Within this shared gene set, numerous MSC-specific genes (CD73, CD90, CD105, and PDGFR β), MSC-associated genes (VEGFA, Vimentin, SerpinE1, and MIF), and differentiation markers (RUNX2 and PPAR γ) were present (Fig. 4a). Clustering analysis of the transcriptomes resulted in the formation of two similarity-based clusters separating iMSCs (irrespective of their source) together with primary MSCs from their corresponding iPSCs and ESC samples (Fig. 4b). Another Venn diagram-based analysis comparing iMSCs (combination of fMSC-iMSCs, aMSC-iMSCs, and ESC-iMSCs), fMSCs, and aMSCs revealed that more genes were expressed in common between iMSCs and fMSCs (534 genes) than between iMSCs and aMSCs (398 genes) with the majority of genes expressed in all three groups (11794). iMSCs proved the most distinct sample set with 923 exclusively expressed genes (Fig. 4c).

Importantly, a heatmap-based clustering analysis of expression of DNA damage repair (such as FEN1 and MSH6) and aging-associated genes (such as *FADS1* and *NOX4*) revealed that iMSCs irrespective of donor age or cell type of origin are more similar to fMSCs compared to aMSCs (Fig. 4d, e).

MSC-iMSCs acquired a rejuvenation signature

Genes expressed in iMSCs and pluripotent stem cells but not expressed in primary MSCs (fMSCs and aMSCs) were identified which we refer to as the rejuvenation signature. On a similar note, genes expressed in primary MSCs but not in pluripotent stem cells and iMSCs are referred to as the aging signature (Fig. 5a). Figure 5b shows a table based on the heatmap from Fig. 5a with the gene names within the rejuvenation and aging signature. To validate our rejuvenation and aging signatures, we carried out an additional analysis incorporating already published datasets of primary human MSCs of different ages [24, 25]. A hierarchical clustering analysis of gene expression including the new samples (MSC1–7) independently confirmed the validity of our rejuvenation signature (e.g., *PM20D2* and *HRASLS*) and aging



signature (e.g. *FAM109B* and *EDIL3*) reflecting the respective expression levels (Fig. 5c).

For further verification of the rejuvenation signature, real-time PCR analysis was carried out using RNA from additional independent adult MSC (56 years) and iMSC samples from distinct age groups (urine-derived iPSC-derived iMSCs (51 years); ESC-iMSCs (prenatal),

fMSC-iMSCs (prenatal), and HFF-iMSCs (human fetal foreskin-derived iPSC-derived iMSCs)) employing primers for genes of the rejuvenation (*IGSF3*, *CXADR*, *FAM84B*, *INHBE*, and *DNMT3B*) and aging signature (*COX7A*, *EZA2*, *EFEMP1*, *ENPP2*, and *TMEM119*) (Fig. 5d). For *IGSF3*, the mRNA expression level in all iMSC preparation was higher than that in the fMSCs

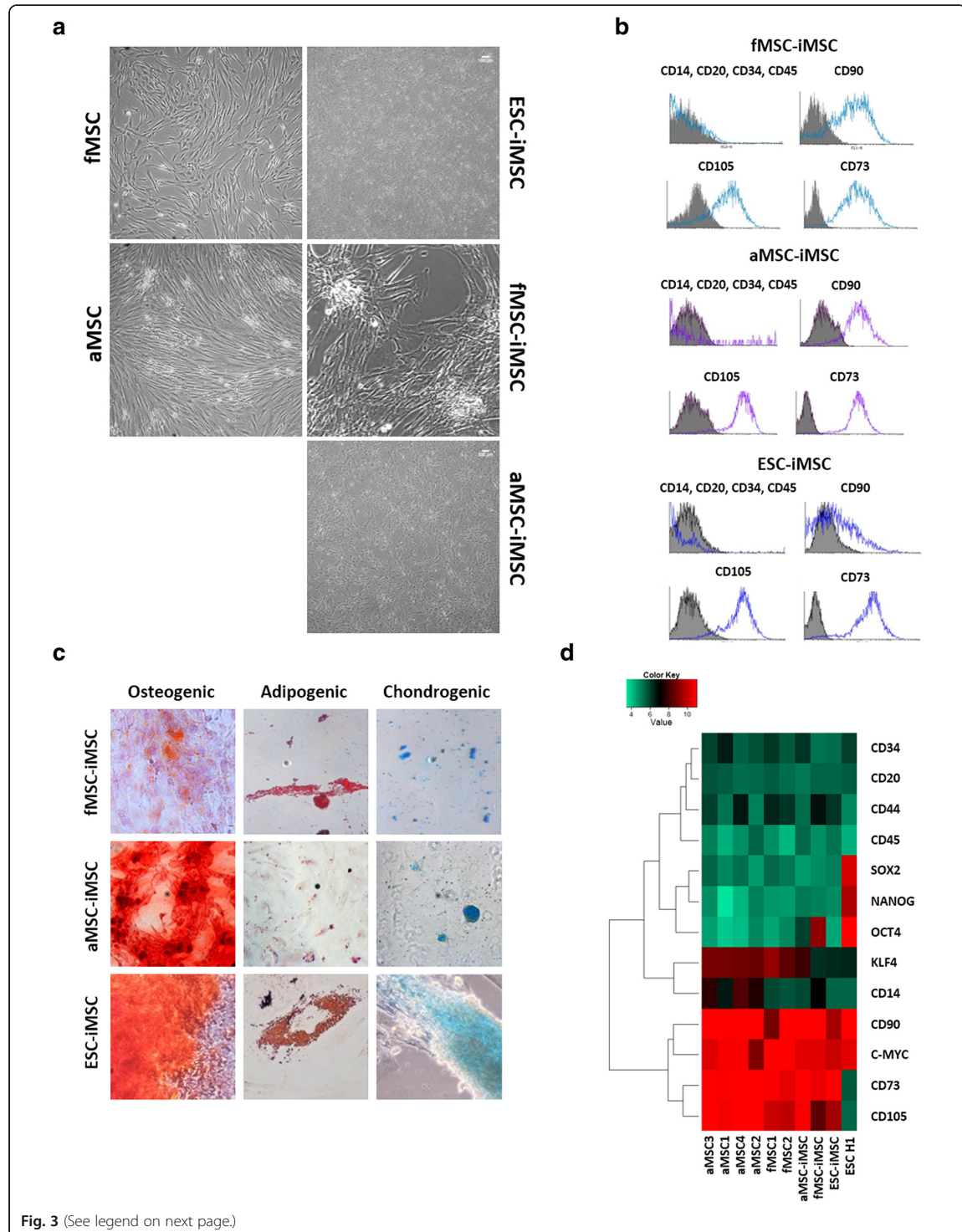


Fig. 3 (See legend on next page.)

(See figure on previous page.)

Fig. 3 Characterization of fMSC-iMSCs, aMSC-iMSCs, and ESC-iMSCs. **a** Morphology of iMSCs compared to native MSCs. **b** Flow cytometry-based analysis of MSC surface marker in iMSCs. Blue/Purple: iMSCs labeled with antibody specific to marker. Gray: isotype control. **c** Differentiation potential of iMSCs in vitro. Osteogenic: Alizarin Red S staining; adipogenic: Oil red O staining; chondrogenic: Alcian Blue staining. **d** Gene expression of MSC, hematopoietic, and pluripotency markers in iMSCs compared to primary MSCs and ESC H1. Representative images of $n = 3$ experiments

and aMSC samples whereas only three of the four iMSC samples showed increased *CXADR* expression levels. For *DNMT3B*, a rejuvenation signature, two of the four iMSC samples showed upregulation. The other two genes of the rejuvenation signature showed comparable levels in aMSCs and iMSCs. For the aging signature, *COX7A*, *EZA2*, *EFEMP1*, and *TMEM119* were expressed at lower levels in iMSCs than in aMSCs with the exception of *ENPP2* (Fig. 5d).

Protein association network analyses confirm rejuvenation and aging signature

Using the genes of the rejuvenation signature as input, a protein association network (PAN) was created adding the $n = 30$ interaction partners with the most interactions from the Biogrid database. We used community clustering to identify densely connected groups of proteins with fewer connections across groups. The rejuvenation signature PAN (Fig. 6a) includes communities characterized by *INHBE* (blue), *TP53*, *CDKN1C*, *IL32* (light blue), *CDK10* (petrol), *ELAVL1* (purple), *DNMT3B* (yellow), and *EEF1A2* (green).

Analogously, we generated a PAN based on the aging signature which revealed genes involved in the TGF β and mTOR-signaling pathways as well as factors associated with oxidative stress including *CAT* (Fig. 6b). The aging signature PAN (Fig. 6b) includes communities characterized by *HSPA5* (blue), *GRB2* (light blue), *CCDC8* (purple), *CAT* (petrol), *EYA2* (yellow), *APP* (green), and *TGFB1* (red).

iMSCs of different age backgrounds show overlapping secretomes with fetal MSCs

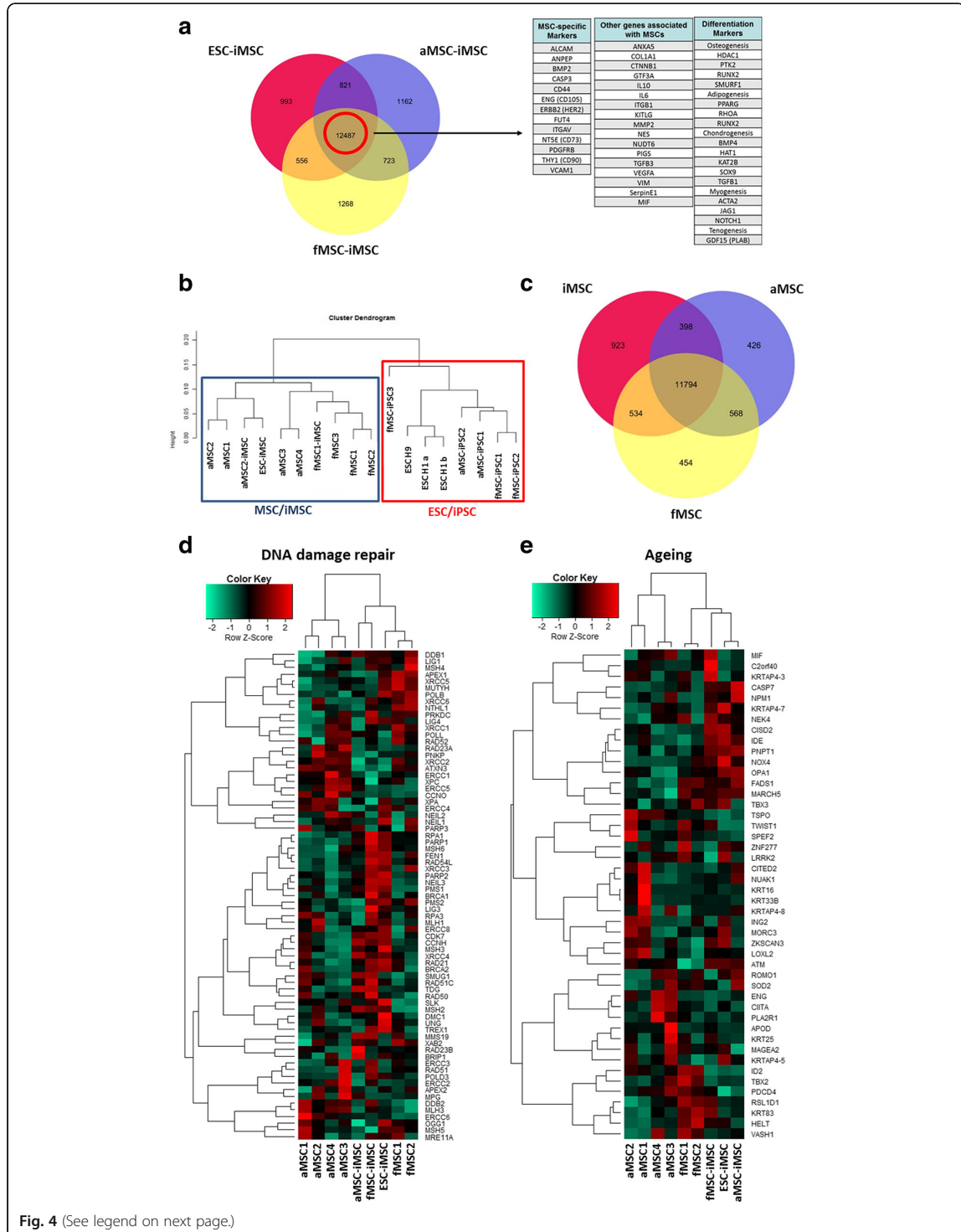
Based on a cytokine array, the secretomes of fMSC-iMSCs, aMSC-iMSCs, and ESC-iMSCs were found to be similar to the secretomes of primary fMSC1, fMSC2, and fMSC3 (Fig. 7a, b). iMSCs, independent from their origin, as well as fetal MSCs showed a large number overlap in the most abundantly secreted cytokines: angiogenin, *BDNF*, *Chitinase 3-like 1*, *Dkk-1*, *EMMPRIN*, *ENA-78*, *endoglin*, *GDF-15*, *GRO α* , *IGFBP-2*, *IGFBP-3*, *IL-6*, *IL-8*, *IL-11*, *LIF*, *MCP-1*, *MCP-3*, *MIF*, *osteopontin*, *PDGF-AA*, *pentraxin-3*, *serpin E1*, *thrombospondin-1*, and *VEGF* (Fig. 7a, Additional file 1: Figure S3). KEGG pathway analysis of the common secreted cytokines showed their involvement in processes like cytokine-cytokine receptor interaction,

TNF signaling pathway, chemokine signaling pathway, PI3K-Akt signaling pathway, HIF-1 signaling pathway, and Jak-STAT signaling pathway (Fig. 7b). Gene Ontology analysis of the common secreted cytokines showed involvement in processes such as regulation of growth factor activity, inflammatory response, positive regulation of ERK1 and ERK2 cascade, positive regulation of angiogenesis, and cell proliferation (Fig. 7c). In addition to this, the secretomes of fMSCs and iMSCs were compared to that of aMSCs (Fig. 7d, Additional file 1: Figure S3). In comparison to fMSCs and iMSCs (independent of the source), MSCs from aged individuals (aMSCs) secreted fewer cytokines and at lower levels except for *IL6*.

Discussion

Derivation and characterization of pluripotent stem cell-derived MSCs (iMSCs) are on the rise [18, 44–46]. iMSCs have been shown to enhance regeneration and healing when applied to a variety of animal models; multiple sclerosis, limb ischemia, arthritis, liver damage, bone defects, wound healing, and hypoxic-ischemia in the brain [46–53]. In this study, we comparatively and critically assessed the effect of donor age and cell type specificity on the iMSC “rejuvenated” signature based on transcriptome analysis and further studied their paracrine signaling potential by secretome analyses. We revealed that fMSCs share a higher transcriptome similarity with ESCs than with aMSCs. This age-related difference may be due to genes involved in cell adhesion (Fig. 1e), which is in agreement with the reported role of adhesion-related processes in pluripotent stem cells [54]. However, the iMSCs generated in this study met the criteria defined for primary MSCs to a certain extent in terms of morphology and surface marker expression (Fig. 3a,b), as previously shown for iMSC generation from fibroblast-derived iPSCs [18]. In agreement with the MSC criteria [2], the generated iMSCs were able to differentiate into bone, cartilage, and fat cells in vitro. In addition, we could successfully confirm a high level of similarity between primary MSCs and iMSCs on transcriptome level and could show that these iMSCs although originating from pluripotent cells are not pluripotent themselves (low similarity to iPSCs) which is important for potential use in future clinical applications.

The expression patterns of genes associated with aging and DNA damage repair in all iMSC populations



(See figure on previous page.)

Fig. 4 Distinct and overlapping gene expression patterns between iMSCs and primary MSCs isolated from donors of distinct ages. **a** Venn diagram-based on expressed genes detected by microarrays of one sample each of fMSC-iMSCs, aMSC-iMSCs, and ESC-iMSCs. MSC-related genes were expressed in all three iMSC preparations. **b** Clustering dendrogram of Illumina gene expression experiments based on Pearson correlation. One cluster consists of iPSCs and ESCs (red box), and the other separated cluster contains primary MSCs as well as all three iMSC preparations (blue box). **c** Venn diagram of iMSCs and MSCs from fetal and aged donors based on expressed genes of one sample each **d** Heatmap showing clustering of primary MSCs and iMSCs for genes related to DNA damage repair. **e** Heatmap showing clustering of primary MSCs and iMSCs for aging-related genes

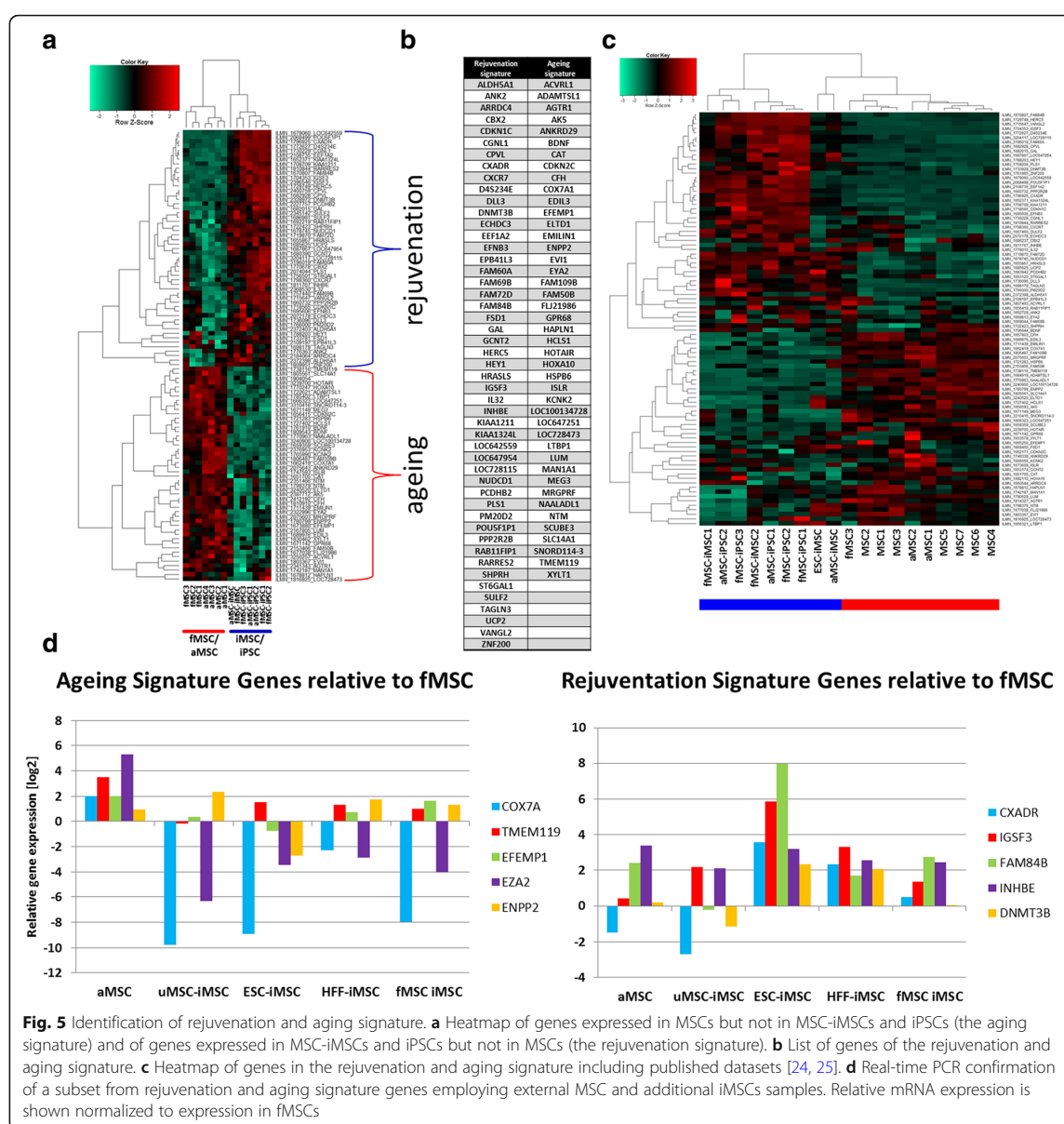
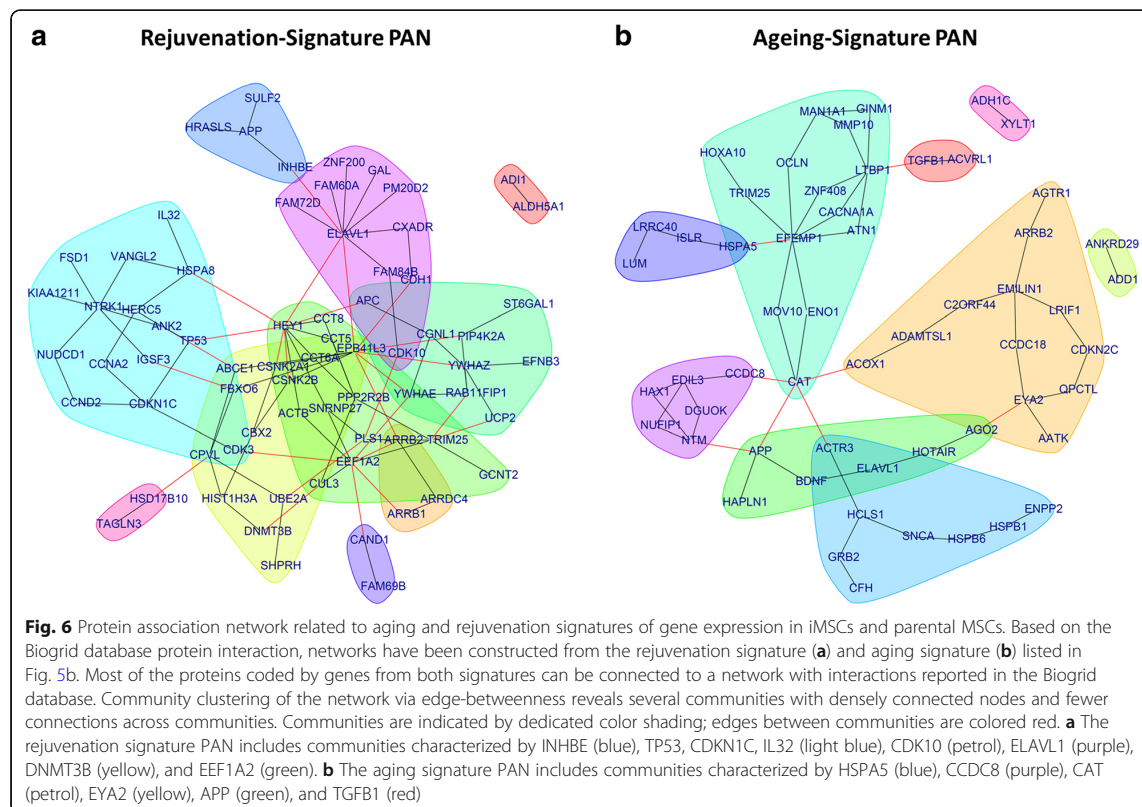
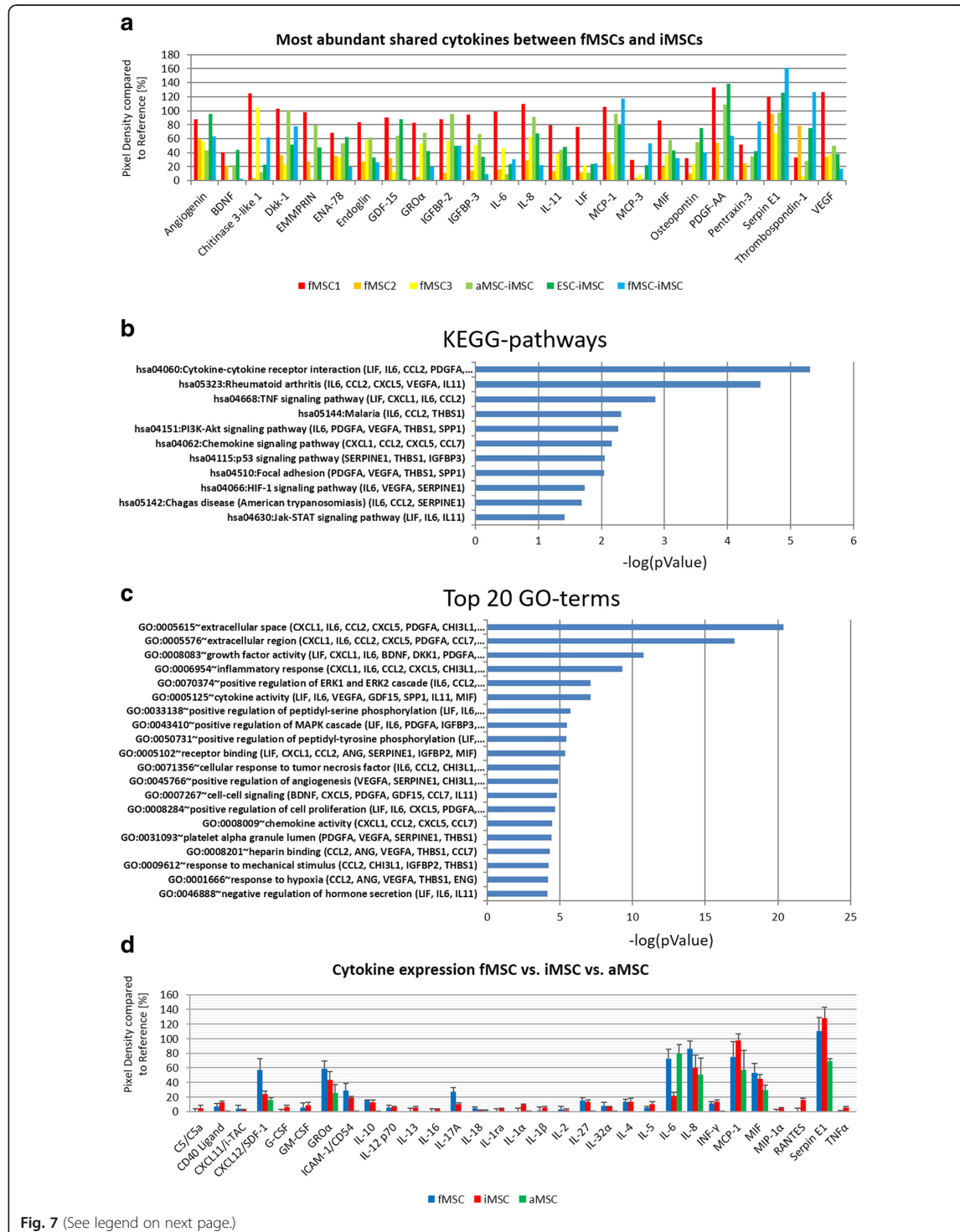


Fig. 5 Identification of rejuvenation and aging signature. **a** Heatmap of genes expressed in MSCs but not in MSC-iMSCs and iPSCs (the aging signature) and of genes expressed in MSC-iMSCs and iPSCs but not in MSCs (the rejuvenation signature). **b** List of genes of the rejuvenation and aging signature. **c** Heatmap of genes in the rejuvenation and aging signature including published datasets [24, 25]. **d** Real-time PCR confirmation of a subset from rejuvenation and aging signature genes employing external MSC and additional iMSCs samples. Relative mRNA expression is shown normalized to expression in fMSCs



clustered closer to fMSCs than to aMSCs (Fig. 4d, e), thus indicating a rejuvenation. DNA damage has been shown to be associated with the complex process of aging before [55]. Irrespective of donor age and cell source, iMSCs acquired a rejuvenation gene signature also present in pluripotent stem cells but not in the parental MSCs (Fig. 5a, b). Conversely, we observed a gene set representing the aging signature comprising genes expressed in primary MSCs but not in pluripotent stem cells and iMSCs. We could independently confirm the extracted aging and rejuvenation signature by including already published datasets of adult MSCs [24, 25] in similarity analyses based on both gene sets (Fig. 5c). Further confirmation of the signatures was carried out at the mRNA level using additional MSC and iMSC samples (Fig. 5d). A large number of the genes within the rejuvenation signature play important roles in embryonic tissues and in development thus indicating the presence of features associated with early development in iMSCs, and therefore, it would appear, endowing iMSCs with enhanced regenerative properties. The rejuvenation signature PAN revealed communities characterized by INHBE, TP53, CDKN1C, IL32, CDK10, ELAVL1, DNMT3B, and EEF1A2. INHBE participates in the

activin/nodal branch of the TGF β signaling pathway which is needed for maintenance of pluripotency [56, 57]. CDK10, CDKN1C, and TP53 are involved in cell cycle control which obviously plays an important role in stem cell self-renewal [58]. However, the detailed cell cycle coordination in order to determine cell fates is not fully uncovered. CDK10 like all members of the CDK family is responsible for cell cycle progression but is limited to the G2-M phase which Vallier et al. describe as necessary to block pluripotency upon induction of differentiation referring to Gonzalez et al. [59]. Gonzales et al. furthermore report that the ATM/ATR-CHEK2-TP53 axis enhances the TGF β pathway to prevent pluripotent state dissolution. In a previous publication, we reported compromised induction of pluripotency in fibroblasts from a Nijmegen Breakage syndrome patient under conditions of impaired DNA damage repair and downregulated TP53 and cell cycle genes [60]. CDKN1C reduces cell proliferation by inhibiting cyclin/Cdk complexes in the G1 phase [61] and is a major regulator of embryonic growth as has been reported by Andrews et al. for the imprinted domain on mouse distal chromosome 7 [62]. ELAVL1 (HuR) has been associated with regulation of growth and proliferation of vascular smooth muscle cells



(See figure on previous page.)

Fig. 7 Comparative analyses of the secretome of fMSCs, iMSCs, and aMSCs. **a** Cytokine expression of fMSC1, fMSC2, fMSC3, and iMSCs (fMSC-iMSCs, aMSC-iMSCs, and ESC-iMSCs) detected using membrane-based cytokine arrays. Expression plot of the most abundant cytokines shared between fMSCs and iMSCs; threshold of expression in comparison to reference spots was set to 20%. **b** KEGG pathway analysis of common cytokines between fMSCs and iMSCs—log(pValue). **c** GO terms associated with common secreted cytokines between fMSCs and iMSCs as –log(pValue). **d** Cytokine expression of fMSCs, iMSCs, and aMSCs (aMSC5, aMSC6, aMSC7)

[63]. DNMT3B has been reported to be essential for de novo methylation and mammalian development [64] and DNMT1 and DNMT3B were shown to decrease upon aging [65].

The aging signature PAN includes communities characterized by HSPA5, CCDC8, CAT, EYA2, APP, and TGFBI. Catalase (CAT) is an antioxidant which has been reported to have decreased activity upon aging in rats [66]. GRB2 is part of the mTOR-signaling pathway which coordinates eukaryotic cell growth and metabolism with environmental inputs [67]. TGF β -signaling plays a major role in young and aging organisms but changes its functionality. Baugé et al. describe a shift of TGF β -signaling from SMAD2/3 to SMAD1/5/8 as cause of a shift from chondrogenic differentiation and maturation in young joints to hypertrophic differentiation in aged or osteoarthritic joints [68]. BDNF has been reported to regulate the amyloid precursor protein APP [69] that is involved in activity-dependent synaptic plasticity and is upregulated after birth but then stays unchanged during aging in rat hippocampus [70].

Accordingly, the loss of the aging signature during iMSC derivation likely contributed to the advantageous features of iMSCs compared to primary MSCs. The observed fetal-like expression pattern of genes involved in DNA damage repair in iMSCs could be due to the involvement of this process in pluripotency induction. An alternative explanation could be that young or progenitor cells have a better capacity to repair DNA damage [71].

A rejuvenated state of processes involved in aging in iMSCs is furthermore likely as the epigenetic rejuvenation of MSCs through pluripotency induction has been described [13].

Of considerable potential significance, from a regenerative medicine perspective, iMSCs should have a similar secretome to that of the corresponding parental MSCs. In line with this, the secretion of GRO α , IL-6, IL-8, MCP-1, MIF, SDF-1, and Serpin E1 in bone marrow-derived MSCs has been described [72]. A further study showed that MSCs derived from bone marrow secrete angiogenin, G-CSF, GM-CSF, GRO α , IL-1 α , IL-6, IL-8, INF γ , MCP-1, oncostatin M, RANTES, and TGF β and do not secrete IL-2, IL-4, IL-10, IL-12, IL-13, MIP-1 β , and SDF-1 α [73], all in agreement with our iMSC secretome profile. Interestingly, we detected the secretion of anti-inflammatory and pro-inflammatory cytokines in iMSCs and fetal mesenchymal populations

confirming findings in MSCs [74]. Gene Ontology analysis revealed overlapping capabilities to interact with the immune system and involvement in regeneration processes of fetal MSCs and iMSCs corroborating studies with MSCs derived from adult donors [75–77]. A KEGG pathway analysis revealed involvement of the overlapping secreted cytokines between fetal MSCs and iMSCs in TNF signaling pathway, Jak-STAT signaling pathway, and PI3K-Akt signaling pathway. Interestingly, we found SerpinE1, thrombospondin-1, IGFBP3, endoglin, and angiogenin to be abundantly secreted in fetal MSCs and iMSCs. The described role of SerpinE1, thrombospondin-1, and endoglin in wound healing [78–80] indicate a putative fetal-like feature of wound healing properties of iMSCs in vivo [81, 82]. Our analyses revealed that aMSCs compared to fMSCs and iMSC secrete a reduced repertoire of cytokines and at significantly lower levels. However, fMSCs, aMSCs, and iMSCs secrete comparable levels of IL6, IL8, SDF-1, MCP-1, MIF, Serpin E1, and GRO α . This once again reinforces the notion that MSCs isolated from the elderly may not be as potent as fetal MSCs and pluripotent stem cell-derived MSCs.

Conclusions

In summary, the current study shows that MSCs of fetal and aged background are not identical and MSCs generated from iPSCs (iMSCs) bear typical characteristics of native MSCs but more in common with fetal MSCs. The key finding from our study is the identification of a rejuvenation gene signature in iMSCs (irrespective of donor age) which also is present in pluripotent stem cells but not in the parental MSCs. Most important for regenerative medicine, iMSCs irrespective of initial age re-acquire a more similar secretome to that of fetal MSCs than aged MSCs. In conclusion, our findings show that the acquisition of a rejuvenated phenotype in iMSCs re-enforces the utility of the “iMSC concept” in regenerative medicine and cell replacement therapy in an ever increasing aging population.

Additional file

Additional file 1: Table S1. List of primary MSC samples. Table S2. List of primers. **Table S3.** List of antibodies. Figure S1 Pluripotency marker staining of generated iPSC line from fMSCs and aMSCs as well as EB formation. **Figure S2.** Correlation coefficient table. Figure S3 Cytokine membranes. (DOCX 2493 kb)

Abbreviations

aMSC: Adult MSC; CD: Cluster of differentiation; DAVID: Database for Annotation, Visualization and Integrated Discovery; EB: Embryoid body; ESCs: Embryonic stem cells; FACS: Fluorescence-activated cell sorting; fMSC: Fetal MSC; GEO: Gene Expression Omnibus; GO: Gene Ontology; iMSCs: iPSC-derived mesenchymal stromal cells; iPSCs: Induced pluripotent stem cells; KEGG: Kyoto Encyclopedia of Genes and Genomes; MSCs: Mesenchymal stem cells; PAN: Protein association network

Acknowledgements

We thank Prof. David Wilson, University of Southampton for access to fetal tissue and Dr. Kelvin Cheung, University of Southampton for derivation of fetal femur explant cultures. We thank Prof. G. Duda for providing MSCs from the 74-year-old.

Funding

Prof. Dr. James Adjaye acknowledges support from the Medical Faculty, Heinrich-Heine-University, Düsseldorf, Germany and support from the Federal Ministry of Education and Research-BMBF (01GN1005) and the Medical Faculty, Heinrich-Heine-University, Düsseldorf. Professor Dr. Richard Oreffo is supported by grants from the BBSRC (LO21072/1) and MRC (MR/K026682/1). In addition, Prof. Dr. James Adjaye and Mr. Md Shaifur Rahman acknowledge support from the German Academic Exchange Service (DAAD-91607303).

Availability of data and materials

The data and cells described in this manuscript can be made available upon request. The transcriptome data is available online at the National Center of Biotechnology Information (NCBI) Gene Expression Omnibus.

Authors contributions

JA, RO, MM, and LSS conceived the idea and designed the experiments. MM and LSS performed the characterization of primary MSCs and generation/characterization of iPSCs/iMSCs. MM, LSS, and MSR analyzed the results and wrote the draft manuscript. OD and RM provided RNA from MSCs of an aged individual (56 years), and JO performed the real-time PCR analysis. WW did the bioinformatical analysis. RVS provided aged MSCs for the cytokine array. JA edited and finally approved the manuscript. All authors reviewed and approved the submitted version.

Ethics approval and consent to participate

Fetal femur-derived MSCs were obtained following informed, written patient consent. Approval was obtained by the Southampton and South West Hampshire Local Research Ethics Committee (LREC 296100). Adult mesenchymal stem cells, used for generation of iPSCs and iMSCs, were isolated from the bone marrow after written informed consent. The corresponding protocol was approved by the research ethics board of the Charité-Universitätsmedizin, Berlin (IRB approval EA2/126/07). Isolation of mesenchymal stem cells from aged individuals was approved under the Southampton and South West Hampshire Local Research Ethics Committee (LREC 194/99). The Ethics commission of the medical faculty at Heinrich Heine University Düsseldorf also approved this study (Study number: 5013).

Consent for publication

Not applicable.

Competing interests

The authors declare that they have no competing interest.

Publisher's Note

Springer Nature remains neutral with regard to jurisdictional claims in published maps and institutional affiliations.

Author details

¹Institute for Stem Cell Research and Regenerative Medicine, Medical Faculty, Heinrich Heine University, Düsseldorf, Moorenstr. 5, 40225 Düsseldorf, Germany. ²Division of Paediatric Stem Cell Therapy, Clinic for Pediatric Oncology, Hematology and Clinical Immunology, Medical Faculty, Heinrich Heine University, Düsseldorf, Moorenstr. 5, 40225 Düsseldorf, Germany. ³Institute for Transplantation Diagnostics and Cell Therapeutics, Heinrich Heine University Hospital, Moorenstr. 5, 40225 Düsseldorf, Germany. ⁴Bone and Joint Research Group, Centre for Human Development, Stem Cells and

Regeneration, Institute of Developmental Sciences, University of Southampton, Southampton SO16 6YD, UK.

Received: 2 October 2018 Revised: 14 February 2019

Accepted: 6 March 2019 Published online: 18 March 2019

References

- Bianco P, Robey PG. Skeletal stem cells. *Development*. 2015;142:1023–7.
- Dominici M, Le Blanc K, Mueller I, Slaper-Cortenbach I, Marini F, Krause D, et al. Minimal criteria for defining multipotent mesenchymal stromal cells. The International Society for Cellular Therapy position statement. *Cytotherapy*. 2006;8:315–7.
- Mirmalek-Sani SH, Tare RS, Morgan SM, Roach HI, Wilson DJ, Hanley NA, et al. Characterization and multipotentiality of human fetal femur-derived cells: implications for skeletal tissue regeneration. *Stem Cells*. 2006;24:1042–53.
- Ito H. Clinical considerations of regenerative medicine in osteoporosis. *Curr Osteoporos Rep*. 2014;12:230–4.
- Zhou S, Greenberger JS, Epperly MW, Goff JP, Adler C, Leboff MS, et al. Age-related intrinsic changes in human bone-marrow-derived mesenchymal stem cells and their differentiation to osteoblasts. *Aging Cell*. 2008;7:335–43.
- Moskalev AA, Shaposhnikov MV, Plyusnina EN, Zhavoronkov A, Budovsky A, Yanai H, et al. The role of DNA damage and repair in aging through the prism of Koch-like criteria. *Ageing Res Rev*. 2013;12:661–84.
- Reuter S, Gupta SC, Chaturvedi MM, Aggarwal BB. Oxidative stress, inflammation, and cancer: how are they linked? *Free Radic Biol Med*. 2010;49:1603–16.
- Brink TC, Demetrius L, Lehrach H, Adjaye J. Age-related transcriptional changes in gene expression in different organs of mice support the metabolic stability theory of aging. *Biogerontology*. 2009;10:549–64.
- Oreffo RO, Bord S, Triffitt JT. Skeletal progenitor cells and ageing human populations. *Clin Sci (Lond)*. 1998;94:549–55.
- Stolzinger A, Scutt A. Age-related impairment of mesenchymal progenitor cell function. *Aging Cell*. 2006;5:213–24.
- Wagner W, Bork S, Horn P, Kronic D, Walenda T, Diehlmann A, et al. Aging and replicative senescence have related effects on human stem and progenitor cells. *PLoS One*. 2009;4:e5846.
- Nasu A, Ikeya M, Yamamoto T, Watanabe A, Jin Y, Matsumoto Y, et al. Genetically matched human iPSC cells reveal that propensity for cartilage and bone differentiation differs with clones, not cell type of origin. *PLoS One*. 2013;8:e53771.
- Frobel J, Hemedda H, Lenz M, Abagnale G, Jousens S, Denecke B, et al. Epigenetic rejuvenation of mesenchymal stromal cells derived from induced pluripotent stem cells. *Stem Cell Reports*. 2014;3:414–22.
- Zhao C, Ikeya M. Generation and applications of induced pluripotent stem cell-derived mesenchymal stem cells. *Stem Cells Int*. 2018;96:1623.
- Lapasset L, Millharet O, Prieur A, Besnard E, Babled A, Ait-Hamou N, et al. Rejuvenating senescent and centenarian human cells by reprogramming through the pluripotent state. *Genes Dev*. 2011;25:2248–53.
- Miller JD, Ganat YM, Kishinevsky S, Bowman RL, Liu B, Tu EY, et al. Human iPSC-based modeling of late-onset disease via progerin-induced aging. *Cell Stem Cell*. 2013;13:691–705.
- Suhr ST, Chang EA, Tjong J, Alcasid N, Perkins GA, Goissis MD, et al. Mitochondrial rejuvenation after induced pluripotency. *PLoS One*. 2010;5:e14095.
- Chen YS, Pelekanos RA, Ellis RL, Horne R, Wolvetang EJ, Fisk NM. Small molecule mesengenic induction of human induced pluripotent stem cells to generate mesenchymal stem/stromal cells. *Stem Cells Transl Med*. 2012;1:83–95.
- Kimbrel EA, Kouris NA, Yavarian GJ, Chu J, Qin Y, Chan A, et al. Mesenchymal stem cell population derived from human pluripotent stem cells displays potent immunomodulatory and therapeutic properties. *Stem Cells Dev*. 2014;23:1611–24.
- Cheung HH, Liu X, Canterel-Thouennon L, Li L, Edmonson C, Rennert OM. Telomerase protects werner syndrome lineage-specific stem cells from premature aging. *Stem Cell Reports*. 2014;2:534–46.
- Hu GW, Li Q, Niu X, Hu B, Liu J, Zhou SM, et al. Exosomes secreted by human-induced pluripotent stem cell-derived mesenchymal stem cells attenuate limb ischemia by promoting angiogenesis in mice. *Stem Cell Res Ther*. 2015;6:10.
- Megges M, Geissler S, Duda GN, Adjaye J. Generation of an iPSC cell line from bone marrow derived mesenchymal stromal cells from an elderly patient. *Stem Cell Res*. 2015;15:565–8.

23. Yang X, Tare RS, Partridge KA, Roach HI, Clarke NM, Howdle SM, et al. Induction of human osteoprogenitor chemotaxis, proliferation, differentiation, and bone formation by osteoblast stimulating factor-1/pleiotrophin: osteoconductive biomimetic scaffolds for tissue engineering. *J Bone Miner Res.* 2003;18:47.
24. Leuning DG, Reinders ME, Li J, Peired AJ, Lievers E, de Boer HC, et al. Clinical-grade isolated human kidney perivascular stromal cells as an organotypic cell source for kidney regenerative medicine. *Stem Cells Transl Med.* 2017;6(2):405–18.
25. Park GC, Song JS, Park HY, Shin SC, Jang JY, Lee JC, et al. Role of fibroblast growth factor-5 on the proliferation of human tonsil-derived mesenchymal stem cells. *Stem Cells Dev.* 2016;25:1149–60.
26. Megges M, Oreffo RO, Adjaye J. Episomal plasmid-based generation of induced pluripotent stem cells from fetal femur-derived human mesenchymal stromal cells. *Stem Cell Res.* 2016;16:128–32.
27. Yu J, Chau KF, Vodyanik MA, Jiang J, Jiang Y. Efficient feeder-free episomal reprogramming with small molecules. *PLoS One.* 2011;6:e17557.
28. Gao Y, Yang L, Chen L, Wang X, Wu H, Ai Z, et al. Vitamin C facilitates pluripotent stem cell maintenance by promoting pluripotency gene transcription. *Biochimie.* 2013;95:2107–13.
29. Hossini AM, Megges M, Prigione A, Lichtner B, Toliat MR, Wruck W, et al. Induced pluripotent stem cell-derived neuronal cells from a sporadic Alzheimer's disease donor as a model for investigating AD-associated gene regulatory networks. *BMC Genomics.* 2015;16:84.
30. Takahashi K, Tanabe K, Ohnuki M, Narita M, Ichisaka T, Tomoda K, et al. Induction of pluripotent stem cells from adult human fibroblasts by defined factors. *Cell.* 2007;131:861–72.
31. Müller FJ, Schuldt BM, Williams R, Mason D, Altun G, Papapetrou EP, et al. A bioinformatic assay for pluripotency in human cells. *Nat Methods.* 2011;8:315–7.
32. Ihaka R, Gentleman RR. A language for data analysis and graphics. *J Comput Graph Stat.* 1996;5:299–314.
33. Gentleman RC, Carey VJ, Bates DM, Bolstad B, Dettling M, Dudoit S, et al. Bioconductor: Open Software Development for Computational Biology and Bioinformatics. *Genome Biol.* 2004;5:R80.
34. Du P, Kibbe WA, Lin SM. Lumi: a pipeline for processing Illumina microarray. *Bioinformatics.* 2008;24:1547–8.
35. Chen H, Boutros PC. VennDiagram: a package for the generation of highly-customizable Venn and Euler diagrams in R. *BMC Bioinformatics.* 2011;12:35.
36. Warnes GR, Bolker B, Bonebakker L, Gentleman R, Huber W, Liaw A, et al. Gplots: Various R Programming Tools for Plotting Data. <http://CRAN.R-project.org/package=gplots>. 2015. Accessed 13 Mar 2019.
37. Ashburner M, Ball CA, Blake JA, Botstein D, Butler H, Cherry JM, et al. Gene ontology: tool for the unification of biology. The Gene Ontology Consortium. *Nat Genet.* 2000;25:25–9.
38. Smyth GK. Linear models and empirical Bayes methods for assessing differential expression in microarray experiments. *Stat Appl Genet Mol Biol.* 2004;3:Article3.
39. Storey JD. A direct approach to false discovery rates. *J R Stat Soc: Series B Stat Methodol.* 2002;64:479–98.
40. Huang DW, Sherman BT, Lempicki RA. Systematic and integrative analysis of large gene lists using DAVID bioinformatics resources. *Nat Protoc.* 2009;4:44–57.
41. Chatri-Aryamontri A, Oughtred R, Boucher L, Rust J, Chang C, Nadine K, et al. The BioGRID Interaction Database: 2017 Update. *Nucleic Acids Res.* 2017;45: D369–79.
42. Butts CT. Network: a package for managing relational data in R. *J Stat Softw.* 2008;24:1–36.
43. Csardi G, Nepusz Z. The Igraph Software Package for complex network research. *Inter J Complex Syst.* 2006;1695:1–9.
44. Liu Y, Goldberg AJ, Dennis JE, Gronowicz GA, Kuhn LT. One-step derivation of mesenchymal stem cell (MSC)-like cells from human pluripotent stem cells on a fibrillar collagen coating. *PLoS One.* 2012;7:e33225.
45. Diederichs S, Tuan RS. Functional comparison of human-induced pluripotent stem cell-derived mesenchymal cells and bone marrow-derived mesenchymal stromal cells from the same donor. *Stem Cells Dev.* 2014;23:1594–610.
46. Sheyn D, Ben-David S, Shapiro G, De Mel S, Bez M, Ornelas L, et al. Human induced pluripotent stem cells differentiate into functional mesenchymal stem cells and repair bone defects. *Stem Cells Transl Med.* 2016;5:1447–60.
47. Wang X, Kimbrel EA, Ijichi K, Paul D, Lazorchak AS, Chu J, et al. Human ESC-derived MSCs outperform bone marrow MSCs in the treatment of an EAE model of multiple sclerosis. *Stem Cell Reports.* 2014;3:115–30.
48. Lian Q, Zhang Y, Zhang J, Zhang HK, Wu X, Zhang Y, et al. Functional mesenchymal stem cells derived from human induced pluripotent stem cells attenuate limb ischemia in mice. *Circulation.* 2010;121:1113–23.
49. Gonzalo-Gil E, Pérez-Lorenzo MJ, Galindo M, Díaz de la Guardia R, López-Millán B, Bueno C, et al. Human embryonic stem cell-derived mesenchymal stromal cells ameliorate collagen-induced arthritis by inducing host-derived indoleamine 2,3 dioxygenase. *Arthritis Res Ther.* 2016;18:77.
50. Spitzhorn LS, Kordes C, Megges M, Sawitza I, Götte S, Reichert D, Schulze-Matz P, Graffmann N, Bohndorf M, Wruck W, Köhler JP, Herebian D, Mayatepek E, Oreffo RO, Häussinger D, Adjaye J. Transplanted human pluripotent stem cell-derived mesenchymal stem cells support liver regeneration in Gunn rats. *Stem Cells Dev.* 2018; <https://doi.org/10.1089/scd.2018.0010>. Epub ahead of print.
51. Kuhn LT, Liu Y, Boyd NL, Dennis JE, Jiang X, Xin X, et al. Developmental-like bone regeneration by human embryonic stem cell-derived mesenchymal cells. *Tissue Eng Part A.* 2014;20:365–77.
52. Zhang J, Guan J, Niu X, Hu G, Guo S, Li Q, et al. Exosomes released from human induced pluripotent stem cells-derived MSCs facilitate cutaneous wound healing by promoting collagen synthesis and angiogenesis. *J Transl Med.* 2015;13:49.
53. Hawkins KE, Corcelli M, Dowding K, Ranzoni AM, Vlahova F, Hau KL, et al. Embryonic stem cell-derived mesenchymal stem cells (MSCs) have a superior neuroprotective capacity over fetal MSCs in the hypoxic-ischemic mouse brain. *Stem Cells Transl Med.* 2018;7:439–49.
54. Taleahmad S, Mirzaei M, Parker LM, Hassani SN, Mollamohammadi S, Sharifi-Zarchi A, et al. Proteome analysis of ground state pluripotency. *Sci Rep.* 2015;5:17985.
55. Freitas AA, Vasieva O, de Magalhães JP. A data mining approach for classifying DNA repair genes into ageing-related or non-ageing-related. *BMC Genomics.* 2011;12:27.
56. Greber B, Lehrach H, Adjaye J. Control of early fate decisions in human ES cells by distinct states of TGFbeta pathway activity. *Stem Cells Dev.* 2008;17: 1065–77.
57. James D, Levine AJ, Besser D, Hemmati-Brivanlou A. TGFbeta/activin/nodal signaling is necessary for the maintenance of pluripotency in human embryonic stem cells. *Development (Cambridge, England).* 2005;132:1273–82.
58. Vallier L. Cell cycle rules pluripotency. *Cell Stem Cell.* 2015;17:131–2.
59. Gonzales KA, Liang H, Lim YS, Chan YS, Yeo JC, Tan CP, et al. Deterministic restriction on pluripotent state dissolution by cell-cycle pathways. *Cell.* 2015; 162:564–79.
60. Mlody B, Wruck W, Martins S, Sperling K, Adjaye J. Nijmegen breakage syndrome fibroblasts and iPSCs: cellular models for uncovering disease-associated signaling pathways and establishing a screening platform for anti-oxidants. *Sci Rep.* 2017;7:Article 7516.
61. Eggemann T, Binder G, Brioude F, Maher ER, Lapunzina P, Cubellis MV, et al. CDKN1C mutations: two sides of the same coin. *Trends Mol Med.* 2014;20:614–22.
62. Andrews SC, Wood MD, Tunster SJ, Barton SC, Surani AM, John RM. Cdkn1c (p57Kip2) is the major regulator of embryonic growth within its imprinted domain on mouse distal chromosome 7. *BMC Dev Biol.* 2007;7:53.
63. Pullmann R, Juhaszova M, de Silanes IL, Kawai T, Mazan-Mamczarz K, Halushka MK, et al. Enhanced proliferation of cultured human vascular smooth muscle cells linked to increased function of RNA-binding protein HuR. *J Biol Chem.* 2005;280:22819–26.
64. Okano M, Bell DW, Haber DA, Li E. DNA methyltransferases Dnmt3a and Dnmt3b are essential for de novo methylation and mammalian development. *Cell.* 1999;99:247–57.
65. Ciccarone F, Malavolta M, Calabrese R, Guastafierro T, Bacalini MG, Reale A, et al. Age-dependent expression of DNMT1 and DNMT3B in PBMCs from a large European population enrolled in the MARK-AGE study. *Aging Cell.* 2016;15:755–65.
66. Tsay HJ, Wang P, Wang SL, Ku HH. Age-associated changes of superoxide dismutase and catalase activities in the rat brain. *J Biomed Sci.* 2000;7:466–74.
67. Saxton RA, Sabatini DM. mTOR signaling in growth, metabolism, and disease. *Cell.* 2017;168:960–76.
68. Baugé C, Girard N, Lhuissier E, Bazille C, Boumediene K. Regulation and role of TGFβ signaling pathway in aging and osteoarthritis joints. *Aging and Disease.* 2014;5:394–405.
69. Ruiz-León Y, Pascual A. Regulation of Beta-amyloid precursor protein expression by brain-derived neurotrophic factor involves activation of both the Ras and phosphatidylinositolide 3-kinase signalling pathways. *J Neurochem.* 2004;88:1010–8.
70. Silhol M, Bonnichon V, Rage F, Tapia-Arancibia L. Age-related changes in brain-derived neurotrophic factor and tyrosine kinase receptor isoforms in the hippocampus and hypothalamus in male rats. *Neuroscience.* 2005;132: 613–24.

71. Rocha CR, Lerner LK, Okamoto OK, Marchetto MC, Menck CF. The role of DNA repair in the pluripotency and differentiation of human stem cells. *Mutat Res*. 2013;752:25–35.
72. Hwang JH, Shim SS, Seok OS, Lee HY, Woo SK, Kim BH, et al. Comparison of cytokine expression in mesenchymal stem cells from human placenta, cord blood, and bone marrow. *J Korean Med Sci*. 2009;24:547–54.
73. Potian JA, Aviv H, Ponzio NM, Harrison JS, Rameshwar P. Veto-like activity of mesenchymal stem cells: functional discrimination between cellular responses to alloantigens and recall antigens. *J Immunol*. 2003;171:3426–34.
74. Aggarwal S, Pittenger MF. Human mesenchymal stem cells modulate allogeneic immune cell responses. *Blood*. 2005;105(4):1815–22.
75. Kalfalah F, Seggewiß S, Walter R, Tigges J, Moreno-Villanueva M, Bürkle A, et al. Structural chromosome abnormalities, increased DNA strand breaks and DNA strand break repair deficiency in dermal fibroblasts from old female human donors. *Aging (Albany NY)*. 2015;7:110–22.
76. Katagiri W, Osugi M, Kawai T, Hibi H. First-in-human study and clinical case reports of the alveolar bone regeneration with the secretome from human mesenchymal stem cells. *Head Face Med*. 2016;12:5.
77. Kawai T, Katagiri W, Osugi M, Sugimura Y, Hibi H, Ueda M. Secretomes from bone marrow-derived mesenchymal stromal cells enhance periodontal tissue regeneration. *Cytotherapy*. 2015 Apr;17:369–81.
78. Jeansson M, Gawlik A, Anderson G, Li C, Kerjaszki D, Henkelman M, et al. Angiopoietin-1 is essential in mouse vasculature during development and in response to injury. *J Clin Invest*. 2011;121:2278–89.
79. Pérez-Gómez E, Jerkic M, Prieto M, Del Castillo G, Martín-Villar E, Letarte M, et al. Impaired wound repair in adult endoglin heterozygous mice associated with lower NO bioavailability. *J Invest Dermatol*. 2014;134:247–55.
80. Sun H, Mi X, Gao N, Yan C, Yu FS. Hyperglycemia-suppressed expression of Serpine1 contributes to delayed epithelial wound healing in diabetic mouse corneas. *Invest Ophthalmol Vis Sci*. 2015;56:3383–92.
81. Marzano F, Ventura A, Caratuzzolo MF, Aiello I, Mastropasqua F, Brunetti G, et al. The p53 family member p73 modulates the proproliferative role of IGFBP3 in short children born small for gestational age. *Mol Biol Cell*. 2015; 26:2733–41.
82. Qu F, Wang J, Xu N, Liu C, Li S, Wang N, et al. WNT3A modulates chondrogenesis via canonical and non-canonical Wnt pathways in MSCs. *Front Biosci (Landmark Ed)*. 2013;18:493–503.

Ready to submit your research? Choose BMC and benefit from:

- fast, convenient online submission
- thorough peer review by experienced researchers in your field
- rapid publication on acceptance
- support for research data, including large and complex data types
- gold Open Access which fosters wider collaboration and increased citations
- maximum visibility for your research: over 100M website views per year

At BMC, research is always in progress.

Learn more biomedcentral.com/submissions



2.10 Transplanted human pluripotent stem cell-derived mesenchymal stem cells support liver regeneration in Gunn rats

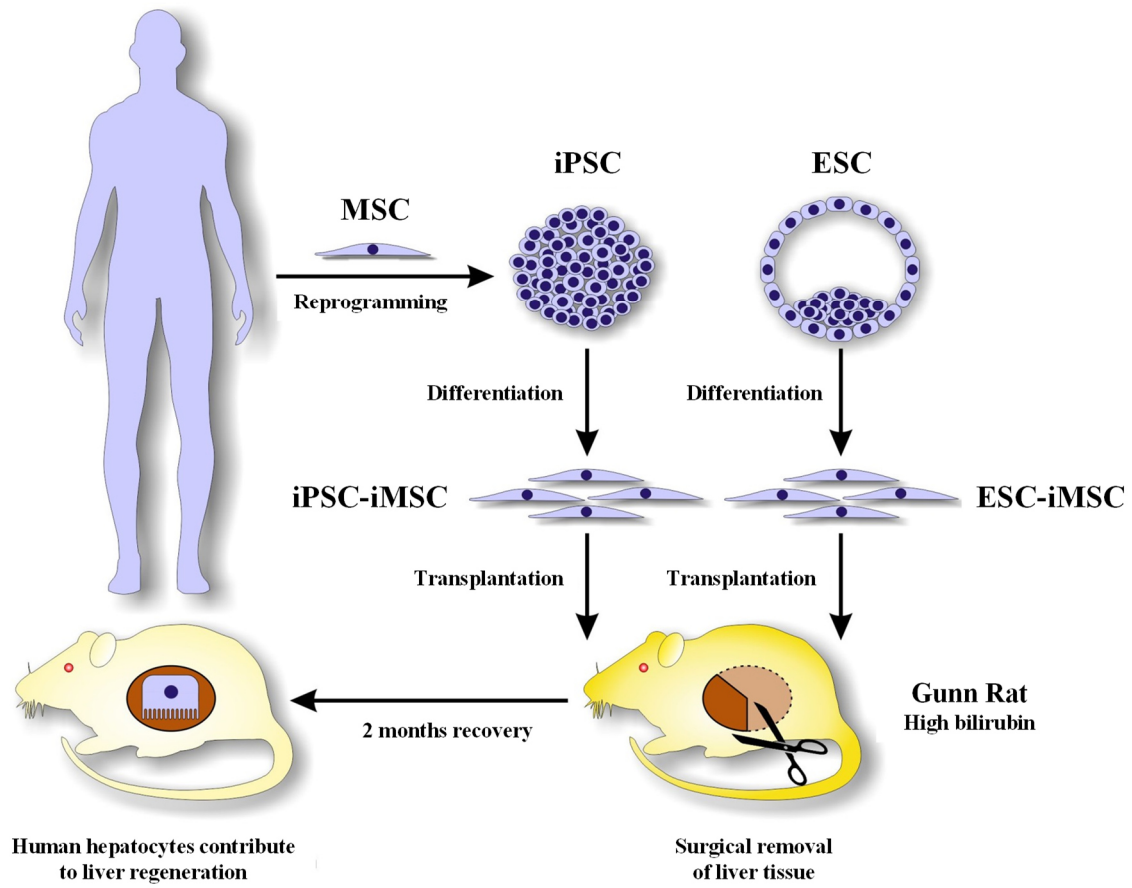
Lucas-Sebastian Spitzhorn*, Claus Kordes*, Matthias Megges, Iris Sawitza, Silke Götze, Doreen Reichert, Peggy Schulze-Matz, Nina Graffmann, Martina Bohndorf, Wasco Wruck, Jan Philipp Köhler, Diran Herebian, Ertan Mayatepek, Richard O.C. Oreffo, Dieter Häussinger and James Adjaye

*These authors contributed equally to this work.

Abstract

Gunn rats bear a mutation within the uridine diphosphate glucuronosyltransferase-1A1 (Ugt1a1) gene resulting in high serum bilirubin levels as seen in Crigler-Najjar syndrome. In the present study, the Gunn rat was used as an animal model for heritable liver dysfunction. Human mesenchymal stem cells (iMSC) derived from embryonic stem cells (H1) and induced pluripotent stem cells were transplanted into Gunn rats after partial hepatectomy. The iMSCs engrafted and survived in the liver for up to 2 months. The transplanted iMSCs differentiated into functional hepatocytes as evidenced by partially suppressed hyperbilirubinemia and expression of multiple human-specific hepatocyte markers such as Albumin, hepatocyte nuclear factor 4 α , UGT1A1, Cytokeratin 18, bile salt export pump, multidrug resistance protein 2, Na/taurocholate-cotransporting polypeptide and α -Fetoprotein. These findings imply that transplanted human iMSCs can contribute to liver regeneration *in vivo* and thus represent a promising tool for the treatment of inherited liver diseases.

Graphical Abstract



Publication Status: published in *Stem Cells and Development*. 2018 Dec 7; 27(24)

Impact Factor: 3.315

This article is reproduced with permission.

Approximated total share of contribution: 40%

Contribution on experimental design, realization and publication:

JA, DH, LSS and CK conceived the idea and designed the experiments. ROCO provided the foetal MSCs. LSS, MM and MB generated and characterized the iPSCs. LSS and MM generated the iMSCs. JPK performed the staining for fibrosis -associated proteins. SG, PSM, NG and DR did the real time PCR analysis. DH and EM were responsible for the bile acid measurements. CK, IS and DR performed the operations and the cell transplantations. CK and LSS performed the serum analysis and the liver tissue stainings. WW did the Bioinformatical analysis. CK and LSS designed the figures and wrote the manuscript. JA and DH edited and finally approved the manuscript. All authors reviewed and approved the submitted version.

Link to the publication:

https://www.liebertpub.com/doi/abs/10.1089/scd.2018.0010?url_ver=Z39.88-2003&rfr_id=ori:rid:crossref.org&rfr_dat=cr_pub%3dpubmed

Transplanted Human Pluripotent Stem Cell-Derived Mesenchymal Stem Cells Support Liver Regeneration in Gunn Rats

Lucas-Sebastian Spitzhorn,^{1,*} Claus Kordes,^{2,*} Matthias Megges,¹ Iris Sawitzka,² Silke Götze,² Doreen Reichert,² Peggy Schulze-Matz,¹ Nina Graffmann,¹ Martina Bohndorf,¹ Wasco Wruck,¹ Jan Philipp Köhler,² Diran Herebian,³ Ertan Mayatepek,³ Richard O.C. Oreffo,⁴ Dieter Häussinger,^{2,†} and James Adjaye^{1,†}

Gunn rats bear a mutation within the uridine diphosphate glucuronosyltransferase-1a1 (*Ugt1a1*) gene resulting in high serum bilirubin levels as seen in Crigler-Najjar syndrome. In this study, the Gunn rat was used as an animal model for heritable liver dysfunction. Induced mesenchymal stem cells (iMSCs) derived from embryonic stem cells (H1) and induced pluripotent stem cells were transplanted into Gunn rats after partial hepatectomy. The iMSCs engrafted and survived in the liver for up to 2 months. The transplanted iMSCs differentiated into functional hepatocytes as evidenced by partially suppressed hyperbilirubinemia and expression of multiple human-specific hepatocyte markers such as albumin, hepatocyte nuclear factor 4 α , *UGT1A1*, cyto-keratin 18, bile salt export pump, multidrug resistance protein 2, Na/taurocholate-cotransporting polypeptide, and α -fetoprotein. These findings imply that transplanted human iMSCs can contribute to liver regeneration in vivo and thus represent a promising tool for the treatment of inherited liver diseases.

Keywords: ESC, iPSC, iMSC, stem cell transplantation, liver regeneration, fetal MSC

Introduction

THE CRIGLER-NAJJAR SYNDROME was first reported in 1952 as an inherited disorder causing jaundice and kernicterus in newborns [1]. To date, phototherapy remains the standard treatment option to prevent the neurotoxic effects of increased bilirubin levels [2]. Phototherapy significantly influences patient's quality of life and can cause DNA damage [3]. Other treatment options such as liver transplantation, liver-directed gene therapy [4], and hepatocyte transplantation [5] require matching donors or involve suppression of the recipient's immune system. Thus, there is an urgent unmet need for alternative treatment options for Crigler-Najjar syndrome. The Gunn rat serves as an animal model to study Crigler-Najjar syndrome 1. Gunn rats have a mutation in the uridine diphosphate glucuronosyltransferase-1a1 (*Ugt1a1*) gene associated with decreased glucuronidation and excretion of bilirubin leading to hyperbilirubinemia [6].

Mesenchymal stem cells (MSCs) are currently under investigation for the treatment of liver diseases. The main

reasons for the application of MSCs reside in their ability to home-in into sites of injury and modulate the immune system by secretion of supportive factors that make them widely used for treating graft-versus-host disease. The potential of MSCs to develop into bone, cartilage, and fat cells and the presence of the cell surface markers CD73, CD90, CD105, CD146, and platelet-derived growth factor receptor β (PDGFR β) are well established and often used as criteria for characterizing them [7,8]. In addition, MSCs are reported to be able to differentiate into other organ-specific cells such as functional liver cells in vitro and in vivo [9,10]. An increasing number of studies have shown that MSCs can contribute to liver regeneration either directly or indirectly through the secretion of beneficial trophic factors [11]. However, some studies have reported that MSCs can also exert adverse effects, such as contributing to fibrosis in several organs [12,13].

Most researchers typically use MSCs from distinct sources such as bone marrow, cord blood, adipose tissue, and amniotic fluid [14]. The use of these MSCs is wrought with

¹Institute for Stem Cell Research and Regenerative Medicine, ²Clinic of Gastroenterology, Hepatology and Infectious Diseases, and ³Department of General Pediatrics, Neonatology and Pediatric Cardiology, Heinrich Heine University, Düsseldorf, Germany.

⁴Centre for Human Development, Stem Cells and Regeneration, Faculty of Medicine, University of Southampton, Southampton, United Kingdom.

*These two authors contributed equally to this work.

[†]Shared senior authorship.

HUMAN iMSCs SUPPORT LIVER REGENERATION IN GUNN RATS**1703**

several limitations such as limited expansion. In light of this, the concept of generating MSCs from induced pluripotent stem cells (iPSCs) is of great interest for stem cell-based therapies given their potential immunosuppressive and regenerative properties, which are maintained in pluripotent stem cell-derived MSCs, termed induced MSCs (iMSCs). It has been shown that iMSCs have the typical mesenchymal morphology, in vitro differentiation potential, cell surface marker expression, and similar transcriptomes to bone marrow-derived MSCs [15]. Interestingly, iMSCs seem to be more potent than their native counterpart [16,17]. Furthermore, the regenerative potential of iMSCs has been demonstrated in animal models of diseases such as multiple sclerosis, limb ischemia, autoimmunity and hypoxic ischemia [16–20].

It has been shown that bone marrow-derived MSCs and hepatocyte-like cells from human iPSCs can improve the disease phenotype in Gunn rats [21,22]. In this study, we addressed the question whether iMSCs from human embryonic stem cells (ESCs) and human iPSCs are an alternative cell source for the regeneration of hereditary liver defects in vivo. The iMSCs derived from both sources were transplanted through the spleen into Gunn rats with an injured liver (partial hepatectomy). By adopting this approach, we could show the ability of the iMSCs to (1) home into the injured liver, (2) bypass rejection by the host immune system, and (3) acquire hepatocyte expression and function, thereby supporting regeneration of the injured liver.

Materials and Methods*Generation of iMSCs*

Fetal MSCs (fMSCs, 55 days postconception) [23,24] were obtained from human femur following informed written patient consent and approval (Southampton and South West Hampshire Local Research Ethics Committee, LREC 296100). The experimental use of human fMSCs was approved by the ethics commission of the Heinrich Heine University, Düsseldorf. The fMSCs were cultured in α -MEM (minimum essential medium Eagle–alpha modified; Sigma-Aldrich, Taufkirchen, Germany) supplemented with 10% fetal bovine serum (FBS), 1% GlutaMAX, and 1% penicillin/streptomycin (fMSC medium). iMSCs were generated from human fMSCs after establishing an iPSC line [24] and from the ESC line H1 (WiCell Research Institute, Madison, WI) as previously described [25]. Experiments with the human ESC line H1 and the derived iMSCs, and their application in this study were approved by the Robert Koch Institute, Germany (AZ:3.04.02/0132). Briefly, iPSCs and ESCs were cultured without feeder cells on Matrigel (Becton Dickinson, Heidelberg, Germany) using StemMACS iPS-Brew XF, human (Miltenyi Biotec, Bergisch Gladbach, Germany), with 1% penicillin/streptomycin in humidified atmosphere with 5% CO₂ at 37°C, with daily change of medium.

When confluency was reached, the medium was changed to α -MEM (see fMSC medium) and the pluripotent cells were treated daily with 10 μ M of the transforming growth factor- β (TGF- β) receptor inhibitor SB-431542 (Miltenyi Biotec) for 14 days. Afterward, the emerged iMSCs were trypsinized using TrypLE Express (Thermo Fisher Scientific, Waltham, MA) for 10 min at 37°C, centrifuged at 300 g for 5 min, and seeded onto uncoated culture dishes in an MSC expansion medium

(see fMSC medium), which led to the depletion of cells with maintained iPSC characteristics. Further passaging was carried out as described above when cells reached about 95% confluency. The cells were seeded at 1×10^6 cells per 175 cm².

Transcriptome analysis

Microarray experiments were performed on the PrimeView Human Gene Expression Array platform (Affymetrix; Thermo Fisher Scientific), the data are provided online at the National Center of Biotechnology Information (NCBI) Gene Expression Omnibus (<https://www.ncbi.nlm.nih.gov/geo/query/acc.cgi?acc=GSE97692>). The unnormalized bead-summary data were further processed through the R/Bioconductor environment employing the package affy (<http://bioconductor.org/packages/release/bioc/html/affy.html>). Using this package, the data were background-corrected, transformed to a logarithmic scale (to the base 2), and normalized by applying the Robust Multi-array Average normalization method.

Immunophenotyping by flow cytometry

The cell surface marker expression of the fMSCs and iMSCs was analyzed by using the human MSC Phenotyping Kit Human (# 130-095-198) from Miltenyi Biotec. To conduct this analysis, 200,000 detached cells were distributed into two 5 mL flow cytometry tubes in 100 μ L phosphate-buffered saline (PBS). The phenotyping cocktail (0.5 μ L) containing antibodies against CD14-PerCP, CD20-PerCP, CD34-PerCP, CD45-PerCP, CD73-APC, CD90-FITC, and CD105-PE or the isotype control cocktail was then applied. After 10 min of incubation at 4°C, the cells were washed and resuspended in 100 μ L paraformaldehyde (PFA 4%) for flow cytometric analysis (FACS Canto from BD Biosciences, Heidelberg, Germany). The histograms were generated using the FlowJo V10 Software (FlowJo LLC, Ashland, OR).

Trilineage differentiation of MSCs

Differentiation of the fMSCs and iMSCs into adipocytes, chondrocytes, and osteoblasts was carried out for 3 weeks using the STEMPRO Adipogenesis/Chondrogenesis/Osteogenesis Differentiation Kit (Thermo Fisher Scientific). Afterward, the cells were fixed with PFA (4%) and stained with 0.2% Oil Red O (adipocyte differentiation), 1% Alcian Blue (chondrocyte differentiation), or 2% Alizarin Red S (osteoblast differentiation) solutions according to standard protocols.

Cell proliferation analyses

The cell proliferation capacity of the fMSCs, iPSC-iMSCs, and ESC-iMSCs was measured by the incorporation of bromodeoxyuridine (BrdU) using the cell proliferation enzyme-linked immunosorbent assay (ELISA), BrdU (colorimetric) kit (Roche, Basel, Switzerland), according to the manufacturer's instructions. The cells were seeded at 30,000 cells per well in a 96-well flat-bottom plate in triplicates. BrdU (100 μ M) was added 24 h later for an incorporation time of 21 h. Cells were fixed, BrdU antibodies coupled with peroxidase were added for 90 min, and the substrate applied for 30 min. The colorimetric reaction was measured using an

1704

SPITZHORN ET AL.

ELISA reader (Biotech Instruments, Heilenpark, Germany) (dual, wavelength 655–490 nm).

Short tandem repeat analysis

The genetic background of cells was analyzed by short tandem repeat (STR) using genomic DNA. For isolation of genomic DNA, the GeneMATRIX DNA/RNA/Protein Universal Purification Kit (Roboclon, Berlin, Germany) was used. For polymerase chain reaction (PCR), 5 μ L 1 \times Go-Taq G2 Hot Start Green PCR buffer, 4 mM MgCl₂, 0.5 μ L dNTP Mix (10 mM each), 1 μ L forward primer (0.3 μ M), 1 μ L reverse primer (0.3 μ M) (sequences are given in Supplementary Table S1; Supplementary Data are available online at www.liebertpub.com/scd), 0.125 μ L (0.625 U) Hotstart Taq Polymerase (5 U/ μ L), and 100 ng genomic DNA were mixed. Water was added to adjust a final volume of 25 μ L. The PCR was performed in a thermal cycler (PEQLAB, Erlangen Germany) starting with 5 min of initial denaturation at 94°C followed by 32 cycles comprising a denaturation step at 94°C for 15 s, an annealing step at 60°C for 30 s, and an extension step at 68°C for 60 s (D7S796 and D21S2055). For other STR primers, the PCR program was used as described [26]. Detection of PCR amplification products was done by gel electrophoresis (2.5% agarose gels).

Liver injury model and cell transplantation

Gunn rats with mutated *Ugt1a1* [6] were obtained from the Rat Resource & Research Centre (RRRC, Columbia, MO) and maintained at the animal facility of the Heinrich Heine University (Düsseldorf, Germany). Immunocompetent female Gunn rats with homozygous mutation were anesthetized by combined ketamine (100 mg/kg) and xylazine (10 mg/kg) injection and the two largest liver lobes were surgically removed (70% of the liver, partial hepatectomy [PHX]) essentially as described [27]. Immediately after PHX, while the abdomen was still open, ~4 million fMSCs ($n=4$), ESC-iMSCs ($n=3$), or iPSC-iMSCs ($n=3$) from male human donors were transplanted into rats through the spleen. For this, the cells were trypsinized, resuspended in 300 μ L Ringer lactate buffer, filtered through a mesh (40 μ m), and injected into the tip of the spleen using G30 syringes. One rat (T7) that received iPSC-iMSCs showed internal bleeding in the uterus with low bilirubin serum levels and was, therefore, excluded from further analysis. Control Gunn rats underwent PHX ($n=4$), but received no cell transplantation. After 2 months of recovery, the animals were sacrificed by loss of blood during anesthesia. The livers were then perfused with physiologic buffer and snap-frozen in liquid nitrogen. The animal experiments were approved by the relevant federal state authority for animal protection (Landesamt für Natur, Umwelt und Verbraucherschutz Nordrhein-Westfalen, Recklinghausen, Germany; Reference No. 84-02.04.2012.A344).

Serum and culture supernatant analysis

To determine the presence of albumin (ALB) in the blood of Gunn rats 2 months after transplantation of human iMSCs and control animals, the blood was collected from the portal vein and diluted 1:10,000. Human serum samples from three

individuals were diluted 1:1,000,000, whereas culture supernatants from fMSCs and iMSCs were taken without dilution. These samples were analyzed by an ELISA specific for human ALB according to the manufacturer's recommendations (human ELISA quantitation set, # E80-129; Bethyl Laboratories, Montgomery). The concentration of total ALB, lactate dehydrogenase (LDH), alanine transaminase (ALT), and aspartate transaminase (AST) in the serum was quantified by a Spotchem EZ SP-4430 using diagnostic test strips for multiparameter analysis (# 77182; Arkray Europe, Amstelveen, Netherlands). The concentration of total bilirubin in the serum was measured using the colorimetric Bilirubin Assay kit (MAK126; Sigma-Aldrich). A cytokine array was performed according to the protocol from Proteome Profiler Human Cytokine Array Panel A (R&D Systems) using 0.4 mL of Gunn rat serum. The emitted chemiluminescence was analyzed by measuring the pixel density of each spot on the array membrane, including reference and negative control spots.

Analysis of bile acids and their conjugates

Bile acids were analyzed by ultra-high performance liquid tandem mass spectrometry (UHPLC-MS/MS) essentially as described [28]. The system consists of a UHPLC-I class (Waters, United Kingdom) coupled to a Xevo TQ-S triple quadrupole mass spectrometer (Waters). Electrospray ionization was performed in the negative ionization mode. Chromatographic separation was performed on a BEH C18 column (2.1 \times 100 mm, 1.7 μ m). The mobile phase consisted of water containing 0.1% formic acid and 5 mM ammonium acetate (Eluent A) and acetonitrile (Eluent B). Analytes were separated by gradient elution. The injection volume was 5 μ L and the column was maintained at 40°C. Detection of the bile acids and their glycine and taurine conjugates was performed in selected reaction monitoring mode. All standards as well as the deuterated internal standard substance (d4-CA, d4-GCA and d5-TCA) were purchased from Sigma-Aldrich and Steraloids (Newport).

Reverse transcriptase-PCR

Human-specific primers (Supplementary Table S1) were generated to detect human mRNA in Gunn rat liver. Total RNA was isolated from five different liver pieces of each rat using the RNeasy Mini kit (Qiagen, Hilden, Germany) according to the manufacturer's recommendations. First-strand cDNA was made from 1 μ g total RNA per 20 μ L reaction volume (RevertAid H Minus First Strand cDNA Synthesis Kit; Thermo Fisher Scientific). A standard protocol using the 2 \times PCR Master Mix (Thermo Fisher Scientific), 0.8 μ M primers, and 5 μ L template cDNA per 25 μ L reaction volume was used to obtain PCR products by conventional PCR. For quantitative real-time PCR (qPCR), 12.5 ng cDNA per sample, 0.6 μ M primers, and the Power Sybr Green Master Mix (Life Technologies) were used. Universal β -actin primers for humans and rats served as a reference gene for the normalization of values calculated by the 2^{- $\Delta\Delta$ CT} method. Human samples of normal liver tissue from patients with tumors were used as a reference to assess the abundance of iMSC-derived cells within Gunn rat tissue. A written consent was given by the patients and the usage of

HUMAN iMSCs SUPPORT LIVER REGENERATION IN GUNN RATS**1705**

liver samples for research was approved by the local ethics committee of the Medical Faculty of the Heinrich Heine University Düsseldorf (Germany).

Immunohistochemistry and immunofluorescence analysis

For immunohistochemistry, tissue sections were made from frozen livers and fixed with 4% formalin for 20 min. The fixed sections were treated with 0.1% Triton X-100, washed in PBS, and endogenous peroxidases were blocked (dual endogenous enzyme block, # S2003; Dako, Glostrup, Denmark). Unspecific binding of antibodies was prevented by the treatment with 10% FBS in PBS supplemented with 0.1% saponin. A mouse antibody against the human cytosolic protein Stem121 (# Y40410; Takara Bio USA, Mountain View, CA) and anti-mouse immunoglobulins coupled with horseradish peroxidase (# AP192P; Merck Millipore, Darmstadt, Germany) were used for diaminobenzidine (DAB) staining (# K346711-2; Dako). The cell nuclei were counterstained by diluted hematoxylin solution (1:5, # 1.05175.0500; Merck Millipore). For the identification of liver cell types, DAB-stained sections were treated with monoclonal antibodies against CK18 (# BM2275P; Acris, Herford, Germany) or HNF4 α (# 3113; Cell Signaling, Danvers, MA). The primary antibodies were then labeled by Cy3-conjugated secondary antibodies directed against mouse or rabbit immunoglobulins (# AP192C, # AP182C; Merck-Millipore). Antibodies against Collagen 1 (# C2456; Sigma-Aldrich), Collagen 4 (# ab6586; Abcam, Cambridge, United Kingdom), OCT4-A (# C30A3; Cell Signaling), and PDGFR β (# 3169S; Cell Signaling) were used for immunofluorescence of liver sections and cultured cells. The sections were fixed with ice-cold methanol, whereas 4% PFA was used to fix cultured cells. Appropriate secondary Cy3-, FITC-, or Alexa Fluor 555-labeled antibodies (# AP182C/F, # AP192C/F; Merck-Millipore, # A-21428; Thermo Fisher Scientific) and 4',6-diamidino-2-phenylindole (DAPI Fluoromount G, # 0100-20; Southern Biotech, Birmingham, AL) or Hoechst 33258 dye (1:5,000; Sigma-Aldrich) were applied to mark primary antibodies and cell nuclei, respectively.

Fluorescence in situ hybridization

Fluorescence in situ hybridization (FISH) was carried out after fixation of liver cryosections with Carnoy's solution (75% methanol and 25% acetic acid) followed by pepsin digestion (0.05 mg/mL pepsin from Roche in 0.01 N chloric acid). Human-specific Y chromosome probe (#D-0324-100-OR; MetaSystems, Altlußheim, Germany) and rat-specific X chromosome probe (#IDRF1067; Empire Genomics, Buffalo, NY) were dissolved in a hybridization solution (Empire Genomics) and hybridized with the sections overnight at 37°C after an initial denaturation at 75°C. After washing with saline sodium citrate, the sections were covered with a mounting medium (DAPI Fluoromount G; Southern Biotech).

Statistics

All data were indicated as arithmetic mean \pm standard error of mean. Statistical analysis was performed by Student's *t*-test and ANOVA (analysis of variance). *P* values of

<0.05 were considered significant and indicated by different letters in the graphs.

Results**Human ESC- and iPSC-derived iMSCs are functional MSCs**

Human iMSCs were derived from the ESC line H1 (ESC-iMSCs) and iPSCs from fetal MSCs (iPSC-iMSCs) by inhibition of TGF- β signaling with SB-431542 for 14 days. This treatment resulted in the downregulation of the pluripotency-regulating octamer-binding transcription factor 4 (OCT4), resulting in the acquisition of the typical fibroblast-like cell morphology as well as expression of MSC surface markers such as PDGFR β (Fig. 1A). The transcriptomes of iMSCs from both sources were compared with the transcriptomes of iPSCs, ESCs, and fMSCs by microarray analysis (Fig. 1B). The iMSCs from ESCs and iPSCs expressed molecular markers typical of MSCs, namely *CD44*, *CD73*, *CD105*, *CD146*, and *PDGFR β* . In addition, expression of pluripotency-regulating transcription factors—*OCT4*, *SRY* (sex-determining region Y)-box 2 (*SOX2*), and *NANOG*—was downregulated in iMSCs both at the mRNA and protein level (Fig. 1A, B). In line with this, Pearson correlation analysis of the transcriptome data showed a low correlation of iMSCs with their pluripotent precursor cells and high correlation (R^2 values 0.944 and 0.966) with fMSCs (Fig. 1C), which was also mirrored by cluster analysis (Supplementary Fig. S1A). STR analysis confirmed the same genetic background for (1) fMSCs, iPSCs, and iPSC-iMSCs, and (2) ESC and ESC-iMSCs, as indicated by distinct banding patterns (Supplementary Fig. S1B).

Flow cytometry-based analysis revealed comparable MSC surface marker expression (*CD73*, *CD90*, and *CD105*) in iMSCs and fMSCs (Fig. 2A–I), and markers of hematopoietic cells were absent (Fig. 2J–L). Statistical analysis revealed no significant differences between iMSCs and the fMSCs with respect to these cell surface markers. Furthermore, the fMSCs as well as the iMSCs displayed a spindle-shaped, fibroblast-like morphology (Fig. 3A1–A3). Similar to fMSCs, iMSCs from ESCs and iPSCs were observed to differentiate into adipocytes with characteristic fat droplets following treatment with an adipocyte differentiation medium, as evidenced by Oil Red O staining (Fig. 3B1–B3). A typical differentiation along the chondrogenic and osteogenic cell lineages was demonstrated for iMSCs, as seen in fMSCs (Fig. 3C1–D3). A BrdU ELISA was performed to determine the relative cell proliferation capacity showing that fMSCs were significantly more proliferative than iPSC-iMSCs and ESC-iMSCs, whereas no significant difference was observed when the two iMSC populations were compared (Supplementary Fig. S2).

The iMSCs neither expressed nor secreted human ALB as investigated by transcriptome analysis and an ELISA specific for human ALB (Fig. 4A, B). In addition, other hepatocyte-specific markers such as hepatocyte nuclear factor 4 α (*HNF4 α*), *UGT1A1*, bile salt export pump (*BSEP*), multidrug resistance protein 2 (*MRP2*), Na/taurocholate-cotransporting polypeptide (*NTCP*), and α -fetoprotein (*AFP*) were also not expressed. In contrast to this, connective tissue proteins such as collagens (*COL1 α 2*, *COL4 α 1*), connective tissue growth factor, and α -smooth muscle actin (α -*SMA*) were detected at the mRNA level (Fig. 4A).

1706

SPITZHORN ET AL.

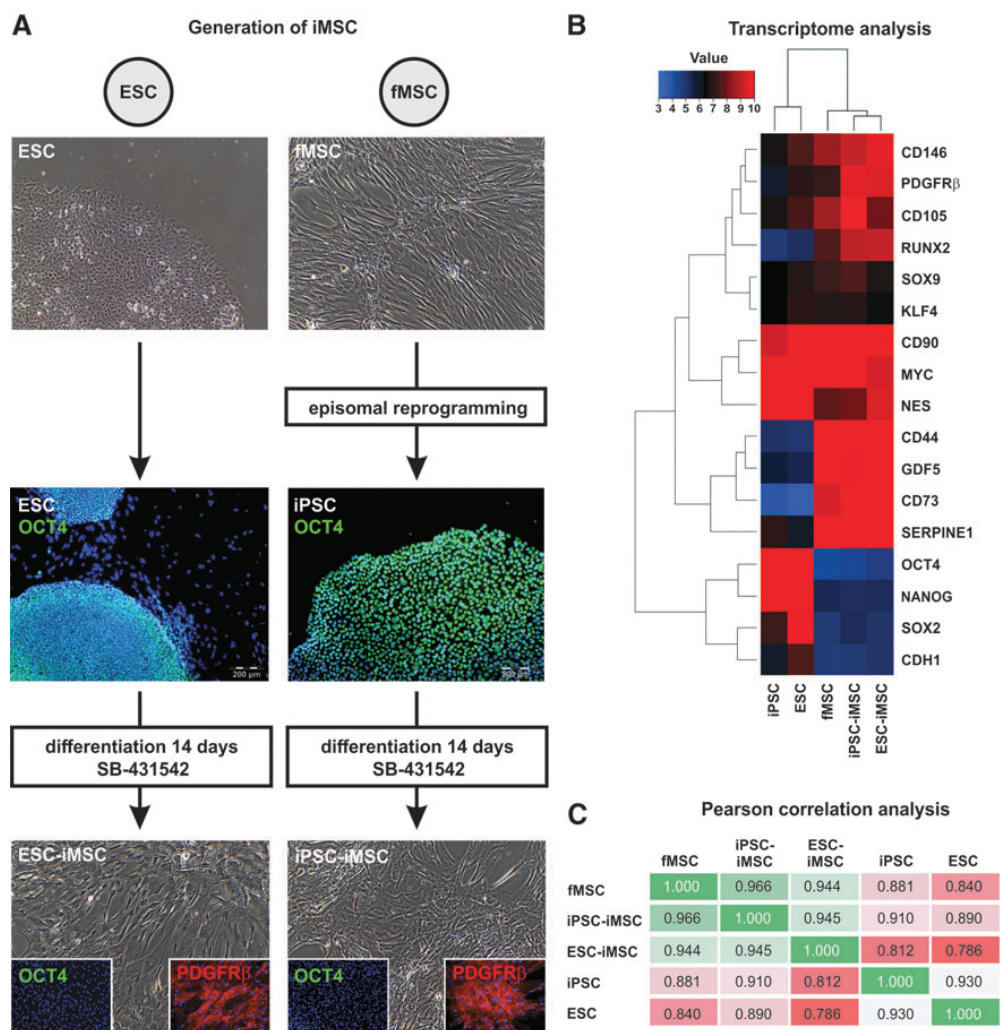


FIG. 1. Characterization of iMSCs by immunofluorescence and transcriptome analysis. **(A)** Scheme of iMSC generation from the human ESC line H1 and fMSCs. ESCs expressing the pluripotency-associated marker OCT4 were treated with the TGF- β receptor inhibitor SB-431542 for 14 days to facilitate their differentiation into iMSCs, concomitant with the loss of OCT4 expression and the appearance of fibroblast-shaped cells expressing the MSC marker PDGFR β . To generate iMSCs from fMSCs, the cells were first reprogrammed into pluripotent OCT4-expressing iPSCs using plasmids encoding the pluripotency factors *OCT4*, *SOX2*, *c-MYC*, *KLF4*, *NANOG*, and *LIN28*. After treatment with SB-431542, the iPSCs differentiated into OCT4⁻/PDGFR β ⁺ iMSCs as observed for ESC-iMSCs. Cell nuclei were stained with Hoechst 33258 (blue), OCT4 with FITC (green), and PDGFR β with Cy3 (red). **(B)** ESC- and iPSC-derived iMSCs were characterized by gene expression array analysis (Euclidean correlation analysis). The transcriptome analysis was performed once for a representative preparation of each cell type. **(C)** Pearson correlation analysis of these transcriptome data revealed a high correlation (green) of both iMSCs with fMSCs, but low correlation (red) with their pluripotent precursors (ESCs and iPSCs). Scale bars indicate 200 μ m. ESC, embryonic stem cell; fMSC, fetal mesenchymal stem cell; iMSC, induced mesenchymal stem cell; iPSC, induced pluripotent stem cell; OCT4, octamer-binding transcription factor 4; PDGFR β , platelet-derived growth factor receptor β ; SOX2, SRY (sex-determining region Y)-box 2; TGF- β , transforming growth factor- β .

Engraftment and differentiation of transplanted iMSCs

After surgical removal of about 70% of the liver (partial hepatectomy/PHX), ESC-iMSCs, iPSC-iMSCs, or fMSCs were immediately transplanted into Gunn rats with homozygous *Ugt1a1* mutation through spleen injection without

immunosuppression. The rats were allowed to recover from liver injury over 2 months, to investigate long-term effects of transplanted human iMSCs. Afterward, engraftment of transplanted ESC- and iPSC-iMSCs was seen in five out of six animals (83%) by analysis of human ALB in Gunn rat blood serum as shown by human-specific ELISA for ALB, whereas ALB was not released by cultured iMSCs (Fig. 4B,

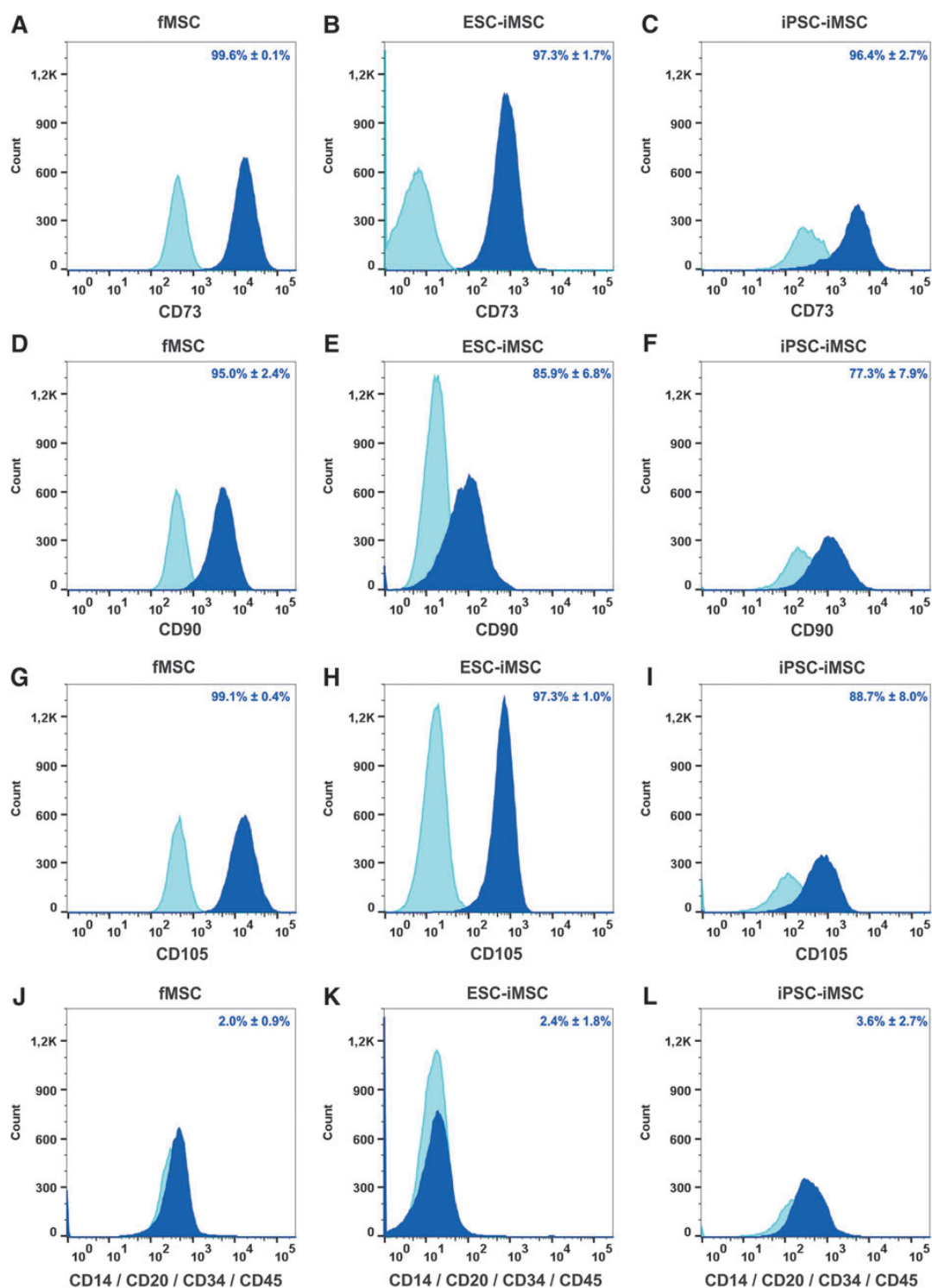


FIG. 2. Characterization of fMSCs and iMSCs by flow cytometry. The MSC markers (A–C) CD73, (D–F) CD90, and (G–I) CD105 were detectable as cell surface proteins on fMSCs and iMSCs derived from ESCs and iPSCs, whereas the expression of hematopoietic markers (J–L) CD14, CD20, CD34, and CD45 was low (dark blue). Light blue histograms represent antibody isotype controls. Representative data of repeated analysis of each cell type are shown (fMSCs $n=4$; ESC-iMSCs $n=3$; and iPSC-iMSCs $n=4$). The percentage of positive cells for particular cell surface markers is indicated as a mean \pm SEM of different analysis. SEM, standard error of mean.

1708

SPITZHORN ET AL.

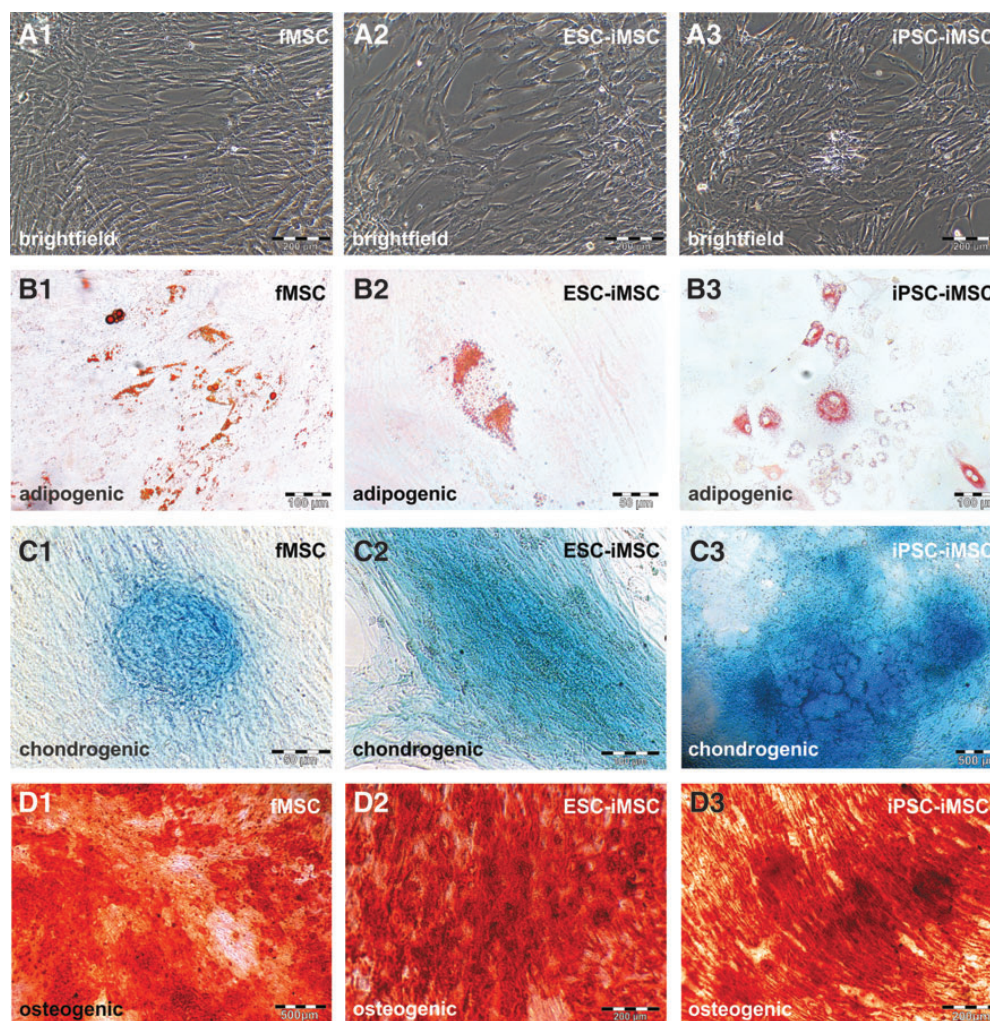


FIG. 3. Functional characterization of fMSCs and iMSCs. To test the developmental potential of iMSCs by qualitative assays, differentiation media for adipogenic (fMSC: $n=7$; ESC-iMSC: $n=3$; and iPSC-iMSC: $n=3$), chondrogenic (fMSC: $n=2$; ESC-iMSC: $n=3$; and iPSC-iMSC: $n=2$), and osteogenic (fMSC: $n=5$; ESC-iMSC: $n=3$; and iPSC-iMSC: $n=3$) development were applied for 21 days. (A1–D1) fMSCs and iMSCs (A2–D2, ESC-iMSCs; A3–D3, iPSC-iMSCs) showed (A1–A3) fibroblast-like morphology and were able to differentiate into (B1–B3) adipocytes (Oil Red O-stained lipid droplets), (C1–C3) chondrocytes (Alcian Blue 8GX marked glycosaminoglycans in cartilage), and (D1–D3) osteoblasts (Alizarin Red stained calcium deposits). Scale bars indicate 50 μm (B2, C1), 100 μm (B1, B3, C2, D1), 200 μm (A1–A3, D2, D3), and 500 μm (C3, D1).

C). Approximately 1%–4% (0.03–0.13 g/dL) of total albumin (rat and human) was of human origin. The total albumin concentration in the transplantation and control groups remained unchanged at 3.2 g/dL. Transplanted iPSC-iMSCs showed lower ALB concentrations in host rat serum (Fig. 4C) and one animal of this group exhibited no signs of engraftment (Supplementary Table S2). Engraftment of transplanted fMSCs was only found in one of four rats and, therefore, not included in detailed analysis (Supplementary Table S2).

To determine the effects of transplanted iMSCs on the disease phenotype of Gunn rats, total bilirubin concentration was measured and found to be reduced by ~31% (ESC-iMSCs) and 22% (iPSC-iMSCs) in Gunn rats of the transplanted

groups compared to control (Fig. 4D), indicating partially suppressed hyperbilirubinemia.

The presence of human ALB in the sera of Gunn rats after iMSC transplantation was confirmed at the mRNA level by qPCR employing human-specific primers (Fig. 5A). The relative amount of human *ALB* mRNA in Gunn rat liver was ~2%–3% when mRNA samples of human liver tissues were used as a reference and set to 100% (Fig. 5A). However, the abundance of human *ALB*-expressing cells was found to be variable in distinct areas of each single liver and varied between 0% and 18%. The expression of human hepatocyte markers within rat liver tissue was further detected by human-specific primer sets for *UGT1A1*,

HUMAN iMSCs SUPPORT LIVER REGENERATION IN GUNN RATS

1709

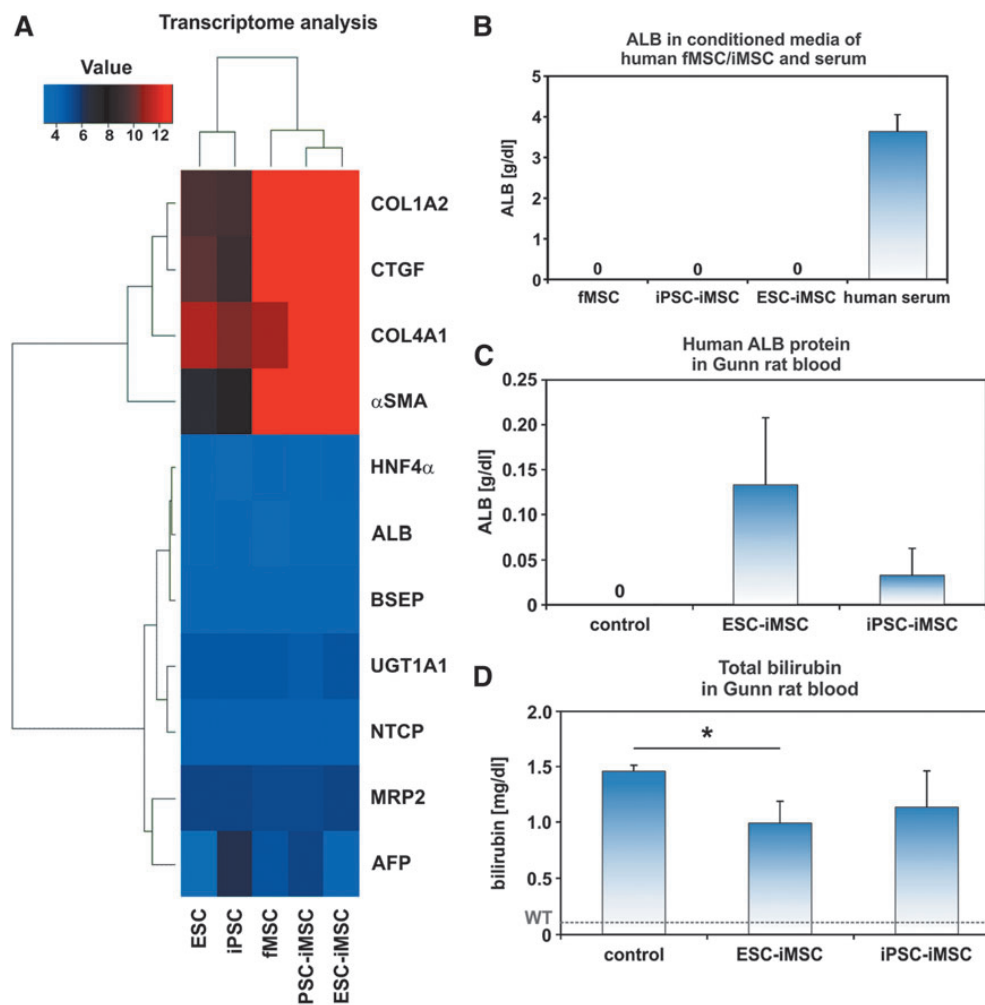


FIG. 4. Transplanted human iMSCs acquired hepatocyte functions in host Gunn rats. **(A)** Transcriptome analysis confirmed the lack of hepatocyte marker expression in pluripotent stem cells as well as fMSCs and iMSCs before transplantation, but indicated an expression of connective tissue markers and α -SMA (Euclidean correlation analysis), which are typically expressed by MSCs. The transcriptome analysis was performed once for a representative preparation of each cell type. **(B)** Moreover, cultured fMSCs and iMSCs did not secrete ALB into the culture medium as determined by a human-specific ALB ELISA. The normal level of ALB in human blood serum of healthy volunteers is indicated as a mean (3.6 g/dL; $n=3$). **(C)** A differentiation of the transplanted human ESC-iMSCs and iPSC-iMSCs into hepatocytes was indicated by the presence of human ALB within the serum of Gunn rats. **(D)** The total bilirubin concentration in blood significantly decreased in Gunn rats after transplantation of human ESC-iMSCs, but reached no significance for iPSC-iMSCs (**C, D**: control $n=4$; ESC-iMSC: $n=3$; iPSC-iMSC: $n=3$; $*P<0.05$). The mean bilirubin level of normal wild-type rats (WT, 0.1 mg/dL) is indicated by a broken line [29]. ALB, albumin; α -SMA, α -smooth muscle actin; ELISA, enzyme-linked immunosorbent assay.

HNF4 α , *BSEP*, *NTCP*, *MRP2*, cytochrome P450 1A2 (*CYP1A2*), *CYP2D6/7*, and *CYP3A4/5/7* (Fig. 5B–I). Accordingly, these hepatocyte-specific mRNAs reached comparable amounts as observed for *ALB* mRNA. The mean value for human *AFP*, a marker for immature hepatocytes, was ~2%–8% (Fig. 5J), and human hypoxanthine phosphoribosyl transferase 1 (*HPRT1*) as a housekeeping gene for human cells reached 16% (ESC-iMSCs) and 7% (iPSC-iMSCs) in Gunn rat liver (Fig. 5K). This suggested that,

in addition to mature and immature hepatocytes, other human cells were present in the Gunn rat livers. Indeed, expression of the MSC marker *CD105* was detectable, indicating persisting human iMSCs (Fig. 5L). To find additional evidence for the presence of human iMSCs, sera from Gunn rats of the transplantation groups and control were analyzed for the presence of human cytokines, employing secretome arrays. Human RANTES (CC motif ligand 5) and SERPIN Family E Member 1 (SERPINE1) could only

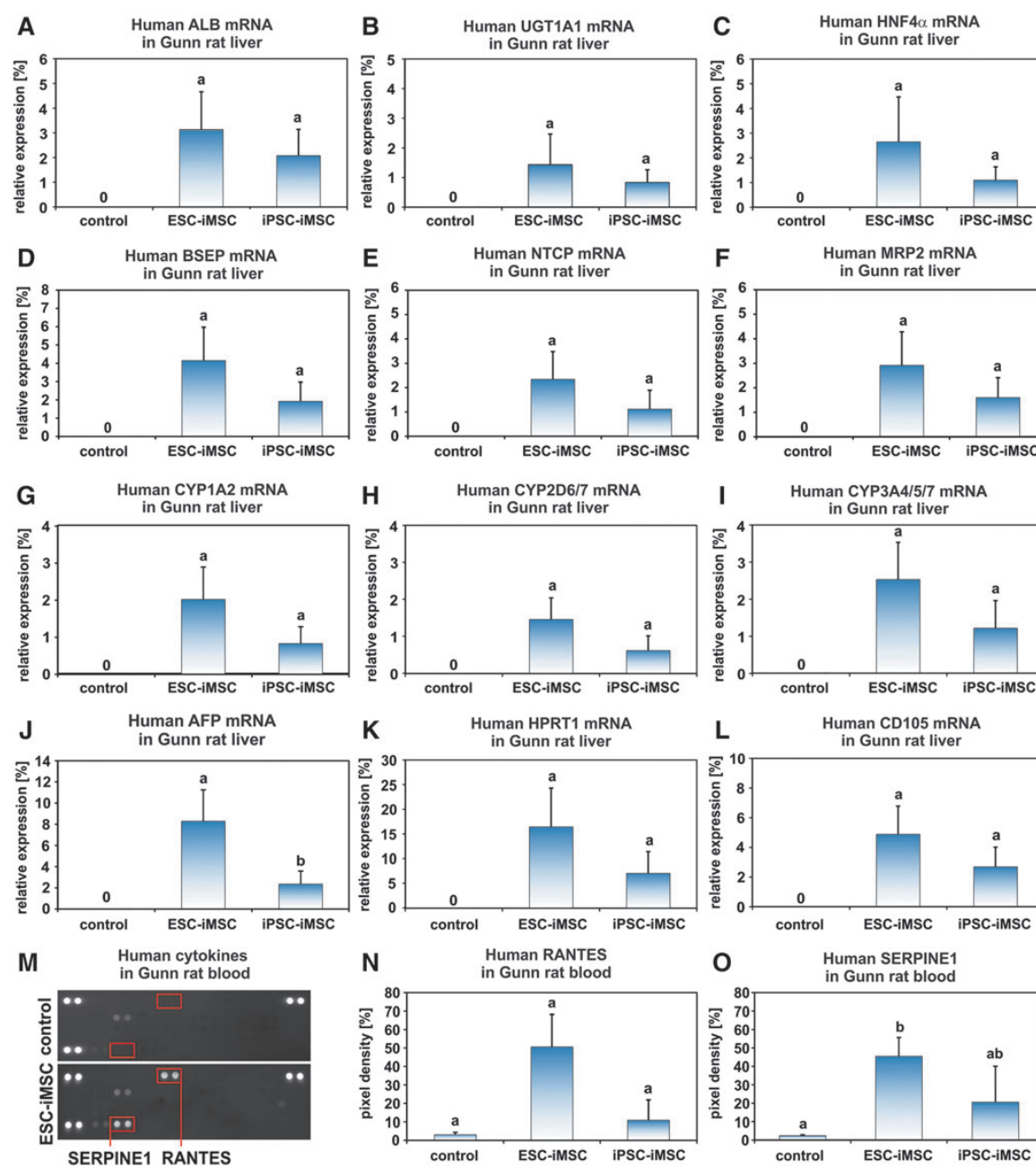


FIG. 5. Transplanted human iMSCs successfully engrafted in Gunn rat liver and expressed hepatocyte markers. Gunn rat liver tissue and serum were analyzed 2 months after iMSC transplantation. (A) The presence of human *ALB* transcripts within Gunn rat liver was analyzed by qPCR. Additional hepatocyte-associated genes such as (B) *UGT1A1*, (C) *HNF4 α* , (D) *BSEP*, (E) *NTCP*, (F) *MRP2*, (G) *CYP1A2*, (H) *CYP2D6/7*, (I) *CYP3A4/5/7*, and (J) *AFP* were found by human-specific primers for qPCR. The results were normalized to human liver samples, which were set to 100%. Thus, the bars represent proportions of the expression values of human liver. (K) Human-specific primers for *HPRT1* were used to assess the total abundance of human cells derived from iMSCs. (L) The MSC marker *CD105* remained detectable by human-specific primers in qPCR within the host Gunn rat livers. (M) Human RANTES and SERPINE1 were detected by protein arrays in the serum of Gunn rats transplanted with human iMSCs. A representative blot of the control and one transplantation group is shown. The three spot pairs in the corners represent protein array quality controls. Densitometric analysis of (N) RANTES and (O) SERPINE1 spots (highlighted by red boxes). The small bar of the control group represents the background pixel density (pixel density in % to the control spots). (A–I, K–L): control $n=4$, ESC-iMSC, passage 10, $n=3$; iPSC-iMSC, passage 10, $n=3$, groups without significant differences share similar letters; $P<0.05$. *AFP*, α -fetoprotein; *BSEP*, bile salt export pump; *HNF4 α* , hepatocyte nuclear factor 4 α ; *MRP2*, multidrug resistance protein 2; *NTCP*, Na/taurocholate-cotransporting polypeptide; qPCR, quantitative real-time polymerase chain reaction; *Ugt1A1*, uridine diphosphate glucuronosyltransferase-1a1.

HUMAN iMSCs SUPPORT LIVER REGENERATION IN GUNN RATS

1711

be detected in the serum of the transplantation groups (Fig. 5M–O), indicating the presence of cytokine-secreting human cells.

Histological analysis of Gunn rat liver

To identify iMSC-derived cells within Gunn rat liver tissue, the human-specific antibody Stem121 directed against a cytoplasmic protein was used for immunohistochemistry analysis (Fig. 6). Stem121-positive cells were mainly located within the rat liver tissue around the central vein zone 3 and 2, as observed after iMSC transplantation (Fig. 6B, C). These cells were polygonal shaped with one or two cell nuclei, which is typical for hepatocytes (Fig. 6C, D1–F1). Costaining of Stem121 immunohistochemistry with fluorescence-labeled antibodies directed against the hepatocyte markers CK18 and HNF4 α further indicated cells with hepatocyte characteristics of human origin (Fig. 6D3–F3). To investigate possible cell fusion events after iMSC transplantation, human-specific Y chromosome probes were combined with rat-specific X chromosome probes in FISH analysis, since pluripotent cells from male donors were used for the generation of iMSCs. Besides cells bearing the Y chromosome, cells with both human Y and rat X were found, indicating fusion of human-derived cells with rat cells in Gunn rat livers after transplantation (Supplementary Fig. S3).

Seemingly, human iMSC-derived hepatocytes were present in Gunn rats and, therefore, we examined and quantified the bile acid composition in rat blood serum using UHPLC-MS/MS, to determine any increase in glycine-conjugated bile acids, typical in human serum. The sum of unconjugated bile acids was increased in the iMSC groups compared to the control group. However, the concentrations of taurine- and glycine-conjugated bile acids were not significantly altered between the groups (Supplementary Fig. S4). To search for adverse effects as a consequence of iMSC transplantation, their possible contribution to fibrosis was analyzed by immunofluorescence and qPCR. As shown by representative immunofluorescent images of Collagen 1 and 4 (Supplementary Fig. S5), no significant scar formation was observed in liver sections of the transplanted groups compared to the control group. In line with this, upregulation of Collagen 1 and α -SMA mRNA was not found in host Gunn rat livers (not shown). However, the relative amount of Collagen 4 mRNA increased significantly by $85\% \pm 15\%$ ($P < 0.05\%$) after ESC-iMSC transplantation, but reached no significance for iPSC-iMSCs. To identify adverse effects imparted by the transplanted iMSCs, serum concentrations of LDH, ALT, and AST were investigated, but these values were not significantly different between the transplanted and control groups (Supplementary Table S2), suggesting no immediate obvious adverse effects by transplanted iMSCs.

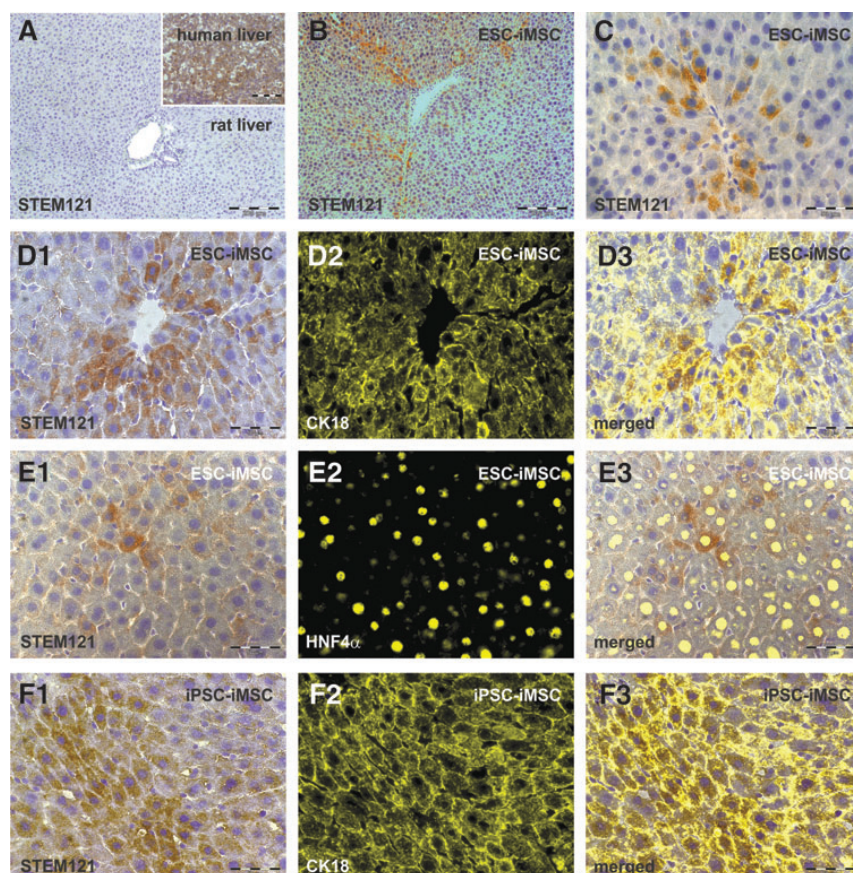


FIG. 6. Histological analysis of human iMSC-derived hepatocytes within the Gunn rat liver. Gunn rat liver tissues were analyzed by immunohistochemistry of the human cytoplasmic protein Stem121 by DAB staining (brown) 2 months after iMSC transplantation. Liver sections of control Gunn rats 2 months after PHX showed no specific Stem121 antibody binding, whereas human liver tissue exhibited intense Stem121 DAB staining, indicating its specificity for human cells (A with insert; $n = 4$). Stem121 DAB staining was also combined with immunofluorescence of the hepatocyte markers CK18 or HNF4 α (yellow). Human iMSC-derived hepatocytes with positive Stem121 staining were found after transplantation of (B–E3) ESC-iMSCs and (F1–F3) iPSC-iMSCs (passage 10, $n = 3$). The presence of Stem121 together with CK18 or HNF4 α confirms the presence of hepatocytes of human origin. Scale bars indicate 50 μm (C–F3) and 200 μm (A, B). DAB, diaminobenzidine; PHX, partial hepatectomy.

Discussion

Human MSCs are widely used in clinical trials and research studies. In a clinical scenario, however, MSCs are often obtained from elderly patients and may have lost their original properties due to changes within the stem cell niches [30]. Moreover, negative influences by prolonged culture without appropriate stem cell niche in vitro could lower their potential to proliferate and differentiate, thereby limiting their therapeutic outcome. Generation of iPSC-derived iMSCs from individual patients may overcome some of these disadvantages and offer significant potential and basis for personalized medicine.

Thus, to date, studies have shown that MSCs generated from either iPSCs or ESCs acquire a rejuvenated phenotype with high proliferative capacity capable of enhancing their therapeutic potential [15–20], and even could outperform primary MSCs [16,17]. We have demonstrated in this study that, iMSCs are similar to fMSCs with respect to their gene expression profile, morphology, cell surface markers, and trilineage differentiation potential at least in vitro. Given their pluripotent origin, it is important to show that iMSCs as derivatives of ESCs and iPSCs are not pluripotent and, thus, do not exhibit tumor formation potential. Expression of *OCT4*, *SOX2*, and *NANOG* was not detected in the iMSCs used in this study and no evidence of tumor formation was found. In contrast, we observed the ability of iMSCs to home into the injured liver and to acquire properties of hepatocytes as indicated by coexpression of human Stem121 (an antibody directed against a human-specific epitope) and hepatocyte markers (CK18 and HNF4 α), as well as the release of ALB into the blood and expression of hepatocyte-associated genes such as *ALB*, *AFP*, *UGT1A1*, *BSEP*, *NTCP*, *MRP2*, *CYP1A2*, *CYP2D6/7*, *CYP3A4/5/7*, and *HNF4 α* . To our knowledge, this is the first study showing the contribution of human iMSCs to liver regeneration. In contrast to this, native fMSCs showed poor contribution to liver regeneration compared to iMSCs. The fMSCs were more proliferative than their iMSC counterparts, which could explain their low differentiation potential since these two processes can influence developmental fate decisions of stem cells. Future studies, including comparative analysis of fetal and adult MSCs as well as iMSCs, will be necessary to investigate possible opposing effects of cell proliferation and differentiation.

The Gunn rat is a well-established model for investigating inherited liver diseases such as Crigler-Najjar syndrome 1, characterized by elevated levels of serum bilirubin caused by the *Ugt1a1* mutation [6]. It was already shown that transplantation of rat bone marrow MSCs [21] as well as human iPSC-derived hepatocytes [22] support liver regeneration and improve the disease phenotype in Gunn rats. In contrast to these studies, immunosuppression of host animals was omitted in our experiments and may explain the variations in engraftment observed in our study. Nevertheless, we could observe the therapeutic potential of human ESC- and iPSC-derived iMSCs for the treatment of liver diseases. Although bilirubin levels in Gunn rat blood serum were reduced in the transplanted groups in comparison to the control, serum bilirubin could not reach the values seen in wild-type rats. However, as previously described by others [31,32], we found evidence for a fusion of cells from human and rat origin. These fusion events may have led to a

gene transfer from human to rat cells, thereby overcoming the host *Ugt1a1* deficiency. With regard to this, cell fusion is apparently not negative per se. Indeed, cell fusion has been discussed as an option for therapeutic use [33,34]. However, we cannot exclude that human iMSCs differentiated into hepatocytes without fusion as described by others [9].

Despite transplanted human iMSCs acquiring hepatocyte functions, no shift from taurine- to glycine-conjugated bile acids was observed in the blood of Gunn rats, which could have mirrored the appearance of cells with properties of human hepatocytes in the rat liver [35]. However, an increased level of unconjugated bile acids was shown in the blood of Gunn rats after iMSC transplantation. Interestingly, in the rat, the blood concentration of unconjugated bile acids is substantially higher than the amount of conjugated bile acids [36]. The reason for elevated concentrations of unconjugated bile acids after iMSC transplantation is unclear.

Evidence for liver injury by the transplanted iMSCs was not observed, since the levels of AST, ALT, nor LDH were found to be elevated in the blood. Although there are publications describing MSC-mediated fibrosis [12] and fibrolysis-inhibiting human SERPINE1 was found in the blood of Gunn rats, we could not find any evidence for liver fibrosis in Gunn rats by histological examination and qPCR analysis of Collagen 1 and α -SMA. However, increased mRNA levels of Collagen 4, which is an essential element of the basement membrane-like structure in the space of Disse of normal liver tissue, were observed in Gunn rats of the transplantation groups. Transplanted iMSCs could have released factors such as connective tissue growth factor that stimulated collagen expression in host liver tissue. Immunofluorescence analysis of liver sections exhibited neither elevated deposition of Collagen 4 nor scar formation. Thus, transplanted iMSCs contributed to liver regeneration of Gunn rats without obvious adverse effects. Since MSCs have been widely reported to release immunomodulatory factors [36–38], no immunosuppression was used in this study. Indeed, the transplanted human iMSCs survived within the Gunn rats for at least 2 months. However, long-term studies are necessary before use of iMSCs in clinical practice to ensure tumor safety for patients. Nevertheless, given their multipotentiality and immunomodulatory capacity, iMSCs seem to represent a valuable cell type for future autologous or allogeneic transplantations [14]. Our findings underpin the potential of iMSCs as an option for treating liver diseases and inherited liver disorders.

Acknowledgments

This study was supported by the German Research Foundation (DFG) through the Collaborative Research Center SFB 974 (“Communication and Systems Relevance during Liver Injury and Regeneration,” Düsseldorf). Professor Dr. James Adjaye acknowledges support from the Federal Ministry of Education and Research-BMBF (01GN1005) and the Medical Faculty, Heinrich-Heine-University, Düsseldorf. Professor Dr. Richard Oreffo is supported by grants from the BBSRC (LO21072/1) and MRC (MR/K026682/1). The authors are grateful to Claudia Rupprecht (Clinic for Gastroenterology, Hepatology and Infectious Diseases) for expert technical assistance and Katharina Raba (Institute of Transplantation

HUMAN iMSCs SUPPORT LIVER REGENERATION IN GUNN RATS

1713

Diagnostics and Cell Therapeutics) of the Heinrich Heine University for the FACS analyses. The authors acknowledge the Rat Resource & Research Center (P40OD011062) for providing Gunn rats.

Author Disclosure Statement

No competing financial interest exists.

References

1. Crigler JF Jr. and VA Najjar. (1952). Congenital familial nonhemolytic jaundice with kernicterus. *Pediatrics* 10:169–180.
2. Ruud Hansen TW. (2010). Phototherapy for neonatal jaundice—therapeutic effects on more than one level? *Semin Perinatol* 34:231–234.
3. Ramy N, EA Ghany, W Alsharany, A Nada, RK Darwish, WA Rabie and H Aly. (2016). Jaundice, phototherapy and DNA damage in full-term neonates. *J Perinatol* 36:132–136.
4. van Dijk R, U Beuers and PJ Bosma. (2015). Gene replacement therapy for genetic hepatocellular jaundice. *Clin Rev Allergy Immunol* 48:243–253.
5. Jorns C, G Nowak, A Nemeth, H Zemack, LM Mörk, H Johansson, R Gramignoli, M Watanabe, A Karadagi, et al. (2016). De novo donor-specific HLA antibody formation in two patients with Crigler–Najjar Syndrome Type I following human hepatocyte transplantation with partial hepatectomy preconditioning. *Am J Transplant* 16:1021–1030.
6. Gunn CK. (1944). Hereditary acholuric jaundice in the rat. *Can Med Assoc J* 50:230–237.
7. Dominici M, K Le Blanc, I Mueller, I Slaper-Cortenbach, F Marini, D Krause, R Deans, A Keating, Dj Prockop and E Horwitz. (2006). Minimal criteria for defining multipotent mesenchymal stromal cells. The International Society for Cellular Therapy position statement. *Cytotherapy* 8:315–317.
8. Crisan M, S Yap, L Casteilla, CW Chen, M Corselli, TS Park, G Andriolo, B Sun, B Zheng, et al. (2008). A perivascular origin for mesenchymal stem cells in multiple human organs. *Cell Stem Cell* 3:301–313.
9. Sato Y, H Araki, J Kato, K Nakamura, Y Kawano, M Kobune, T Sato, K Miyanishi, T Takayama, et al. (2005). Human mesenchymal stem cells xenografted directly to rat liver are differentiated into human hepatocytes without fusion. *Blood* 106:756–763.
10. Kuo TK, SP Hung, CH Chuang, CT Chen, YR Shih, SC Fang, VW Yang and OK Lee. (2008). Stem cell therapy for liver disease: parameters governing the success of using bone marrow mesenchymal stem cells. *Gastroenterology* 134:2111–2121, 2121.e1.
11. van Poll D, B Parekkadan, CH Cho, F Berthiaume, Y Nahmias, AW Tilles and ML Yarmush. (2008). Mesenchymal stem cell-derived molecules directly modulate hepatocellular death and regeneration in vitro and in vivo. *Hepatology* 47:1634–1643.
12. Kramann R, RK Schneider, DP DiRocco, F Machado, S Fleig, PA Bondzie, JM Henderson, BL Ebert and BD Humphreys. (2015). Perivascular Gli1+ progenitors are key contributors to injury-induced organ fibrosis. *Cell Stem Cell* 16:51–66.
13. Walker N, L Badri, S Wettlaufer, A Flint, U Sajjan, PH Krebsbach, VG Keshamouni, M Peters-Golden and VN Lama. (2011). Resident tissue-specific mesenchymal progenitor cells contribute to fibrogenesis in human lung allografts. *Am J Pathol* 178:2461–2469.
14. Jung Y, G Bauer and JA Nolte. (2012). Concise review: induced pluripotent stem cell-derived mesenchymal stem cells: progress toward safe clinical products. *Stem Cells* 30:42–47.
15. Froebel J, H Hemeda, M Lenz, G Abagnale, S Jousens, B Denecke, T Sarić, M Zenke and W Wagner. (2014). Epigenetic rejuvenation of mesenchymal stromal cells derived from induced pluripotent stem cells. *Stem Cell Rep* 3:414–422.
16. Wang X, EA Kimbrel, K Ijichi, D Paul, AS Lazorchak, J Chu, NA Kouris, GJ Yavarian, SJ Lu, et al. (2014). Human ESC-derived MSCs outperform bone marrow MSCs in the treatment of an EAE model of multiple sclerosis. *Stem Cell Rep* 3:115–130.
17. Hawkins KE, M Corcelli, K Dowding, AM Ranzoni, F Vlahova, KL Hau, A Hunjan, D Peebles, P Gressens, et al. (2018). Embryonic stem cell-derived mesenchymal stem cells (MSCs) have a superior neuroprotective capacity over fetal MSCs in the hypoxic-ischemic mouse brain. *Stem Cells Transl Med* 7:439–449.
18. Lian Q, Y Zhang, J Zhang, HK Zhang, X Wu, Y Zhang, FF Lam, S Kang, JC Xia, et al. (2010). Functional mesenchymal stem cells derived from human induced pluripotent stem cells attenuate limb ischemia in mice. *Circulation* 121:1113–1123.
19. Gruenloh W, A Kambal, C Sondergaard, J McGee, C Nacey, S Kalomoiris, K Pepper, S Olson, F Fierro and JA Nolte. (2011). Characterization and in vivo testing of mesenchymal stem cells derived from human embryonic stem cells. *Tissue Eng Part A* 17:1517–1525.
20. Kimbrel EA, NA Kouris, GJ Yavarian, J Chu, Y Qin, A Chan, RP Singh, D McCurdy, L Gordon, RD Levinson and R Lanza. (2014). Mesenchymal stem cell population derived from human pluripotent stem cells displays potent immunomodulatory and therapeutic properties. *Stem Cells Dev* 23:1611–1624.
21. Muraca M, C Ferrareso, MT Vilei, A Granato, M Quarta, E Cozzi, M Rugge, KA Pauwelyn, M Caruso, et al. (2007). Liver repopulation with bone marrow derived cells improves the metabolic disorder in the Gunn rat. *Gut* 56:1725–1735.
22. Chen Y, Y Li, X Wang, W Zhang, V Sauer, CJ Chang, B Han, T Tchaikovskaya, Y Avsar, et al. (2015). Amelioration of hyperbilirubinemia in Gunn rats after transplantation of human induced pluripotent stem cell-derived hepatocytes. *Stem Cell Rep* 5:22–30.
23. Mirmalek-Sani SH, RS Tare, SM Morgan, HI Roach, DI Wilson, NA Hanley and RO Oreffo. (2006). Characterization and multipotentiality of human fetal femur-derived cells: implications for skeletal tissue regeneration. *Stem Cells* 24:1042–1053.
24. Megges M, RO Oreffo and J Adjaye. (2016). Episomal plasmid-based generation of induced pluripotent stem cells from fetal femur-derived human mesenchymal stromal cells. *Stem Cell Res* 16:128–132.
25. Chen YS, RA Pelekanos, RL Ellis, R Horne, EJ Wolvetang and NM Fisk. (2012). Small molecule mesengenic induction of human induced pluripotent stem cells to generate mesenchymal stem/stromal cells. *Stem Cells Transl Med* 1:83–95.
26. Dirks WG and HG Drexler. (2013). STR DNA typing of human cell lines: detection of intra- and interspecies cross-contamination. *Methods Mol Biol* 946:27–38.
27. Higgins GM and RM Anderson. (1931). Experimental pathology of the liver. I. Restoration of the liver of the white rat following partial surgical removal. *Arch Pathol Lab Med* 12:186–202.

1714

SPITZHORN ET AL.

28. Herebian D and E Mayatepek. (2012). Analysis of bile acids by tandem mass spectrometry. In: *Hepatobiliary Transport in Health and Disease*. Häussinger D, V Keitel, R Kubitz, eds. Walter De Gruyter GmbH Co. KG, Berlin/Boston, pp 277–287.
29. Kordes C, I Sawitza, S Götze, D Herebian and D Häussinger. (2014). Hepatic stellate cells contribute to progenitor cells and liver regeneration. *J Clin Invest* 124:5503–5515.
30. O'Hagan-Wong K, S Nadeau, A Carrier-Leclerc, F Apablaza, R Hamdy, D Shum-Tim, F Rodier and I Colmegna. (2016). Increased IL-6 secretion by aged human mesenchymal stromal cells disrupts hematopoietic stem and progenitor cells' homeostasis. *Oncotarget* 7:13285–13296.
31. Vassilopoulos G, PR Wang and DW Russell. (2003). Transplanted bone marrow regenerates liver by cell fusion. *Nature* 422:901–904.
32. Wang X, H Willenbring, Y Akkari, Y Torimaru, M Foster, M Al-Dhalimy, E Lagasse, M Finegold, S Olson and M Grompe. (2003). Cell fusion is the principal source of bone marrow-derived hepatocytes. *Nature* 422:897–901.
33. Vassilopoulos G and DW Russell. (2003). Cell fusion: an alternative to stem cell plasticity and its therapeutic implications. *Curr Opin Genet Dev* 13:480–485.
34. Sullivan S and K Eggan. (2006). The potential of cell fusion for human therapy. *Stem Cell Rev* 2:341–349.
35. García-Cañaveras JC, MT Donato, JV Castell and A Lahoz. (2012). Targeted profiling of circulating and hepatic bile acids in human, mouse, and rat using a UPLC-MRM-MS-validated method. *J Lipid Res* 53:2231–2241.
36. Aggarwal S and MF Pittenger. (2005). Human mesenchymal stem cells modulate allogeneic immune cell responses. *Blood* 105:1815–1822.
37. Kaplan JM, ME Youd and TA Lodie. (2011). Immunomodulatory activity of mesenchymal stem cells. *Curr Stem Cell Res Ther* 6:297–316.
38. Trounson A and C McDonald. (2015). Stem cell therapies in clinical trials: progress and challenges. *Cell Stem Cell* 17:11–22.

Address correspondence to:

Prof. Dr. James Adjaye
Institute for Stem Cell Research and Regenerative Medicine
Heinrich Heine University, Düsseldorf
Moorenstraße 5
Düsseldorf 40225
Germany

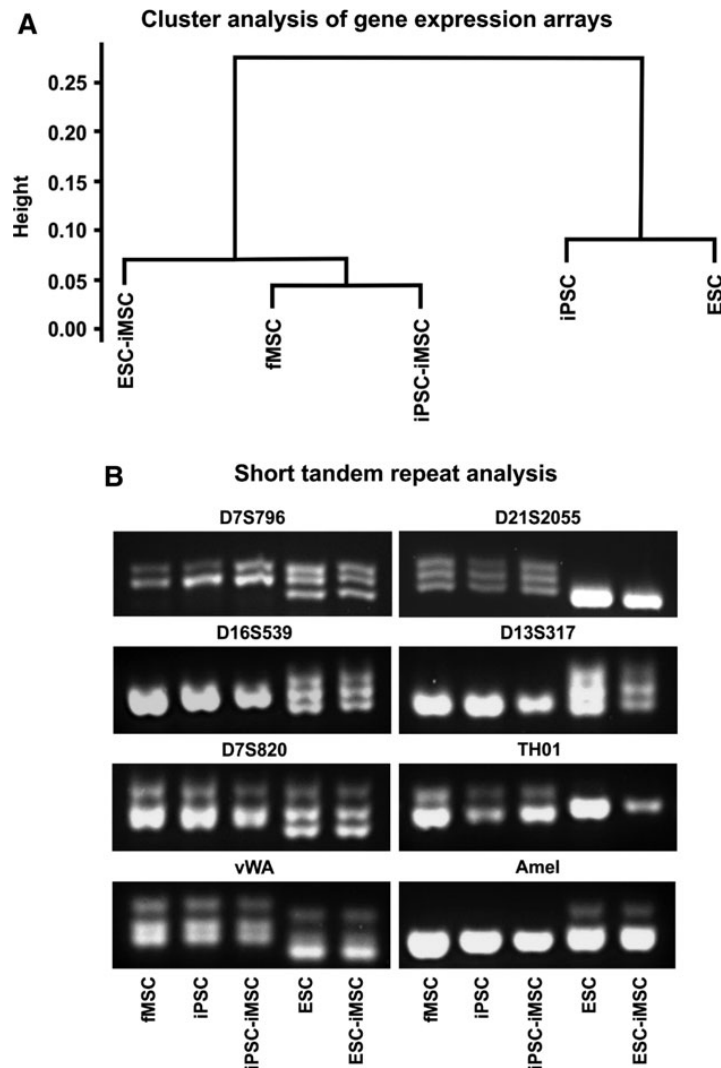
E-mail: james.adjaye@med.uni-duesseldorf.de

Prof. Dr. Dieter Häussinger
Clinic of Gastroenterology, Hepatology
and Infectious Diseases
Heinrich Heine University, Düsseldorf
Moorenstraße 5
Düsseldorf 40225
Germany

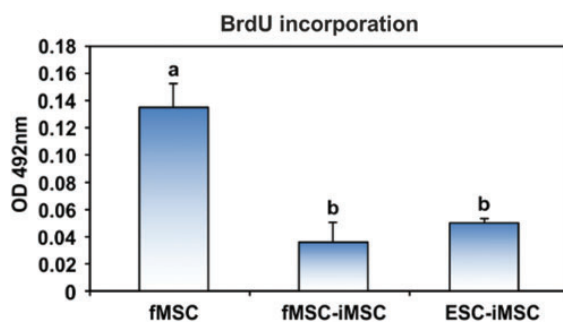
E-mail: haeussin@uni-duesseldorf.de

Received for publication January 15, 2018
Accepted after revision September 29, 2018
Prepublished on Liebert Instant Online October 3, 2018

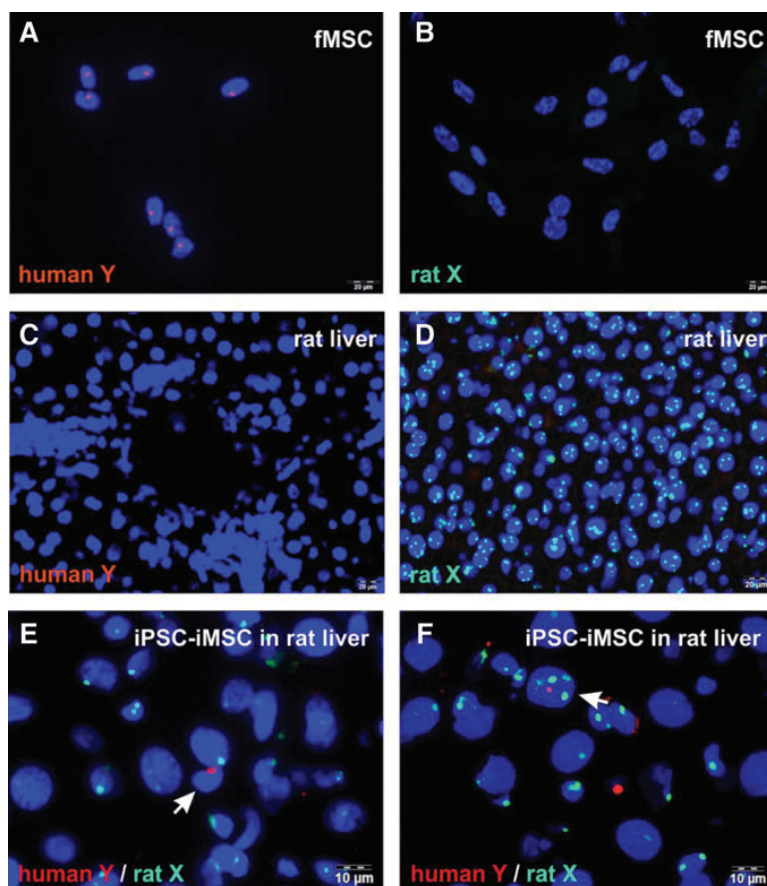
Supplementary Data



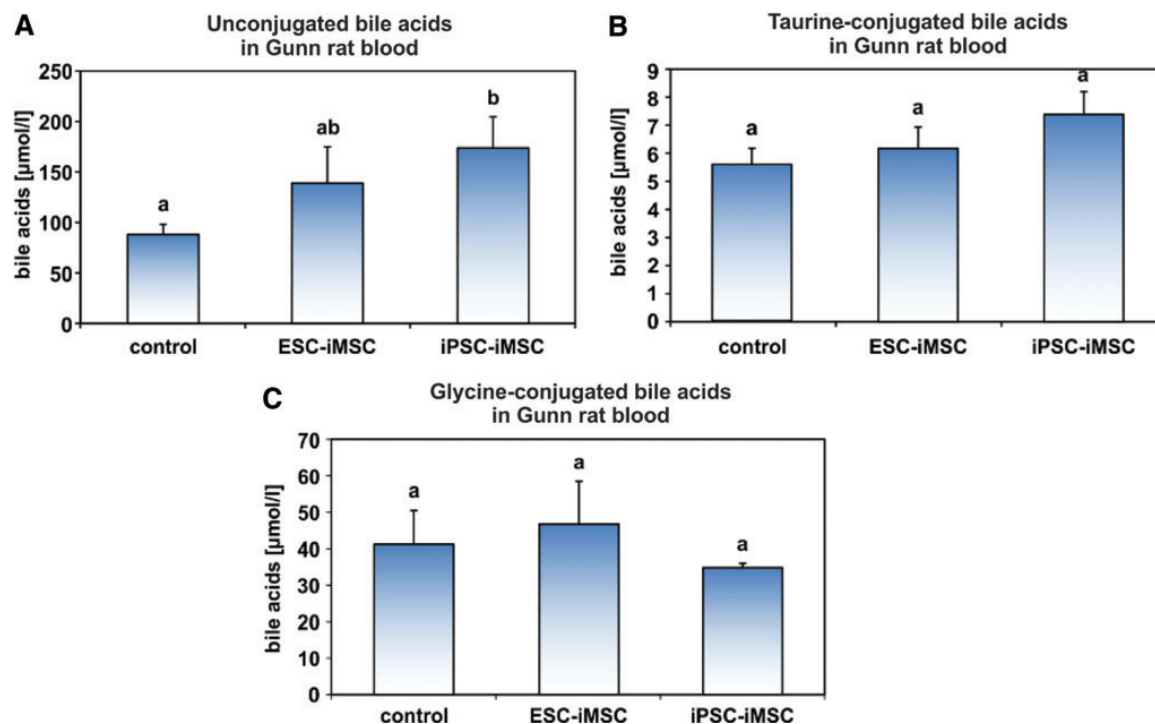
SUPPLEMENTARY FIG. S1. Cluster analysis of gene expression arrays and short tandem repeat analysis. (A) Cluster analysis of microarray data (Fig. 1B, generated once for a representative preparation of each cell type) revealed high similarity of ESC-iMSCs and iPSC-iMSCs to native fMSCs, and they clustered away from their pluripotent precursor cells (ESCs and iPSCs). (B) STR analysis using specific primers for eight different STR loci resulted in distinct banding patterns. Two groups were identified: (1) fMSCs, iPSCs, and fMSC-iMSCs; and (2) ESCs and ESC-iMSCs. STR analysis confirmed same genetic background for fMSCs and fMSC-iMSCs as well as for ESCs and ESC-iMSCs. ESC, embryonic stem cell; fMSC, fetal mesenchymal stem cell; iMSC, induced mesenchymal stem cells; STR, short tandem repeat.



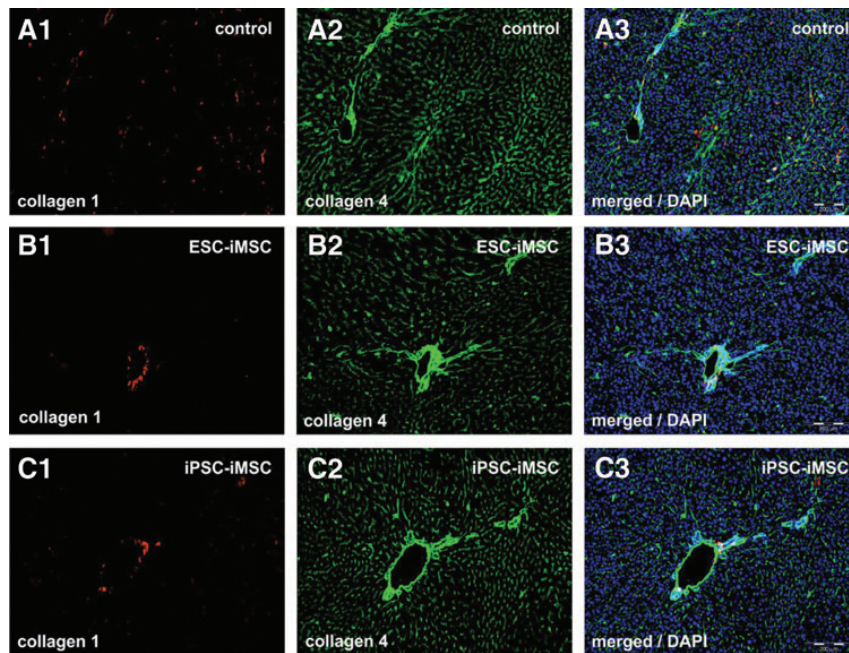
SUPPLEMENTARY FIG. S2. Assessment of cell proliferation by BrdU incorporation. BrdU was added to the culture medium for 21 h and measured using ELISA. The highest proliferation rate was measured for native fMSCs at passage 8 in comparison to fMSC-iMSCs and ESC-iMSCs at passage 10 ($n=3$, groups without significant differences share similar letters; $P < 0.05$). The iMSC preparations showed equal BrdU incorporation. BrdU, bromodeoxyuridine; ELISA, enzyme-linked immunosorbent assay.



SUPPLEMENTARY FIG. S3. FISH analysis of human- and rat-specific sex chromosomes. To investigate possible cell fusion events between host rat hepatocytes and human iMSCs, FISH analysis was performed. Before this, (A) the specificity of human Y chromosome probes (*red*) was tested on cultured fMSCs of a male donor. The positive staining of a single chromosome in the cells suggests specificity of the Y chromosome probe. The cell nuclei are shown in *blue* by DAPI staining. (B) The rat X chromosome probe failed to bind to human chromosomes (absence of *green* staining), when applied to male fMSCs, confirming the specificity of the X probe for rat cells. (C) The human Y chromosome probe was also tested on rat liver. The lack of any significant binding confirmed its specificity for human cells. (D) The rat X chromosome probe successfully stained the nuclei of rat liver cells (*green*). A possible cell fusion was analyzed by combined application of human-specific Y (*red*) and rat-specific X (*green*) chromosome probes. Hints for transplanted iMSCs (E) without and (F) with cell fusion were found (*arrows*). iPSC-iMSCs and ESC-iMSCs were used at passage 10. Scale bars indicate 20 μm (A–D) and 10 μm (E, F).



SUPPLEMENTARY FIG. S4. Human iMSC transplantation caused no shift from taurine- to glycine-conjugated bile acids typical for humanized bile acid serum profile. Unconjugated as well as taurine- and glycine-conjugated bile acids in serum of Gunn rats were quantified by UHPLC-MS/MS 2 months after PHX in the control and transplantation group. (A) The concentration of unconjugated bile acids was elevated in the blood of Gunn rats that received iPSC-iMSCs compared to the control group, whereas the sums of the (B) taurine- and (C) glycine-conjugated bile acids remained similar. iPSC-iMSCs and ESC-iMSCs were used at passage 10 ($n=3$ and 4; similar *letters* indicate groups without significant differences, $P<0.05$). UHPLC-MS/MS, ultra-high performance liquid tandem mass spectrometry.



SUPPLEMENTARY FIG. S5. Fibrosis-associated genes remained unchanged after human iMSC transplantation. Gunn rat liver tissue sections were analyzed 2 months after iMSC transplantation, to evaluate their possible contribution to fibrosis. (A1, B1, C1) Collagen 1 (*red*) and (A2, B2, C2) Collagen 4 (*green*) were analyzed by immunofluorescence to detect excessive extracellular matrix deposition within Gunn rat liver. Neither the control nor transplantation groups exhibited significantly elevated levels of Collagens 1 and 4 after 2 months of liver regeneration (control $n=4$; ESC-iPSC, passage 10, $n=3$; iPSC-iMSC, passage 10, $n=3$). (A3, B3, C3) The immunofluorescence images of Collagen 1 and 4 were merged with DAPI staining (*blue*). Scale bars indicate 200 μm .

SUPPLEMENTARY TABLE S1. PRIMER SEQUENCES

Gene	Acc. No./Ref.	Primer forward	Primer reverse
α -SMA ^a	NM_001613.2	TTGACATCAGGAAGGACCTC	TCCTGTTTGCTGATCCACAT
β -Actin ^a	NM_001101.3	TCTACAAATGAGCTGCGTGTGG	AGATGGGCACAGTGTGGGTGA
ALB ^b	NM_000477.5	AGTCCACACGGAATGCTGCC	TTCCACTTCGGCAATGCAGTG
AFP ^b	NM_001134.2	GCCACTGTGTGCCAAGCTCAG	TGTTTCATCCACCAACCAAGCT
BSEP ^b	NM_003742.2	TTATTGCGAAATCTGCTTCC	TTTTGCATAACTTGGGGTGT
CD105 ^b	NM_00114753.2	TGACAAAGTTTGTCTTGCGCAG	GACACTGACCTGCACAAAAG
COL1 α 2 ^a	NM_000089.3	GTGGTGACCAAGGTCCAGTT	CCAGGGAGACCCAGAATACC
COL4 α 1 ^b	NM_001845.5	TGAGATACTTGCCCATGTGC	TTGTCCCTTTTCCACCTGGAG
COL4 α 1 ^a	NM_000092.4	CTGGCTGTGGAAAATGTGACTG	TCACCCCTTTTGTCTGCTGGTG
CTGF ^b	NM_001901.2	TTGCGAAAGCTGACCTGGAA	CTTCATGACCTCGCCGTC
CYP1A2	NM_000761.5	CAGAGGTTCTCTGTTGCTTCC	AGGCTTGGTCAACAAGGTACA
CYP2D6/7	NM_000106.6	GACCTAGCTCAGGAGGGACT	AAAGCCCTTTTGGAAAGCGTAG
CYP3A4/5/7	NM_017460.5	TGGAGATGTGTGGTGAGAA	GGGTCTTGTGGATTGTTGAG
HNF4 α ^b	NM_178849.2	AGCTTCTGCGGAGCTCCC	TCGTCAAAGGATGCGTATGGA
HPRT1 ^b	NM_000194.2	CCACGAAAGTGTGGATATAAG	CTCCAGATGTTTCCAAACTCA
MRP2 ^b	NM_000392.4	GAGCTGGCCCTTGTACTCAC	TAGGGACAGGAACCCAGGAGT
NTCP ^b	NM_003049.3	AAATCCAAACGGCCACAATAC	GAGGAGGTGGCAATCAAGAG
UGT1A1 ^b	NM_000463.2	CCGTGCTTTTATCACCCTATG	CAAATCCACCCAGAACACCG
D7S796	[S1]	TTTTGGTATTGGCCATCCTA	GAAAGGAACAGAGAGACAGGG
D21S2055	[S1]	AAAGAAACCAATAGGCTATCTATC	TACAGTAAATCCTTGGTAGGAGA
D16S539	[S2]	GGGGTCTAAAGAGCTGTAAAAAG	GTTTGTGTGTCATCTGTAAAGCATGTATC
D13S317	[S2]	ACAGAAAGTCTGGGATGTGGAGGA	GGCAGCCCAAAAAGACAGA
D7S820	[S2]	ATGTTGGTCAAGGCTGACTATG	GATCCACATTTATCCTCATTTGAC
TH01	[S2]	ATTCAAAGGTAATCTGGGCTCTGG	GTGGGCTGAAAAGCTCCCGATTAT
vWA	[S2]	CTAGTGGATGATAAGAATAATCAGTATGTG	GGACAGATGATAAATACATAGGATGGATGG
Amel	[S2]	ACCTCATCTGGGACCCCTGGTT	AGGCTTGAGGGCCAACCATCAG

^aPrimer set for human and rat.^bHuman-specific primer set.

SUPPLEMENTARY TABLE S2. RESULTS OF TRANSPLANTATION EXPERIMENTS WITH HUMAN FETAL MESENCHYMAL STEM CELLS, EMBRYONIC STEM CELL-iMSCS, AND INDUCED PLURIPOTENT STEM CELL-iMSCS IN GUNN RATS

Animal	Cell type	Total bilirubin in serum (mg/dL)	Total albumin in serum (g/dL)	Human HPRT1 mRNA in liver (%)	Human ALB in serum (g/dL)	Human ALB in liver (% of human liver)	Human UGT1A1 mRNA in liver (%)	Human HNF1 α mRNA in liver (%)	Human BSEP mRNA in liver (% of human liver)	Human NTCP mRNA in liver (%)	Human MRP2 mRNA in liver (%)	Human CYP1A2 mRNA in liver (%)	Human CYP2D6 mRNA in liver (%)	Human CYP3A4 mRNA in liver (%)	Human AFP mRNA in liver (%)	Human CD73 mRNA in liver (%)	Human CD105 mRNA in liver (%)	Unconjugated bile acids in serum (μ M)	Glycine-conjugated bile acids in serum (μ M)	Taurine-conjugated bile acids in serum (μ M)	AST in serum (IU/L)	ALT in serum (IU/L)	LDH in serum (IU/L)	Liver/body weight ratio (%)
C1	—	1.4	3.2	0	0	0	0	0	0	0	0	0	0	0	0	0	0	91.5	63.1	4.5	83	79	1282	3.8
C2	—	1.5	3.1	0	0	0	0	0	0	0	0	0	0	0	0	0	0	82.7	49.4	6.6	50	68	533	4.5
C3	—	1.6	3.4	0	0	0	0	0	0	0	0	0	0	0	0	0	0	112.6	30.4	6.5	56	49	448	4.1
C4	—	1.4	3.2	0	0	0	0	0	0	0	0	0	0	0	0	0	0	64.0	23.4	4.7	55	63	100	4.4
T1	ESC-iMSC	0.6	3.0	2.8	0.053	1.3	0.5	1.6	0.8	0.4	0.5	0.4	0.4	0.7	3.4	0.3	2.5	82.5	66.6	7.6	47	56	100	4.8
T2	ESC-iMSC	1.1	2.9	30.2	0.28	6.2	3.5	6.2	7.1	4.4	5.3	3.6	2.3	4.0	13.7	3.8	8.7	127.8	26.4	5.4	64	86	403	4.6
T3	ESC-iMSC	1.3	3.2	16.5	0.065	1.8	0.3	0.1	4.5	2.1	3.0	1.9	1.8	3.2	7.7	2.4	3.4	205.3	48.0	5.5	81	87	123	4.5
T4	iPSC-iMSC	1.0	3.4	5.7	0.006	2.5	1.1	1.8	2.1	0.7	2.0	1.3	1.2	2.4	2.8	2.3	4.5	120.7	33.5	7.1	87	113	109	4.7
T5	iPSC-iMSC	0.3	3.2	15.2	0.093	3.7	1.5	1.4	3.7	2.6	2.8	1.9	1.5	2.7	4.3	2.5	3.6	172.6	37.2	6.2	96	106	166	4.3
T6	iPSC-iMSC	1.8	3.8	0	0	0	0	0	0	0	0	0	0	0	0	0	0	227.2	34.2	8.8	80	68	51	5.1
T7 ^a	iMSC	1.5	3.7	0	0	0	0	0	0	0	0	0	0	0	0	0	0	164.5	26.3	9.5	66	43	28	4.4
T8	iMSC	1.5	3.3	0	0	0	0	0	0	0	0	0	0	0	0	0	0	154.4	18.7	5.8	56	59	120	4.4
T9	iMSC	1.2	3.3	0.4	0	1.6	3.2	2.4	1.0	0.4	0.9	0.5	0.4	0.5	18.6	6.2	2.4	161.5	33.2	10.3	49	52	100	4.0
T10	iMSC	1.7	3.8	0	0	0	0	0	0	0	0	0	0	0	0	0	0	215.8	12.5	3.8	67	67	127	4.4
T11	iMSC	1.3	3.5	0	0	0	0	0	0	0	0	0	0	0	0	0	0	224.4	11.5	5.0	102	60	150	4.7

^aNot included in further analysis (internal bleeding of the uteri after 2 months)—not conducted.

C, control (PHX without transplantation); ESC, embryonic stem cell; iMSC, fetal mesenchymal stem cell; iMSC, induced mesenchymal stem cell; T, PHX with transplantation.

2.11 Human iPSC-derived iMSCs improve bone regeneration in mini-pigs

Pascal Jungbluth*, Lucas-Sebastian Spitzhorn*, Jan Grassmann, Stephan Tanner, David Latz, Md Shaifur Rahman, Martina Bohndorf, Wasco Wruck, Martin Sager, Vera Grotheer, Patric Kröpil, Mohssen Hakimi, Joachim Windolf, Johannes Schnependahl and James Adjaye

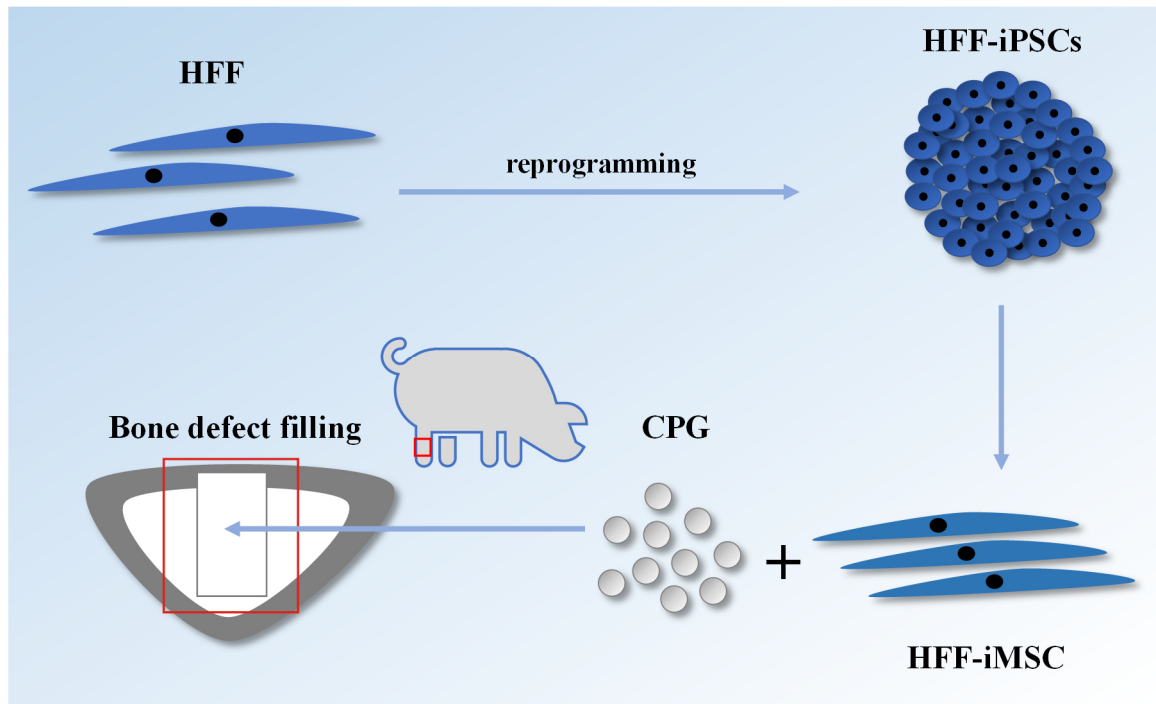
*These authors contributed equally to this work.

Abstract

Autologous bone marrow concentrate (BMC) as well as mesenchymal stem cells (MSCs) have beneficial outcomes in healing bone defects. To address the shortcoming associated with the use of primary MSCs, induced pluripotent stem cell (iPSCs) derived MSCs (iMSCs) are seen as an alternative. The aim of this study was to investigate bone regeneration potential of human iMSCs combined with calcium phosphate granules (CPG) in a critical-size defect at the proximal tibia of mini-pigs in the early phase of bone healing compared to previously reported autograft treatment- a composite made of autologous BMC and CPG, and CPG alone.

iMSCs were derived from iPSCs originating from human fetal foreskin fibroblasts (HFF). They were able to differentiate into osteoblasts *in vitro*, express a plethora of bone morphogenic proteins (BMPs) and secrete paracrine signaling-associated cytokines such as PDGF-AA and Osteopontin. Radiologically and histomorphometrically, HFF-iMSC+CPG transplantation resulted in a significantly better osseous consolidation than CPG alone and showed no significantly different outcome compared to autologous BMC+CPG after 6 weeks. The results of this translational study imply that iMSCs represent a valuable future treatment option for load-bearing bone defects in human.

Graphical Abstract



Publication Status: published in *Bone Research*; 2019 Oct 24;7:32.

Impact Factor: 12.354

This article is reproduced with permission.

Approximated total share of contribution: 40%

Contribution on experimental design, realization and publication:

JA, JS, JW, PJ and LSS conceived the ideas and designed the experiments. PJ, JS, JG, ST, MH and MS were responsible for the animal well-being, the operation procedure and the post-operative care. PJ, JS, JG, PK and ST performed the explantations and subsequent histomorphometrical and radiological analyses. LSS, MSR, MB performed the characterization of the HFF-iPSCs as well as the generation and characterization of the HFF-iMSCs. WW performed the transcriptome analyses. DL evaluated and processed the images of the histomorphometrical and radiological analyses. All authors contributed to the writing of the manuscript and JA and JW finally approved the manuscript.

Link to the publication:

<https://www.nature.com/articles/s41413-019-0069-4>



ARTICLE OPEN

Human iPSC-derived iMSCs improve bone regeneration in mini-pigs

Pascal Jungbluth¹, Lucas-Sebastian Spitzhorn², Jan Grassmann¹, Stephan Tanner¹, David Latz¹, Md Shaifur Rahman^{1b}, Martina Bohndorf², Wasco Wruck², Martin Sager³, Vera Grotheer¹, Patric Kröpil⁴, Mohssen Hakimi⁵, Joachim Windolf¹, Johannes Schnependahl¹ and James Adjaye²

Autologous bone marrow concentrate (BMC) and mesenchymal stem cells (MSCs) have beneficial effects on the healing of bone defects. To address the shortcomings associated with the use of primary MSCs, induced pluripotent stem cell (iPSC)-derived MSCs (iMSCs) have been proposed as an alternative. The aim of this study was to investigate the bone regeneration potential of human iMSCs combined with calcium phosphate granules (CPG) in critical-size defects in the proximal tibias of mini-pigs in the early phase of bone healing compared to that of a previously reported autograft treatment and treatment with a composite made of either a combination of autologous BMC and CPG or CPG alone. iMSCs were derived from iPSCs originating from human fetal foreskin fibroblasts (HFFs). They were able to differentiate into osteoblasts *in vitro*, express a plethora of bone morphogenic proteins (BMPs) and secrete paracrine signaling-associated cytokines such as PDGF-AA and osteopontin. Radiologically and histomorphometrically, HFF-iMSC + CPG transplantation resulted in significantly better osseous consolidation than the transplantation of CPG alone and produced no significantly different outcomes compared to the transplantation of autologous BMC + CPG after 6 weeks. The results of this translational study imply that iMSCs represent a valuable future treatment option for load-bearing bone defects in humans.

Bone Research (2019)7:32

; <https://doi.org/10.1038/s41413-019-0069-4>

INTRODUCTION

The majority of bone fractures heal without complications. However, cases involving bone nonunion and large skeletal bone defects represent a challenge for orthopedic surgery. Despite its significant drawbacks, including donor site morbidity, limited availability, and poor bone quality, autologous bone grafting remains the gold standard for treatment.¹ The use of autologous bone marrow concentrate (BMC) or mesenchymal stem cells (MSCs) have been described as alternative treatment options for improving bone regeneration.^{2,3}

BMC contains stem cells, growth factors, and immune cells and have been shown to improve bone regeneration.⁴ MSCs are multipotent, which is manifested in their ability to differentiate into adipocytes, chondrocytes and osteoblasts *in vitro*.^{5–8}

MSCs, as well as BMC, have been used in large animal studies for bone regeneration in weight-bearing and nonweight-bearing conditions.^{4,9} However, the availability of MSCs is restricted and associated with complications such as donor site comorbidity related to the invasive isolation from bone marrow or other tissues such as fat.¹⁰ Furthermore, it has been demonstrated that their differentiation and proliferation capacity decreases with donor age and the duration of culture.^{11–13}

MSCs differentiated from embryonic or induced pluripotent stem cells (ESCs, iPSCs), termed iMSCs, represent an alternative

to primary MSCs. As the use of ESCs is associated with ethical concerns, iPSC-derived iMSCs have been identified as a promising source of transplantable donor cells for regenerative therapies. The advantage of the use of iMSCs is that they can be generated from well-characterized and banked iPSCs with known HLA types. Another advantage of iMSCs over their native counterparts is that iMSCs have been characterized as rejuvenated MSCs.¹⁴ Although they are derived from pluripotent cells (which are by definition tumorigenic), iMSCs themselves are free from the risk of tumor formation since they do not express oncogenic pluripotency-associated genes such as OCT4.¹⁵ Moreover, iMSCs outperformed native MSCs in the treatment of multiple sclerosis in a rodent model.¹⁶ More importantly, iMSCs have been successfully used *in vivo* to improve bone regeneration by their direct differentiation into bone cells and their recruitment of host cells in a radial defect model in mice.¹⁰ The aim of this study was to evaluate the feasibility and impact of the use of a composite made of human iMSCs and calcium phosphate granules (CPG) for bone regeneration compared with that of a previously investigated autograft treatment, a composite made of autologous BMCs and CPG, and CPG alone in a critical-size long bone defect in mini-pigs under weight-bearing conditions in the early phase of bone healing. To the best of our knowledge, this investigation is the first to evaluate

¹Department of Trauma and Hand Surgery, Heinrich Heine University Hospital Düsseldorf, Moorenstr. 5, 40225 Düsseldorf, Germany; ²Institute for Stem Cell Research and Regenerative Medicine, Medical Faculty, Heinrich Heine University, Düsseldorf, Moorenstr. 5, 40225 Düsseldorf, Germany; ³Animal Research Institute, Heinrich Heine University, Düsseldorf, Moorenstr. 5, 40225 Düsseldorf, Germany; ⁴Department of Diagnostic and Interventional Radiology, Medical Faculty, Heinrich Heine University, Düsseldorf, Moorenstr. 5, 40225 Düsseldorf, Germany and ⁵Vivantes Klinikum Am Urban, Dieffenbachstraße 1, 10967 Berlin, Germany

Correspondence: Johannes Schnependahl (Johannes.Schnependahl@med.uni-duesseldorf.de) or James Adjaye (james.adjaye@med.uni-duesseldorf.de)

These authors contributed equally: Pascal Jungbluth, Lucas-Sebastian Spitzhorn

Received: 22 October 2018 Revised: 4 June 2019 Accepted: 22 July 2019

Published online: 24 October 2019

Human iMSCs improve bone regeneration in mini-pigs
P Jungbluth et al.

2

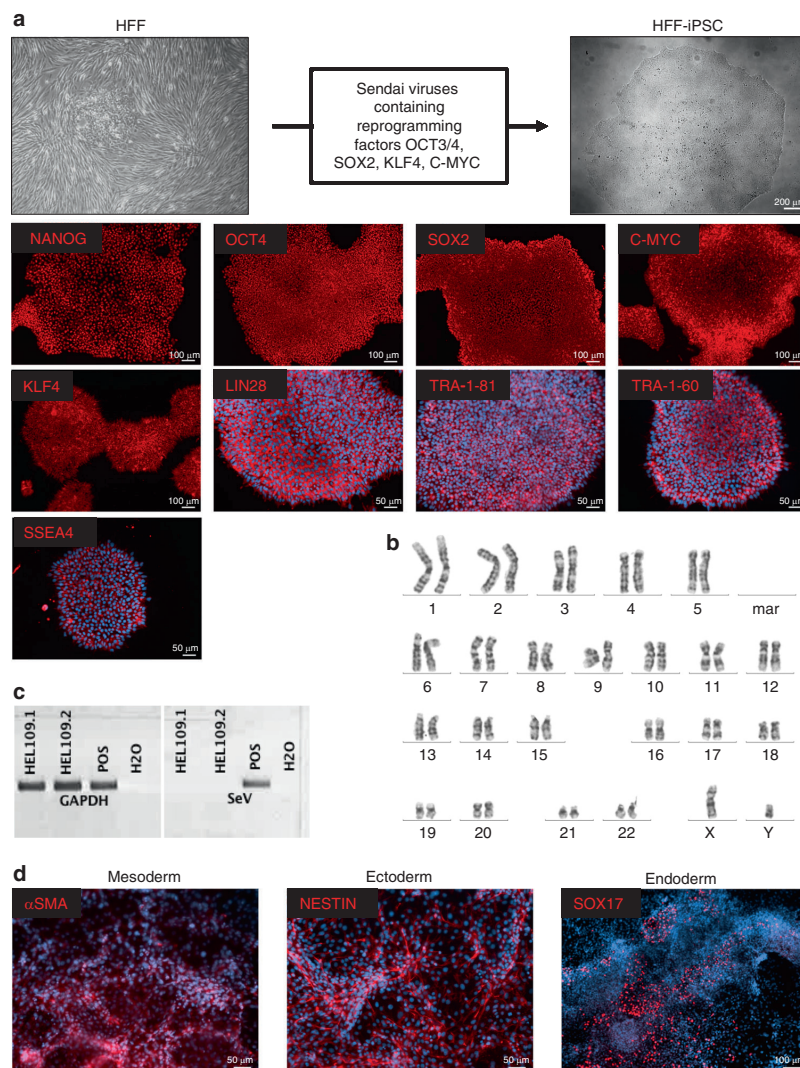


Fig. 1 Characterization of HFF-derived iPSCs. **a** Protocol used for the generation of HFF-iPSCs and the confirmation of pluripotency marker expression by immunofluorescence-based detection. **b** Karyotype of the HFF-iPSCs. **c** Viral vector dilution PCR. **d** Evaluation of embryoid body formation by using immunofluorescence-based staining. Cell nuclei are stained using Hoechst stain (blue)

the regenerative potential of human iMSCs in a large animal model under the aforementioned conditions.

RESULTS

Reprogramming of HFFs into iPSCs

Human fetal foreskin fibroblasts (HFFs) were used to generate iPSCs by employing Sendai viruses encoding the reprogramming factors OCT3/4, SOX2, KLF4, and C-MYC. The HFF-iPSCs grew as colonies and expressed the pluripotency-regulating transcription factors OCT4, SOX2, NANOG, C-MYC, and KLF4 in addition to LIN28, SSEA4, TRA-1-60, and TRA-1-81 (Fig. 1a). A normal human male karyotype (46, XY) with no chromosomal aberrations was observed (Fig. 1b), and the absence of viral DNA was confirmed by

PCR (Fig. 1c). Embryoid body formation assays demonstrated the capability of the HFF-iPSCs to differentiate into mesoderm (α SMA), ectoderm (NESTIN) and endoderm (SOX17) (Fig. 1d).

Characterization of the HFF-iMSCs

The HFF-iPSCs were differentiated into HFF-iMSCs using a 14-day protocol that utilized the inhibition of the TGF β pathway by SB431542.¹⁷ HFF-iMSCs showed a typical fibroblast spindle-shaped morphology and expressed the MSC markers PDGFR β and Vimentin. Importantly, in contrast to the HFF-iPSCs, they were devoid of OCT4 expression (Fig. 2a). Cell surface marker analysis revealed that they exhibited a typical MSC immunophenotype by expressing CD73, CD90, and CD105 versus the hematopoietic markers CD14, CD20, CD34, and CD45 (Fig. 2b). The HFF-iMSCs

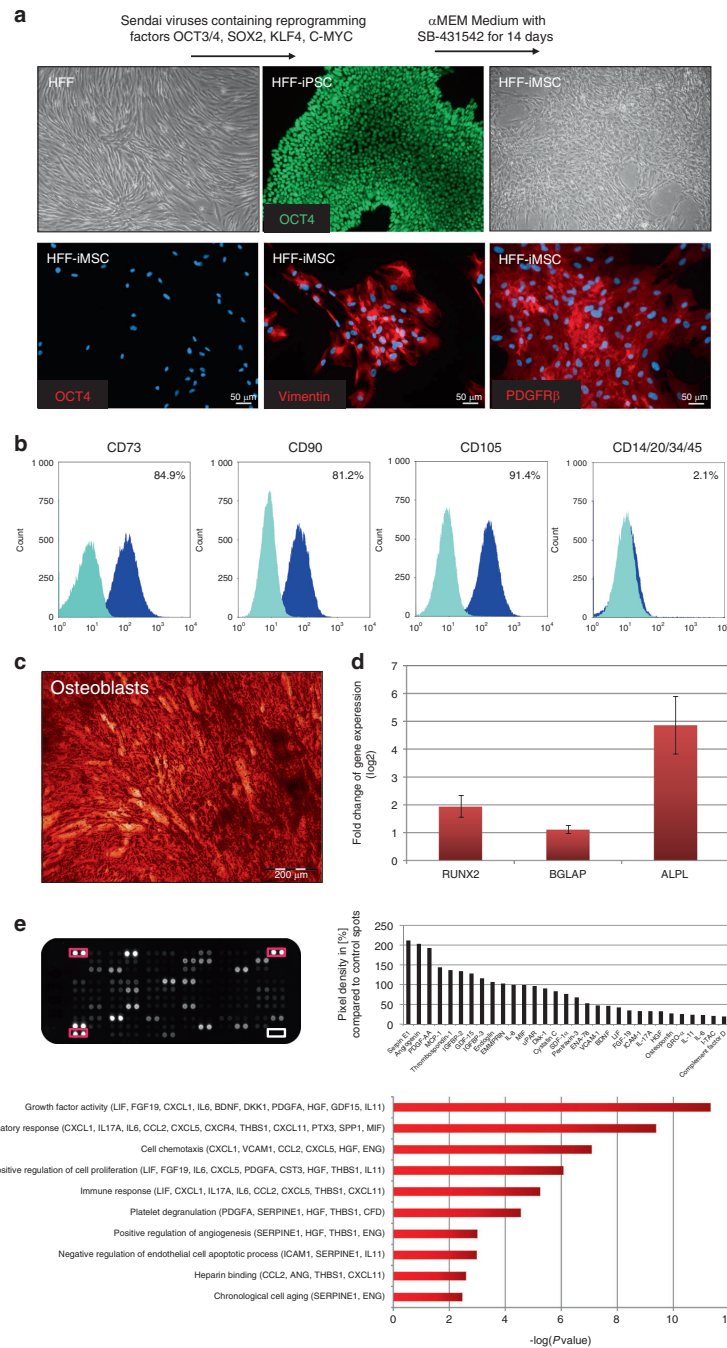


Fig. 2 Properties of HFF-iPSC-derived iMSCs. **a** HFF-iMSCs were analyzed with respect to their morphology and protein expression. The cell nuclei were stained with Hoechst. **b** Flow cytometric analysis using MSC cell surface markers (dark blue: specific cell surface markers; light blue: antibody isotype controls). **c** Alizarin Red S staining after osteogenic differentiation for 3 weeks. **d** Quantitative real-time PCR results for bone-related genes (in triplicate, normalized to the levels in untreated cells). **e** Cytokine membrane incubated with HFF-iMSC-conditioned media (left) and the background-corrected top 31 detected cytokines representing each of the selected associated GO terms; *P*-value < 0.05 (right)

Human iMSCs improve bone regeneration in mini-pigs
P Jungbluth et al.

4

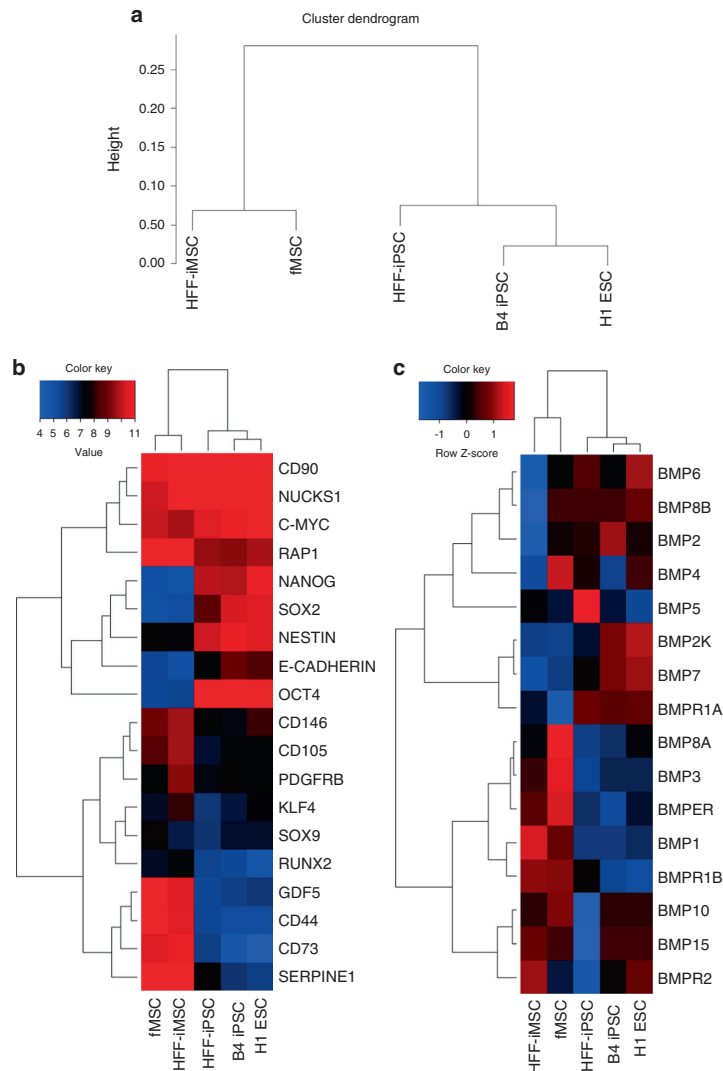


Fig. 3 Microarray analysis of the HFF-iMSCs. **a** Cluster dendrogram of the HFF-iMSCs, fMSCs and pluripotent stem cells. **b** Heatmap depicting differential gene expression in HFF-iMSCs, fMSCs and pluripotent stem cells (iPSCs and ESCs). **c** Heatmap displaying the differential expression of BMPs and their corresponding receptors

were able to differentiate into adipocytes and chondrocytes (Fig. S1). More importantly, osteoblast differentiation in vitro was confirmed by Alizarin Red S staining of the emerged calcium deposits (Fig. 2c) and also by the upregulated expression of the bone-related genes *RUNX2*, *BGLAP*, and *ALPL* (Fig. 2d). The secretome of the HFF-iMSCs was investigated using a cytokine membrane assay able to detect 103 distinct cytokines. The top 31 secreted cytokines included serpin E1, angiogenin, PDGF-AA, and osteopontin, which are known to play an important role in skeletal regeneration processes. The associated GO terms “growth factor activity”, “cell chemotaxis” and “positive regulation of angiogenesis” imply the beneficial properties of these factors that are secreted by HFF-iMSCs (Fig. 2e).

Transcriptome and STR analysis of HFF-iMSCs

The transcriptomes of the HFF-iMSCs were compared with the transcriptomes of iPSCs, ESCs, and fMSCs by microarray analysis. Cluster analysis revealed two groups: one that included the pluripotent cells, including the HFF-iPSCs, B4-iPSCs, and H1-ESCs, and the other that included the MSCs, HFF-iMSCs and primary fetal MSCs (fMSCs) (Fig. 3a). The expression of the MSC marker genes *CD44*, *CD73*, *CD105*, *CD146*, and *PDGFRB* was confirmed. Notably, the expression of the key pluripotency-associated transcription factors, *OCT4*, *NANOG*, and *SOX2* was downregulated in HFF-iMSCs compared to iPSCs and ESCs (Fig. 3b). Furthermore, transcriptome analysis revealed the expression of several BMPs and their corresponding receptors (Fig. 3c). Pearson correlation

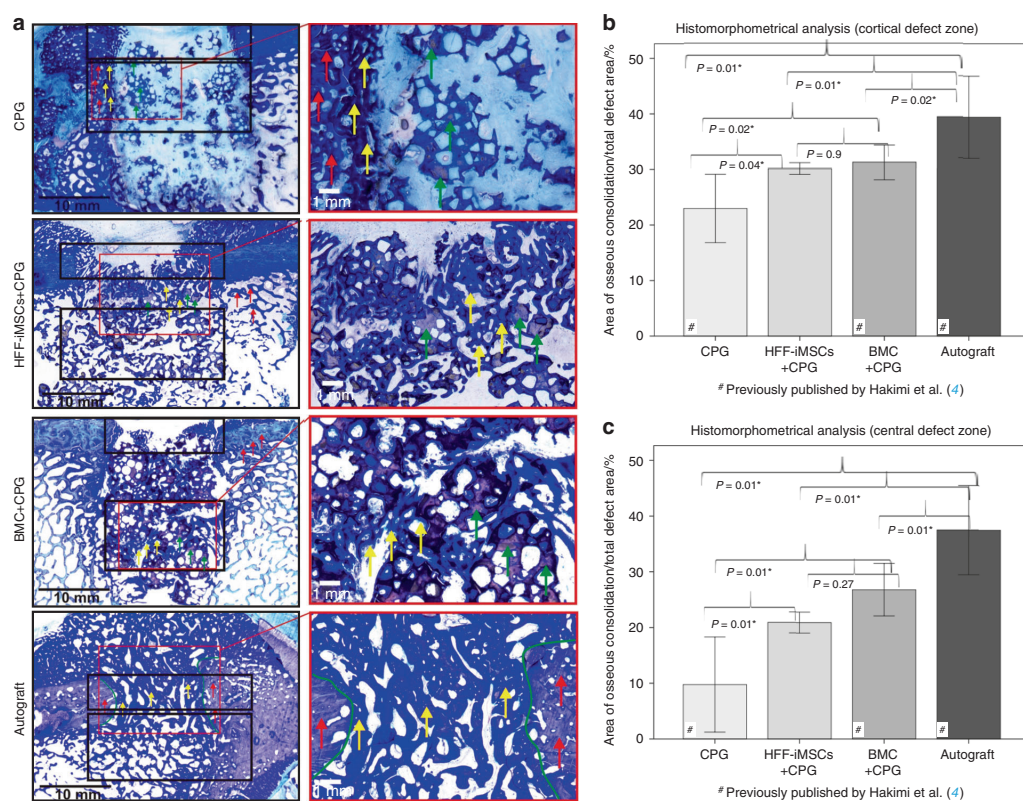


Fig. 4 Histomorphometrical and radiological analysis of regenerated bone defects after 6 weeks. **a** Representative histological bone sections from all experimental groups after a regeneration period of six weeks (left: overview image depicting the cortical (upper black box) and central defect zones (lower black box); right: detailed image); yellow arrows: newly formed bone (royal blue); red arrows: former cortical bone (purple); green arrows: nonresorbed remnants of the CPG. **b** Histomorphometrical evaluation of the cortical defect zone. **c** Histomorphometrical evaluation of the central defect zone. The results for the CPG, BMC + CPG and Autograft groups were previously published by our group.⁴ $n = 8$ for each group; values are presented with the standard deviation)

analysis of the transcriptome data showed a high correlation of HFF-iMSCs with fMSCs (R^2 value 0.947) and a low correlation with pluripotent stem cells (Fig. S2). Short-tandem-repeat (STR) analysis of the parental HFFs, HFF-iPSCs, and HFF-iMSCs verified their common genetic background (Fig. S3).

Multilevel analysis of bone defect regeneration

CPG loaded with HFF-iMSCs were transplanted into a critical-size bone defect in the proximal tibia (see Fig. S5) in 8 mini-pigs. The results of the multilevel analysis were compared to those of the analysis of the three previously described standardized experimental groups, CPG, BMC + CPG and Autograft,⁴ which were used as controls within the present study to reduce the unnecessary sacrifice of mini-pigs.

Histological evaluation

Defect closure in all 4 experimental groups was confirmed by radiographic analysis after 6 weeks of regeneration (Fig. 4a). According to the histomorphometrical analysis of the cortical area, new bone formation was significantly lower in the CPG group compared to that in the CPG + HFF-iMSC ($P < 0.04$), CPG + BMC ($P < 0.02$), and Autograft groups ($P < 0.01$). The area of new bone formation was $23.0 \pm 6.2\%$ in the CPG group and $31.2 \pm 3.1\%$ in the BMC + CPG group, and in the HFF-iMSCs + CPG group, the defect

filling area was $30.1 \pm 1\%$. This, however, was significantly inferior (vs. HFF-iMSCs + CPG $P < 0.01$, vs. BMC + CPG $P < 0.02$) compared to the mean osseous consolidation of $39.4 \pm 7.4\%$ observed in the Autograft group. No significant differences were observed between the HFF-iMSCs + CPG and BMC + CPG groups ($P = 0.9$).

Similar results were observed in the central defect area. A mean osseous consolidation of $9.8 \pm 8.5\%$ was observed when using CPG alone. This was significantly lower than that in all other groups ($P < 0.01$). The area of new bone formation in the central defect area of the HFF-iMSC + CPG group was $20.9 \pm 1.9\%$, and it was $26.8 \pm 4.7\%$ in the BMC + CPG group and $37.4 \pm 8\%$ in the Autograft group. The values observed in the Autograft group were significantly greater than those observed in all other groups ($P < 0.01$). No significant differences were observed between the HFF-iMSCs + CPG and the BMC + CPG group ($P = 0.27$). Relevant histological signs of inflammation caused by the grafting materials/cells were not found in any of the specimens (Fig. 4a–c).

Multidetector computed tomography (MDCT) volumetry

The mean extent of bone defect consolidation was $46\% \pm 10.1\%$ in the CPG + HFF-iMSCs group, $53.5\% \pm 19.1\%$ in the BMC + CPG group, and $81.1\% \pm 5.1\%$ in the Autograft group. The volume of new bone formation within the defect was $26.1\% \pm 5.1\%$ in the CPG group, which was significantly inferior compared to that in all

Human iMSCs improve bone regeneration in mini-pigs
P Jungbluth et al.

6

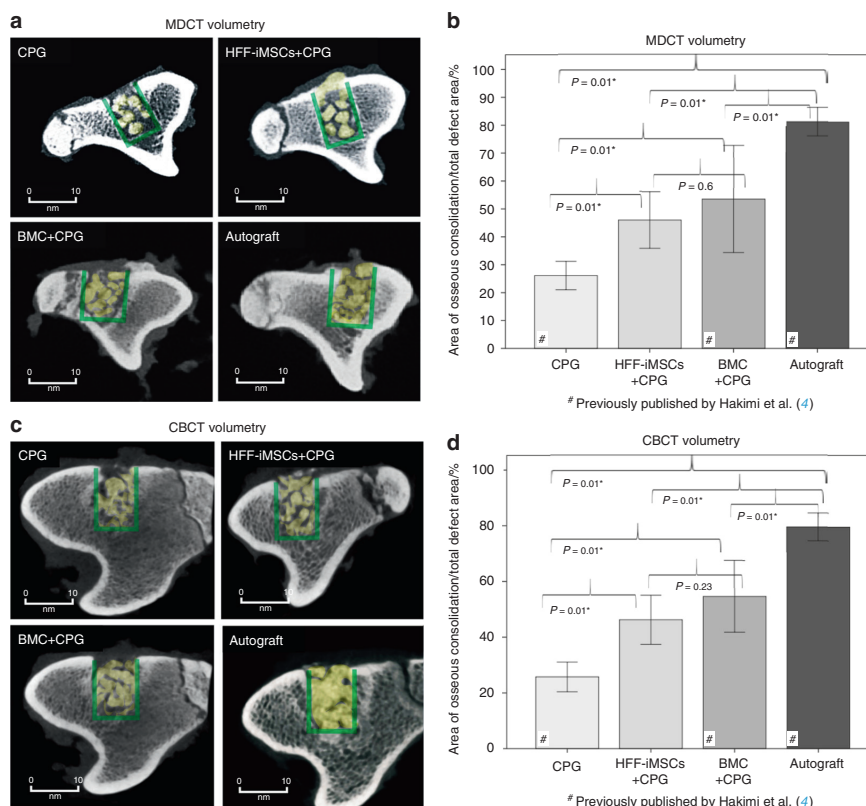


Fig. 5 Radiological analysis of regenerated bone defects after 6 weeks. **a** Axial MDCT volumetry images of the tibial defect; only areas with a density >500 HU are indicated (yellow area). The green circled area represents the defect zone. **b** MDCT volumetry evaluation of bone defect consolidation. **c** Axial CBCT volumetry images of the tibial defect; only areas with a density >2 350 HU are indicated (yellow area). The green circled area represents the defect zone. **d** CBCT volumetry evaluation of bone defect consolidation. The results for the CPG, BMC + CPG and Autograft groups were previously published by our group.⁴ $n = 8$ for each group; values are presented with the standard deviation

other groups ($P < 0.01$). Concerning the volume of new bone formation, the HFF-iMSCs + CPG group was similar to the BMC + CPG group ($P = 0.6$), and the volume in both groups was significantly lower compared to that of the Autograft group ($P < 0.01$) (Fig. 5a, b)

Cone-beam computed tomography (CBCT) volumetry

CBCT volumetry analysis of the mean osseous consolidation in the HFF-iMSCs + CPG group, the BMC + CPG group, and the Autograft group found a volume of new bone formation of $46.3\% \pm 8.8\%$, $54.7\% \pm 12.8\%$, and $79.5\% \pm 5\%$, respectively, in the defect area. The volume of new bone formation was significantly greater in the Autograft group compared to the HFF-iMSCs + CPG and BMC + CPG groups ($P < 0.01$). There were no significant differences between the HFF-iMSCs + CPG and BMC + CPG groups ($P = 0.23$). The reconstructed area in the CPG group was $25.8\% \pm 5.3\%$ and was significantly lower compared to that in all other groups ($P < 0.01$) (Fig. 5c, d).

DISCUSSION

Within the limitations of this translational study, it could be demonstrated that a composite containing human HFF-iMSCs and CPG was potent in inducing bone regeneration in the early phase of bone healing during the first six weeks. This *in vivo* model

approximates the preclinical setting, as the species-specific (mini-pig) bone regeneration capacity (1.2–1.5 mm per day) mimics that found in humans under normal anatomical and physiological conditions.¹⁸ In current clinical practice, the treatment of large bone defects and bone nonunion in humans relies on bone grafting.¹⁹ Bone marrow-derived MSC (BM-MS) transplantation has been proposed as a possible alternative.^{20–22} However, the scarcity of bone grafts, donor-associated disorders, the invasiveness of BM-MS collection and immune rejection are possible drawbacks. Recently, the craniofacial bone regeneration potential of autologous MSCs was reported in small-animal models.⁹ For long bone reconstruction in sheep and for human facial remodeling, the utility of BM-MSCs has also been demonstrated in combination with scaffolds and BMP7.^{21,23} However, to date, only a limited number of studies have implemented preclinical animal models for weight-bearing long bone defect regeneration.

In this study, human iMSCs were used, as it has been reported that the differentiation and proliferation potential of primary MSCs *in vitro* diminish upon aging.¹² In contrast, iMSCs generated from iPSCs or ESCs, when compared to BM-MSCs, show a similar phenotype but have a longer life span.²⁴ Human iMSCs are characterized by a superior molecular signature in terms of rejuvenation compared to adult MSCs.¹⁴ Furthermore, iMSCs are currently in use in a human phase 1 clinical trial of GvHD [NCT02923375].

In this investigation, HFFs were used for iPSC generation by employing nonintegrating Sendai viruses; thus, the resulting HFF-iPSC line was devoid of transgenes. The HFF-iPSCs were positive for the Yamanaka factors²⁵ and were chromosomally normal. The HFF-iMSCs that differentiated from the HFF-iPSCs expressed typical MSC markers, such as CD105 and Vimentin, and were devoid of the pluripotency-associated markers OCT4 and NANOG; subsequently, they did not result in tumor formation, as also observed in our earlier study.¹⁵ However, to ensure patient safety, long-term studies need to be conducted to evaluate the probability of tumor formation.

Upon osteogenic differentiation *in vitro*, the HFF-iMSCs showed a high rate of calcification and expressed high levels of the key transcription factor *RUNX2*²⁶ and other important bone-related genes, including *BGLAP* and *ALPL*. Furthermore, they secreted immune-modulatory and osteo-regenerative cytokines such as PDGF-AA and osteopontin, thus avoiding the necessity for additional supplementation in cell culture. It was previously reported that BM-MSC supernatants induce the expression of bone-related genes, such as *BGLAP* and *ALPL*,²⁷ and iPSC-MSCs have been shown to inhibit caspase activity in T-cells by producing TGF- β .²⁸

To attain significance and clinical impact, we used 32 skeletally mature mini-pigs that were split into four groups of eight. Of these four groups, three groups were previously described by our group⁷ and were used as references in the present study: the autologous spongiosa group was used as the gold standard autograft control, the autologous BMC (bone marrow concentrate) combined with CPG group served as the positive control and the CPG alone group was used as the negative control. For the present study, HFF-iMSCs loaded on calcium phosphate granules were transplanted into a surgically induced bone defect in 8 mini-pigs. In all cases, even though no immunosuppression was administered to the pigs, obvious postoperative events, such as inflammatory reactions were not observed histologically. By applying histomorphometric, MDCT and CBCT analyses, we observed the successful reconstruction of bone mass. To mimic the surgical procedures used in humans, the implantation and explantation were performed by an expert group of orthopedic surgeons according to standard clinical protocols used for human patients.

In the current study, a minimal number of cells (1×10^6) was transplanted to simulate the conditions typical to clinical settings, where the feasibility of long-term *in vitro* cell expansion is limited due to the amount of restricted time available for the treatment of the patient. Radiologically and histomorphometrically, the transplantation of the HFF-iMSCs loaded on CPG led to significantly better osseous consolidation in the central and cortical defect zones compared to that obtained with the use of CPG alone. Furthermore, in comparison with the composite of autologous BMC + CPG, no significant differences could be found in the cortical and central defect areas. These results are noteworthy since BMCs contain platelets and growth factors in addition to bone marrow MSCs,^{4,29} whereas the iMSCs were transplanted without the addition of exogenous factors. Furthermore, autologous BMC was used when the iMSCs were of human origin, and no administration of immune suppression was necessary. As expected, both radiologically and histomorphometrically, autologous bone transplantation resulted in the highest rate of new bone formation, which was significantly higher compared to that observed in all other groups. In a rat model of critical-size cranial defects, human iMSCs performed comparably to human MSCs (bone marrow and umbilical cord) and showed 2.8-fold improved regeneration compared to calcium phosphate cement alone after 12 weeks.³⁰ Another study demonstrated that human iMSCs contributed to substantial bone formation and produced a significantly better outcome than primary human BM-MSCs in a mouse radial defect model.¹⁰ In addition to the use of iMSC in

in vivo studies, a protocol has been described for generating bone substitutes by the incubation of iMSC-loaded scaffolds in a perfusion bioreactor system with the aim of using these in personalized bone tissue engineering in the near future.³¹ In addition to the use of different scaffold materials, the supplementation of BM-MSCs with growth factors such as BMP-7 has been used to stimulate osteogenic reconstruction.²³

Moreover, the transplantation of primed or osteogenic-differentiated MSCs into bone defect models has also been reported.^{9,32} In the current study, human iMSCs were transplanted without the addition of growth factors and at their full multipotent capacity to enable HFF-iMSCs to function as immunosuppressors and inducers of regeneration (paracrine effects) and to directly contribute to bone formation. The successful outcome of the transplantation of the composite of HFF-iMSCs and micro- and macroporous calcium phosphate granules (CPG) may have been due to the characteristics of the specific scaffold material used. An *in vitro* compatibility test of HFF-iMSCs and CPG (see Fig. S4) showed that HFF-iMSCs can be absorbed by CPG and remain alive and functional within the scaffold material. The CPGs that were utilized are composed of carbonated, calcium-deficient apatite calcium phosphate. They mimic human bone material more closely than HA or TCP cement.³³ Another advantage of CPG is the presence of both small and large pores, which enable the three-dimensional ingrowth of newly formed bone mass into the scaffold material.³⁴ Furthermore, the use of granules leads to a faster resorption rate *in vivo* when compared to the use of compact blocks of identical material.³⁵ The reported high wicking capability of CPG³³ enabled the transplantation of iMSCs into bone defects after absorption into the scaffold material. CPG was used as a scaffold material because it has been shown to have beneficial effects on bone reconstruction.³⁶ Furthermore, CPG have been used successfully as a scaffold material in combination with other fluid osteoinductive substances, such as platelet-rich plasma (PRP), BMC and a combination of both in the animal model used by our group.

One limitation of our study is the use of CT to evaluate the newly formed bone; this method cannot discriminate between the bone substitute material CPG and newly formed bone mass because both structures have comparable densities. However, the radiological and histomorphometrical analyses used in this study represent well-established evaluation methods that have been used by our group in previous studies with this type of animal model.^{4,37-39} Under these circumstances, a high correlation between the results of the histomorphometrical analysis and the two independent CT analyses confirmed the reliability of our system for evaluating osseous consolidation noninvasively, as previously shown.⁴ Furthermore, this investigation did not make an exact determination of the molecular mechanism(s) associated with bone regeneration and did not evaluate whether neo-bone formation was a direct effect of the implanted cells or the effects of secreted factors, such as immune modulation and pro-angiogenic signaling factors. Since the factors secreted from MSCs and iMSCs have been described as significantly influencing the therapeutic effect via interaction with immune cells,^{40,41} immune modulation and paracrine signaling might have played a pivotal role, as indicated by the analysis of the secretome of the HFF-iMSCs that revealed the presence of serpin E1, angiogenin, PDGF-AA and osteopontin; in addition, the transcriptome analysis showed the expression of several BMPs associated with bone regeneration.^{23,42} Furthermore, it must be taken into account that the BMP2/4 and NF- κ B signaling pathways play important roles in the paracrine pathways involved in the bone regeneration process by regulating the secretory profile of MSCs.^{43,44} Key components of these pathways, RAP1 and NUCKS1, were shown to be expressed by HFF-iMSCs (see Fig. 3b). We postulate that there are potential mechanisms whereby HFF-iMSCs might contribute to the

Human iMSCs improve bone regeneration in mini-pigs
P Jungbluth et al.

8

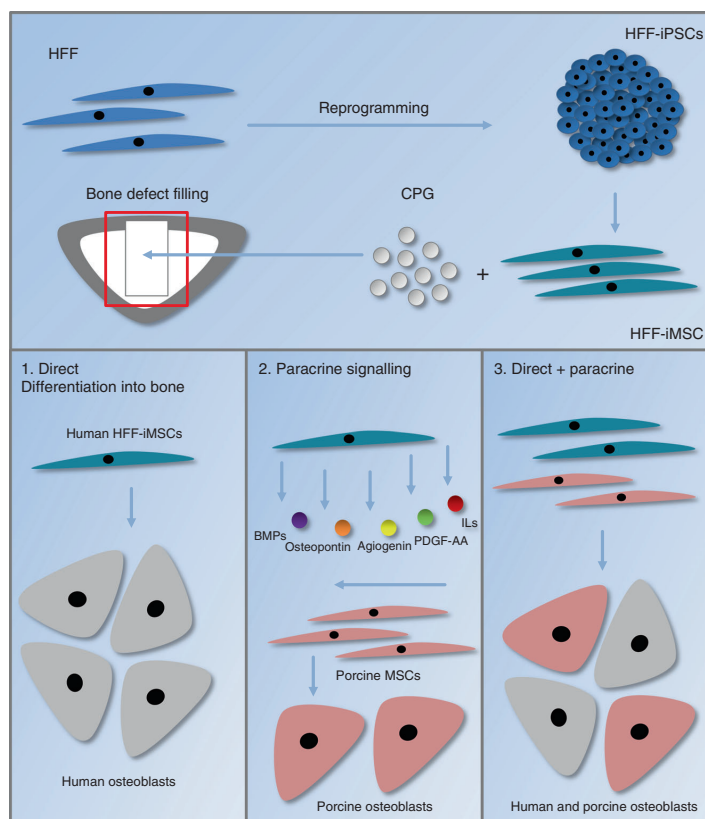


Fig. 6 Possible modes of action of the HFF-iMSCs. We propose three potential mechanisms whereby HFF-iMSCs contribute to the regeneration of critical-size bone defects. 1: Niche-induced differentiation into human osteoblasts; 2: paracrine signaling-induced regeneration by the activation and recruitment of resident stem cells; 3: a combination of niche-induced differentiation and paracrine signaling

regeneration of critical-size bone defects, including (i) their niche-induced differentiation into human osteoblasts, (ii) their paracrine signaling-induced regeneration via the activation and recruitment of resident porcine stem cells, and (iii) a combination of differentiation and paracrine signaling (Fig. 6). Ultimately, iMSC tracing experiments will be required to investigate the homing/chemotactic effects of iMSCs and the efficiency of their expansion *in vivo* in subsequent studies.

The positive effects of the human HFF-iMSC composite in the early phase of bone healing could possibly lead to follow-up experiments that would be conducted for longer than 6 weeks. Additionally, the monitoring of defect healing, biomechanical evaluation and an increase in the numbers of transplanted cells could be of use in future studies.

Using the iPSC approach, it is possible to generate HLA-matched iMSCs for treating distinct bone defects, thus reducing the need for patient-derived BMCs as well as BM-MSCs. Human HFF-iMSC engrafting was shown *in vivo* to lead to the formation of new bone six weeks posttransplantation, thus demonstrating the usefulness of iMSCs for the future treatment of large bone defects. However, clinical applications will require significant improvements to optimize applicability, ensure patient safety and increase the in-depth understanding of the basic biomolecular processes involved in regeneration and the long-term posttransplantation effects.

MATERIALS AND METHODS

Generation of HFF-iPSCs

Human fetal foreskin fibroblasts were reprogrammed at the Biomedicum Stem Cell Center (Helsinki, Finland) using Sendai virus vectors encoding the reprogramming factors OCT3/4, SOX2, KLF4, and C-MYC. The reprogramming and culture of the iPSCs were carried out under feeder-free conditions using Matrigel (Becton Dickinson, Heidelberg, Germany) and E8 medium (Thermo Fisher Scientific, Darmstadt, Germany) or StemMACS IPS BREW medium (Miltenyi Biotec, Bergisch Gladbach, Germany). The clearance of the Sendai virus was confirmed by PCR; we referred to the HFF-derived iPSCs as HFF-iPSCs.

Embryoid body formation

The pluripotency of the iPSCs was confirmed by an embryoid body assay demonstrating the ability of the iPSCs to spontaneously differentiate into cell types representative of the three germ layers (ectoderm, mesoderm, and endoderm) as described previously.⁴⁵ Please refer to Table S1 for a list of the antibodies used. Further details are provided in the Supplementary Methods.

Karyotyping of the HFF-iPSCs

The karyotype analysis was carried out by the Institute of Human Genetics and Anthropology, Heinrich-Heine-University, Düsseldorf, Germany.

Generation of HFF-iMSCs

iMSCs were generated from HFF-iPSCs by using a modified version of an already published protocol¹⁷ that utilized the TGF β pathway inhibitor SB 431542 to facilitate epithelial to mesenchymal transition. The iPSCs were cultured under feeder-free conditions on Matrigel (Becton Dickinson, New Jersey, USA) using human StemMACS iPS BREW XF medium (Miltenyi Biotec). When the cell layer covered ~50% of the well, the medium was switched to α -MEM (alpha-modified minimum essential medium; Sigma-Aldrich, Taufkirchen, Germany) supplemented with 10% FBS, 1% GlutaMAX and 1% P-S⁻¹ without basic fibroblast growth factor. This medium was supplemented with 10 $\mu\text{mol}\cdot\text{L}^{-1}$ SB 431542 (Miltenyi Biotec). For 14 days, the cell culture medium was changed daily. The cells were harvested using TrypLE Express and were reseeded onto uncoated culture dishes in α -MEM without SB 431542 supplementation. After several passaging steps, the cells were characterized as iMSCs. The general cell culture reagents were obtained from Gibco (Thermo Fisher Scientific, Darmstadt, Germany).

Transcriptome analysis

The microarray analysis was performed by using the PrimeView Human Gene Expression Array platform (Affymetrix, Thermo Fisher Scientific). The data are accessible online via the National Center of Biotechnology Information (NCBI) Gene Expression Omnibus. Further processing of the nonnormalized bead summary data was performed using R/Bioconductor software⁴⁶ with the affy package (<http://bioconductor.org/packages/release/bioc/html/affy.html>).⁴⁷ After background correction, the values were converted to a logarithmic scale (to base 2), and normalization was performed using the robust multi-array average method. Ethically approved fetal MSCs (kindly provided by Prof. Richard O.C. Oreffo, University of Southampton-UK) were used as the reference cells.

Flow cytometry

The MSC Phenotyping Kit Human (# 130-095-198) from Miltenyi Biotec was used to identify the cell surface profile of the HFF-iMSCs according to the manufacturer's instructions. The labeled cells were analyzed using a FACSCanto from BD Biosciences (Heidelberg, Germany). The histograms were generated using Summit 4.3.02 software. The protocol used for cell preparation can be found in the Supplementary Methods.

Demonstration of the multipotency of HFF-iMSCs

The differentiation of HFF-iMSCs into adipocytes, chondrocytes, and osteoblasts was performed with the STEMPRO Adipogenesis, Chondrogenesis and Osteogenesis Differentiation Kit (Thermo Fisher Scientific). The differentiation was carried out for 3 weeks with media changes every 2–3 days. After this period, the cells were fixed with PFA and stained as described previously.⁴⁸ The staining procedures are described in the Supplementary Methods.

Secretome analysis of the HFF-iMSC-conditioned media

The molecules secreted from the HFF-iMSCs were identified using the Proteome Profiler Human Cytokine Array Panel A (R&D Systems), which consists of a membrane with 103 different spotted antibodies, according to the user manual. For the detection of cytokines, 1.5 mL of conditioned medium from HFF-iMSCs was incubated on the cytokine membrane. The membrane was analyzed by detecting the emitted chemiluminescence. The pixel density of each spot, representing the amount of bound cytokine, was analyzed using ImageJ software. The value of the negative control was subtracted from all other values. Then, every value was divided by the mean of the values of the reference spots and multiplied by 100 to determine the percentage value in comparison to the reference spots.

Immunofluorescence staining

The cells were stained as described previously.⁴⁸ Please refer to the Supplementary Methods for a detailed description. The list of primary antibodies used can be found in the Supplementary Material (Table S1).

Real-time reverse transcriptase-polymerase chain reaction (qRT-PCR)

Real-time quantitative PCR was performed for each technical triplicate using the Power SYBR Green Master Mix (Life Technologies) with a ViiA7 instrument (Life Technologies). The program used consisted of the denaturation of the samples at 95 °C for 2 min, followed by 40 cycles of amplification (30 s of denaturation at 95 °C, annealing at the primer-specific temperature (57 °C–63 °C) for 30 s, and extension at 72 °C for 30 s). The primers were purchased from MWG, and the specific sequences, as well as the amplicon sizes, are provided in the Supplementary Material (Table S2). For the analysis of the qRT-PCR data, the housekeeping gene encoding ribosomal protein L37A was used to normalize the values of the tested genes. The expression levels were calculated using the $\Delta\Delta\text{CT}$ method and are shown as the mean value with the standard error of mean. The procedures used for RNA isolation and cDNA synthesis are described in the Supplementary Methods.

Bone defect model and cell transplantation

All animals were handled in compliance with the guidelines for the care and use of animals at our institution and in accordance with the EU Directive 2010/63/EU for animal experiments. Approval from the regional ethics committee for animal experiments (LANUV NRW, Recklinghausen, Germany) was obtained (Permit Number: 84-02.04.2015.A042). In this study, 8 female Goettingen mini-pigs (aged 20–28 months, weight 24 kg–35 kg) were used. Based on previous studies performed by our group utilizing a similar animal model and an a priori power analysis, a sample size of 8 was determined to have a power of 80%, and a *P*-value of 0.05 denoted significance.⁴⁹

The animals were randomly assigned to one of the study groups (each group consisted of eight Goettingen mini-pigs). All defects were filled entirely using a volume of 2.4 cm³. In the CPG group, the defects were filled with calcium granules alone, and in the BMC + CPG group, the defects were filled with autologous BMCs in combination with CPG. In the autograft group, the defects were filled with autologous bone harvested from the iliac crest. For this, the iliac crest was exposed, and a Kirschner guide wire (K-wire) was inserted. Using a cannulated reamer placed on the guide wire, cancellous bone was harvested. The results from these 3 groups have been reported by our group⁴ and were used as controls in the present study to avoid the loss of additional animals and for ethical reasons. Preliminary experiments were carried out by our group in which the same defect was created in the proximal tibia of four mini-pigs without the addition of any filling material. Because of a proximal tibia fracture that occurred within 3 days after operation, all of these animals had to be sacrificed prematurely.⁵⁰ Therefore, the defect model used in the current study fulfills the criteria of a critical-size defect model. To prevent the unnecessary sacrifice of additional animals and for ethical reasons, the present study was carried out without a no treatment control.

In accordance with the animal model developed by our group,⁴⁹ a cylindrical defect of 11 mm diameter and 25 mm depth was created in the right proximal tibia medially using a cannulated reamer (Aesculap AG & Co. KG, Tuttlingen, Germany). In the CPG, BMC + CPG and HFF-iMSCs + CPG groups spherical, micro- and macroporous (micro: 2 μm –10 μm ; macro: 150 μm –550 μm), carbonated, and apatite calcium phosphate granules 2 mm–4 mm in size (Calcibon[®] Granules, Biomet Deutschland GmbH, Berlin, Germany) were used.

Human iMSCs improve bone regeneration in mini-pigs
P Jungbluth et al.

10

All surgical procedures were performed with single anesthesia by the same experienced surgeon under strict aseptic conditions. Further methodological details are described in the Supplementary Methods. Using a medial approach in the right proximal tibia, the defect was created 10 mm distal to the joint line and 12 mm anterior to the most posterior aspect of the tibia. In the BMC group, bone marrow was harvested from the iliac crest, and mononuclear cells were concentrated to generate bone marrow concentrate (BMC) using a point-of-care device (MarrowStim® mini concentration system, Biomet Biologics, Inc., Warsaw, Indiana, USA) as described previously.⁴ In the HFF-iMSCs + CPG group, the CPG were soaked with a mixture of 1×10^6 HFF-iMSCs (passage numbers 5, 7, and 9) for five minutes prior to implantation. The soft tissues were closed in layers.

Postoperatively, all animals were allowed to bear their full weight. At 42 days after the procedure, the animals were sacrificed using 3% sodium pentobarbital (Eutha 77, Essex Pharma GmbH, München, Germany). The proximal tibia was harvested by a sharp dissection tool and fixed in 10% neutral buffered formalin solution for 14 days. Figure S5 shows a schematic of the bone defect.

Statistical analysis

The statistical analysis was performed using SPSS software (version 21.0, SPSS Inc., Chicago, IL, USA). The mean values and standard deviations were calculated. The outcome measures of the radiological and histomorphometrical evaluations were examined by one-way analysis of variance (ANOVA). Differences between the independent variables were checked with post hoc tests [Tukey's HSD (honestly significant difference) test]. Significance was defined at a *P*-value < 0.05.

Multidetector computed tomography (MDCT)

Using a 64-detector row CT scanner (SOMATOM Sensation Cardiac 64, Siemens Medical Solutions, Germany), radiographic analysis was performed as described previously.³⁹ In brief, volumetric measurements were performed with respect to density in Hounsfield units (HU) according to axial images. A threshold value of 500 HU was defined for osseous consolidation, and the defect volume was measured three times at different HU ranges:

- (i) Overall size of the defect: measured by including all pixels with an density between -100 and +3 000 HU.
- (ii) Areas of consolidation: measurement of pixels with densities between 500 and 3 000 HU.
- (iii) Nonconsolidated areas: measurement of all pixels with densities between -100 and 500 HU.

Quantitative cone-beam CT (CBCT) volumetry

Using a CBCT scanner with a flat panel detector (PaX-Duo3D, Vatech, Korea), images were obtained as described previously.³⁸ The bone defect volume and extent of new bone formation were evaluated quantitatively using DICOM viewer (Osirix Imaging Software, 64-Bit extended version, Pixmeo, Geneva, Switzerland). With respect to the density values, the volumetric measurements were performed after semiautomatic selection and by marking pixels with predefined density values on the axial images. Based on the mean density values of cortical and trabecular bone, a threshold value of 2 350 was defined for bone consolidation, and volumetric measurements of the defect were performed three times with three different settings:

- (i) Overall size of defect: measured by including all pixels in the outlined defect
- (ii) Areas of consolidation: measurement of pixels with densities >2 350

- (iii) Nonmineralized areas: measurement of all pixels with densities <2 350.

The relative extent of bone regeneration and the absolute volumes of bone consolidation were determined.

Histological preparation of the bone segments

For nondecalfied sectioning, all specimens were dehydrated using an ascending series of graded alcohol and xylene prior to infiltration and embedding in methylmethacrylate. Serial sections were cut in the axial direction using a diamond wire saw (Exakt®, Apparatebau, Norderstedt, Germany). Before staining, the toluidine blue-stained sections were ground to a final thickness of approximately 50 µm.

Histomorphometrical analysis

Two experienced investigators who were blinded to the experimental groups performed all histomorphometric analyses and microscopic observations as described previously.⁴⁹ In brief, the areas of new bone formation (µm²) and the percentage of total new bone formation were measured in the cortical and central defect areas (see Fig. S5). After visual identification, the tissue type was determined manually and assigned a color on three sections from each specimen. Based on this, the areas of newly formed bone, connective tissue, and CPG were calculated according to the total bone defect area.

DATA AVAILABILITY

The HFF, HFF-iPSC and HFF-iMSC transcriptome data are accessible online via the National Center of Biotechnology Information (NCBI) Gene Expression Omnibus.

ACKNOWLEDGEMENTS

Prof. Dr. James Adjaye and Prof. Dr. Joachim Windolf acknowledge support from the medical faculty at Heinrich-Heine-University, Düsseldorf, Germany. In addition, Prof. Dr. James Adjaye and Mr. Md Shaifur Rahman, acknowledge support from the German Academic Exchange Service (DAAD-91607303). We thank Prof. Richard O.C. Oreffo at the Center for Human Development, Stem Cells and Regeneration, Faculty of Medicine, University of Southampton, United Kingdom, for providing the fMSCs. We acknowledge Dr. Claus Kordes at the Clinic of Gastroenterology, Hepatology and Infectious Diseases, Heinrich Heine University, Düsseldorf, Germany, for his assistance with the osteogenic differentiation imaging and Katharina Raba at the Institute of Transplantation Diagnostics and Cell Therapeutics, Heinrich Heine University, for her assistance with the FACS analyses.

AUTHOR CONTRIBUTIONS

J.A., J.S., J.W., P.J. and L.S.S. conceived the ideas and designed the experiments. P.J., J.S., J.G., S.T., M.H. and M.S. were responsible for the care of the animals, the operation procedure and the postoperative care. P.J., J.S., J.G., P.K. and S.T. performed the explantations and subsequent histomorphometrical and radiological analyses. L.S.S., M.S.R. and M.B. performed the characterization of the HFF-iPSCs and the generation and characterization of the HFF-iMSCs. W.W. performed the transcriptome analyses. D.L. evaluated and processed the images of the histomorphometrical and radiological analyses. All authors contributed to the writing of the manuscript, and J.A. and J.W. approved the final version of the manuscript.

ADDITIONAL INFORMATION

The online version of this article (<https://doi.org/10.1038/s41413-019-0069-4>) contains supplementary material, which is available to authorized users.

Competing interests: The authors declare no competing interests.

REFERENCES

1. Faour, O., Dimitriou, R., Cousins, C. A. & Giannoudis, P. V. The use of bone graft substitutes in large cancellous voids: any specific needs? *Injury* **42**, 87–90 (2011).

2. Herten, M. et al. Bone marrow concentrate for autologous transplantation in minipigs. Characterization and osteogenic potential of mesenchymal stem cells. *Vet. Comp. Orthop. Traumatol.* **26**, 34–41 (2013).
3. Grayson, W. L. et al. Stromal cells and stem cells in clinical bone regeneration. *Nat. Rev. Endocrinol.* **11**, 140–150 (2015).
4. Hakimi, M. et al. The composite of bone marrow concentrate and PRP as an alternative to autologous bone grafting. *PLoS ONE* **9**, e100143 (2014).
5. Friedenstein, A. J., Chailakhyan, R. K. & Gerasimov, U. V. Bone marrow osteogenic stem cells: in vitro cultivation and transplantation in diffusion chambers. *Cell Tissue Kinet.* **20**, 263–272 (1987).
6. Pittenger, M. F. et al. Multilineage potential of adult human mesenchymal stem cells. *Science* **284**, 143–147 (1999).
7. Bianco, P., Riminucci, M., Gronthos, S. & Robey, P. G. Bone marrow stromal stem cells: nature, biology, and potential applications. *Stem Cells* **19**, 180–192 (2001).
8. Dominici, M. et al. Minimal criteria for defining multipotent mesenchymal stromal cells. The International Society for Cellular Therapy position statement. *Cytotherapy* **8**, 315–317 (2006).
9. Bhumiratana, S. et al. Tissue-engineered autologous grafts for facial bone reconstruction. *Sci. Transl. Med.* **8**, 343ra83 (2016).
10. Sheyn, D. et al. Human induced pluripotent stem cells differentiate into functional mesenchymal stem cells and repair bone defects. *Stem Cells Transl. Med.* **5**, 1447–1460 (2016).
11. Duscher, D. et al. Aging disrupts cell subpopulation dynamics and diminishes the function of mesenchymal stem cells. *Sci. Rep.* **4**, 7144 (2014).
12. Yang, Y. K., Ogando, C. R., Wang See, C., Chang, T. Y. & Barabino, G. A. Changes in phenotype and differentiation potential of human mesenchymal stem cells aging in vitro. *Stem Cell Res Ther.* **9**, 131 (2018).
13. Palumbo, S., Tsai, T. L. & Li, W. J. Macrophage migration inhibitory factor regulates AKT signaling in hypoxic culture to modulate senescence of human mesenchymal stem cells. *Stem Cells Dev.* **23**, 852–865 (2014).
14. Frobel, J. et al. Epigenetic rejuvenation of mesenchymal stromal cells derived from induced pluripotent stem cells. *Stem Cell Rep.* **3**, 414–422 (2014).
15. Spitzhorn, L. S. et al. Transplanted human pluripotent stem cell-derived mesenchymal stem cells support liver regeneration in Gunn rats. *Stem Cells Dev.* **27**, 1702–1714 (2018).
16. Wang, X. et al. Human ESC-derived MSCs outperform bone marrow MSCs in the treatment of an EAE model of multiple sclerosis. *Stem Cell Rep.* **3**, 115–130 (2014).
17. Chen, Y. S. et al. Small molecule mesengenic induction of human induced pluripotent stem cells to generate mesenchymal stem/stromal cells. *Stem Cells Transl. Med.* **1**, 83–95 (2012).
18. Schlegel, K. A., Lang, F. J., Donath, K., Kulow, J. T. & Wiltfang, J. The monocortical critical size bone defect as an alternative experimental model in testing bone substitute materials. *Oral. Surg. Oral. Med. Oral. Pathol. Oral. Radio. Endod.* **102**, 7–13 (2006).
19. Li, Y. et al. Bone defect animal models for testing efficacy of bone substitute biomaterials. *J. Orthop. Transl.* **3**, 95–104 (2015).
20. Quarto, R. et al. Repair of large bone defects with the use of autologous bone marrow stromal cells. *N. Engl. J. Med.* **344**, 385–386 (2001).
21. Warnke, P. H. et al. Growth and transplantation of a custom vascularised bone graft in a man. *Lancet* **364**, 766–770 (2004).
22. Ismail et al. Mesenchymal stem cell implantation in atrophic nonunion of the long bones: a translational study. *Bone Jt. Res.* **5**, 287–293 (2016).
23. Reichert, J. C. et al. A tissue engineering solution for segmental defect regeneration in load-bearing long bones. *Sci. Transl. Med.* **4**, 141ra93 (2012).
24. Lian, Q. et al. Functional mesenchymal stem cells derived from human induced pluripotent stem cells attenuate limb ischemia in mice. *Circulation* **121**, 1113–1123 (2010).
25. Takahashi, K. et al. Induction of pluripotent stem cells from adult human fibroblasts by defined factors. *Cell* **131**, 861–872 (2007).
26. Komori, T. Requisite roles of Runx2 and Cbfb in skeletal development. *J. Bone Min. Metab.* **21**, 193–197 (2003).
27. Zhou, W., Liu, Q. & Xu, B. Improvement of bone defect healing in rats via mesenchymal stem cell supernatant. *Exp. Ther. Med.* **15**, 1500–1504 (2018).
28. Li, C. L. et al. Human iPSC-MSC-derived xenografts modulate immune responses by inhibiting the cleavage of caspases. *Stem Cells* **35**, 1719–1732 (2017).
29. Jungbluth, P. et al. Concentration of platelets and growth factors in platelet-rich plasma from Goettingen minipigs. *GMS Inter. Plast. Reconstr. Surg. Dgpw.* **3**, Doc11 (2014).

Human iMSCs improve bone regeneration in mini-pigs

P Jungbluth et al.

11

30. Wang, P. et al. Bone tissue engineering via nanostructured calcium phosphate biomaterials and stem cells. *Bone Res.* **2**, 14017 (2014).
31. de Peppo, G. M., Vunjak-Novakovic, G. & Marolt, D. Cultivation of human bone-like tissue from pluripotent stem cell-derived osteogenic progenitors in perfusion bioreactors. *Methods Mol. Biol.* **1202**, 173–184 (2014).
32. Schubert, T. et al. The enhanced performance of bone allografts using osteogenic-differentiated adipose-derived mesenchymal stem cells. *Biomaterials* **32**, 8880–8891 (2011).
33. Tas, A. C. Preparation of porous apatite granules from calcium phosphate cement. *J. Mater. Sci. Mater. Med.* **19**, 2231–2239 (2008).
34. Weiss, P. et al. Synchrotron X-ray microtomography (on a micron scale) provides three-dimensional imaging representation of bone ingrowth in calcium phosphate biomaterials. *Biomaterials* **24**, 4591–4601 (2003).
35. Bohner, M. & Baumgart, F. Theoretical model to determine the effects of geometrical factors on the resorption of calcium phosphate bone substitutes. *Biomaterials* **25**, 3569–3582 (2004).
36. Zhang, J., Liu, W., Schnitzler, V., Tancret, F. & Bouler, J. M. Calcium phosphate cements for bone substitution: chemistry, handling and mechanical properties. *Acta Biomater.* **10**, 1035–1049 (2014).
37. Jungbluth, P. et al. The early phase influence of bone marrow concentrate on metaphyseal bone healing. *Injury* **44**(Oct), 1285–1294 (2013).
38. Kröpil, P. et al. Cone beam CT in assessment of tibial bone defect healing: an animal study. *Acad. Radiol.* **19**, 320–325 (2012).
39. Riegger, C. et al. Quantitative assessment of bone defect healing by multidetector CT in a pig model. *Skelet. Radiol.* **41**, 531–537 (2012).
40. Li, X. et al. iPSC-derived mesenchymal stem cells exert SCF-dependent recovery of cigarette smoke-induced apoptosis/proliferation imbalance in airway cells. *J. Cell Mol. Med.* **21**, 265–277 (2017).
41. Li, X. et al. Mesenchymal stem cells alleviate oxidative stress-induced mitochondrial dysfunction in the airways. *J. Allergy Clin. Immunol.* **141**, 1634–1645 (2018).
42. Schmidt-Bleek, K., Willie, B. M., Schwabe, P., Seemann, P. & Duda, G. N. BMPs in bone regeneration: Less is more effective, a paradigm-shift. *Cytokine Growth Factor Rev.* **27**, 141–148 (2016).
43. Ding, Y. et al. Rap1 deficiency-provoked paracrine dysfunction impairs immunosuppressive potency of mesenchymal stem cells in allograft rejection of heart transplantation. *Cell Death Dis.* **9**, 386 (2018).
44. Zhang, Y. et al. Absence of NUCKS augments paracrine effects of mesenchymal stem cells-mediated cardiac protection. *Exp. Cell Res.* **356**, 74–84 (2017).
45. Bohndorf, M. et al. Derivation and characterization of integration-free iPSC line ISRM-UM51 derived from SIX2-positive renal cells isolated from urine of an African male expressing the CYP2D6 *4/*17 variant which confers intermediate drug metabolizing activity. *Stem Cell Res.* **25**, 18–21 (2017).
46. Gentleman, R. C. et al. Bioconductor: open software development for computational biology and bioinformatics. *Genome Biol.* **5**, R80 (2004).
47. Gautier, L., Cope, L., Bolstad, B. M. & Irizarry, R. A. Affy-analysis of Affymetrix GeneChip data at the probe level. *Bioinformatics* **20**, 307–315 (2004).
48. Rahman, M. S. et al. The presence of human mesenchymal stem cells of renal origin in amniotic fluid increases with gestational time. *Stem Cell Res Ther.* **9**, 113 (2018).
49. Hakimi, M. et al. Combined use of platelet-rich plasma and autologous bone grafts in the treatment of long bone defects in mini-pigs. *Injury* **41**, 717–723 (2010).
50. Jungbluth, P. et al. Platelet-rich plasma on calcium phosphate granules promotes metaphyseal bone healing in mini-pigs. *J. Orthop. Res.* **28**, 1448–1455 (2010).



Open Access This article is licensed under a Creative Commons Attribution 4.0 International License, which permits use, sharing, adaptation, distribution and reproduction in any medium or format, as long as you give appropriate credit to the original author(s) and the source, provide a link to the Creative Commons license, and indicate if changes were made. The images or other third party material in this article are included in the article's Creative Commons license, unless indicated otherwise in a credit line to the material. If material is not included in the article's Creative Commons license and your intended use is not permitted by statutory regulation or exceeds the permitted use, you will need to obtain permission directly from the copyright holder. To view a copy of this license, visit <http://creativecommons.org/licenses/by/4.0/>.

© The Author(s) 2019

Supplementary Material

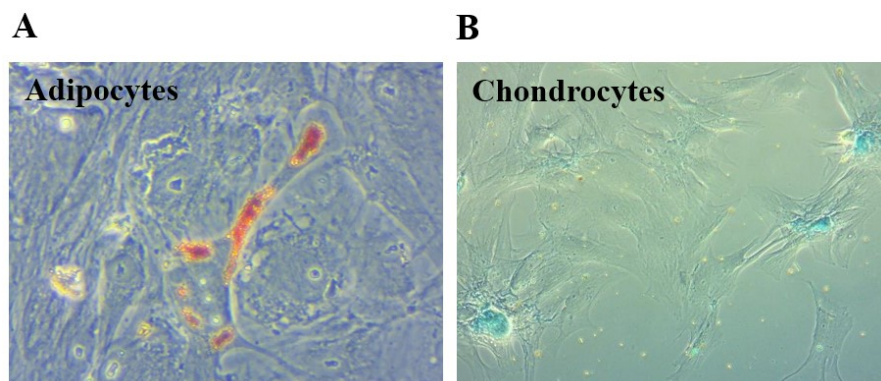


Figure S1. HFF-iMSC differentiations. (A) Oil Red O Staining of evolved fat droplets upon adipogenic differentiation. (B) Alcian Blue staining of proteoglycans within the chondrocyte clusters.

Sample	HFF-iMSC	fMSC	HFF-iPSC	B4 iPSC	H1 ESC
HFF-iMSC	1	0.947	0.833	0.790	0.788
fMSC	0.947	1	0.893	0.837	0.834
HFF-iPSC	0.833	0.893	1	0.953	0.944
B4 iPSC	0.790	0.837	0.953	1	0.982
H1 ESC	0.788	0.834	0.944	0.982	1

Figure S2. Pearson correlation values.

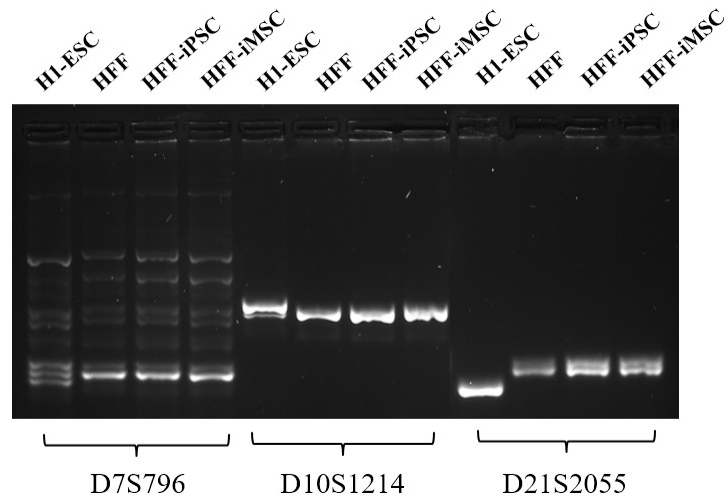


Figure S3. Short-tandem-repeat Analysis. Short-tandem-repeat PCR of HFF, HFF-iPSCs and HFF-iMSCs based on the primers D7S796, D10S1214 and D21S2055 confirms a common genetic background and origin.

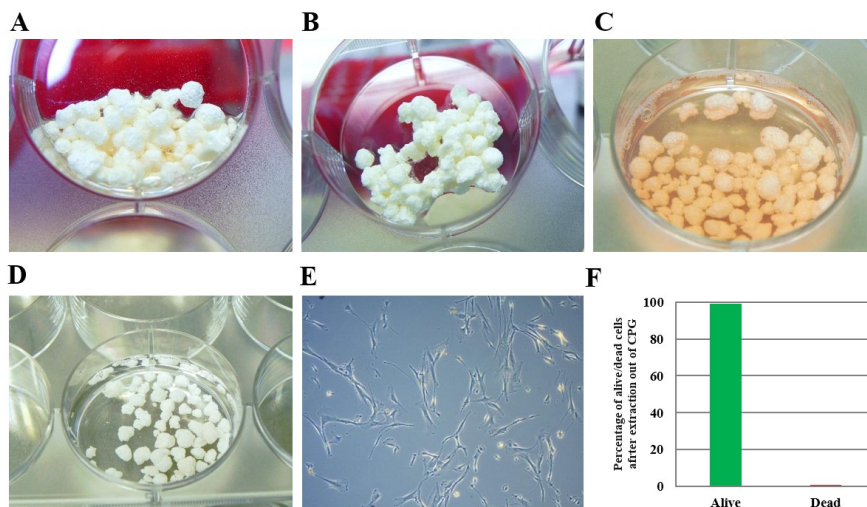


Figure S4. *In vitro* compatibility test of HFF-iMSC and CPG. (A) Loading of CPG with HFF-iMSC suspension. (B) CPGs after absorption of HFF-iMSC suspension. (C) Incubation of loaded CPGs at 37°C and 5% CO₂ for 24h in MSC medium. (D) Extraction of HFF-iMSCs out of CPG with TrypLE. (E) HFF-iMSC reattachment and growth on plastic dish. (F) Plot of alive/dead cells after extraction out of CPG.

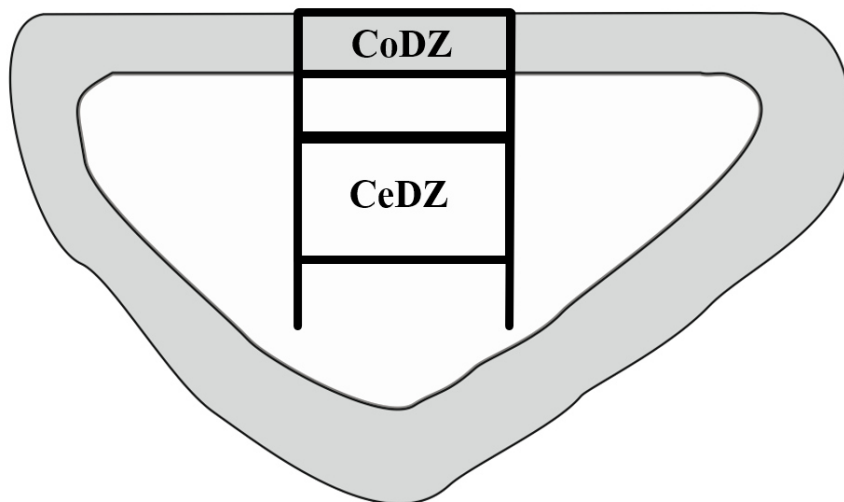


Figure S5. Schematic of a histological section with the critical-size bone defect in the proximal tibia. Histomorphometrical quantification of new bone formation was carried out for two distinct regions- the cortical defect zone (CoDZ) and the central defect zone (CeDZ). Adapted from Hakimi et al., 2014 (4).

Table S1. List of antibodies

Primary Antibodies	Providing Company	Dilution
OCT-4A (C30A3) rabbit mAb number 2840	Cell Signaling Technology, USA	1:400
SSEA4 (MC813) mouse mAb number 4755		1:1000
E-cadherin (24E10) rabbit mAb number 3195		1:200
Vimentin (5G3F10) mouse mAb number 3390		1:200
TRA-1-60 mouse mAb number 4746		1:1000
TRA-1-81 mouse mAb number 4745		1:1000
Rabbit anti-NANOG Cat# 4903S		1:800
Rabbit anti-SOX2 Cat# 3579S		1:400
c-Myc (D84C12) Rabbit mAb #5605		1:400
KLF4 Antibody #4038		1:400
LIN28A (D84C11) XP® Rabbit mAb #3695		1:400
PDGF Receptor β (28E1) Rabbit mAb #3169		1:100
CD133 PA2049	Boster Bio, USA	1:500
C-Kit (H-300) rabbit polyclonal IgG	Tebu Bio, Germany	1:200
rb PODXL, sc33138	Santa Cruz Biotechnology, USA	1:200
aSMA Cat# M0851, RRID:AB_2223500	Dako (Agilent), USA	1:1000
Nestin Cat# N5413, RRID:AB_1841032	Sigma-Aldrich, USA	1:1000
Mouse anti-Sox17 Cat# AF1924, RRID:AB_355060	R and D Systems, USA	1:250

Table S2. List of primers

Gene	Primer Sequences	
RUNX2	F1: CAGACCAGCAGCACTCCATA	R1: CAGCGTCAACACCATCATTC
BGLAP	F1: AAGGTGCAGCCTTTGTGTCC	R1: GGCTCCCAGCCATTGATACA
ALPL	F1: CTATCCTGGCTCCGTGCTC	R1: ACTGATGTTCCAATCCTGCG
D7S796	F1: TTTTGGTATTGGCCATCCTA	R1: GAAAGGAACAGAGAGACAGGG
D10S1214	F1: ATTGCCCAAAACTTTTTTG	R1: TTGAAGACCAGTCTGGGAAG
D21S2055	F1: AACAGAACCAATAGGCTATCTATC	R1: TACAGTAAATCACTTGGTAGGAGA

Supplementary Methods

Staining of differentiated HFF-iMSCs

For adipocyte staining, a 0.2 % Oil-Red-O working solution was prepared by diluting the 0.5 % stock solution with distilled water followed by filtration using whatman paper. The medium was aspirated completely and the cells washed with PBS followed by 50 % ethanol. The cells were stained with 0.2 % Oil-Red-O Solution for 10 min at room temperature. After two washing steps with 50 % ethanol and distilled water, PBS was added to the cells to enable microscopic analysis. For chondrocyte staining, the cells were washed with

PBS and then stained with 1 % Alcian Blue solution (prepared in 0.1 N HCl) for 30 min at room temperature on a rocking platform. Afterwards, the cells were rinsed three times with 0.1 N HCl, covered with distilled water and analysed by light microscopy. For osteoblast staining, the cells were rinsed with distilled water and stained with 2 % Alizarin Red S solution (prepared in distilled water) for 30 min at room temperature on a rocking platform. Afterwards, the wells were washed three times with distilled water and PBS was finally added to allow their visualization by light microscopy.

Embryoid body formation

Initially, the iPSCs were cultured on matrigel using StemMACS IPS BREW medium. After reaching confluence they were detached using PBS (without Calcium and Magnesium) and then cultured in T25 flasks as a suspension culture using high glucose DMEM, containing 10% FBS, 1% P/S, 1% GlutaMAX and 1% NEAA. The emerging embryoid bodies were collected and settled on a gelatin-coated well. After 3-4 days the embryoid bodies were fixed using 4% PFA then stained with antibodies specific to the three germ layers (see Table S1).

Immunofluorescence staining

To block unspecific binding sites blocking buffer was applied to the fixed (4% PFA) cells for 2h at RT. If intracellular proteins were to be stained, blocking buffer containing 10% normal goat serum (NGS, Sigma), 0.5% Triton X-100 (Carl Roth GmbH & Co. KG, Karlsruhe, Germany), 1% BSA (Sigma), and 0.05% Tween 20 (Sigma), all dissolved in PBS, was used. When extracellular proteins were stained, Triton and Tween were omitted. Primary antibodies were added to the cells for 1h at RT followed by 3 washing steps. Afterwards the corresponding secondary antibodies (Thermo Fisher Scientific) and DAPI (Southern Biotech) or Hoechst 33258 dye (Sigma-Aldrich Chemie GmbH, Taufkirchen, Germany) were applied to the cells and incubated for 1h at RT in the dark. A fluorescence microscope (LSM700; Zeiss, Oberkochen, Germany) was used for imaging. Picture processing was done using the ZenBlue 2012 Software Version 1.1.2.0. (Carl Zeiss Microscopy GmbH, Jena, Germany).

Cell preparation for flow cytometry

The cells were detached using TrypLE Express (Gibco) for 7 min at 37°C. After centrifugation at 300 g for 5 min, 200,000 cells were distributed into two 5 ml flow cytometry tubes in 2 ml phosphate buffered saline (PBS). The cells were then centrifuged for 10 min at 300 g, the supernatants were discarded, and the pellets were resuspended in 100 µl PBS. The phenotyping cocktail (0.5 µl) was then applied to the first of the two tubes. The cocktail contains antibodies directed against CD14-PerCP, CD20-PerCP, CD34-PerCP, CD45-PerCP, CD73-APC, CD90-FITC, and CD105-PE. In the second tube, the Isotype Control Cocktail was applied. After 10 min of incubation at 4°C in the

dark, the cells were washed with PBS and centrifuged at 300 g for 10 min. Afterwards, the pellets were resuspended in 100 µl paraformaldehyde (PFA 4 %) for storage until flow cytometric analysis.

RNA Isolation and cDNA Synthesis

RNA isolation was performed using the Direct-zol RNA Miniprep Kit (Zymo Research, CA, USA) according to manufacturer's instruction. Complementary DNA (cDNA) synthesis from 500ng mRNA was done applying the TaqMan Reverse Transcription Kit (Applied Biosystems). The reaction mixture (20µl per sample) included 7.70µl H₂O, 2µl reverse transcriptase buffer, 4.4µl MgCl₂ (25mM), 1µl Oligo (dT)/ Random hexamer (50µM), 4µl dNTP mix (10mM), 0.4µl RNase Inhibitor (20U/µl) and 0.5µl Reverse Transcriptase (50U/µl).

In vitro compatibility test of HFF-iMSC and CPG

First, 2.4cm³ CPGs were loaded with 1100µl of a suspension of 1x10⁶ HFF-iMSC. After cell suspension was completely absorbed by the CPGs the cell-loaded granules were covered with 5 ml αMEM medium and incubated at 37°C and 5% CO₂ for 24h. Afterwards the CPGs were washed with PBS and incubated in TrypLE for 15 min at 37°C with repeatedly shaking. Alive/dead ratio of the extracted cells was determined by trypan blue staining and cells were reseeded onto a plastic culture dish.

Animal preparation for cell transplantation

All mini-pigs fasted for a minimum of 12 h before surgery and peri-operative antibiotic prophylaxis was attained by daily administration of 3.3 ml Lincomycin (Lincomycin 20%, WDT, Garbsen, Germany) for three days starting immediately prior to surgery. Animals were primed by an intramuscularly applied sedation with 0.5 mg/kg Atropin (Atropinsulfat, B Braun, Melsungen, Germany), 5 mg/kg Azaperon (Stresnil®, Janssen-Cilag GmbH, Neuss, Germany) and 10 mg/kg Ketamin (Ketavet®, Pharmacia GmbH, Karlsruhe, Germany). Anesthesia was started with 0.5 g Thiopental (Inresa Arzneimittel GmbH, Freiburg, Germany) and maintained by inhalation of oxygen, nitrous oxide, and isoflurane. Infusion of 5 % Glucose's solution (Delta-Select, Pfullingen, Germany), 10 ml Inzolen (Koehler Chemie GmbH,

Alsbach-Hähnlein, Germany), and 5 ml Lidocain 2 % (Lidocain-HCl, B. Braun, Melsungen, Germany) was administered at a rate during the procedure to maintain hydration and cardiac protection. By an intravenous injection of 0.4 mg/kg Pirtramid (Dipidolor®, Janssen-Cilag GmbH, Neuss, Germany) and 4.5 mg/kg Carprofene (Rimadyl®, Pfizer Pharma GmbH, Karlsruhe, Germany) intra-operative analgesia was ensured. For the treatment of post-operative pain Pirtramid and Carprofene were applied subcutaneously for three days.

DNA-Fingerprinting analysis

DNA isolation was done using the QIAamp® DNA Mini KIT following the manufacture's instruction. The analysis of the short-tandem-repeats (STR) was by PCR using distinct primers (D7S796, D10S1214 and D21S2055). Primer sequences are provided in supplementary table 2. The PCR reaction contained 5 µl 1x Go-Taq G2 Hot Start Green PCR buffer, 4 µl 4 mM MgCl₂, 0.5 µl dNTP-Mix (10 mM each), 1 µl forward primer (0.3 µM), 1 µl reverse primer (0.3 µM), 0.125 µl (0.625 U) Hotstart Taq polymerase (5 U/µl), and 100 ng genomic DNA were mixed. Water was added to adjust a final volume of 25 µl. A thermal cycler (PEQLAB, Erlangen Germany) was utilized for the PCR reaction. The 5 min initial denaturation at 94°C were followed by 32 cycles consisting of a denaturation step at 94°C for 15 s, an annealing step at 60°C for 30 s, and an extension step at 68°C for 60 s. Gel electrophoresis (2.5% agarose gel) was used to detect the PCR amplification products. The used primers are listed in Table S2.

2.12 Human mesenchymal factors induce rat hippocampal- and human neural stem cell dependent oligodendrogenesis

Janusz J. Jadasz, Lena Tepe, Felix Beyer, Iria Samper Agrelo, Rainer Akkermann, Lucas-Sebastian Spitzhorn, Maria Elena Silva, Richard O. C. Oreffo, Hans-Peter Hartung, Alessandro Prigione, Francisco J. Rivera, James Adjaye and Patrick Küry

Abstract

The generation of new oligodendrocytes is essential for adult brain repair in diseases such as multiple sclerosis. We previously identified the multifunctional p57kip2 protein as a negative regulator of myelinating glial cell differentiation and as an intrinsic switch of glial fate decision in adult neural stem cells (aNSCs). In oligodendroglial precursor cells (OPCs), p57kip2 protein nuclear exclusion was recently found to be rate limiting for differentiation to proceed. Furthermore, stimulation with mesenchymal stem cell (MSC)-derived factors enhanced oligodendrogenesis by yet unknown mechanisms. To elucidate this instructive interaction, we investigated to what degree MSC secreted factors are species dependent, whether hippocampal aNSCs respond equally well to such stimuli, whether apart from oligodendroglial differentiation also tissue integration and axonal wrapping can be promoted and whether the oligodendrogenic effect involved subcellular translocation of p57kip2. We found that CC1 positive oligodendrocytes within the hilus express nuclear p57kip2 protein and that MSC dependent stimulation of cultured hippocampal aNSCs was not accompanied by nuclear p57kip2 exclusion as observed for parenchymal OPCs after spontaneous differentiation. Stimulation with human MSC factors was observed to equally promote rat stem cell oligodendrogenesis, axonal wrapping and tissue integration. As forced nuclear shuttling of p57kip2 led to decreased CNPase- but elevated GFAP expression levels, this indicates heterogenic oligodendroglial mechanisms occurring between OPCs and aNSCs. We also show for the first time that dominant pro-oligodendroglial factors derived from human fetal MSCs can instruct human induced pluripotent stem cell-derived NSCs to differentiate into O4 positive oligodendrocytes.

Publication Status: published in *Glia*. 2018 Jan;66(1):145-160.

Impact Factor: 5.846

This article is reproduced with permission.

Approximated total share of contribution: 5%

Contribution on experimental design, realization and publication:

LSS was responsible for the expansion of the human MSCs as well as for the production of the conditioned medium. All authors contributed to the writing of the manuscript.

Link to the publication:

<https://onlinelibrary.wiley.com/doi/full/10.1002/glia.23233>

Received: 15 February 2017 | Revised: 4 August 2017 | Accepted: 29 August 2017

DOI: 10.1002/glia.23233



RESEARCH ARTICLE

Human mesenchymal factors induce rat hippocampal- and human neural stem cell dependent oligodendrogenesis

Janusz J. Jadasz¹ | Lena Tepe¹ | Felix Beyer¹ | Iria Samper Agrelo¹ |
 Rainer Akkermann¹ | Lucas-Sebastian Spitzhorn² | Maria Elena Silva^{3,4} |
 Richard O. C. Oreffo⁵ | Hans-Peter Hartung¹ | Alessandro Prigione⁶ |
 Francisco J. Rivera^{3,7,8} | James Adjaye² | Patrick Küry¹

¹Department of Neurology, Neuroregeneration, Medical Faculty, Heinrich-Heine-University, Düsseldorf, D-40225, Germany²Institute for Stem Cell Research and Regenerative Medicine, Medical Faculty, Heinrich-Heine University, Düsseldorf, D-40225, Germany³Laboratory of Stem Cells and Neuroregeneration, Institute of Anatomy, Histology and Pathology, Faculty of Medicine, Universidad Austral de Chile, Valdivia, Chile⁴Institute of Pharmacy, Faculty of Sciences, Universidad Austral de Chile, Valdivia, Chile⁵Bone and Joint Research Group, Centre for Human Development, Stem Cells and Regeneration, Institute of Developmental Sciences, University of Southampton, Southampton, SO16 6YD, United Kingdom⁶Max Delbrueck Center for Molecular Medicine (MDC), Berlin, D-13125, Germany⁷Center for Interdisciplinary Studies on the Nervous System (CISNe), Universidad Austral de Chile, Valdivia, Chile⁸Institute of Molecular Regenerative Medicine & Spinal Cord Injury and Tissue Regeneration Center Salzburg (SCI-TReCS), Paracelsus Medical University Salzburg, Salzburg, Austria**Correspondence**

Janusz Jadasz, Department of Neurology,
 Heinrich-Heine-University Düsseldorf,
 Moorenstrasse 5, D-40225 Düsseldorf,
 Germany.
 Email: janusz.jadasz@uni-duesseldorf.de

Funding information

This work was supported by the German Research Foundation (DFG; SPP1757/KU1934/2_1, KU1934/5-1), the Christiane and Claudia Hempel Foundation for clinical stem cell research, DMSG Ortsvereinigung Düsseldorf und Umgebung e.V., iBrain, YoungGlia, the German Academic Exchange Service (DAAD) and FONDECYT-CONICYT (Chile; regular grant number 1161787). A.P. is supported by a young investigator grant from the Bundesministerium für Bildung und Forschung (BMBF e:Bio). The MS Center at the Department of Neurology is supported in part by the Walter and Ilse Rose Foundation and the James and Elisabeth Cloppenburg, Peek & Cloppenburg Düsseldorf Foundation. R. O. is supported by grants from the BBSRC (LO21072/1) and MRC (MR/K026682/1). J. A acknowledges funding from the medical faculty of Heinrich Heine University, Düsseldorf.

Abstract

The generation of new oligodendrocytes is essential for adult brain repair in diseases such as multiple sclerosis. We previously identified the multifunctional p57kip2 protein as a negative regulator of myelinating glial cell differentiation and as an intrinsic switch of glial fate decision in adult neural stem cells (aNSCs). In oligodendroglial precursor cells (OPCs), p57kip2 protein nuclear exclusion was recently found to be rate limiting for differentiation to proceed. Furthermore, stimulation with mesenchymal stem cell (MSC)-derived factors enhanced oligodendrogenesis by yet unknown mechanisms. To elucidate this instructive interaction, we investigated to what degree MSC secreted factors are species dependent, whether hippocampal aNSCs respond equally well to such stimuli, whether apart from oligodendroglial differentiation also tissue integration and axonal wrapping can be promoted and whether the oligodendrogenic effect involved subcellular translocation of p57kip2. We found that CC1 positive oligodendrocytes within the hilus express nuclear p57kip2 protein and that MSC dependent stimulation of cultured hippocampal aNSCs was not accompanied by nuclear p57kip2 exclusion as observed for parenchymal OPCs after spontaneous differentiation. Stimulation with human MSC factors was observed to equally promote rat stem cell oligodendrogenesis, axonal wrapping and tissue integration. As forced nuclear shuttling of p57kip2 led to decreased CNPase- but elevated GFAP expression levels, this indicates heterogenic oligodendroglial mechanisms occurring between OPCs and aNSCs. We also show for the first time that dominant pro-oligodendroglial factors derived from human fetal MSCs can instruct human induced pluripotent stem cell-derived NSCs to differentiate into O4 positive oligodendrocytes.

KEYWORDS

heterogeneity, inhibitors, intracellular protein shuttling, multiple sclerosis, myelin repair, neuroregeneration, oligodendrocyte

1 | INTRODUCTION

Upon demyelination in the adult central nervous system (CNS) as observed in multiple sclerosis (MS), a certain degree of myelinating glial cell replacement and of *de novo* generation of myelin sheaths can be observed (Franklin, 2002). Resident oligodendroglial precursor cells (OPCs) and adult neural stem cells (aNSCs) are the two major sources for myelin repair (Akkermann, Jadasz, Azim, & Küry, 2016). The efficiency of this endogenous regeneration process remains limited due to the fact that these cells often fail in terminal maturation, most likely due to the presence of multiple differentiation inhibitors (de Castro, Bribian, & Ortega, 2013; Kremer, Aktas, Hartung, & Küry, 2011; Kuhlmann, Miron, Cui, Wegner, Antel, & Brück, 2008). Moreover, the oligodendrogenic potential of aNSCs of both neurogenic niches differs as mainly cells of the subventricular zone (SVZ) of the lateral ventricles were found to differentiate into oligodendrocytes (OLs) in demyelination animal models (Nait-Oumesmar, Picard-Riera, Kerninon, & Baron-Van Evercooren, 2008; Picard-Riera et al., 2002; Xing et al., 2014) and in MS brain tissue (Nait-Oumesmar et al., 2007). While aNSCs possess the capacity to differentiate into neurons, astrocytes and oligodendrocytes, evidence is missing that hippocampal stem cells generate oligodendrocytes (OLs) or OPC-like cells *in vivo*, unless genetically manipulated (Jadasz et al., 2012; Jessberger, Toni, Clemenson, Ray, & Gage, 2008; Rolando et al., 2016). We previously discovered p57kip2 as a key negative regulator of oligodendroglial differentiation and acting as determinant of glial fate decision in aNSCs (Jadasz et al., 2012; Kremer et al., 2009). Furthermore, p57kip2 protein translocation from nucleus to cytoplasm was recently observed to be a rate-limiting step in parenchymal OPC maturation (Göttle et al., 2015), which raised the question whether a similar shuttling process is also essential for oligodendroglial fate specification in aNSCs.

Another efficient approach to promote oligodendrogenesis is by administering trophic factor cocktails such as secreted by bone marrow-derived mesenchymal stem cells (MSCs) (Kassis et al., 2008; Uccelli, Moretta, & Pistoia, 2008). Both cell types, aNSCs as well as OPCs, were shown to respond to MSC-derived factors when grown in co-cultures or when supplied with conditioned media. For instance, the incubation of aNSCs with rat mesenchymal stem cell conditioned medium (MSC-CM) resulted in an increased percentage of oligodendrocyte cells (Rivera et al., 2006) and, furthermore, ameliorated and stabilized OPC maturation (Jadasz et al., 2013). *In vivo* administration of human adult MSC-CM to the demyelinated CNS improved its recovery (Bai et al., 2012) and MSCs were found to modulate hippocampal stem cells into oligodendrocytes (Bai et al., 2009; Munoz, Stoutenger, Robinson, Spees, & Prockop, 2005; Rivera et al., 2006). However, a number of questions regarding MSC-mediated specification of aNSCs and their oligodendroglial progeny remain unaddressed. Currently the identity of MSC-CM derived compounds as well as the underlying mode of action are unknown, which is of additional interest considering the observation that not all MSCs are able to potentiate oligodendroglial processes (Lindsay, Johnstone, McGrath, Mallinson, & Barnett, 2016; Lindsay et al., 2013). Moreover, it is important to note that the majority

of studies were performed with adult MSCs and it remains therefore to be shown whether the oligodendrogenic potential is restricted to adult cells or whether it strictly correlates with its bone (cell-) origin.

We present data which provides evidence that intrinsic oligodendroglial differentiation mechanisms of parenchymal precursor- and neural stem cells differ but that extrinsic (MSC-derived) stimuli are not restricted to specific stages or ages. Moreover, we show for the first time that also fetal human MSC-derived factors are equally potent in stimulating oligodendrogenesis and in preventing astrocyte formation and that they can potently instruct human induced pluripotent stem cell-derived NSCs. Our findings can thus contribute to the overall understanding of instructive stem/stem cell interactions and to the possible development of future myelin repair strategies.

2 | MATERIALS AND METHODS

2.1 | Adult rat mesenchymal stem cell culture

Preparation and culture of adult rat mesenchymal stem cells were performed according to previous descriptions (Jadasz et al., 2013). Briefly, one 12-week old female Wistar rat was anesthetized using isoflurane (DeltaSelect, Langenfeld, Germany) and killed by decapitation. Femoral and tibial bones were separated from the body, exposed and cleaned from remaining tissue before femoral head and tibial plateau were cut off and bone marrow was flushed out into Minimum Essential Medium alpha Medium (α -MEM) (Gibco Cell Culture, Life Technologies, Germany) using a cannula. Bone marrow clumps were dissociated by repeated resuspension with the cannula and recovered by centrifugation at 800 g for 10 min. Cell pellets were resuspended in α -MEM containing 10% fetal bovine serum (FBS; PAN Biotech GmbH, Germany) and seeded at 1×10^6 cells/cm² in a humidified incubator at 37°C with 5% CO₂. After three days, adherent cells were further incubated in fresh α -MEM-10%FBS until 90–100% confluency was reached. To achieve a confluent monolayer after three days of incubation, 4×10^5 cells per 100 mm culture dish were seeded for cells from 10 week old rats. For experiments, α -MEM-10%FBS incubated for three to four days on rMSC populations was used as rat mesenchymal stem cell conditioned medium (MSC-CM) to stimulate adult neural stem cells after sterile filtration (20 μ m filter).

2.2 | Adult rat neural stem cell culture and transfection

Preparation and culture methods of adult neural stem cells were conducted as previously described (Jadasz et al., 2012). Briefly, brains of five adult Wistar rats (12-week old) were used for preparation of hippocampal stem cells. Isoflurane anesthetized animals were killed by decapitation and after removal of the brains hippocampal areas were prepared, mechanically digested and put in 4°C phosphate buffered saline (PBS; PAA Laboratories, Pasching, Austria). After washing the cell suspension in PBS, cells were enzymatically digested in PDD solution containing papain (0.01%, Worthington Biochemicals, Lakewood, USA), 0.1% dispase II (Boehringer, Ingelheim, Germany), DNase I

(0.01%, Worthington Biochemicals) and 12.4 mM MgSO₄, dissolved in HBSS (PAA Laboratories) for 30 min at 37°C with 10 min trituration steps in between. After additional washing steps in neurobasal (NB) medium (Gibco BRL, Karlsruhe, Germany) supplemented with B27 (Gibco), 2 mM L-glutamine (Gibco), 100 U/ml penicillin/0.1 mg/l streptomycin (PAN Biotech, Aidenbach, Germany) and centrifugation at 200 g for 5 min, cells were resuspended in NB medium supplemented with 2 µg/ml heparin (Sigma-Aldrich, Taufkirchen, Germany), 20 ng/ml FGF-2 (R&D Systems, Wiesbaden-Nordenstadt, Germany) and 20 ng/ml EGF (R&D Systems). This protocol allows the cells, seeded at 7×10^4 cells/ml density, to form neurospheres in uncoated T75 culture flasks at 37°C in a humidified incubator with 5% CO₂. Every two days medium was changed and adult neural stem cells were passaged once a week using accutase (PAA Laboratories) for separation (10 min at 37°C). For experiments, cells were dispersed by an accutase step and plated on poly-L-ornithine/laminin (100 µg/ml and 5 µg/ml, Sigma-Aldrich) coated and acid-pretreated 13 mm glass cover slips ($5-8 \times 10^4$ cells/coverslip), or on ethanol activated Mimetix aligned 12-well plate fibre scaffold inserts (2×10^5 cells/insert; Electrospinning company, Harwell Oxford, UK) for 24 hr in proliferation medium containing FGF2, EGF and heparin before changing to control medium (α -MEM), rat mesenchymal stem cell conditioned medium (rMSC-CM) or to human fetal MSC-CM from two different cell lines (H36, H37) all of which containing 10% FBS.

For transplantation studies onto cerebral slice cultures, adult neural stem cells were transfected with pmaxGFP plasmid (LONZA) for visualization. To do so, accutase-dispersed NSCs from neurosphere cultures of passages three to nine were subjected to nucleofection of using a Lonza nucleofection device and the adult rat NSC nucleofector kit (Lonza, Basel, Switzerland). In detail, 2.5×10^6 cells were transfected using program A-033 (high-efficiency) resuspended in 100 µl nucleofection solution and 3.4 µg plasmid.

To modulate the expression of the p57kip2 gene in adult neural stem cells nucleofections were performed with overexpression constructs pIRES (empty vector control), pIRES-p57kip2 (wild type p57kip2) and pIRES-NLS (p57kip2 with mutated NLS sequence) as published previously (Göttle et al., 2015). For visualization expression vectors were cotransfected with pmaxGFP (Lonza; a green fluorescent protein expression vector) at a ratio of 13.6:1.

2.3 | iPSC-derived NSC preparation

Human NSCs were derived from induced pluripotent stem cell (iPSC) lines that were previously generated from healthy neonatal foreskin fibroblasts (BJ line from ATCC) using episomal plasmids containing the reprogramming factors OCT4, KLF4, SOX2, c-MYC, NANOG, LIN28, and SVLT (Lorenz et al., 2017). NSCs were induced following a small molecule-mediated protocol (Li et al., 2011). Briefly, iPSCs were split and plated onto feeder-free Matrigel-coated plates in DMEM/F12 medium. The next day, the cells were cultured in 1:1 Neurobasal: DMEM/F12 medium with 1x N2, 1x B27, 10 ng/ml hLIF (ThermoFisher), 4 µM CHIR99021 (Cayman Chemical), 3 µM SB431542 (SelleckChem), 0.05% BSA, pen/strep, MycoZap, and L-glutamine. In

addition, 0.1 µM Compound E (Calbiochem) was included for the first week of differentiation. NSCs were maintained on matrigel-coated plates and split by scraping with a cell spatula at 80–100% confluence at ratios of 1:2 to 1:5. All cultures were kept in a humidified atmosphere of 5% CO₂ at 37°C under atmospheric oxygen condition and were regularly monitored against mycoplasma contamination.

2.4 | Human fetal bone marrow-derived mesenchymal stem cell culture

Human fetal (hf) femur-derived MSC cells (H36, H37) were obtained at 55 days postconception following informed, written patient consent. Approval was obtained by the Southampton and South West Hampshire Local Research Ethics Committee (LREC 296100). Their derivation and characterization has been described previously (Mirmalek-Sani et al., 2006). Human fetal MSCs were cultured in MEM medium with α -modifications (Minimum Essential Medium Eagle-Alpha Modified α -MEM; Sigma-Aldrich Chemie GmbH, Steinheim, Germany). 500 ml of α -MEM were supplemented with 10% FBS (FBS Gibco® by life technologies, California, USA), 1% GlutaMAX® (Glutamax®, ThermoFisher Scientific, Darmstadt, Germany) and 1% penicillin/streptomycin (ThermoFisher Scientific, Darmstadt, Germany). This mixture was then vacuum filtered with a 0.2 µm sieve. Medium was replenished every three days and kept as conditioned medium for further experiments. Cells were harvested at 90% confluency. For cell detachment, TrypLE Select 1x (TrypLE or Trypsin Gibco®, ThermoFisher Scientific, Darmstadt, Germany) was added (8 ml for T175) and the dish was placed into the incubator (36°C, 5% CO₂) for 7 minutes. To stop the enzymatic reaction fresh α -MEM medium was added (20 ml in T175). The cell suspension was then placed into a 50 ml falcon tube and centrifuged (550 g, 7 min, room temperature). The supernatant was discarded and the resulting cell pellet was solved in 10 ml α -MEM for cell counting.

2.5 | Immunohistochemistry

After rats were deeply anesthetized and transcardially perfused using 4% paraformaldehyde (PFA), brains were extracted, postfixed in 4% PFA for 24 hr and cryoprotected in 30% sucrose. Subsequently, brains were quick-frozen in -35°C to -50°C cold methylbutan. Brain slices (14 µm) were cut and stained according to standard protocols: rabbit anti-p57kip2 (1:250, SIGMA), mouse anti-GFAP (1:500, Millipore), mouse anti-adenomatous polyposis coli for oligodendrocytes (APC, CC1; 1:500, GeneTex), anti-mouse and anti-rabbit antibodies conjugated with either Alexa Fluor594 or Alexa Fluor488 (1:500, ThermoFisher Scientific, Darmstadt, Germany). The nuclei were stained with 4',6-diamidino-2-phenylindole (DAPI, 1:100, Roche). Brain slices were mounted under fluoromount-G® (SouthernBiotech) and analyzed using a confocal CLSM microscope (Zeiss, Jena, Germany).

2.6 | Immunocytochemistry

To evaluate marker expression, immunocytochemical analysis was performed as previously described (Jadasz et al., 2012, 2013). Briefly, the cells were fixed for 10 min using 4% PFA and unspecific binding of



antibody was prevented by incubation for 45 min in 1% normal goat serum (NGS; in PBS, 0.1% Triton). Subsequently, cells were subjected to primary antibody solution (0.1% NGS, 0.03% Triton or 10% NGS for O4 staining) and following dilutions were used overnight at 4°C: rabbit anti-p57kip2 (1:250, Sigma-Aldrich), mouse anti-myelin basic protein (MBP; 1:500, Sternberger Monoclonals, Lutherville, MD), mouse anti-2',3'-cyclic-nucleotide 3'-phosphodiesterase (CNPase; 1:500, Sternberger Monoclonals), mouse anti-GFAP (1:1000, Millipore), rabbit anti-GFAP (1:1000, Dako, Hamburg, Germany), rabbit anti-Olig2 (1:1000, Millipore, 1:250 for staining of human cells), mouse anti-O4 (1:40, Millipore) and anti-mouse and anti-rabbit antibodies conjugated with either Alexa Fluor594 or Alexa Fluor488 (1:500, ThermoFisher Scientific, Darmstadt, Germany). Secondary antibodies were applied for 2 hr at room temperature following washing steps with PBS. The nuclei were stained with DAPI (1:100, Roche). Cells were mounted under Citifluor (Citifluor, Leicester, UK) and analyzed using an Axioplan2 or a confocal CLSM microscope (Zeiss, Jena, Germany). The statistical analyses of the positive cells normalized to DAPI using two-tailed unpaired t-test were made with Image J, Excel and GraphPad Prism 5.0c software.

2.7 | RNA preparation, cDNA synthesis and quantitative RT-PCR

RNA preparation, cDNA synthesis and quantitative RT-PCR were performed as recently described (Jadasz et al., 2013). Briefly, reverse transcription was done using the high capacity cDNA Reverse Transcription Kit ThermoFisher Scientific, Darmstadt, Germany) after total RNA was purified from cultured stem cells via the RNeasy procedure (Qiagen, Hilden, Germany). For quantitative RT-PCR, SYBRGreen universal master mix (ThermoFisher Scientific, Darmstadt, Germany) was mixed with cDNA and gene expression levels were determined on a 7900HT sequence detection system (Applied Biosystems). Using PrimerExpress 2.0 software (Applied Biosystems), we generated, tested and determined primer sequences for specific amplicon generation: AQP4 forward: CAT GGC CAG CAG TGA GGT TT, AQP4 reverse: CAT CGC CAA GTC CGT CTT CT, CGT forward: CCG GCC ACC CTG TCA AT, CGT reverse: TCC GTC GTG GCG AAG AA, CNPase forward: GCC GTT GTG GTA CTT CTC CA, CNPase reverse: GCC CGA AAA AGC CAC ACA TT, GAPDH forward: GAA CGG GAA GCT CAC TGG C, GAPDH reverse: GCA TGT CAG ATC CAC AAC GG, GFAP forward: CTG GTG TGG AGT GCC TTC GT, GFAP reverse: CAC CAA CCA GCT TCC GAG AG, GST-pi forward: TTG CAT CGA AGG TCC TCC AC, GST-pi reverse: CAC CTG GGT CGC TCT TTA GG, Id2 forward: AGA ACC AAA CGT CCA GGA CG, Id2 reverse: TGC TGA TGT CCG TGT TCA GG, Id4 forward: CAG CTG CAG GTC CAG GAT GT, Id4 reverse: AAA GTG GAG ATC CTG CAG CAC, MBP forward: CAA TGG ACC CGA CAG GAA AC, MBP reverse: TGG CAT CTC CAG CGT GTT C, NG2 forward: GTA CGC CAT CAG AGA GGT CG, NG2 reverse: ATC TGG GAG GGG GCT ATT GT, Olig2 forward: CCC CGT CTG GGC TTA GAA G, Olig2 reverse: CTC CTA CCC CGC CCA AAA.

We used GAPDH as reference gene, which proved to be the most accurate and stable normalization gene among a number of others such as β -actin, β -2-microglobulin, hydroxymethyl-bilane synthase,

hypocanthine phosphoribosyl-transferase I, ribosomal protein L13a, succinate dehydrogenase complex subunit A, TATA box binding protein, ubiquitin C, tyrosine 3-monooxygenase/tryptophan 5-monooxygenase activation protein zeta polypeptide as referenced in (Vandesompele et al., 2002). Relative gene expression levels were determined according to the $\Delta\Delta Ct$ method (ThermoFisher Scientific, Darmstadt, Germany). Each sample was measured in quadruplicate; data are shown as mean values \pm SEM.

2.8 | Slice culture preparation

For slice cultures Wistar rats of both sexes, aged between 7 and 10 days were used. Animals were anaesthetized with isoflurane before decapitation. Upon removal, the whole brain was transferred into a petri dish filled with ice cold HEPES buffered Ringer solution (135 mM NaCl, 5.4 mM KCl, 1 mM MgCl₂ x6H₂O, 1.8 mM CaCl₂2H₂O, 5 mM HEPES, pH: 7.2). For the generation of cerebellar slices, the cortex was fixed with forceps while a parasagittal cut was made with a scalpel, chopping off one lateral edge of the cerebellum. Afterwards, the cerebellum was separated from the rest of the brain and carefully dried on a Whatman paper. The cutting edge of the sagittal cut was then fixed to the magnetic platform of the HM 650V microtome (ThermoFisher Scientific, Darmstadt, Germany) with a drop of superglue (UHU, Mannheim, Germany). The magnetic platform was then transferred into the basin of the microtome filled with Ringer solution so that the cerebellum was covered with liquid. The cooling element, previously stored at -20°C was introduced to keep the buffer temperature down. A razor blade was placed into the cutting segment and the brain was positioned with the dorsal part pointing toward the razor blade. Finally, 350 μm thick sagittal sections were made (cutting frequency: 50 Hz, cutting amplitude: 1 mm, cutting speed: 0.9 mm/s). The slices were collected in a petri dish filled with ice cold Ringer solution and plated onto the membrane of Millicell cell culture inserts (hydrophilic PTFE, pore size: 0.4 μm , diameter 30 mm; Merck Millipore, Darmstadt, Germany) in 6-well plates before one washing step with sterile Ringer solution and one washing step with slice medium were performed. Nutrition of slices was provided by 1 ml of slice medium [50% basal medium eagle (BME), 25% HBSS +/+, 25% heat inactivated horse serum; containing 1% penicillin/streptomycin (ThermoFisher Scientific), and 5 mg/ml D-Glucose monohydrate (Merck, Darmstadt, Germany)] underneath the membrane. All fluid on top of the slice was carefully removed to enable gas exchange. Medium was changed completely the next day and then every 3–4 days. Tissue slices were kept in culture for a maximum time of 20 days.

2.9 | Transplantation of adult neural stem cells on slice cultures

Before transplantation onto slices, NSCs were transfected with pmaxGFP to mark cells as described above. After transfection, a small pipette was used to transfer the cells into 10 ml of prewarmed NB all medium thereby omitting dead cell debris. After one centrifugation step, cells were resuspended in slice medium. Onto each tissue slice, prepared and transferred to membranes the day before, 2×10^5 cells in 5 μl slice medium were

transplanted. At the same time, the medium was changed from slice medium to 50% slice medium/50% α -MEM as control condition or 50% slice medium/50% H37 MSC-CM. Slices with transplanted aNSCs and treated with control or MSC conditioned media were kept in culture for 4 days before fixation. Slices were once washed with PBS and fixed with 4% PFA for 15 minutes. To cover the whole slice with liquid, 1 ml was added underneath the membrane and 1 ml was added on top of the slice and the membrane. The slices were washed with PBS three times to remove remaining PFA. Each slice was then carefully cut out of the membrane with a scalpel and transferred to a wet chamber. To make the slice permeable for antibodies, they were incubated over night at 4°C in permeabilization solution (0.5% Triton x-100 in PBS). Unspecific binding was then prevented by incubation in blocking solution (10% NGS, 1% BSA, 0.2% Triton x-100 in PBS) over night at 4°C. Primary antibodies were diluted in antibody solution (1% NGS, 1% BSA, 0.1% Triton x-100 in PBS) and added to the slices over night at 4°C at following concentrations: mouse anti-MBP (1:500), rabbit anti-GFAP (1:1000). Secondary antibodies were diluted in the same antibody solution and added after the excess primary antibody had been washed off: goat anti-mouse Alexa 488 (1:500), goat anti-rabbit Alexa 488 (1:500), goat anti-rabbit Alexa 594 (1:500), goat anti-mouse Alexa 594 (1:500), goat anti-rabbit Alexa 647 (1:500). Secondary antibodies were also incubated over night at 4°C and protected from light to avoid bleaching of the fluorescent dyes. After washing with PBS for three times, the slices were transferred to a microscope slide facing upwards. Slices were mounted with coverslips under Citifluor, secured by small drops of nail varnish and analyzed using the confocal laser scanning microscope 510 (CLSM 510, Zeiss, Jena, Germany). Z-stack pictures with a 20 \times magnification were collected and for analysis of transplanted cells, Z-stacks were fused to a maximum intensity Z-stack with Image J. For live cell imaging, transplanted aNSCs were photographed every ten minutes starting at time point 2 hr post-transfection/transplantation lasting up to 96 hr.

2.10 | Statistical analysis

Statistical analysis and graphs were performed using Excel and GraphPad Prism 5.0c software. To determine statistical significance, Student's *t*-test was applied for groups of two, one-way ANOVA with Bonferroni post-test for multiple comparisons was applied comparing three or more groups and two-way ANOVA with Bonferroni post-test for groups of three or four with different conditions/variables. Statistical significance thresholds were set as follows: **p* < .05; ***p* < .01; ****p* < .001. All data are shown as mean values \pm SEM and "n" represents the number of independent experiments performed.

3 | RESULTS

3.1 | Heterogeneous subcellular localization of the p57kip2 protein in the hippocampal neurogenic niche of the adult brain

We examined p57kip2 protein localization in cells of adult neurogenic niche regions and applied immunohistochemical staining on sagittal

brain sections of wild type rats. We placed emphasis on analyzing and comparing cells from corresponding areas of both neurogenic zones as others have shown that niche architecture and differentiating cells are both heterogeneous (Doetsch et al., 2002). Therefore, we investigated cells within the hilus of the inner tapering area of the subgranular zone (SGZ) and scored CC1 positive or GFAP positive cells according to the nature of their p57kip2 signals. Inspection of the hilus of the SGZ area revealed that the majority of CC1 positive oligodendrocytes expressed this protein and that predominantly nuclear p57kip2 localization could be observed (Figure 1a–c). Conversely, fewer astrocytes (as revealed by the GFAP signals outside the granular zone, as opposed to neural stem cells within the zone) expressed this factor and these cells almost equally displayed nuclear in combination with cytoplasmic p57kip2 signals (Figure 1d–f). Furthermore, we analyzed cells within the inferior horn as subregion of the SVZ scoring CC1 positive cells according to the nature of their p57kip2 signals. Inspection of the SVZ revealed predominantly cytoplasmic p57kip2 localization in CC1 positive oligodendrocytes (Figure 1g–i). These observations suggest that oligodendroglial derivatives of the two stem cell niches differently depend on the endogenous p57kip2 translocation and that cells of the SGZ follow an opposite localization mechanism as compared with myelinating cells derived from parenchymal OPCs (Göttle et al., 2015; Kremer et al., 2009), which is why we focused in all of our following experiments on the analysis of hippocampal adult neural stem cells.

3.2 | Nuclear localization of the p57kip2 protein during adult neural stem cell dependent oligodendrogenesis

To correlate the subcellular localization of p57kip2 with the oligodendroglial differentiation of hippocampal aNSCs, we exposed cultured stem cells to strong oligodendroglial stimuli provided by adult rat bone marrow mesenchymal stem cell conditioned media (MSC-CM; Rivera et al., 2006; Steffenhagen et al., 2012). Using the differentiating aNSCs, we studied whether this stimulation affects p57kip2 protein shuttling from nucleus to cytoplasm as it occurs in differentiating parenchymal OPCs (Göttle et al., 2015). Three and seven days after MSC-CM treatment cells were fixed and immunocytochemical stainings confirmed the generation of oligodendrocytes as the majority of cells expressed 2',3'-cyclic-nucleotide 3'-phosphodiesterase (CNase) as well as myelin basic protein (MBP; Figure 2a–b'). By applying the anti-p57kip2 antibody (Figure 2c–e), we could discriminate between three distinct patterns of p57kip2 localization: (1) exclusively nuclear localization (Figure 2c–c',f; red bars), (2) ubiquitous localization in which the intensity of p57kip2 staining was similar for nuclear and cytoplasmic signals (Figure 2d–d',f; grey bars), and (3) exclusively extranuclear localization (Figure 2e–e',f; white bars). We observed that nuclear p57kip2 localization was more prominent in MBP positive cells as compared with negative cells. Over time, i.e., with continued MSC-CM stimulation, the degree of cells with nuclear signals decreased and the majority of OLS featured ubiquitous protein localization (Figure 2f). Almost none of the cells at

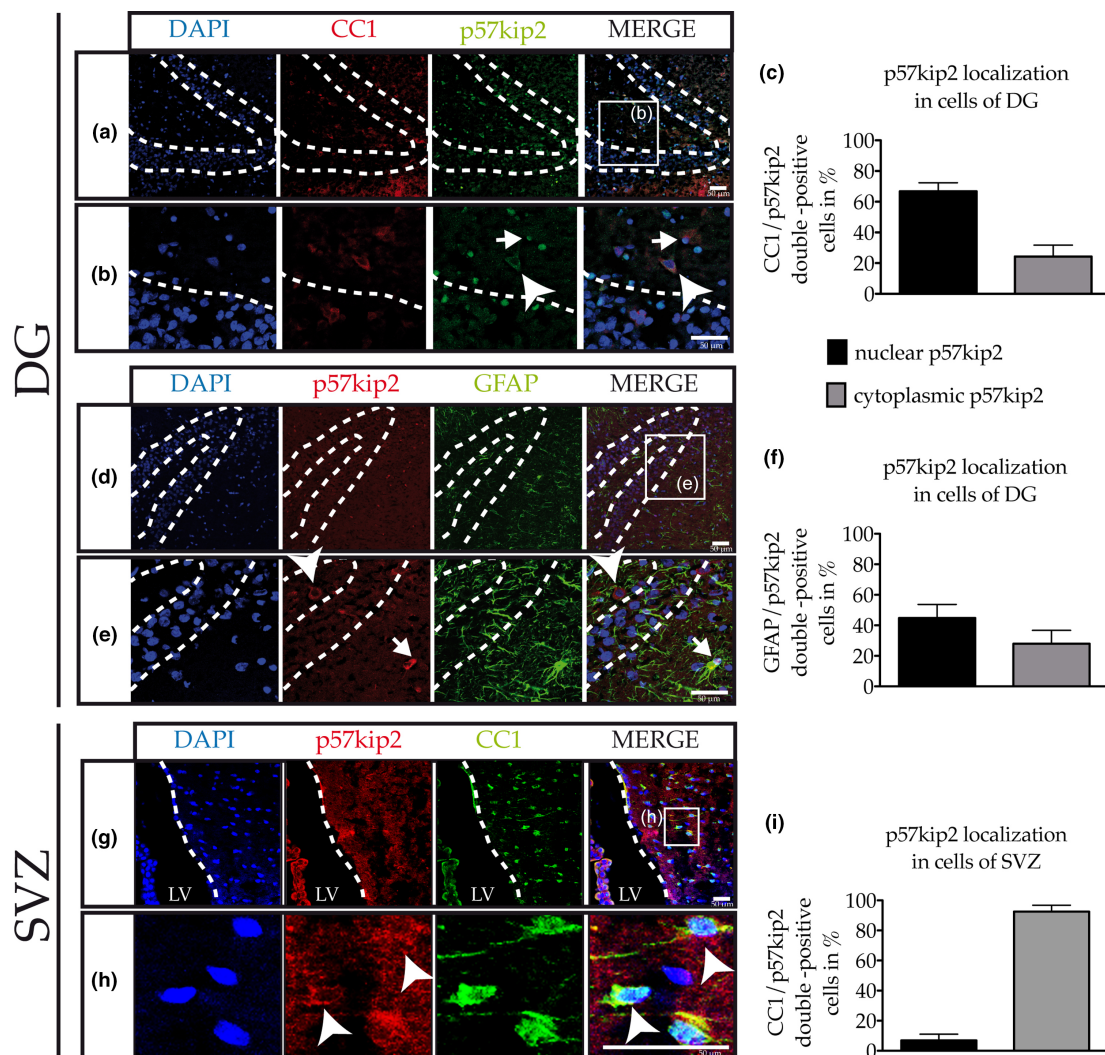


FIGURE 1 Localization of p57kip2 protein in the dentate gyrus of the rat adult brain. (a,b) Immunohistochemical staining in the dentate gyrus of the hippocampal formation and in the subventricular zone of the lateral ventricle revealed that p57kip2 and the oligodendroglial marker anti-adenomatous polyposis coli (CC1) are co-expressed. (c) We quantified oligodendroglial cells in the vicinity of the hippocampal stem cell niche lying in the tapering triangle of the inner dentate gyrus and found the p57kip2 protein was mainly localized in nuclei (60% of CC1/p57kip2 positive cells; indicated by arrows) rather than cytoplasm (22%; indicated by arrowheads). (d-f) Fewer GFAP positive cells expressed this factor and both subcellular localizations were equally detected. (g-i) In contrast, antibody stainings revealed that the localization of p57kip2 within cells lying in the inferior horn of the SVZ is mainly found in the cytoplasm indicated by arrowheads and that the co-expressing with CC1 was higher than compared with nuclear CC1/p57kip2 positive cells. Data are shown as mean values \pm SEM derived from $n = 5$ rat brains. Scale bars: 50 μ m [Color figure can be viewed at wileyonlinelibrary.com]

day three as well as day seven displayed exclusive cytoplasmic p57kip2 signals, which is in strong contrast to the clear re-patterning that was observed during parenchymal OPC differentiation and myelination (Göttle et al., 2015).

For functional assessment, we transfected aNSCs prior to MSC-CM stimulation with an expression vector that carries a p57kip2 variant with a mutated nuclear localization signal (NLS), confining it to the cytoplasm.

Overexpression of this mutant protein was shown to induce a dominant negative effect and to substantially promote parenchymal OPC differentiation, whereas the wild type protein (with sustained nuclear localization) blocked oligodendroglial maturation (Göttle et al., 2015). aNSCs were transfected with either empty control vector (pIRES), the full-length wild type p57kip2 overexpression construct (pIRES-p57kip2), or with the NLS mutant expression construct (pIRES-NLS) along with a

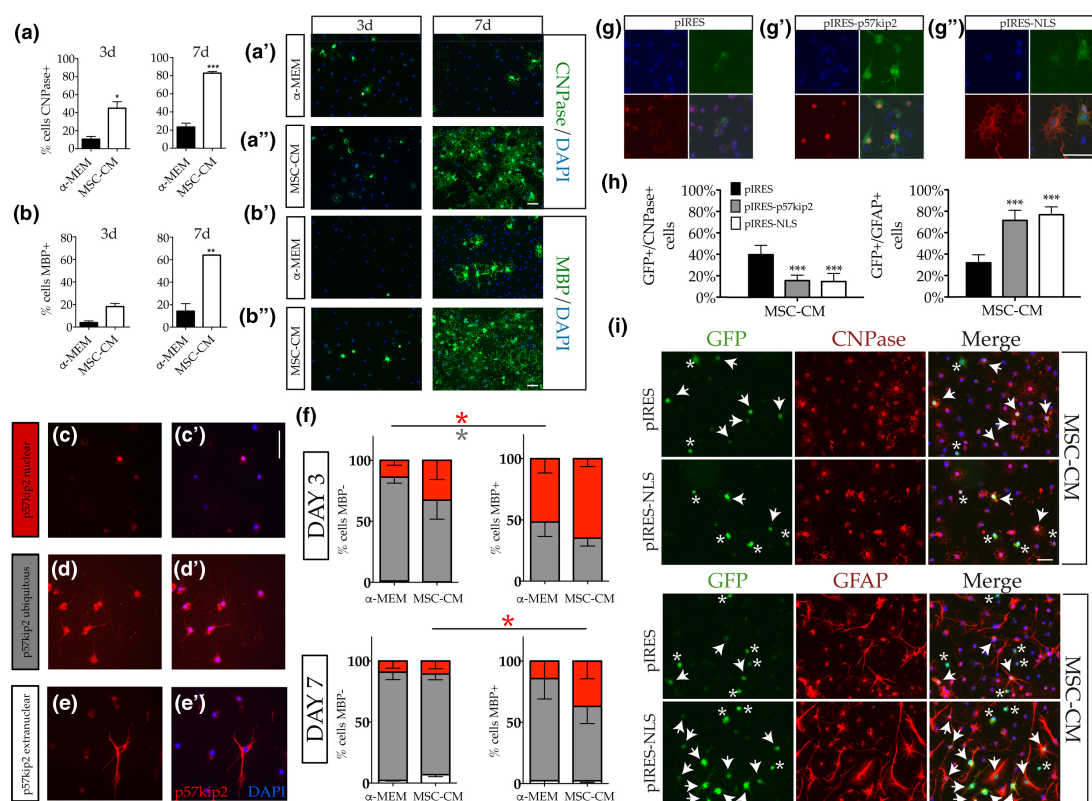


FIGURE 2 p57kip2 protein localization under oligodendroglial differentiation promoting conditions. (a–b'') Adult neural stem cells were treated with adult rat bone marrow-derived mesenchymal stem cell conditioned medium (MSC-CM) to direct and promote oligodendrocyte differentiation as revealed by increased degrees of CNPase and MBP expressing cells. (c–e'') Representative anti-p57kip2 stainings of cultured aNSCs revealed three different p57kip2 localization patterns: predominantly nuclear localization (c–c'), ubiquitous localization in the nucleus as well as in the cytoplasm (d–d') and extranuclear localization (e–e'). (f) p57kip2 immunofluorescent stainings in MBP negative and MBP positive cells revealed that in the oligodendroglial lineage more cells displayed nuclear p57kip2 protein signals (as compared with MBP negative cells) and that during further maturation a shift toward ubiquitous protein localization was observed. Almost none of the cells displayed exclusive cytoplasmic signals. (g–g'') Anti-p57kip2 immunofluorescent staining three days after transfection of aNSCs (visualized by means of maxGFP expression) showed that control transfected cells (pIRES) expressed low p57kip2 signals (g) pIRES-p57kip2 transfected aNSCs displayed strong nuclear signals (g') and that pIRES-NLS transfected NSCs displayed strong signals exclusively in the cytoplasm (g''). Anti-CNPase and anti-GFAP stainings (h,i) showed that three days after p57kip2 overexpression and modulation of nuclear entry, the degree of CNPase positive cells significantly decreased in all treatments and that, concomitantly, the GFAP positivity increased. Asterisks indicate GFP positive cells devoid of CNPase or GFAP, arrows point to CNPase or GFAP expressing cells. Data are mean values \pm SEM derived from $n = 3$ –6 independent experiments. Statistical analysis: one-way ANOVA analysis of variance with Bonferroni's multiple comparison post-test, two-way ANOVA analysis of variance with Bonferroni post-test and student's t -test ($*p < .05$; $**p < .01$; $***p < .001$). Scale bars: 50 μ m [Color figure can be viewed at wileyonlinelibrary.com]

GFP expression vector to detect transfected cells. Immunofluorescent staining confirmed increasing nuclear signal intensities in cells with wild type protein overexpression (Figure 2g–g') but also revealed that the NLS mutant protein was localized mainly in the cytoplasm (Figure 2g''), indicating that the mutation abolished NLS functionality. Under MSC-CM dependent differentiation the degree of CNPase vs. GFAP expressing cells was determined as a function of the molecular modulation. In contrast to reactions of parenchymal OPCs (Göttle et al., 2015), introduction of the NLS mutant led to significant decrease of CNPase

positivity as much as upon overexpression of the wild type p57kip2 protein (Figure 2h,i). We next asked whether directed protein localization can affect the astrocyte-oligodendrocyte determination axis of aNSCs and evaluated the degree of GFAP positive astrocytes. GFAP positive cells similarly increased following expression of the p57kip2 protein with NLS mutation or the wild type p57kip2 protein (Figure 2h,i), the latter of which is in line with our previous observations (Jadasz et al., 2012). Together, overexpression of p57kip2 proteins severely interfered with the MSC induced oligodendroglial induction.



3.3 | Human fetal mesenchymal stem cell secreted factors facilitate the oligodendroglial differentiation of adult neural stem cells

Reproduced observations on rat MSC activities promoting the generation of oligodendroglial cell derivatives from NSCs, prompted us to assess the oligodendroglial potential of supernatants derived from human MSC cultures. In xenoreactive approaches, human MSC-CM from different origins were reported to be limited in their repair capacity (Lindsay et al., 2013). Therefore, in light of the recently discovered embryonic origin of adult neural stem cells (Furutachi et al., 2015), we wondered whether human fetal MSCs were also able to direct and stimulate oligodendrocyte differentiation and to modulate intracellular distribution of the p57kip2 protein.

To answer this question, we included two different human fetal mesenchymal stem cell populations, termed H36 and H37 in our experiments. Human fetal MSCs were obtained from femurs at gestation ages of 8–9 weeks and cultured for 21 days before clonal multipotent populations were produced with the potential to differentiate into adipocytes, osteocytes and chondrocytes (Mirmalek-Sani et al., 2006). Stimulation of aNSCs with either H36 or H37 conditioned media resulted in increased levels of NG2 transcripts after one day of incubation and decreased thereafter (Figure 3a). Gene expression levels of ceramide galactosyltransferase (CGT), Olig2, CNPase and MBP were also increased and eventually maintained at later stages (Figure 3a). Concomitantly, we also detected robust inductions of the cellular fractions expressing oligodendroglial specific proteins such as Olig2, CNPase and MBP (Figure 3b–d). Along the oligodendroglial lineage (i.e., in MBP positive cells), H36 and H37 MSC-CM similarly promoted an initial nuclear presence of p57kip2 protein, which upon longer application was altered to a more ubiquitous distribution pattern (Figure 3e) almost identical to what was observed for rat MSC-CM (Figure 2f), indicating that the identified mesenchymal instructive capacity is conserved across species. Conversely, transcript levels for early astrocytic genes such as Id2 and Id4 were timely and efficiently downregulated by both human MSC-CM and late astrocytic transcripts encoding AQP4 and GFAP experienced robust and significant downregulations mainly at later time points (Figure 3f). Of note, GFAP protein expression, being a hallmark of both adult neural stem cells as well as astrocytes, was initially increased in response to rat and human MSC-CMs and then downregulated along with the induction of late oligodendroglial markers (Figure 3g).

3.4 | Nuclear p57kip2 protein localization upon stimulation with human fetal MSC-CM

Our findings showed that the subcellular localization of the p57kip2 protein is affected over time in presence of human MSC-derived factors characterized by a transition to ubiquitous nuclear and cytoplasmic signals (Figure 3e). We next challenged adult hippocampal neural stem cells with p57kip2 overexpression constructs and H36 or H37 MSC-CM stimuli. Similar to the reactions of transfected cells observed in the presence of rat MSC-CM, overexpression of both p57kip2

protein variants, wild type as well as the NLS mutant, led to decreased numbers of CNPase positive oligodendrocytes (Figure 4a,b) and to an increase of GFAP positivity (Figure 4c,d), thus interfering with MSC directed oligodendrogenesis and boosting expression of astrocytic markers.

3.5 | Myelination and tissue integration of hippocampal adult neural stem cells

To evaluate the myelination potential of fate-directed hippocampal stem cell progeny by mesenchymal stem cell secreted stimuli, we incubated aNSCs with rat and human MSC-CM on 2 μ m thick myelination competent nanofibers [Aligned Mimetix microfibers; (Bechler, Byrne, & Ffrench-Constant, 2015)]. Supernatants of rat and human origin were equally potent in enhancing the generation of MBP positive internode-like structures (Figure 5c–h,i,l), which were only occasionally observed upon treatment with control medium (α -MEM; Figure 5a–b,i,l). In the control condition most of the cells significantly upregulated GFAP in contrast to aNSCs subjected to mesenchymal secreted factors, in which MBP was significantly upregulated (Figure 5i). Concomitantly, aNSCs cultured for seven days demonstrated a significant increase in sheath length after exposure to human fetal conditioned medium (Figure 5j,k,l). To reveal whether these observations hold true in a more physiological model, we transplanted hippocampal aNSCs onto organotypic slice cultures. Cerebelli from seven to ten day old rats were cut into 350 μ m thick slices and incubated on cell culture inserts which allowed observation and discrimination of white and grey matter structures (Figure 6b,c). Slices were incubated without aNSCs for 24 hr, then GFP expressing cells were added (for identification and visualization of transplanted cells) followed by stimulation with either a mix of 50% α -MEM/50% slice culture medium (as control condition) or with 50% human fetal H37 MSC-CM/50% slice culture medium. Four days after treatment, slice cultures were fixed and stained for GFAP and MBP to detect astrocytes and oligodendrocytes, respectively. We observed that hippocampal aNSCs integrated into slices and readily initiated differentiation into myelin forming MBP positive oligodendrocytes in the presence of human MSC conditioned medium (H37) whereas integration, cellular process outgrowth and MBP formation were almost not detectable under control conditions (Figure 6a). Furthermore, we detected that transplanted hippocampal aNSCs developed parallel MBP positive processes when exposed to human MSC-CM indicating the differentiation into myelinating mature oligodendrocytes (Figure 6d–d’). We then asked how fast aNSCs diversify their morphology toward mature OLs and observed that the initiation of parallel process morphologies started between 18 and 28 hr after exposure to human fetal H37 medium (Figure 6e,f). We reproducibly observed aNSCs with such a mature morphology on each cerebellar slice upon H37 treatment across all eight experiments and furthermore noticed that mature OLs did not vanish after 4 days of treatment (Figure 6g). In contrast, under control conditions we did not observe such a cellular phenotype within this time frame and found only one cell with parallel processes after 4 days of incubation across all experiments. These data therefore suggest that secreted factors of human

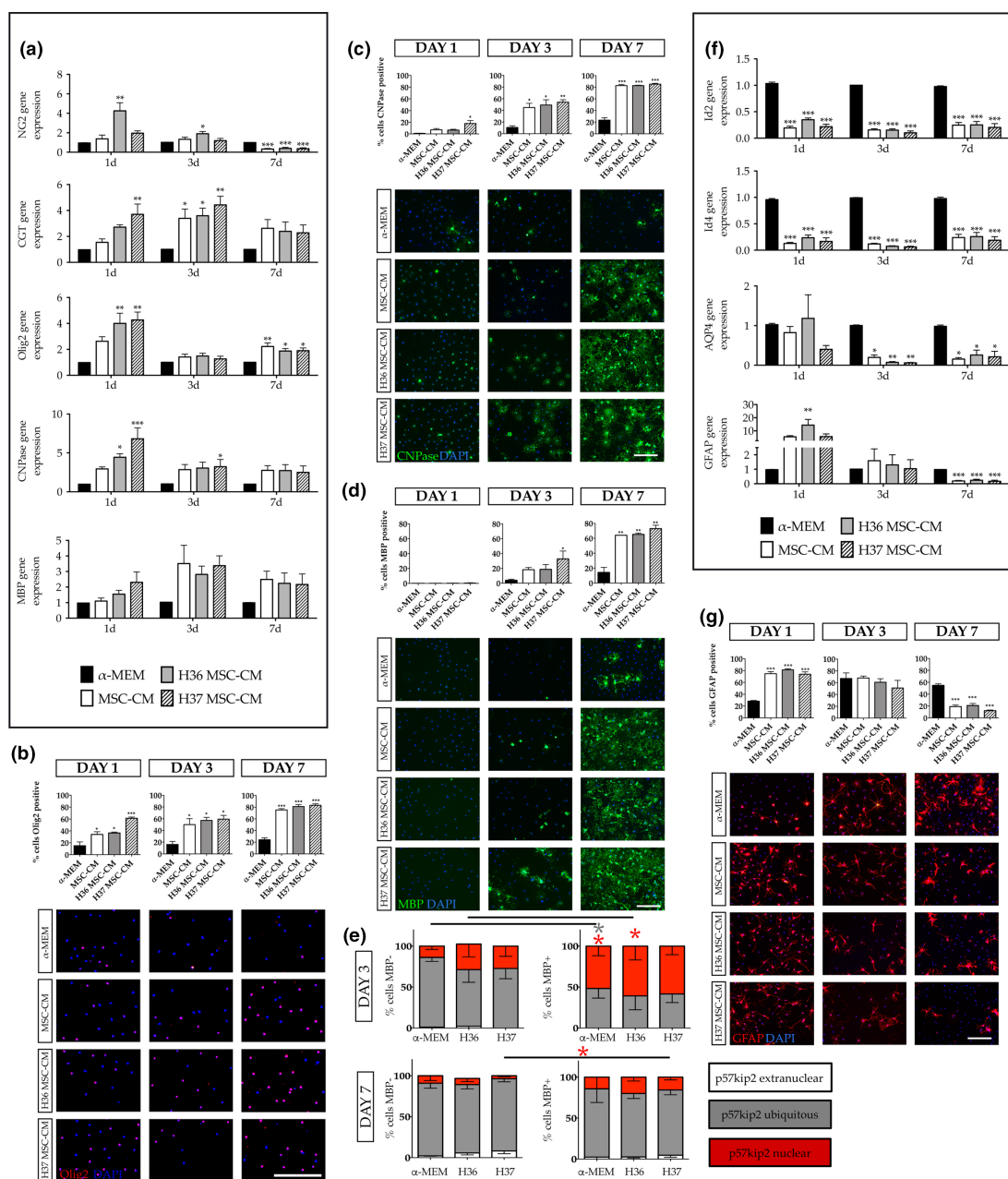


FIGURE 3 Induction of oligodendroglial differentiation by human mesenchymal stem cell factors. (a) Determination of transcript levels by means of quantitative real-time RT-PCR revealed upregulated gene expression levels of oligodendroglial factors NG2, CGT, Olig2, CNPase and MBP upon rat and human MSC-CM treatment. (b-d) Determination of the degree of Olig2+ (b), CNPase+ (c), and MBP positive (d) cells revealed increasing numbers among all MSC-CM treated cells with H37 MSC-CM exerting the most potent effect. (e) Human fetal mesenchymal stem cell secreted factors consolidated an early nuclear and later on ubiquitous p57kip2 protein localization in MBP positive cells. (f) Astrocytic gene expression levels for Id2, Id4, AQP4, and GFAP were almost equally downregulated by rat and human MSC-CM preparations. (g) Representative anti-GFAP immunofluorescent staining revealed an initial increase in expressing cells which decreased later on. Glyceraldehyde-3-phosphate dehydrogenase (GAPDH) expression was used as reference gene, and data are shown as mean values \pm SEM derived from $n = 3$ for both, q-RT-PCR as well as staining experiments. Statistical analysis: one-way ANOVA analysis of variance with Bonferroni's multiple comparison post-test (stainings) and two-way ANOVA analysis of variance with Bonferroni post-test (q-RT-PCR) ($*p < .05$; $**p < .01$; $***p < .01$). Scale bars: 200 μ m [Color figure can be viewed at wileyonlinelibrary.com]

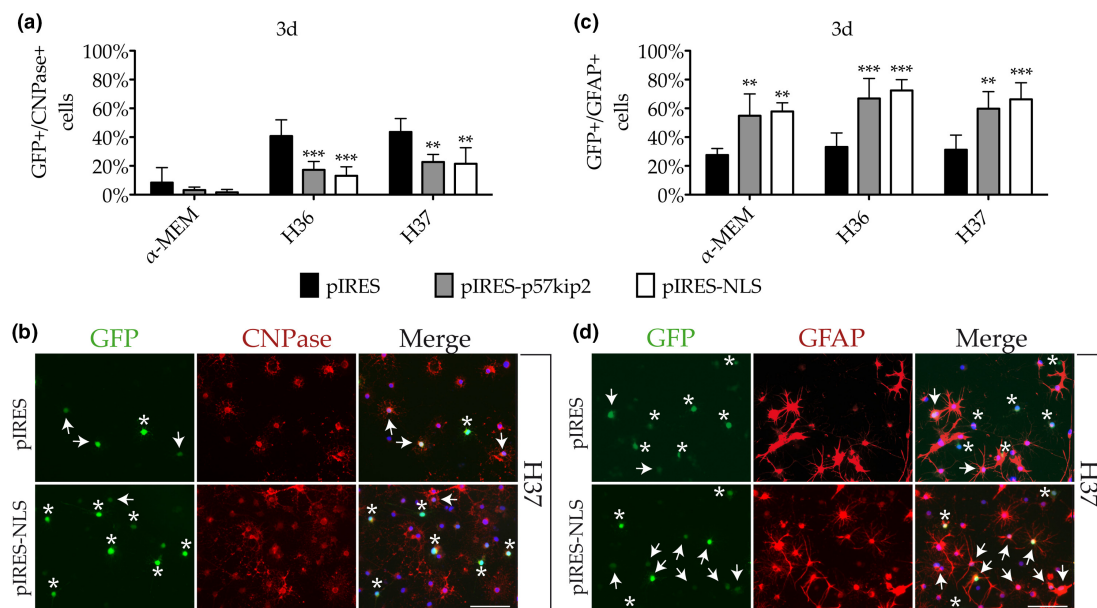


FIGURE 4 p57kip2 protein overexpression interferes with human MSC-derived oligodendrogenesis. Anti-CNPase (a,b) and anti-GFAP (c,d) immunofluorescent staining showed that three days after p57kip2 wild type or NLS mutant overexpression oligodendrogenesis (CNPase positive cells) was significantly impaired and astrocyte generation was promoted, for both cells kept in control medium (α -MEM) as well as when treated with H36 and H37 MSC-CM. Asterisks indicate GFP positive cells devoid of CNPase or GFAP, arrows point to CNPase- or GFAP expressing cells. Data are mean \pm SEM derived from $n = 3$ independent experiments. Statistical analysis: two-way ANOVA analysis of variance with Bonferroni post-test (** $p < .01$; *** $p < .001$). Scale bars: 100 μ m [Color figure can be viewed at wileyonlinelibrary.com]

fetal MSC origin support integration of hippocampal aNSCs into neuronal networks and promote hippocampal stem cells to initiate oligodendrogenesis.

3.6 | Human iPSC-derived NSCs express Olig2 after stimulation with human fetal mesenchymal stem cell factors

In contrast to rat neural stem cells, human NSC differentiation into oligodendrocytes appears to be impaired and delayed (Jadasz et al., 2016) indicating that research efforts should be dedicated to the derivation of improved new protocols for iPSC-derived oligodendrocyte generation. To study possible MSC dependent pro-oligodendroglial effects in a purely human system, i.e., responses of human neural stem cells following supply of human fetal mesenchymal stem cell secreted factors, we stimulated human iPSC-derived NSCs with H37 MSC-CM. After six days, human neural stem cells were fixed and stained using an anti-Olig2 antibody to see whether these cells adopt an oligodendroglial fate. Importantly, H37 MSC-CM was able to significantly elevate the degree of cells with nuclear Olig2 expression in comparison to human NSCs subjected to control medium (Figure 7a-c'). Concomitantly, we observed a significant downregulation of GFAP after seven days (Figure 7d-f'). To investigate whether human fetal secreted factors further promote differentiation along the oligodendroglial lineage, we stained for the early oligodendrocyte marker O4 and found significantly

elevated degrees of O4 expressing cells upon H37 treatment after 14 days in culture (Figure 7g-k).

4 | DISCUSSION

An appropriate description of the oligodendrogenic progeny of adult neural stem cells is essential to understand events leading to functional recovery in the injured or diseased CNS. Although respective determination and differentiation mechanisms are still unclear, there is increasing evidence that stem cell-derived OLs significantly contribute to myelin repair but also differ in their ability to remyelinate axons. As aNSC-derived OLs revealed different activation kinetics and thicker myelin sheaths in response to demyelination as compared with parenchymal-derived cells (Xing et al., 2014), this suggests that a certain degree of heterogeneity among repair mediating cells may exist. Conversely, aNSCs from the SGZ are primarily involved in the maintenance of neurogenesis (Goncalves, Schafer, & Gage, 2016; Spalding et al., 2013) and are therefore less likely to differentiate into OLs compared with SVZ-derived stem cells (Levison & Goldman, 1993), further contributing to this heterogeneous picture. It is therefore of interest to identify the molecular basis of these differences and to describe their responses to intrinsic and extrinsic regulators previously shown to control stem cell dependent oligodendrogenesis.

We here demonstrate that the p57kip2 protein localization of CC1 positive cells within the subgranular stem cell niche differs from

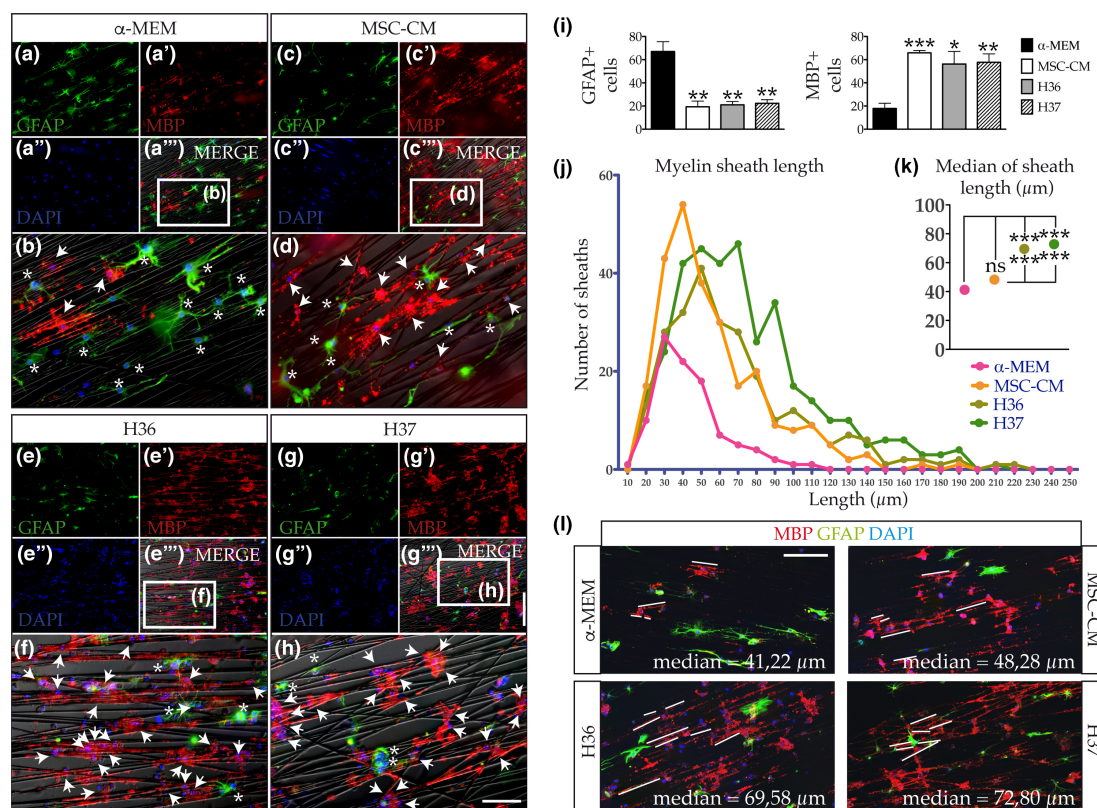


FIGURE 5 Myelination of adult neural stem cells. (a-h) Adult neural stem cells from the subgranular zone myelinate aligned Mimetix microfibers after stimulation with rat and human conditioned medium *in vitro* for seven days, whereas α-MEM stimulated cells mainly expressed GFAP. Arrows mark MBP expressing- and asterisks mark cells GFAP expressing cells. (i) Immunocytochemical staining revealed significant downregulation of GFAP and an increase in MBP expression under the influence of mesenchymal secreted factors on nanofibers after seven days concomitant with (j) an increase of the number of myelin sheaths as well as (j,k) the significant extension of the myelin sheath lengths (median) under human fetal conditioning (H36, H37) of aNSCs. (l) Representative photographs show the difference in myelin sheath length highlighted by redrawn white lines corresponding to myelin sheaths. In total, 3157 sheaths (α-MEM: 468, MSC-CM: 795, H36: 810, H37: 1084) were measured and data are shown as mean ± SEM (i) and as median (k) derived from n=3 independent experiments. Statistical analysis: one-way ANOVA analysis of variance with Bonferroni's multiple comparison post-test (* $p < .05$; ** $p < .01$; *** $p < .01$). Scale bars: 200 μm (g), 100 μm (h,l) [Color figure can be viewed at wileyonlinelibrary.com]

parenchymal OLs (Göttle et al., 2015) as well as from cells in SVZ subregions. Moreover, in contrast to cultured OPCs stem cell dependent oligodendrogenesis cannot be enforced by expression of a mutant version of the p57kip2 protein that is restricted to the cytoplasm. We also found that a nonphysiological overexpression of wild type p57kip2 proteins (directed to the nucleus) blocks MSC dependent oligodendrogenesis and promotes the accumulation of astrocytic markers, which is in contrast to p57kip2 nuclear localization during parenchymal oligodendrogenesis. Furthermore, this suggests that a complete nuclear exclusion of the p57kip2 protein is not necessary for stem cells to generate a myelinating glial cell type, but that this process underlies a more complex space- and likely also time-dependent redistribution of p57kip2. These are likely cell autonomous differences and probably not related to the niche environment as SGZ cells maintain this feature *ex vivo*. Shuttling of CDK2, Hes5 and LIMK-1, which we found to bind

p57kip2, appear therefore to be OPC specific (Göttle et al., 2015) while stem cell oligodendrogenesis relies on a different mechanism. A release of the inhibitory interaction between p57kip2 and Ascl1, which was found to drive differentiation of OLs (Göttle et al., 2015), might also be valid in the stem cell context as overexpression of this transcription factor was previously shown to instruct oligodendrogenic differentiation in SGZ-derived aNSCs (Braun et al., 2015; Jessberger et al., 2008). It remains to be shown whether the p57kip2 inferred blockade of Ascl1's transactivation properties—given that this very mechanism is also valid in the stem cell context—can be released by means other than nuclear export, or whether the observed redistribution from nucleus to nucleus plus cytoplasm still results in a net release of Ascl1, sufficient to allow for oligodendrogenesis to proceed. Moreover, using stem cell specific protein/protein interaction assays, it will be of interest to identify the nature of aNSC specific binding proteins.

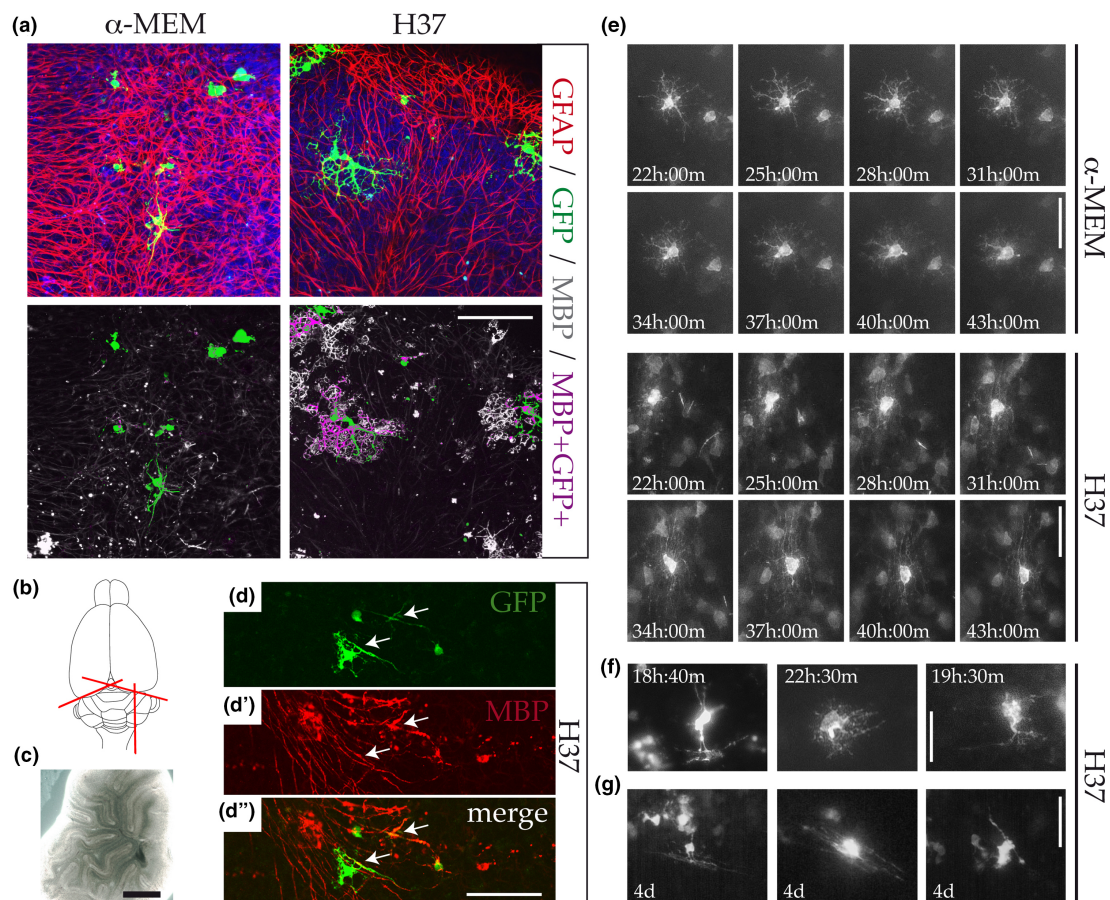


FIGURE 6 Transplantation of hippocampal aNSCs on cerebellar slices. Transplantation of GFP-transfected aNSCs on freshly prepared P7 cerebellar slices showed that after oligodendroglial stimulation with human MSC-CM (H37) such cells integrated into the network and started to express MBP after 4 days (a). Brains were cut parasagittal into 350 μm thick slices using a vibrating microtome and cultured on a Biopore membrane (Millicell; b,c). (d-d'') Representative pictures of transplanted GFP marked cells upon human fetal H37 MSC-CM stimulation revealing the development of parallel MBP positive processes marked by arrows and, therefore, indicating a mature oligodendrocyte positive for MBP. (e) Live cell imaging of representative aNSCs under control (α -MEM) and stimulating (H37) conditions during the time window of 22 hr to 43 hr post-transplantation and medium change. After 28 hr morphological changes become apparent and the representative cell under H37 conditions starts to develop oligodendrocyte-characteristic parallel processes, which was not observed under control conditions (α -MEM). (f) Photographs showing individual aNSCs of further independent experiments developing a parallel processes-bearing morphology after transplantation onto slices and concomitant medium change to H37 at early time-points. (g) Representative pictures of H37 treated aNSCs on cerebellar slices after four days in culture. Cells are shown from eight independent experiments, four of which were conducted using live cell imaging. Scale bars: 100 μm (a,d,e-g), 1 mm (c) [Color figure can be viewed at wileyonlinelibrary.com]

Alternatively, *Ascl1* might as well be blocked in aNSCs as it is a key regulator of hippocampal neurogenesis in CC1 positive cells that are still able to differentiate into neurons (Imura, Wang, Noda, Sofroniew, & Fushiki, 2010). This could explain the observed and unexpected nuclear p57kip2 localization in CC1 positive cells *in vivo* and in MBP positive cells *in vitro*.

Besides the *Ascl1* enforced oligodendrogenic program, we and others showed that hippocampal stem cells can efficiently be driven into oligodendroglial cells in the presence of MSC-derived trophic factors (Bai et al., 2009; Munoz et al., 2005; Rivera et al., 2006; Steffenhagen et al., 2012). This is strong evidence that SGZ-derived aNSCs are

capable of generating myelinating glia and that this process can be induced via exogenous stimulation. In a MSC stimulated environment, not only expression of oligodendroglial vs. astrocyte markers is tightly controlled, but also tissue integration as well as the myelin (wrapping) process are prominently enhanced. Whether the observed elongation of myelin sheath length is a consequence of rejuvenation by fetal factors or due to humanization by human factors remains to be addressed in future experiments. Studies have reported myelin sheath lengths of OL lineage cells and these were much shorter than those we measured after incubation with H36/37 (Bechler et al., 2015; Hamilton et al., 2017). This may have implications regarding the regeneration of lost

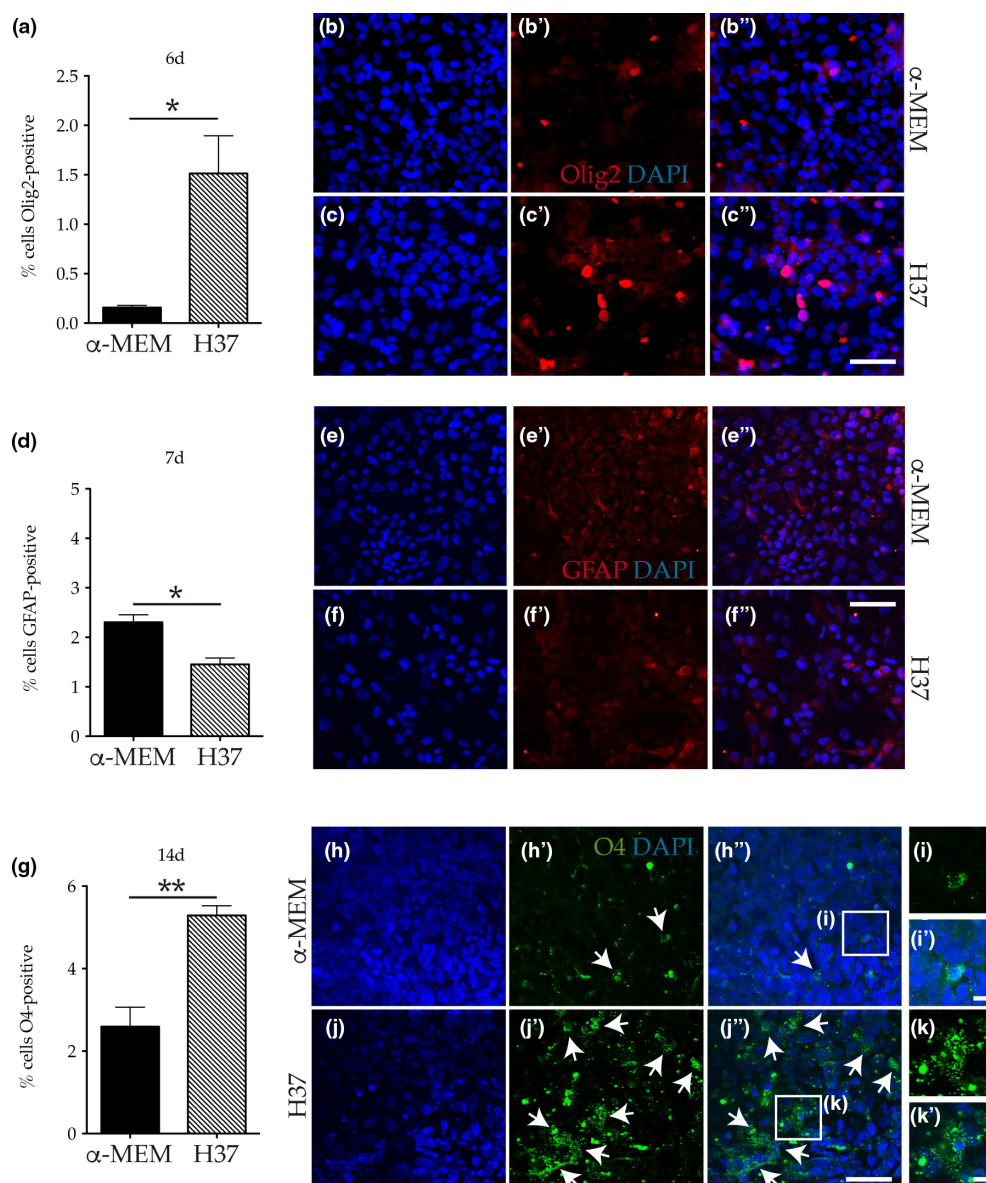


FIGURE 7 Human MSC-CM enhances nuclear Olig2 protein expression in human iPSC-derived NSCs (hiPSC-NSCs). (a) Quantitative assessment of the percentage of nuclear Olig2 expressing human NSCs as a consequence of control medium and H37 MSC-CM treatment for six days. (b-c) Representative immunofluorescent staining of cultured human NSCs after six days in either control medium (b-b) or H37 MSC-CM (c-c). After seven days of treatment with H37, GFAP is significantly downregulated (d-f'') in comparison to control medium. (g-k') At later time points, the oligodendrocyte marker O4 (marked by arrows) became evident and was elevated upon H37 treatment after 14 days of incubation. Data are shown as mean \pm SEM and derived from $n = 3$ independent experiments. Student's t -test (* $p < .05$; ** $p < .01$). Scale bars: 50 μ m (c'', f'', j''), 10 μ m (i', k') [Color figure can be viewed at wileyonlinelibrary.com]

myelin, e.g., in MS patients, as it might impact conduction velocity and/or axonal support (Ford et al., 2015).

Since fetal human and rodent MSC-derived factors revealed to be equally potent in promoting SGZ aNSC dependent oligodendrogenesis, this demonstrates a strong conservation across species. This was

corroborated by the observed fast induction of oligodendrogenesis in human iPSC-derived neural stem cells which we report here for the first time. As compared with other iPSC dependent oligodendrogenesis protocols that take 60 or 130 days for O4 generation (Douvaras et al., 2014; Wang et al., 2013) mesenchymal factors induced a rather fast



differentiation process taking 14 days for O4 expression, which is even more remarkable in light of the fact that the high serum content of the mesenchymal stem cell medium, used for conditioning, dominantly induces astrocyte features.

As MSC-CM was also shown to exert a positive effect on iPSC-derived hepatoblast maturation (Takagi et al., 2016), it can be speculated that pluripotent stem cells, once directed toward multipotency, may become sensitive to MSC factors. This observation is of particular interest in light of the development of future autologous stem cell therapies in that reprogramming fibroblasts from a single patient into both MSCs and NSCs could be used to generate OLs for exogenous supply.

Finally, also in the presence of dominant MSC-derived factors, the intracellular distribution of the p57kip2 protein was not changed as much as previously seen in maturing OPCs, with on-going nuclear presence and additional cytoplasmic signals to emerge. However, the fact that nuclear p57kip2 signals are more prominent in MBP positive cells at early time points leads to the assumption that it is mandatory for initiation phases of oligodendrogenesis as it changed to ubiquitous distribution after seven days. Nuclear accumulation of endogenous p57kip2 protein might exert such a function, which however, can be blocked upon nonphysiologic overexpression of wild type p57kip2 protein. Moreover, the observation that the NLS mutant p57kip2 protein cannot dominantly instruct oligodendrogenic processes as clearly shown in parenchymal OPCs (Göttle et al., 2015) further indicates different functional or dose/subcellular localization specific roles among the two cell types. Hence, it is likely that in NSCs, oligodendrogenesis is regulated differently (Akkermann et al., 2016) or that mesenchymal secreted factors act by a different oligodendrogenic pathway. Of note, when parenchymal OPCs were treated with MSC-CM H37, cells previously shown to rapidly export the p57kip2 protein during spontaneous and chemokine driven differentiation (Göttle et al., 2015), only weak or incomplete protein translocation or a generally reduced nuclear p57kip2 signal were observed (data not shown), indicating that mesenchymal cues employ different molecular mechanisms. Such mechanistic differences need to be addressed in upcoming investigations.

Such analyses will certainly also help identifying the secreted MSC factor cocktail acting on cell fate determination as well as on the promotion of oligodendroglial maturation along the different cellular stages. In addition, it must be assumed that anti-astrocytic components are also present and act in parallel. Contained factors are likely to influence glial transcription either in the sense of myelin gene induction or repression of oligodendroglial related inhibitory components (Kremer et al., 2011) or of pro-astrocytic regulators such as the non-DNA binding transcriptional regulators Id2 and Id4 (Jadasz et al., 2013; Rivera et al., 2006). Of note, recent studies have addressed the role of some specific factors that might be secreted by MSCs such as insulin-like growth factor-1 (IGF-1), sonic hedgehog (SHH), transforming growth factor beta 1 (TGF β -1), vascular endothelial growth factor (VEGF), ciliary neurotrophic factor (CNTF) and hepatocyte growth factor (HGF) (Jadasz et al., 2013; Rivera et al., 2006, 2008), which are also secreted by human MSCs (Chen, Tredget, Wu, & Wu, 2008; Lin et al., 2008;

Razavi, Razavi, Zarkesh Esfahani, Kazemi, & Mostafavi, 2013). However, none of them revealed to contribute to MSC-mediated oligodendrogenesis of adult neural stem cells (Rivera et al., 2006, 2008). Previously reported differential IL-6 expression levels between human embryonic- and adult bone marrow stem cells (Wang et al., 2014) could also account for such differences and therefore be part of the active cocktail. Since experiments using single factors only revealed to be negative in terms of favoring oligodendrogenesis, cocktails of different factors should be considered for future aNSC dependent oligodendrogenesis assays. In this regard one has to appreciate that NSCs are not homogeneously distributed within the brain which could be the spatio-temporal basis for synergistic or subsequent trophic actions. In this way SHH and VEGF might be important for the initial migration step to colonize damaged areas before HGF, for example, may act as a OL developing factor (de Castro & Bribian, 2005).

Finally, MSCs can also produce microRNAs (Chen et al., 2010), which are packed and delivered via exosomes to target cells (Tomasoni et al., 2013). Taking this signaling into account, one recent study compared microRNA levels of human olfactory mucosa- and bone-marrow-derived mesenchymal stromal cells and revealed that miR-146-5p correlates with CXCL12 secretion and with its role in facilitating myelination (Lindsay et al., 2016), as this chemokine was previously shown to be responsible for OPC maturation (Göttle et al., 2010). Further studies will show to what extent miR-146-5p/CXCL12 are part of the pro-oligodendroglial secretome.

Our findings unraveled a certain degree of heterogeneity among myelin repair mediating cells when it comes to intrinsic regulators and mechanisms but at the same time showed a remarkable stability of potent exogenous stimuli acting across species. Based on their immunomodulatory actions, systemic application of mesenchymal stem cells is currently under investigation in clinical trials (Jadasz et al., 2016; Oh et al., 2015). However, for a prospective biomedical translation, it would be desirable that active pro-oligodendrogenic and anti-astrocytic components are identified first and then applied specifically—a strategy to which our here described findings might contribute.

ACKNOWLEDGMENT

We thank Dr. Sebastian Illes for discussion, Dr. Matthias Megges for initial experiments with human mesenchymal stem cell conditioned medium, Raul Bukowiecki for initial help with the human iPSC-derived NSC culture and Julia Jadasz for technical support.

ETHICAL GUIDELINES

The Ethics commission of the medical faculty at Heinrich-Heine-University also approved the use of the human fetal MSCs for this study (Study number: 5013).

CONFLICT OF INTERESTS

The authors declare that there is no conflict of interests regarding the publication of this article.

ORCID

Janusz J. Jadasz  <http://orcid.org/0000-0002-5505-4570>

Rainer Akkermann  <http://orcid.org/0000-0003-1583-9987>

Patrick Küry  <http://orcid.org/0000-0002-2654-1126>

REFERENCES

- Akkermann, R., Jadasz, J. J., Azim, K., & Küry, P. (2016). Taking advantage of nature's gift: Can endogenous neural stem cells improve myelin regeneration? *International Journal of Molecular Sciences*, *17*. pii: E1895. doi:10.3390/ijms17111895
- Bai, L., Lennon, D. P., Caplan, A. I., DeChant, A., Hecker, J., Kranso, J., ... Miller, R. H. (2012). Hepatocyte growth factor mediates mesenchymal stem cell-induced recovery in multiple sclerosis models. *Nature Neuroscience*, *15*, 862–870.
- Bai, L., Lennon, D. P., Eaton, V., Maier, K., Caplan, A. I., Miller, S. D., & Miller, R. H. (2009). Human bone marrow-derived mesenchymal stem cells induce Th2-polarized immune response and promote endogenous repair in animal models of multiple sclerosis. *Glia*, *57*, 1192–1203.
- Bechler, M. E., Byrne, L., & Ffrench-Constant, C. (2015). CNS myelin sheath lengths are an intrinsic property of oligodendrocytes. *Current Biology*, *25*, 2411–2416.
- Braun, S. M., Pilz, G. A., Machado, R. A., Moss, J., Becher, B., Toni, N., & Jessberger, S. (2015). Programming hippocampal neural stem/progenitor cells into oligodendrocytes enhances remyelination in the adult brain after injury. *Cell Reports*, *11*, 1679–1685.
- Chen, L., Tredget, E. E., Wu, P. Y., & Wu, Y. (2008). Paracrine factors of mesenchymal stem cells recruit macrophages and endothelial lineage cells and enhance wound healing. *PLoS One*, *3*, e1886.
- Chen, T. S., Lai, R. C., Lee, M. M., Choo, A. B., Lee, C. N., & Lim, S. K. (2010). Mesenchymal stem cell secretes microparticles enriched in pre-microRNAs. *Nucleic Acids Research*, *38*, 215–224.
- de Castro, F., & Bribian, A. (2005). The molecular orchestra of the migration of oligodendrocyte precursors during development. *Brain Research Reviews*, *49*, 227–241.
- de Castro, F., Bribian, A., & Ortega, M. C. (2013). Regulation of oligodendrocyte precursor migration during development, in adulthood and in pathology. *Cellular and Molecular Life Sciences*, *70*, 4355–4368.
- Doetsch, F., Verdugo, J. M., Caille, I., Alvarez-Buylla, A., Chao, M. V., & Casaccia-Bonnel, P. (2002). Lack of the cell-cycle inhibitor p27Kip1 results in selective increase of transit-amplifying cells for adult neurogenesis. *Journal of Neuroscience*, *22*, 2255–2264.
- Douvaras, P., Wang, J., Zimmer, M., Hanchuk, S., O'Bara, M. A., Sadiq, S., ... Fossati, V. (2014). Efficient generation of myelinating oligodendrocytes from primary progressive multiple sclerosis patients by induced pluripotent stem cells. *Stem Cell Reports*, *3*, 250–259.
- Ford, M. C., Alexandrova, O., Cossell, L., Stange-Marten, A., Sinclair, J., Kopp-Scheinflug, C., ... Grothe, B. (2015). Tuning of Ranvier node and internode properties in myelinated axons to adjust action potential timing. *Nature Communications*, *6*, 8073.
- Franklin, R. J. (2002). Why does remyelination fail in multiple sclerosis? *Nature Reviews Neuroscience*, *3*, 705–714.
- Furutachi, S., Miya, H., Watanabe, T., Kawai, H., Yamasaki, N., Harada, Y., ... Gotoh, Y. (2015). Slowly dividing neural progenitors are an embryonic origin of adult neural stem cells. *Nature Neuroscience*, *18*, 657–665.
- Goncalves, J. T., Schafer, S. T., & Gage, F. H. (2016). Adult neurogenesis in the hippocampus: From stem cells to behavior. *Cell*, *167*, 897–914.
- Göttle, P., Kremer, D., Jander, S., Ödemis, V., Engele, J., Hartung, H. P., & Küry, P. (2010). Activation of CXCR7 receptor promotes oligodendroglial cell maturation. *Annals of Neurology*, *68*, 915–924.
- Göttle, P., Sabo, J. K., Heinen, A., Venables, G., Torres, K., Tzekova, N., ... Küry, P. (2015). Oligodendroglial maturation is dependent on intracellular protein shuttling. *Journal of Neuroscience*, *35*, 906–919.
- Hamilton, N. B., Clarke, L. E., Arancibia-Carcamo, I. L., Kougoumtzidou, E., Matthey, M., Karadottir, R., ... Attwell, D. (2017). Endogenous GABA controls oligodendrocyte lineage cell number, myelination, and CNS internode length. *Glia*, *65*, 309–321.
- Imura, T., Wang, X., Noda, T., Sofroniew, M. V., & Fushiki, S. (2010). Adenomatous polyposis coli is essential for both neuronal differentiation and maintenance of adult neural stem cells in subventricular zone and hippocampus. *Stem Cells*, *28*, 2053–2064.
- Jadasz, J. J., Kremer, D., Göttle, P., Tzekova, N., Domke, J., Rivera, F. J., Adjaye, J., Hartung, H. P., Aigner, L., & Küry, P. (2013). Mesenchymal stem cell conditioning promotes rat oligodendroglial cell maturation. *PLoS One*, *8*, e71814.
- Jadasz, J. J., Lubetzki, C., Zalc, B., Stankoff, B., Hartung, H. P., & Küry, P. (2016). Recent achievements in stem cell-mediated myelin repair. *Current Opinion in Neurology*, *29*, 205–212.
- Jadasz, J. J., Rivera, F. J., Taubert, A., Kandasamy, M., Sandner, B., Weidner, N., ... Küry, P. (2012). p57kip2 regulates glial fate decision in adult neural stem cells. *Development*, *139*, 3306–3315.
- Jessberger, S., Toni, N., Clemenson, G. D., Jr., Ray, J., & Gage, F. H. (2008). Directed differentiation of hippocampal stem/progenitor cells in the adult brain. *Nature Neuroscience*, *11*, 888–893.
- Kassis, I., Grigoriadis, N., Gowda-Kurkalli, B., Mizrahi-Kol, R., Ben-Hur, T., Slavin, S., ... Karussis, D. (2008). Neuroprotection and immunomodulation with mesenchymal stem cells in chronic experimental autoimmune encephalomyelitis. *Archives of Neurology*, *65*, 753–761.
- Kremer, D., Aktas, O., Hartung, H. P., & Küry, P. (2011). The complex world of oligodendroglial differentiation inhibitors. *Annals of Neurology*, *69*, 602–618.
- Kremer, D., Heinen, A., Jadasz, J., Göttele, P., Zimmermann, K., Zickler, P., ... Küry, P. (2009). p57kip2 is dynamically regulated in experimental autoimmune encephalomyelitis and interferes with oligodendroglial maturation. *Proceedings of the National Academy of Sciences of the United States of America*, *106*, 9087–9092.
- Kuhlmann, T., Miron, V., Cui, Q., Wegner, C., Antel, J., & Brück, W. (2008). Differentiation block of oligodendroglial progenitor cells as a cause for remyelination failure in chronic multiple sclerosis. *Brain*, *131*, 1749–1758.
- Levison, S. W., & Goldman, J. E. (1993). Both oligodendrocytes and astrocytes develop from progenitors in the subventricular zone of postnatal rat forebrain. *Neuron*, *10*, 201–212.
- Li, W., Sun, W., Zhang, Y., Wei, W., Ambasadhan, R., Xia, P., ... Ding, S. (2011). Rapid induction and long-term self-renewal of primitive neural precursors from human embryonic stem cells by small molecule inhibitors. *Proceedings of the National Academy of Sciences of the United States of America*, *108*, 8299–8304.
- Lin, N., Tang, Z., Deng, M., Zhong, Y., Lin, J., Yang, X., ... Xu, R. (2008). Hedgehog-mediated paracrine interaction between hepatic stellate cells and marrow-derived mesenchymal stem cells. *Biochemical and Biophysical Research Communications*, *372*, 260–265.
- Lindsay, S. L., Johnstone, S. A., McGrath, M. A., Mallinson, D., & Barnett, S. C. (2016). Comparative miRNA-based fingerprinting reveals biological differences in human olfactory mucosa- and bone-marrow-derived mesenchymal stromal cells. *Stem Cell Reports*, *6*, 729–742.



- Lindsay, S. L., Johnstone, S. A., Mountford, J. C., Sheikh, S., Allan, D. B., Clark, L., & Barnett, S. C. (2013). Human mesenchymal stem cells isolated from olfactory biopsies but not bone enhance CNS myelination in vitro. *Glia*, *61*, 368–382.
- Lorenz, C., Lesimple, P., Bukowiecki, R., Zink, A., Inak, G., Mlody, B., ... Prigione, A. (2017). Human iPSC-derived neural progenitors are an effective drug discovery model for neurological mtDNA disorders. *Cell Stem Cell*, *20*, 659–674 e9.
- Mirmalek-Sani, S. H., Tare, R. S., Morgan, S. M., Roach, H. I., Wilson, D. I., Hanley, N. A., & Oreffo, R. O. (2006). Characterization and multipotentiality of human fetal femur-derived cells: implications for skeletal tissue regeneration. *Stem Cells*, *24*, 1042–1053.
- Munoz, J. R., Stoutenger, B. R., Robinson, A. P., Spees, J. L., & Prockop, D. J. (2005). Human stem/progenitor cells from bone marrow promote neurogenesis of endogenous neural stem cells in the hippocampus of mice. *Proceedings of the National Academy of Sciences of the United States of America*, *102*, 18171–18176.
- Nait-Oumesmar, B., Picard-Riera, N., Kerninon, C., & Baron-Van Evercooren, A. (2008). The role of SVZ-derived neural precursors in demyelinating diseases: from animal models to multiple sclerosis. *Journal of Neurology*, *265*, 26–31.
- Nait-Oumesmar, B., Picard-Riera, N., Kerninon, C., Decker, L., Seilhean, D., Hoglinger, G. U., ... Baron-Van Evercooren, A. (2007). Activation of the subventricular zone in multiple sclerosis: Evidence for early glial progenitors. *Proceedings of the National Academy of Sciences of the United States of America*, *104*, 4694–4699.
- Oh, K. W., Moon, C., Kim, H. Y., Oh, S. I., Park, J., Lee, J. H., ... Kim, S. H. (2015). Phase I trial of repeated intrathecal autologous bone marrow-derived mesenchymal stromal cells in amyotrophic lateral sclerosis. *Stem Cells Translational Medicine*, *4*, 590–597.
- Picard-Riera, N., Decker, L., Delarasse, C., Goude, K., Nait-Oumesmar, B., Liblau, R., ... Evercooren, A. B. (2002). Experimental autoimmune encephalomyelitis mobilizes neural progenitors from the subventricular zone to undergo oligodendrogenesis in adult mice. *Proceedings of the National Academy of Sciences of the United States of America*, *99*, 13211–13216.
- Razavi, S., Razavi, M. R., Zarkesh Eshfahani, H., Kazemi, M., & Mostafavi, F. S. (2013). Comparing brain-derived neurotrophic factor and ciliary neurotrophic factor secretion of induced neurotrophic factor secreting cells from human adipose and bone marrow-derived stem cells. *Development, Growth & Differentiation*, *55*, 648–655.
- Rivera, F. J., Couillard-Despres, S., Pedre, X., Ploetz, S., Caioni, M., Lois, C., ... Aigner, L. (2006). Mesenchymal stem cells instruct oligodendrogenic fate decision on adult neural stem cells. *Stem Cells*, *24*, 2209–2219.
- Rivera, F. J., Kandasamy, M., Couillard-Despres, S., Caioni, M., Sanchez, R., Huber, C., ... Aigner, L. (2008). Oligodendrogenesis of adult neural progenitors: differential effects of ciliary neurotrophic factor and mesenchymal stem cell derived factors. *Journal of Neurochemistry*, *107*, 832–843.
- Rolando, C., Erni, A., Grison, A., Beattie, R., Engler, A., Gokhale, P. J., ... Taylor, V. (2016). Multipotency of Adult Hippocampal NSCs In Vivo Is Restricted by Droscha/NFIB. *Cell Stem Cell*, *19*, 653–662.
- Spalding, K. L., Bergmann, O., Alkass, K., Bernard, S., Salehpour, M., Huttner, H. B., ... Frisen, J. (2013). Dynamics of hippocampal neurogenesis in adult humans. *Cell*, *153*, 1219–1227.
- Steffenhagen, C., Dechant, F. X., Oberbauer, E., Furtner, T., Weidner, N., Küry, P., ... Rivera, F. J. (2012). Mesenchymal stem cells prime proliferating adult neural progenitors toward an oligodendrocyte fate. *Stem Cells Development*, *21*, 1838–1851.
- Takagi, C., Yagi, H., Hieda, M., Tajima, K., Hibi, T., Abe, Y., ... Kitagawa, Y. (2016). Mesenchymal stem cells contribute to hepatic maturation of human induced pluripotent stem cells. *European Surgical Research*, *58*, 27–39.
- Tomasoni, S., Longaretti, L., Rota, C., Morigi, M., Conti, S., Gotti, E., ... Benigni, A. (2013). Transfer of growth factor receptor mRNA via exosomes unravels the regenerative effect of mesenchymal stem cells. *Stem Cells Development*, *22*, 772–780.
- Uccelli, A., Moretta, L., & Pistoia, V. (2008). Mesenchymal stem cells in health and disease. *Nature Reviews Immunology*, *8*, 726–736.
- Vandesompele, J., De Preter, K., Pattyn, F., Poppe, B., Van Roy, N., De Paepe, A., & Speleman, F. (2002). Accurate normalization of real-time quantitative RT-PCR data by geometric averaging of multiple internal control genes. *Genome Biology*, *3*, RESEARCH0034.
- Wang, S., Bates, J., Li, X., Schanz, S., Chandler-Militello, D., Levine, C., ... Goldman, S. A. (2013). Human iPSC-derived oligodendrocyte progenitor cells can myelinate and rescue a mouse model of congenital hypomyelination. *Cell Stem Cell*, *12*, 252–264.
- Wang, X., Kimbrel, E. A., Ijichi, K., Paul, D., Lazorchak, A. S., Chu, J., ... Xu, R. H. (2014). Human ESC-derived MSCs outperform bone marrow MSCs in the treatment of an EAE model of multiple sclerosis. *Stem Cell Reports*, *3*, 115–130.
- Xing, Y. L., Roth, P. T., Stratton, J. A., Chuang, B. H., Danne, J., Ellis, S. L., ... Merson, T. D. (2014). Adult neural precursor cells from the subventricular zone contribute significantly to oligodendrocyte regeneration and remyelination. *Journal of Neuroscience*, *34*, 14128–14146.

How to cite this article: Jadasz JJ, Tepe L, Beyer F, et al. Human mesenchymal factors induce rat hippocampal- and human neural stem cell dependent oligodendrogenesis. *Glia*. 2018;66:145–160. <https://doi.org/10.1002/glia.23233>

2.13 Additional Publications

Fabrication of biocompatible porous scaffolds based on hydroxyapatite/collagen/chitosan composite for restoration of defected maxillofacial mandible bone

Md Shaifur Rahman, Md Masud Rana, Lucas-Sebastian Spitzhorn, Naznin Akhtar, Md Zahid Hasan, Naiyyum Choudhury, Tanja Fehm, Jan T. Czernuszka, James Adjaye and Sikder M. Asaduzzaman

Abstract

Fabrication of scaffolds from biomaterials for restoration of defected mandible bone has attained increased attention due to limited accessibility of natural bone for grafting. Hydroxyapatite (Ha), collagen type 1 (Col1) and chitosan (Cs) are widely used biomaterials which could be fabricated as a scaffold to overcome the paucity of bone substitutes. Here, rabbit Col1, shrimp Cs and bovine Ha were extracted and characterized with respect to physicochemical properties. Following the biocompatibility, degradability and cytotoxicity tests for Ha, Col1 and Cs a hydroxyapatite/collagen/chitosan (Ha·Col1·Cs) scaffold was fabricated using thermally induced phase separation technique. This scaffold was cross-linked with (1) either glutaraldehyde (GTA), (2) dehydrothermal treatment (DTH), (3) irradiation (IR) and (4) 2-hydroxyethyl methacrylate (HEMA), resulting in four independent types (Ha·Col1·Cs-GTA, Ha·Col1·Cs-IR, Ha·Col1·Cs-DTH and Ha·Col1·Cs-HEMA). The developed composite scaffolds were porous with 3D interconnected fiber microstructure. However, Ha·Col1·Cs-IR and Ha·Col1·Cs-GTA showed better hydrophilicity and biodegradability. All four scaffolds showed desirable blood biocompatibility without cytotoxicity for brine shrimp. In vitro studies in the presence of human amniotic fluid-derived mesenchymal stem cells revealed that Ha·Col1·Cs-IR and Ha·Col1·Cs-DHT scaffolds were non-cytotoxic and compatible for cell attachment, growth and mineralization. Further, grafting of Ha·Col1·Cs-IR and Ha·Col1·Cs-DHT was performed in a surgically created non-load-bearing rabbit maxillofacial mandible defect model. Histological and radiological observations indicated the restoration of defected bone. Ha·Col1·Cs-IR and Ha·Col1·Cs-DHT could be used as

an alternative treatment in bone defects and may contribute to further development of scaffolds for bone tissue engineering.

Publication Status: published in *Progress in Biomaterials*. 2019 May 29.

Impact Factor: -

Approximated total share of contribution: 5%

Contribution on experimental design, realization and publication:

MSR, MMR, LSS, NA, SMA, NC, JTC and JA conceived the idea. MMR, MSR, NA, and LSS designed and performed the experimental work and analyses the data. JTC analyzed the physical characterization of the scaffold and scaffold constituents data. MZH performed the in vitro brine shrimp cytotoxicity and RBC haemolysis assay. MMR, MSR, MZH and LSS wrote the manuscript. NC, SMA, JTC and JA edited the manuscript. NC, SMA and JA supervised the work. All the authors read and approved the final manuscript.

Link to the publication:

<https://link.springer.com/article/10.1007%2Fs40204-019-0113-x>

Characterization of burn wound healing gel prepared from human amniotic membrane and Aloe vera extract

Md Shaifur Rahman, Rashedul Islam, Md Masud Rana, Lucas-Sebastian Spitzhorn, Mohammad Shahedur Rahman, James Adjaye and Sikder M. Asaduzzaman

Abstract

Background

Skin burn wound is a notable medical burden worldwide. Rapid and effective treatment of burnt skin is vital to fasten wound closure and healing properly. Amniotic graft and Aloe vera are widely used as wound managing biomaterials. Sophisticated processing, high cost, availability, and the requirement of medics for transplantation limit the application of amnion grafts. We aim to prepare a novel gel from amnion combined with the Aloe vera extract for burn wound healing which overcome the limitations of graft.

Methods

Two percent human amniotic membrane (AM), Aloe vera (AV) and AM+AV gels were prepared. In vitro cytotoxicity, biocompatibility, cell attachment, proliferation, wound healing scratch assays were performed in presence of the distinct gels. After skin irritation study, second-degree burns were induced on dorsal region of Wistar rats; and gels were applied to observe the healing potential in vivo. Besides, macroscopical measurement of wound contraction and re-epithelialization; gel treated skin was histologically investigated by Hematoxylin and eosin (H&E) staining. Finally, quantitative assessment of angiogenesis, inflammation, and epithelialization was done.

Results

The gels were tested to be non-cytotoxic to nauplii and compatible with human blood and skin cells. Media containing 500 µg/mL AM+AV gel were observed to promote HaCaT and HFF1 cells attachment and proliferation. In vitro scratch assay demonstrated that AM+AV significantly accelerated wound closure through migration of HaCaT cells. No erythema and edema were observed in skin irritation experiments confirming the applicability of the gels. AV and AM+AV groups showed significantly accelerated

wound closure through re-epithelialization and wound contraction with $P < 0.01$. Macroscopically, AM and AM+AV treated wound recovery rates were 87 and 90% respectively with $P < 0.05$. Histology analysis revealed significant epithelialization and angiogenesis in AM+AV treated rats compared to control ($P < 0.05$). AM+AV treated wounds had thicker regenerated epidermis, increased number of blood vessels, and greater number of proliferating keratinocytes within the epidermis.

Conclusion

We demonstrated that a gel consisting of a combination of amnion and Aloe vera extract has high efficacy as a burn wound healing product. Amniotic membrane combined with the carrier Aloe vera in gel format is easy to produce and to apply.

Publication Status: published in *BMC Complementary and Alternative Medicine*. 2019 19:115

Impact Factor: 2.109

Approximated total share of contribution: 5%

Contribution on experimental design, realization and publication:

MSR1 and MSR2 conceived the idea. MSR1, RI, and MSR2 designed the experiment. MSR1, MMR, LSS and RI performed the experimental work and analysis the data. MSR1 and RI wrote the initial draft and SMA, MSR2, LSS, JA edited the manuscript. SMA and MSR2 supervised the work from start to end. JA supervised the in vitro study. All authors read and approved the final manuscript.

Link to the publication:

[https://bmccomplementalternmed.biomedcentral.com/articles/10.1186/s12906-019-2525-](https://bmccomplementalternmed.biomedcentral.com/articles/10.1186/s12906-019-2525-5)

Discussion

Caesarean Section as Alternative Process to Obtain AF-MSCs

Although different cell types of epithelial or mesenchymal lineage were reported to be present in amniotic fluid (AF) [Hoehn et al., 1974; Hoehn and Salk, 1982], in this study we have focused on the Vimentin expressing mesenchymal-like AF cells (AF-MSCs) since epithelial cells have been described to be senescent and to have lower differentiation and proliferation potential [Wolfrum et al., 2010]. In contrast to our approach, most of the AF-related works obtain the AF during amniocentesis which is flawed with a potential danger for the foetus and the mother and which is limited in availability [Hamid et al., 2017]. Within the present work, caesarean sections were described as a mode of AF derivation which reveals a good alternative and furthermore give a better chance to study cells from healthy diploid individuals. The AF-MSCs were able to differentiate into bone and cartilage cells making them potential candidates for regenerative therapies [Spitzhorn et al., 2017; Rahman et al., 2018]. Although the AF-MSCs cell surface marker pattern was not completely in agreement with standards raised by the ISCT [Dominici and Le Blanc, 2006], we still consider them as MSCs as it has been reported that MSCs from different tissues may vary in their immunophenotype [Tsai et al., 2007]. In contrast to studies describing AFCs from different trimesters to express pluripotency factors such as OCT4 [Prusa et al., 2003; Hamid et al., 2017; Tsai et al., 2004], we could only observe the expression of pluripotency associated marker such as SSEA4 and C-Kit. This fact makes these cells attractive for reprogramming events [Spitzhorn et al., 2017; Rahman et al., 2018]. Various studies have reported that AF-MSCs express OCT4, but this finding is discussed very critically since self-renewal experiments are missing [Babaie et al., 2007]. Paracrine signalling via chemokines and their corresponding receptors is key for attracting immune cells to the site of injury or inflammation [Miyasaka and Tanaka, 2004]. In accordance with previously published results, we could show that AF-MSCs secrete pro-angiogenic factors as well as pro- and anti-inflammatory factors as well as tissue repair supportive factors [Spitzhorn et al., 2017; Mirabella et al., 2013; Zagoura et al., 2012].

On transcriptome level AF-MSCs were shown to be not pluripotent but close to fMSCs and to be involved in biological processes such as skeletal development. The AF-MSC-specific gene set which was identified could be a pool of genes leading to potential AF

markers such as Pregnancy-specific beta-1-glycoprotein 5 (PSG5) discriminating them from other MSCs [Spitzhorn et al., 2017].

All these features and the fact that AF-MSCs are at a very early developmental stage make these cells very valuable. But the derivation of these cells by invasive procedures is a risk for the foetus and the mother. In this study, it was shown that AF can also be obtained during Caesarean section without any additional risk for the mother and the baby. The provided data suggests that indeed full-term AF-MSCs also are of tremendous clinical potential and comparable to AF cells obtained by amniocentesis or cord blood-derived cells [Spitzhorn et al., 2017].

Amniotic Fluid as Source for Kidney-derived Stem Cells

The management of kidney-associated diseases is a big challenge for today's doctors. Functioning kidneys filter toxins from the blood and metabolise drugs [Perazella, 2009] and are thereby important for the general health. Millions of people all over the world are affected by acute or chronic kidney failure which is caused by acute kidney injury or a chronic diseased kidney. These conditions can result from ischemia, sepsis, trauma, toxins or hypothermia. Due to impaired kidney functions whole organ transplantations or dialysis are done for millions of patients worldwide [Kellum and Hoste, 2008; Hoste and Schurgers, 2008]. These treatment options are facing high costs and the restricted availability of donor organs [Saidi and Kenari, 2014]. Increasing rates of acute kidney injury (AKI) represent a major health and economic burden [Koyner et al., 2014]. AKI, of which a quarter results from drug side effects, can cause chronic kidney disease (CKD) [Mehta et al., 2015; Chawla et al., 2014] which itself increases the risk of developing renal cell carcinoma [Izzedine and Perazella, 2015]. CKD is often a secondary disease triggered by other pathological conditions such as diabetes, high blood pressure, infections or inflammations [Chhabra and Brayman, 2009; <https://www.kidney.org>]. First symptoms include anaemia, decreased bone strength, impaired nerve function and insufficient supply of nutrients. In a later stage of the disease, kidney transplantation or dialysis are the only treatment options so far but are only available for 10% of the effected patients [<https://www.kidney.org>]. Kidney donor organ shortage and the massive influence of the daily life by undergoing dialysis lead to hopes in stem cell-based therapies to improve the patients' health. Drug-induced nephrotoxicity is an important

risk factor to develop pathological kidney conditions and is one reason that novel drugs are not approved [Sanchez-Romero et al., 2016]. This emphasizes the need for better *in vitro* testing systems to identify potential risks as early as possible in the drug-developmental pipeline.

Due to pathological kidney conditions, millions of patients worldwide are in need for dialysis or kidney transplantation [Kellum and Hoste, 2008, Hoste and Schurgers, 2008]. This is conflicted by low number of good quality available donor organs and high costs [Saidi and Kenari, 2014]. Within the last years the researches interest in kidney relates studies has increased. Cell transplantations are considered as potential alternatives. Renal cells were shown to be derived from ESCs and iPSCs [Xia et al., 2013; Taguchi et al., 2014; Lam et al., 2014; Schutgens et al., 2016; Little, 2016]. But there are also approaches which do not include pluripotent stem cell-derived cells such as amniotic fluid- and urine-derived stem cells.

Although the characteristics and features from AF-MSCs are well described, the origin of these cells needs to be identified to solve the controversial opinions [Loukogeorgakis et al., 2017]. In this work, we wanted to address the question from which organ the AF-MSCs are originating from since heterogenous reports on their cell identity exist [Da Sacco et al., 2017]. Morphological the AF-MSCs were similar to cells obtained from kidney biopsy and urine derived cells [Rahman et al., 2018]. Cell types from the amniotic fluid were reported to originate mostly from the foetal urine [Sutherland and Bain, 1972; Underwood et al., 2005]. In recent years, urine cells were described to have their origin in the kidney [Arcolino et al., 2015; Zhang et al., 2014; Da Sacco et al., 2017; Bohndorf et al., 2017; Spitzhorn et al., 2018]. We could proof that the AF-MSCs really are kidney cells [Rahman et al., 2018] as already assumed in 1970s [Sutherland and Bain, 1972]. We identified renal marker expression such as SIX2, CITED1, LIM homeobox 1 (LHX1) and paired-box-protein 8 (PAX8) in the analysed cells which was described before for kidney progenitor cells and neonatal urine-derived cells [Arcolino et al., 2016, Metsuyanin et al., 2009; Rosenblum, 2008; Tong et al., 2009; Schedl, 2007]. On functionality level we could show that AF-MSCs were able to endocytose albumin comparable to commercial bought kidney cells. Upon WNT signalling activation using a GSK3 inhibitor we observed a morphological change, a change of protein location as well as of marker expression, hinting towards a more differentiated cell stage [Rahman et al., 2018].

Since the embryonal kidney development takes place during the second and third trimester [Little and McMahon; 2012] we analysed a potential synergistic relation between gestation time at which AFCs were obtained and renal marker expression. This hypothesis was confirmed *in silico* by comparison of previously published data sets from first and second trimesters [Moschidou et al., 2013; Spitzhorn et al., 2017] with our cells from the third trimester. Additionally, we checked expression of several kidney markers on PCR level. Both analyses confirmed that the presence of human mesenchymal stem cells of renal origin in amniotic fluid increases with gestational time [Rahman et al., 2018]. In further studies the specification of the cells should be further investigated to dissect the exact kidney cell type these cells represent considering that the kidney is a complex organ with over 23 different cells types.

Although the renal regeneration capacity of MSCs has been reported [Casiraghi et al., 2016; Hamza et al., 2017; Večerić-Haler et al., 2017] the use of MSCs (especially from elderly donors) is wrought with limiting factors such as ageing-associated potential loss, decreased proliferation, telomere shorting and finally decreased differentiation capacity [Guillot et al., 2007]. Due to this and the increasing prevalence of kidney-associated diseases other cell sources for renal repair are in need. Although big efforts have been made for the usage of iPSCs and their derivatives to be used in clinical applications, long-term safety studies and further research will be required until routinely applications in patients are possible. To overcome this gap other cell types without tumorigenic potential are needed to be used in renal repair treatments. This work contributes a milestone for studying nephrogenesis, for usage in *in vitro* models of kidney diseases, for screening of drugs and toxins, for the use in renal organoid formation and possible clinical applications.

Urine as a Source of Kidney Stem Cells with Industrial Potential for Personalized Research

Biopsies to derive kidney cells are wrought with several risks and high costs. Therefore, other sources of renal cells are under investigation. One possible way is to derive kidney cells from iPSCs or ESCs [Xia et al., 2013; Taguchi et al., 2014; Little, 2016]. Also, non-kidney stem cells such as MSCs could be of value for future therapies since cell transplantation of MSCs has been beneficial in a model of impaired kidney function

[Hamza et al., 2017]. It was reported that AF is composed of foetal urine [Underwood et al., 2005] and AF-derived stem cells have been used to generate podocytes [Xinaris et al., 2016]. Based on these facts and on our results that amniotic fluid contains MSCs of renal origin [Rahman et al., 2018], urine was investigated in this work as a potential source for kidney-derived cells.

As an alternative to the established stem cells sources such as bone marrow or amniotic fluid, urine was qualified to be a source for renal stem cells. The beauty of this source is that it can be accessed non-invasively thereby omitting any risk or pain for the patient. For the researcher it is advantageous since no clinician has to be involved in the derivation of the material and the sample acquisition could be done in new ways; for example, postal delivery. All these facts make the urine approach very cost-effective. Of high significance was the finding that the urine-derived stem cells originate from the kidney. This makes them valuable for future kidney related research or potential candidates for cell replacement therapy thereby overcoming the donor organ shortage. They are valuable for *in vitro* drug screening and disease modelling approaches [Spitzhorn et al., 2018; Nguyen et al., 2019].

In this work, it was described that these urine-derived stem cells are exhibiting MSC features and kidney features. They were able to differentiate into bone, cartilage and fat cells *in vitro* by parallel expression of kidney markers SIX2 and Nephhrin, which represent key-regulators of nephrogenesis. Furthermore, they directly could be converted into the functional filtration cells of the kidney, the podocytes. Alongside with this, urine-derived stem cells could be reprogrammed into iPSCs which further on were able to differentiate into iMSCs, neurons, hepatocytes and endothelial cells [Spitzhorn et al., 2018; Nguyen et al., 2019]

Urine-derived stem cells have several key advantages compared to other stem cells such as MSCs: (i) they can be derived from human in all age groups (from infants until elderly people), both genders and nearly every health condition (ii) sample collection is non-invasive and can be done very cost-effective (iii) no need for enzymes for the isolation of homogenous cell population (iv) they can be obtained autologous for personalized therapies or research [Zhang et al., 2014]. Also, for diagnostic screening urine-derived stem cells are of high interest when urine samples are collected at various time points during disease progression. They are perfectly suitable for treatment of patients suffering

from kidney-associated disease since they are able to differentiate into functional kidney cells [Arcolino et al., 2015].

The beauty of urine as source for stem cells lies in the possibility to easily derive patient-specific cells. These autologous cells or also HLA-matched cells are suitable for transplantations without the risk of immune rejection. Furthermore, using *in vitro* propagation it is possible to generate critical numbers of these cells in GMP quality which is needed for in patient use. The fact that the procedure is non-invasive allows it to obtain cells from without the risk of co-morbidity.

The possibility of generating iPSCs from urine-derived stem cells is of high significance for further research studies using iPSC-derived cell types. Especially the analysis of the expressed Cytochromes P450 (CYP) variant, which is an enzyme complex within the liver, and the HLA profile are of high interest for future application and therefore were performed in the present work [Bohndorf et al., 2017]. The CYP variant is crucial for drug metabolism within the liver. Thus, the individual can be identified as poor, intermediate, high or ultra-high metabolizer of distinct drugs [Dagostino et al., 2018]. In addition to that, the HLA type was determined which is very important for future clinical use of the iPSC-derived cell products to enable allogenic cell transplantations which decrease the risk of immune rejection within the recipient.

In conclusion, this work qualified urine as a source for stem cells which represent a considerable alternative to established stem cells sources such as bone marrow. It has several advantages over the invasive procedures and is ideal for kidney related studying. Combined with HLA typing and analysis of CYP variants and metabolism activity of drugs this can be used to develop protocols for personalised drug screening [Spitzhorn et al., 2018].

All these findings and our ongoing research prompted us to set up a business model for developing and selling urine-derived kidney (stem) cell products for nephrotoxicity studies, drug screenings and other fields of (personalized) research. With our concept of “UriCell” we have won the audience award at the Heinrich Heine University Idea Competition 2016, the second prize and the audience award at the NUK Business Plan Competition 2017. In 2018 we have won the “Rheinischer Innovationspreis 2018” and raised over 266.000€ of European Regional Development Fund support from the economic development scheme “START-UP-Hochschulausgründungen” to enable the

transition from the research level to the industrial level and to prepare the founding of the UriCell GmbH [<https://www.uricell.de/>].

The Future of iPSCs in Clinical Applications

The top priority for new therapeutic applications in humans is the safety of the therapy or the cellular product. iPSC research has made great steps towards the broad clinical use. But international standards are yet to be set. Standardized iPSC lines would improve consistent and comparable outcome of therapies. HLA-specific generation of iPSCs would be of great use as well [Travernier et al., 2013; Bohndorf et al., 2017]. Since the derivation of iPSCs from the various cell types is possible, it enables broad personalized research with the aim of individualized results. Combined with already established methods which enable gene editing such as CRISPR/Cas9 and TALENs, iPSCs from a patient with a distinct genetic disease can be generated, the gene defect could be corrected *in vitro* and the cells carrying the functional gene could be transplanted to the patient [Smith, 2015].

A critical point is that so far iPSC-derived organ-specific cells are lacking full maturity. This issue must be overcome to enable higher *in vitro* prediction reliability and a better outcome after transplantations. Alongside with the maturity comes the improved functionality of the cells which allows better results in drug screening and toxicology studies [Davidson, 2015].

The number of medical innovations within the last year is quite limited. Only 5% of the drug candidates receive the approval for the market and before so research and development have tremendous costs exceeding billions of dollars [Giri and Bader, 2015]. Therefore, industry is in search for reducing the costs. This could be achieved by focussing on common disease or to reduce the number of animal studies although they often represent the best choice since primary human cells are hard to obtain. iPSC-based research may represent a great alternative for medical application and could circumvent the ethical issues connected with the use of ESCs.

But so far very limited in-patient applications of iPSC-derived cells exist. In 2014 a Japanese woman was treated for AMD using autologous iPSC-derived retinal cell sheet which survived for at least one year in the patient and which did not cause obvious side effects

[Mandai et al., 2017]. One big hurdle for the medical application of iPSCs is the lack of international standards for safety. It is expected for other iPSC-based treatments such as Parkinson's disease to commerce by 2020 [Karagiannis et al., 2017]. iPSCs could serve as perfect cells to study patient-specific drug responses *in vitro* since iPSCs were successful replacing mouse models in a clinical study to evaluate drugs against amyotrophic lateral sclerosis [McNeish et al., 2015]. Furthermore, iPSCs have been used to identify new biomarkers for example in Kawasaki's disease an inflammatory disease affecting the arterial endothelial cells [Ikeda et al., 2016]. Probably, iPSCs will not completely replace animal models rather they will be a valuable addition [Karagiannis et al., 2017]. Nevertheless, many countries have established new policies to extend the academical and industrial cooperation for the translation of iPSC research from bench to bedside. In 2017, for example the Japan Agency for Medical Research and Development (AMED) was initiated. One of its mayor goals is to build up stocks of iPSCs. The Center for iPS Cell Research and Application (CiRA) at Kyoto University, which is under the lead of Shinya Yamanaka, is contributing to this program by generating iPSCs of clinical-grade as well as disease-specific iPSCs [<https://www.cira.kyoto-u.ac.jp/e/>; Karagiannis et al., 2017]. These cells are then given to cooperation partners for developing new therapeutic approaches and novel drugs. Another way of iPSC use is not only drug testing but also repurposing of already established drugs for application in other diseases. This was successfully done in 2014. This approach could save up two thirds of time and costs [Nosengo, 2016].

Multicellular Organoids as Better *in vitro* Instruments for Disease Modelling

As mentioned above the two-dimensional cell culture is lacking maturity of the iPSC-derived cells. Within the last years several protocols for organoid formation of different organs have been developed including brain [Lancaster and Knoblich, 2014], liver [Takebe et al., 2014] and eye [Eiraku et al., 2011]. So far, most of these organoids do not have the level of complexity as the original organ which affects *in vitro* function [Taguchi and Nishinakamura, 2017]. In this work, it could be shown that liver organoids are good tools to model liver-associated diseases such as NAFLD [Spitzhorn et al., 2016]. Renal organoids were shown to have renal structures such as renal tubule [Taguchi et al., 2014] and nephrons [Takasato et al., 2014] but still were not able to fully mimic organ function.

Nevertheless, they are seen as a model to be used for studying kidney development *in vitro* [Takebe et al., 2015]. Transplanted kidney organs integrated into the rat body and connected to the host's vasculature as well as urine system [Song et al., 2013].

One big challenge of the generation of organoids is the sufficient supply of nutrients and oxygen for the whole cell complex which can be ensured by vascularization [van den Berg et al., 2018]. In many of these protocols MSCs are used since, by expression of myosin II proteins, MSCs are relevant for self-condensation for organoid formation where the contractions are triggered by the actomyosin-cytoskeletal axis [Takebe et al., 2015]. Since tree-dimensional *in vitro* models are on the rise we also showed data indicating the possibility to generate kidney organoids from the urine-derived cells in combination with endothelial cells and MSCs both generated from urine stem cell-derived iPSCs. Thus, we were able to generate a multi-cellular organoid from the same genetic background. This technique could contribute to improving disease modelling, drug screening and nephrotoxicity tests since it may provide a higher level of maturity and a such can be closer to mimic the in-human situation [Nguyen et al., 2019].

Ethical issues as well as restricted reliability of translation from research studies from one species to the other (human) are emphasizing the need for good *in vitro* models as alternative for *in vivo* studies. Three-dimensional cell culture models can increase the relevance of *in vitro* assays but need further improvements [Nguyen and Pentoney, 2017].

iMSCs as Rejuvenated MSCs with Clinical Application Potential

Many clinical trials and research studies use MSCs. In a realistic clinical scenario MSCs would be often obtained from elderly patients and thus may have decreased regenerative potential [O'Hagan-Wong et al., 2016]. Apart from the negative effects of ageing on the cells, *in vitro* culture also can influence the cells' potency which would restrict their therapeutic effect. The generation of MSCs from iPSCs of a patient could be an alternative to the usage of primary MSCs. Indeed, MSCs generated from iPSCs or ESCs were reported to be rejuvenated cells which are more proliferative coming along with increased potential in clinical applications [Frobel et al., 2014; Wang et al., 2014; Hawkins et al., 2018; Lian et al., 2010; Gruenloh et al., 2011; Kimbrel et al., 2014; Chen et al., 2012; Liu et al., 2012; Diederichs and Tuan, 2014; Sheyn et al., 2016] which was

underlined by outperforming primary MSCs in a setting of hind limb ischemia [Wang et al., 2014; Hawkins et al., 2018]. Due to their broad differentiation capacity and modes of actions they have been used in various settings such as multiple sclerosis, limb ischemia, arthritis, cartilage defects, bone defects, wound healing and hypoxic-ischemia in the brain [Sheyn et al., 2016; Wang et al., 2014; Lian et al., 2010; Gonzalo-Gil et al., 2016; Nejadnik et al., 2015; Kuhn et al., 2014; Zhang et al., 2015; Hawkins et al., 2018].

Although several reports exist, the detailed analysis of features in iMSCs compared to primary MSCs on transcriptome, secretome and functional level has to be addressed. In this work fetal MSCs (fMSCs), adult MSCs (aMSCs) and fMSC-iMSCs, aMSCs-iMSCs as well as ESC-iMSCs were compared. We addressed the question of possible rejuvenation events which occur when iMSCs are derived from native MSCs from elderly patients. First of all, we could show that fMSCs represent MSCs in a younger state than aMSCs by transcriptome analysis and their closer relationship to ESCs. The generated iMSCs from either ESCs or fMSC-derived iPSCs met the MSC criteria with regard to cell surface marker expression, morphology and differentiation capacity. On transcriptome level, these iMSCs irrespective of their origin were similar to primary MSCs and distinct from pluripotent cells. The fact, that these iMSCs are not expressing pluripotency genes, is of high relevance to ensure transplantation safety by avoiding the risk of tumour formation. On transcriptional level the iMSCs were detailed compared to fMSCs and aMSCs revealing interesting differences. Using gene sets involved in DNA damage repair and ageing it was observed that the iMSCs clustered together with the foetal MSCs and away from the aMSCs implying rejuvenation since DNA damage is a known to be involved in ageing processes and accumulates over time [Spitzhorn et al., 2019; Freitas et al., 2011].

To further investigate this rejuvenation event, genes were identified which are shared between iMSCs and pluripotent cells but not the native MSCs. This gene set (e.g. *INHBE*, *DNMT3B*, *POU5F1P1*, *CDKN1C*, *GCNT2*) we described as the rejuvenation signature. The counterpart of this was the ageing signature which was only present in the native MSCs but not in the iMSCs and pluripotent cells. The reliability of these signatures was shown by applying it to additional previously published data sets of adult MSCs [Leuning et al., 2017; Park et al., 2016] and on mRNA level using additional MSC and iMSC samples. By downstream computational analyses it was shown that the genes from the rejuvenation signature are associated with embryonic tissue and development underlining

acquired feature of early development. The gain of the rejuvenation signature by parallel loss of the ageing signature could explain the beneficial properties of iMSCs compared to native MSCs [Spitzhorn et al., 2019]. Upon generation of iPSCs, DNA damage is reverted, and the epigenetics also change [Drews et al., 2012] which could explain the fMSC-like expression of genes involved in DNA damage repair in the iMSCs.

As not only the cells itself but also their secreted factors are considered valuable for future applications, we could show that the secretome of the iMSCs irrespective of their source is similar to that of their parental cells thereby extending the transcriptome analysis by a functional component [Spitzhorn et al., 2019]. The plethora of secreted factors is in accordance with previous published secretomes of bone marrow derived MSCs [Hwang et al., 2009; Potian et al., 2003; Aggarwal and Pittenger, 2005] and includes pro- as well as anti-inflammatory cytokines and pro-angiogenic factors such as angiogenin.

We could proof that iMSCs have typical MSCs features. Moreover, we could identify that iMSCs have special gene signature setting them apart from native MSCs and insinuate a potential rejuvenated state. In combination with the broad range of secreted factors, it can be stated that the iMSC-concept has a high relevance for the clinical environment especially taken into account that we are living in a rising ageing society. Identification of the crucial factors within the secretome could be an important step towards clinical use. Since the secretome of the MSCs is rich in beneficial factors one could assume that transplantations of cells could be substituted by transplantation of the factors only [Spitzhorn et al., 2019]. The increasing number of MSC-based clinical trials in phase I or II [<https://www.clinicaltrials.gov/>] underlines the therapeutic significance of MSCs for regenerative medicine and even for iMSCs there are two clinical trials for Graft versus host disease as well as meniscus injury, showing that the iMSC concept already has found its way into the clinic. The bottleneck so far in the use native MSCs is the availability of matching cells [Sheyn et al., 2016]. The beauty of the iMSC-concept is that clinicians are independent from expansion of native cells by generating iMSCs on demand from the pool of unlimited expandable iPSCs.

iMSCs as Promising Cells for Treatment of Liver Diseases

The prevalence for liver injuries and liver diseases is increasing. One particular example for an inherited liver disease is the Crigler-Najjar syndrome. First reported in 1952, this disease is manifesting in elevated bilirubin levels and resulting in kernicterus and jaundice in new-borns [Crigler and Najjar, 1952]. The standard therapeutic choice is phototherapy to break down bilirubin and to avoid the chance for neurotoxicity [Ruud Hansen, 2010] which is significantly decreasing the life quality of the patients and itself can cause DNA damage [Ramy et al., 2016]. This is why alternative treatment options are under consideration. The alternatives such as liver transplantation, liver focused gene therapy [van Dijk et al., 2015] or transplantation of hepatocytes [Jorns et al., 2016] are restricted by availability of matching organs/cells and necessary immune-suppression. To elaborate new therapeutic strategies the Gunn rat is the animal model of choice. These animals bear a mutation in the uridine diphosphate glucuronosyltransferase-1a1 (Ugt1a1) gene which is crucial for the glucuronidation and thus the excretion of bilirubin by the liver. Since this gene is not functional in these rats, they exhibit hyperbilirubinemia and as such represent an animal model for Crigler-Najjar syndrome 1 [Gunn, 1944]. In previous studies in the Gunn rat, bone marrow MSCs as well as HLCs from human iPSCs had a beneficial effect on the hyperbilirubinemia [Muraca et al., 2007; Chen et al., 2015].

In this work, iMSCs from fMSC-derived iPSCs as well as ESCs were generated and showed their similarity to native MSCs on gene expression, morphology, cell surface marker expression as well as on differentiation level. Transcriptome analysis further revealed that these cells are not pluripotent which is crucial for transplantation applications. After partial hepatectomy in Gunn rats, the human iMSCs were transplanted to analyse the contribution to liver regeneration as well as their effect on the inherited enzyme defect within this rat strain [Spitzhorn et al., 2018]. The mode of MSCs application into test objects or patients varies. Many studies have shown beneficial outcomes after intravenous infusion in animal models [Akiyama et al., 2002] and in humans [Koç et al., 2002]. But lethal embolies have been identified as potential risks, since MSCs express high levels of cell adhesion molecules and thus are prone to form cell aggregates which can be found within the lungs [Horwartz et al., 1999; Gao et al., 2001]. In the present scenario of intra-splenic transplantation we tried to minimize the risks of possible pulmonary embolisms by carefully filtration of the MSCs using a fine mesh to isolate only single cells.

By employing human specific antibodies and primers we could show that the transplanted human iMSCs home into the site of injury within rat liver and differentiate into human hepatocytes. The level of maturity and functionality was addressed by analysis of mature hepatocyte marker such as bile salt export pump (BSEP) and sodium-taurocholate cotransporting polypeptide (NTCP) and the detection of human albumin within the rat serum. More importantly these iMSCs derived hepatocytes expressed UGT1A which led to reduced levels of bilirubin in the animals upon iMSC transplantation. Since humans have higher glycine-conjugated bile acids concentration [García-Cañaveras et al., 2012] than rats a shift in the bile salt profile was expected. But only elevated levels of unconjugated bile acids were observed. Also, liver-associated blood markers AST, ALT and LDH were not elevated after iMSC transplantation. Although some studies have reported adverse effects of MSCs transplantation by contributing to fibrosis [Kramann et al, 2015; Walker et al., 2011] we did not observe side effects during the experimental time frame (2 months) [Spitzhorn et al., 2018].

The animal model in this work was also used in other studies in which beneficial effects of rat MSCs [Muraca et al., 2007] as well as human HLCs [Chen et al., 2015] to liver regeneration and improvement of the disease phenotype were shown. These studies used immunosuppressive reagents alongside with the cell transplantation which was omitted in this work to investigate the immune-modulatory potential of the iMSCs. After 2 months, human MSC marker were still present as indicated on mRNA level as well as human cytokines were detected in the rat serum indicating that a subpopulation of transplanted iMSCs did not contribute directly to liver regeneration but could be participating as paracrine effector cells protection the human cells from the hosts immune system or promoting the human cells to differentiated into liver cells [Spitzhorn et al., 2018]. The human cells survived in the rat body for the experimental time period of two month which can be explained by the well-described MSC feature to release immunomodulatory factors [Aggerwal and Pittenger, 2005; Kaplan et al., 2010; Trounson and McDonald, 2015].

In contrast to iMSCs, fMSCs showed much lower beneficial effect on liver regeneration which could be explained by their preference to proliferate than to differentiate, further studies including MSCs of different age groups as well as iMSCs should be done to analyse the influence of proliferate capacity on the cell fate decisions. Furthermore, the way of action for the transplanted MSCs is not fully clear since evidences for fused and

not-fused cells of human and rat origin. Cell fusion events have been described before [Vassilopoulos et al., 2003; Wang et al., 2003] as well as the absence of cell fusion after MSC transplantation [Sato et al., 2005].

However, human iMSCs were able to contribute to liver regeneration in a rat model without noticed side effects. Since a limited time frame of 2 months was analysed a next step towards clinical studies would be long-term studies to ensure that no tumour formation occurs. Nevertheless, their differentiation potential as well as their immunomodulatory properties make iMSCs a promising cell type for transplantations and treatment of (inherited) liver diseases [Spitzhorn et al., 2018].

iMSC Transplantation as a Feasible Way to Regenerate Bone

In this work, it was shown that iMSCs from human foetal foreskin (HFF) derived iPSCs in combination with calcium phosphate granules (CPG) contributed to bone regeneration in critical size defect within mini pigs during the early phase of bone healing [Jungbluth et al., 2019].

In today's clinical practice bone grafting is the standard way of therapy for large bone defects [Li et al., 2015] but the availability of suitable grafts is limited. Alternative Use of stem cells such as bone marrow-derived MSCs has been described [Quarto et al., 2001; Warnke et al., 2004] which are associated with risk during the collection. Both ways are further flawed with possible immune rejections. In this study iMSCs were used, as iMSCs represent an alternative to primary MSCs which are losing their therapeutic potential upon *in vitro* ageing [Yang et al., 2018]. On the contrary, iMSCs from pluripotent stem cells have typical MSCs features alongside with a pro-longed life span [Lian et al., 2010].

Most studies on bone regeneration are employing small animal models. So far, human iMSCs were successfully used in a critical size cranial defect in rats [Wang et al., 2014] and in a mice radial defect model [Sheyn et al., 2016] where they performed as good or even better than their native counterparts. For studies of bone regeneration in larger animals such as sheep or even human, primary bone marrow MSCs have been shown to be effective with or without the use of scaffolds or supplementation with growth factors [Warnke et al., 2004; Reichert et al., 2012]. But studies in human-size animal models for weight bearing bone reconstruction are very rare. For this reason, we have chosen the

Göttingen mini-pig as an *in vivo* model for this work. The significance of this work is underlined by the fact that mini pigs represent a human-scale preclinical animal model due to their bone regeneration capacity of 1.2-1.5 mm/per day which is comparable to the human values [Schlegel et al., 2006]. If animal experiments are conducted their significance should be ensured. The reliability and way of significance of this study was ensured by the fact that groups of 8 pigs were used after a priori power analysis for a power of 80 % with a p value of 0.05 [Hakimi et al., 2010].

As a first step for generating iMSCs, iPSCs have to be generated. In this study these iPSCs were generated from human foreskin fibroblasts (a routinely obtained clinical side product) using non-integrating Sendai viruses containing the Yamanaka factors thereby omitting integration events in the cells. The HFF-iPSCs expressed the pluripotency factors and showed no chromosomal aberrations. The iMSCs generated from the HFF-iPSCs expressed the typical MSC cell surface markers and were able to differentiate into bone cells *in vitro* as shown by alizarin red staining and expression of RUNX2 [Jungbluth et al., 2019] which represents a key player in bone differentiation [Komori, 2003]. Importantly, for transplantation safety these cells were negative for pluripotency-associated factors.

These HFF-iMSCs were shown to release factors beneficial for bone regeneration and angiogenesis events such as PDGF-AA and osteopontin. Thereby it was not necessary to supplement these factors. In a previous study, it has been reported that MSCs from the bone marrow contribute to expression of bone related genes via paracrine effects [Zhou et al., 2018]. Furthermore, the ability of HFF-iMSCs to secrete immunomodulatory factors is of high interest since no experimental induced immunosuppression was administered to the pig. This might indicate that human iMSCs escaped the rejection of the host's immune system.

In this work only 1×10^6 human cells were transplanted into the bone defects thereby mimicking possible shortage of cells in a clinical scenario. Future studies could aim for the usage of higher cell number to identify an optimal ratio of defect size and transplanted cell number.

The effect of the transplanted human iMSCs was analysed on histomorphometrical level as well as on radiological level. It could be shown that human iMSCs in combination with CPG significantly improved bone regeneration. The level of bone restoration was

comparable to the outcome of autologous bone marrow concentrate (BMC) but could not reach the level of regeneration as autologous bone tissue [Jungbluth et al., 2019]. The fact that iMSCs perform as good as autologous BMC is remarkable for two reasons. First, the BMC used originated from the same pig and autologous cell transplantations are expected to be better than allogenic once. Second, BMC contains not only bone marrow MSCs but also platelets and various growth factors [Jungbluth et al., 2014; Hakimi et al., 2014]. Another valuable point is that cross-species transplantation was done using human cells within the pig without external suppression of the host immune system.

Especially for reconstruction bone *in vitro*, tissue engineering approaches are on the rise. iMSCs have been successfully used to generate bone substitutes by loading on scaffolds and subsequent incubation in a perfusion bioreactor system [De Peppo et al., 2014]. Scaffolds as artificial bone matrices are highly important for bone reconstruction but only perform sufficiently when used in combination with stem cells. Calcium phosphate scaffolds resemble the mineral phase of bone tissue and create a beneficial microenvironment within the site of injury [Barrère et al., 2006]. It was shown that iMSCs are able to attach to calcium scaffolds and differentiate into mineralized bone cells [TheinHan et al, 2013; Chen et al, 2012; Jeon et al, 2016]. Using these advances in tissue engineering and the iMSCs concept personalized bone substitutes are possible.

However, further experiments have to be done to identify the way in which the human iMSCs contributed to bone regeneration. Although they were shown to be able to differentiate into bone cells *in vitro* the analysis of the pig bones after 6 weeks of regeneration time does not allow to tell whether the human cells contribute directly by differentiation or indirectly by paracrine signalling and thereby recruiting host cells. A combination of both processes may be also possible alongside with fusion events. The CT analyses can only identify bone tissue but not its origin. The high correlation of the histomorphometrical and the radiological analysis proof the reliability of these evaluation methods as previously described [Hakimi et al., 2014]. One way of accessing the way of action cell tracking experiments should be considered to specifically detect the human cells within the defect zone.

With these additional experiments one also could try to address the molecular mechanisms underlying the bone regeneration events. BMPs which are involved in bone regeneration processes [Reichert et al., 2012; Schmidt-Bleek et al., 2016] were found to

be present on transcriptome level. In the future the presence of BMPs could be analysed on different levels such as mRNA or protein.

To my knowledge, this work is the first to evaluate the therapeutic potential of human iMSCs in a pre-clinical animal model of bone regeneration. Long-term studies will be needed to analyse their potential in later stages of bone regeneration as well contribute to ensure their transplantation safety by not observation of tumours [Jungbluth et al., 2019].

MSCs for Treatment of Neurodegenerative Diseases

Although it is known that MSCs can contribute to oligodendrogenesis of aNSCs by release of paracrine factors, the specific cytokines and molecular mechanisms involved are no clear yet [Lindsay et al., 2013, 2016]. Another aspect which was addressed by this work is whether MSCs from foetal tissue can promote oligodendrogenesis as reported for adult MSCs.

In this work it was shown that conditioned medium from human fMSCs prevents astrocytic differentiation, promotes oligodendrogenesis of aNSCs in rats and facilitate differentiation of iPSCs-derived NSCs into oligodendrocytes [Jadasz et al., 2018].

The contribution of adult neural stem cells to oligodendrogenesis is crucial for advances in analysis and treatment of neurodegenerative diseases. Recent data suggest that oligodendrocytes which originate from stem cells of the subventricular zone are involved in myelin repair [Xing et al., 2014]. It was previously reported that oligodendrogenesis of stem cells from the hippocampus can be induced by secreted factors of MSCs [Bai et al., 2009; Munoz et al., 2005; Rivera et al., 2006; Steffenhagen et al., 2012] underlining the fact that neuronal stem cells from the subgranular zone are able to generate myelinating glia. The trophic factors released by MSCs are influencing the myelin wrapping process as well as the expression of oligodendrial markers. This could be explained by response to human factors directly or an indirect rejuvenation process taking part in the cells upon stimulation with fMSCs conditioned medium. They way of action can be either pro-oligodendric or anti-astrocytic [Kremer et al., 2011, Jadasz et al., 2013; Rivera et al., 2006]. Although some studies were done dealing with distinct factors secreted by MSCs such as HGF or VEGF [Jadasz et al., 2013; Rivera et al., 2006, 2008] which were also found in conditioned medium of human MSCs [Chen et al., 2008; Lin et al., 2008; Razavi

et al., 2013] none of these factors were proven to be involved in the MSC-dependent oligodendrogenesis of adult neural stem cells [Rivera et al., 2006, 2008]. It is very probable that a cocktail of factors causes the oligodendrogenesis [Jadasz et al., 2018]. In addition to chemokines, MSCs also release microRNAs [Chen et al., 2010] which can influence cells from the environment [Tomasoni et al., 2013]. For example, miR-146-5p was shown to be involved in myelination via CXCL12 secretion [Lindsay et al., 2016] which is important for development of oligodendrocytes from their progenitors [Göttle et al., 2010].

Since rat as well as human MSCs were able to enhance oligodendrogenesis in this study, it can be assumed that this event has an underlying conserved mechanism. Furthermore, the ability of MSC conditioned medium on differentiation of iPSCs into oligodendrocytes was shown and represents a faster alternative when compared to previously reported protocols [Douvaras et al., 2014; Wang et al., 2013]. Using the iPSCs approach it will be possible to generate neural stem cells as well as MSCs from the same genetic background which can be used for additional applications [Jadasz et al., 2018].

The data presented in this work emphasize the broad potential of MSCs to contribute to regenerative processes in the brain. For selective use in therapeutic approach further studies are necessary to identify the factor combination in the MSC secretome which is responsible for oligodendrogenesis. By identification of the distinct factors which are driving the neuronal repair it would be possible to invent new therapeutic strategies. These for example could go away from transplantations of cells but rather go into the direction of transplanting/injection only these distinct factors. This could be done with patient specific cells which are maintained under GMP conditions.

Further Research

Due to the fact that amniotic fluid- and urine-derived stem cells have shown great differentiation and paracrine potential *in vitro*, these cell types should be tested in the established *in vivo* models to elucidate their potential for regeneration of liver and bone. Especially their use in bone regeneration seems promising as both cell types were able to differentiate into bone *in vitro*. In addition to the application in these two models, the

cells should be applied in *in vivo* models of kidney-associated diseases since they are of renal origin.

This renal origin should be further investigated to dissect the exact renal cell types present in amniotic fluid and urine. In line with this, their molecular and cellular identities should be defined more precisely. This also would allow developing robust protocols to differentiate these kidney progenitor cells in differentiated kidney cells such as renal proximal tubular cells or podocytes which exhibit the important functions associated with the kidney.

Furthermore, follow up studies for the iMSCs experiments could be done in which a longer time period is covered to address the long-term effects of these cells and to further evaluate their transplantation safety. Future studies should have the aim to identify the underlying biomolecular mechanisms of the iMSCs in regeneration processes and should clarify if their mode of action is direct and/or via paracrine signalling. For the latter it could be of high value to quantitatively assess the factors secreted by the iMSCs. Additionally, it is planned to compare iMSCs derived from iPSCs from different sources (MSCs, AF-MSCs, uMSCs, HFF, epicardial cells, etc.) to reveal similarities and potentially differences manifested through their initial cell source. Upcoming *in vivo* studies should include tracing of the transplanted cells. This can be done by labelling of the cell with fluorochromes such as GFP or super magnetic iron oxides which can be stained or read using magnetic resonance which can even be done *in vivo* [Frank et al., 2002] and would allow to identify their exact location. To minimize the risk for the patient future research should also focus on their role as paracrine effector cells going towards transplantations of secreted factors only. For MSCs this was done in the last years by analysing their secreted extracellular vesicles [Giebel et al., 2017].

Since the hepatic differentiation potential of human iMSCs was shown, they have been used in preliminary experiments for the development of artificial livers. Therefore, rat livers were decellularized and loaded with human iMSCs. It was shown that these cells differentiated into hepatocytes, probably driven by the micro-architecture provided by the rat liver matrix. This approach could contribute to the generation of mature *ex vivo* livers for basic research or even transplantation experiments.

Since conditioned medium of human fMSCs has a positive effect on oligodendrogenesis in rats, the potency of human iMSCs conditioned medium is under investigation in preliminary experiments using the established rodent models.

In addition to the *in vivo* application of the different stem cell types it should be targeted to optimize *in vitro* usage of the cells. Therefore, the different cell types should be considered for generating multi-cellular organoids consisting of iMSCs and endothelial cells and organ-specific cells to develop cell culture tools for increasing the prediction reliability. When maturity and functionality are given, these *in vitro* generated organoids could be the bases for further transplantation experiments. Further advanced engineering approaches such as bio-printing or organ-on-a-chip technology which have to be shown for kidney related work [Homan et al., 2016; Wilmer et al., 2016] should be considered in future experiments as well as distinct cell culture topographies which have been shown to influence differentiation processes of MSCs [Abagnale et al., 2015].

Conclusion

In the present work, amniotic fluid derived from caesarean sections was identified as a source of stem cells. These cells were shown to be similar to bone marrow MSCs on cellular as well as on transcriptional level. In addition to that, they expressed pluripotency associated factors. They were further shown to be paracrine effector cells by releasing various trophic factors. Thus, caesarean sections represent a great alternative to amniocentesis which is without risk for the foetus and the mother and provides researchers with potent cells to be used in clinical applications. In additional experiments we could show that these AF-MSCs originate from the foetal kidney as shown by expression of kidney-associated genes and function. These results add important insights into the ongoing controversial discussion about the origin of cells harboured in amniotic fluid. These findings underpin the potency of AF-MSCs for kidney-related research, disease modelling and for generating iPSCs. Additionally, it was shown that urine also contains MSCs which express renal markers. These urine-derived stem cells could be successfully reprogramed into iPSCs. iPSCs represent a highly powerful tool in toxicology studies and were shown to be useful in (liver) disease modelling. It is possible to use iPSCs for the generation of MSCs (iMSCs) which irrespective of their origin (fMSCs, aMSCs, or pluripotent cells) show typical MSCs features. These iMSCs are rejuvenated MSCs as shown by the identified rejuvenation signature. Especially meaningful for future experimental use of the iMSCs, they were shown to be paracrine active in a similar way than fMSCs. These findings additionally underline the magnitude of the iMSC concept for usage in regeneration and therapeutically applications in an ever-increasing ageing society. In an animal of inherited liver disease and liver injury human iMSCs differentiated into functional liver cells and contributed to liver regeneration and the partially rescue of the disease phenotype. Furthermore, mini-pig experiments have provided evidence for the potential of iMSCs to be used in the treatment of bone defects. Combined with the iPSCs approach it is feasible to produce HLA-matched iMSCs which can be used in the patients without the risk of rejection and as such are an alternative to BMC or bone marrow concentrate. However, long-term studies and detailed analysis of the mode of action of these stem cells and their derivatives are necessary for possible future applications in humans. Taken all these results together, application of stem cells in the clinical scenario can be considered as a key-driver in transforming healthcare.

Appendix – Talks, Poster Presentations and Prizes

Conference Talks:

2nd International Annual Conference of the German Stem Cell Network, Heidelberg, 2014
Mesenchymal stem cells derived from iPS cells from aged individuals acquire fetal characteristics

3rd International Annual Conference of the German Stem Cell Network, Frankfurt, 2015
Regenerative potential of human pluripotent stem cell-derived MSCs in a Gunn rat liver injury model

Stem Cell Network NRW Meeting, Herne, 2016
Human pluripotent stem cell derived MSCs regenerate injured Gunn rat liver and trans-differentiate into functional hepatocytes and reduce bilirubin levels

German Association of the Study of the Liver Meeting, Essen, 2017
Generation of a 3D model to better mimic NAFLD in vitro

SFB 974 Retreat, Trier, 2017
Human pluripotent stem cell-derived MSCs regenerate injured Gunn rat liver

DeLiver Symposium Düsseldorf, 2017
Transplanted human pluripotent stem cell-derived mesenchymal stem cells differentiate into hepatocytes and improve hyperbilirubinemia in Gunn rats

Next-Gen Regenerative Medicine & Tissue Engineering Conference, Frankfurt, 2018
Amniotic fluid and urine as Sources of renal stem cells

13th BMFZ Retreat, Düsseldorf, 2019
iMSCs – a promising cell population for translational medicine

Kick-Off Meeting StemCell Network NRW, Düsseldorf, 2019
MSCs for translational research and regenerative medicine

23rd Surgical Research Days of the German Society of Surgery, Aachen, 2019
Human fetal foreskin fibroblast derived iMSCs support regeneration of a critical size bone defect in mini-pigs

German Congress for Orthopaedics and traumatology, Berlin, 2019
Human iPSC-derived iMSCs improve bone regeneration in mini-pigs

Conference Poster:

2nd International Annual Conference of the German Stem Cell Network, Heidelberg, 2014
Mesenchymal stem cells derived from iPS cells from aged individuals acquire fetal characteristics.

8th International Meeting of the Stem Cell Network NRW, Bonn, 2015
Acquisition of fetal features in mesenchymal stem cells derived from iPS cells from aged individuals.

International Society for Stem Cell Research Annual Meeting, Stockholm, 2015
Acquisition of fetal features in mesenchymal stem cells derived from iPS cells from aged individuals.

3rd International Annual Conference of the German Stem Cell Network, Frankfurt, 2015
(i) Characterization and banking of human third trimester amniotic fluid-derived mesenchymal stem cells obtained from cesarean sections.
(ii) Regenerative potential of human pluripotent stem cell-derived MSCs in a Gunn rat liver injury model.

German Association of the Study of the Liver Meeting, Düsseldorf, 2016
Regenerative potential of human pluripotent stem cell-derived MSCs in a Gunn rat liver injury model.

CECAD 2nd Cologne Ageing Conference, Cologne, 2016
Rejuvenation of mesenchymal stem cells derived from iPS cells originating from aged individuals.

24th International Bile Acid Meeting: Bile Acids in Health and Disease, Düsseldorf, 2016
Generation of liver buds by self-condensation of human iPSC-derived MSCs, HLCs and endothelial cells.

German Stem Cell Network Meeting, Hannover, 2016
(i) Dissecting the complexity of cell types present in urine, identifies renal progenitor cells with regenerative potential.
(ii) Generation of liver buds by self-condensation of human iPSC-derived MSCs, HLCs and endothelial cells.

German Association of the Study of the Liver Meeting, Essen, 2017
Generation of a 3D model to better mimic NAFLD in vitro.

DeLiver Symposium Düsseldorf, 2017
Transplanted human pluripotent stem cell-derived mesenchymal stem cells differentiate into hepatocytes and improve hyperbilirubinemia in Gunn rats.

9th International Meeting Stem Cell Network NRW, Münster, 2017

(i) *Human ESC and iPSC-derived MSCs regenerate injured Gunn rat liver: a comparative study.*

(ii) *Dissecting the complexity of cell types present in urine, identifies renal progenitor cells with regenerative potential.*

(iii) *Human iPSC-derived iMSCs improve regeneration in a Goettingen mini-pig bone defect model.*

(iv) *Dissecting the Complexity in Amniotic Fluid-Derived Cells Obtained from Cesarean Sections.*

(v) *Generation of a 3D model to better mimic NAFLD in vitro.*

Stem Cell Community Day, Düsseldorf, 2018

Human fetal foreskin iPSC-derived iMSCs support regeneration in a Goettingen mini-pig bone defect model.

6th Annual German Stem Cell Network Meeting, Heidelberg, 2018

Human fetal foreskin iPSC-derived iMSCs support regeneration in a Goettingen mini-pig bone defect model.

7th Annual German Stem Cell Network Meeting, Berlin, 2019

UriCell: Human urine as an innovative source of kidney progenitor cells amenable for drug testing and toxicity studies

Prizes:

Poster Award: 9th International Meeting Stem Cell Network NRW, Münster, 2017

Human ESC and iPSC-derived MSCs regenerate injured Gunn rat liver: a comparative study.

3rd Place Poster Award: Stem Cell Community Day, Düsseldorf, 2018

Human fetal foreskin iPSC-derived iMSCs support regeneration in a Goettingen mini-pig bone defect model.

Hans-Jürgen-Bretschneider-Prize, 23rd Surgical Research Days of the German Society of Surgery, Aachen, 2019

Human fetal foreskin fibroblast-derived iMSCs support regeneration of a critical size bone defect in mini-pigs.

Research Award of the AO Germany, German Congress for Orthopaedics and Traumatology, Berlin, 2019

Human iPSC-derived iMSCs improve bone regeneration in mini-pigs.

Bibliography

Abagnale G, Steger M, Nguyen VH, Hersch N, Sechi A, Joussen S, Denecke B, Merkel R, Hoffmann B, Dreser A, Schnakenberg U, Gillner A, Wagner W. Surface topography enhances differentiation of mesenchymal stem cells towards osteogenic and adipogenic lineages. *Biomaterials*. 2015 Aug;61:316-26.

Abdel Aziz MT, Atta HM, Mahfouz S, Fouad HH, Roshdy NK, Ahmed HH, Rashed LA, Sabry D, Hassouna AA, Hasan NM. Therapeutic potential of bone marrow-derived mesenchymal stem cells on experimental liver fibrosis. *Clin Biochem*. 2007 Aug;40(12):893-9.

Aggarwal S, Pittenger MF. Human mesenchymal stem cells modulate allogeneic immune cell responses. *Blood*. 2005 Feb 15;105(4):1815-22

Akiyama Y, Radtke C, Honmou O, Kocsis JD. Remyelination of the spinal cord following intravenous delivery of bone marrow cells. *Glia*. 2002 Sep;39(3):229-36.

Akkermann R, Jadasz JJ, Azim K, Küry P. Taking Advantage of Nature's Gift: Can Endogenous Neural Stem Cells Improve Myelin Regeneration? *Int J Mol Sci*. 2016 Nov 14;17(11). pii: E1895.

Al-Awqati Q, Oliver JA. Stem cells in the kidney. *Kidney Int*. 2002 Feb;61(2):387-95.

Alvarez CV, Garcia-Lavandeira M, Garcia-Rendueles ME, Diaz-Rodriguez E, Garcia-Rendueles AR, Perez-Romero S, Vila TV, Rodrigues JS, Lear PV, Bravo SB. Defining stem cell types: understanding the therapeutic potential of ESCs, ASCs, and iPS cells. *J Mol Endocrinol*. 2012 Aug 30;49(2):R89-111.

Antonucci I, Di Pietro R, Alfonsi M, Centurione MA, Centurione L, Sancilio S, Pelagatti F, D'Amico MA, Di Baldassarre A, Piattelli A, Tetè S, Palka G, Borlongan CV, Stuppia L. Human second trimester amniotic fluid cells are able to create embryoid body-like structures in vitro and to show typical expression profiles of embryonic and primordial germ cells. *Cell Transplant*. 2014;23(12):1501-15.

Arcolino FO, Zia S, Held K, Papadimitriou E, Theunis K, Bussolati B, Raaijmakers A, Allegaert K, Voet T, Deprest J, Vriens J, Toelen J, van den Heuvel L, Levchenko E. Urine of Preterm Neonates as a Novel Source of Kidney Progenitor Cells. *J Am Soc Nephrol*. 2016 Sep;27(9):2762-70.

Babaie Y, Herwig R, Greber B, Brink TC, Wruck W, Groth D, Lehrach H, Burdon T, Adjaye J. Analysis of Oct4-dependent transcriptional networks regulating self-renewal and pluripotency in human embryonic stem cells. *Stem Cells*. 2007 Feb;25(2):500-10.

Bai L, Lennon DP, Caplan AI, DeChant A, Hecker J, Kranso J, Zaremba A, Miller RH. Hepatocyte growth factor mediates mesenchymal stem cell-induced recovery in multiple sclerosis models. *Nat Neurosci*. 2012 Jun;15(6):862-70.

Barrère F, van Blitterswijk CA, de Groot K. Bone regeneration: molecular and cellular interactions with calcium phosphate ceramics. *Int J Nanomedicine*. 2006;1(3):317-32.

Bexell D, Gunnarsson S, Svensson A, Tormin A, Henriques-Oliveira C, Siesjö P, Paul G, Salford LG, Scheduling S, Bengzon J. Rat multipotent mesenchymal stromal cells lack long-distance tropism to 3 different rat glioma models. *Neurosurgery*. 2012 Mar;70(3):731-9.

Bhumiratana S, Bernhard JC, Alfi DM, Yeager K, Eton RE, Bova J, Shah F, Gimble JM, Lopez MJ, Eisig SB, Vunjak-Novakovic G. Tissue-engineered autologous grafts for facial bone reconstruction. *Sci Transl Med*. 2016 Jun 15;8(343):343ra83.

- Bianco P, Cao X, Frenette PS, Mao JJ, Robey PG, Simmons PJ, Wang CY. The meaning, the sense and the significance: translating the science of mesenchymal stem cells into medicine. *Nat Med*. 2013 Jan;19(1):35-42.
- Bohndorf M, Neube A, Spitzhorn LS, Enczmann J, Wruck W, Adjaye J. Derivation and characterization of integration-free iPSC line ISRM-UM51 derived from SIX2-positive renal cells isolated from urine of an African male expressing the CYP2D6 *4/*17 variant which confers intermediate drug metabolizing activity. *Stem Cell Res*. 2017 Dec;25:18-21.
- Bork S, Pfister S, Witt H, Horn P, Korn B, Ho AD, Wagner W. DNA methylation pattern changes upon long-term culture and aging of human mesenchymal stromal cells. *Aging Cell*. 2010 Feb;9(1):54-63.
- Boyd NL, Robbins KR, Dhara SK, West FD, Stice SL. Human embryonic stem cell-derived mesoderm-like epithelium transitions to mesenchymal progenitor cells. *Tissue Eng Part A*. 2009 Aug;15(8):1897-907.
- Brink TC, Demetrius L, Lehrach H, Adjaye J. Age-related transcriptional changes in gene expression in different organs of mice support the metabolic stability theory of aging. *Biogerontology*. 2009;10:549-564.
- Bussolati B, Camussi G. Therapeutic use of human renal progenitor cells for kidney regeneration. *Nat Rev Nephrol*. 2015 Dec;11(12):695-706.
- Buzhor E, Omer D, Harari-Steinberg O, Dotan Z, Vax E, Pri-Chen S, Metsuyanin S, Pleniceanu O, Goldstein RS, Dekel B. Reactivation of NCAM1 defines a subpopulation of human adult kidney epithelial cells with clonogenic and stem/progenitor properties. *Am J Pathol*. 2013 Nov;183(5):1621-1633.
- Campagnoli C, Roberts IA, Kumar S, Bennett PR, Bellantuono I, Fisk NM. Identification of mesenchymal stem/progenitor cells in human first-trimester fetal blood, liver, and bone marrow. *Blood*. 2001 Oct 15;98(8):2396-402.
- Cananzi M, Atala A, De Coppi P. Stem cells derived from amniotic fluid: new potentials in regenerative medicine. *Reprod Biomed Online*. 2009;18 Suppl 1:17-27.
- Caplan AI. Mesenchymal stem cells. *J Orthop Res*. 1991 Sep;9(5):641-50.
- Carey BW, Markoulaki S, Hanna J, Saha K, Gao Q, Mitalipova M, Jaenisch R. Reprogramming of murine and human somatic cells using a single polycistronic vector. *Proc Natl Acad Sci U S A*. 2009 Jan 6;106(1):157-62.
- Casiraghi F, Perico N, Cortinovis M, Remuzzi G. Mesenchymal stromal cells in renal transplantation: opportunities and challenges. *Nat Rev Nephrol*. 2016;12(4):241-53.
- Chambers I, Smith A. Self-renewal of teratocarcinoma and embryonic stem cells. *Oncogene*. 2004 Sep 20;23(43):7150-60.
- Chan CKF, Gulati GS, Sinha R, Tompkins JV, Lopez M, Carter AC, Ransom RC, Reinisch A, Wearda T, Murphy M, Brewer RE, Koepke LS, Marecic O, Manjunath A, Seo EY, Leavitt T, Lu WJ, Nguyen A, Conley SD, Salhotra A, Ambrosi TH, Borrelli MR, Siebel T, Chan K, Schallmoser K, Seita J, Sahoo D, Goodnough H, Bishop J, Gardner M, Majeti R, Wan DC, Goodman S, Weissman IL, Chang HY, Longaker MT. Identification of the Human Skeletal Stem Cell. *Cell*. 2018 Sep20;175(1):43-56.e21.
- Charbord P, Livne E, Gross G, Häupl T, Neves NM, Marie P, Bianco P, Jorgensen C. Human bone marrow mesenchymal stem cells: a systematic reappraisal via the genostem experience. *Stem Cell Rev*. 2011 Mar;7(1):32-42
- Chatterjee I, Li F, Kohler EE, Rehman J, Malik AB, Wary KK. Induced Pluripotent Stem (iPS) Cell Culture Methods and Induction of Differentiation into Endothelial Cells. *Methods Mol Biol*. 2016;1357:311-27.

Chatzipantelis P, Lazaris AC, Kafiri G, Nonni A, Papadimitriou K, Xiromeritis K, Patsouris ES. CD56 as a useful marker in the regenerative process of the histological progression of primary biliary cirrhosis. *Eur J Gastroenterol Hepatol*. 2008 Sep;20(9):837-42.

Chawla LS, Eggers PW, Star RA, Kimmel PL. Acute kidney injury and chronic kidney disease as interconnected syndromes. *N Engl J Med*. 2014;371:58-66.

Chen L, Tredget EE, Wu PY, Wu Y. Paracrine factors of mesenchymal stem cells recruit macrophages and endothelial lineage cells and enhance wound healing. *PLoS One*. 2008 Apr 2;3(4):e1886.

Chen TS, Lai RC, Lee MM, Choo AB, Lee CN, Lim SK. Mesenchymal stem cell secretes microparticles enriched in pre-microRNAs. *Nucleic Acids Res*. 2010 Jan;38(1):215-24.

Chen W, Zhou H, Weir MD, Tang M, Bao C, Xu HH. Human embryonic stem cell-derived mesenchymal stem cell seeding on calcium phosphate cement-chitosan-RGD scaffold for bone repair. *Tissue Eng Part A*. 2013 Apr;19(7-8):915-27.

Chen Y, Li Y, Wang X, Zhang W, Sauer V, Chang CJ, Han B, Tchaikovskaya T, Avsar Y, Tafaleng E, Madhusudana Girija S, Tar K, Polgar Z, Strom S, Bouhassira EE, Guha C, Fox IJ, Roy-Chowdhury J, Roy-Chowdhury N. Amelioration of Hyperbilirubinemia in Gunn Rats after Transplantation of Human Induced Pluripotent Stem Cell-Derived Hepatocytes. *Stem Cell Reports*. 2015 Jul 14;5(1):22-30.

Chen YS, Pelekanos RA, Ellis RL, Horne R, Wolvetang EJ, Fisk NM. Small molecule mesengenic induction of human induced pluripotent stem cells to generate mesenchymal stem/stromal cells. *Stem Cells Transl Med*. 2012 Feb;1(2):83-95.

Cheung HH, Liu X, Canterel-Thouennon L, Li L, Edmonson C, Rennert OM. Telomerase protects werner syndrome lineage-specific stem cells from premature aging. *Stem Cell Reports*. 2014;2:534-546.

Chhabra P, Brayman KL. The use of stem cells in kidney disease. *Curr Opin Organ Transplant*. 2009 Feb;14(1):72-8.

Chivu M, Dima SO, Stancu CI, Dobrea C, Uscatescu V, Necula LG, Bleotu C, Tanase C, Albulescu R, Ardeleanu C, Popescu I. In vitro hepatic differentiation of human bone marrow mesenchymal stem cells under differential exposure to liver-specific factors. *Transl Res*. 2009 Sep;154(3):122-32.

Chopp M, Zhang XH, Li Y, Wang L, Chen J, Lu D, Lu M, Rosenblum M. Spinal cord injury in rat: treatment with bone marrow stromal cell transplantation. *Neuroreport*. 2000 Sep 11;11(13):3001-5.

Chou BK, Mali P, Huang X, Ye Z, Dowey SN, Resar LM, Zou C, Zhang YA, Tong J, Cheng L. Efficient human iPS cell derivation by a non-integrating plasmid from blood cells with unique epigenetic and gene expression signatures. *Cell Res*. 2011 Mar;21(3):518-29.

Chuah JKC, Zink D. Stem cell-derived kidney cells and organoids: Recent breakthroughs and emerging applications. *Biotechnol Adv*. 2017 Mar - Apr;35(2):150-167.

Combes AN, Wilson S, Phipson B, Binnie BB, Ju A, Lawlor KT, Cebrian C, Walton SL, Smyth IM, Moritz KM, Kopan R, Oshlack A, Little MH. Haploinsufficiency for the *Six2* gene increases nephron progenitor proliferation promoting branching and nephron number. *Kidney Int*. 2018 Mar;93(3):589-598.

Cowan CA, Atienza J, Melton DA, Eggan K. Nuclear reprogramming of somatic cells after fusion with human embryonic stem cells. *Science*. 2005 Aug 26;309(5739):1369-73.

Crigler JF Jr, Najjar VA. Congenital familial nonhemolytic jaundice with kernicterus. *Pediatrics*. 1952 Aug;10(2):169-80.

Crisan M, Yap S, Casteilla L, Chen CW, Corselli M, Park TS, Andriolo G, Sun B, Zheng B, Zhang L, Norotte C, Teng PN, Traas J, Schugar R, Deasy BM, Badylak S, Buhning HJ, Giacobino JP, Lazzari L, Huard J, Péault B. A perivascular origin for mesenchymal stem cells in multiple human organs. *Cell Stem Cell*. 2008 Sep 11;3(3):301-13.

Cruz NM, Song X, Czerniecki SM, Gulieva RE, Churchill AJ, Kim YK, Winston K, Tran LM, Diaz MA, Fu H, Finn LS, Pei Y, Himmelfarb J, Freedman BS. Organoid cystogenesis reveals a critical role of microenvironment in human polycystic kidney disease. *Nat Mater*. 2017 Nov;16(11):1112-1119.

Cyranoski D. Japanese man is first to receive 'reprogrammed' stem cells from another person. *Nature*. 2017 Mar.

Da Sacco S, Perin L, Sedrakyan S. Amniotic fluid cells: current progress and emerging challenges in renal regeneration. *Pediatr Nephrol*. 2017 Jun 15.

Dagostino C, Allegri M, Napolioni V, D'Agnelli S, Bignami E, Mutti A, van Schaik RH. CYP2D6 genotype can help to predict effectiveness and safety during opioid treatment for chronic low back pain: results from a retrospective study in an Italian cohort. *Pharmgenomics Pers Med*. 2018 Oct 24;11:179-191.

Das A, Segar CE, Hughley BB, Bowers DT, Botchwey EA. The promotion of mandibular defect healing by the targeting of SIP receptors and the recruitment of alternatively activated macrophages. *Biomaterials*. 2013 Dec;34(38):9853-62.

Davidson MD, Ware BR, Khetani SR. Stem cell-derived liver cells for drug testing and disease modeling. *Discov Med*. 2015 May;19(106):349-58.

De Coppi P, Bartsch G Jr, Siddiqui MM, Xu T, Santos CC, Perin L, Mostoslavsky G, Serre AC, Snyder EY, Yoo JJ, Furth ME, Soker S, Atala A. Isolation of amniotic stem cell lines with potential for therapy. *Nat Biotechnol*. 2007 Jan;25(1):100-6.

De Peppo GM, Vunjak-Novakovic G, Marolt D. Cultivation of human bone-like tissue from pluripotent stem cell-derived osteogenic progenitors in perfusion bioreactors. *Methods Mol Biol*. 2014;1202:173-84.

Diederichs S and Tuan RS. Functional comparison of human-induced pluripotent stem cell-derived mesenchymal cells and bone marrow-derived mesenchymal stromal cells from the same donor. *Stem Cells Dev*. 2014;23:1594-1610.

Dominici M, Le Blanc K, Mueller I, Slaper-Cortenbach I, Marini F, Krause D, Deans R, Keating A, Prockop Dj, Horwitz E. Minimal criteria for defining multipotent mesenchymal stromal cells. The International Society for Cellular Therapy position statement. *Cytotherapy*. 2006;8(4):315-7.

Douvaras P, Wang J, Zimmer M, Hanchuk S, O'Bara MA, Sadiq S, Sim FJ, Goldman J, Fossati V. Efficient generation of myelinating oligodendrocytes from primary progressive multiple sclerosis patients by induced pluripotent stem cells. *Stem Cell Reports*. 2014 Aug 12;3(2):250-9.

Drews K, Jozefczuk J, Prigione A, Adjaye J. Human induced pluripotent stem cells--from mechanisms to clinical applications. *J Mol Med (Berl)*. 2012 Jul;90(7):735-45.

Duijvestein M, Vos AC, Roelofs H, Wildenberg ME, Wendrich BB, Verspaget HW, Kooy-Winkelaar EM, Koning F, Zwaginga JJ, Fidder HH, Verhaar AP, Fibbe WE, van den Brink GR, Hommes DW. Autologous bone marrow-derived mesenchymal stromal cell treatment for refractory luminal Crohn's disease: results of a phase I study. *Gut*. 2010 Dec;59(12):1662-9.

Duncan AW, Dorrell C, Grompe M. Stem cells and liver regeneration. *Gastroenterology*. 2009 Aug;137(2):466-81

Duscher D, Rennert RC, Januszyk M, Anghel E, Maan ZN, Whittam AJ, Perez MG, Kosaraju R, Hu MS, Walmsley GG, Atashroo D, Khong S, Butte AJ, Gurtner GC. Aging disrupts cell subpopulation dynamics and diminishes the function of mesenchymal stem cells. *Sci Rep*. 2014 Nov 21;4:7144.

Ellinger I, Ellinger A. Smallest Unit of Life: Cell Biology. In: Jensen-Jarolim E. (eds) *Comparative Medicine*. Springer, Vienna. 2014.

Faour O, Dimitriou R, Cousins CA, Giannoudis PV. The use of bone graft substitutes in large cancellous voids: any specific needs? *Injury*. 2011 Sep;42 Suppl 2:S87-90.

Frank JA, Zywicke H, Jordan EK, Mitchell J, Lewis BK, Miller B, Bryant LH Jr, Bulte JW. Magnetic intracellular labeling of mammalian cells by combining (FDA-approved) superparamagnetic iron oxide MR contrast agents and commonly used transfection agents. *Acad Radiol*. 2002 Aug;9 Suppl 2:S484-7.

Franklin RJ. Why does remyelination fail in multiple sclerosis? *Nat Rev Neurosci*. 2002 Sep;3(9):705-14.

Freitas AA, Vasieva O, de Magalhães JP. A data mining approach for classifying DNA repair genes into ageing-related or non-ageing-related. *BMC Genomics*. 2011;12:27

Friedenstein AJ, Chailakhjan RK, Lalykina KS. The development of fibroblast colonies in monolayer cultures of guinea-pig bone marrow and spleen cells. *Cell Tissue Kinet*. 1970 Oct;3(4):393-403.

Frobel J, Hemeda H, Lenz M, Abagnale G, Joussem S, Denecke B, Sarić T, Zenke M, Wagner W. Epigenetic rejuvenation of mesenchymal stromal cells derived from induced pluripotent stem cells. *Stem Cell Reports*. 2014 Sep 9;3(3):414-22.

Fuchs E, Tumber T, Guasch G. Socializing with the neighbors: stem cells and their niche. *Cell*. 2004 Mar 19;116(6):769-78. Review.

Gao J, Dennis JE, Muzic RF, Lundberg M, Caplan AI. The dynamic in vivo distribution of bone marrow-derived mesenchymal stem cells after infusion. *Cells Tissues Organs*. 2001;169(1):12-20.

García-Cañaveras JC, Donato MT, Castell JV, Lahoz A. Targeted profiling of circulating and hepatic bile acids in human, mouse, and rat using a UPLC-MRM-MS-validated method. *J Lipid Res*. 2012 Oct;53(10):2231-41.

Georgas KM, Chiu HS, Lesieur E, Rumballe BA, Little MH. Expression of metanephric nephron-patterning genes in differentiating mesonephric tubules. *Dev Dyn*. 2011;240(6):1600-12.

Giebel B, Kordelas L, Börger V. Clinical potential of mesenchymal stem/stromal cell-derived extracellular vesicles. *Stem Cell Investig*. 2017 Oct 24;4:84.

Giri S, Bader A. A low-cost, high-quality new drug discovery process using patient-derived induced pluripotent stem cells. *Drug Discov Today*. 2015 Jan;20(1):37-49.

Gonzalo-Gil E, Pérez-Lorenzo MJ, Galindo M, Díaz de la Guardia R, López-Millán B, Bueno C, Menéndez P, Pablos JL, Criado G. Human embryonic stem cell-derived mesenchymal stromal cells ameliorate collagen-induced arthritis by inducing host-derived indoleamine 2,3 dioxygenase. *Arthritis Res Ther*. 2016 Apr 1;18:77.

Göttle P, Kremer D, Jander S, Odemis V, Engele J, Hartung HP, Küry P. Activation of CXCR7 receptor promotes oligodendroglial cell maturation. *Ann Neurol*. 2010 Dec;68(6):915-24.

Graffmann N, Matz P, Wruck W, Adjaye J. The promise of induced pluripotent stem cells for liver disease, toxicology and drug discovery. *Drug Target Review*. 2015 2 (1).

- Grayson WL, Bunnell BA, Martin E, Frazier T, Hung BP, Gimble JM. Stromal cells and stem cells in clinical bone regeneration. *Nat Rev Endocrinol*. 2015 Mar;11(3):140-50.
- Gruenloh W, Kambal A, Sondergaard C, McGee J, Nacey C, Kalomoiris S, Pepper K, Olson S, Fierro F, Nolte JA. Characterization and in vivo testing of mesenchymal stem cells derived from human embryonic stem cells. *Tissue Eng Part A*. 2011 Jun;17(11-12):1517-25.
- Guillot PV, Gotherstrom C, Chan J, Kurata H, Fisk NM. Human first-trimester fetal MSC express pluripotency markers and grow faster and have longer telomeres than adult MSC. *Stem Cells*. 2007;25(3):646-54.
- Gunn CK. Hereditary Acholuric Jaundice in the Rat. *Can Med Assoc J*. 1944 Mar;50(3):230-7.
- Hakimi M, Grassmann JP, Betsch M, Schnependahl J, Gehrman S, Hakimi AR, Kröpil P, Sager M, Herten M, Wild M, Windolf J, Jungbluth P. The composite of bone marrow concentrate and PRP as an alternative to autologous bone grafting. *PLoS One*. 2014 Jun 20;9(6):e100143.
- Hakimi M, Jungbluth P, Sager M, Betsch M, Herten M, Becker J, Windolf J, Wild M. Combined use of platelet-rich plasma and autologous bone grafts in the treatment of long bone defects in mini-pigs. *Injury*. 2010 Jul;41(7):717-23.
- Hamid AA, Joharry MK, Mun-Fun H, Hamzah SN, Rejali Z, Yazid MN, Thilakavathy K, Nordin N. Highly potent stem cells from full-term amniotic fluid: A realistic perspective. *Reprod Biol*. 2017 Mar;17(1):9-18.
- Hamza AH, Al-Bishri WM, Damiati LA, Ahmed HH. Mesenchymal stem cells: a future experimental exploration for recession of diabetic nephropathy. *Ren Fail*. 2017;39(1):67-76.
- Haque N, Rahman MT, Abu Kasim NH, Alabsi AM. Hypoxic culture conditions as a solution for mesenchymal stem cell based regenerative therapy. *ScientificWorldJournal*. 2013 Aug 27;2013:632972.
- Harding R, Hooper SB. Regulation of lung expansion and lung growth before birth. *J Appl Physiol* (1985). 1996 Jul;81(1):209-24.
- Hariharan K, Kurtz A, Schmidt-Ott KM. Assembling Kidney Tissues from Cells: The Long Road from Organoids to Organs. *Front Cell Dev Biol*. 2015 Nov 11;3:70.
- Hauser PV, De Fazio R, Bruno S, Sdei S, Grange C, Bussolati B, Benedetto C, Camussi G. Stem cells derived from human amniotic fluid contribute to acute kidney injury recovery. *Am J Pathol*. 2010;177(4):2011-21.
- Hawkins KE, Corcelli M, Dowding K, Ranzoni AM, Vlahova F, Hau KL, Hunjan A, Peebles D, Gressens P, Hagberg H, de Coppi P, Hristova M, Guillot PV. Embryonic Stem Cell-Derived Mesenchymal Stem Cells (MSCs) Have a Superior Neuroprotective Capacity Over Fetal MSCs in the Hypoxic-Ischemic Mouse Brain. *Stem Cells Transl Med*. 2018 May;7(5):439-449.
- Hawkins KE, Moschidou D, Faccenda D, Wruck W, Martin-Trujillo A, Hau KL, Ranzoni AM, Sanchez-Freire V, Tommasini F, Eaton S, De Coppi P, Monk D, Campanella M, Thrasher AJ, Adjaye J, Guillot PV. Human Amniocytes Are Receptive to Chemically Induced Reprogramming to Pluripotency. *Mol Ther*. 2017 Feb 1;25(2):427-442.
- Hendry C, Rumballe B, Moritz K, Little MH. Defining and redefining the nephron progenitor population. *Pediatr Nephrol*. 2011;26(9):1395-406.
- Herten M, Grassmann JP, Sager M, Benga L, Fischer JC, Jäger M, Betsch M, Wild M, Hakimi M, Jungbluth P. Bone marrow concentrate for autologous transplantation in minipigs. Characterization and osteogenic potential of mesenchymal stem cells. *Vet Comp Orthop Traumatol*. 2013;26(1):34-41.

Higgins JP, Wang L, Kambham N, Montgomery K, Mason V, Vogelmann SU, Lemley KV, Brown PO, Brooks JD, van de Rijn M. Gene expression in the normal adult human kidney assessed by complementary DNA microarray. *Mol Biol Cell*. 2004 Feb;15(2):649-56.

Hoehn H, Bryant EM, Karp LE, Martin GM. Cultivated cells from diagnostic amniocentesis in second trimester pregnancies. I. Clonal morphology and growth potential. *Pediatr Res*. 1974 Aug;8(8):746-54.

Hoehn H, Salk D. Morphological and biochemical heterogeneity of amniotic fluid cells in culture. *Methods Cell Biol*. 1982;26:11-34. Review.

Homan KA, Kolesky DB, Skylar-Scott MA, Herrmann J, Obuobi H, Moisan A, Lewis JA. Bioprinting of 3D Convuluted Renal Proximal Tubules on Perfusable Chips. *Sci Rep*. 2016 Oct 11;6:34845.

Horwitz EM, Gordon PL, Koo WK, Marx JC, Neel MD, McNall RY, Muul L, Hofmann T. Isolated allogeneic bone marrow-derived mesenchymal cells engraft and stimulate growth in children with osteogenesis imperfecta: Implications for cell therapy of bone. *Proc Natl Acad Sci U S A*. 2002 Jun 25;99(13):8932-7.

Horwitz EM, Prockop DJ, Fitzpatrick LA, Koo WW, Gordon PL, Neel M, Sussman M, Orchard P, Marx JC, Pyeritz RE, Brenner MK. Transplantability and therapeutic effects of bone marrow-derived mesenchymal cells in children with osteogenesis imperfecta. *Nat Med*. 1999 Mar;5(3):309-13.

Hoste EA, Schurgers M. Epidemiology of acute kidney injury: how big is the problem? *Crit Care Med* 2008;36(4 Suppl):S146-S151.

<https://www.cira.kyoto-u.ac.jp/e/>

<https://www.clinicaltrials.gov>

<https://www.kidney.org>

<https://www.uricell.de/>

Hu Q, Friedrich AM, Johnson LV, Clegg DO. Memory in induced pluripotent stem cells: reprogrammed human retinal-pigmented epithelial cells show tendency for spontaneous redifferentiation. *Stem Cells*. 2010 Nov;28(11):1981-91.

Hwang JH, Shim SS, Seok OS, Lee HY, Woo SK, Kim BH, Song HR, Lee JK, Park YK. Comparison of cytokine expression in mesenchymal stem cells from human placenta, cord blood, and bone marrow. *J Korean Med Sci*. 2009 Aug;24(4):547-54.

Ikeda K, Mizoro Y, Ameku T, Nomiya Y, Mae SI, Matsui S, Kuchitsu Y, Suzuki C, Hamaoka-Okamoto A, Yahata T, Sone M, Okita K, Watanabe A, Osafune K, Hamaoka K. Transcriptional Analysis of Intravenous Immunoglobulin Resistance in Kawasaki Disease Using an Induced Pluripotent Stem Cell Disease Model. *Circ J*. 2016 Dec 22;81(1):110-118.

Illich DJ, Demir N, Stojković M, Scheer M, Rothamel D, Neugebauer J, Hescheler J, Zöllner JE. Concise review: induced pluripotent stem cells and lineage reprogramming: prospects for bone regeneration. *Stem Cells*. 2011 Apr;29(4):555-63.

In 't Anker PS, Scherjon SA, Kleijburg-van der Keur C, de Groot-Swings GM, Claas FH, Fibbe WE, Kanhai HH. Isolation of mesenchymal stem cells of fetal or maternal origin from human placenta. *Stem Cells*. 2004;22(7):1338-45.

In 't Anker PS, Scherjon SA, Kleijburg-van der Keur C, Noort WA, Claas FH, Willemze R, Fibbe WE, Kanhai HH. Amniotic fluid as a novel source of mesenchymal stem cells for therapeutic transplantation. *Blood*. 2003 Aug 15;102(4):1548-9.

Israel MA, Yuan SH, Bardy C, Reyna SM, Mu Y, Herrera C, Hefferan MP, Van Gorp S, Nazor KL, Boscolo FS, Carson CT, Laurent LC, Marsala M, Gage FH, Remes AM, Koo EH, Goldstein LS. Probing sporadic and familial Alzheimer's disease using induced pluripotent stem cells. *Nature*. 2012 Jan 25;482(7384):216-20.

Izzedine H, Perazella MA. Onco-nephrology: an appraisal of the cancer and chronic kidney disease links. *Nephrol Dial Transplant*. 2015;30: 1979–1988.

Jadasz JJ, Kremer D, Göttle P, Tzekova N, Domke J, Rivera FJ, Adjaye J, Hartung HP, Aigner L, Küry P. Mesenchymal stem cell conditioning promotes rat oligodendroglial cell maturation. *PLoS One*. 2013 Aug 12;8(8):e71814.

Jadasz JJ, Tepe L, Beyer F, Samper Agrelo I, Akkermann R, Spitzhorn LS, Silva ME, Oreffo ROC, Hartung HP, Prigione A, Rivera FJ, Adjaye J, Küry P. Human mesenchymal factors induce rat hippocampal- and human neural stem cell dependent oligodendrogenesis. *Glia*. 2018 Jan;66(1):145-160.

Jeon OH, Panicker LM, Lu Q, Chae JJ, Feldman RA, Elisseeff JH. Human iPSC-derived osteoblasts and osteoclasts together promote bone regeneration in 3D biomaterials. *Sci Rep*. 2016 May 26;6:26761.

Jessen KR, Mirsky R. Glial cells in the enteric nervous system contain glial fibrillary acidic protein. *Nature*. 1980 Aug 14;286(5774):736-7.

Jin HK, Carter JE, Huntley GW, Schuchman EH. Intracerebral transplantation of mesenchymal stem cells into acid sphingomyelinase-deficient mice delays the onset of neurological abnormalities and extends their life span. *J Clin Invest*. 2002 May;109(9):1183-91.

Jin ZB, Okamoto S, Osakada F, Homma K, Assawachananont J, Hiram Y, Iwata T, Takahashi M. Modeling retinal degeneration using patient-specific induced pluripotent stem cells. *PLoS One*. 2011 Feb 10;6(2):e17084.

Jorns C, Nowak G, Nemeth A, Zemack H, Mörk LM, Johansson H, Gramignoli R, Watanabe M, Karadagi A, Alheim M, Hauzenberger D, van Dijk R, Bosma PJ, Ebbesen F, Szakos A, Fischler B, Strom S, Ellis E, Ericzon BG. De Novo Donor-Specific HLA Antibody Formation in Two Patients With Crigler-Najjar Syndrome Type I Following Human Hepatocyte Transplantation With Partial Hepatectomy Preconditioning. *Am J Transplant*. 2016 Mar;16(3):1021-30.

Jung KH, Shin HP, Lee S, Lim YJ, Hwang SH, Han H, Park HK, Chung JH, Yim SV. Effect of human umbilical cord blood-derived mesenchymal stem cells in a cirrhotic rat model. *Liver Int*. 2009 Jul;29(6):898-909.

Jungbluth P, Grassmann JP, Thelen S, Wild M, Sager M, Windolf J, Hakimi M. Concentration of platelets and growth factors in platelet-rich plasma from Goettingen minipigs. *GMS Interdiscip Plast Reconstr Surg DGPW*. 2014 Nov 24;3:Doc11.

Jungbluth P, Spitzhorn LS, Grassmann J, Tanner S, Latz D, Rahman MS, Bohndorf M, Wruck W, Sager M, Grotheer V, Kröpil P, Hakimi M, Windolf J, Schnependahl J, Adjaye J. Human iPSC-derived iMSCs improve bone regeneration in mini-pigs. *BoneRes*. 2019 Oct 24;7:32.

Kang NH, Hwang KA, Kim SU, Kim YB, Hyun SH, Jeung EB, Choi KC. Potential antitumor therapeutic strategies of human amniotic membrane and amniotic fluid-derived stem cells. *Cancer Gene Ther*. 2012 Aug;19(8):517-22.

Kang, Yan Zhou, Shuang Tan, Guangqian Zhou, Lars Aagaard, Lin Xie, Cody Bünger, Lars Bolund, Yonglun Luo. Mesenchymal stem cells derived from human induced pluripotent stem cells retain adequate osteogenicity and chondrogenicity but less adipogenicity. *Stem Cell Res Ther.* 2015; 6(1): 144.

Kaplan JM, Youd ME, Lodie TA. Immunomodulatory activity of mesenchymal stem cells. *Curr Stem Cell Res Ther.* 2011 Dec;6(4):297-316.

Karagiannis P, Onodera A, Yamanaka S. New Models for Therapeutic Innovation from Japan. *EBioMedicine.* 2017 Apr;18:3-4.

Karoui M, Penna C, Amin-Hashem M, Mitry E, Benoist S, Franc B, Rougier P, Nordlinger B. Influence of preoperative chemotherapy on the risk of major hepatectomy for colorectal liver metastases. *Ann Surg.* 2006 Jan;243(1):1-7.

Karussis D, Kassis I, Kurkalli BG, Slavin S. Immunomodulation and neuroprotection with mesenchymal bone marrow stem cells (MSCs): a proposed treatment for multiple sclerosis and other neuroimmunological/neurodegenerative diseases. *J Neurol Sci.* 2008 Feb 15;265(1-2):131-5.

Kasper G, Mao L, Geissler S, Draycheva A, Trippens J, Kuhnisch J, Tschirschmann M, Kaspar K, Perka C, Duda GN, Klose J. Insights into mesenchymal stem cell aging: involvement of antioxidant defense and actin cytoskeleton. *Stem Cells.* 2009 Jun;27(6):1288-97.

Kassis I, Grigoriadis N, Gowda-Kurkalli B, Mizrachi-Kol R, Ben-Hur T, Slavin S, Abramsky O, Karussis D. Neuroprotection and immunomodulation with mesenchymal stem cells in chronic experimental autoimmune encephalomyelitis. *Arch Neurol.* 2008 Jun;65(6):753-61.

Katsara O, Mahaira LG, Iliopoulou EG, Moustaki A, Antsaklis A, Loutradis D, Stefanidis K, Baxeavanis CN, Papamichail M, Perez SA. Effects of donor age, gender, and in vitro cellular aging on the phenotypic, functional, and molecular characteristics of mouse bone marrow-derived mesenchymal stem cells. *Stem Cells Dev.* 2011 Sep;20(9):1549-61.

Kaviani A, Perry TE, Dzakovic A, Jennings RW, Ziegler MM, Fauza DO. The amniotic fluid as a source of cells for fetal tissue engineering. *J Pediatr Surg.* 2001 Nov;36(11):1662-5.

Kellum JA, Hoste EA. Acute kidney injury: epidemiology and assessment. *Scand J Clin Lab Invest Suppl* 2008;241:6-11.

Kimbrel EA, Kouris NA, Yavarian GJ, Chu J, Qin Y, Chan A, Singh RP, McCurdy D, Gordon L, Levinson RD, Lanza R. Mesenchymal stem cell population derived from human pluripotent stem cells displays potent immunomodulatory and therapeutic properties. *Stem Cells Dev.* 2014 Jul 15;23(14):1611-24.

Kloskowski T, Nowacki M, Pokrywczyńska M, Drewa T. Urine--a waste or the future of regenerative medicine? *Med Hypotheses.* 2015 Apr;84(4):344-9.

Kobayashi A, Mugford JW, Krautzberger AM, Naiman N, Liao J, McMahon AP. Identification of a multipotent self-renewing stromal progenitor population during mammalian kidney organogenesis. *Stem Cell Reports.* 2014;3(4):650-62.

Koç ON, Day J, Nieder M, Gerson SL, Lazarus HM, Krivit W. Allogeneic mesenchymal stem cell infusion for treatment of metachromatic leukodystrophy (MLD) and Hurler syndrome (MPS-IH). *Bone Marrow Transplant.* 2002 Aug;30(4):215-22.

Koike C, Zhou K, Takeda Y, Fathy M, Okabe M, Yoshida T, Nakamura Y, Kato Y, Nikaido T. Characterization of amniotic stem cells. *Cell Reprogram.* 2014 Aug;16(4):298-305.

- Komori, T. Requisite roles of Runx2 and Cbfb in skeletal development. *J Bone Miner Metab.* 2003, 21, 193-197.
- Kordes C, Sawitza I, Götze S, Häussinger D. Hepatic stellate cells support hematopoiesis and are liver-resident mesenchymal stem cells. *Cell Physiol Biochem.* 2013;31(2-3):290-304.
- Kordes C, Sawitza I, Götze S, Herebian D, Häussinger D. Hepatic stellate cells contribute to progenitor cells and liver regeneration. *J Clin Invest.* 2014 Dec;124(12):5503-15.
- Kordes C, Sawitza I, Götze S, Schumacher E, Häussinger D. Beyond fibrosis: stellate cells as liver stem cells. *Z Gastroenterol.* 2015 Dec;53(12):1425-31.
- Koyner JL, Cerdá J, Goldstein SL, Jaber BL, Liu KD, Shea JA, Faubel S; Acute Kidney Injury Advisory Group of the American Society of Nephrology. The daily burden of acute kidney injury: a survey of U.S. nephrologists on World Kidney Day. *Am J Kidney Dis.* 2014 Sep;64(3):394-401.
- Kramann R, Schneider RK, DiRocco DP, Machado F, Fleig S, Bondzie PA, Henderson JM, Ebert BL, Humphreys BD. Perivascular Gli1+ progenitors are key contributors to injury-induced organ fibrosis. *Cell Stem Cell.* 2015 Jan 8;16(1):51-66.
- Kremer D, Aktas O, Hartung HP, Küry P. The complex world of oligodendroglial differentiation inhibitors. *Ann Neurol.* 2011 Apr;69(4):602-18.
- Kuhn LT, Liu Y, Boyd NL, Dennis JE, Jiang X, Xin X, Charles LF, Wang L, Aguila HL, Rowe DW, Lichtler AC, Goldberg AJ. Developmental-like bone regeneration by human embryonic stem cell-derived mesenchymal cells. *Tissue Eng Part A.* 2014 Jan;20(1-2):365-77.
- Kuo TK, Hung SP, Chuang CH, Chen CT, Shih YR, Fang SC, Yang VW, Lee OK. Stem cell therapy for liver disease: parameters governing the success of using bone marrow mesenchymal stem cells. *Gastroenterology.* 2008 Jun;134(7):2111-21, 2121.e1-3.
- Kuroda R, Matsumoto T, Kawakami Y, Fukui T, Mifune Y, Kurosaka M. Clinical impact of circulating CD34-positive cells on bone regeneration and healing. *Tissue Eng Part B Rev.* 2014 Jun;20(3):190-9.
- Lam AQ, Freedman BS, Morizane R, Lerou PH, Valerius MT, Bonventre JV. Rapid and efficient differentiation of human pluripotent stem cells into intermediate mesoderm that forms tubules expressing kidney proximal tubular markers. *J Am Soc Nephrol.* 2014;25(6):1211-25.
- Lancaster MA, Knoblich JA. Generation of cerebral organoids from human pluripotent stem cells. *Nat Protoc.* 2014 Oct;9(10):2329-40.
- Lange C, Bassler P, Lioznov MV, Bruns H, Kluth D, Zander AR, Fiegel HC. Hepatocytic gene expression in cultured rat mesenchymal stem cells. *Transplant Proc.* 2005 Jan-Feb;37(1):276-9.
- Le Blanc K, Frassoni F, Ball L, Locatelli F, Roelofs H, Lewis I, Lanino E, Sundberg B, Bernardo ME, Remberger M, Dini G, Egeler RM, Bacigalupo A, Fibbe W, Ringdén O; Developmental Committee of the European Group for Blood and Marrow Transplantation. Mesenchymal stem cells for treatment of steroid-resistant, severe, acute graft-versus-host disease: a phase II study. *Lancet.* 2008 May 10;371(9624):1579-86.
- Lee KD, Kuo TK, Whang-Peng J, Chung YF, Lin CT, Chou SH, Chen JR, Chen YP, Lee OK. In vitro hepatic differentiation of human mesenchymal stem cells. *Hepatology.* 2004 Dec;40(6):1275-84.

- Leuning DG, Reinders ME, Li J, Peired AJ, Lievers E, de Boer HC, Fibbe WE, Romagnani P, van Kooten C, Little MH, Engelse MA, Rabelink TJ. Clinical-Grade Isolated Human Kidney Perivascular Stromal Cells as an Organotypic Cell Source for Kidney Regenerative Medicine. *Stem Cells Transl Med.* 2017 Feb;6(2):405-418.
- Li CY, Wu XY, Tong JB, Yang XX, Zhao JL, Zheng QF, Zhao GB, Ma ZJ. Comparative analysis of human mesenchymal stem cells from bone marrow and adipose tissue under xeno-free conditions for cell therapy. *Stem Cell Res Ther.* 2015 Apr 13;6:55.
- Li DL, He XH, Zhang SA, Fang J, Chen FS, Fan JJ. Bone marrow-derived mesenchymal stem cells promote hepatic regeneration after partial hepatectomy in rats. *Pathobiology.* 2013;80(5):228-34.
- Li L, Xie T. Stem cell niche: structure and function. *Annu Rev Cell Dev Biol.* 2005;21:605-31.
- Li R, Liang J, Ni S, Zhou T, Qing X, Li H, He W, Chen J, Li F, Zhuang Q, Qin B, Xu J, Li W, Yang J, Gan Y, Qin D, Feng S, Song H, Yang D, Zhang B, Zeng L, Lai L, Esteban MA, Pei D. A mesenchymal-to-epithelial transition initiates and is required for the nuclear reprogramming of mouse fibroblasts. *Cell Stem Cell.* 2010 Jul 2;7(1):51-63.
- Li Y, Chen SK, Li L, Qin L, Wang XL, Lai YX. Bone defect animal models for testing efficacy of bone substitute biomaterials. *J Orthop Translat.* 2015 Jun 16;3(3):95-104.
- Lian Q, Zhang Y, Zhang J, Zhang HK, Wu X, Zhang Y, Lam FF, Kang S, Xia JC, Lai WH, Au KW, Chow YY, Siu CW, Lee CN, Tse HF. Functional mesenchymal stem cells derived from human induced pluripotent stem cells attenuate limb ischemia in mice. *Circulation.* 2010 Mar 9;121(9):1113-23.
- Lichtner B, Matz P, Adjaye J. Generation of iPSC lines from primary human chorionic villi cells. *Stem Cell Res.* 2015 Nov;15(3):697-9.
- Lin N, Tang Z, Deng M, Zhong Y, Lin J, Yang X, Xiang P, Xu R. Hedgehog-mediated paracrine interaction between hepatic stellate cells and marrow-derived mesenchymal stem cells. *Biochem Biophys Res Commun.* 2008 Jul 18;372(1):260-5.
- Lindsay SL, Johnstone SA, McGrath MA, Mallinson D, Barnett SC. Comparative miRNA-Based Fingerprinting Reveals Biological Differences in Human Olfactory Mucosa- and Bone-Marrow-Derived Mesenchymal Stromal Cells. *Stem Cell Reports.* 2016 May 10;6(5):729-742.
- Lindsay SL, Johnstone SA, Mountford JC, Sheikh S, Allan DB, Clark L, Barnett SC. Human mesenchymal stem cells isolated from olfactory biopsies but not bone enhance CNS myelination in vitro. *Glia.* 2013 Mar;61(3):368-82.
- Little MH, McMahon AP. Mammalian kidney development: Principles, progress, and projections. *Cold Spring Harb Perspect Biol.* 2012;4:4.
- Little MH. Generating kidney tissue from pluripotent stem cells. *Cell Death Discovery.* 2016;2:16053.
- Liu Y, Goldberg AJ, Dennis JE, Gronowicz GA, Kuhn LT. One-step derivation of mesenchymal stem cell (MSC)-like cells from human pluripotent stem cells on a fibrillar collagen coating. *PLoS One.* 2012;7:e33225.
- Loukogeorgakis SP, De Coppi P. Amniotic fluid stem cells: the known, the unknown, and potential regenerative medicine applications. *Stem Cells.* 2017;35:1663-1673.

Mah N, Wang Y, Liao MC, Prigione A, Jozefczuk J, Lichtner B, Wolfrum K, Haltmeier M, Flöttmann M, Schaefer M, Hahn A, Mrowka R, Klipp E, Andrade-Navarro MA, Adjaye J. Molecular insights into reprogramming-initiation events mediated by the OSKM gene regulatory network. *PLoS One*. 2011;6(8):e24351.

Mahmoudi S, Brunet A. Aging and reprogramming: a two-way street. *Curr Opin Cell Biol*. 2012 Dec;24(6):744-56.

Makino S, Fukuda K, Miyoshi S, Konishi F, Kodama H, Pan J, Sano M, Takahashi T, Hori S, Abe H, Hata J, Umezawa A, Ogawa S. Cardiomyocytes can be generated from marrow stromal cells in vitro. *J Clin Invest*. 1999 Mar;103(5):697-705.

Mandai, M., Watanabe, A., Kurimoto, Y., Hirami, Y., Morinaga, C., Daimon, T., Fujihara, M., Akimaru, H., Sakai, N., Shibata, Y., Terada, M., Nomiya, Y., Tanishima, S., Nakamura, M., Kamao, H., Sugita, S., Onishi, A., Ito, T., Fujita, K., Kawamata, S., Go, M.J., Shinohara, C., Hata, K.-I., Sawada, M., Yamamoto, M., Ohta, S., Ohara, Y., Yoshida, K., Kuwahara, J., Kitano, Y., Amano, N., Umekage, M., Kitaoka, F., Tanaka, A., Okada, C., Takasu, N., Ogawa, S., Yamanaka, S., Takahashi, M., 2017. Autologous induced stem-cell-derived retinal cells for macular degeneration. *N. Engl. J. Med.* 376, 1038–1046.

Mark P, Kleinsorge M, Gaebel R, Lux CA, Toelk A, Pittermann E, David R, Steinhoff G, Ma N. Human Mesenchymal Stem Cells Display Reduced Expression of CD105 after Culture in Serum-Free Medium. *Stem Cells Int*. 2013;2013:698076.

Maximow AA. Relation of blood cells to connective tissues and endothelium. *Physiological Reviews* 1924 4;4, 533-563.

McCaffrey LM, Macara IG. Epithelial organization, cell polarity and tumorigenesis. *Trends Cell Biol*. 2011 Dec;21(12):727-35.

McMahon AP. Development of the Mammalian Kidney. In: Paul Wassarman (Hg.): *Essays on Developmental Biology*. 2016; Part B, Bd. 117: Elsevier (Current Topics in Developmental Biology), pp. 31–64.

McNeish J, Gardner JP, Wainger BJ, Woolf CJ, Eggan K. From Dish to Bedside: Lessons Learned While Translating Findings from a Stem Cell Model of Disease to a Clinical Trial. *Cell Stem Cell*. 2015 Jul 2;17(1):8-10.

Megges M, Geissler S, Duda GN, Adjaye J. Generation of an iPS cell line from bone marrow derived mesenchymal stromal cells from an elderly patient. *Stem Cell Res*. 2015 Nov;15(3):565-8.

Mehta RL, Awdishu L, Davenport A, Murray PT, Macedo E, Cerda J, Chakaravarthi R, Holden AL, Goldstein SL. Phenotype standardization for drug-induced kidney disease. *Kidney Int*. 2015 Aug;88(2):226-34.

Metsuyanin S, Harari-Steinberg O, Buzhor E, Omer D, Pode-Shakked N, Ben-Hur H, Halperin R, Schneider D, Dekel B. Expression of stem cell markers in the human fetal kidney. *PLoS One*. 2009 Aug 21;4(8):e6709.

Michelotti GA, Xie G, Swiderska M, Choi SS, Karaca G, Krüger L, Premont R, Yang L, Syn WK, Metzger D, Diehl AM. Smoothed is a master regulator of adult liver repair. *J Clin Invest*. 2013 Jun;123(6):2380-94.

Miller JD, Ganat YM, Kishinevsky S, Bowman RL, Liu B, Tu EY, Mandal PK, Vera E, Shim JW, Kriks S, Taldone T, Fusaki N, Tomishima MJ, Krainc D, Milner TA, Rossi DJ, Studer L. Human iPSC-based modeling of late-onset disease via progerin-induced aging. *Cell Stem Cell*. 2013 Dec 5;13(6):691-705.

- Mirabella T, Cilli M, Carlone S, Cancedda R, Gentili C. Amniotic liquid derived stem cells as reservoir of secreted angiogenic factors capable of stimulating neo-arteriogenesis in an ischemic model. *Biomaterials*. 2011 May;32(15):3689-99.
- Mirabella T, Gentili C, Daga A, Cancedda R. Amniotic fluid stem cells in a bone microenvironment: driving host angiogenic response. *Stem Cell Res*. 2013 Jul;11(1):540-51.
- Mirmalek-Sani SH, Tare RS, Morgan SM, Roach HI, Wilson DI, Hanley NA, Oreffo RO. Characterization and multipotentiality of human fetal femur-derived cells: implications for skeletal tissue regeneration. *Stem Cells*. 2006 Apr;24(4):1042-53.
- Miyasaka M, Tanaka T. Lymphocyte trafficking across high endothelial venules: dogmas and enigmas. *Nat Rev Immunol*. 2004 May;4(5):360-70.
- Moschidou D, Drews K, Eddaoudi A, Adjaye J, De Coppi P, Guillot PV. Molecular signature of human amniotic fluid stem cells during fetal development. *Curr Stem Cell Res Ther*. 2013 Jan;8(1):73-81.
- Moschidou D, Mukherjee S, Blundell MP, Drews K, Jones GN, Abdulrazzak H, Nowakowska B, Phoolchund A, Lay K, Ramasamy TS, Cananzi M, Nettersheim D, Sullivan M, Frost J, Moore G, Vermeesch JR, Fisk NM, Thrasher AJ, Atala A, Adjaye J, Schorle H, De Coppi P, Guillot PV. Valproic acid confers functional pluripotency to human amniotic fluid stem cells in a transgene-free approach. *Mol Ther*. 2012 Oct;20(10):1953-67.
- Moskalev AA, Shaposhnikov MV, Plyusnina EN, Zhavoronkov A, Budovsky A, Yanai H, Fraifeld VE. The role of DNA damage and repair in aging through the prism of Koch-like criteria. *Ageing Res Rev*. 2013 Mar;12(2):661-84.
- Munoz JR, Stoutenger BR, Robinson AP, Spees JL, Prockop DJ. Human stem/progenitor cells from bone marrow promote neurogenesis of endogenous neural stem cells in the hippocampus of mice. *Proc Natl Acad Sci U S A*. 2005 Dec 13;102(50):18171-6.
- Muraca M, Ferraresso C, Vilei MT, Granato A, Quarta M, Cozzi E, Rugge M, Pauwelyn KA, Caruso M, Avital I, Inderbitzin D, Demetriou AA, Forbes SJ, Realdi G. Liver repopulation with bone marrow derived cells improves the metabolic disorder in the Gunn rat. *Gut*. 2007 Dec;56(12):1725-35.
- Nejadnik H, Diecke S, Lenkov OD, Chapelin F, Donig J, Tong X, Derugin N, Chan RC, Gaur A, Yang F, Wu JC, Daldrop-Link HE. Improved approach for chondrogenic differentiation of human induced pluripotent stem cells. *Stem Cell Rev*. 2015 Apr;11(2):242-53.
- Nesselmann C, Kaminski A, Steinhoff G. Cardiac stem cell therapy. Registered trials and a pilot study in patients with dilated cardiomyopathy. *Herz*. 2011 Mar;36(2):121-34.
- Nguyen DG, Pentoney SL Jr. Bioprinted three dimensional human tissues for toxicology and disease modeling. *Drug Discov Today Technol*. 2017 Mar;23:37-44.
- Nguyen L, Spitzhorn LS, Adjaye J. Constructing an Isogenic 3D Human Nephrogenic Progenitor Cell Model Composed of Endothelial, Mesenchymal, and SIX2-Positive Renal Progenitor Cells. *Stem Cells Int*. 2019 May 2;2019:3298432.
- Nosengo N. Can you teach old drugs new tricks? *Nature*. 2016 Jun 16;534(7607):314-6.
- Nussler A, Konig S, Ott M, Sokal E, Christ B, Thasler W, Brulport M, Gabelein G, Schormann W, Schulze M, Ellis E, Kraemer M, Nocken F, Fleig W, Manns M, Strom SC, Hengstler JG. Present status and perspectives of cell-based therapies for liver diseases. *J Hepatol*. 2006 Jul;45(1):144-59

- O'Brien LL, McMahon AP. Induction and patterning of the metanephric nephron. *Semin Cell Dev Biol.* 2014 Dec;36:31-8.
- O'Hagan-Wong K, Nadeau S, Carrier-Leclerc A, Apablaza F, Hamdy R, Shum-Tim D, Rodier F, Colmegna I. Increased IL-6 secretion by aged human mesenchymal stromal cells disrupts hematopoietic stem and progenitor cells' homeostasis. *Oncotarget.* 2016 Mar 22;7(12):13285-96.
- Oliveira Arcolino F, Tort Piella A, Papadimitriou E, Bussolati B, Antonie DJ, Murray P, van den Heuvel L, Levchenko E. Human Urine as a Noninvasive Source of Kidney Cells. *Stem Cells Int.* 2015;2015:362562.
- Olver RE, Strang LB. Ion fluxes across the pulmonary epithelium and the secretion of lung liquid in the foetal lamb. *J Physiol.* 1974 Sep;241(2):327-57.
- Oreffo RO, Bord S, Triffitt JT. Skeletal progenitor cells and ageing human populations. *Clin Sci (Lond).* 1998;94:549-555.
- Oreffo RO, Cooper C, Mason C, Clements M. Mesenchymal stem cells: lineage, plasticity, and skeletal therapeutic potential. *Stem Cell Rev.* 2005;1(2):169-78.
- Palumbo S, Tsai TL, Li WJ. Macrophage migration inhibitory factor regulates AKT signaling in hypoxic culture to modulate senescence of human mesenchymal stem cells. *Stem Cells Dev.* 2014 Apr 15;23(8):852-65.
- Park GC, Song JS, Park HY, Shin SC, Jang JY, Lee JC, Wang SG, Lee BJ, Jung JS. Role of Fibroblast Growth Factor-5 on the Proliferation of Human Tonsil-Derived Mesenchymal Stem Cells. *Stem Cells Dev.* 2016 Aug 1;25(15):1149-60.
- Parolini O, Alviano F, Bagnara GP, Bilic G, Bühring HJ, Evangelista M, Hennerbichler S, Liu B, Magatti M, Mao N, Miki T, Marongiu F, Nakajima H, Nikaido T, Portmann-Lanz CB, Sankar V, Soncini M, Stadler G, Surbek D, Takahashi TA, Redl H, Sakuragawa N, Wolbank S, Zeisberger S, Zisch A, Strom SC. Concise review: isolation and characterization of cells from human term placenta: outcome of the first international Workshop on Placenta Derived Stem Cells. *Stem Cells.* 2008 Feb;26(2):300-11.
- Paulitschek C, Schulze-Matz P, Hesse J, Schmidt T, Wruck W, Adjaye J, Schrader J. Generation and characterization of two iPSC lines from human epicardium-derived cells. *Stem Cell Res.* 2017 Apr;20:50-53.
- Perazella MA. Renal vulnerability to drug toxicity. *Clin J Am Soc Nephrol.* 2009;4:1275-1283.
- Perin L, Giuliani S, Jin D, Sedrakyan S, Carraro G, Habibian R, Warburton D, Atala A, De Filippo RE. Renal differentiation of amniotic fluid stem cells. *Cell Prolif.* 2007 Dec;40(6):936-48.
- Perin L, Sedrakyan S, Giuliani S, Da Sacco S, Carraro G, Shiri L, Lemley KV, Rosol M, Wu S, Atala A, Warburton D, De Filippo RE. Protective effect of human amniotic fluid stem cells in an immunodeficient mouse model of acute tubular necrosis. *PLoS One.* 2010 Feb 24;5(2):e9357.
- Perry BC, Zhou D, Wu X, Yang FC, Byers MA, Chu TM, Hockema JJ, Woods EJ, Goebel WS. Collection, cryopreservation, and characterization of human dental pulp-derived mesenchymal stem cells for banking and clinical use. *Tissue Eng Part C Methods.* 2008 Jun;14(2):149-56.
- Phinney DG, Prockop DJ. Concise review: mesenchymal stem/multipotent stromal cells: the state of transdifferentiation and modes of tissue repair-current views. *Stem Cells.* 2007 Nov;25(11):2896-902.
- Potian JA, Aviv H, Ponzio NM, Harrison JS, Rameshwar P. Veto-like activity of mesenchymal stem cells: functional discrimination between cellular responses to alloantigens and recall antigens. *J Immunol.* 2003;171:3426-3434.

Prigione A, Adjaye J. Modulation of mitochondrial biogenesis and bioenergetic metabolism upon in vitro and in vivo differentiation of human ES and iPS cells. *Int J Dev Biol*. 2010;54(11-12):1729-41.

Prusa AR, Marton E, Rosner M, Bernaschek G, Hengstschlager M. Oct-4-expressing cells in human amniotic fluid: a new source for stem cell research? *Hum Reprod*. 2003 Jul;18(7):1489-93.

Quarto R, Mastrogiacomo M, Cancedda R, Kutepov SM, Mukhachev V, Lavroukov A, Kon E, Marcacci M. Repair of large bone defects with the use of autologous bone marrow stromal cells. *N Engl J Med*. 2001 Feb 1;344(5):385-6.

Rahman MS, Spitzhorn LS, Wruck W, Hagenbeck C, Balan P, Graffmann N, Bohndorf M, Ncube A, Guillot PV, Fehm T, Adjaye J. The presence of human mesenchymal stem cells of renal origin in amniotic fluid increases with gestational time. *Stem Cell Res Ther*. 2018 Apr 25;9(1):113.

Ramy N, Ghany EA, Alsharany W, Nada A, Darwish RK, Rabie WA, Aly H. Jaundice, phototherapy and DNA damage in full-term neonates. *J Perinatol*. 2016 Feb;36(2):132-6.

Ranzoni AM, Corcelli M, Hau KL, Kerns JG, Vanleene M, Shefelbine S, Jones GN, Moschidou D, Dala-Ali B, Goodship AE, De Coppi P, Arnett TR, Guillot PV. Counteracting bone fragility with human amniotic mesenchymal stem cells. *Sci Rep*. 2016 Dec 20;6:39656.

Razavi S, Razavi MR, Zarkesh Esfahani H, Kazemi M, Mostafavi FS. Comparing brain-derived neurotrophic factor and ciliary neurotrophic factor secretion of induced neurotrophic factor secreting cells from human adipose and bone marrow-derived stem cells. *Dev Growth Differ*. 2013 Aug;55(6):648-55.

Reichert JC, Cipitria A, Epari DR, Saifzadeh S, Krishnakanth P, Berner A, Woodruff MA, Schell H, Mehta M, Schuetz MA, Duda GN, Hutmacher DW. A tissue engineering solution for segmental defect regeneration in load-bearing long bones. *Sci Transl Med*. 2012 Jul 4;4(141):141ra93.

Reuter S, Gupta SC, Chaturvedi MM, Aggarwal BB. Oxidative stress, inflammation, and cancer: how are they linked? *Free Radic Biol Med*. 2010;49:1603-1616.

Rivera FJ, Couillard-Despres S, Pedre X, Ploetz S, Caioni M, Lois C, Bogdahn U, Aigner L. Mesenchymal stem cells instruct oligodendrogenic fate decision on adult neural stem cells. *Stem Cells*. 2006 Oct;24(10):2209-19.

Rosada C, Justesen J, Melsvik D, Ebbesen P, Kassem M. The human umbilical cord blood: a potential source for osteoblast progenitor cells. *Calcif Tissue Int*. 2003 Feb;72(2):135-42.

Rose FR, Oreffo RO. Bone tissue engineering: hope vs hype. *Biochem Biophys Res Commun*. 2002 Mar 22;292(1):1-7.

Rosenblum ND. Developmental biology of the human kidney. *Semin Fetal Neonatal Med*. 2008;13(3):125-132.

Rosner M, Schipany K, Gundacker C, Shanmugasundaram B, Li K, Fuchs C, Lubec G, Hengstschlager M. Renal differentiation of amniotic fluid stem cells: perspectives for clinical application and for studies on specific human genetic diseases. *Eur J Clin Invest*. 2012 Jun;42(6):677-84.

Roubelakis MG, Pappa KI, Bitsika V, Zagoura D, Vlahou A, Papadaki HA, Antsaklis A, Anagnostou NP. Molecular and proteomic characterization of human mesenchymal stem cells derived from amniotic fluid: comparison to bone marrow mesenchymal stem cells. *Stem Cells Dev*. 2007 Dec;16(6):931-52.

Ruud Hansen TW. Phototherapy for neonatal jaundice--therapeutic effects on more than one level? *Semin Perinatol*. 2010 Jun;34(3):231-4.

- Saidi RF, Kenari SKH. Challenges of Organ Shortage for Transplantation: Solutions and Opportunities. *Int J Organ Transplant Med.* 2014;5(3):87–96.
- Sanchez-Romero N, Schophuizen CM, Gimenez I, Masereeuw R. In vitro systems to study nephropharmacology: 2D versus 3D models. *Eur J Pharmacol* 2016;790:36–45.
- Sato Y, Araki H, Kato J, Nakamura K, Kawano Y, Kobune M, Sato T, Miyanishi K, Takayama T, Takahashi M, Takimoto R, Iyama S, Matsunaga T, Ohtani S, Matsuura A, Hamada H, Niitsu Y. Human mesenchymal stem cells xenografted directly to rat liver are differentiated into human hepatocytes without fusion. *Blood.* 2005 Jul 15;106(2):756-63.
- Savickiene J, Treigyte G, Baronaite S, Valiulienė G, Kaupinis A, Valius M, Arlauskienė A, Navakauskienė R. Human Amniotic Fluid Mesenchymal Stem Cells from Second- and Third-Trimester Amniocentesis: Differentiation Potential, Molecular Signature, and Proteome Analysis. *Stem Cells Int.* 2015;2015:319238.
- Schedl A. Renal abnormalities and their developmental origin. *Nat Rev Gen.* 2007;8:791-802.
- Schlegel KA, Lang FJ, Donath K, Kulow JT, Wiltfang J. The monocortical critical size bone defect as an alternative experimental model in testing bone substitute materials. *Oral Surg Oral Med Oral Pathol Oral Radiol Endod.* 2006 Jul;102(1):7-13.
- Schmidt-Bleek K, Willie BM, Schwabe P, Seemann P, Duda GN. BMPs in bone regeneration: Less is more effective, a paradigm-shift. *Cytokine Growth Factor Rev.* 2016 Feb;27:141-8.
- Schöbel A, Rösch K, Herker E. Functional innate immunity restricts Hepatitis C Virus infection in induced pluripotent stem cell-derived hepatocytes. *Sci Rep.* 2018 Mar 1;8(1):3893.
- Schutgens F, Verhaar MC, Rookmaaker MB. Pluripotent stem cell-derived kidney organoids: An in vivo-like in vitro technology. *Eur J Pharmacol.* 2016;790:12-20.
- Schwartz RE, Reyes M, Koodie L, Jiang Y, Blackstad M, Lund T, Lenvik T, Johnson S, Hu WS, Verfaillie CM. Multipotent adult progenitor cells from bone marrow differentiate into functional hepatocyte-like cells. *J Clin Invest.* 2002 May;109(10):1291-302.
- Scruggs BA, Semon JA, Zhang X, Zhang S, Bowles AC, Pandey AC, Imhof KM, Kalueff AV, Gimble JM, Bunnell BA. Age of the donor reduces the ability of human adipose-derived stem cells to alleviate symptoms in the experimental autoimmune encephalomyelitis mouse model. *Stem Cells Transl Med.* 2013 Oct;2(10):797-807.
- Sedrakyan S, Da Sacco S, Milanesi A, Shiri L, Petrosyan A, Varimezova R, Warburton D, Lemley KV, De Filippo RE, Perin L. Injection of amniotic fluid stem cells delays progression of renal fibrosis. *J Am Soc Nephrol.* 2012 Apr;23(4):661-73.
- Seeberger KL, Eshpeter A, Korbitt GS. Isolation and culture of human multipotent stromal cells from the pancreas. *Methods Mol Biol.* 2011;698:123-40.
- Shand J, Berg J, Bogue C; Committee for Pediatric Research; Committee on Bioethics. Human embryonic stem cell (hESC) and human embryo research. *Pediatrics.* 2012 Nov;130(5):972-7.
- Sheyn D, Ben-David S, Shapiro G, De Mel S, Bez M, Ornelas L, Sahabian A, Sareen D, Da X, Pelled G, Tawackoli W, Liu Z, Gazit D, Gazit Z. Human Induced Pluripotent Stem Cells Differentiate Into Functional Mesenchymal Stem Cells and Repair Bone Defects. *Stem Cells Transl Med.* 2016 Nov;5(11):1447-1460.
- Siegel N, Rosner M, Unbekandt M, Fuchs C, Slabina N, Dolznig H, Davies JA, Lubec G, Hengstschläger M. Contribution of human amniotic fluid stem cells to renal tissue formation depends on mTOR. *Hum Mol Genet.* 2010 Sep 1;19(17):3320-31.

- Siegel N, Valli A, Fuchs C, Rosner M, Hengstschläger M. Induction of mesenchymal/epithelial marker expression in human amniotic fluid stem cells. *Reprod Biomed Online*. 2009;19(6):838-46.
- Simoni G, Colognato R. The amniotic fluid-derived cells: the biomedical challenge for the third millennium. *J Prenat Med*. 2009 Jul;3(3):34-6.
- Smith C, Abalde-Atristain L, He C, Brodsky BR, Braunstein EM, Chaudhari P, Jang Y-Y, Cheng L, Ye Z. Efficient and Allele-Specific Genome Editing of Disease Loci in Human iPSCs. *Mol Ther* 23(3):570-577, 2015.
- Song JJ, Guyette JP, Gilpin SE, Gonzalez G, Vacanti JP, Ott HC. Regeneration and experimental orthotopic transplantation of a bioengineered kidney. *Nat Med*. 2013 May;19(5):646-51.
- Song L, Webb NE, Song Y, Tuan RS. Identification and functional analysis of candidate genes regulating mesenchymal stem cell self-renewal and multipotency. *Stem Cells*. 2006 Jul;24(7):1707-18.
- Spitzhorn LS, Kawala MA, Adjaye J. Generation of a 3D model to better mimic NAFLD in vitro. *Z Gastroenterol* 2016; 54(12): 1343-1404.
- Spitzhorn LS, Kordes C, Megges M, Sawitza I, Götze S, Reichert D, Schulze-Matz P, Graffmann N, Bohndorf M, Wruck W, Köhler JP, Herebian D, Mayatepek E, Oreffo RO, Häussinger D, Adjaye J. Transplanted human pluripotent stem cell-derived mesenchymal stem cells support liver regeneration in Gunn rats. *Stem Cells Dev*. 2018 Oct 3.
- Spitzhorn LS, Megges M, Wruck W, Rahman MS, Otte J, Degistirici Ö, Meisel R, Sorg RV, Oreffo ROC, Adjaye J. Human iPSC-derived MSCs (iMSCs) from aged individuals acquire a rejuvenation signature. *Stem Cell Res Ther*. 2019 Mar 18;10(1):100.
- Spitzhorn LS, Rahman MS, Nguyen L, Ncube A, Bohndorf M, Wruck W, Adjaye J. Urine-derived stem cells as innovative platform for drug testing and disease modelling. *Drug Target Review*. Summer 2018; Issue 02.
- Spitzhorn LS, Rahman MS, Schwindt L, Ho HT, Wruck W, Bohndorf M, Wehrmeyer S, Ncube A, Beyer I, Hagenbeck C, Balan P, Fehm T, Adjaye J. Isolation and Molecular Characterization of Amniotic Fluid-Derived Mesenchymal Stem Cells Obtained from Caesarean Sections. *Stem Cells Int*. 2017;2017:5932706.
- Squillaro T, Peluso G, Galderisi U. Clinical Trials With Mesenchymal Stem Cells: An Update. *Cell Transplant*. 2016;25(5):829-48.
- Starzl TE, Fung J, Tzakis A, Todo S, Demetris AJ, Marino IR, Doyle H, Zeevi A, Warty V, Michaels M, Kusne S, Rudert WA, Trucco M. Baboon-to-human liver transplantation. *Lancet*. 1993 Jan 9;341(8837):65-71.
- Steffenhagen C, Dechant FX, Oberbauer E, Furtner T, Weidner N, Küry P, Aigner L, Rivera FJ. Mesenchymal stem cells prime proliferating adult neural progenitors toward an oligodendrocyte fate. *Stem Cells Dev*. 2012 Jul 20;21(11):1838-51.
- Stolzing A and Scutt A. Age-related impairment of mesenchymal progenitor cell function. *Aging Cell*. 2006;5:213-224.
- Stolzing A, Jones E, McGonagle D, Scutt A. Age-related changes in human bone marrow-derived mesenchymal stem cells: consequences for cell therapies. *Mech Ageing Dev*. 2008 Mar;129(3):163-73.

- Sun Q, Li F, Li H, Chen RH, Gu YZ, Chen Y, Liang HS, You XR, Ding SS, Gao L, Wang YL, Qin MD, Zhang XG. Amniotic fluid stem cells provide considerable advantages in epidermal regeneration: B7H4 creates a moderate inflammation microenvironment to promote wound repair. *Sci Rep.* 2015 Jun 23;5:11560.
- Sutherland GR, Bain AD: Culture of cells from the urine of newborn children. *Nature.* 1972;239:231.
- Tada M, Takahama Y, Abe K, Nakatsuji N, Tada T. Nuclear reprogramming of somatic cells by in vitro hybridization with ES cells. *Curr Biol.* 2001 Oct 2;11(19):1553-8.
- Taguchi A, Kaku Y, Ohmori T, Sharmin S, Ogawa M, Sasaki H, Nishinakamura R. Redefining the in vivo origin of metanephric nephron progenitors enables generation of complex kidney structures from pluripotent stem cells. *Cell Stem Cell.* 2014 Jan 2;14(1):53-67.
- Taguchi A, Nishinakamura R. Higher-Order Kidney Organogenesis from Pluripotent Stem Cells. *Cell Stem Cell.* 2017 Dec 7;21(6):730-746.e6.
- Takahashi K, Tanabe K, Ohnuki M, Narita M, Ichisaka T, Tomoda K, Yamanaka S. Induction of pluripotent stem cells from adult human fibroblasts by defined factors. *Cell.* 2007 Nov 30;131(5):861-72.
- Takahashi K, Yamanaka S. Induction of pluripotent stem cells from mouse embryonic and adult fibroblast cultures by defined factors. *Cell.* 2006 Aug 25;126(4):663-76.
- Takahashi Y, Sekine K, Kin T, Takebe T, Taniguchi H. Self-Condensation Culture Enables Vascularization of Tissue Fragments for Efficient Therapeutic Transplantation. *Cell Rep.* 2018 May 8;23(6):1620-1629.
- Takasato M, Er PX, Chiu HS, Maier B, Baillie GJ, Ferguson C, Parton RG, Wolvetang EJ, Roost MS, Chuva de Sousa Lopes SM, Little MH. Kidney organoids from human iPS cells contain multiple lineages and model human nephrogenesis. *Nature.* 2015 Oct 22;526(7574):564-8.
- Takebe T, Enomura M, Yoshizawa E, Kimura M, Koike H, Ueno Y, Matsuzaki T, Yamazaki T, Toyohara T, Osafune K, Nakauchi H, Yoshikawa HY, Taniguchi H. Vascularized and Complex Organ Buds from Diverse Tissues via Mesenchymal Cell-Driven Condensation. *Cell Stem Cell.* 2015 May 7;16(5):556-65.
- Takebe T, Zhang RR, Koike H, Kimura M, Yoshizawa E, Enomura M, Koike N, Sekine K, Taniguchi H. Generation of a vascularized and functional human liver from an iPSC-derived organ bud transplant. *Nat Protoc.* 2014 Feb;9(2):396-409.
- Taranger CK, Noer A, Sørensen AL, Håkelién AM, Boquest AC, Collas P. Induction of dedifferentiation, genomewide transcriptional programming, and epigenetic reprogramming by extracts of carcinoma and embryonic stem cells. *Mol Biol Cell.* 2005 Dec;16(12):5719-35.
- Tavernier G, Mlody B, Demeester J, Adjaye J, De Smedt SC. Current methods for inducing pluripotency in somatic cells. *Adv Mater.* 2013 May 28;25(20):2765-71.
- TheinHan W, Liu J, Tang M, Chen W, Cheng L, Xu HH. Induced pluripotent stem cell-derived mesenchymal stem cell seeding on biofunctionalized calcium phosphate cements. *Bone Res.* 2013;4:371-384.
- Thomson JA, Itskovitz-Eldor J, Shapiro SS, Waknitz MA, Swiergiel JJ, Marshall VS, Jones JM. Embryonic stem cell lines derived from human blastocysts. *Science.* 1998 Nov 6;282(5391):1145-7.
- Tögel F, Hu Z, Weiss K, Isaac J, Lange C, Westenfelder C. Administered mesenchymal stem cells protect against ischemic acute renal failure through differentiation-independent mechanisms. *Am J Physiol Renal Physiol.* 2005 Jul;289(1):F31-42.

Toma JG, McKenzie IA, Bagli D, Miller FD. Isolation and characterization of multipotent skin-derived precursors from human skin. *Stem Cells*. 2005 Jun-Jul;23(6):727-37.

Tomasoni S, Longaretti L, Rota C, Morigi M, Conti S, Gotti E, Capelli C, Introna M, Remuzzi G, Benigni A. Transfer of growth factor receptor mRNA via exosomes unravels the regenerative effect of mesenchymal stem cells. *Stem Cells Dev*. 2013 Mar 1;22(5):772-80.

Tong GX, Yu WM, Beaubier NT, Weeden EM, Hamele-Bena D, Mansukhani MM, O'Toole KM. Expression of PAX8 in normal and neoplastic renal tissues: an immunohistochemical study. *Mod Pathol*. 2009 Sep;22(9):1218-27.

Torricelli F, Brizzi L, Bernabei PA, Gheri G, Di Lollo S, Nutini L, Lisi E, Di Tommaso M, Cariatì E. Identification of hematopoietic progenitor cells in human amniotic fluid before the 12th week of gestation. *Ital J Anat Embryol*. 1993 Apr-Jun;98(2):119-26.

Trounson A, McDonald C. Stem Cell Therapies in Clinical Trials: Progress and Challenges. *Cell Stem Cell*. 2015 Jul 2;17(1):11-22.

Tsai MS, Hwang SM, Chen KD, Lee YS, Hsu LW, Chang YJ, Wang CN, Peng HH, Chang YL, Chao AS, Chang SD, Lee KD, Wang TH, Wang HS, Soong YK. Functional network analysis of the transcriptomes of mesenchymal stem cells derived from amniotic fluid, amniotic membrane, cord blood, and bone marrow. *Stem Cells*. 2007 Oct;25(10):2511-23.

Uccelli A, Laroni A, Freedman MS. Mesenchymal stem cells for the treatment of multiple sclerosis and other neurological diseases. *Lancet Neurol*. 2011 Jul;10(7):649-56.

Uccelli A, Moretta L, Pistoia V. Mesenchymal stem cells in health and disease. *Nat Rev Immunol*. 2008 Sep;8(9):726-36.

Underwood MA, Gilbert WM, Sherman MP. Amniotic fluid: not just fetal urine anymore. *J Perinatol*. 2005 May;25(5):341-8.

van den Berg CW, Ritsma L, Avramut MC, Wiersma LE, van den Berg BM, Leuning DG, Liewers E, Koning M, Vanslambrouck JM, Koster AJ, Howden SE, Takasato M, Little MH, Rabelink TJ. Renal Subcapsular Transplantation of PSC-Derived Kidney Organoids Induces Neo-vasculogenesis and Significant Glomerular and Tubular Maturation In Vivo. *Stem Cell Reports*. 2018 Mar 13;10(3):751-765.

van Dijk R, Beuers U, Bosma PJ. Gene replacement therapy for genetic hepatocellular jaundice. *Clin Rev Allergy Immunol*. 2015 Jun;48(2-3):243-53.

van Poll D, Parekkadan B, Cho CH, Berthiaume F, Nahmias Y, Tilles AW, Yarmush ML. Mesenchymal stem cell-derived molecules directly modulate hepatocellular death and regeneration in vitro and in vivo. *Hepatology*. 2008 May;47(5):1634-43.

Vassilopoulos G, Wang PR, Russell DW. Transplanted bone marrow regenerates liver by cell fusion. *Nature*. 2003 Apr 24;422(6934):901-4.

Večerić-Haler Ž, Cerar A, Perše M. (Mesenchymal) Stem cell-based therapy in cisplatin induced acute kidney injury animal model: risk of immunogenicity and tumorigenicity. *Stem Cells International*. vol. 2017, Article ID 7304643.

Villa-Diaz LG, Brown SE, Liu Y, Ross AM, Lahann J, Parent JM, Krebsbach PH. Derivation of mesenchymal stem cells from human induced pluripotent stem cells cultured on synthetic substrates. *Stem Cells*. 2012 Jun;30(6):1174-81.

Vogel S, Trapp T, Börger V, Peters C, Lakbir D, Dilloo D, Sorg RV. Hepatocyte growth factor-mediated attraction of mesenchymal stem cells for apoptotic neuronal and cardiomyocytic cells. *Cell Mol Life Sci*. 2010 Jan;67(2):295-303.

Wagner W, Bork S, Horn P, Kronic D, Walenda T, Diehlmann A, Benes V, Blake J, Huber FX, Eckstein V, Boukamp P, Ho AD. Aging and replicative senescence have related effects on human stem and progenitor cells. *PLoS One*. 2009 Jun 9;4(6):e5846.

Wagner W, Ho AD, Zenke M. Different facets of aging in human mesenchymal stem cells. *Tissue Eng Part B Rev*. 2010 Aug;16(4):445-53.

Wagner W, Horn P, Castoldi M, Diehlmann A, Bork S, Saffrich R, Benes V, Blake J, Pfister S, Eckstein V, Ho AD. Replicative senescence of mesenchymal stem cells: a continuous and organized process. *PLoS One*. 2008 May 21;3(5):e2213.

Walker N, Badri L, Wettlaufer S, Flint A, Sajjan U, Krebsbach PH, Keshamouni VG, Peters-Golden M, Lama VN. Resident tissue-specific mesenchymal progenitor cells contribute to fibrogenesis in human lung allografts. *Am J Pathol*. 2011 Jun;178(6):2461-9.

Wang P, Zhao L, Liu J, Weir MD, Zhou X, Xu HH. Bone tissue engineering via nanostructured calcium phosphate biomaterials and stem cells. *Bone Res*. 2014 Sep 30;2:14017.

Wang S, Qu X, Zhao RC. Clinical applications of mesenchymal stem cells. *J Hematol Oncol*. 2012 Apr 30;5:19.

Wang X, Kimbrel EA, Ijichi K, Paul D, Lazorchak AS, Chu J, Kouris NA, Yavarian GJ, Lu SJ, Pachter JS, Crocker SJ, Lanza R, Xu RH. Human ESC-derived MSCs outperform bone marrow MSCs in the treatment of an EAE model of multiple sclerosis. *Stem Cell Reports*. 2014 Jun 6;3(1):115-30.

Wang X, Willenbring H, Akkari Y, Torimaru Y, Foster M, Al-Dhalimy M, Lagasse E, Finegold M, Olson S, Grompe M. Cell fusion is the principal source of bone-marrow-derived hepatocytes. *Nature*. 2003 Apr 24;422(6934):897-901.

Warnke PH, Springer IN, Wiltfang J, Acil Y, Eufinger H, Wehmöller M, Russo PA, Bolte H, Sherry E, Behrens E, Terheyden H. Growth and transplantation of a custom vascularised bone graft in a man. *Lancet*. 2004 Aug 28-Sep 3;364(9436):766-70.

Weissman IL. Translating stem and progenitor cell biology to the clinic: barriers and opportunities. *Science*. 2000 Feb 25;287(5457):1442-6.

Wenceslau CV, Miglino MA, Martins DS, Ambrósio CE, Lizier NF, Pignatari GC, Kerkis I. Mesenchymal progenitor cells from canine fetal tissues: yolk sac, liver, and bone marrow. *Tissue Eng Part A*. 2011 Sep;17(17-18):2165-76.

Williams AR, Hare JM. Mesenchymal stem cells: biology, pathophysiology, translational findings, and therapeutic implications for cardiac disease. *Circ Res*. 2011 Sep 30;109(8):923-40.

Wilmer MJ, Ng CP, Lanz HL, Vulto P, Suter-Dick L, Masereeuw R. Kidney-on-a-Chip Technology for Drug-Induced Nephrotoxicity Screening. *Trends Biotechnol*. 2016 Feb;34(2):156-170.

Wilmot I, Schnieke AE, McWhir J, Kind AJ, Campbell KH. Viable offspring derived from fetal and adult mammalian cells. *Cloning Stem Cells*. 2007 Spring;9(1):3-7.

Wilson A, Shehadeh LA, Yu H, Webster KA. Age-related molecular genetic changes of murine bone marrow mesenchymal stem cells. *BMC Genomics*. 2010 Apr 7;11:229.

Wolfrum K, Wang Y, Prigione A, Sperling K, Lehrach H, Adjaye J. The LARGE principle of cellular reprogramming: lost, acquired and retained gene expression in foreskin and amniotic fluid-derived human iPS cells. *PLoS One*. 2010 Oct 29;5(10):e13703.

Woodbury D, Schwarz EJ, Prockop DJ, Black IB. Adult rat and human bone marrow stromal cells differentiate into neurons. *J Neurosci Res*. 2000 Aug 15;61(4):364-70.

Wu Y, Zhao RC, Tredget EE. Concise review: bone marrow-derived stem/progenitor cells in cutaneous repair and regeneration. *Stem Cells*. 2010 May;28(5):905-15.

Xia Y, Nivet E, Sancho-Martinez I, Gallegos T, Suzuki K, Okamura D, Wu MZ, Dubova I, Esteban CR, Montserrat N, Campistol JM, Izpisua Belmonte JC. Directed differentiation of human pluripotent cells to ureteric bud kidney progenitor-like cells. *Nat Cell Biol*. 2013 Dec;15(12):1507-15.

Xinaris C, Benedetti V, Novelli R, Abbate M, Rizzo P, Conti S, Tomasoni S, Corna D, Pozzobon M, Cavallotti D, Yokoo T, Morigi M, Benigni A, Remuzzi G. Functional Human Podocytes Generated in Organoids from Amniotic Fluid Stem Cells. *J Am Soc Nephrol*. 2016 May;27(5):1400-11.

Xing YL, Röth PT, Stratton JA, Chuang BH, Danne J, Ellis SL, Ng SW, Kilpatrick TJ, Merson TD. Adult neural precursor cells from the subventricular zone contribute significantly to oligodendrocyte regeneration and remyelination. *J Neurosci*. 2014 Oct 15;34(42):14128-46.

Yang YK, Ogando CR, Wang See C, Chang TY, Barabino GA. Changes in phenotype and differentiation potential of human mesenchymal stem cells aging in vitro. *Stem Cell Res Ther*. 2018 May 11;9(1):131.

Yu J, Chau KF, Vodyanik MA, Jiang J, Jiang Y. Efficient feeder-free episomal reprogramming with small molecules. *PLoS One*. 2011 Mar 1;6(3):e17557.

Zagoura DS, Roubelakis MG, Bitsika V, Trohatou O, Pappa KI, Kapelouzou A, Antsaklis A, Anagnostou NP. Therapeutic potential of a distinct population of human amniotic fluid mesenchymal stem cells and their secreted molecules in mice with acute hepatic failure. *Gut*. 2012 Jun;61(6):894-906.

Zeiser R, Blazar BR. Acute Graft-versus-Host Disease - Biologic Process, Prevention, and Therapy. *N Engl J Med*. 2017 Nov 30;377(22):2167-2179.

Zhang D, Wei G, Li P, Zhou X, Zhang Y. Urine-derived stem cells: A novel and versatile progenitor source for cell-based therapy and regenerative medicine. *Genes Dis*. 2014;1(1):8-17.

Zhang J, Guan J, Niu X, Hu G, Guo S, Li Q, Xie Z, Zhang C, Wang Y. Exosomes released from human induced pluripotent stem cells-derived MSCs facilitate cutaneous wound healing by promoting collagen synthesis and angiogenesis. *J Transl Med*. 2015 Feb 1;13:49.

Zhang S, Chen S, Li W, Guo X, Zhao P, Xu J, Chen Y, Pan Q, Liu X, Zychlinski D, Lu H, Tortorella MD, Schambach A, Wang Y, Pei D, Esteban MA. Rescue of ATP7B function in hepatocyte-like cells from Wilson's disease induced pluripotent stem cells using gene therapy or the chaperone drug curcumin. *Hum Mol Genet*. 2011 Aug 15;20(16):3176-87.

Zhang Y, McNeill E, Tian H, Soker S, Andersson KE, Yoo JJ, Atala A. Urine derived cells are a potential source for urological tissue reconstruction. *J Urol*. 2008 Nov;180(5):2226-33.

Zhao W, Li JJ, Cao DY, Li X, Zhang LY, He Y, Yue SQ, Wang DS, Dou KF. Intravenous injection of mesenchymal stem cells is effective in treating liver fibrosis. *World J Gastroenterol*. 2012 Mar 14;18(10):1048-58.

Zhou S, Greenberger JS, Epperly MW, Goff JP, Adler C, Leboff MS, Glowacki J. Age-related intrinsic changes in human bone-marrow-derived mesenchymal stem cells and their differentiation to osteoblasts. *Aging Cell*. 2008 Jun;7(3):335-43.

Zhou W, Freed CR. Adenoviral gene delivery can reprogram human fibroblasts to induced pluripotent stem cells. *Stem Cells*. 2009 Nov;27(11):2667-74.

Zhou W, Liu Q, Xu B. Improvement of bone defect healing in rats via mesenchymal stem cell supernatant. *Exp Ther Med*. 2018 Feb;15(2):1500-1504.

Zuk PA, Zhu M, Ashjian P, De Ugarte DA, Huang JI, Mizuno H, Alfonso ZC, Fraser JK, Benhaim P, Hedrick MH. Human adipose tissue is a source of multipotent stem cells. *Mol Biol Cell*. 2002 Dec;13(12):4279-95.

Acknowledgements

I am deeply grateful to Prof. Dr. James Adjaye who was my supervisor during my PhD work. He supported me in my scientific and personal development. In his Institute for Stem Cell Research and Regenerative Medicine he has created a great scientific unit which is known all over the world. I really enjoyed working under his lead and am looking forward to the next years of our collaboration. Furthermore, I would like to thank Prof. Dr. Henrike Heise for being the co-supervisor of my thesis. She was always very open and supportive.

Next, I would like to thank all co-authors I was allowed to publish with. Especially, I want to emphasize the role of Dr. Claus Kordes from the Clinic of Gastroenterology, Hepatology and Infectious Diseases (Director Prof. Dr. Dieter Häussinger), who was like a mentor for me. He taught me numerous things making me a better scientist. We worked together as a strong team and had always a very positive and productive time.

I also appreciate the still ongoing collaborations with Prof. Dr. Pascal Jungbluth and Dr. Jan Grassmann from the Department of Trauma and Hand Surgery (Director Prof. Dr. Joachim Windolf) and with Prof. Dr. Tanja Fehm and Dr. Carsten Hagenbeck from the Department of Obstetrics and Gynaecology. I am very thankful to Prof. Dr. Richard O. C. Oreffo from the Bone and Joint Research Group (University of Southampton) for providing the fetal MSCs.

Of course, I also thank all my colleagues in the institute. We really created a harmonic and friendly atmosphere and supported each other as a team. Especially I would like to mention Md Shaifur Rahman, Audrey Ncube, Wasco Wruck, Dr. Nina Graffmann, Martina Bohndorf, Silke Wehrmeyer, Rita Ofterdinger, Dr. Jörg Otte, Lisa Nguyen, Dr. Matthias Megges, Soraia Martins, Dr. Lars Erichsen, Aurelian Robert Fiszl, Dragana Malic and Dr. Peggy Schulze-Matz. Furthermore, I would like to thank Katharina Raba for her support and Dr. Janusz Jadasz, who gave great advice during my PhD time.

In addition to that, I thank my family and friends, who always were interested in my work and supported me during my studies.

Most importantly, with all my heart, I sincerely thank my parents. They supported me my whole life and taught me all important values which allowed me to become the man I am now.

Curriculum Vitae

Personal Details

Name Lucas-Sebastian Spitzhorn
Address Yorckstraße 10, 40476 Düsseldorf
Telephone 0171/1532095
E-Mail-Address lucas-sebastian.spitzhorn@med.uni-duesseldorf.de
Date of Birth, Place 26/06/1989, Düsseldorf, Germany



Professional Experience

2014 – 2020 PhD in Biology; Heinrich Heine University Düsseldorf

Institute for Stem Cell Research and Regenerative Medicine; University Hospital Düsseldorf

Theme of the PhD Thesis:
Derivation, characterization and application of human primary stem cells, iPSCs, and iPSC-derived MSCs for regenerative medicine and disease modelling

Education

2012 – 2014 Biology (Master of Science); Heinrich Heine University Düsseldorf

Institute for Stem Cell Research and Regenerative Medicine; University Hospital Düsseldorf; Theme of the Master Thesis:
Comparative characterization of human native mesenchymal stem cells and mesenchymal stem cells derived from induced pluripotent stem cells
(Grade: 1.3)
Final Grade: 1.60

2009 – 2012 Biology (Bachelor of Science); Heinrich Heine University Düsseldorf

Institute of Transplantation Diagnostics and Cell Therapeutics; University Hospital Düsseldorf; Theme of the Bachelor Thesis:
Definition of critical parameters for the detection of the immunosuppressive activity of human mesenchymal stem cells
(Grade: 1.3)
Final Grade: 1.87

2008 – 2009 RWTH Aachen University
Course of Studies: Mechanical Engineering (Bachelor of Science)

1999 – 2008 Humboldt-Gymnasium, Düsseldorf
Final Abitur (equivalent to A level) Grade: 1.4

Internships

03/04/2012 – 15/05/2012 Institute of Transplantation Diagnostics and Cell Therapeutics; University Hospital Düsseldorf
Practical Course:
Isolation and characterization of human mesenchymal stem cells

12/03/2012 – 16/03/2012	Medizinische Laboratorien Düsseldorf Department: Microbiology: Diagnostics for stool and smears
09/03/2010 – 29/03/2010	Medizinische Laboratorien Düsseldorf Department: Molecular Biology
16/06/2008 – 27/07/2008	Hille & Müller GmbH, Düsseldorf Machining skills like chiselling, making screw threads etc.; generating complete working pieces; welding; engineering drawing on the drawing board and with a CAD system
16/01/2006 – 27/01/2006	Bayer Industry Services, Wuppertal Basic chemical reactions; Generation of Aspirin powder
Languages	German (native speaker), English (fluent)
Activities and Interests	sports (intensive cardio and strength workouts four times a week), music, personal development, reading, family and friends, photography, art
Advanced Qualifications	“Good Scientific Practice for PhD Students”; 2015 “GASL Hands on workshop 2016. Isolation of non-parenchymal liver cells from mice/rats: HSC, LSEC, BEC” iGRAD Course “Self and time Management”; 2016 iGRAD Course “Leadership Skills”; 2017 iGRAD Course “Emotional Intelligence”; 2017 CEDUS Businessplan-Workshop; 2017 Course: “The GMP-Quality Standard and Its Benefits for Research and Development”, 2019 Course: “The Two Faces of Processing ATMPs”, 2019
Additional Effort	Ideenwettbewerb Heinrich Heine University Düsseldorf, Audience Award for the concept „Urinstammzellbank“, 2016 BioRiver Boost; One of the eight winners with the concept “Urinstammzellbank/-service”, Neuss, 2016 Poster Award at the 9 th International Meeting Stem Cell Network NRW, Münster, 2017 NUK Businessplan Competition 2 nd Prize and Audience Award for UriCell 3 rd Place Poster Award at Stem Cell Community Day, Düsseldorf, 2018 Rheinischer Innovationspreis for UriCell, 2018 Hans-Jürgen-Bretschneider-Prize, 23 rd Surgical Research Days of the German Society of Surgery, Aachen, 2019 Research Award of the AO Germany, German Congress for Orthopaedics and Traumatology, Berlin, 2019 Winner of the Future Life Science Award of the Handelsblatt University Innovation Challenge with the project UriCell, 2019 Finalist: BioRiver Boost with the project UriCell, Bergisch-Gladbach, 2019

Lucas-Sebastian Spitzhorn

Düsseldorf, 19th January 2020

Declaration of Authorship

Ich, Lucas-Sebastian Spitzhorn, versichere an Eides Statt, dass die Dissertation von mir selbständig und ohne unzulässige fremde Hilfe unter Beachtung der „Grundsätze zur Sicherung guter wissenschaftlicher Praxis an der Heinrich-Heine-Universität Düsseldorf“ erstellt worden ist. Ich habe bisher keine erfolglosen Promotionsversuche unternommen.

Signature:

Lucas-Sebastian Spitzhorn

Düsseldorf, January 2020